A Dehydrogenative Dehydro-Diels-Alder Reaction and its Application to Fluorescent Tools and Natural Product Synthesis

by

Laura S. Kocsis

B.S. Chemistry, Carnegie Mellon University, 2009

Submitted to the Graduate Faculty of the

Kenneth P. Dietrich School of Arts and Sciences in partial fulfillment

of the requirements for the degree of

Doctor of Philosophy

University of Pittsburgh

2014

UNIVERSITY OF PITTSBURGH

Kenneth P. Dietrich School of Arts and Sciences

This dissertation was presented

by

Laura S. Kocsis

It was defended on

August 26th, 2014

and approved by

Dennis P. Curran, Bayer Professor, Department of Chemistry

W. Seth Horne, Assistant Professor, Department of Chemistry

Bruce Armitage, Professor, Department of Chemistry, Carnegie Mellon University

Dissertation Advisor: Kay M. Brummond, Professor, Department of Chemistry

A Dehydrogenative Dehydro-Diels-Alder Reaction and its Application to Fluorescent Tools and Natural Product Synthesis

Laura S. Kocsis, PhD

University of Pittsburgh, 2014

Functionalized naphthalenes are valuable building blocks in many areas of chemistry, such as natural products, drugs, and fluorescent dyes, but advances in new synthetic methods to generate naphthalenes have been limited. We have developed a microwave-assisted, intramolecular dehydrogenative dehydro-Diels–Alder (DDDA) reaction of styrenyl derivatives which affords cyclopenta[*b*]naphthalene products that cannot be accessed using existing synthetic strategies. The DDDA reaction can be performed in as little as 30 minutes to provide diverse naphthalene compounds exclusively and in high yields; only in examples involving heteroatom substitution of the styrene-yne tether were mixtures of naphthalene and dihydronaphthalene products obtained.

In order to better understand and control the selectivity of DDDA reactions resulting in product mixtures, the mechanisms of formation for the naphthalene and dihydronaphthalene substrates were investigated. Isotopic labeling experiments and gas detection studies revealed that these two products were generated via diverging mechanisms of a common intermediate, where dihydronaphthalene substrates were produced via a radical pathway, while naphthalene compounds were yielded by unimolecular elimination of hydrogen gas. As an additional outcome of these mechanistic studies, reaction conditions were established for the selective production of either naphthalene or dihydronaphthalene products in high yields.

The synthetic utility of the DDDA reaction was demonstrated by its application to the synthesis of eight aryldihydronaphthalene and arylnaphthalene lignan natural products, including

taiwanin C and justicidin B. Computational methods for chemical shift assignment were developed, which showed good correlation with experimental spectra and allowed for regioisomeric lignans to be distinguished. The synthetic utility of DDDA reaction was realized by a single-step conversion of halogenated cyclopenta[*b*]naphthalene substrates to solvatochromic fluorophores. These fluorescent dyes displayed red-shifted spectral properties compared to PRODAN, a commonly used and structurally related fluorescent biological probe, making them potentially valuable for study in biological systems. Moreover, structure-photophysical property relationships (SPPR) of cyclopenta[*b*]naphthalene dyes were determined by utilizing the DDDA reaction to introduce systematic variations in fluorophore structure, such as changes in donor position, which significantly altered the dyes' photophysical properties. The SPPR determined will allow for the future rational design and tuning of fluorophore structure and photophysical properties to address specific needs in biological applications.

TABLE OF CONTENTS

LIST OF TABLES

LIST OF FIGURES

LIST OF SCHEMES

LIST OF EQUATIONS

LIST OF ABBREVIATIONS

$\Delta\delta$	chemical shift deviation
^{1}H NMR	proton nuclear magnetic resonance
^{13}C NMR	carbon nuclear magnetic resonance
Ac_2O	acetic anhydride
ASAP	atmospheric solids analysis probe
B3LYP	Becke, 3-parameter, Lee-Yang-Parr
BDE	bond dissociation energy
BOP-Cl	bis(2-oxo-3-oxazolidinyl)phosphinic chloride
Bz	benzoyl
$CDCl_3$	deuterated chloroform
Cs_2CO_3	cesium carbonate
Cy	cyclohexane
DA	Diels-Alder
DCC	*N,N'*-dicyclohexylcarbodiimide
DCM	dichloromethane
DCE	1,2-dichloroethane
DDA	dehydro-Diels-Alder
DDDA	dehydrogenative dehydro-Diels-Alder

DDQ	2,3-dichloro-5,6-dicyanobenzoquinone
DFT	density functional theory
DIBAL-H	diisobutylaluminum hydride
DIPEA	*N*,*N*-diisopropylethylamine
DMAP	4-dimethylaminopyridine
DMF	*N*,*N*-dimethylformamide
DMSO	dimethylsulfoxide
EDCI•HCl	1-ethyl-3-(3-dimethylaminopropyl)carbodiimide hydrochloride
EDG	electron-donating group
ES	electrospray
Et_2O	diethyl ether
Et_3N	triethylamine
EtOH	ethanol
EWG	electron-withdrawing group
GC	gas chromatography
HCl	hydrochloric acid
HOMO	highest occupied molecular orbital
HPLC	high performance liquid chromatography
HRMS	high resolution mass spectrometry
IL	ionic liquid
IR	infrared spectroscopy
KIE	kinetic isotope effect
LHMDS	lithium hexamethyldisilylazide

LRMS	low resolution mass spectrometry
LUMO	lowest unoccupied molecular orbital
MeCN	acetonitrile
MMFF	Merck Molecular Force Field
MP	melting point
MS	mass spectrometry
MWI	microwave irradiation
*n*BuLi	*n*-butyllithium
NMP	N-methyl-2-pyrrolidone
o-DCB	1,2-dichlorobenzene
o-DCB-d_4	1,2-dichlorobenzene-d_4
PCC	pyridinium chlorochromate
PhMe	toluene
$PhNO_2$	nitrobenzene
PICT	planar intramolecular charge transfer
PTP	push-triazole-pull
R^2	coefficient of determination
SPPR	structure-photophysical property relationships
rt	room temperature
tan δ	loss tangent
TBAF	tetra-*n*-butylammonium fluoride
TD	time dependent
TICT	twisted intramolecular charge transfer

THF	tetrahydrofuran
TLC	thin layer chromatography
TMS	trimethysilyl
TOF	time-of-flight
Ts	tosyl
UV	ultraviolet light

ACKNOWLEDGEMENTS

There are numerous people that I need to thank for supporting me throughout my time as a graduate student. First, I would like to thank my adviser, Professor Kay Brummond, who has supported and challenged me over the past five years. She believed in me more than I believed in myself at times, and everything that I accomplished along the way is due to her pushing me to be better. I have always appreciated the freedom that Kay gave me to pursue my own ideas and to think outside the box, and I have become a better scientist as a result. Her ability to see the bigger picture and to always work toward it has been a constant inspiration to me, and it is something that I hope I can carry on as I move on to my next endeavor.

I cannot thank Kay without thanking the members of the Brummond group past and present who have helped me along the way, either by teaching me, answering my questions, doing me favors, or dealing with my latest practical joke. In particular, I would like to thank Erica Benedetti and Mélanie Charpenay who I had the pleasure to collaborate with. I have learned a great deal from them, and without their hard work this thesis would be much shorter. I would also like to acknowledge Ashley Bober, Paul Jackson, Lauren Parrette, and Sarah Wells for helping me to correct my thesis. When I needed an extra set of eyes, they offered to help me without hesitation. I would like to give special thanks to Ashley; she went above and beyond to assist me with my thesis and to set my mind at ease during this stressful time, and I am so

grateful to her. Josh Osbourn also deserves recognition. He always answered every question I asked of him during and after his time in the Brummond group, but more importantly, he has been a great friend and role model.

There have been other people that I have had the chance to learn from and work with that have been instrumental to my success in graduate school. These include my committee members Professor Dennis Curran, Professor Seth Horne, and Professor Bruce Armitage, as well as my collaborators Sharlene Chin and Professor Dean Tantillo from UC Davis, Kristy Elbel and Professor Emmanuel Theodorakis from UC San Diego, Billie Hardigree and Professor Mark Haidekker from University of Georgia, Xing Yin and Professor David Waldeck from University of Pittsburgh, and Husain Kagalwala and Professor Stefan Bernhard from Carnegie Mellon University. I would also like to thank the staff of the instrumental facilities at the University of Pittsburgh, including Sage Bowser, Viswanathan Elumalai, Steve Geib, Joel Gillespie, Bhaskar Godugu, and Damodaran Krishnan, who not only taught me new methods, but performed experiments for me that I would not have been able to do alone. I am fortunate to have had the opportunity to work with each of you during my time at Pitt.

I cannot talk about my graduate school experience with mentioning the friends that have supported me along the way. These include my "first year" friends Upamanyu Basu, Kevin Bivona, Conor Haney, Ben Hay, Nicole Kennedy, George Lengyel, Everett Merling, and Robin Sloan as well as those from high school, college, and graduate school who have made an effort to stay in touch with me, even when I have all but disappeared from the social scene. I appreciate their endless patience and acceptance of my schedule, and thank them for the time they spent visiting me when I could not come to see them. I would especially like to thank Silvia Bezer, Anatolie Bratu, Kyle Magocs, and the many people that have offered to open their homes to me

during my last month at Pitt. It has been a great comfort knowing that I always have somewhere to call home.

As I move on from my time in graduate school to the next stage of my life and career, I realize that the transition would have been much more difficult without the efforts of a network of chemists that have assisted me. Matt Curry, Ben Dugan, Jamie Mccabe Dunn, and Jay Theroff all helped me to find career opportunities, and it was a great relief to have them in my corner. I would also like to thank Catalina Achim and Craig Zificsak, who have become mentors to me throughout both my undergraduate and graduate studies. The advice that they have shared, and the help that they have provided allowed me to become a better chemist. Craig always made himself available to me, especially as graduation approached, and he answered every question I passed his way. He has been a great friend and an even better mentor.

Lastly, and most importantly, I would like to acknowledge my parents, Susan and Keith, for their endless love, support, and patience. They have not only encouraged me to always perform at my best, but they have also helped me make every difficult decision I have encountered along the way. My parents have displayed endless understanding for the missed holidays and special occasions that came along with my pursuit of graduate school, and I can only promise that I will make up for all my absences in the time to come. I am eternally grateful for everything that they have done for me to get me to where I am today, and I would not be the person I am without their guidance. Graduate school has not been easy, but it was much easier with their help.

1.0 DEVELOPMENT OF A MICROWAVE-ASSISTED INTRAMOLECULAR DEHYDROGENATIVE DEHYDRO-DIELS-ALDER REACTION FOR THE SYNTHESIS OF NOVEL NAPHTHALENE FRAMEWORKS

This chapter is based on results present in:

Kocsis, L. S.; Benedetti, E.; Brummond, K. M. A Thermal Dehydrogenative Diels–Alder Reaction of Styrenes for the Concise Synthesis of Functionalized Naphthalenes. *Org. Lett.* **2012**, *14*, 4430-4433.

1.1 INTRODUCTION

Design and synthesis of small molecules for the purpose of function enables advancement in fields ranging from pharmaceuticals to pesticides. Unfortunately, modern synthetic method development has not matched the demand for certain classes of small molecules, one example being novel naphthalene substrates. Functionalized naphthalenes can serve as valuable building blocks in many important areas of chemistry, which has increased their appeal as synthetic targets. For example, several natural products that show desirable biological activity and contain a naphthalene core have been isolated, including rifampicin, michellamines, and gossypol (Figure 1.1). Rifampicin (**1.1**) is an antiviral and antibacterial agent that is used in the treatment of tuberculosis, while biaryl dimer michellamine B (**1.2**) behaves as a potent HIV inhibitor. Both

of these drugs act through inhibition of viral replication.[1] The atropisomers of gossypol are especially interesting because they show independent biological properties, with (*R*)-gossypol (not shown) being active against tumor cells and HIV-1,[2] and (*S*)-gossypol (**1.3**) inhibiting viruses such as herpes and influenza.[3] In addition to natural products, small molecule naphthalene-containing drugs have been developed, such as the antifungal agents tolnaftate (**1.4**) and terbinafine (**1.5**),[4] the anti-inflammatory compound naproxen (**1.6**),[5] and the penicillin derivative nafcillin (**1.7**),[6] which is used in the treatment of bacterial infections that are pencillin resistant (Figure 1.2). Many fluorescent dyes are also based on a naphthalene scaffold, with two of the most well-known being PRODAN (**1.8**), used predominantly for the study of lipid membrane environments,[7] and dansyl chloride (**1.9**), an amino acid label for investigation of protein structure and interactions (Figure 1.3).[8] The membrane potential probe JC-9 (**1.10**) and the pH indicators 5(6)-carboxynaphthofluorescein (**1.11**) and 5(6)-SNARF (**1.12**) are further examples of naphthalene-based fluorophores.[9]

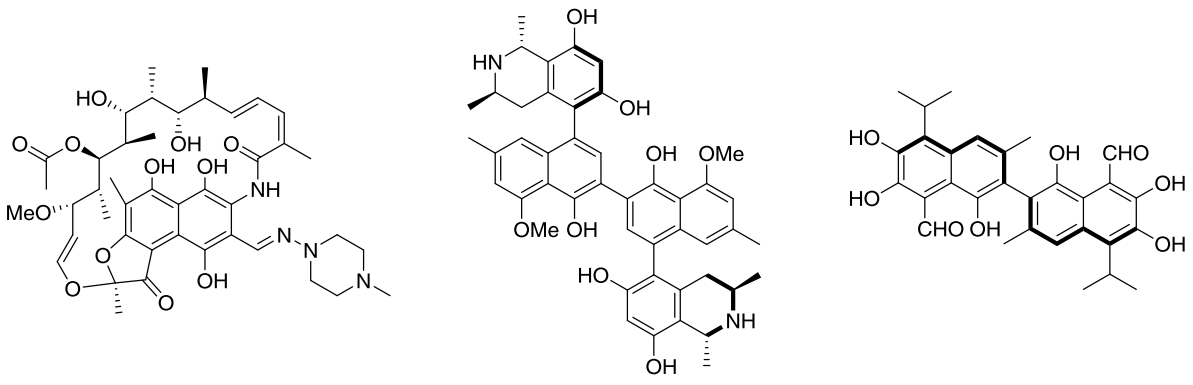

Figure 1.1. Bioactive natural products containing a naphthalene framework

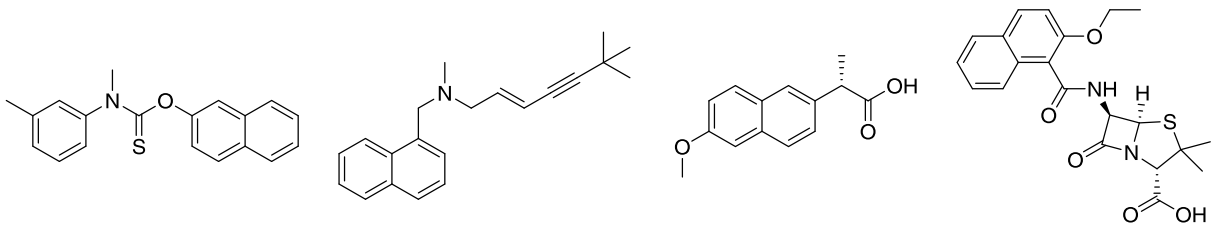

Tolnaftate (1.4)
Antifungal

Terbinafine (1.5)
Antifungal

Naproxen (1.6)
Antiinflammatory

Nafcillin (1.7)
Antibacterial

Figure 1.2. Naphthalene-containing drugs

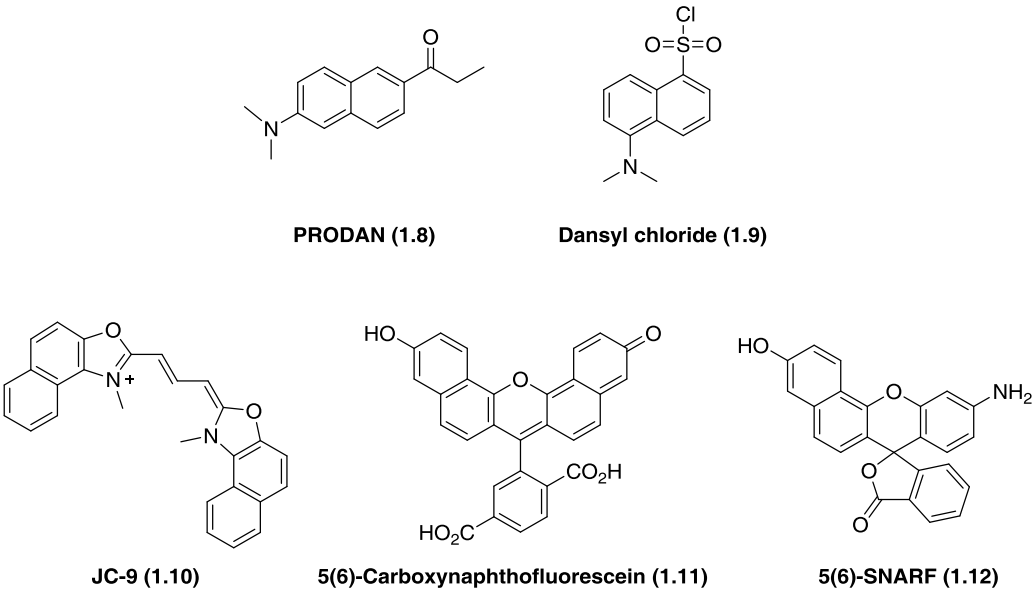

PRODAN (1.8)

Dansyl chloride (1.9)

JC-9 (1.10)

5(6)-Carboxynaphthofluorescein (1.11)

5(6)-SNARF (1.12)

Figure 1.3. Naphthalene-based fluorophores

Despite the many functions of naphthalene, synthetic routes to access naphthalene derivatives have traditionally relied on substitution reactions of commercially available naphthalene substrates; however, this approach provides products of limited diversity and is often hampered by lack of regiochemical control. To generate more functionalized and varied naphthalene compounds, reactions of benzene derivatives in the form of benzannulation strategies have been explored, but as a general means of accessing diverse naphthalene frameworks, these protocols are still restricted.[10] Phthalide annulations have been implemented for the generation of naphthalene structures, with one prominent example being the reaction of homophthalic anhydride **1.13** with the enolizable enone **1.14**,[11] a variant of which was utilized as a key step in the first asymmetric total synthesis of fredericamycin A (**1.15**) by Kita et al. (Scheme 1.1).[12] Naphthalenes are also produced by Lewis acid or acid-catalyzed cyclizations. For example, cyclization of Stobbe condensation products **1.16** with acetic acid is one method of naphthalene formation that has found application in the synthesis of (*S*)-gossypol by Meyers et al. (for structure see Figure 1.1).[13] The rearrangement of strained rings has also found utility in naphthalene synthesis, whereby photochemical conversion of benzobicyclo[3.1.0]hexanones **1.17** produces naphthol derivatives.[14]

Transition metal-catalyzed cyclizations are a more common route to access functionalized naphthalenes by using chromium, palladium, nickel, cobalt, or rhodium transition metals, among others.[10] One example is a palladium-catalyzed [2 + 2 + 2] cocyclotrimerization reaction of benzyne **1.18**, generated *in situ*, with dimethyl acetylenedicarboxylate;[15] a similar method has been adapted to access arylnaphthalene lignan natural products including taiwanin E (**1.19**) (Scheme 1.1).[16] Phosphorous ylides have also been utilized in the synthesis of functionalized naphthalenes, with a representative reaction being a tandem Horner-Emmons-

Claisen condensation sequence of ketoaldehyde **1.20** and phosphonate **1.21**.[17] In this case, the naphthalene product was also carried on to afford arylnaphthalene lignans, such as chinensin (**1.22**). One final benzannulation method of naphthalene formation is Diels-Alder (DA) reactions, which have been achieved through addition of quinones and benzynes to dienes, or *o*-quinodimethanes to acetylenes. An example of the latter is the DA reaction of dimethyl fumarate with acetic acid and isobenzofuran **1.23**, generated *in situ*.[18] Subsequent addition of trifluoroacetic acid serves to aromatize the DA cycloadduct to the naphthalene product. This methodology was utilized in the synthesis of a library of naphthalenes that were then used to generate arylnaphthalene lignan derivatives.

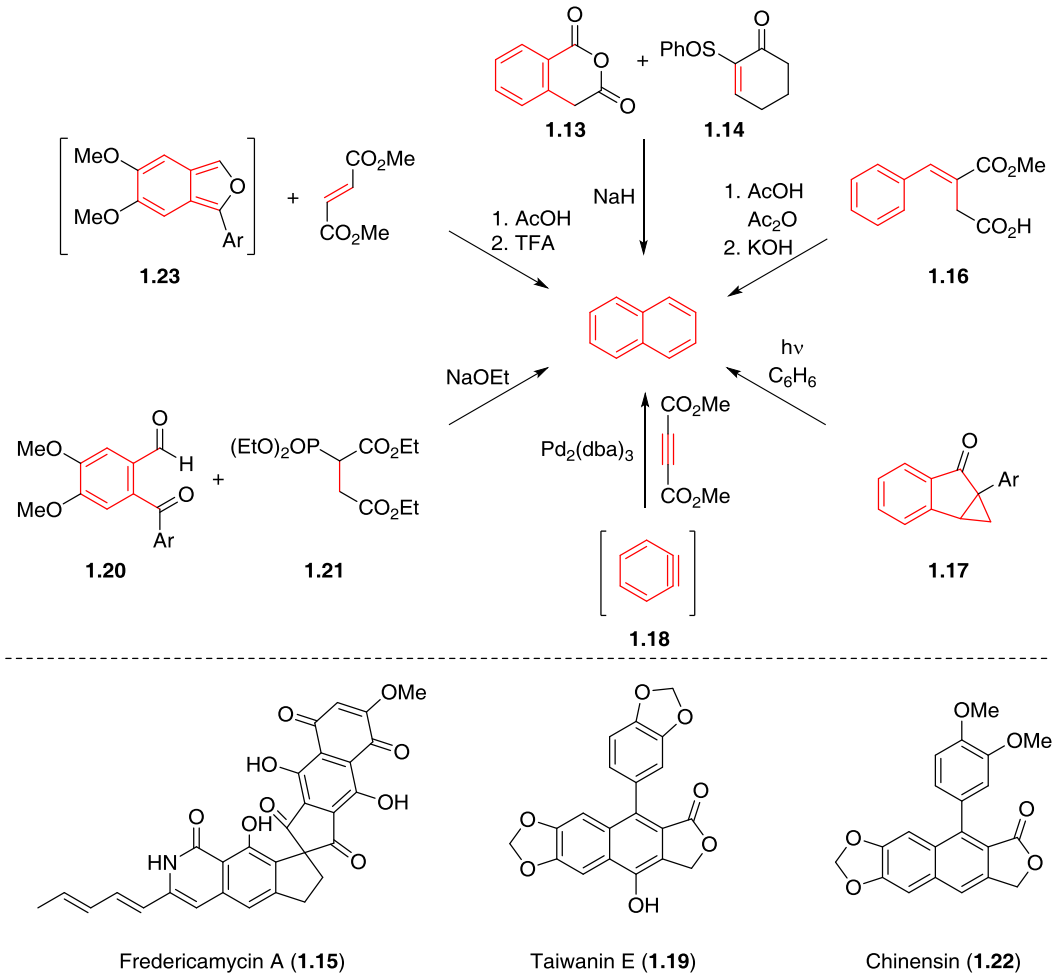

Scheme 1.1. Previously reported benzannulation strategies to access naphthalenes

Dehydro-Diels-Alder (DDA) reactions, or DA reactions where one, two, or all three of the double bonds of the classic diene and dienophile are replaced with triple bonds, are another method commonly employed in the synthesis of naphthalene compounds.[19] The energy price to incorporate the high degree of precursor unsaturation required for the formation of aromatic products can be mitigated by the propensity of cyclohexadiene derivatives to aromatize. Often, the DDA reaction is performed thermally and in an intramolecular fashion using tethered diynes, one or both of which is aryl-substituted, to produce polycyclic naphthalene substrates. In these cases, an arylacetylene acts as the diene in the DDA reaction, while the second alkyne is the dienophile (Scheme 1.2). This naphthalene producing strategy has found limited application in the synthesis of arylnaphthalene lignans and some more complex polycyclic frameworks. As representative examples, arylnaphthalene lignans **1.25** are generated via a thermal DDA reaction of 3-arylpropiolic acid propargyl esters **1.24**,[20] and polycyclic naphthalenes **1.27** can be produced similarly from diynes **1.26** (Scheme 1.3).[21] A drawback of this methodology is that substitution of both alkynes with aryl moieties results in selectivity issues within the reaction, and mixtures of retro- and/or regioisomers are formed. Although most DDA reactions are carried out intramolecularly, intermolecular examples have also been demonstrated utilizing photochemical reaction conditions.[22] Additionally, while DDA reactions to form naphthalenes are usually conducted between two alkynes and one arene or alkene, naphthalenes may also be produced by DDA reactions of a styrene and an alkyne, which will be described in the following section.

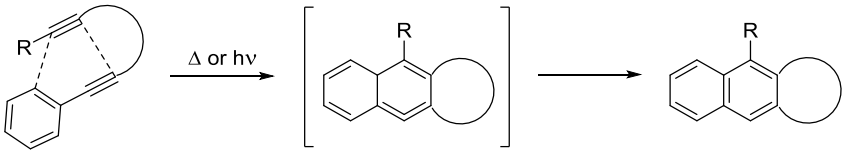

Scheme 1.2. Intramolecular DDA reactions of aryldiynes to generate naphthalenes

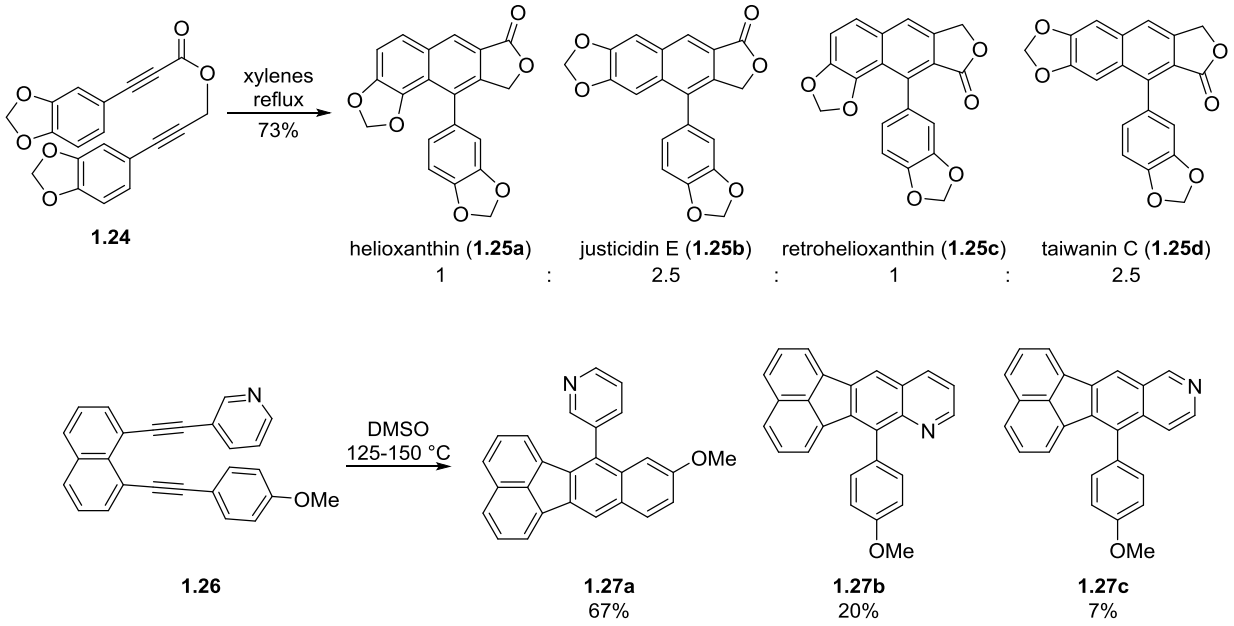

Scheme 1.3. DDA reactions to form polycyclic naphthalene frameworks

1.2 REACTION DISCOVERY

1.2.1 Intramolecular [2 + 2] cycloaddition reactions of allene-ynes

Our initial interest in the synthesis of novel naphthalene frameworks evolved from previous research in our laboratory centered on transformations of allene-ynes. Over the past decade, the Brummond group has developed methodology for the formation of alkylidene cyclobutene substrates by means of thermal intramolecular [2 + 2] cycloaddition reactions of allene-ynes. While similar reactions had been reported prior to disclosure of this method by Brummond and Chen in 2005, they were scattered and showed limited substrate scope.[23] Brummond and Chen demonstrated the first systematic study of intramolecular [2 + 2] cycloaddition reactions of allene-ynes **1.28**, highlighting the generality of the reaction by making various substitutions to the allene-yne tether, as well as to the termini of the alkyne and allene. Alkylidene cyclobutene products **1.29** were generated in moderate to high yields upon microwave irradiation (Scheme 1.4).[24] Others, including Oh,[25] Ohno,[26] Ovaska,[27] Ma,[28] Mukai,[29] and Malacria,[30] also explored the potential of this reaction either concurrent with or shortly after the initial report by Brummond and Chen, and further expanded the scope of allene-yne precursors and reaction conditions that could be utilized in the thermal intramolecular [2 + 2] cycloaddition reaction.

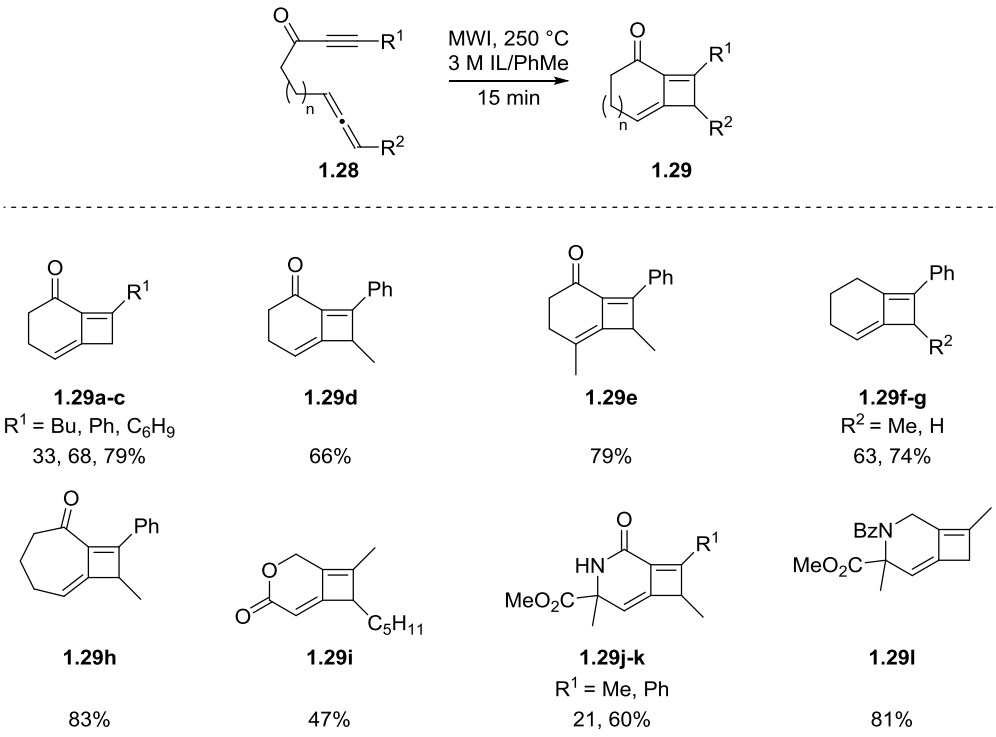

Scheme 1.4. Scope of allene-yne [2 + 2] cycloaddition reaction by Brummond and Chen

With conditions in hand to successfully produce alkylidene cyclobutene products, Brummond and Osbourn investigated the application of the intramolecular [2 + 2] cycloaddition reaction of allene-ynes to the synthesis of more complex molecular frameworks; specifically, to the generation of spirooxindoles. Beyond the ability to produce such complex substrates in a single step, the resulting products would contain a core structure similar to that of welwitindolinone A isonitrile (**1.30**), a spirooxindole targeted for total synthesis[31] because of its unique structure and biological properties, which include reversal of P-glycoprotein-mediated multiple drug resistance (Figure 1.4).[32] An advantage of utilizing intramolecular [2 + 2] cycloaddition reactions of allene-ynes to access spirooxindoles over other protocols is the greater degree of diversity that can be incorporated into the products by modifying the allene-yne

precursor. Additionally, the double bonds of the spirocyclic alkylidene cyclobutene can serve as handles for further structural variation. In the procedure reported by Brummond and Osbourn, a tandem [3,3]-sigmatropic rearrangement of propargyl acetates **1.31** yields intermediate allenyl acetates **1.32** which can then undergo the intramolecular [2 + 2] cycloadditon reaction to generate spirooxindoles **1.33** (Scheme 1.5). Modifications to the oxindole nitrogen, propargyl ester, alkyne terminus, and diyne tether length of **1.31** led to a variety of spirooxindole substrates.

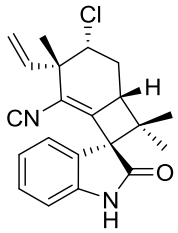

Figure 1.4. Structure of welwitindolinone A isonitrile (**1.30**)

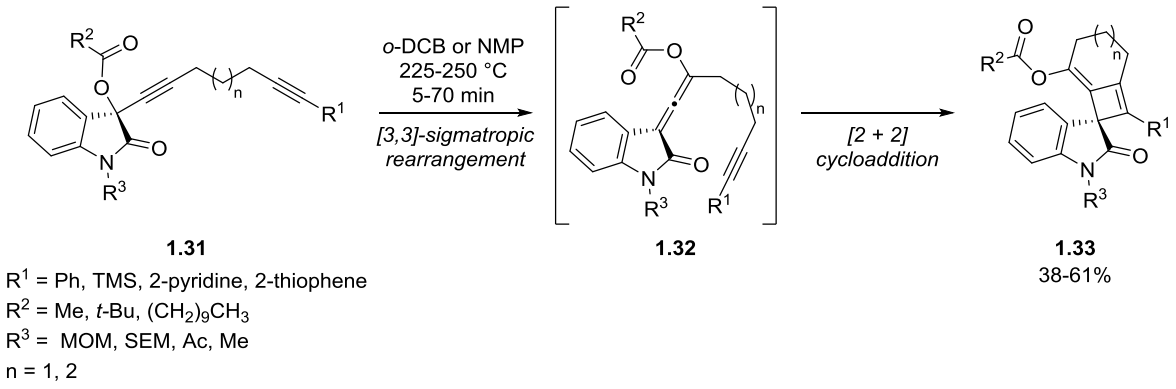

Scheme 1.5. Synthesis of spirooxindoles.
Performed via a tandem [3,3]-sigmatropic rearrangement/[2 + 2] cycloaddition reaction

1.2.2 Evidence for a diradical mechanism in the intramolecular [2 + 2] cycloaddition reaction of allene-ynes

In addition to expanding the scope and applications of the intramolecular [2 + 2] cycloaddition reaction of allene-ynes, Brummond and Osbourn investigated the mechanism of this reaction by employing both experimental and computational methods. Similar thermal reactions of ene-diynes and ene-allene-ynes are presumed to proceed via the formation of diradical intermediates, but evidence substantiating this mechanism is rare; only in a few examples by Bergman,[33] Myers-Saito,[34] and Schmittel[35] is there experimental support for the presence of diradical intermediates. In the [2 + 2] cycloaddition reaction of allene-yne **1.34** to form alkylidene cyclobutene **1.40**, the reaction may potentially occur via a concerted transition state **1.35**, or through generation of diradical intermediates **1.36** or **1.37** or zwitterionic intermediates **1.38** or **1.39** (Scheme 1.6). However, based on B3LYP density functional theory calculations of the possible transition states of the [2 + 2] cycloaddition reaction performed by Tantillo and Siebert at UC Davis, only a diradical transition state was identified as a reasonable pathway for the

reaction to proceed.[36] Further computational studies of the diradical pathway showed that the activation energy of the first bond-forming step to produce the smaller ring diradical intermediate **1.36** was 18.1 kcal/mol lower than that to generate the larger ring diradical intermediate **1.37**. This lower barrier to bond formation is attributed to the greater stability of the radicals of **1.36**.

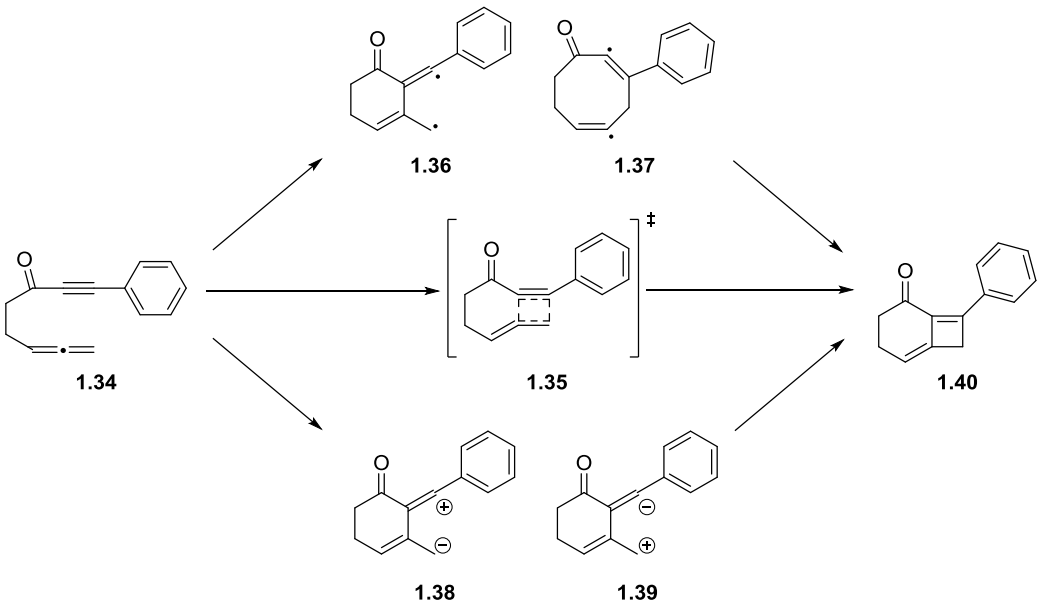

Scheme 1.6. Potential mechanisms of the [2 + 2] cycloaddition reaction of allene-ynes

To lend additional support to the computational evidence promoting a diradical mechanism in the intramolecular [2 + 2] cycloaddition reaction of allene-ynes, Brummond and Osbourn conducted diradical trapping experiments utilizing cyclopropyl radical clocks appended to the alkynyl terminus of the allene-yne.[36] Diradical formation during the [2 + 2] cycloaddition reaction would lead to positioning of a vinyl radical adjacent to the cyclopropyl ring, which

would subsequently open to generate alternate products to the expected alkylidene cyclobutene substrates (Scheme 1.7). As an example, allene-yne **1.41** was irradiated in the presence of the hydrogen atom donor γ-terpinene to produce the triene **1.43**; no alkylidene cyclobutene product **1.42** was observed. The proposed mechanism to form **1.43** proceeds by initial bond formation between the distal allene bond and the alkyne to generate diradical **1.44**, which is followed by opening of the cyclopropyl ring to produce allene **1.45** (Scheme 1.8). Hydrogen atom abstraction from γ-terpinene by the allylic radical of **1.45**, as well as quenching of the remaining radical by hydrogen atom abstraction from **1.45**, results in production of intermediate **1.46**. A final 4π electrocyclization of **1.46** yields trienes **1.43** as a 1:1.2 mixture of *E*:*Z* isomers. The formation of triene **1.43** via the opening of the cyclopropyl radical clock of **1.41** further supports the diradical mechanism proposed as a result of the computational studies.

Scheme 1.7. Cyclopropane rings as radical clocks

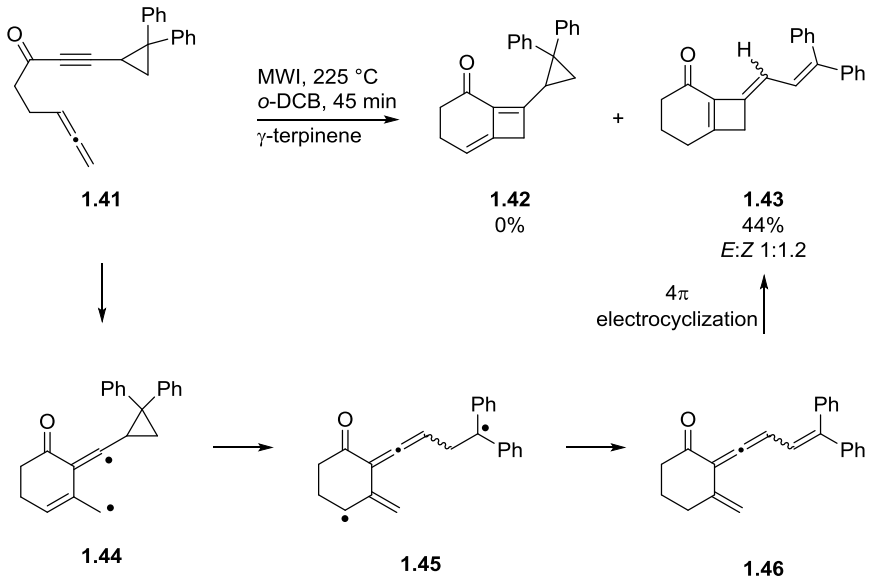

Scheme 1.8. Diradical trapping experiments.
Example of diradical trapping in an intramolecular [2 + 2] cycloaddition reaction of allene-yne **1.41** and the proposed mechanism for formation of the triene product **1.43**

1.2.3 Thermal [2 + 2 + 2] cycloaddition reactions of ene-allene-ynes

With computational and experimental evidence in hand supporting a diradical mechanism for the formation of alkylidene cyclobutenes in the [2 + 2] cycloaddition reaction of allene-ynes, our interest was turned towards applying this information to the synthesis of more complex polycyclic frameworks. Rather than expand the scope of alkylidene cyclobutene products, as was done in the preparation of the spirooxindoles via the [2 + 2] cycloaddition reaction, we were interested in trapping the diradical intermediate via an intramolecular, formal [2 + 2 + 2] cycloaddition reaction to afford tricycles. We envisioned that tethering an alkene to the allene-yne substrate, as in **1.47**, would lead to a diradical intermediate **1.48** upon irradiation. One radical of **1.48** could then be trapped by the alkene to produce a second diradical intermediate **1.49** and form a five-membered ring (Scheme 1.9). Subsequent recombination of the diradicals

would then result in formation of the tricyclic ring system **1.50**. Radical trapping by the alkene would be competitive with the initial radical recombination of **1.48** to produce the traditional alkylidene cyclobutene products **1.51**; therefore, the alkene would need to be functionalized with radical stabilizing groups that promote formation of the [2 + 2 + 2] cycloadduct **1.50**.

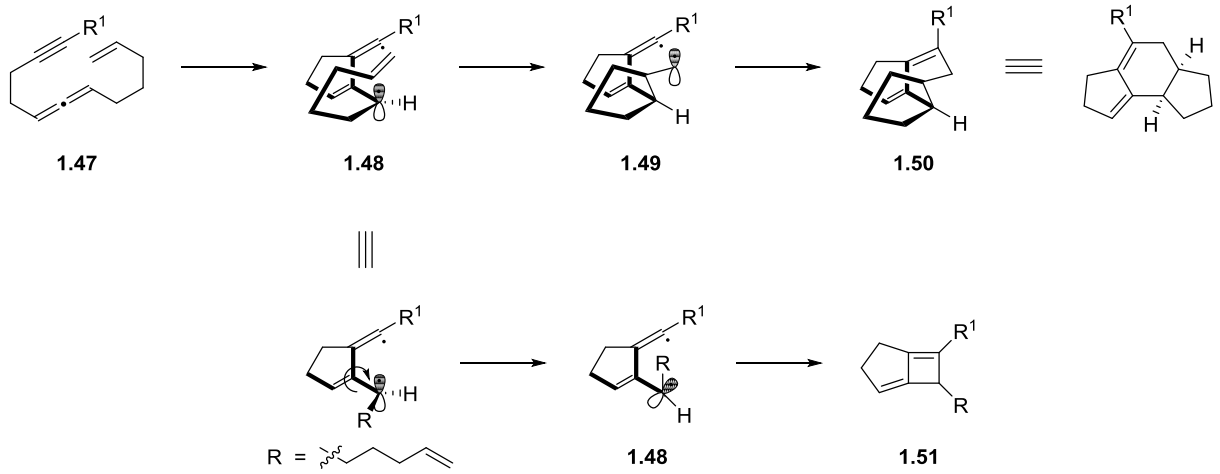

Scheme 1.9. Proposed mechanism for a [2 + 2 + 2] cycloaddition reaction of ene-allene-ynes. [2 + 2 + 2] cycloaddition reaction to form tricyclic substrates (top) and competing radical recombination to provide alkylidene cyclobutene products (bottom)

To test the feasibility of the intramolecular [2 + 2 + 2] cycloaddition reaction, a variety of ene-allene-yne substrates with diversity in both structure and functionality were synthesized. However, despite modifications to the alkene functionality or the allene-yne tether, irradiation of ene-allene-yne **1.52** resulted in only [2 + 2] cycloaddition reactions of either the alkyne or the alkene with the allene to produce alkylidene cyclobutene and/or cyclobutane products **1.53** and **1.54**, respectively; the generation of the [2 + 2 + 2] cycloadduct **1.55** was not observed (Scheme 1.10, A). In an effort to prevent the formation of cyclobutane products and promote the [2 + 2 +

2] cycloaddition reaction, the allene was placed at a terminal position in the ene-allene-yne substrate **1.56**, which upon irradiation would generate a diradical intermediate **1.57**. For this example, it was predicted that the vinyl radical formed would add to the alkene to produce the tricyclic substrate **1.59**. However, only the [2 + 2] cycloaddition reaction occurred to provide cyclobutene **1.58** (Scheme 1.10, B).

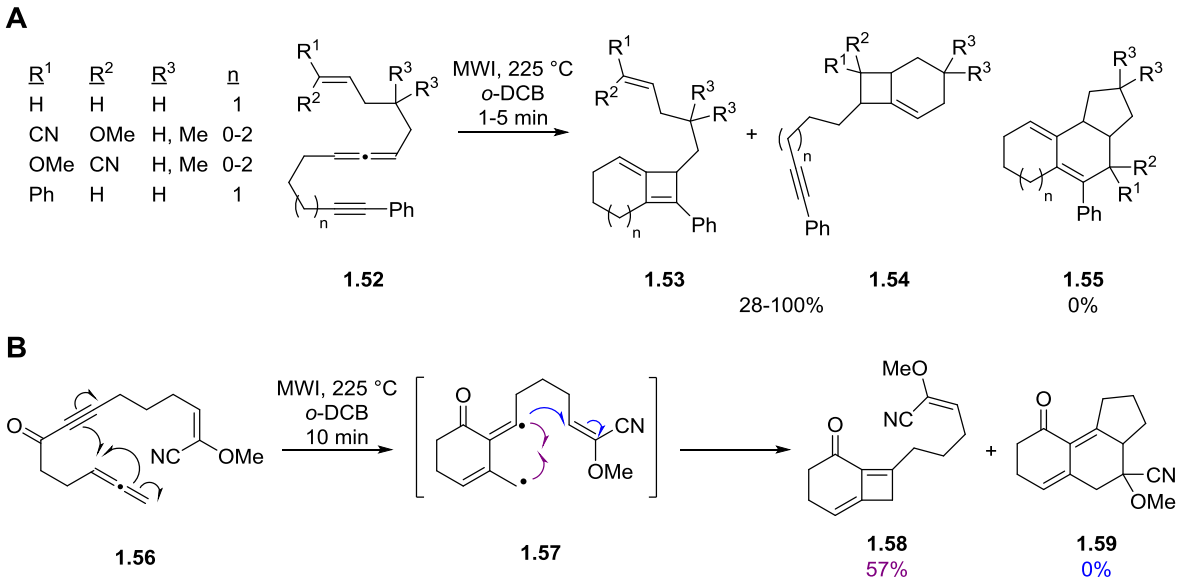

Scheme 1.10. Irradiation of ene-allene-ynes to explore the [2 + 2 + 2] cycloaddition reaction. (A) Irradiation of a variety of ene-allene-yne substrates **1.52** containing a central allene moiety; (B) irradiation of redesigned ene-allene-yne substrates **1.56** containing a terminal allene

1.2.4 Discovery of a thermal dehydrogenative dehydro-Diels-Alder reaction

Despite the observed inability of the ene-allene-yne substrates to undergo the intramolecular [2 + 2 + 2] cycloaddition reaction, one variant of the ene-allene-yne substrates did take part in an unexpected cycloaddition reaction of potentially significant synthetic utility. Irradiation of ene-

allene-yne **1.60** containing a styrene moiety for 10 min at 225 °C in *o*-DCB resulted in the formation of naphthalene **1.61** in 68% yield; the expected alkylidene cyclobutene product **1.62** produced from a [2 + 2] cycloaddition reaction of the allene and alkyne, as well as the desired [2 + 2 + 2] cycloadduct **1.63** were not observed (Scheme 1.11). The isolated naphthalene is believed to form via a DDA reaction in which the styrene is acting as a diene and the ynone as a dienophile. Surprisingly, the allene which is often very reactive under thermal conditions in the presence of alkynes and alkenes, as previously demonstrated, did not partake in the reaction. This was evidenced by analysis of the crude reaction mixture by ^{1}H NMR spectroscopy, which showed allene resonances at δ 4.7 and 5.3 that were similar to those of the starting material **1.60** (Figure 1.5). The disappearance of the olefinic resonances at δ 6.2 and 6.4 signified full conversion of the starting material to product, while the presence of distinct resonances in the aromatic region of the ^{1}H NMR spectrum were diagnostic of formation of naphthalene **1.61**. Overall, the ^{1}H NMR spectrum of the crude reaction mixture was very clean and showed one product, the naphthalene **1.61**. Conversion of **1.61** to a tosyl hydrazone **1.64** allowed for confirmation of the naphthalene structure by X-ray crystallography (Scheme 1.12).

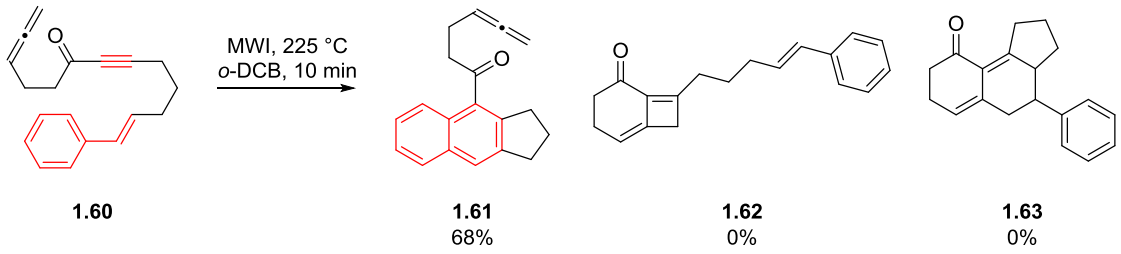

Scheme 1.11. Unexpected DDA reaction of styrene-yne **1.60** to produce naphthalene **1.61**

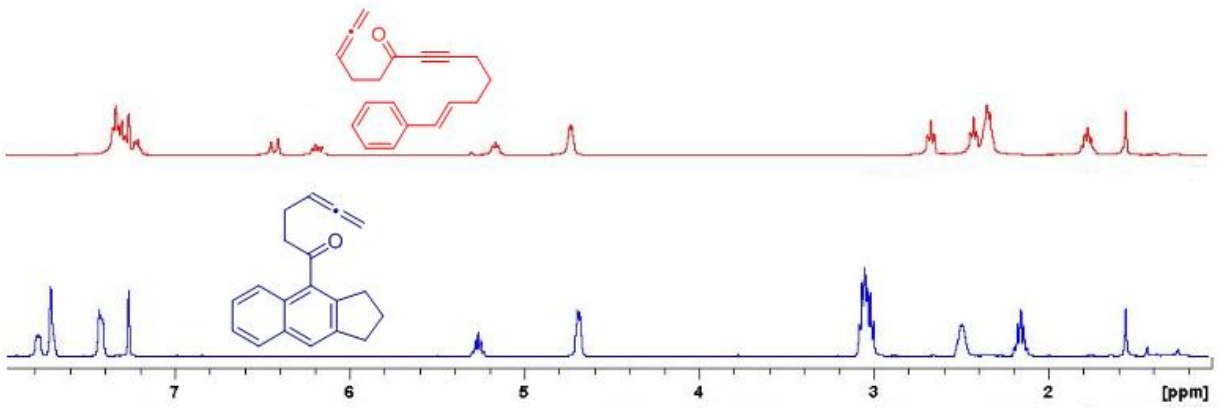

Figure 1.5. ^{1}H NMR analysis of DDA reaction.
^{1}H NMR spectrum of styrene-yne **1.60** (top) and crude reaction mixture after microwave irradiation showing only naphthalene product **1.61** (bottom)

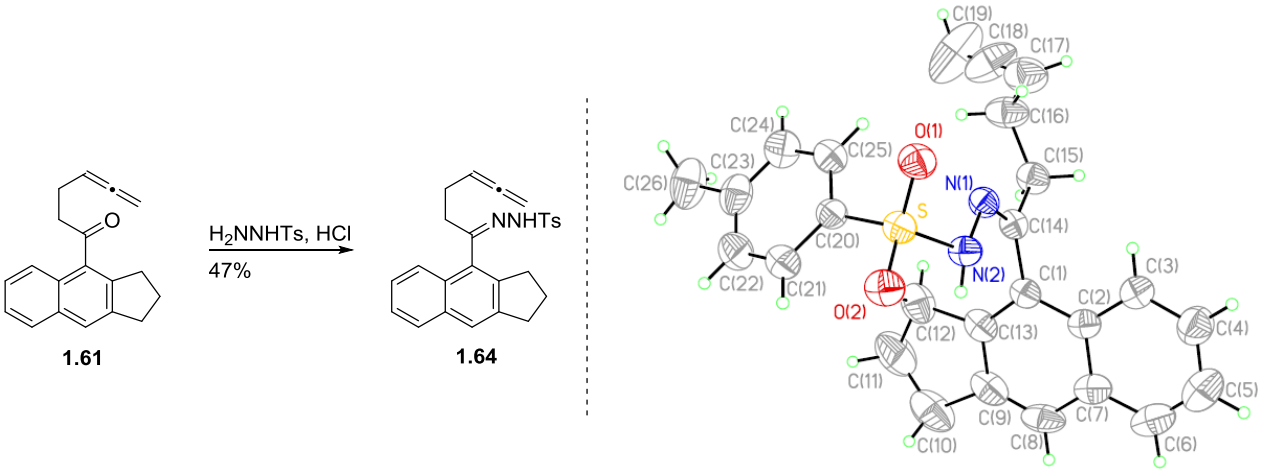

Scheme 1.12. Confirmation of naphthalene structure.
Conversion of naphthalenone **1.61** to hydrazone **1.64** (left) and X-ray crystal structure of **1.64** (right)

The effectiveness and selectivity associated with the thermal conversion of styrene-yne **1.60** to naphthalene **1.61** was surprising for a number of reasons, the first being that the styrene is acting as a diene for the DDA reaction. Problems that can arise when employing styrene as a diene include a lack of regioselectivity, as well as undesired polymerization[37] and [2 + 2] cycloaddition reactions.[38] An example of the latter is observed in the intermolecular reaction of *trans*-anethole (**1.65**) with tetracyanoethylene (**1.66**), where the dienophile reacts exclusively with the styrene olefin to produce cyclobutanes **1.67** (Scheme 1.13).[38a] Similar [2 + 2] cycloaddition reactions are also associated with styrenes in intramolecular examples.[38b] To circumvent problems related to using styrene as a diene in DA reactions, intramolecular variants of the reaction can be utilized to control regioselectivity, and more reactive dienophiles can be employed to prevent undesired, competitive reactions. However, in the latter case, the desired cycloadducts are often obtained in low yields because the reactivity of these dienophiles leads to a second DA reaction with the newly formed diene of the first cycloadduct. This is depicted in the DA reaction of 1,1-diphenylethylene (**1.68**) and maleic anhydride (**1.69**), which generates the cycloadduct **1.70** in 42% yield (Scheme 1.14).[39] While selectivity problems commonly accompany the use of styrene as a diene in DA reactions, no byproducts attributed to polymerization or [2 + 2] cycloaddition were observed in the DDA reaction of styrene-yne **1.60** (Scheme 1.11).

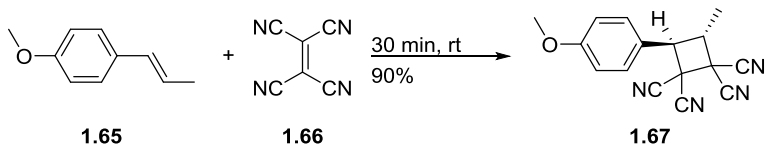

1.65 **1.66** **1.67**

Scheme 1.13. Participation of styrenes in [2 + 2] cycloaddition reactions

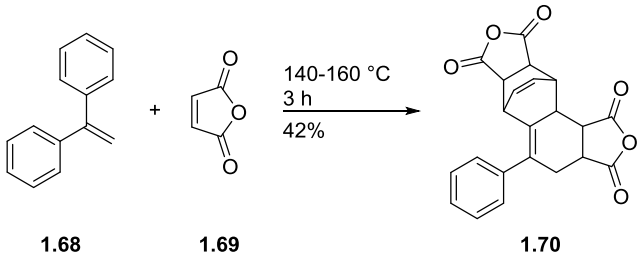

Scheme 1.14. Reactions of reactive dienophiles with styrenes

Another unique and unexpected aspect of the DDA reaction of styrene-yne **1.60** was the occurrence of a dehydrogenation during the reaction to produce the naphthalene **1.61**. In traditional DDA reactions to produce naphthalenes, arylacetylenes are employed as dienes rather than styrenes because they have additional unsaturation that allows for the generation of the naphthalene products via aromatization of a cyclic allene intermediate (Scheme 1.2). When styrene is utilized instead of arylacetylene in the intramolecular DDA reaction, a tetraene intermediate is produced that subsequently aromatizes to the dihydronaphthalene product (Scheme 1.15).[40] In order to form naphthalene, a second oxidative reaction must be performed to aromatize the dihydronaphthalene to naphthalene.[41] However, in our thermal dehydrogenative dehydro-Diels-Alder (DDDA) reaction of styrene-yne **1.60**, no oxidants were necessary to achieve exclusive formation of the naphthalene product **1.61**, highlighting the novelty of this reaction (Scheme 1.11).

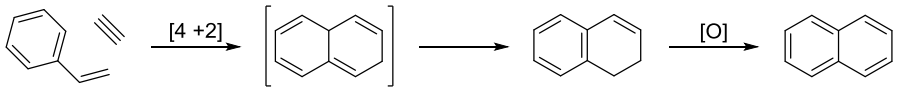

Scheme 1.15. Two-step formation of naphthalene via DDA reactions of styrene

While DDDA reactions of styrenes to produce naphthalenes are rare, previous examples have been reported that demonstrate variable yields and selectivity. In 1971, Klemm et al. were the first to discover the DDDA reaction by refluxing styrene-yne **1.71** in acetic anhydride to produce naphthalene lactone **1.72** in low yield (Scheme 1.16, A).[42] Klemm later improved upon this methodology in the synthesis of arylnaphthalene lactams **1.74** by reflux of the styrene-yne **1.73** in xylenes; however, the yield of the naphthalene product was moderate at best (Scheme 1.16, B).[43] More recently, Chackalamannil et al.[44] and Ruijter et al.[45] have also employed the DDDA reaction of styrene-ynes **1.75** and **1.78** to the synthesis of naphthalene lactones **1.76** and lactams **1.79**, respectively (Scheme. 1.16, C and D). These reactions showed limited success because only low to moderate yields of the naphthalene were obtained, and also because the naphthalene was generated as a mixture with dihydronaphthalene that was inseparable by column chromatography. A common feature of each of these reactions was the incorporation of heteroatoms into the styrene-yne tether in the form of esters or amides.

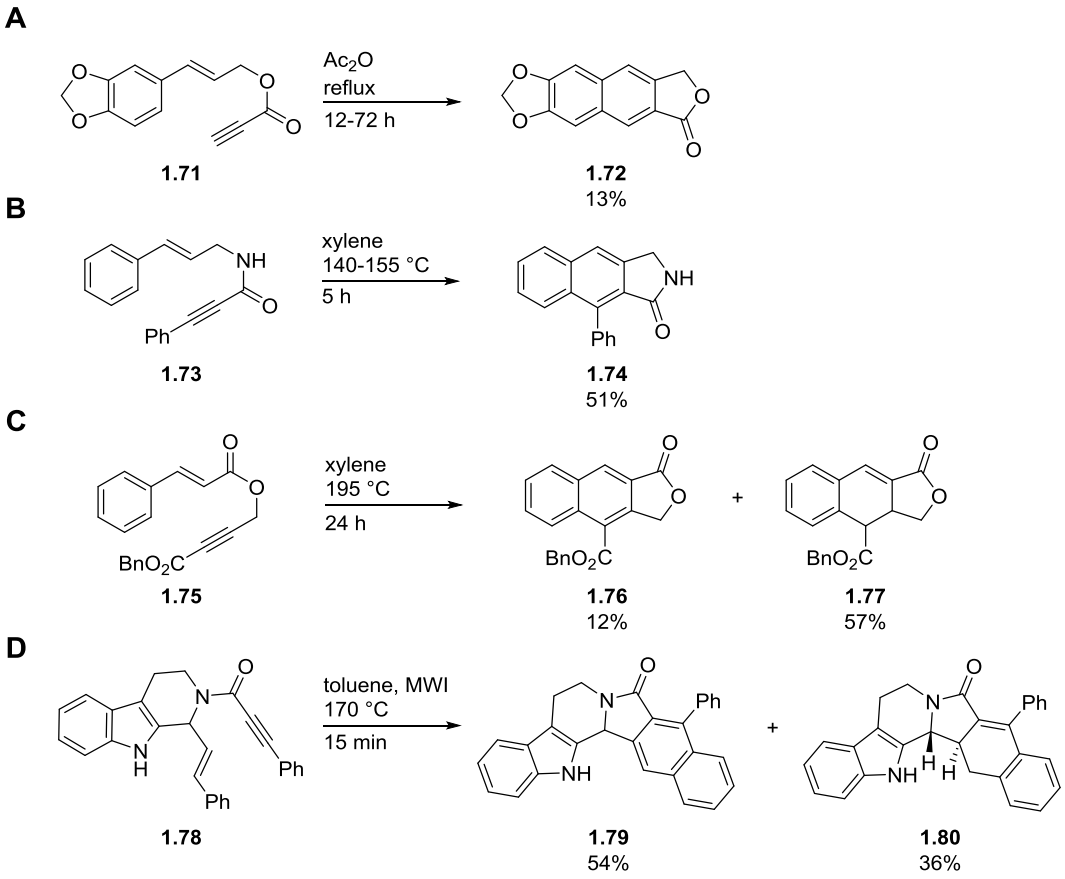

Scheme 1.16. Previous DDDA reactions of styrene-ynes.
Previous reactions reported low yields of naphthalene and mixtures of dihydronaphthalene and naphthalene products

Despite the poor yields and selectivity initially associated with DDDA reactions, two additional reports highlight the ability of this methodology to generate naphthalenes exclusively and in high yields, but only when the alkynyl terminus of the precursor is substituted with a trimethylsilyl (TMS) moiety. Terashima et al. were the first to show selective formation of cyclopentenone-fused naphthalenes **1.82** from styrene-ynes **1.81** with the intention of employing this reaction in the synthesis of fredericamycin A (Scheme 1.17, A).[46] In 2011, Matsubara et al. also reported exclusive production of naphthalenes **1.84** from styrene-ynes **1.83** that contained heteroatoms within the styrene-yne tether, as well as a TMS-substituted alkyne (Scheme 1.17,

B).[47] Exchange of the TMS of **1.83** for an ester or phenyl substituent resulted in the formation of a mixture of naphthalene and dihydronaphthalene substrates with dihydronaphthalene being the major product. Based upon these results, Matsubara et al. proposed that the silyl substituent was key to the exclusive production of the naphthalenes, and that this bulky substituent promoted a dehydrogenative retro-Diels-Alder reaction and loss of hydrogen gas from the initial DA cycloadduct to yield the naphthalene.[47]

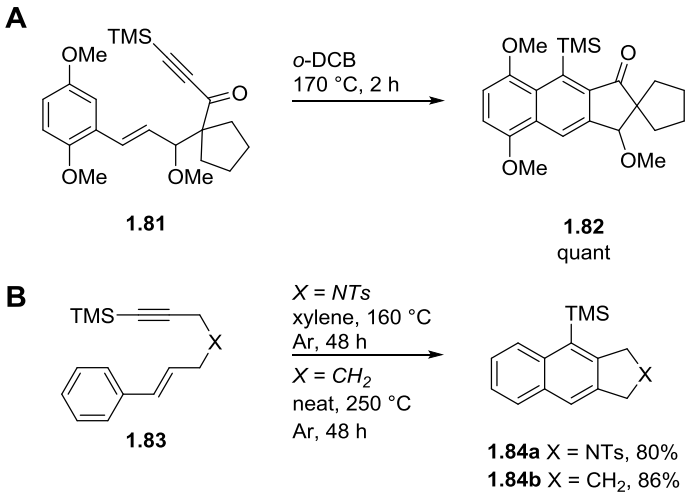

Scheme 1.17. DDDA reactions of TMS-substituted styrene-ynes.
DDDA reactions of TMS-substituted styrene-ynes produced naphthalenes exclusively

Of significant note, Matsubara also performed the DDDA reaction with a styrene-yne containing an unsubstituted all carbon tether to generate the naphthalene **1.84b** in 86% yield (Scheme 1.17, B). However, this reaction required harsh conditions of 250 °C for 48 h in order to complete. The reaction time observed in this case is considerably longer than that determined for our DDDA reaction of styrene-yne **1.60,** containing a similar styrene-yne tether, in which

naphthalene **1.61** was formed after only 10 min of microwave irradiation at 225 °C (Scheme 1.11). Additionally, comparing our initial result to the other aforementioned DDDA reactions, we achieved selective production of naphthalene in high yield when an electron-withdrawing carbonyl moiety was appended to the alkyne terminus of the styrene-yne **1.60**; no dihydronaphthalene product was observed. This is in contrast to the proposal by Matsubara that a TMS group on the alkyne promotes exclusive production of naphthalene,[47] and also to the results of Chackalamannil, where an electron-withdrawing ester on the alkyne terminus of the styrene-yne **1.75** gave mixtures of naphthalene and dihydronaphthalene products.[44]

1.2.5 Optimization of DDDA reaction conditions

The results obtained from our initial DDDA reaction were promising, especially when compared with the literature precedent for DDDA reactions of styrene-ynes, which led to our pursuit and optimization of this reaction. We envisioned that the original reaction conditions could be modified in order to lower the reaction temperature and possibly increase the reaction yield. To simplify the structure of the styrene-yne and naphthalene product, a model system was chosen in which a methyl ketone was appended to the alkyne terminus of the styrene-yne, rather than a ketone containing a tethered allene as in **1.60**. This structural modification was not expected to have an impact on the reactivity of the styrene-yne in the DDDA reaction because the allene does not participate in the reaction. Synthesis of the methyl ketone-substituted styrene-yne **1.88** was performed by first oxidizing commercially available 5-hexyn-1-ol (**1.85**) to 5-hexyn-1-al (**1.86**) using PCC, followed by a Horner-Wadsworth-Emmons reaction of the aldehyde with diethyl benzylphosphonate to yield the styrene-yne **1.87** (Scheme 1.18). Subsequent addition of

dimethylacetamide and boron trifluoride diethyl etherate to the lithium acetylide of **1.87** resulted in acylation of the alkyne to generate styrene-yne **1.88** in 69% yield.

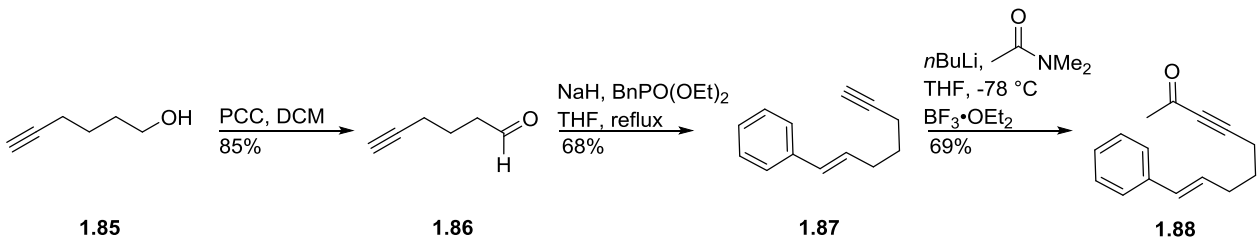

1.85 **1.86** **1.87** **1.88**

Scheme 1.18. Synthesis of styene-yne **1.88**

To test the DDDA reaction on the model system, irradiation of styrene-yne **1.88** was performed using 1,2-dichloroethane (DCE) and trifluorotoluene as reaction solvents. Although irradiation of our initial styrene-yne **1.60** was performed in *o*-DCB with good results, DCE and trifluorotoluene were deemed preferable reaction solvents to *o*-DCB because of their lower boiling points, which would allow for removal of the solvent under reduced pressure. Reactions performed in *o*-DCB, due to its high boiling point, require purification by column chromatography to remove solvent from the product, or concentration under high vacuum. Irradiation of **1.88** in both DCE and trifluorotoluene (0.06 M) at 180 °C provided the naphthalene in quantitative yield (Scheme 1.19). The reaction time in DCE was only 30 min, which was significantly shorter than the reaction time in trifluorotoluene of 175 min. Removal of the solvent resulted in a crude product that was of very high quality by ^{1}H NMR analysis, showing no additional products or impurities in the spectrum. If the product was purified by

filtering through a small column of silica gel, only an approximate 5% decrease in the yield was observed. It should be noted that the temperature of the DDDA reaction was reduced to 180 °C for the model study from 225 °C, which was used in the initial DDDA reaction of ene-allene-yne **1.60** to generate naphthalene **1.61** (Scheme 1.11). This decrease in reaction temperature when the reaction was performed in DCE did not significantly prolong the reaction time, highlighting 180 °C in DCE as optimal reaction conditions for further studies of the DDDA reaction.

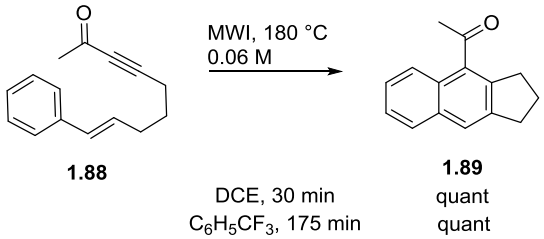

Scheme 1.19. Optimization of DDDA reaction conditions

1.3 EXPLORING THE SCOPE AND LIMITATIONS OF THE DDDA REACTION

An examination of previous DDDA reactions represented in the literature shows that no general or systematic studies have been performed to test and expand upon the scope of this reaction. Of the examples reported, most involve DDDA reaction of styrene-ynes with heteroatom-containing tethers and with phenyl or TMS moieties appended to the alkyne terminus; little has been explored in terms of functionality or structural changes to the styrene-yne tether, alkyne terminus, or styrene itself of the DDDA reaction precursor. Immediately our DDDA reaction to

produce naphthalenes **1.61** and **1.89** was recognized as different because the styrene-yne precursors contained an electron-withdrawing group on the alkyne terminus, no dihydronaphthalene was observed along with formation of the naphthalene, and cyclopenta[*b*]naphthalene frameworks were readily synthesized in high yields and short reaction times. Based upon these initial results and the ideal reactions conditions determined during our optimization studies, we envisioned that a systematic study could be undertaken to expand the scope and explore the limitations of the DDDA reaction, which would allow for a more general synthesis of functionalized naphthalenes via this methodology. Expanding the scope of the DDDA reaction may result in the ability to apply this reaction to the synthesis of cyclopenta[*b*]naphthalene-based natural products, such as those depicted in Figure 1.6, which have not yet been synthesized or studied for biological activity.[48]

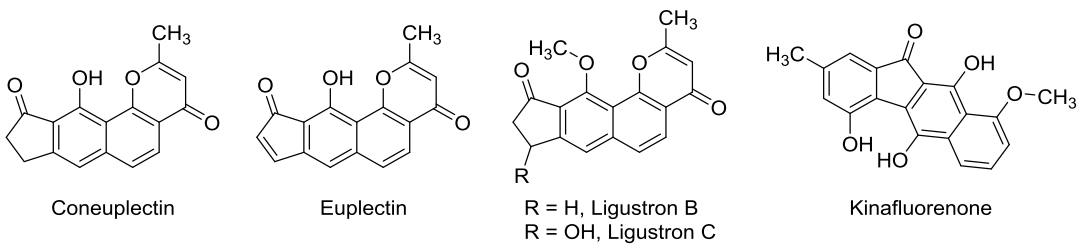

Figure 1.6. Cyclopenta[*b*]naphthalene-containing natural products

1.3.1 Variations to the styrene of the styrene-yne

Primary efforts to expand the scope of the DDDA reaction focused on utilizing substituted styrenes to generate cyclopenta[*b*]naphthalene substrates containing substitution at various

positions of the naphthalene. Halogenated styrenes were chosen to test the feasibility of this DDDA reaction because of the ease of incorporation of halogens into the styrene, and also because the halogen could later be used as a handle for subsequent transformations of the naphthalene, such as in cross-coupling reactions. One method in which the halogen could be readily integrated into the styrene at the *ortho*-, *meta*- and *para*-positions is by a Horner-Wadsworth-Emmons reaction of suitably substituted aryl phosphonates with 5-hexyn-1-al, which could be performed in an analogous fashion to the synthesis of styrene-yne **1.87** (Scheme 1.20).

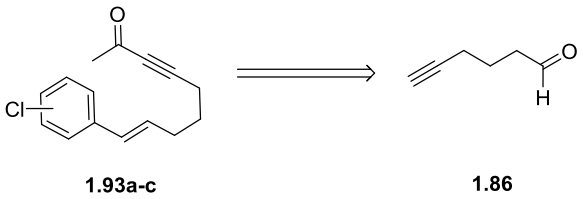

Scheme 1.20. Retrosynthetic analysis of the synthesis of halogenated styrenes

In order to perform the Horner-Wadsworth-Emmons reaction, preparation of the diethyl chlorobenzylphosphonates reagents was required. This was accomplished by utilizing Arbuzov reactions of triethyl phosphite with 2- or 3-chlorobenzyl bromides (**1.90a-b**) to produce diethyl 2-chlorobenzylphosphonate (**1.91a**) and diethyl 3-chlorobenzylphosphonate (**1.91b**) in 81 and 98% yield, respectively (Scheme 1.21). Diethyl 4-chlorobenzylphosphonate (**1.91c**) was commercially available. With these reagents in hand, the Horner-Wadsworth-Emmons reaction was conducted with 5-hexyn-1-al (**1.86**) and *n*-butyllithium to afford **1.92a-c** in 67-78% yield. Subsequent acylation of the lithium acetylides of **1.92a-c** was executed by addition of either *N*-

methoxy-*N*-methylacetamide or dimethylacetamide in the presence of boron trifluoride diethyl etherate to yield the styrene-ynes **1.93a-c** in 50-87% yield.

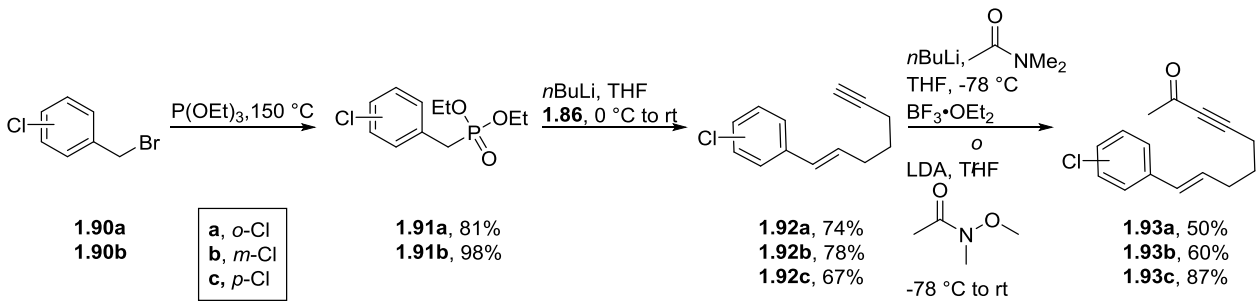

Scheme 1.21. Synthesis of halogenated styrene-ynes **1.93a-c**

Styrene-ynes **1.93a-c** all successfully underwent the DDDA reaction by irradiation at 180 °C to produce halogenated cyclopenta[*b*]naphthalenes **1.94a-d** in high yields (Scheme 1.22). Irradiation of *o*-chlorostyrene-yne **1.93a** in *o*-DCB generated 5-subsituted chloronaphthalene **1.94a** in 86% yield after 180 min. While DCE was previously found to be an optimal DDDA reaction solvent due to its low boiling point and easy removal from the reaction mixture, irradiation of DCE at high temperatures of 180 °C or greater often required extended time to reach the desired temperature due to the lower tan δ of DCE. In such cases, it was found that *o*-DCB could be utilized, rather than DCE, with minimal effect on the reaction time and yield. Irradiation of *m*-chlorostyrene-yne **1.93b** in *o*-DCB also required 180 min of reaction time, but resulted in the formation of both the 6- and 8-chloronaphthalenes **1.94b** and **1.94c** in a 1.4:1 ratio and 79% combined yield. The observation of these two naphthalene products is a consequence of a lack of regioselectivity in the DA reaction, where the styrene can react as two distinct dienes.

The diene leading to the generation of the 6-substituted naphthalene **1.94b** is slightly favored because the chloro group in the product is less sterically encumbered, whereas the 8-substituted chloronaphthalene **1.94c** has the chloro group in a *peri* position to the methyl ketone. Irradiation of the *para*-substituted styrene **1.93c** for 200 min at 180 °C in DCE resulted in a quantitative yield of 7-chloronaphthalene **1.94d**, demonstrating that the DDDA reaction can proceed successfully with substitution at all positions of the A ring of the cyclopentab[*b*]naphthalene substrates. In addition, it should be noted that chloro groups were not the only halogens to show success in the DDDA reaction; bromo groups were also well tolerated and produced cyclopenta[*b*]naphthalenes in comparable yields.

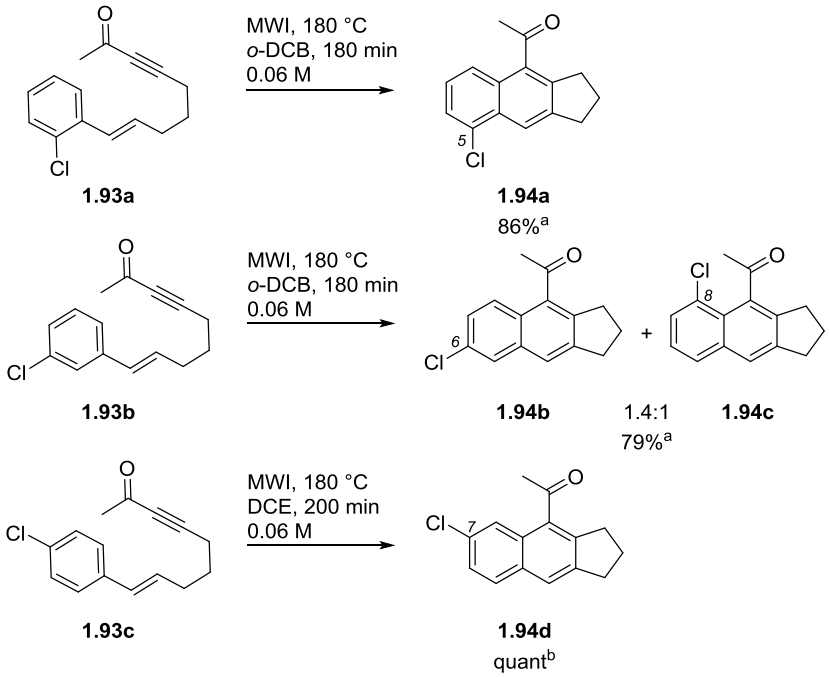

Scheme 1.22. DDDA reaction of halogenated styrene-ynes.
[a]Isolated yields after purification by silica gel column chromatography.[b]Crude yields where no byproducts or impurities were observed by ^{1}H NMR spectroscopy.

The difference in reaction times between halogenated and non-halogenated styrene-ynes in the DDDA reaction can be explained electronically. In a normal demand DA reaction, such as the DDDA reaction, electron-donating groups (EDG) on the diene and electron-withdrawing groups (EWG) on the dienophile raise and lower the energies of their HOMO and LUMO, respectively, resulting in a smaller HOMO-LUMO energy gap and better orbital interaction. A methyl ketone on the dienophile, as in **1.88**, serves to lower the LUMO energy and accelerate the DA reaction. However, incorporation of an electron-withdrawing chloro group into the styrene of **1.93** results in a decrease in the energy of the HOMO of the diene. This creates a larger energy gap between the HOMO and LUMO than exists for the non-halogenated styrene, and leads to a slower rate of DA reaction.

1.3.2 Variations to the alkyne of the styrenyl precursor

In addition to modifications to the styrene moiety of styrene-ynes employed in DDDA reactions to produce cyclopenta[*b*]naphthalene substrates, changes to functionality on the alkyne terminus were also investigated. Our examples of DDDA reactions are unique in that an electron-withdrawing methyl ketone is appended to the alkyne terminus of the styrene-yne and exclusive formation of naphthalene is obtained in high yield. Almost all previous reports of DDDA reactions of styrene-ynes involved substitution of the alkynyl terminus with phenyl or TMS moieties, and only for TMS substitution were naphthalenes exclusively produced upon heating. We envisioned that the scope of the DDDA reaction of styrene-ynes could be greatly expanded by changing the functionality appended to the alkyne terminus to include a variety of EWGs. The limitations of the reaction could also be explored in this manner, by testing the effectiveness of

electron-withdrawing and non-electron-withdrawing functionality on the alkyne of the styrene-yne in the DDDA reaction.

By utilizing the unsubstituted styrene-ynes **1.88** and **1.93c**, modifications could readily be made to the alkyne terminus either by cross-coupling reactions or by addition of various electrophiles to the lithium acetylides of **1.88** and **1.93c** (Scheme 1.23). For example, the phenyl ketone-substituted styrene-yne **1.95** was produced in 71% yield by a palladium-catalyzed cross-coupling reaction of benzoyl chloride with styrene-yne **1.88**. Additionally, aldehyde **1.96** and ester **1.97** were generated in 82 and 79% yield, respectively, by addition of DMF and methyl chloroformate to the lithium acetylides of **1.93c** and **1.88**. In a similar fashion, addition of methanesulfonyl chloride to the lithium acetylide of **1.88** formed methyl sulfone **1.98**, but in only 17% yield. As an alternative approach to producing alkynyl sulfones, the lithium acetylide of **1.93c** was first treated with diphenyl disulfide, and the resulting sulfide was oxidized with *meta*-chloroperoxybenzoic acid to generate a mixture of sulfoxide **1.99** and sulfone **1.100** in a 1.3:1 ratio and combined 75% yield. Even though this new approach did not significantly improve the yield of the sulfone-substituted styrene-yne, it did allow for the formation of two different precursors that could be utilized in the DDDA reaction. Finally, phosphonate **1.101** was synthesized in 91% yield by addition of diethyl chlorophosphate to the lithium acetylide of **1.93c**.

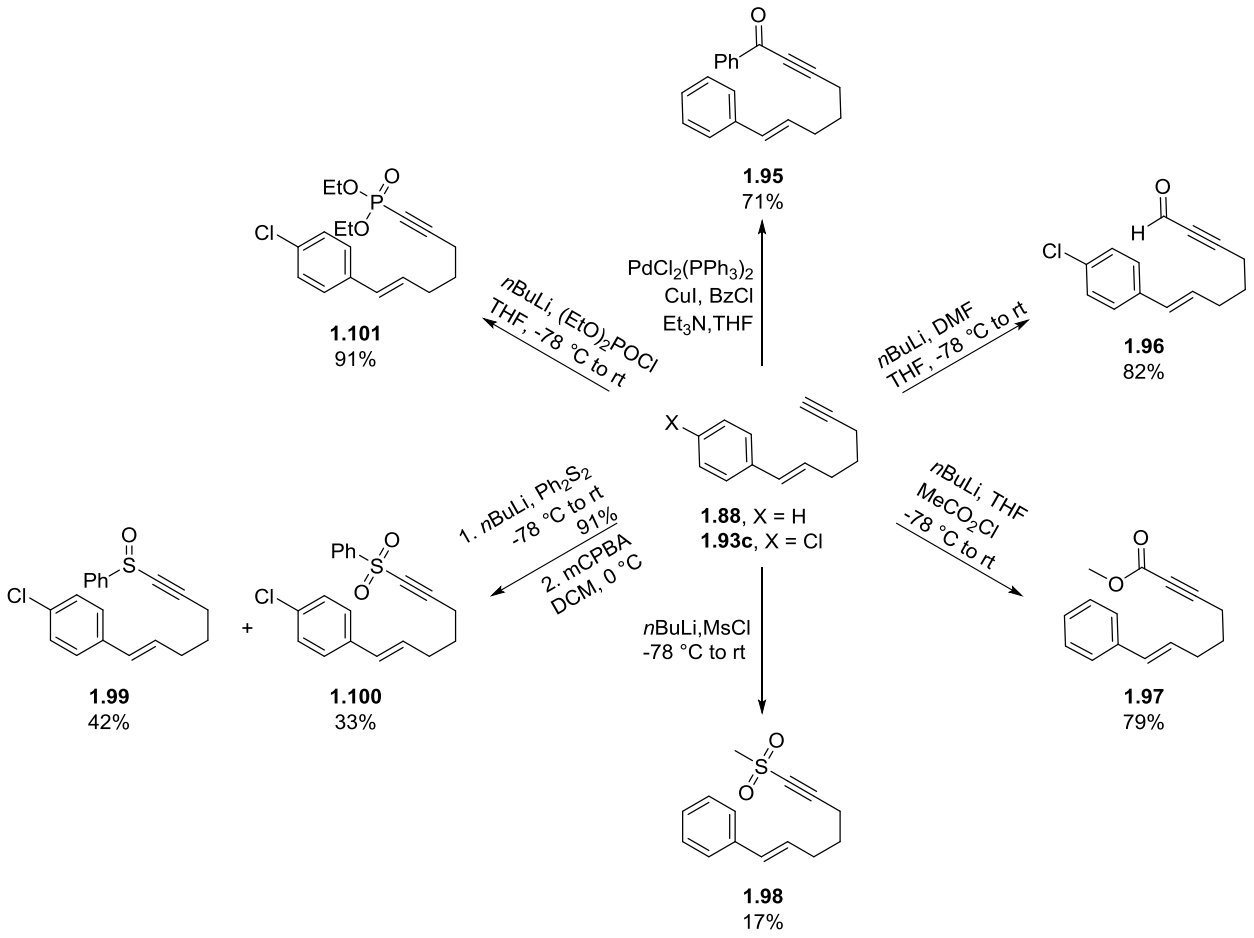

Scheme 1.23. Substitution of styrene-ynes with varied EWGs

In addition to electron-withdrawing substituents, a TMS group was also investigated as an alkynyl substituent in the DDDA reaction. This would not only allow for a study of the effect of electronics of the dienophile on the DDDA reaction, but also for a direct comparison to the results of Matsubara et al. who utilized the same substrate in their DDDA reaction studies.[47] The TMS-substituted styrene-yne **1.104** was synthesized by first treating 5-hexyn-1-ol (**1.85**) with excess *n*-butyllithium and trimethylsilyl chloride, followed by 5% acetic acid to afford the trimethysilylacetylene derivative **1.102** in 94% yield (Scheme 1.24). The alcohol of **1.102** was then oxidized to an aldehyde in 71% yield using PCC, and a Horner-Emmons-Wadsworth reaction was performed on the aldehyde **1.103** with *n*-butyllithium and diethyl

benzylphosphonate to produce styrene-yne **1.104** in 20% yield. Alternative reaction conditions may lead to an improved yield for the formation of **1.104** based upon previous syntheses where yields of the Horner-Emmons-Wadsworth reaction with non-halogenated aryl phosphonates were increased by employing sodium hydride as base rather than *n*-butyllithium (Scheme 1.18).

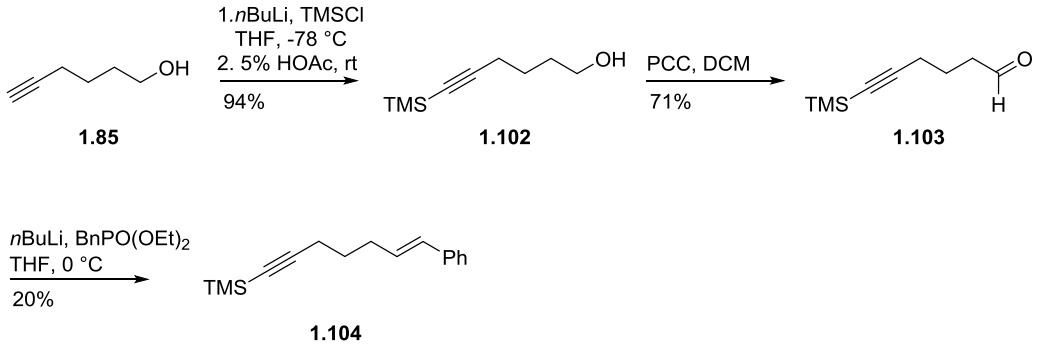

Scheme 1.24. Synthesis of TMS-substituted styrene-yne **1.104**

Irradiation of styrene-ynes containing electron-withdrawing substituents on the terminus of the alkyne resulted in the successful formation of cyclopenta[*b*]naphthalenes via the DDDA reaction in high yields and variable reaction times (Scheme 1.25). For each reaction, the styrenyl precursor was initially irradiated for 5 min. Based upon the conversion of the starting material to product as estimated by TLC, the irradiation time was periodically increased until the reaction appeared complete. The reaction was then performed a second time without periodic stopping to ensure that the total reaction time determined in the first experiment was adequate for the reaction to complete. Using this procedure, styrene-ynes **1.95**, **1.96**, **1.99**, and **1.100** containing a phenyl ketone, aldehyde, sulfone, and sulfoxide, respectively, were found to undergo the DDDA

reaction in DCE at 180 °C in 15-90 min to produce naphthalenes **1.105**, **1.106**, **1.109**, and **1.110** in 75% to quantitative yields. Certain examples, such as phenyl ketone-substituted styrene-yne **1.95**, required longer irradiation times of 90 min, possibly due to steric hindrance attributed to the additional phenyl group. Other DDDA reactions showed enhanced reaction rates, such as for the formation of phenyl sulfone-containing naphthalene **1.109** which was generated in only 15 min. This rate enhancement can be explained by the stronger electron-withdrawing ability of the sulfone, which would serve to further decrease the LUMO energy of the dienophile and increase HOMO/LUMO orbital interaction. For ester and phosphonate-substituted styrene-ynes **1.97** and **1.101**, in which the substituent on the dienophile was not as electron-withdrawing, DDDA reaction rates were significantly slowed at 180 °C, requiring multiple hours. To perform the DDDA reaction in reasonable microwave irradiation times of less than 3 h, the reaction was conducted at 225 °C in *o*-DCB, which afforded naphthalenes **1.107** and **1.111** in 90 and 150 min, respectively. Increasing the temperature did not affect the yield of the DDDA reaction. Finally, EWGs on the dienophile were determined to be essential to the success of the DDDA reaction. Replacing the EWGs with a TMS moiety, as in styrene-yne **1.104**, or using styrene-yne **1.88** with an unsubstituted alkyne terminus in the DDDA reaction resulted in trace amounts or no formation of cyclopenta[*b*]naphthalene products **1.112** and **1.113**. This is in contrast to the reports by Matsubara et al. where TMS-substituted naphthalene **1.112** was isolated in 86% yield.[47] However, the DDDA reaction by Matsubara was conducted at 250 °C, whereas our study was performed at 180 °C, so a direct comparison of the results was not made. Higher temperatures may be required for DDDA reactions of TMS-substituted styrene-ynes to achieve naphthalene formation, which is also evidenced by the higher temperatures and longer reaction

times required for styrene-ynes containing weaker electron-withdrawing dienophile substituents, such as the ester and phosphonate, to undergo the DDDA reaction.

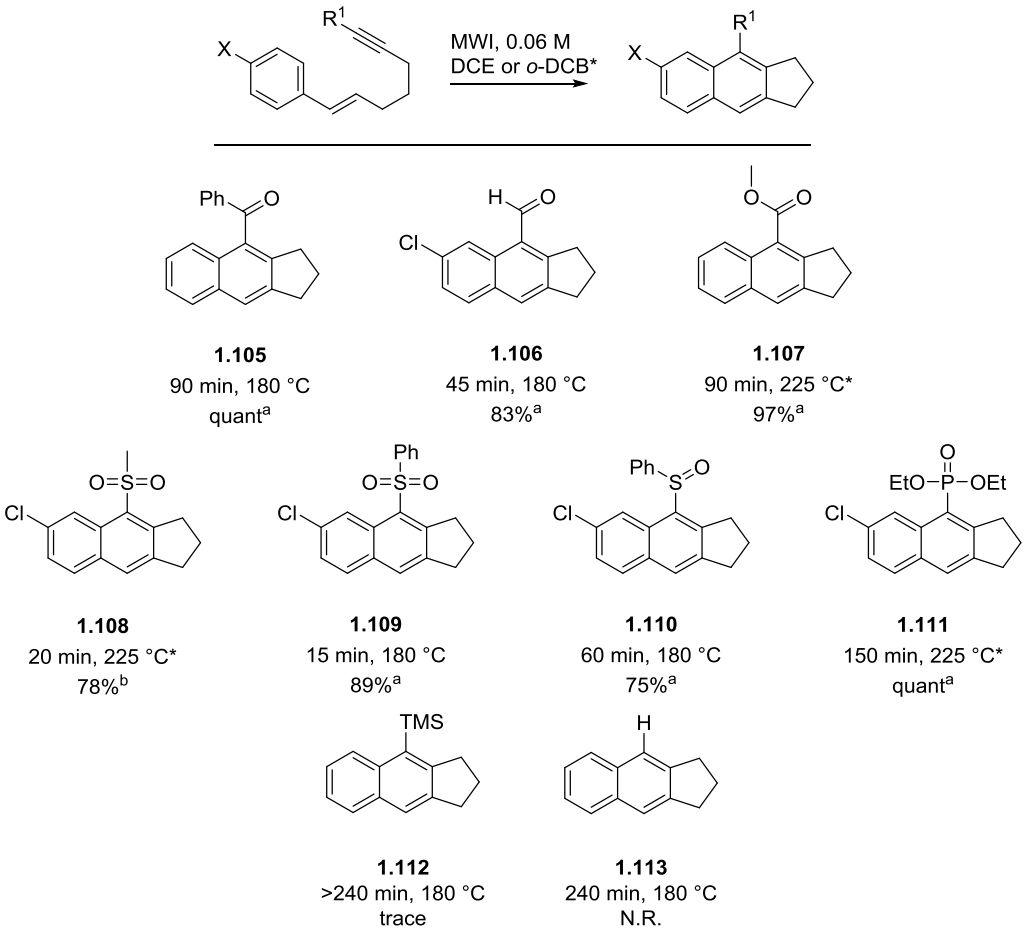

Scheme 1.25. DDDA reactions of styrene-ynes containing variable EWGs.
[a]Crude yields where no byproducts or impurities were observed by ^{1}H NMR spectroscopy. [b]Isolated yields after purification by silica gel column chromatography.

1.3.3 Variations to the styrene-yne tether of the styrenyl precursor

To further expand the scope of the DDDA reaction, modifications were made to the styrene-yne tether in the form of additional substitution to the tether, incorporation of heteroatoms into the tether, and extension of the tether length. Until this point, the DDDA reactions that we explored contained an all carbon tether that contained no substituents; however, almost all previously reported DDDA reactions were performed on styrene-ynes that contained heteroatoms in their tether, usually in the form of esters, amides, or amines, or contained some form of substitution, such as a carbonyl. A typical limitation of DDDA reactions that contained heteroatoms in their styrene-yne tether was the formation of dihydronaphthalene along with the desired naphthalene product. In order to determine if our DDDA reaction would have comparable limitations, in addition to potentially expanding the reaction's scope, changes were made to the styrene-yne tether of the styrenyl precursor.

As an initial study, modifications were made to styrenyl precursors containing an all carbon styrene-yne tether. First, increasing the tether length by one methylene unit was explored. The synthesis of the styrene-yne **1.118** commenced by subjecting commercially available hept-3-yn-1-ol (**1.114**) to a zipper reaction with sodium hydride and ethylenediamine to provide hept-6-yn-1-ol (**1.115**) in 72% yield (Scheme 1.26). The remainder of the synthesis of styrene-yne **1.118** was carried out in an analogous manner to that conducted for the synthesis **1.88** and in comparable yield (Scheme 1.18); however, the Horner-Wadsworth-Emmons reaction to produce **1.117** proceeded in a significantly reduced yield of 20% (Scheme 1.26).

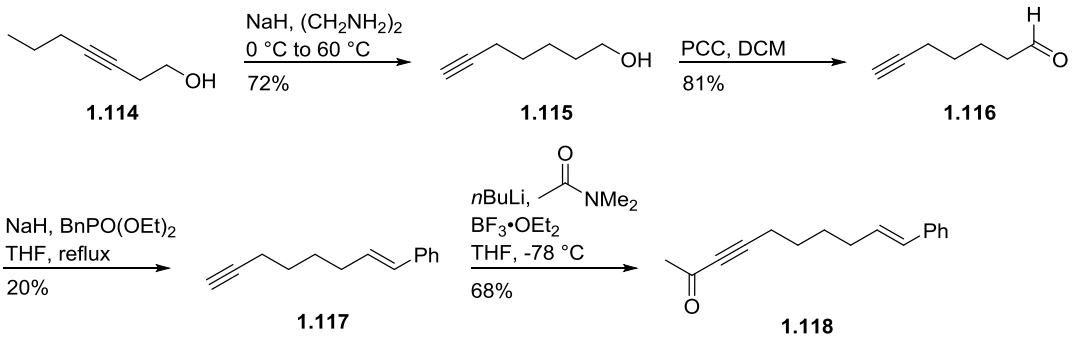

Scheme 1.26. Synthesis of styrene-yne **1.118** containing an elongated styrenyl tether

A series of styrenyl precursors containing carbonyl substitution within the styrene-yne tether, rather than on the terminus of the alkyne, were also synthesized to provide substrates with tethers similar to those utilized in DDDA reactions by Terashima.[46] The benefit of this modification to the styrene-yne tether is that an EWG is still appended to the dienophile, but other substituents can easily be incorporated at the alkyne terminus. The commercially available chlorobenzaldehydes **1.119** were employed as starting materials and converted to allylic alcohols **1.120** in 60-78% yield by addition of vinyl magnesium bromide (Scheme 1.27). Subsequent treatment of the allylic alcohols **1.120** with phosphorous tribromide provided 70 -83% yield of cinnamyl bromides **1.121**, which were then transformed to dimethylamides **1.122** in 73-74% yield by addition to dimethylacetamide and LDA. To access the desired styrenyl precursors, the dimethylamides of **1.122** were substituted with phenyl or trimethylsilylacetylides, producing styrene-ynes **1.123** in 80 -96% or 40-55% yield, respectively.

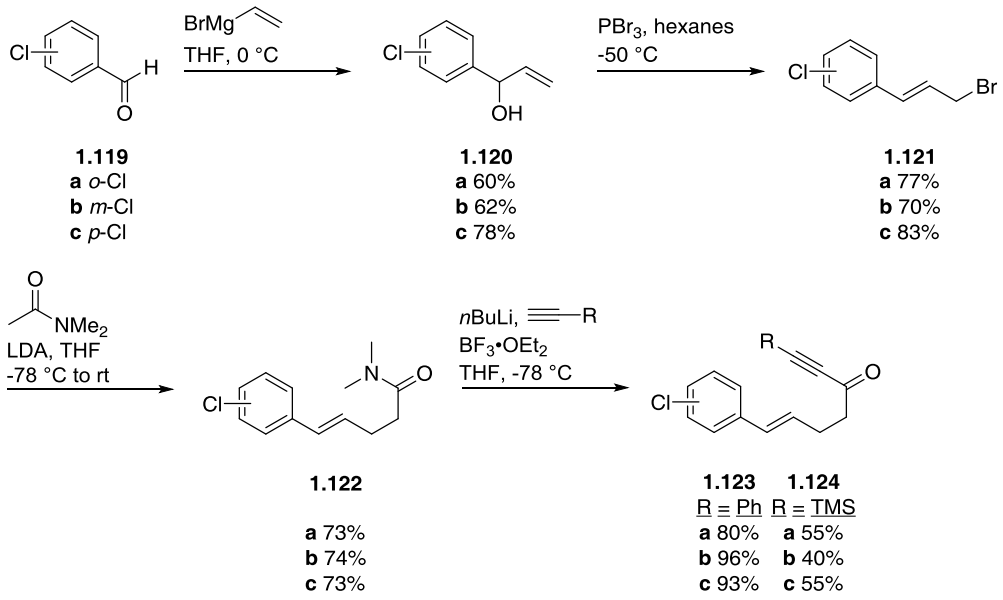

Scheme 1.27. Synthesis of styrene-ynes containing carbonyl substitution in the styrenyl tether

One final modification to styrenyl precursors containing all carbon styrene-yne tethers was the incorporation of a central diester group. Generation of the enolate of diethyl 2-(prop-2-yn-1-yl)malonate (**1.125**) and subsequent reaction with cinnamyl bromide **1.126** yielded the styrene-yne **1.127** in 81% yield (Scheme 1.28). Acylation of the lithium acetylide of **1.127** was achieved by addition of *N*-methoxy-*N*-methylacetamide to produce the styrene-yne **1.128** in 86% yield.

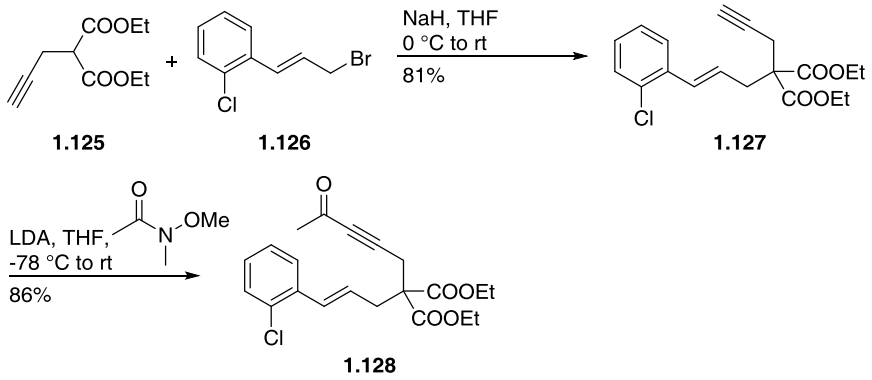

Scheme 1.28. Synthesis of styrene-yne containing diester substitution in the styrenyl tether

In addition to styrenyl precursors in which modifications were made to styrene-yne tethers consisting exclusively of methylene units, variants of the precursors in which heteroatoms were incorporated into the styrene-yne tether were also synthesized. A more concise and convergent synthesis could be employed to access these heteroatom-containing substrates by combination of commercially available propargyl amines or alcohols and cinnamyl derivatives (Scheme 1.29). To test this proposed synthetic pathway, propargyl amine (**1.129**) was first tosylated to generate sulfonamide **1.130** in quantitative yield (Scheme 1.30). Subsequent treatment of **1.130** with potassium carbonate and cinnamyl bromide formed styrene-yne **1.131** in 94% yield, the lithium acetylide of which was then acylated in 45% yield using dimethylacetamide and boron trifluoride diethyl etherate to afford styrene-yne **1.132a**. An *ortho*-chloro derivative of this styrene-yne **1.132b** was also generated via an analogous synthetic route. Additionally, a styrene-yne containing an oxygen atom in its tether was synthesized via a coupling of propargyl alcohol (**1.133**) and cinnamyl acetate using diethyl zinc and tetrakis(triphenylphosphine)palladium(0) to generate the styrene-yne **1.134**, which was then

subjected to a second palladium-catalyzed cross-coupling reaction with benzoyl chloride to produce the benzoyl-substituted styrene-yne **1.135** in 68% yield.

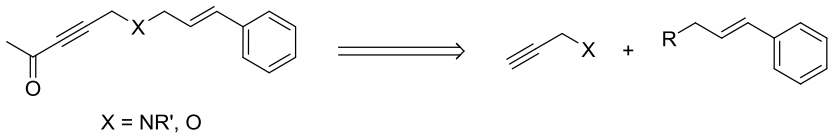

Scheme 1.29. Retrosynthetic analysis of styrene-ynes with heteroatom-substituted tethers

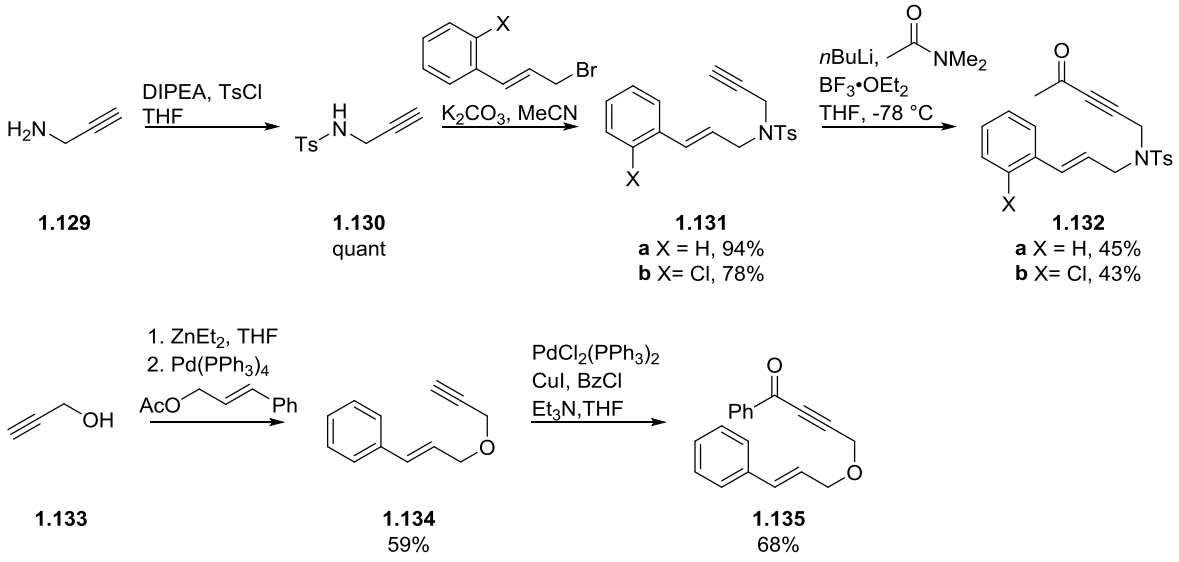

Scheme 1.30. Synthesis of styrene-ynes containing heteroatoms in the styrenyl tether

To test the effect of the DDDA reaction on styrene-ynes containing modified carbon tethers, styrenyl precursors **1.118**, **1.123a-c**, **1.124a-c**, and **1.128** were subjected to microwave irradiation. Irradiation of **1.118** containing an elongated carbon tether for 50 min at 300 °C formed the cyclohexane-fused naphthalene **1.136** in quantitative yield (Scheme 1.31). Irradiation of **1.118** at lower temperatures of 225-250 °C only resulted in recovery of starting material. Although these reaction conditions to produce naphthalene **1.136** are harsh, this is the first example, to our knowledge, of a cyclohexane-fused naphthalene being generated via a DDDA reaction of styrenes. Irradiation of **1.128** for 30 min at 180 °C in *o*-DCB produced naphthalene **1.137** in quantitative yield, while irradiation of the phenyl-substituted alkynones **1.123a-c** at 225 °C in *o*-DCB generated cyclopenta[*b*]naphthalenones **1.138**-**1.141** in high yields of 77-96% after only 40 min; higher reaction temperatures were necessary for product formation in reasonable irradiation times. Under the same DDDA reaction conditions, TMS-substituted alkynones **1.124a-c** required 90 min of irradiation time to afford cyclopenta[*b*]naphthalenones **1.142**-**1.145** in comparable yields. Similar to the chloronaphthalenes **1.94** described in Scheme 1.22, halogens could be incorporated at all positions of the A ring of the cyclopenta[*b*]naphthalenones, and irradiation of *meta*-chlorostyrene-ynes resulted in a mixture of 6- and 8-substituted chloronaphthalenes, the ratio of which depended upon the steric bulk of the substituent at the 1-position. In contrast to phenyl and TMS-substituted examples, an unsubstituted alkynone was relatively unsuccessful in the DDDA reaction, providing the cyclopenta[*b*]naphthalenone in low yields after long reaction time.

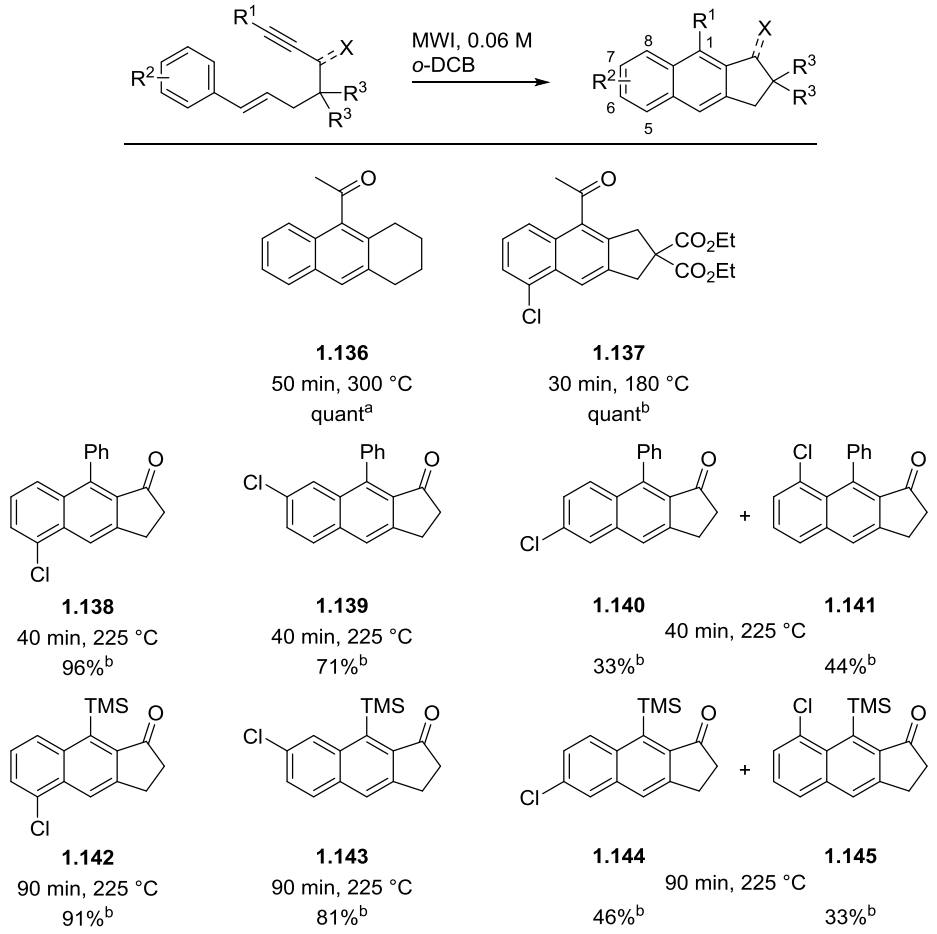

Scheme 1.31. DDDA reaction of styrene-ynes with varied carbon tethers.
[a]Crude yields where no byproducts or impurities were observed by ^{1}H NMR spectroscopy. [b]Isolated yields after purification by silica gel column chromatography.

While modifications to the all carbon tether of styrene-ynes were well tolerated in the DDDA reaction and allowed for the formation of naphthalene products exclusively and in high yields, introduction of heteroatoms into the styrene-yne tether resulted in mixtures of naphthalene and dihydronaphthalene products that were inseparable by column chromatography. This is in line with previously reported DDDA results where mixtures of naphthalene and dihydronaphthalene substrates were commonly obtained from styrene-ynes containing esters, amides, or nitrogen atoms in their tethers.[44-45,47] Irradiation at 180 °C for only 10 min of both the non-halogenated and halogenated styrenyl precursors **1.132a** and **1.132b** containing a sulfonamide in their styrene-yne tethers produced an approximate 1:2 ratio of the naphthalenes **1.146** or **1.148** to the dihydronaphthalenes **1.147** or **1.149** in high combined yields of 72-86% (Scheme 1.32). These product ratios and yields are comparable to those reported by Matsubara et al. for when the alkyne terminus of the styrene-yne was substituted with an ester.[47] As an additional example, styrenyl precursor **1.135** containing an oxygen atom in the styrene-yne tether was irradiated at 180 °C for 30 min, producing naphthalene **1.150** and dihydronaphthalene **1.151** in a 1.8:1 ratio and 43% combined yield. Although the yield of the naphthalene products was similar for both sulfonamide- and oxygen-containing tethers, the yield of dihydronaphthalene **1.151** was significantly reduced when compared to **1.147** and **1.149**, which was attributed to decomposition of the dihydronaphthalene product upon the longer irradiation time of 30 min. Similar decomposition of sulfonamide-substituted dihydronaphthalene **1.147** was also observed upon prolonged irradiation. Attempts to oxidize the mixture of **1.146** and **1.147** using cerric ammonium nitrate, dichlorodicyanobenzoquinone, and palladium on carbon to provide naphthalene **1.146** exclusively resulted in either complete decomposition of the reaction mixture or selective decomposition of the dihydronaphthalene **1.147**.

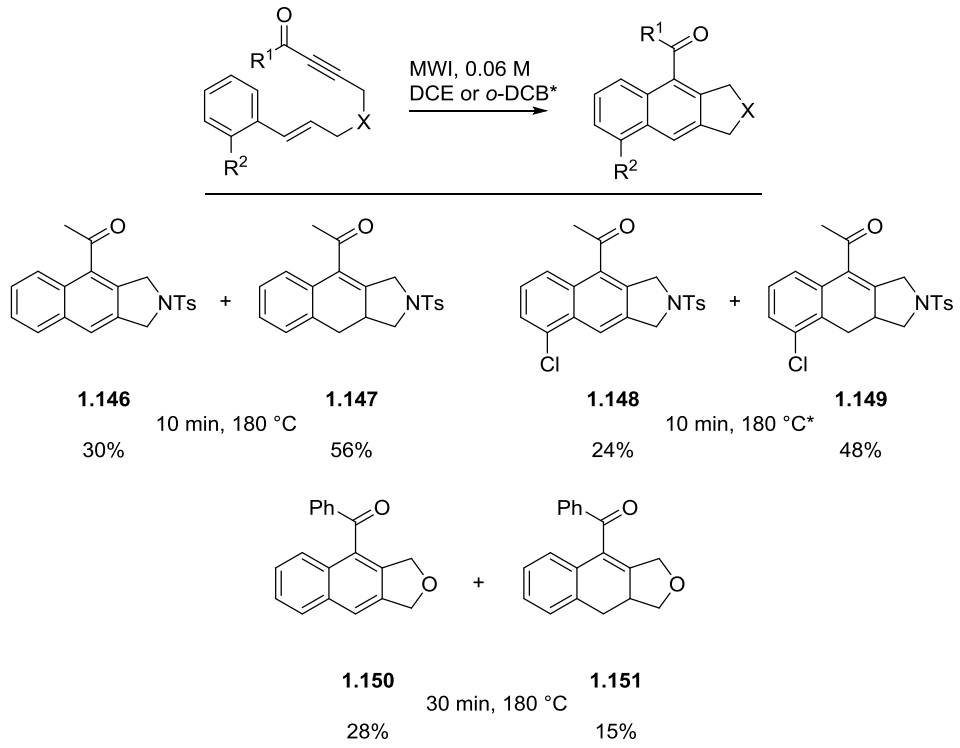

Scheme 1.32. DDDA reaction of styrene-ynes with heteroatom-containing tethers.
Yields shown are isolated yields for the product mixture after purification by column chromatography. Ratio of naphthalene and dihydronaphthalene products was determined by ^{1}H NMR spectroscopy.

1.3.4 Controlling regioselectivity in the DDDA reaction of *meta*-substituted styrenes

Although DDDA reactions of styrenyl precursors containing carbon tethers successfully produced cyclopenta[*b*]naphthalenes exclusively and in high yields, examples of styrene-ynes, such as **1.93b** and **1.124b** which incorporated chloro groups at the *meta*-position of the styrenes produced mixtures of 6- and 8-chloronaphthalene regioisomers upon irradiation, resulting in a reduced yield of each individual naphthalene (Scheme 1.22 and Scheme 1.31). To improve the regioselectivity of the DDDA reaction of *meta*-substituted styrenes for the 6-chloronaphthalene product, additional modifications were made to the styrenyl precursor. One such change was the incorporation of a methyl group at the *ortho*-position of the styrene, adjacent to the chloro

substituent. By placing a methyl group at this position, only one DA pathway was possible upon irradiation of the styrene-yne to afford the 6-chloronaphthalene substrate; the other DA route would result in a tetraene intermediate that would not be able to aromatize to the 8-chloronaphthalene product due to the location of the methyl group (Scheme 1.33).

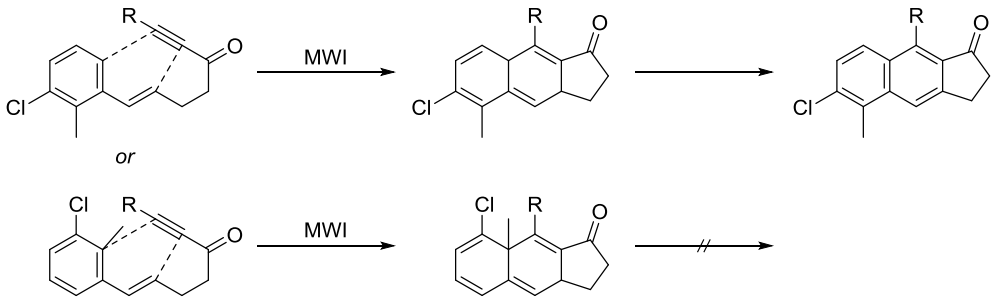

Scheme 1.33. Controlling the regioselectivity of the DDDA reaction.
Regioselectivity controlled through *ortho*-methyl substitution of styrenes

To test the feasibility of this strategy for controlling regioselectivity in the DDDA reaction, the styrene-ynes **1.158a** and **1.158b** containing a 2-methyl-3-chloro-substituted styrene were synthesized from commercially available 3-chloro-2-methylbenzoic acid (**1.152**) by reduction of the acid with LAH to yield 96% of the primary alcohol **1.153**, which was then oxidized to aldehyde **1.154** in 91% yield by employing PCC (Scheme 1.34). To access the styrene-ynes **1.158a** and **1.158b**, an analogous synthesis was performed on **1.154** as was conducted to afford the substituted alkynones **1.123** and **1.124** (Scheme 1.27), and each step provided the products in comparable, if not higher yields (Scheme 1.34). The DDDA reactions of styrene-yne **1.158a** and **1.158b** proved to be a success in that only the 6-chloronaphtahlenes **1.159a** and **1.159b** were formed in high yields of 86 and 92%, respectively; no additional

products were observed or isolated. This indicates that substituting the *ortho*- as well as the *meta*-position of the styrene allows for regiocontrol in the DDDA reaction.

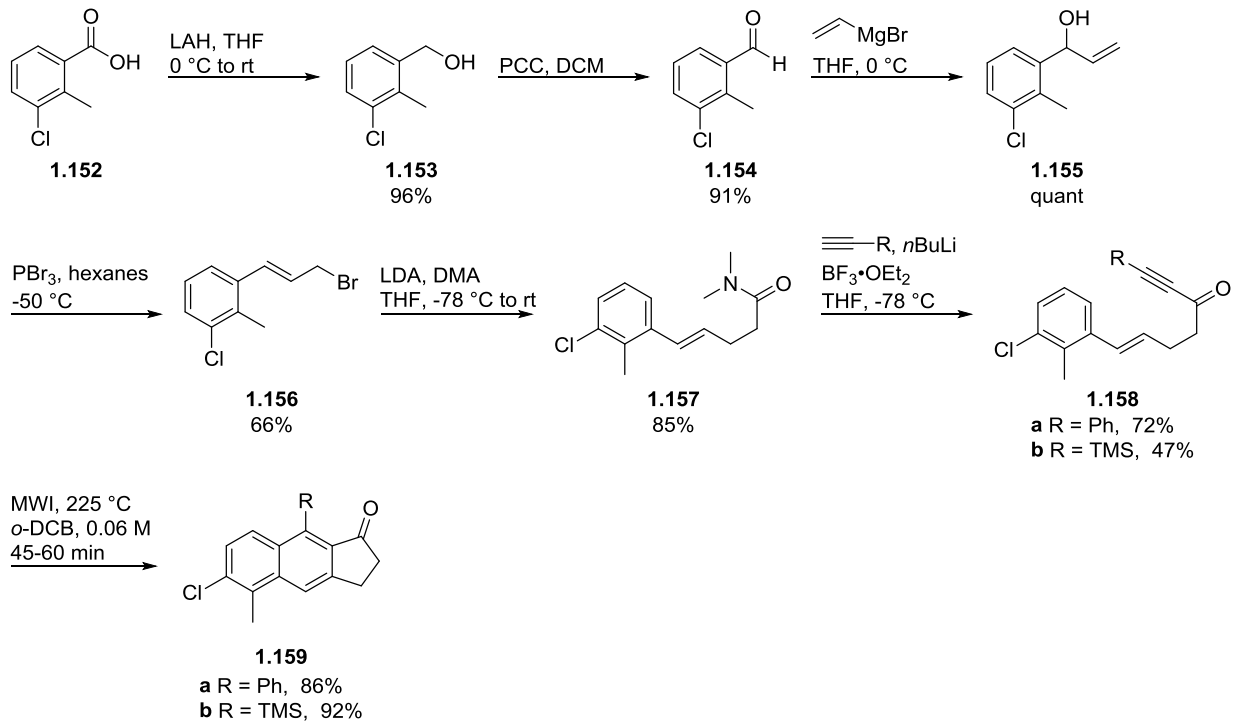

Scheme 1.34. Synthesis and DDDA reaction of styrene-ynes **1.158**. Provided regioselective formation of 6-chloronaphthalenes **1.159**

In addition to substituting the *ortho*-position of the styrenyl precursors, regioselectivity for the 6-chloronaphtahlene product may also be obtained by increasing the steric bulk of the substituent on the alkyne of the styrene-yne. In previous DDDA reactions, it was observed that increasing the bulkiness of the alkynyl substituent from a phenyl to a TMS moiety resulted in a preference for formation of the 6-chloronaphthalene over the 8-chloronaphthalene. For example,

irradiation of phenyl-substituted styrene-yne **1.123b** afforded a 1:1.3 ratio of **1.140** to **1.141**, favoring the 8-chloronaphthalne product, while irradiation of **1.124b**, containing a bulkier TMS group on the alkyne, reversed product selectivity, now with the 6-chloronapthalene as the major product in a 1.4:1 ratio of **1.144** to **1.145** (Scheme 1.31). We envisioned that by further increasing the steric bulk of the alkynyl substituent, a higher degree of regioselectivity would be obtained in the DDDA reaction to generate the 6-chloronaphthalene product. To this end, the triphenylsilyl-substituted alkynone **1.160** was synthesized in 62% yield by addition of triphenysilylacetylide to the dimethylamide **1.122b** (Scheme 1.35). The DDDA reaction of **1.160** provided the 6-chloronaphthalene **1.161** exclusively in 67% yield; no 8-chloronaphthalene **1.162** was observed. This supports the hypothesis that appending a bulkier substituent to the alkyne terminus of the styrene-yne results in undesirable steric interactions with the chloro group in the transition state that disfavors the formation of the 8-chloronaphthalene product.

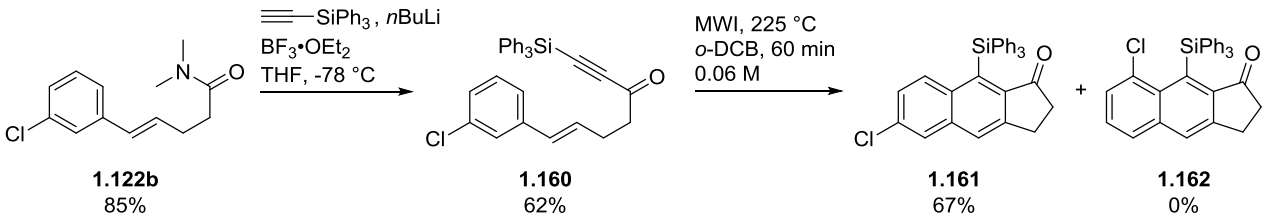

Scheme 1.35. Synthesis and DDDA reaction of styrene-yne **1.160**

1.3.5 Comparison of microwave-assisted DDDA reaction to conventional heating methods

All examples of the DDDA reaction reported above were performed employing microwave irradiation rather than conventional heating methods, such as heating by an oil bath. By using these microwave-assisted reaction conditions, it was found that naphthalene products were obtained exclusively, in high yields, and in brief reaction times. This is in contrast to many previous reports of DDDA reactions where conventional heating methods were utilized only to afford the naphthalene in low to moderate yields, in long reaction times of multiple hours to days, or as a mixture with the dihydronaphthalene substrate.[42-47] Only one other previously studied DDDA reaction by Ruijter et al. utilized microwave irradiation, and it was also observed that the complete reaction of the styrene-yne occurred in only 15 min to produce high combined yields of the naphthalene and dihydronaphthalene products.[45]

To determine whether the high yielding and selective results we obtained in the DDDA reaction were a result of the microwave conditions employed, or were from purely thermal effects, conventional heating experiments were conducted. The first experiment performed was heating of halogenated styrene-yne **1.93c** in DCE to 180 °C in an oil bath using a sealed microwave vial. The DDDA reaction to produce naphthalene **1.94d** required 2 d to complete, and only resulted in 61% yield of the naphthalene. This reaction time is much longer and the yield lower than for the microwave-assisted conditions, which provided quantitative yield of **1.94d** in only 180 min (Scheme 1.36). While this may allude to a specific microwave effect,[49] DCE is a low-boiling solvent and is not suited for prolonged heating at very high temperature of 180 °C in an oil bath; vigorous boiling and evaporation of the solvent into the headspace occurred throughout the reaction period. Utilizing microwave irradiation provides an advantage over

conventional heating when employing low boiling reaction solvents due to superheating of the solvent, which allows for higher reaction temperatures to be more easily and rapidly attained.[50]

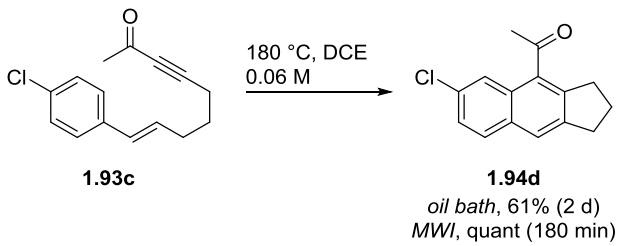

Scheme 1.36. Conventional versus microwave heating of styrene-yne **1.93c** in DCE

In a second experiment, styrene-yne **1.96** in *o*-DCB was heated to 180 °C in an oil bath. By using *o*-DCB as a reaction solvent, higher temperatures are more easily reached under conventional thermal conditions because of the solvent's much higher boiling point and higher tan δ, which allows for a more accurate comparison of microwave to conventional heating conditions. As a result of heating styrene-yne **1.96** under conventional conditions, naphthalene **1.106** was afforded in 53% yield after 100 min. Microwave irradiation of styrene-yne **1.96** at 180 °C, on the hand, produced naphthalene **1.106** in 73% yield after 60 min (Scheme 1.37). These results once again demonstrate that the microwave-assisted DDDA reaction leads to higher yields and shorter reaction times when compared with conventional heating methods. However, whether the source of these increased yields and faster reaction times may be attributed to the purely thermal effect of rapid and efficient heating provided by microwave irradiation, or to a non-thermal microwave effect, is still debatable.[49,51]

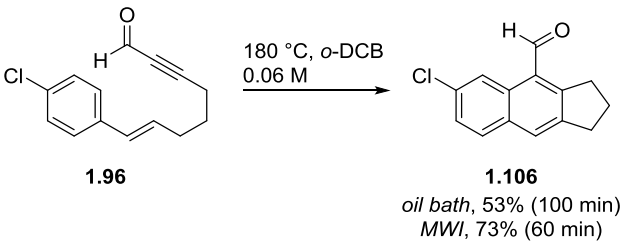

Scheme 1.37. Conventional versus microwave heating of styrene-yne **1.96** in *o*-DCB

To rule out a non-thermal microwave effect as a source of the shortened reaction times, one final microwave irradiation experiment was conducted using a silicon carbide, rather than borosilicate glass, reaction vessel. Silicon carbide is used for ruling out microwave effects because it is a ceramic material that absorbs microwaves, essentially shielding the reaction mixture from the electromagnetic field.[52] Upon absorption of the microwaves, silicon carbide acts as a semiconductor and the reaction vessel becomes rapidly heated, which then heats the reaction mixture. This allows for heating of the reaction mixture under thermal conditions with the same efficiency as traditional microwave irradiation, but without exposure to the electromagnetic field. Subjecting styrene-yne **1.96** to irradiation in a silicon carbide vial at 180 °C for 60 min resulted in a 71% yield of the naphthalene **1.106**, a comparable value to the 73% yield of **1.106** obtained when **1.96** was irradiated in a glass reaction vessel under the same reaction conditions (Scheme 1.38). Based upon these results, the high yields and short reaction times attained in the DDDA reaction are attributed to the rapid and efficient heating caused by microwave irradiation, rather than non-thermal microwave effects. However, it should be noted that there is debate regarding the microwave-absorbing ability of silicon carbide, where some researchers believe that it still allows transmission of microwaves.[51] To conclusively determine if

there is a specific microwave effect for the DDDA reaction, alternate experiments will need to be conducted using a reaction vessel that is proven to be more strongly microwave absorbing.

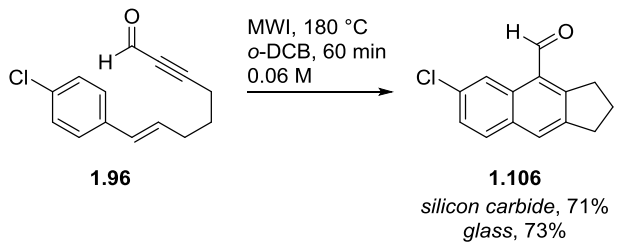

1.96 **1.106**
silicon carbide, 71%
glass, 73%

Scheme 1.38. MWI of styrene-yne **1.96** in silicon carbide versus borosilicate glass vessels

1.4 CONCLUSIONS

In conclusion, initial investigations of a formal, thermal [2 + 2 + 2] cycloaddition reaction of ene-allene-yne substrates led to the discovery of a microwave-assisted intramolecular dehydrogenative dehydro-Diels-Alder (DDDA) reaction of styrenes. Notably, these primary results showed that the DDDA reaction was performed in higher yield, shorter reaction time, and with excellent product selectivity compared to DDDA reactions previously reported in the literature. Additionally, the styrene-yne used in our reaction contained an EWG substituted on the alkyne terminus, as well as an all carbon styrene-yne tether, which are two variants of the DDDA reaction that have been scarcely explored.

These primary results prompted our further study of the DDDA reaction, which could potentially be optimized and utilized as a general method to access novel cyclopenta[*b*]naphthalene frameworks. With this in mind, the scope of the DDDA reaction was

explored, and it was determined that modifications to the styrene, tether, and alkyne terminus of styrenyl precursors containing carbon tethers were all well tolerated in the DDDA reaction to generate naphthalenes exclusively and in high yields. Limitations to the DDDA reaction were observed in that an EWG group was required on the alkyne dienophile in order for the reaction to proceed in high yield, and also incorporation of heteroatoms into the styrene-yne tether resulted in mixtures of naphthalene and dihydronaphthalene products that were inseparable by column chromatography. One further limitation to this methodology was that *meta*-substituted styrenyl precursors showed minimal regioselectivity in the DDDA reaction, a problem which could be overcome by incorporating an *ortho*-substituent on the styrene or by appending a bulkier group to the alkyne terminus of the styrene-yne. Finally, the high yields, short reaction times, and product selectivity demonstrated by the microwave-assisted DDDA reaction of styrenes attributed to the more efficient and rapid heating allowed by microwave irradiation, rather than non-thermal microwave effects.

This research on expanding the scope of the DDDA reaction was not performed alone, and Dr. Erica Benedetti contributed significantly to this work by synthesizing the cyclopenta[*b*]naphthalene analogs **1.94a-c**, **1.137**, **1.148** and **1.149**.

1.5 EXPERIMENTAL

1.5.1 General methods

All commercially available compounds were purchased and used as received unless otherwise specified. THF, Et_2O, and DCM were purified by passing through alumina using a Sol-Tek ST-

002 solvent purification system. Triethylamine and acetonitrile (MeCN) were distilled over calcium hydride, and deuterated chloroform ($CDCl_3$) was dried over 3 Å molecular sieves. Purification of the compounds by flash column chromatography was performed using silica gel (40-63 μm particle size, 60 Å pore size), or by using a Biotage Horizon flash purification system with either Biotage SNAP KP-SIL or Silicycle SiliaSep silica flash cartridges. TLC analyses were performed on silica gel F_{254} glass plates (250 μm thickness). ^{1}H NMR and ^{13}C NMR spectra were recorded on Bruker Avance 300, 400, 500, 600, or 700 MHz spectrometers. Spectra were referenced to residual chloroform (7.26 ppm, ^{1}H; 77.16 ppm, ^{13}C), benzene (7.16 ppm, ^{1}H; 128.0 ppm, ^{13}C), or dichloromethane (5.32 ppm, ^{1}H; 53.84 ppm, ^{13}C). Chemical shifts are reported in ppm, multiplicities are indicated by s (singlet), d (doublet), t (triplet), q (quartet), p (pentet), m (multiplet), and broad singlet (bs). Coupling constants, *J*, are reported in hertz (Hz). All NMR spectra were obtained at room temperature unless otherwise specified. ^{1}H and ^{13}C NMR spectra can be found in Appendix B. IR spectra were obtained using a Nicolet Avatar E.S.P. 360 FT-IR. EI mass spectroscopy was performed on a Waters Micromass GCT high resolution mass spectrometer, while ES mass spectroscopy was performed on a Waters Q-TOF Ultima API, Micromass UK Limited high resolution mass spectrometer. All microwave-mediated reactions were carried out in sealed vessels using a Biotage Initiator Exp or Anton Paar Monowave 300 microwave synthesizer. All microwave-mediated reactions were conducted in either a Biotage Initiator Exp microwave synthesizer using 0.5-2 mL conical and 2-5 mL cylindrical microwave irradiation vials, or in an Anton-Paar Monowave 300 microwave synthesizer using G4 and G10 cylindrical microwave irradiation vials. The temperature of reactions in the Monowave 300 was monitored internally by a ruby sensor fiber optic probe, unless otherwise specified. The microwave parameters were set to variable power, constant

temperature, stirring on, and a fixed hold time. Separation of naphthalene and dihydronaphthalene products was performed on a Varian Prostar HPLC chromatograph using a Varian Dynamax Microsorb 100-5 Si column.

1.5.2 Experimental procedures detailed in published papers

Characterization and conditions for the preparation of the following naphthalenes, including syntheses and characterization of all precursors and spectral data, were previously published and can be found in the Supporting Information of Kocsis, L. S.; Benedetti, E.; Brummond, K. M. A Thermal Dehydrogenative Diels–Alder Reaction of Styrenes for the Concise Synthesis of Functionalized Naphthalenes. *Org. Lett.* **2012**, *14*, 4430-4433 (Figure 1.7).

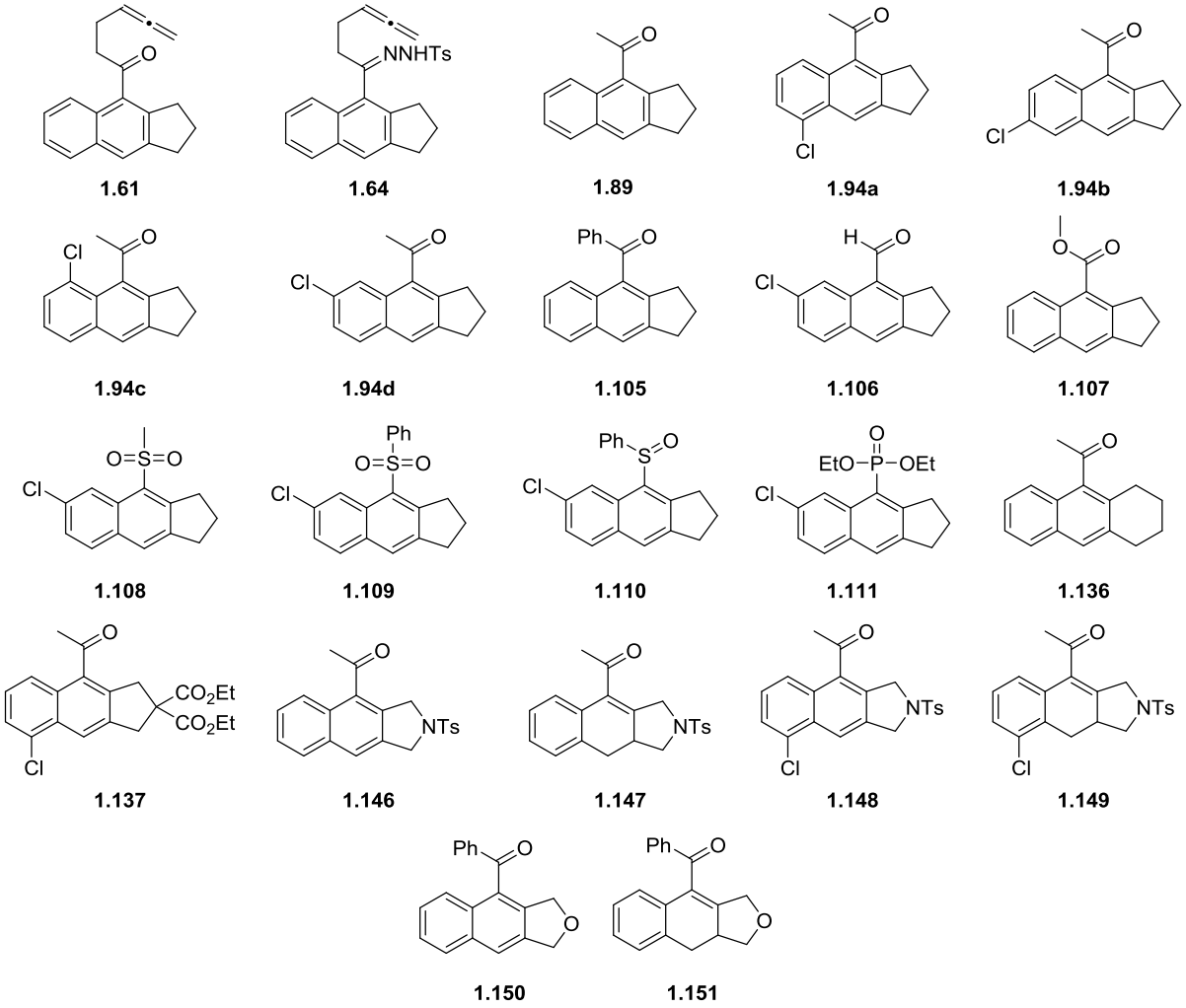

Figure 1.7. Previously published naphthalenes.
Syntheses and characterization can be found in *Org. Lett.* **2012**, *14*, 4430-4433.

Characterization and conditions for the preparation of the following naphthalenes, including syntheses and characterization of all precursors and spectral data, were previously published and can be found in the Supporting Information of Benedetti, E.; Kocsis, L. S.; Brummond, K. M. Synthesis and Photophysical Properties of a Series of Cyclopenta[*b*]naphthalene Solvatochromic Fluorophores. *J. Am. Chem. Soc.* **2012**, *134*, 12418-12421 (Figure 1.8).

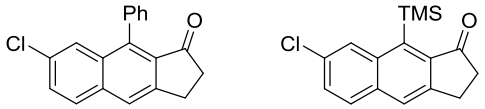

1.139 **1.143**

Figure 1.8. Previously published naphthalenes.
Syntheses and characterization can be found in in *J. Am. Chem. Soc.* **2012**, *134*, 12418-12421.

1.5.3 General procedures

General procedure A: conversion of aldehydes to allylic alcohols.[53] To a flame-dried two-neck round-bottomed flask equipped with an argon inlet adapter, a septum, and a stir bar was added aldehyde (1.0 equiv) and THF (0.6 M) with stirring. The solution was cooled to 0 °C in an ice bath, and vinylmagnesium bromide (1.2 equiv of a 1.0 M solution in THF) was added dropwise via syringe turning the reaction mixture yellow. The reaction mixture was warmed to rt and stirred for 3 h, followed by transfer to a separatory funnel containing sat'd aq ammonium chloride. Et_2O was added, and the aqueous layer was separated and extracted with Et_2O (2x). The combined organic layers were washed with brine, dried over magnesium sulfate, gravity filtered,

and concentrated under reduced pressure to yield the title compound. The crude product was either carried on without further purification or purified by silica gel flash column chromatography.

General procedure B: conversion of allylic alcohols to cinnamyl bromides.[53] To a flame-dried two-neck round-bottomed flask equipped with an argon inlet adapter, a septum, and a stir bar was added allylic alcohol (1.0 equiv) and hexanes (0.3 M) with stirring. The solution was cooled to -50 °C (bath temperature) in a dry ice/acetone bath, and phosphorous tribromide (1.0 equiv) in hexanes (1.6-1.8 M) was added dropwise via syringe. The reaction mixture was stirred at -50 °C for 1 h, and then was poured into brine. The aqueous layer was separated, and the organic layer was washed with water (3x). The combined aqueous layers were then extracted with hexanes (2x), and the combined organic layers were washed with brine, dried over magnesium sulfate, gravity filtered, and concentrated under reduced pressure. The crude material was filtered through a pad of silica gel with 10% ethyl acetate/hexanes washings to yield the title compound.

General procedure C: conversion of cinnamyl bromides to dimethylacetamides. To a flame-dried two-neck round-bottomed flask equipped with an argon inlet adapter, a septum, and a stir bar was added dimethylacetamide (1.0 equiv) in THF (0.3 M). The solution was cooled at -78 °C (bath temperature) in a dry ice/acetone bath and LDA (1.1 equiv of a 2.0 M solution in heptane/THF/ethylbenzene) was added dropwise via syringe with stirring, turning the reaction mixture light brown. The reaction mixture was stirred at -78 °C for 1-2 h and became yellow in color. Cinnamyl bromide (1.3-1.5 equiv) dissolved in minimal THF was added to the reaction all

at once, turning the reaction mixture a deeper yellow. The reaction mixture was warmed to rt slowly over 3 h, and then stirred at rt for 16 h becoming cloudy and orange. The reaction mixture was poured into brine (15 mL), and the aqueous layer was separated and extracted with Et_2O (3x). The combined organic layers were washed with brine, dried over magnesium sulfate, gravity filtered, and concentrated under reduced pressure. The crude product was purified by silica gel flash column chromatography to yield the title compound.

General procedure D: conversion of dimethylacetamides to alkynones. To a flame-dried two-neck round-bottomed flask equipped with an argon inlet adapter, a septum, and a stir bar was added alkyne (1.2-4.0 equiv) in THF (0.4 M). The solution was cooled at -78 °C (bath temperature) in a dry ice/acetone bath, and *n*-butyllithium (1.1-3.5 equiv of a 1.6 M solution in hexanes) was added dropwise via syringe with stirring. The reaction mixture was stirred at -78 °C for 1 h, then amide (1.0 equiv) in THF (0.3 M) followed by boron trifluoride diethyl etherate (1.1-1.25 equiv) was added dropwise via syringe. The reaction mixture was stirred at -78 °C for 1 h, and a second portion of boron trifluoride diethyl etherate (1.1-1.25 equiv) followed by acetic acid (1.1-1.25 equiv) was added. The reaction mixture was warmed to -20 °C and quenched with sat'd aq ammonium chloride solution. The aqueous layer was separated and extracted with Et_2O (2x). The combined organic layers were washed with brine, dried over magnesium sulfate, gravity filtered, and concentrated under reduced pressure. The crude product was purified by silica gel flash column chromatography to yield the title compound.

General procedure E: dehydrogenative dehydro-Diels-Alder reaction. To a 2-5 mL microwave irradiation vial was added styrene-yne in *o*-DCB (0.05-0.07 M). The solution was

irradiated at 225 °C until complete by TLC. The reaction mixture was then concentrated under high vacuum to remove *o*-DCB and purified by silica gel flash column chromatography to yield the title compound. Alternatively, the reaction mixture could be purified directly by silica gel column chromatography by first eluting with 100% hexanes to separate *o*-DCB, and then increasing the polarity of the eluent to yield the title compound.

1.5.4 Synthesis of cyclopenta[*b*]naphthalenones and their styrenyl precursors

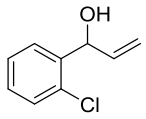

1.120a

1-(2-Chlorophenyl)prop-2-en-1-ol (1.120a). Follows general procedure A: 2-chlorobenzaldehyde (**1.119a**) (2.50 mL, 22.2 mmol), THF (37 mL), vinylmagnesium bromide (26.6 mL, 26.6 mmol). The crude material was purified by silica gel flash column chromatography (40 g silica cartridge, 0-15% ethyl acetate/hexanes) to yield the title compound as a light yellow oil (2.23 g, 60%). Compound **1.120a** was previously characterized.[54]

Data **1.120a**

^{1}H NMR (300 MHz, $CDCl_3$)

7.55 (dd, *J* = 7.5, 1.5 Hz, 1H), 7.36 (dd, *J* = 7.5, 1.5 Hz, 1H), 7.31 (td, *J* = 7.5, 1.5 Hz, 1H), 7.23 (td, *J* = 7.5, 1.5 Hz, 1H), 6.05 (ddd, *J* = 16.0, 10.4, 5.6 Hz, 1H), 5.68-5.65 (m, 1H), 5.40 (dt, *J* = 17.2, 1.5 Hz, 1H), 5.24 (dt, *J* = 10.4, 1.5 Hz, 1H), 2.10 (d, *J* = 3.9 Hz, 1H) ppm

TLC R_f = 0.2 (10% ethyl acetate/hexanes) [silica gel, UV, PAA stain]

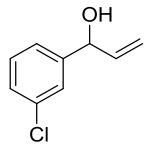

1.120b

1-(3-Chlorophenyl)prop-2-en-1-ol (1.120b). Follows general procedure A: 3-chlorobenzaldehyde (**1.119b**) (5.00 mL, 44.1 mmol), THF (74 mL), vinylmagnesium bromide (53.0 mL, 53.0 mmol). The crude material was purified by silica gel flash column chromatography (5.0 cm column, 10% ethyl acetate/hexanes) to yield the title compound as a light yellow oil (4.62 g, 62%). Compound **1.120b** was previously characterized.[55]

Data **1.120b**

^{1}H NMR (300 MHz, $CDCl_3$)

7.38 (s, 1H), 7.29-7.22 (m, 3H), 6.01 (ddd, *J* = 16.5, 10.3, 6.2 Hz, 1H), 5.36 (dt, *J* = 17.1, 1.2 Hz, 1H), 5.24 (dt, *J* = 10.3, 1.2 Hz, 1H), 5.20-5.18 (m, 1H), 1.99-1.97 (t, *J* = 3.3 Hz, 1H) ppm

TLC R_f = 0.2 (10% ethyl acetate/hexanes) [silica gel, UV, $KMnO_4$ stain]

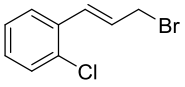

1.121a

(*E*)-1-(3-Bromoprop-1-en-1-yl)-2-chlorobenzene (1.121a). Follows general procedure B: allylic alcohol **1.120a** (2.20 g, 13.0 mmol), hexanes (47 mL), phosphorous tribromide (1.23 mL, 13.0 mmol), hexanes (9 mL). The crude material was purified by silica gel flash column chromatography (3.0 cm column, 5-10% ethyl acetate/hexanes) to yield the title compound as a golden oil (2.30 g, 77% yield). Compound **1.121a** was previously characterized.[56]

Data **1.121a**

^{1}H NMR (400 MHz, $CDCl_3$)

7.59 (d, *J* = 7.3 Hz, 1H), 7.41 (d, *J* = 7.3 Hz, 1H), 7.31-7.23 (m, 2H), 7.09 (d, *J* = 15.6 Hz, 1H), 6.44 (dt, *J* = 15.6, 7.9 Hz, 1H), 4.23 (d, *J* = 7.9 Hz, 2H) ppm

TLC R_f = 0.7 (10% ethyl acetate/hexanes) [silica gel, UV, $KMnO_4$ stain]

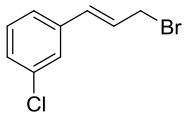

1.121b

(*E*)-1-(3-Bromoprop-1-en-1-yl)-3-chlorobenzene (1.121b). Follows general procedure B: allylic alcohol **1.120b** (1.56 g, 9.28 mmol), hexanes (34 mL), phosphorous tribromide (0.88 mL, 9.28 mmol), hexanes (6 mL). The crude material was purified by silica gel flash column chromatography (2.5 cm column, 5% ethyl acetate/hexanes) to yield the title compound as a yellow oil (1.50 g, 70% yield).

Data **1.121b**

^{1}H NMR (300 MHz, $CDCl_3$)

7.38 (s, 1H), 7.27-7.25 (m, 3H), 6.59 (d, *J* = 15.6 Hz, 1H), 6.41 (dt, *J* = 15.6, 7.6 Hz, 1H), 4.15 (d, *J* = 7.6 Hz, 2H) ppm

TLC R_f = 0.7 (10% ethyl acetate/hexanes) [silica gel, UV, $KMnO_4$ stain]

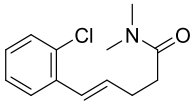

1.122a

(*E*)-5-(2-Chlorophenyl)-*N*,*N*-dimethylpent-4-enamide (1.122a). Follows general procedure C: dimethylacetamide (0.40 mL, 4.30 mmol), THF (14 mL), LDA (2.37 mL, 4.73 mmol), and

cinnamyl bromide **1.121a** (1.48 g, 6.45 mmol, 1.50 equiv). The crude product was purified by silica gel flash column chromatography (25 g silica cartridge, 0-80 % ethyl acetate/hexanes) to yield the title compound as a yellow oil (0.750 g, 73%). ^{1}H NMR spectroscopy showed traces of DCM and ethyl acetate solvents.

Data **1,122a**

^{1}H NMR (300 MHz, $CDCl_3$)

7.51 (dd, *J* = 7.5, 1.8 Hz, 1H), 7.33 (dd, *J* = 7.5, 1.8 Hz, 1H), 7.17 (dt, *J* = 7.5, 1.8 Hz, 2H), 6.81 (d, *J* = 15.8 Hz, 1H), 6.30 (dt, *J* = 15.8, 6.6 Hz, 1H), 3.04 (s, 3H), 2.98 (s, 3H), 2.66-2.49 (m, 4H) ppm

^{13}C NMR (100 MHz, $CDCl_3$)

172.0, 135.5, 132.6 (2C), 132.5, 129.5, 128.1, 126.8, 126.7, 37.2, 35.4, 32.9, 28.6 ppm

IR (thin film)

3059, 3038, 2930, 1653, 1591, 1496, 1143, 753, 694 cm^{-1}

LRMS (TOF MSMS ES+ ASAP)

m/z (%): 238 (100)

HRMS (TOF MS ES+ ASAP)

$[M+H]^+$ calcd for $C_{13}H_{17}NOCl$: 238.0999; found, 238.0997

TLC R_f = 0.2 (70% ethyl acetate/hexanes) [silica gel, UV, $KMnO_4$ stain]

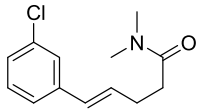

1.122b

(*E*)-5-(3-Chlorophenyl)-*N*,*N*-dimethylpent-4-enamide (1.122b). Follows general procedure C: dimethylacetamide (0.47 mL, 5.05 mmol), THF (16 mL), LDA (2.78 mL, 5.56 mmol), and cinnamyl bromide **1.121b** (1.51 g, 6.57 mmol, 1.30 equiv). The crude product was purified by silica gel flash column chromatography (25 g silica cartridge, 0-80 % ethyl acetate/hexanes) to yield the title compound as a golden oil (0.894 g, 74%).

Data **1.122b**

^{1}H NMR (300 MHz, $CDCl_3$)

7.34 (bs, 1H), 7.27-7.15 (m, 3H), 6.39 (d, J = 16.0 Hz, 1H), 6.26 (dt, J = 16.0, 6.0 Hz, 1H), 3.02 (s, 3H), 2.97 (s, 3H), 2.58-2.45 (m, 4H) ppm

^{13}C NMR (100 MHz, $CDCl_3$)

172.0, 139.4, 134.4, 131.3, 129.7, 129.3, 126.9, 125.9, 124.3, 37.2, 35.4, 32.9, 28.5 ppm

IR (thin film)

3051, 2932, 2902, 1639, 1593, 1142, 752, 735 cm^{-1}

LRMS (TOF MSMS ES+ ASAP)

m/z (%): 238 (100)

HRMS (TOF MS ES+ ASAP)

$[M+H]^+$ calcd for $C_{13}H_{17}NOCl$: 238.0999; found, 238.0995

TLC R_f = 0.2 (70% ethyl acetate/hexanes) [silica gel, UV, $KMnO_4$ stain]

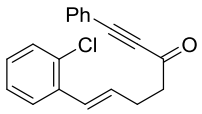

1.123a

(*E*)-7-(2-Chlorophenyl)-1-phenylhept-6-en-1-yn-3-one (1.123a). Follows general procedure D: phenylacetylene (81 μL, 0.74 mmol, 1.2 equiv), THF (2.0 mL), *n*-butyllithium (0.43 mL, 0.68 mmol, 1.1 equiv), amide **1.122a** (0.150 g, 0.63 mmol), THF (2.0 mL), two portions of boron trifluoride diethyl etherate (89 μL, 0.71 mmol, 1.1 equiv), acetic acid (41 μL, 0.71 mmol, 1.1 equiv). The crude product was purified by silica gel flash column chromatography (12 g silica cartridge, 0-10% ethyl acetate/hexanes) to yield the title compound as a light yellow oil (0.148 g, 80%).

Data **1.123a**

^{1}H NMR (300 MHz, $CDCl_3$)

7.61-7.58 (m, 2H), 7.52-7.45 (m, 2H), 7.41 (app d, *J* = 7.7 Hz, 2H), 7.38-7.32 (m, 1H), 7.23-7.13 (m, 2H), 6.86 (d, *J* = 15.6 Hz, 1H), 6.24 (dt, *J* = 15.6, 6.9 Hz, 1H), 2.90 (t, *J* = 7.2 Hz, 2H), 2.71 (q, *J* = 7.2 Hz, 2H) ppm

^{13}C NMR (100 MHz, $CDCl_3$)

186.9, 135.4, 133.1 (2C), 132.7, 131.1, 130.8, 129.6, 128.7 (2C), 128.2, 127.5, 126.8, 126.7, 119.9, 91.3, 87.8, 44.9, 27.6 ppm

IR (thin film)

3062, 2899, 2848, 2200, 1667, 1591, 1489, 755 cm^{-1}

LRMS (TOF MSMS ES+ ASAP)

m/z (%): 294 (73), 293 (98), 259 (100)

HRMS (TOF MS ES+ ASAP)

[M] calcd for $C_{19}H_{15}OCl$: 294.0811; found, 294.0803

TLC R_f = 0.4 (10% ethyl acetate/hexanes) [silica gel, UV, $KMnO_4$ stain]

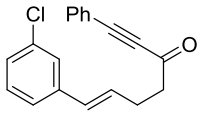

1.123b

(*E*)-7-(3-Chlorophenyl)-1-phenylhept-6-en-1-yn-3-one (1.123b). Follows general procedure D: phenylacetylene (0.12 mL, 1.09 mmol, 1.3 equiv), THF (3.0 mL), *n*-butyllithium (0.63 mL, 1.01 mmol, 1.2 equiv), amide **1.122b** (0.200 g, 0.84 mmol), THF (3.0 mL), two portions of boron trifluoride diethyl etherate (0.13 mL, 1.05 mmol, 1.25 equiv), acetic acid (60 μL, 1.05 mmol, 1.25 equiv). The crude product was purified by silica gel flash column chromatography (3 cm column, 10% ethyl acetate/hexanes) to yield the title compound as a yellow oil (0.239 g, 96%).

Data **1.123b**

^{1}H NMR (300 MHz, $CDCl_3$)

7.61-7.57 (m, 2H), 7.50-7.37 (m, 3H), 7.33 (s, 1H), 7.23-7.16 (m, 3H), 6.42 (d, *J* = 16.0 Hz, 1H), 6.26 (dt, *J* = 16.0, 6.6 Hz, 1H), 2.87 (t, *J* = 7.2 Hz, 2H), 2.66 (app q, *J* = 7.2 Hz, 2H) ppm

^{13}C NMR (100 MHz, $CDCl_3$)

186.7, 139.2, 134.5, 133.1 (2C), 130.8, 130.0, 129.8, 129.7, 128.7 (2C), 127.1, 126.0, 124.3, 119.9, 91.2, 87.8, 44.8, 27.3 ppm

IR (thin film)

3061, 3023, 2923, 2851, 2202, 1668, 1593, 1489, 758, 688 cm^{-1}

LRMS (TOF MSMS ES+ ASAP)

m/z (%): 294 (100), 293 (50), 259 (20)

HRMS (TOF MS ES+ ASAP)

$[M+H]^+$ calcd for $C_{19}H_{16}OCl$: 294.0890; found, 294.0895

TLC R_f = 0.4 (10% ethyl acetate/hexanes) [silica gel, UV, $KMnO_4$ stain]

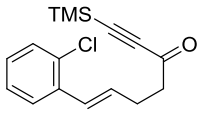

1.124a

(*E*)-7-(2-Chlorophenyl)-1-(trimethylsilyl)hept-6-en-1-yn-3-one (1.124a). Follows general procedure D: trimethylsilylacetylene (0.28 mL, 1.99 mmol, 1.2 equiv), THF (5.4 mL), *n*-butyllithium (1.15 mL, 1.84 mmol, 1.1 equiv), amide **1.122a** (0.400 g, 1.68 mmol), THF (5.4 mL), two portions of boron trifluoride diethyl etherate (0.24 mL, 1.91 mmol, 1.1 equiv), acetic acid (0.11 mL, 1.91 mmol, 1.1 equiv). The crude product was purified by silica gel flash column chromatography (12 g silica cartridge, 0-10% ethyl acetate/hexanes) to yield the title compound as a light yellow oil (0.268 g, 55%).

Data **1.124a**

^{1}H NMR (300 MHz, $CDCl_3$)

7.48 (dd, *J* = 7.5, 1.8 Hz, 1H), 7.34 (dd, *J* = 7.5, 1.8 Hz, 1H), 7.23-7.13 (m, 2H), 6.82 (d, *J* = 15.8 Hz, 1H), 6.19 (dt, *J* = 15.8, 6.8 Hz, 1H), 2.79 (t, *J* = 7.2 Hz, 2H), 2.63 (app q, *J* = 7.2 Hz, 2H), 0.26 (s, 9H) ppm

^{13}C NMR (100 MHz, $CDCl_3$)

187.4, 136.1, 133.4, 131.7, 130.4, 129.0, 128.2, 127.6, 127.5, 102.6, 99.2, 45.4, 28.2, 0.0 (3C) ppm

IR (thin film)

3062, 2961, 2901, 2150, 1677, 1591, 1469, 1252, 847, 751 cm^{-1}

LRMS (TOF MS ES+ ASAP)

m/z (%): 293 (30), 291 (100), 290 (32), 276 (25), 275 (79), 255 (20), 239 (15)

HRMS (TOF MS ES+ ASAP)

$[M+H]^+$ calcd for $C_{16}H_{20}OSiCl$: 291.0972; found, 291.0961

TLC R_f = 0.3 (10% ethyl acetate/hexanes) [silica gel, UV, $KMnO_4$ stain]

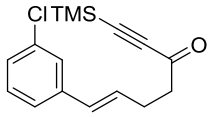

1.124b

(*E*)-7-(3-Chlorophenyl)-1-(trimethylsilyl)hept-6-en-1-yn-3-one (1.124b). Follows general procedure D: trimethylsilylacetylene (0.29 mL, 2.02 mmol, 1.2 equiv), THF (5.6 mL), *n*-butyllithium (1.16 mL, 1.85 mmol, 1.1 equiv), amide **1.122b** (0.400 g, 1.68 mmol), THF (5.6 mL), two portions of boron trifluoride diethyl etherate (0.24 mL, 1.93 mmol, 1.15 equiv), acetic acid (0.11 mL, 1.93 mmol, 1.15 equiv). The crude product was purified by silica gel flash column chromatography 3.0 cm column, 5% ethyl acetate/hexanes) to yield the title compound as a light yellow oil (0.193 g, 40%).

Data **1.124b**

^{1}H NMR (300 MHz, $CDCl_3$)

7.32 (bs, 1H), 7.20-7.16 (m, 3H), 6.38 (d, *J* = 16.0 Hz, 1H), 6.21 (dt, *J* = 16.0, 6.7 Hz, 1H), 2.78 (t, *J* = 6.6 Hz, 2H), 2.58 (app q, *J* = 6.6 Hz, 2H), 0.26 (s, 9H) ppm

^{13}C NMR (100 MHz, $CDCl_3$)

186.8, 139.1, 134.4, 129.9, 129.7, 129.7, 127.1, 126.0, 124.3, 101.8, 98.4, 44.6, 27.1, 0.0 (3C) ppm

IR (thin film)

3055, 3025, 2960, 2901, 2150, 1677, 1252, 846, 762 cm^{-1}

LRMS (TOF MS ES+ ASAP)

m/z (%): 293 (29), 291 (100), 290 (10), 276 (20), 275 (56), 255 (25), 239 (5)

HRMS (TOF MS ES+ ASAP)

$[M+H]^+$ calcd for $C_{16}H_{20}OSiCl$: 291.0972; found, 291.0981

TLC R_f = 0.5 (10% ethyl acetate/hexanes) [silica gel, UV, $KMnO_4$ stain]

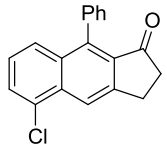

1.138

5-Chloro-9-phenyl-2,3-dihydro-1*H*-cyclopenta[*b*]naphthalen-1-one (1.138). Follows general procedure E: styrene-yne **1.123a** (0.110 g, 0.37 mmol) and *o*-DCB (5.0 mL, 0.07 M). The solution was irradiated at 225 °C for 40 min turning the reaction mixture amber. The reaction mixture was purified directly by silica gel flash column chromatography (2.5 cm column, 0-10% ethyl acetate/hexanes) to yield the title compound as a yellow solid (0.105 g, 96%).

Data **1.138**

MP 210-213 °C

^{1}H NMR (300 MHz, $CDCl_3$)

8.42 (s, 1H), 7.68 (d, *J* = 7.2 Hz, 1H), 7.63 (d, *J* = 8.7 Hz, 1H), 7.53-7.50 (m, 3H), 7.32-7.26 (m, 3H), 3.41-3.36 (m, 2H), 2.79-2.74 (m, 2H) ppm

^{13}C NMR (100 MHz, $CDCl_3$)

205.7, 149.2, 140.2, 135.7, 134.0, 133.5, 131.7, 131.4, 129.7 (2C), 128.4, 128.0 (2C), 127.9, 127.8, 125.5, 121.3, 37.5, 25.1 ppm

IR (thin film)

3060, 3025, 2958, 2924, 1710, 1595, 1483, 1111 cm^{-1}

LRMS (TOF MSMS ES+ ASAP)

m/z (%): 293 (100), 251 (63), 230 (5), 216 (10), 215 (12)

HRMS (TOF MS ES+ ASAP)

$[M+H]^+$ calcd for $C_{19}H_{14}OCl$: 293.0733; found, 293.0728

TLC R_f = 0.2 (10% ethyl acetate/hexanes) [silica gel, UV, $KMnO_4$ stain]

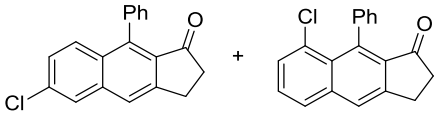

1.140 **1.141**

6-Chloro-9-phenyl-2,3-dihydro-1*H*-cyclopenta[*b*]naphthalen-1-one (1.140) and 8-chloro-9-phenyl-2,3-dihydro-1*H*-cyclopenta[*b*]naphthalen-1-one (1.141). Follows general procedure E: styrene-yne **1.123b** (0.110 g, 0.37 mmol) and *o*-DCB (5.0 mL, 0.07 M). The solution was irradiated at 225 °C for 40 min turning the reaction mixture amber. The reaction mixture was purified directly by silica gel flash column chromatography (25 g silica cartridge, 0-10% ethyl acetate/hexanes) to yield the title compounds as beige solids (combined yield of 0.083 g, 77%).

Data **1.140**

Yield 0.036 g, 33% yield

MP 220-221 °C

^{1}H NMR (400 MHz, C_6D_6)

7.60 (s, 1H), 7.57 (d, *J* = 9.2 Hz, 1H), 7.33-7.29 (m, 2H), 7.27-7.24 (m, 3H), 7.11 (s, 1H), 7.03 (d, *J* = 9.2 Hz, 1H), 2.54-2.50 (m, 2H), 2.20-2.16 (m, 2H) ppm

^{13}C NMR (100 MHz, C_6D_6)

203.5, 149.3, 140.0, 137.5, 136.2, 134.4, 131.6, 130.8 (2C), 130.5 (2C), 130.2, 126.9 (2C), 126.5 (2C), 123.8, 37.2, 24.6 ppm

IR (KBr pellet)

3084, 3038, 2935, 1710, 1616, 1572, 1494 cm^{-1}

LRMS (TOF MSMS ES+ ASAP)

m/z (%): 292 (48), 291 (100), 257 (5), 215 (2)

HRMS (TOF MS ES+ ASAP)

$[M+H]^+$ calcd for $C_{19}H_{14}OCl$: 293.0733; found, 293.0723

TLC R_f = 0.3 (15% ethyl acetate/hexanes) [silica gel, UV, $KMnO_4$ stain]

Data **1.141**

Yield 0.048 g, 44% yield

MP 160-162 °C

^{1}H NMR (300 MHz, $CDCl_3$)

7.94 (s, 1H), 7.82 (dd, *J* = 7.8, 1.9 Hz, 1H), 7.50-7.37 (m, 5H), 7.26-7.23 (m, 2H), 3.30-3.25 (m, 2H), 2.72-2.68 (m, 2H) ppm

^{13}C NMR (100 MHz, $CDCl_3$)

205.2, 148.1, 139.8, 138.9, 138.0, 134.2, 133.0, 130.0, 129.3 (2C), 128.1, 127.9, 127.8, 127.3, 127.2 (2C), 125.9, 37.5, 24.1 ppm

IR (thin film)

3056, 3028, 2928, 2864, 1708, 1612, 1497, 1182 cm^{-1}

LRMS (TOF MSMS ES+ ASAP)

m/z (%): 292 (100), 291 (12), 257 (44)

HRMS (TOF MS ES+ ASAP)

$[M+H]^+$ calcd for $C_{19}H_{14}OCl$: 293.0733; found, 293.0727

TLC R_f = 0.1 (15% ethyl acetate/hexanes) [silica gel, UV, $KMnO_4$ stain]

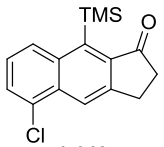

1.142

5-Chloro-9-(trimethylsilyl)-2,3-dihydro-1*H*-cyclopenta[*b*]naphthalen-1-one (1.142). Follows general procedure E: styrene-yne **1.124a** (0.052 g, 0.18 mmol) and *o*-DCB (3.0 mL, 0.06 M). The solution was irradiated at 225 °C for 90 min turning the reaction mixture amber. The reaction mixture was purified directly by silica gel flash column chromatography (2.5 cm column, 0-5% ethyl acetate/hexanes) to yield the title compound as an off-white solid (0.047 g, 91%).

Data **1.142**

MP 128-130 °C

^{1}H NMR (400 MHz, $CDCl_3$)

8.42-8.40 (m, 2H), 7.65 (d, *J* = 7.8 Hz, 1H), 7.37 (t, *J* = 7.8 Hz, 1H), 3.37-3.34 (m, 2H), 2.81-2.78 (m, 2H), 0.55 (s, 9H) ppm

^{13}C NMR (100 MHz, $CDCl_3$)

207.9, 148.7, 143.3, 142.4, 138.5, 133.3, 132.0, 130.1, 127.9, 124.7, 123.1, 36.9, 25.5, 3.1 (3C) ppm

IR (thin film)

3089, 2966, 2939, 2889, 1714, 1591, 1487, 1249, 1240 cm^{-1}

LRMS (TOF MS ES+ ASAP)

m/z (%): 289 (22), 275 (28), 273 (100)

HRMS (TOF MS ES+ ASAP)

$[M+H]^+$ calcd for $C_{16}H_{18}OSiCl$: 289.0815; found, 289.0791

TLC R_f = 0.6 (10% ethyl acetate/hexanes) [silica gel, UV, $KMnO_4$ stain]

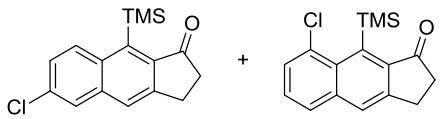

1.144 1.145

6-Chloro-9-(trimethylsilyl)-2,3-dihydro-1*H*-cyclopenta[*b*]naphthalen-1-one (1.144) and 8-chloro-9-(trimethylsilyl)-2,3-dihydro-1*H*-cyclopenta[*b*]naphthalen-1-one (1.145). Follows general procedure E: styrene-yne **1.124b** (0.073 g, 0.25 mmol) and *o*-DCB (4.2 mL, 0.06 M). The solution was irradiated at 225 °C for 90 min turning the reaction mixture brown. The reaction mixture was concentrated under high vacuum, and the crude products were separated by silica gel flash column chromatography (12 g silica cartridge, 0-10% ethyl acetate/hexanes) to yield the title compounds as white solids (combined yield of 0.057 g, 79%).

Data **1.144**

Yield 0.033 g, 46% yield

MP 125-128 °C

^{1}H NMR (300 MHz, $CDCl_3$)

8.42 (d, *J* = 9.2 Hz, 1H), 7.82 (d, *J* = 2.2 Hz, 1H), 7.79 (s, 1H), 7.40 (dd, *J* = 9.2, 2.2 Hz, 1H), 3.32-3.28 (m, 2H), 2.80-2.75 (m, 2H), 0.54 (s, 9H) ppm

^{13}C NMR (100 MHz, $CDCl_3$)

207.6, 148.6, 142.8, 141.8, 136.7, 135.5, 133.5, 132.2, 126.9, 126.0, 125.6, 36.8, 25.2, 2.94 (3C) ppm

IR (thin film)

2966, 2943, 2884, 1706, 1607, 1485, 1249, 1241 cm^{-1}

LRMS (TOF MSMS ES+ ASAP)

m/z (%): 273 (100), 243 (18), 229 (25), 199 (48)

HRMS (TOF MS ES+ ASAP)

[M-CH_3] calcd for $C_{15}H_{14}OSiCl$: 273.0502; found, 273.0498

TLC R_f = 0.4 (10% ethyl acetate/hexanes) [silica gel, UV, $KMnO_4$ stain]

Data **1.145**

Yield 0.024 g, 33% yield

MP 145-147 °C

^{1}H NMR (300 MHz, $CDCl_3$)

7.78 (s, 1H), 7.73 (d, *J* = 8.1 Hz, 1H), 7.55 (d, *J* = 7.2 Hz, 1H), 7.42 (app t, *J* = 8.1 Hz, 1H), 3.31-3.26 (m, 2H), 2.81-2.76 (m, 2H), 0.44 (s, 9H) ppm

^{13}C NMR (100 MHz, $CDCl_3$)

207.9, 146.8, 145.3, 144.1, 137.5, 136.8, 135.3, 127.4, 127.3, 127.3, 126.4, 37.0, 25.2, 2.96 (3C) ppm

IR (thin film)

2953, 2941, 2913, 1707, 1601, 1479, 1250, 1239 cm^{-1}

LRMS (TOF MSMS ES+ ASAP)

m/z (%): 273 (51), 257 (23), 231 (100), 199 (31)

HRMS (TOF MS ES+ ASAP)

[M-Me] calcd for $C_{15}H_{14}OSiCl$: 273.0502; found, 273.0476

TLC R_f = 0.3 (10% ethyl acetate/hexanes) [silica gel, UV, $KMnO_4$ stain]

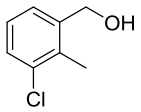

1.153

(3-Chloro-2-methylphenyl)methanol (1.153). To a flame-dried two-neck 25 mL round-bottomed flask equipped with an argon inlet adapter, a septum, and a stir bar was added lithium aluminum hydride (0.178 g, 4.69 mmol). The round-bottomed flask was evacuated and refilled with argon (3x). THF (6 mL) was added slowly via syringe with stirring, and the suspension was cooled to 0 °C in an ice bath. 3-Chloro-2-methylbenzoic acid (**1.152**) (0.200 g, 1.17 mmol) in THF (6 mL) was then added slowly dropwise via syringe. The reaction mixture was warmed to rt and stirred for 1 h, followed by cooling once again to 0 °C in an ice bath and quenching slowly dropwise with water. The aqueous layer was separated and extracted with Et_2O (2x). The combined organic layers were washed with water, dried over magnesium sulfate, gravity filtered, and concentrated under reduced pressure to yield the title compound as an off-white solid (0.175 g, 96%). The crude product was carried on without further purification. Compound **1.153** was previously characterized.[57]

Data **1.153**

^{1}H NMR (300 MHz, $CDCl_3$)

7.33-7.26 (m, 2H), 7.13 (t, J = 7.8 Hz, 1H), 4.72 (d, J = 5.4 Hz, 2H), 2.39 (s, 3H), 1.58 (t, J = 5.4 Hz, 1H) ppm

TLC R_f = 0.2 (10% ethyl acetate/hexanes) [silica gel, UV]

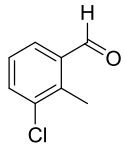

1.154

3-Chloro-2-methylbenzaldehyde (1.154). To a one-neck 50 mL round-bottomed flask equipped with a septum pierced with a needle and a stir bar was added pyridinium chlorochromate (3.51 g, 16.3 mmol) and DCM (30 mL) with stirring. Alcohol **1.153** (1.67 g, 10.7 mmol) in minimal DCM was added all at once via syringe, and the reaction turned dark brown and thick. The reaction mixture was stirred at rt for 4 h until complete by TLC, followed by addition of diethyl ether and silica gel. The suspension was stirred for 30 min, filtered through a pad of silica gel with diethyl ether washings, and then concentrated under reduced pressure to yield the title compound as a yellow oil (1.50 g, 91%). The crude product was carried on without further purification. Compound **1.154** was previously characterized.[57]

Data **1.154**

^{1}H NMR (300 MHz, $CDCl_3$)

10.28 (s, 1H), 7.72 (dd, J = 7.8, 1.2 Hz, 1H), 7.60 (dd, J = 7.8, 1.2 Hz, 1H), 7.31 (t, J = 7.8 Hz, 1H), 2.72 (s, 3H) ppm

TLC R_f = 0.5 (10% ethyl acetate/hexanes) [silica gel, UV]

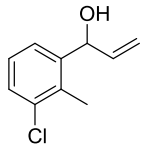

1.155

1-(3-Chloro-2-methylphenyl)prop-2-en-1-ol (1.155). Follows general procedure A: aldehyde **1.154** (1.45 g, 9.38 mmol), THF (16 mL), and vinylmagnesium bromide (11.3 mL, 11.3 mmol).

The title compound was an orange oil (1.71 g, quant.). The crude material was carried on without further purification.

Data **1.155**

^{1}H NMR (300 MHz, $CDCl_3$)

7.38 (d, *J* = 7.8 Hz, 1H), 7.31 (dd, *J* = 7.8, 1.2 Hz, 1H), 7.15 (t, *J* = 7.8 Hz, 1H), 6.01 (ddd, *J* = 16.2, 10.5, 5.7 Hz, 1H), 5.45-5.42 (m, 1H), 5.30 (dt, *J* = 17.1, 1.2 Hz, 1H), 5.23 (dt, *J* = 10.5, 1.2 Hz, 1H), 2.39 (s, 3H), 1.94 (bs, 1H) ppm

^{13}C NMR (100 MHz, $CDCl_3$)

142.5, 139.1, 135.2, 133.5, 128.6, 127.0, 124.6, 115.9, 72.4, 15.7 ppm

IR (thin film)

3364, 3415, 2923, 1638, 1569, 1443, 784, 728 cm^{-1}

HRMS (TOF MS ES+)

$[M\text{-}OH]^+$ calcd for $C_{10}H_{10}Cl$, 165.0471; found, 165.0478

TLC R_f = 0.2 (10% ethyl acetate/hexanes) [silica gel, UV]

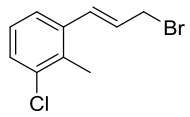

1.156

(*E*)-1-(3-Bromoprop-1-en-1-yl)-3-chloro-2-methylbenzene (1.156). Follows general procedure B: allylic alcohol **1.155** (1.75 g, 9.58 mmol), hexanes (35 mL), phosphorous tribromide (0.90 mL, 9.58 mmol), and hexanes (6 mL). The title compound was an orange sticky solid (1.55 g, 66%).

Data **1.156**

^{1}H NMR (300 MHz, $CDCl_3$)

7.33-7.28 (m, 2H), 7.10 (t, *J* = 8.1 Hz, 1H), 6.88 (d, *J* = 15.3 Hz, 1H), 6.25 (dt, *J* = 15.3, 7.8 Hz, 1H), 4.16 (dd, *J* = 7.8, 0.9 Hz, 2H), 2.40 (s, 3H) ppm

^{13}C NMR (100 MHz, $CDCl_3$)

137.3, 135.2, 133.8, 132.3, 129.0, 128.3, 126.8, 125.0, 33.1, 16.3 ppm

IR (thin film)

3041, 2925, 1642, 1563, 1456, 1434, 1202, 963, 778 cm^{-1}

HRMS (TOF MS ES+)

$[M\text{-}Br]^+$ calcd for $C_{10}H_{10}Cl$, 165.0471; found, 165.0475

TLC R_f = 0.7 (10% ethyl acetate/hexanes) [silica gel, UV]

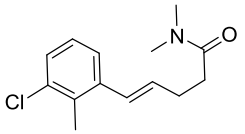

1.157

(*E*)-5-(3-Chloro-2-methylphenyl)-*N*,*N*-dimethylpent-4-enamide (1.157). Follows general procedure C: dimethylacetamide (0.45 mL, 4.84 mmol), THF (17 mL), LDA (2.68 mL, 5.35 mmol), cinnamyl bromide **1.156** (1.55 g, 6.31 mmol). The crude product was purified by silica gel flash column chromatography (5.0 cm column, 65-100% ethyl acetate/hexanes) to yield the title compound as a yellow oil (1.04 g, 85%).

Data **1.157**

^{1}H NMR (300 MHz, $CDCl_3$)

7.28-7.22 (m, 2H), 7.05 (t, *J* = 7.8 Hz, 1H), 6.64 (d, *J* = 15.3 Hz, 1H), 6.10 (dt, *J* = 15.3, 6.6 Hz, 1H), 3.03 (s, 3H), 2.97 (s, 3H), 2.58 (q, *J* = 6.9 Hz, 2H), 2.49 (t, *J* = 6.9 Hz, 2H), 2.36 (s, 3H) ppm

^{13}C NMR (100 MHz, $CDCl_3$)

172.1, 139.1, 134.8, 132.9, 132.6, 128.6, 127.8, 126.6, 124.6, 37.3, 35.5, 33.1, 28.8, 16.2 ppm

IR (thin film)

3062, 2928, 1649, 1562, 1495, 1138, 778, 711 cm^{-1}

HRMS (TOF MS ES+)

$[M+H]^+$ calcd for $C_{14}H_{19}NOCl$, 252.1155; found, 252.1164

TLC R_f = 0.3 (65% ethyl acetate/hexanes) [silica gel, UV]

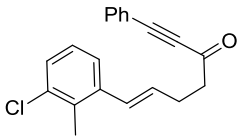

1.158a

(*E*)-7-(3-Chloro-2-methylphenyl)-1-phenylhept-6-en-1-yn-3-one (1.158a). Follows general procedure D: phenylacetylene (0.12 mL, 1.09 mmol), THF (3 mL), *n*-butyllithium (0.63 mL, 1.01 mmol), amide **1.157** (0.200 g, 0.79 mmol), THF (3 mL), two portions of boron trifluoride diethyl etherate (0.13 mL, 1.05 mmol), and acetic acid (60 μL, 1.05 mmol). The crude material was purified by silica gel flash column chromatography (1.5 cm column, 5-10% ethyl acetate/hexanes) to yield the title compound as a yellow oil (0.175 g, 72%).

Data **1.1.158a**

^{1}H NMR (300 MHz, $CDCl_3$)

7.58 (d, *J* = 6.6 Hz, 2H), 7.47-7.36 (m, 3H), 7.26-7.23 (m, 2H), 7.05 (t, *J* = 7.5 Hz, 1H), 6.67 (d, *J* = 15.0 Hz, 1H), 6.06 (dt, *J* = 15.0, 7.2 Hz, 1H), 2.88 (t, *J* = 7.2 Hz, 2H), 2.68 (app q, *J* = 7.2 Hz, 2H), 2.36 (s, 3H) ppm

TLC R_f = 0.5 (10% ethyl acetate/hexanes) [silica gel, UV]

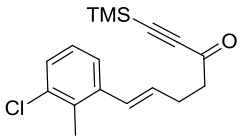

1.158b

***(E)*-7-(3-Chloro-2-methylphenyl)-1-(trimethylsilyl)hept-6-en-1-yn-3-one (1.158b)**. Follows general procedure D: trimethysilylacetylene (0.23 mL, 1.64 mmol), THF (5 mL), *n*-butyllithium (0.94 mL, 1.51 mmol), amide **1.157** (0.300 g, 1.26 mmol), THF (5 mL), two portions of boron trifluoride diethyl etherate (0.20 mL, 1.58 mmol), and acetic acid (90 μL, 1.58 mmol). The crude material was purified by silica gel flash column chromatography (1.5 cm column, 3% ethyl acetate/hexanes) to yield the title compound as a yellow oil (0.180 g, 47%).

Data **1.1.158b**

^{1}H NMR (400 MHz, $CDCl_3$)

7.25 (d, *J* = 7.8 Hz, 2H), 7.06 (t, *J* = 7.8 Hz, 1H), 6.64 (d, *J* = 15.6 Hz, 1H), 6.01 (dt, *J* = 15.6, 6.9 Hz, 1H), 2.76 (t, *J* = 6.3 Hz, 2H), 2.59 (dt, *J* = 6.9, 5.4 Hz, 2H), 2.36 (s, 3H), 0.25 (s, 9H) ppm

^{13}C NMR (100 MHz, $CDCl_3$)

186.8, 139.0, 134.9, 133.1, 131.2, 129.4, 128.0, 126.7, 124.7, 102.0, 98.4, 44.8, 27.5, 16.3, -0.7 (3C) ppm

IR (thin film)

3034, 2961, 2151, 2093, 1679, 1591, 1436, 1252, 1113, 847, 763 cm^{-1}

HRMS (TOF MS ES+)

[M] calcd for $C_{17}H_{21}OSiCl$, 304.1050; found, 304.1060

TLC R_f = 0.5 (10% ethyl acetate/hexanes) [silica gel, UV]

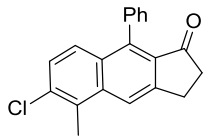

1.159a

6-Chloro-5-methyl-9-phenyl-2,3-dihydro-1*H*-cyclopenta[*b*]naphthalen-1-one (1.159a). Follows general procedure E: styrene-yne **1.158a** (0.050 g, 0.16 mmol) and *o*-DCB (2.7 mL, 0.06 M). The solution was irradiated at 225 °C for 45 min. The reaction mixture was concentrated under high vacuum and purified by silica gel flash column chromatography (1.5 cm column, 10% ethyl acetate/hexanes) to yield the title compound as a white solid (0.043 g, 86%).

Data **1.1.159b**

MP 219-220 °C

^{1}H NMR (300 MHz, CD_2Cl_2)

8.14 (s, 1H), 7.51-7.48 (m, 3H), 7.45 (d, J = 9.1 Hz, 1H), 7.33 (d, J = 9.1 Hz, 1H), 7.28-7.25 (m, 2H), 3.37-3.33 (m, 2H), 2.82 (s, 3H), 2.74-2.69 (m, 2H) ppm

^{13}C NMR (100 MHz, $CDCl_3$)

205.8, 149.4, 140.4, 137.0, 136.1, 134.4, 130.9, 130.8, 130.7, 129.8 (2C), 128.1 (2C), 128.0, 127.8, 127.4, 121.1, 37.6, 25.2, 16.2 ppm

IR (thin film)

3062, 2923, 1713, 1609, 1444, 1239, 699 cm^{-1}

HRMS (TOF MS ES+)

$[M+H]^+$ calcd for $C_{20}H_{16}OCl$, 307.0890; found, 307.0896

TLC R_f = 0.2 (10% ethyl acetate/hexanes) [silica gel, UV]

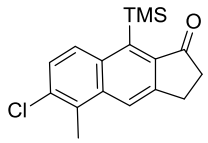

1.159b

6-Chloro-5-methyl-9-(trimethylsilyl)-2,3-dihydro-1*H*-cyclopenta[*b*]naphthalen-1-one (1.159b). Follows general procedure E: styrene-yne **1.158b** (0.085 g, 0.28 mmol) and *o*-DCB (4.6 mL, 0.06 M). The solution was irradiated at 225 °C for 60 min turning the reaction mixture yellow. The reaction mixture was concentrated under high vacuum and purified by silica gel flash column chromatography (1.5 cm column, 5% ethyl acetate/hexanes) to yield the title compound as a light yellow solid (0.077 g, 92%).

Data **1.1.159b**

MP 178-181 °C

^{1}H NMR (300 MHz, $CDCl_3$)

8.24 (d, J = 9.3 Hz, 1H), 8.07 (d, J = 0.9 Hz, 1H), 7.41 (d, J = 9.3 Hz, 1H), 3.35-3.30 (m, 2H), 2.80-2.75 (m, 5H), 0.52 (s, 9H) ppm

^{13}C NMR (100 MHz, $CDCl_3$)

208.0, 140.9, 143.5, 141.4, 136.4, 136.2, 133.7, 131.1, 130.2, 126.5, 122.9, 37.1, 25.7, 16.3, 3.2 (3C) ppm

IR (thin film)

2923, 1710, 1603, 1249, 870, 852 cm^{-1}

HRMS (ESI)

$[M+H]^+$ calcd for $C_{17}H_{20}OClSi$, 303.0972; found, 303.0957

TLC R_f = 0.4 (10% ethyl acetate/hexanes) [silica gel, UV]

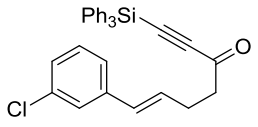

1.160

(*E*)-7-(3-Chlorophenyl)-1-(triphenylsilyl)hept-6-en-1-yn-3-one (1.160). Follows general procedure D: triphenylsilylacetylene (0.478 g, 1.68 mmol, 4.0 equiv), THF (4.2 mL), *n*-butyllithium (0.92 mL, 1.47 mmol, 3.5 equiv), amide **1.122b** (0.100 g, 0.42 mmol), THF (1.4 mL), two portions of boron trifluoride diethyl etherate (67 μL, 0.53 mmol, 1.25 equiv), and acetic acid (30 μL, 0.53 mmol, 1.25 equiv). The crude product was purified by silica gel flash column chromatography 1.5 cm column, 2-4% ethyl acetate/hexanes) to yield the title compound as a clear oil (0.124 g, 62%). The product was contaminated with a small amount of triphenylsilylacetylene that was carried through the subsequent cyclization step and removed by purification of the cyclized product.

Data **1.160**

^{1}H NMR (300 MHz, $CDCl_3$)

7.68-7.61 (m, 6H), 7.50-7.37 (m, 9H), 7.28-7.26 (m, 1H), 7.20-7.16 (m, 3H), 6.35 (d, J = 16.2 Hz, 1H), 6.19 (dt, J = 16.2, 6.6 Hz, 1H), 2.84 (t, J = 7.0 Hz, 2H), 2.58 (app q, J = 7.0 Hz, 2H) ppm

TLC R_f = 0.5 (10% ethyl acetate/hexanes) [silica gel, UV, $KMnO_4$ stain]

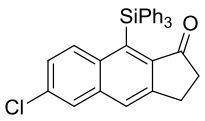

1.161

6-Chloro-9-(triphenylsilyl)-2,3-dihydro-1*H*-cyclopenta[*b*]naphthalen-1-one (1.161) Follows general procedure E: styrene-yne **1.160** (0.083 g, 0.17 mmol) and *o*-DCB (3.5 mL, 0.05 M). The

solution was irradiated at 225 °C for 110 min turning the reaction mixture brown. The reaction mixture was concentrated under high vacuum, and the crude material was purified by silica gel flash column chromatography (1.5 cm column, 2-5% ethyl acetate/hexanes) to yield the title compound as a white solid (0.054 g, 67%).

Data **1.161**

MP 225-226 °C

^{1}H NMR (600 MHz, $CDCl_3$)

7.93 (s, 1H), 7.84-7.81 (m, 2H), 7.58 (d, *J* = 7.2 Hz, 6H), 7.35 (t, *J* = 7.2 Hz, 3H), 7.30 (t, *J* = 7.2 Hz, 6H), 6.93 (dd, *J* = 9.0, 1.8 Hz, 1H), 3.31-3.28 (m, 2H), 2.51-2.49 (m, 2H) ppm

^{13}C NMR (150 MHz, $CDCl_3$)

205.7, 148.3, 143.9, 137.3, 137.0 (3C), 136.7, 135.6, 135.5 (6C), 133.8, 133.3, 129.1 (3C), 127.9 (6C), 127.3, 127.0, 126.2, 36.5, 25.5 ppm

IR (thin film)

3068, 3049, 2924, 2854, 2247, 1714, 1607, 1485, 732, 700 cm^{-1}

LRMS (TOF MSMS ES+ ASAP)

m/z (%): 217 (10), 397 (100), 399 (75)

HRMS (TOF MS ES+ ASAP)

$[M-H]^+$ calcd for $C_{31}H_{22}OSiCl$: 473.1128; found, 473.1119

TLC R_f = 0.3 (10% ethyl acetate/hexanes) [silica gel, UV, $KMnO_4$ stain]

2.0 MECHANISTIC INVESTIGATION OF THE DEHYDROGENATIVE DEHYDRO-DIELS-ALDER REACTION

2.1 INTRODUCTION

The importance of functionalized naphthalenes as key structural components for various material, chemical, and biological applications has led to a need in the synthetic community for new methods to access naphthalene derivatives; a sampling of the applications of naphthalenes as natural products, drugs, and fluorescent dyes are shown in Figures 1.1, 1.2, and 1.3. As mentioned previously, this need has been partially met by classical methods of naphthalene synthesis, such as electrophilic aromatic substitution[58] and transition metal-catalyzed cross-coupling reactions;[59] however, the former suffers from regiocontrol issues,[60] and both are limited by precursor availability. A more versatile approach involves a *de novo* construction of naphthalenes from benzene precursors by benzannulation strategies,[10,61] representative examples of which are shown in Scheme 1.1.

We have developed a DDDA reaction of styrenes that complements other benzannulation strategies, and allows for the formation of a unique class of functionalized cyclopenta[*b*]naphthalene substrates in high yields and short reaction times (see Chapter 1.3). The selectivity of our reaction for the naphthalene product, rather than dihydronaphthalene, exceeds the selectivity observed in many previous examples, as thermal reactions of styrene-ynes

often primarily lead to generation of the dihydronaphthalene product.[20,40b,41,43,62] For example, refluxing of the cinnamyl arylpropiolate ester **2.1** in acetic anhydride provided only γ-apopicropodophyllin (**2.2**) in 48% yield (Scheme 2.1, A).[40a] Selectivity for the dihydronaphthalene product was also observed in the formation of heterocycles, where microwave irradiation of **2.3** in toluene at 150 °C for 2.5 h produced 99% yield of dihydronaphthalene **2.4** (Scheme 2.1, B).[63]

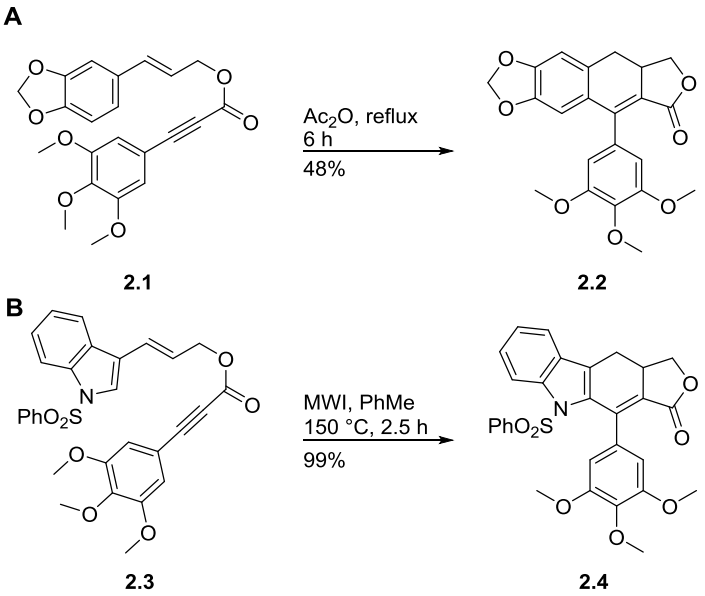

Scheme 2.1. Previous DDA reactions of styrenes to produce dihydronaphthalene compounds

While our DDDA reaction of styrene-ynes selectively provided naphthalene compounds upon irradiation of precursors containing all carbon tethers, the reaction was not as successful for precursors in which the tether contained heteroatoms (Scheme 2.2). In fact, the dihydronaphthalene **1.147** was observed as the major product in a 1.9:1 ratio with naphthalene

1.146 upon heating of **1.132a** at 180 °C in DCE.[64] Mixtures of naphthalene and dihydronaphthalene products are not uncommon in DDDA reactions of styrene-ynes that have heteroatom-containing tethers (as depicted in Scheme 1.16, C and D),[44-45] and a similar example to that reported by our group was also published by Matsubara et al.[47] In Matsubara's example, the alkynyl terminus of the styrene-yne **2.6** was substituted with an ethyl ester, rather than a methyl ketone, and upon heating at 160 °C for 96 h in xylenes a 1:1.7 ratio of products **2.7**:**2.8** was obtained, which was comparable to our results. Attempts by other research groups,[45] as well as our own,[64] to oxidize these product mixtures to naphthalenes were unsuccessful, often leading to decomposition of the mixture and limiting the synthetic utility of the reaction.

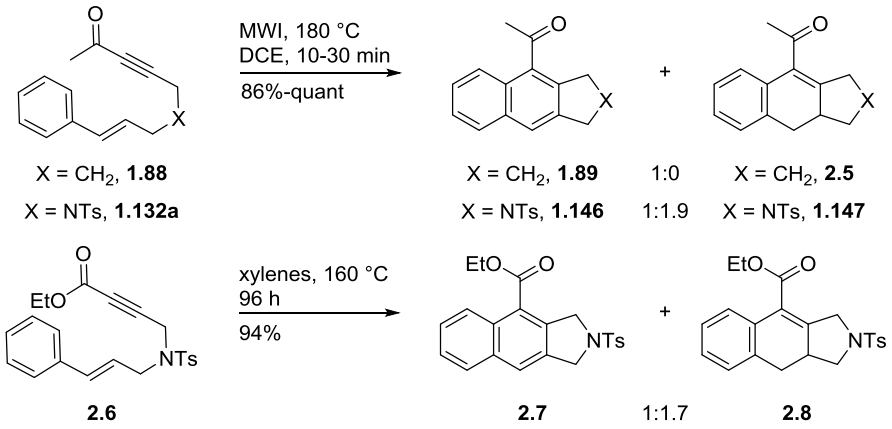

Scheme 2.2. DDDA reactions showing effect of precursor on product selectivity obtained

Despite the numerous reports of DDA reactions to produce dihydronaphthalene substrates, and the less common examples of DDDA reactions to generate mixtures of naphthalene and dihydronaphthalene compounds,[44-45] or naphthalene products exclusively

(Scheme 1.17),[46-47] little has been done to understand the mechanism of formation of these products. Previous reports either allude to naphthalene formation in the DDDA reaction arising from an oxidation of the dihydronaphthalene product via adventitious air,[44] or no explanation is provided. The reactions performed in our own laboratory where the type of styrene-yne tether dictates the selectivity of the DDDA reaction suggest that the process by which these two products are generated may be more complicated than previously presumed (Scheme 2.2). Given the importance of naphthalene and dihydronaphthalene compounds as synthetic targets, a reconsideration of the DDA and DDDA reactions as general methods for preparing these classes of compounds is warranted. Our first step toward increasing the synthetic utility of these reactions involved acquiring a deeper understanding of the mechanism of our DDDA reaction.

2.2 RESULTS AND DISCUSSION

2.2.1 Varying the DDDA reaction conditions

In order to learn more about the mechanism of the DDDA reaction, we were initially interested in testing a variety of reaction conditions to see how different factors would affect the product selectivity of the reaction. The primary conditions that we chose to alter were reaction time, temperature, concentration, atmosphere, and solvent. By making these modifications to the environment of the DDDA reaction, we were optimistic that we could not only begin to gain an understanding of the mechanisms of formation of both the dihydronaphthalene and products based on changes in product selectivity observed, but also start to control the selectivity of the reaction toward either product.

Reaction Time. As previously demonstrated, irradiation of styrene-yne **1.132a** at 180 °C in 1,2-dichloroethane (DCE) for 10 min resulted in a mixture of 30% naphthalene **1.146** and 56% dihydronaphthalene **1.147** (Scheme 2.2).[64] Subjecting **1.132a** to prolonged irradiation for 1 h in a separate experiment increased the ratio of **1.146**:**1.147** from 1:1.9 to 4.8:1; however, the yield of naphthalene **1.146** increased only marginally from 30 to 38%, while the yield of the dihydronaphthalene **1.147** decreased from 56 to 8% (entries 1 and 2, Table 2.1). The disappearance of dihydronaphthalene **1.147** upon longer reaction times without a proportionate increase in the yield of naphthalene **1.146** indicated that **1.147** was decomposing rather than converting to naphthalene **1.146**. This same trend was also observed when the reaction was heated at 120 °C over 45 min in *o*-dichlorobenzene-d_4 (*o*-DCB-d_4). For example, irradiating styrene-yne **1.132a** for 15 min yielded 7% **1.146** and 53% **1.147**, along with 34% remaining starting material; these yields were determined by ^{1}H NMR spectroscopy using *p*-dimethoxybenzene as an internal standard (entry 3). Continued irradiation of the sample for 30 min (45 min total) led to complete conversion of the starting material; however, the quantity of naphthalene **1.146** only slightly increased, whereas the amount of dihydronaphthalene **1.147** decreased (entry 5). This once again signified that dihydronaphthalene **1.147** was decomposing and was not converted to naphthalene **1.146** with longer reaction times. It should be noted that performing the DDDA reaction of **1.132a** using conventional heating at 180 °C with an oil bath, rather than microwave irradiation, did not significantly alter the reaction time, yield, or ratio of **1.146** and **1.147** (see Experimental, section 2.4.5).

Table 2.1. DDDA conditions and resulting naphthalene and dihydronaphthalene ratios

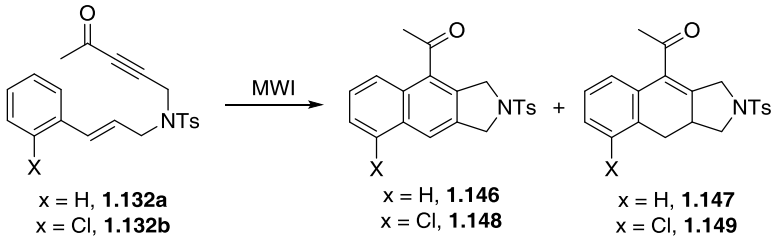

x = H, **1.132a**
x = Cl, **1.132b**

x = H, **1.146**
x = Cl, **1.148**

x = H, **1.147**
x = Cl, **1.149**

entry	conditions	**1.132a**[a] (%)	**1.146** (%)	**1.147** (%)	total yield (%)	**1.146**:**1.147**[b]
1	DCE (0.06 M), 180 °C, 10 min[c]	-	30[d]	56	86	1:1.9
2	DCE (0.06 M), 180 °C, 60 min[e]	-	38[d]	8	46	4.8:1
3	*o*-DCB-d_4 (0.06 M), 120 °C, 15 min[e]	34	7	53	94[f]	1:7.6
4	*o*-DCB-d_4 (0.06 M), 120 °C, 30 min[e]	10	11	52	73[f]	1:4.7
5	*o*-DCB-d_4 (0.06 M), 120 °C, 45 min[e]	-	13	44	57[f]	1:3.4
6	*o*-DCB-d_4 (0.06 M), 180 °C, 1 min[e]	-	36	45	81[f]	1:1.3
7	*o*-DCB-d_4 (0.06 M), 225 °C, 1 min[c]	-	48[d]	33	81[f]	1.5:1
8	*o*-DCB (0.06 M), 180 °C, 10 min[c,g]	-	24[d]	48	72	1:2
9	*o*-DCB (0.06 M), 225 °C, 10 min[c,g]	-	59[d]	6	65	9.8:1
10	*o*-DCB-d_4 (0.12 M), 180 °C, 1 min[e]	-	27	57	84[f]	1:2.1
11	*o*-DCB-d_4 (0.50 M), 180 °C, 1 min[e]	-	16	60	76[f]	1:3.8
12	DCE (0.06 M), 180 °C, 2 min[c]	-	-	-	-	1:1.9
13	DCE (0.06 M), 180 °C, 2 min, Ar[c]	-	-	-	-	1:1.9

[a]Percent unreacted starting material; [b]product ratios determined by ^{1}H NMR spectroscopy; [c]reactions were performed in a Biotage Initiator microwave reactor; [d]products were isolated as a mixture, and individual product yields were approximated based on the ratio of products as determined by ^{1}H NMR spectroscopy; [e]reactions were performed in an Anton-Paar Monowave 300 microwave reactor; [f]yields were determined by ^{1}H NMR spectroscopy using *p*-dimethoxybenzene as an internal standard; [g]styrene-yne **1.132b** was used to give products **1.148** and **1.149**.

Reaction Temperature. Changing the reaction temperature of the DDDA reaction considerably altered the ratio of naphthalene to dihydronaphthalene products. Heating styrene-yne **1.132a** at 120 °C in *o*-DCB-d_4 for 15 min resulted in a 1:7.6 ratio of **1.146**:**1.147**, while

raising the reaction temperature to 180 °C afforded a 1:1.3 product ratio of naphthalene **1.146** to dihydronaphthalene **1.147** (compare entries 3 and 6, Table 2.1). When the reaction was heated at 225 °C for 1 min, naphthalene **1.146** was formed as the major product in a 1.5:1 ratio with dihydronaphthalene **1.147** (entry 7). More dramatic results were obtained for heating of chloro-substituted styrene-yne **1.132b**. Performing the DDDA reaction at 180 °C generated a 1:2 mixture of **1.148**:**1.149**, whereas increasing the reaction temperature to 225 °C produced naphthalene **1.148** in an approximate 10:1 ratio with dihydronaphthalene **1.149**, significantly shifting the selectivity of the DDDA reaction in favor of naphthalene formation (entries 8 and 9).

Concentration Effect. Increasing the concentration of the DDDA reaction from 0.06 to 0.12 M resulted in a near doubling of the amount of dihydronaphthalene **1.147** produced, which changed the product ratio of **1.146**:**1.147** from 1:1.3 to 1:2.1 (compare entries 6 and 10, Table 2.1). Concentration of the reaction mixture to 0.50 M further increased the ratio of **1.146** to **1.147**, yielding a 1:3.8 mixture of naphthalene and dihydronaphthalene products (entry 11). Thus, more concentrated reaction conditions afforded more of the dihydronaphthalene substrate.

Atmosphere. Heating styrene-yne **1.132a** at 180 °C in DCE either under air or after degassing the reaction mixture with argon both generated a 1:1.9 mixture of naphthalene **1.146** to dihydronaphthalene **1.147** in as little as 2 min (entries 12 and 13, Table 2.1). While these conditions did not ensure rigorous exclusion of oxygen, this experiment suggests that performing the reaction in the presence or absence of oxygen had no effect on the product selectivity.

Solvent Studies. In order to test the effect of solvent on the DDDA reaction, the reaction was carried out at a constant temperature of 180 °C in solvents of increasing dielectric constant ranging from *o*-DCB (ε = 9.93) to water (ε = 80.1). Regardless of the solvent employed, each reaction was complete within 1 min. The dielectric constant of the solvent also had only a

moderate effect on the selectivity of the reaction, with product ratios of **1.146**:**1.147** ranging from 1:1 to 1:4 (entries 1-4, Table 2.2). However, when nitrobenzene ($PhNO_2$) and *N*,*N*-dimethylformamide (DMF) were utilized as solvents, greater selectivity in the DDDA reaction was observed. Performing the DDDA reaction in $PhNO_2$ generated exclusively naphthalene **1.146** in 84% yield (entry 7). Alternatively, heating of styrene-yne **1.132a** in DMF resulted in a 70% yield of a mixture of dihydronaphthalene **1.147** and naphthalene **1.146**, where **1.147** was now the major product by a >10:1 ratio (entry 8). Small amounts of unidentified byproducts as determined by ^{1}H NMR spectroscopy were also formed along with **1.146** and **1.147** under the DMF reaction conditions. By simply employing $PhNO_2$ or DMF as the reaction solvent, we have shown that selective formation of the naphthalene or dihydronaphthalene products can be obtained in high yields for the DDDA or DDA reactions, respectively, thus enhancing the synthetic utility of these reactions. It should be noted that DMF has previously been used as a solvent for DDA reactions of cinnamyl arylpropiolate esters and *N*-(cinnamyl)cinnamamides, which formed dihydronaphthalene lactones exclusively; however, no explanation was provided for the selectivity observed.[43,62b,65]

Table 2.2. Effect of solvent on the product selectivity obtained in the DDDA reaction

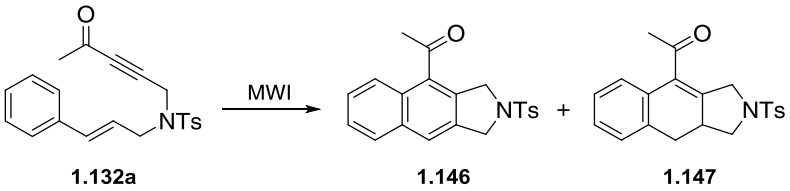

1.132a **1.146** **1.147**

entry[a]	solvent (tan δ)	dielectric constant	**1.146**:**1.147**[b]
1	*o*-DCB (0.28)	9.93	1:1.2
2	DCE (0.127)	10.36	1:1.8
3	MEK (0.079)	18.50	1:2.6
4	*i*PrOH (0.799)	20.18	1:4.4
5	$EtNO_2$ (0.064)[c]	28.06	1:1
6	NMP (0.275)	32.20	1:3
7	$PhNO_2$ (0.589)	34.82	1:0
8	DMF (0.161)	36.71	1:10
9	H_2O (0.123)	80.10	1:2

[a]Irradiated reaction mixture (0.06 M) at 180 °C for 1 min; [b]ratio of products determined by ^{1}H NMR spectroscopy; [c]the reported tan δ is for $MeNO_2$.

Next, we determined the minimum amount of $PhNO_2$ required to achieve successful selectivity for the naphthalene over the dihydronaphthalene product in the DDDA reaction by varying the amount of $PhNO_2$ used. It was discovered that exclusive use of $PhNO_2$ as solvent was not necessary, and that as little as 5% $PhNO_2$/*o*-DCB (8 equiv $PhNO_2$) resulted in selective naphthalene formation (entry 3, Table 2.3). Reducing the quantity of $PhNO_2$ to 4 equiv in the reaction mixture resulted in a 4:1 ratio of naphthalene **1.146** to dihydronaphthalene **1.147**, while reducing the amount of $PhNO_2$ by half to 2 equiv showed a proportional increase in the quantity of dihydronaphthalene **1.147** observed (entries 5 and 6). A number of examples in which $PhNO_2$ was employed as a reaction solvent for the purpose or aromatization have been reported,[66] as

well as mechanisms by which $PhNO_2$ functions as an electron or hydrogen atom acceptor have been described.[67]

Table 2.3. Minimal amount of $PhNO_2$ required for exclusive naphthalene formation

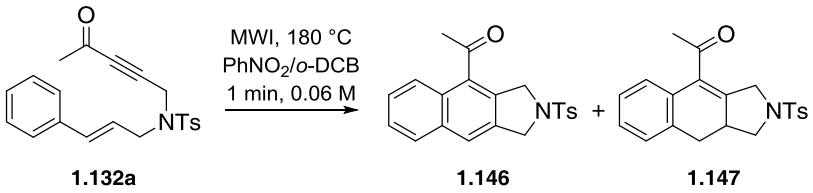

1.132a **1.146** **1.147**

entry	$PhNO_2$ (equiv)	yield	**1.146**:**1.147**[a]
1	32	77%	1:0
2	16	81%	1:0
3	8	73%	1:0
4	6	70%	12:1
5	4	70%	4:1
6	2	73%	2:1

[a]Ratio of products determined by ^{1}H NMR spectroscopy.

2.2.2 Isotopic labeling experiments

While making variations to the solvent of the DDDA reaction led to the development of conditions for the selective production of either the naphthalene or dihydronaphthalene product, elucidation of the mechanism was not possible from these results. In further efforts to determine the mechanism of the DDDA reaction, isotopic labeling experiments were conducted.

Synthetic protocols. A monodeuterated styrene-yne **2.14** was prepared by first reducing 3-phenyl-2-propyn-1-ol (**2.9**) using lithium aluminum deuteride to afford the monodeuterated cinnamyl alcohol **2.10** in quantitative yield; the stereochemistry was inferred based on ^{1}H NMR

spectroscopy (Scheme 2.3). Subjecting **2.10** to the Mitsonobu reaction conditions of triphenylphosphine, diisopropyl azodicarboxylate and 4-methyl-*N*-(prop-2-yn-1-yl)benzenesulfonamide (**2.11**) gave styrene-yne **2.12** in 85% yield. *N*-methoxy-*N*-methylacetamide (**2.13**) was then employed to acylate the lithium acetylide of **2.12**, and provided 46% yield of monodeuterated alkynone **2.14**.

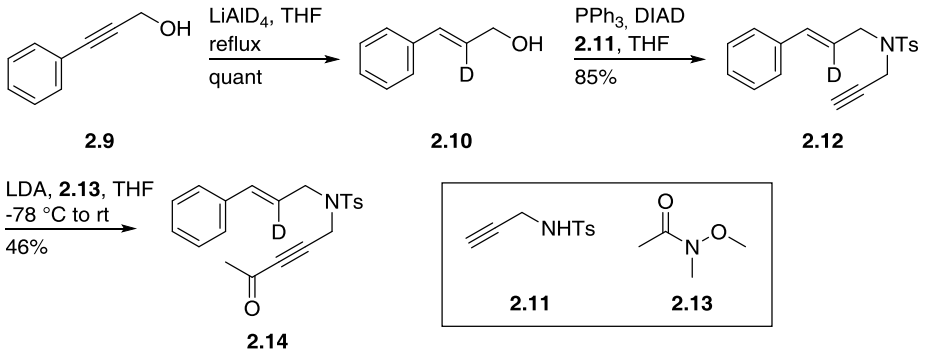

Scheme 2.3. Synthesis of monodeuterated styrene-yne **2.14**

The pentadeuterated substrates **2.19** and **2.20** were prepared in a similar manner as **2.14**; however, the synthesis began by a Sonogashira cross-coupling reaction of bromobenzene-d_5 (**2.15**) with propargyl alcohol (**2.16**) using tetrakis(triphenylphosphine)palladium(0), copper(I) iodide, and pyrrolidine to generate 3-(phenyl-d_5)prop-2-yn-1-ol in 50% yield (Scheme 2.4). Subsequent reduction of the alkyne using lithium aluminum hydride produced 56% yield of cinnamyl alcohol **2.17**. Identical Mitsunobu reaction conditions to those utilized in the transformation of **2.10** to **2.12** were utilized for conversion of **2.17** to styrene-yne **2.18** in 86% yield. Finally, to the lithium acetylide of **2.18** was added either *N*-methoxy-*N*-methylacetamide

(**2.13**) or methyl chloroformate, which produced pentadeuterated alkynone **2.19** and alkynoate **2.20** in 80 or 55% yield, respectively.

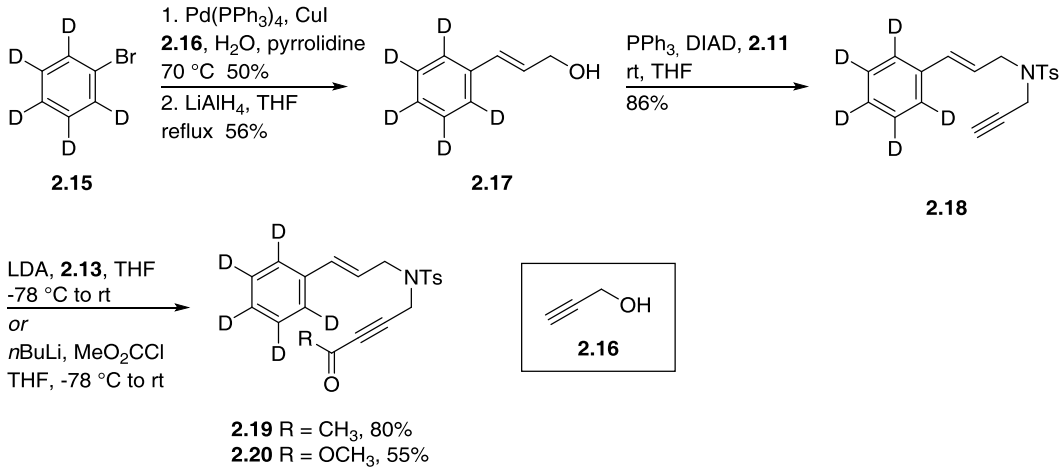

Scheme 2.4. Synthesis of pentadeuterated styrene-ynes **2.19** and **2.20**

Deuterated solvents and additives. The 10:1 selectivity observed in favor of the dihydronaphthalene product **1.147** when the DDDA reaction was performed in DMF implied that DMF was somehow affecting the reaction. DMF has previously been shown to act as a hydrogen atom donor,[68] and we initially postulated that the selectivity for **1.147** obtained in DMF was because of the hydrogen donating ability of the solvent. To determine whether the dihydronaphthalene product **1.147** was formed selectively in DMF due to hydrogen atom abstraction from the solvent by a radical intermediate, the reaction was performed in deuterated DMF (DMF-d_7). However, executing the reaction in DMF-d_7 produced only the non-deuterated product **1.147**, as determined by ^{1}H NMR spectroscopy (Scheme 2.5). Dihydronaphthalene **1.147** is characterized by distinct resonances in its ^{1}H NMR spectrum in the region of δ 4.6-2.4 (Figure

2.1). The protons adjacent to both the sulfonamide and the α,β-unsaturated ketone are represented in the ^{1}H NMR spectrum as two doublet of doublets at δ 4.53 and 3.90 that each have a large coupling constant of 18.0 Hz, which denotes geminal proton-proton coupling (H_a). The second set of protons that are adjacent to the sulfonamide (H_b) are found in the ^{1}H NMR spectrum as resonances at δ 3.95 and 2.86. The resonance at δ 3.95 is split as a doublet of doublets with coupling constants of 9.2 and 8.4 Hz; the 9.2 Hz coupling constant matches that of the apparent triplet at δ 2.86. The proton labeled as H_c appears as a multiplet at δ 3.02-2.93 due to complex splitting by the neighboring protons. Finally, the resonances representing benzyl protons H_d and H_e are located at δ 2.82 and 2.51 in the ^{1}H NMR spectrum, respectively. The resonance designated as H_d is characterized as a doublet of doublets with coupling constants of 14.8 and 6.4 Hz that correspond to geminal coupling with H_e and vicinal coupling with H_c, respectively. The coupling constant of 14.8 Hz observed for the apparent triplet at δ 2.51 (H_e) is representative of both geminal coupling to H_d, as well as large vicinal coupling to H_c. Despite performing the reaction in DMF-d_7, none of these resonances showed any change in the ^{1}H NMR spectrum of **1.147**, signifying that no deuterium incorporation had occurred (compare top and bottom spectra, Figure 2.1). These results indicate that production of dihydronaphthalene **1.147** was occurring by a different mechanism than abstraction of a hydrogen atom from the solvent.

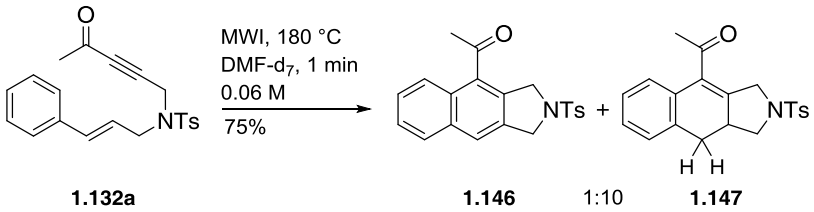

Scheme 2.5. DDDA reaction performed in DMF-d_7

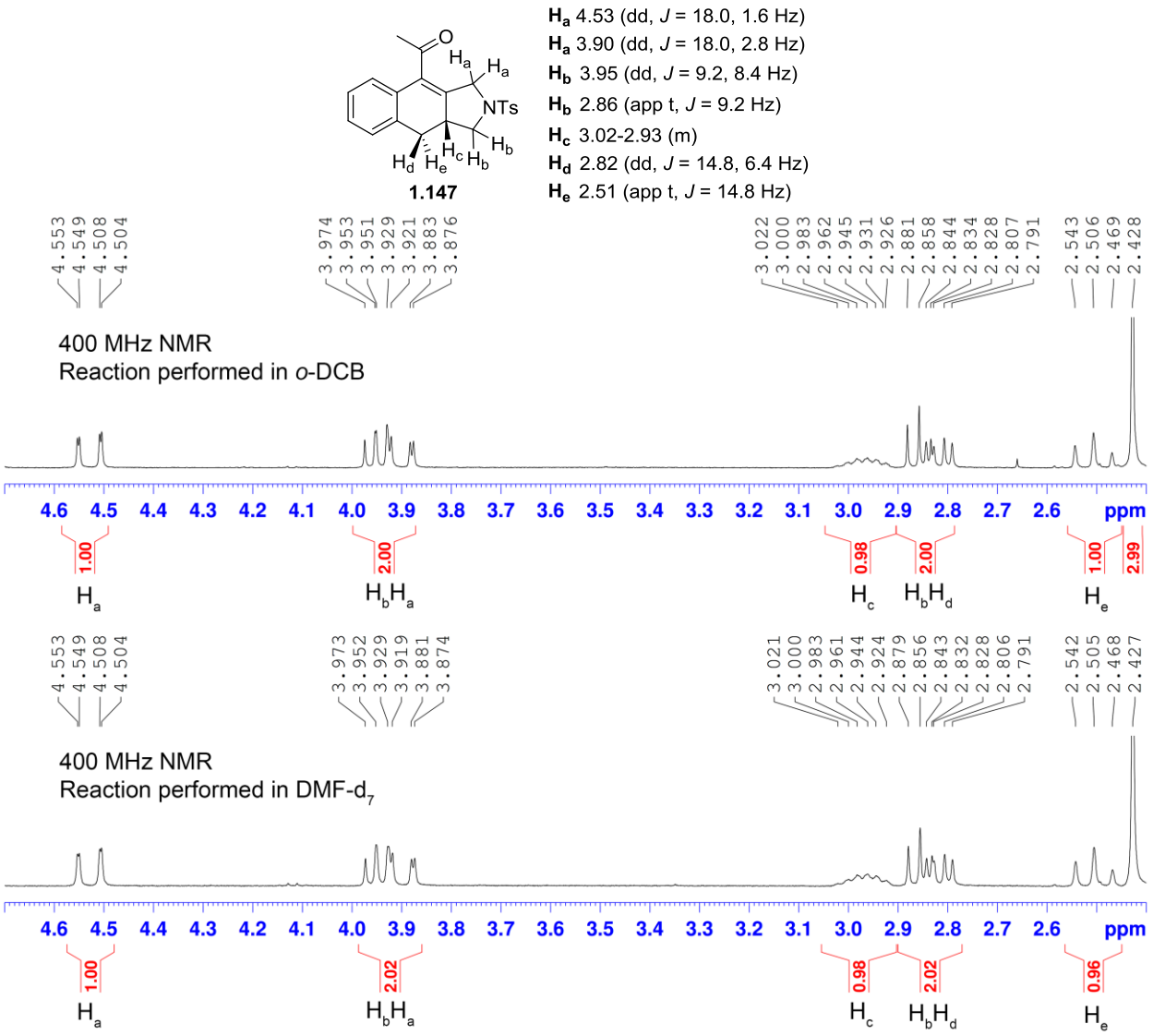

Figure 2.1. ^{1}H NMR spectrum of **1.147** after DDDA reaction of **1.132a**.
Performed in *o*-DCB (top) versus in DMF-d_7 (bottom)

Attempts were also made to capture potential radical intermediates with radical trapping agents. First, 1,4-cyclohexadiene was added to the reaction as a hydrogen atom donor; a large excess of 1,4-cyclohexadiene (10 equiv) was employed to ensure that hydrogen atom abstraction would occur by radical intermediates if they were present. Utilizing the standard DDDA reaction conditions of heating **1.132a** for 1 min at 180 °C in *o*-DCB-d_4, a 1:1.2 ratio of naphthalene and dihydronaphthalene products **1.146**:**1.147** was obtained in 72% combined yield, which was comparable to results of DDDA reactions that did not include 1,4-cyclohexadiene (Scheme 2.6). No byproducts resulting from trapping of radical or biradical intermediates were observed. Increasing the concentration of 1,4-cyclohexadiene further to 50% v/v 1,4-cyclohexadiene (88 equiv) led to problems reaching the reaction's target temperature due to the lower boiling point of 1,4-cyclohexadiene; therefore, conclusive results were not obtained at this concentration.

Alternatively, attempts to trap radical intermediates of the DDDA reaction were made by utilizing (2,2,6,6-tetramethylpiperidin-1-yl)oxyl (TEMPO) as a trapping agent.[69] Heating of **1.132a** in DCE at 180 °C for 2 min in the presence of excess TEMPO (1.5 equiv) resulted in a 52% yield of naphthalene **1.146**; no dihydronaphthalene **1.147** or TEMPO-trapped product was detected (Scheme 2.6) The increase in yield of **1.146** from 30% when the reaction was performed in the absence of TEMPO to 52% in the presence of TEMPO may be explained by TEMPO acting as an oxidant during the reaction, rather than as a radical trap.[70] The overall lower yield of the reaction and the lack of dihydronaphthalene product observed was attributed to decomposition of dihydronaphthalene under the reaction conditions, and was evidenced by tosyl and unresolved aliphatic impurities observed in the crude ^{1}H NMR spectrum of the reaction mixture.

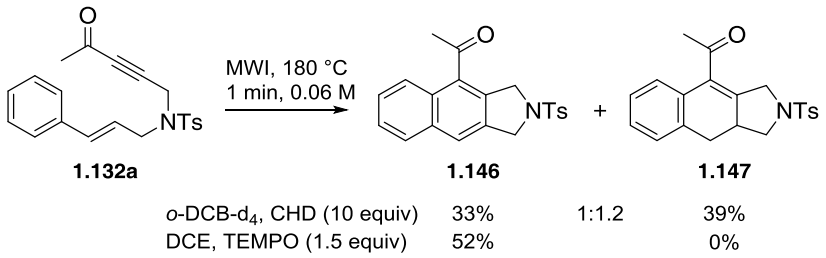

Scheme 2.6. DDDA reactions in the presence of 1,4-cyclohexadiene (CHD) or TEMPO

Deuterated DDDA Substrates. The failure of radical trapping experiments using deuterated solvents or additives, such as DMF-d_7, 1,4-cyclohexadiene and TEMPO, to provide evidence for the existence of radical intermediates in the DDDA reaction encouraged us to pursue other avenues in order to elucidate the mechanism of naphthalene and dihydronaphthalene formation. As an alternate approach, the deuterated styrene-ynes, for which the syntheses were previously shown (Schemes 2.3 and 2.4), were subjected to the thermal conditions of the DDDA reaction. First, alkynone-d_1 **2.14** was heated at 180 °C for 1 min in *o*-DCB-d_4, which generated naphthalene **1.146** and dihydronaphthalene-d_1 **2.21** in a combined 81% yield and in a 1:5.2 ratio, as determined by ^{1}H NMR spectroscopy (Scheme 2.7). By incorporation of deuterium onto the double bond of the styrene, a significant change in the product ratio was observed when compared to heating of the non-deuterated precursor **1.132a**, which only produced a 1:1.2 mixture of **1.146**:**1.147**. This change in product distribution in favor of dihydronaphthalene **2.21** was representative of a large primary kinetic isotope effect (KIE), where the bond-breaking that needed to occur at the carbon-deuterium bond in order to form naphthalene **1.146** was slower compared to the breaking of a carbon-hydrogen bond at this position. The slower breaking of the carbon-deuterium bond, which does not need to occur for

production of the dihydronaphthalene **2.21**, led to a slower rate of naphthalene formation and a higher ratio of the dihydronaphthalene product.

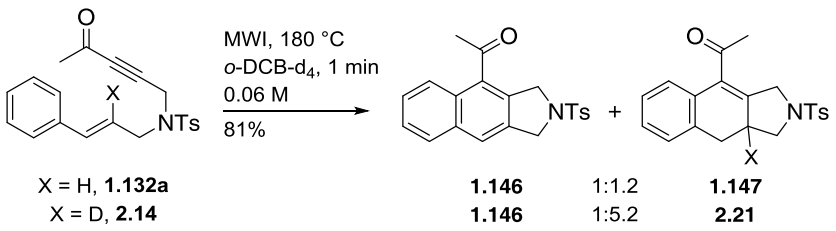

Scheme 2.7. DDDA reaction of alkynone-d_1 **2.14** showing a primary KIE

In an additional isotopic labeling experiment, heating of alkynone-d_5 **2.19** for 1 min at 180 °C in *o*-DCB-d_4 resulted in a 1:1 mixture of naphthalene **2.22** and dihydronaphthalene **2.23** in 68% yield (Scheme 2.8). Naphthalene **2.22** was separated from dihydronaphthalene **2.23** by HPLC, and characterization of **2.23** by ^{1}H NMR and COSY spectroscopy showed the presence of two diastereomers in a 1.5:1 ratio. The formation of these dihydronaphthalene products that contained a deuterium label at the 4-position indicated that deuterium atom migration had occurred from the aryl ring of **2.19** during the reaction.

Incorporation of a deuterium atom at the 4-position of the dihydronaphthalene **2.23** considerably altered the ^{1}H NMR spectrum of **2.23** compared to non-deuterated dihydronaphthalene **1.147**. For example, the doublet of doublets and apparent triplet found at δ 2.82 (H_d) and 2.51 (H_e), representative of the two protons at the 4-position of **1.147** (top spectrum, Figure 2.2), each changed upon deuterium incorporation in **2.23** and became two doublets that integrated for 0.69 and 0.47 protons, respectively; the coupling constants were

reflective of coupling only to the neighboring proton (H_c) and not geminal coupling (middle spectrum, Figure 2.2). Not only did this indicate that deuterium migration had occurred during the DDDA reaction of **2.19**, but each doublet represented an individual diastereomer, the ratio of which could then be measured. Additional smaller resonances at δ 2.89, 2.86, 2.81, 2.80, and 2.54 were also noted in the ^{1}H NMR spectrum of **2.23**, which were similar to the resonances observed for **1.147**.

Not surprisingly, heating **2.19** in DMF under the same reaction conditions resulted in a 70% combined yield of **2.22** and **2.23** in a 1:7 ratio; however, dihydronaphthalene **2.23** was now generated in a much greater diastereomeric ratio of 14:1 in favor of the opposite diastereomer (Scheme 2.8). This change in diastereoselectivity was also obvious from the ^{1}H NMR spectrum because the doublet at δ 2.50 (H_e) was now more prominent in comparison to the doublet at δ 2.80 (H_d), with integrations of 0.95 and 0.07, respectively (bottom spectrum, Figure 2.2).

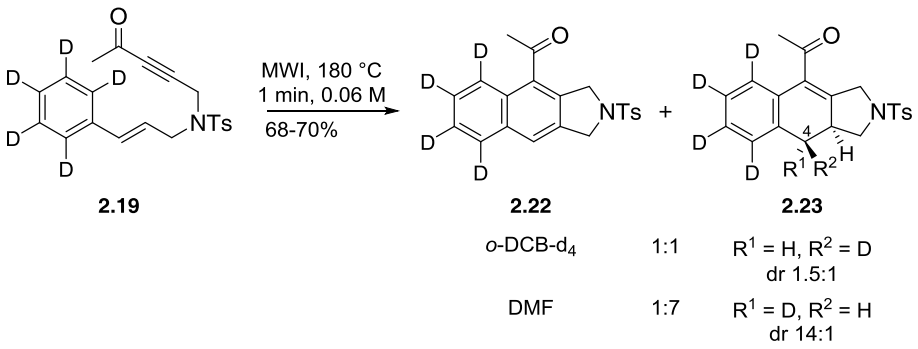

Scheme 2.8. Deuterium atom transfer in the DDDA reaction.
DDDA reaction of styrene-yne-d_5 **2.19** leading to the formation of dihydronaphthalene **2.23** with unique labeling of the 4-position by deuterium

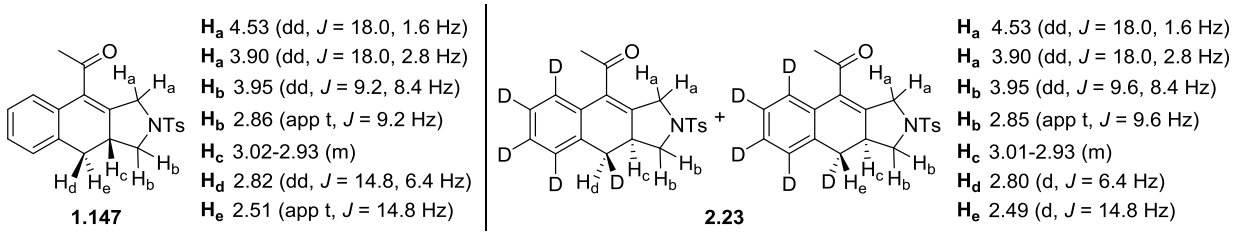

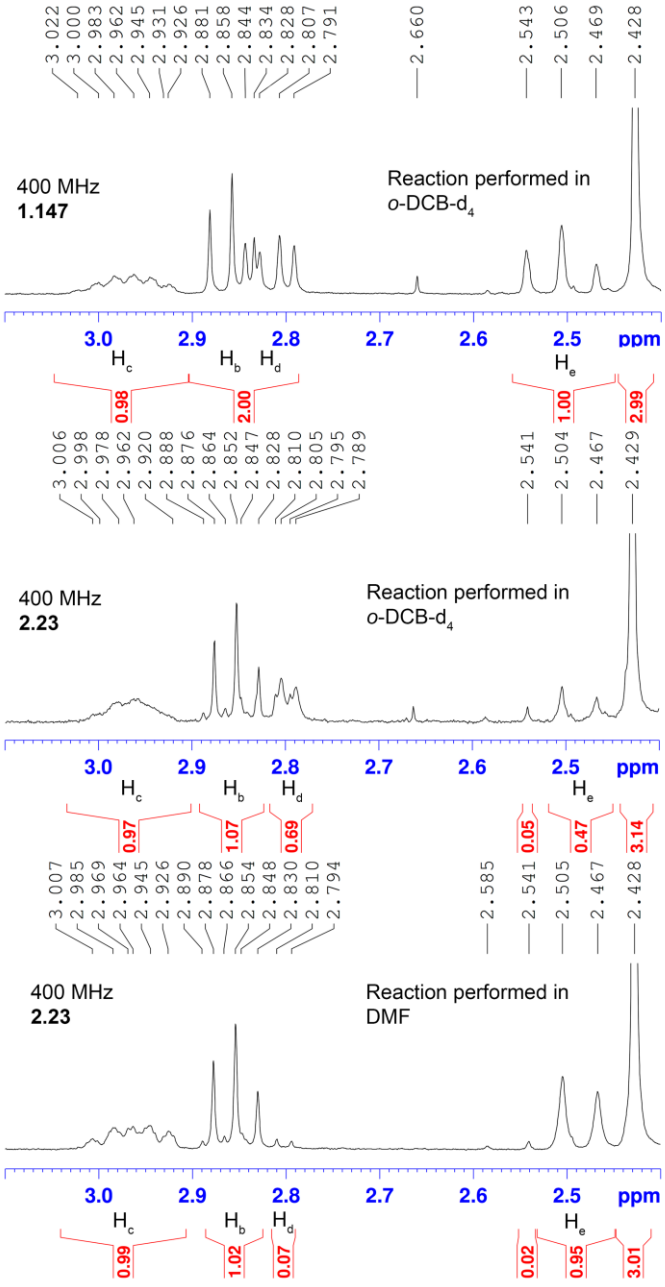

Figure 2.2. [1]H NMR spectra of non-deuterated and deuterated dihydronaphthalenes.
[1]H NMR spectra of non-deuterated dihydronaphthalene **1.147** (top) and deuterium-labeled dihydronaphthalene **2.23** synthesized via irradiation of **2.19** in *o*-DCB (middle) and DMF (bottom)

Crossover experiment. While the above isotopic labeling experiments indicated that dihydronaphthalene **2.23** was being formed via transfer of a deuterium atom from the arene of **2.19** during the reaction, these results did not allow for elaboration on the mechanism of this deuterium migration. The incorporation of the deuterium atom at the 4-position of dihydronaphthalene **2.23** could occur via either an inter- or intramolecular transfer mechanism, and to determine which mechanism was operative, a crossover experiment was performed employing alkynoate **2.20**, containing a styrene with a deuterated aryl group, and alkynone **1.132a**, which was not deuterated. To test for intermolecular hydrogen/deuterium atom transfer, these two styrene-ynes together were subjected to the DDDA reaction, which would allow for the formation of six possible products if crossover was occurring (Scheme 2.9). Irradiation of a 1:1 mixture of **1.132a** and **2.20** for 3 min at 180 °C in *o*-DCB afforded a mixture of six compounds that were separated as four peaks by HPLC (Figure 2.3). Characterization by ESI-MS revealed two of the isolated chromatogram peaks as naphthalenes **2.25** (t_r = 27.3 min) and **1.146** (t_r = 34.2 min), while analysis of the remaining two chromatogram peaks showed a mixture of dihydronaphthalenes **2.26** and **2.27** in one peak (t_r = 28.7 min), in addition to a mixture of **1.147** and **2.24** (t_r = 38.2 min) in the other peak; the HPLC chromatogram peaks corresponding to the dihydronaphthalenes also contained naphthalene, but to a lesser degree (Table 2.4). The $(M+H)^+$ ions of the deuterated products **2.24** and **2.26** were observed with relative intensities of greater than 55%, thus differentiating these peaks from those that result from the natural abundance of carbon-13 for **1.147** and **2.27**, which would appear with similar masses, but with much lower relative intensities. The observation of all possible crossover products indicated that transfer of hydrogen/deuterium to the 4-position of the dihydronaphthalene was taking place via an intermolecular process.

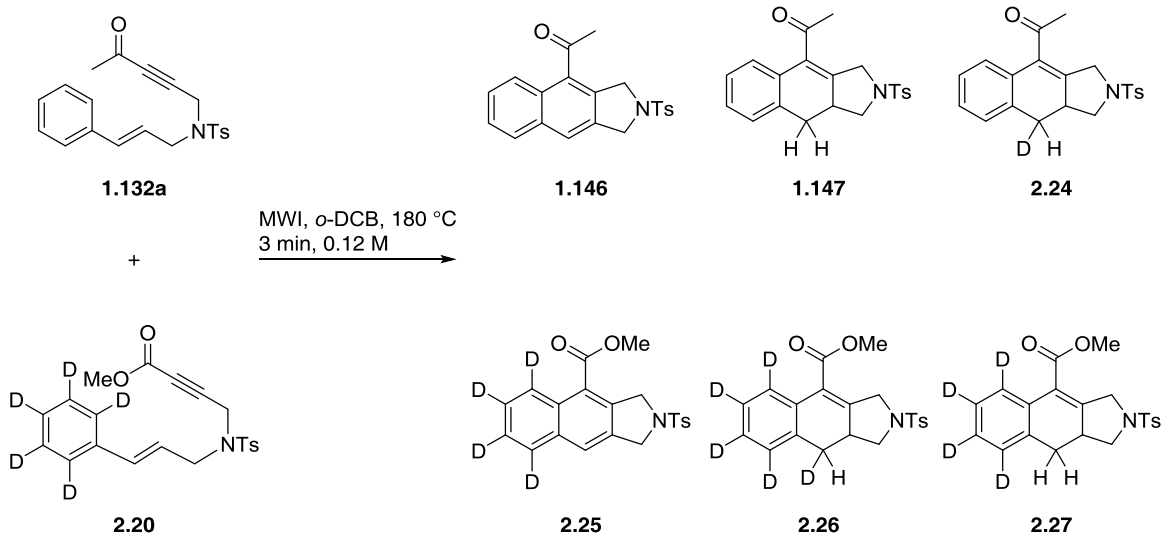

Scheme 2.9. Crossover experiment.
Crossover experiment conducted with alkynone **1.132a** and alkynoate **2.20** to provide six products

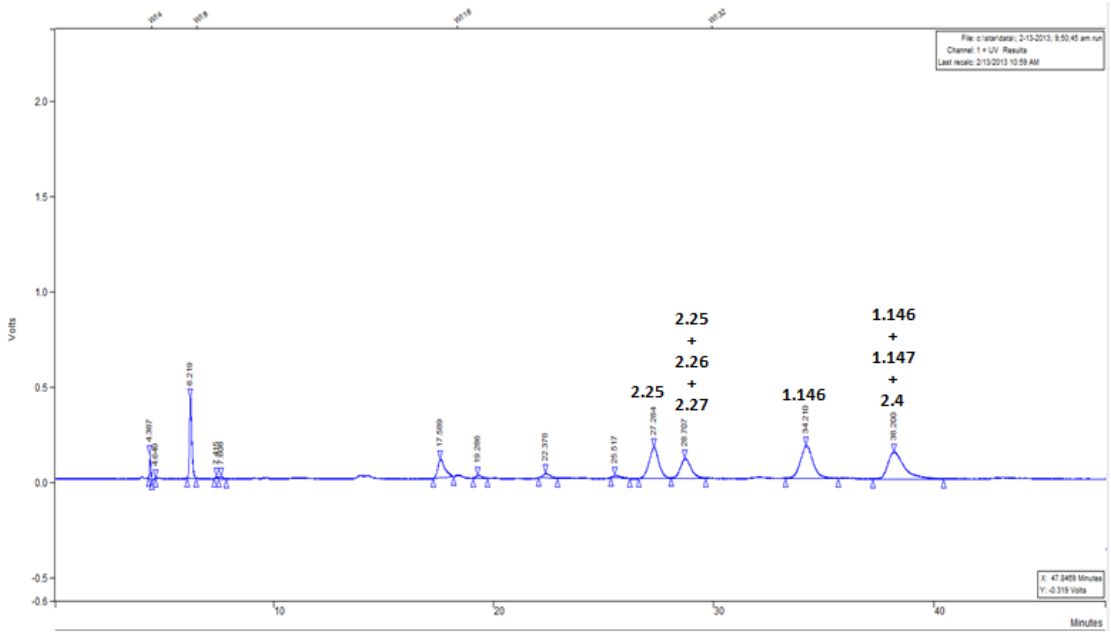

Figure 2.3. HPLC chromatogram showing separation of products from crossover experiment

Table 2.4. Results of ESI-MS for products isolated from the crossover experiment

HPLC retention time (min)	product	mass calculated (m/z)	mass found (m/z)	relative intensity
27.3	**2.25**	386.13586	386.13497	100.00
28.7	**2.25**	386.13586	386.13489	49.58
28.7	**2.27**	388.15151	388.15065	79.66
28.7	**2.26**	389.15779	389.15581	100.00
34.2	**1.146**	366.11584	366.11483	100.00
38.2	**1.146**	366.11584	366.11539	8.84
38.2	**1.147**	368.13149	368.13046	100.00
38.2	**2.24**	369.13777	369.13489	54.67

2.2.3 Mechanism of dihydronaphthalene formation

As a result of our mechanistic studies, we propose that the dihydronaphthalene product **1.147** is formed via an initial [4 + 2] cycloaddition reaction of **1.132a** to produce the tetraene intermediate **2.28** (Scheme 2.10, A). The tris-allylic hydrogen atom of **2.28** is then abstracted to generate a carbon-centered radical, which is represented by the two resonance structures **2.29** and **2.30**. Next, the carbon-centered radical **2.30** proceeds to abstract a hydrogen atom from another equivalent of **2.28** to afford the dihydronaphthalene substrate **1.147**, along with an additional radical **2.30** which will propagate the reaction. Support for this mechanistic proposal is provided by the crossover study (Scheme 2.9), which indicated that intermolecular hydrogen/deuterium atom abstraction was occurring to produce the dihydronaphthalene products **1.147** and **2.27** (Scheme 2.10, B). Concentration studies also lend support to a radical mechanism because more concentrated reaction mixtures resulted in an increased ratio of dihydronaphthalene to naphthalene products.

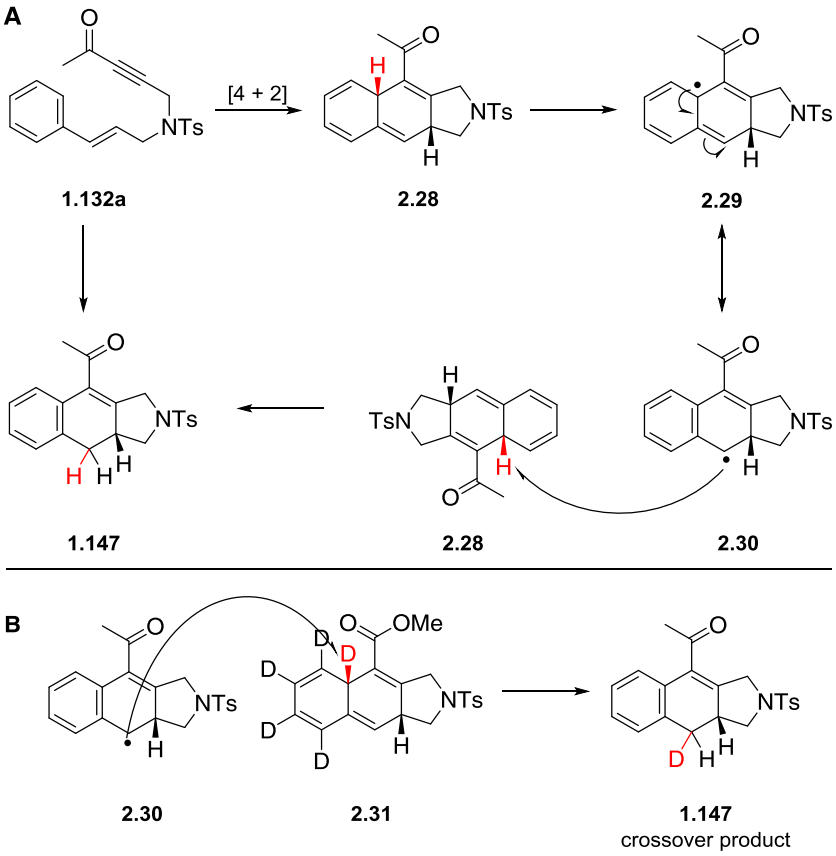

Scheme 2.10. Proposed mechanism of dihydronaphthalene formation.
(A) Proposed mechanism; (B) support for mechanism provided by the crossover experiment

The diastereoselectivity observed in the formation of dihydronaphthalene **2.23** when alkynone-d_5 **2.19** was heated in DMF also supports the intermolecular hydrogen atom transfer mechanism (Scheme 2.8). An X-ray crystal structure was obtained of the dihydronaphthalene product **1.147** and is represented by the structure in Figure 2.4, A. This structure showed that the N-S-C angle of the *N*-tosyl group was 107°, which placed the aromatic ring of the tosyl group below one face of the dihydronaphthalene. A similar conformation of the tosyl group in the carbon-centered radical intermediate would cause hindrance on one face of the intermediate, which would promote the radical to intermolecularly abstract a deuterium atom using its

unhindered face, thus achieving the observed diastereoselectivity (Figure 2.4, B). What remains unclear is why an almost equal mixture of diastereomers is formed when the DDA reaction is conducted in *o*-DCB, while a much greater diastereoselectivity is realized when the reaction takes place in DMF (Scheme 2.8). Additionally, what has yet to be determined and explained in terms of our mechanistic proposal is why the dihydronaphthalene is selectively produced over the naphthalene product when DMF is employed as the reaction solvent. One potential reason for the observed product selectivity could be due to the much higher dielectric constant of DMF compared to other solvents utilized, as more polar solvents have been previously demonstrated to have an effect on selectivity in radical reactions;[71] however no conclusions can yet be drawn regarding the effect of DMF on the DDA reaction. To better understand the above results, we plan to enlist Professor Dean Tantillo and his group at UC Davis to perform calculations that may shine light on this matter.

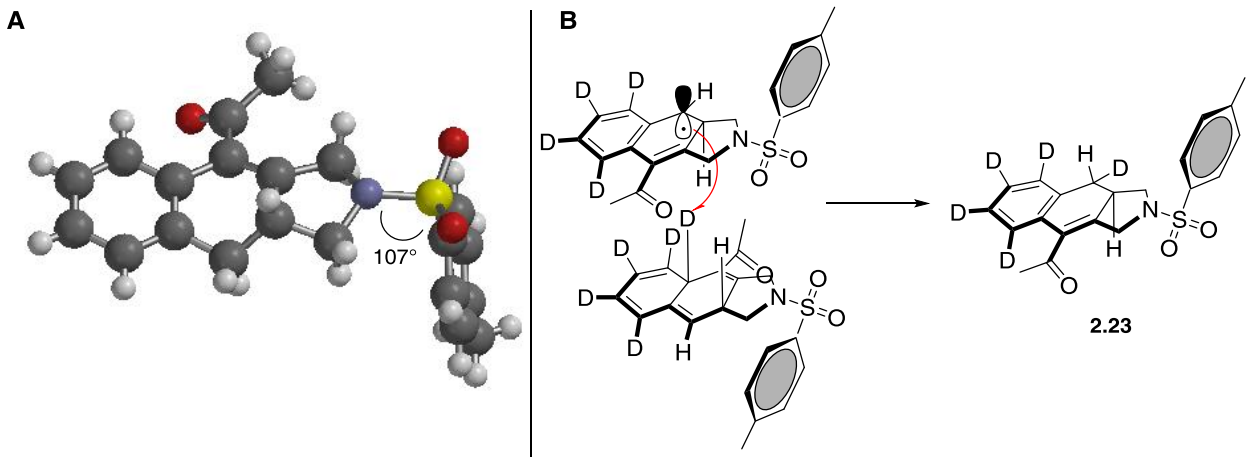

Figure 2.4. Understanding the observed diastereoselectivity of the DDA reaction in DMF. (A) Structure of dihydronaphthalene **1.147** determined by X-ray crystallography; (B) proposed mechanism for why diastereoselectivity is observed in the reaction of **2.19** in DMF to produce **2.23**

In order to initiate the radical process proposed for the formation of dihydronaphthalene **1.147**, the tris-allylic hydrogen atom of **2.28** must first be abstracted (Scheme 2.10). It is unlikely that this bond is spontaneously broken at the temperatures that we perform the reaction, which can be as low as 120 °C, because the bond dissociation energy (BDE) of the carbon hydrogen bond of 1,4-cyclohexadiene, a related system, was calculated as 71-78 kcal/mol.[72] Instead, we propose that the radical reaction to form dihydronaphthalene **1.147** is initiated by abstraction of the tris-allylic hydrogen from **2.28** by triplet oxygen (Scheme 2.11, A). This hypothesis is supported by the work of Hendry et al., who studied the thermal dehydrogenation of 1,4-cyclohexadiene to benzene by oxygen, and showed that only substoichiometric amounts of oxygen were required for aromatization.[73] Based on kinetic data and quantitative water analysis of the reaction mixture, Hendry provided the mechanism in Scheme 2.11, B for the aromatization of 1,4-cyclohexadiene by triplet oxygen, in which oxygen is regenerated during the reaction by decomposition of the hydrogen peroxide formed. When we conducted the DDDA reaction in the presence or absence of oxygen, the same product selectivity, reaction rates, and yields of naphthalene **1.146** and dihydronaphthalene **1.147** were observed (entries 12 and 13, Table 2.1); this data is supported by Hendry's results, which indicated that stoichiometric quantities of oxygen are not necessary to achieve aromatization. It should be noted that to remove oxygen from the reaction mixture, bubbling with argon was performed; however this method does not rigorously exclude oxygen, and residual oxygen may have been present in the reaction mixture.

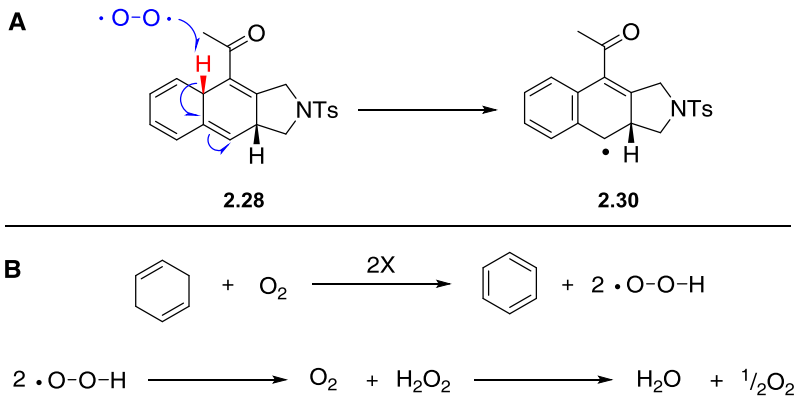

Scheme 2.11. Proposed mechanism of hydrogen abstraction from **2.28**.
(A) Abstraction of tris-allylic hydrogen atom of **2.28** by triplet oxygen to initiate a radical mechanism; (B) Hendry's mechanism for dehydrogenation of 1,4-cyclohexadiene by triplet oxygen

2.2.4 Mechanism of naphthalene formation

The data described within this chapter provides substantial support for the proposed mechanism of formation of dihydronaphthalene substrates (Scheme 2.10); however, this data does not allow for an explanation of how the naphthalene product is generated, aside from evidence which indicates that the naphthalene is not produced directly from dihydronaphthalene (entries 3-5, Table 2.1). The lack of evidence for oxidation of dihydronaphthalene to naphthalene, along with the large primary KIE effect observed for the DDDA reaction of **2.14** (Scheme 2.7), suggests that the naphthalene and dihydronaphthalene products are being formed by diverging mechanistic pathways.

One possible pathway by which the naphthalene could be formed is a concerted noncatalytic elimination of hydrogen gas via the same tetraene intermediate **2.28** that we proposed in the formation of dihydronaphthalene **1.147** (Scheme 2.12). By envisioning **2.28** in a different boat-like conformation, we noted that the hydrogen atoms may be in close enough spacial proximity to undergo concerted intramolecular elimination, which is an allowed process

for our system according to the rules of conservation of orbital symmetry reported by Woodward and Hoffman.[74]

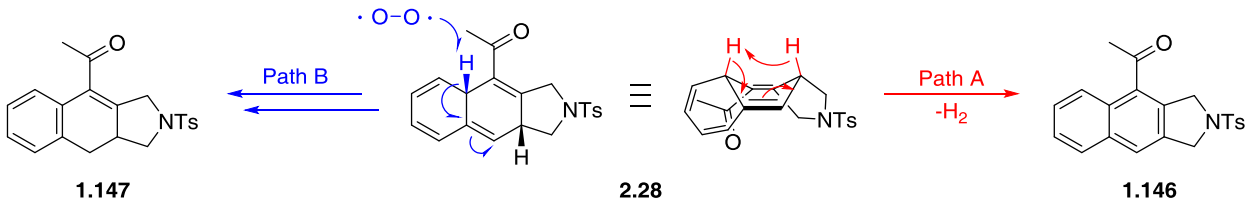

Scheme 2.12. Diverging strategy for formation of naphthalene and dihydronaphthalene from a common intermediate, where generation of naphthalene is postulated to occur by loss of H_2 gas

Woodward and Hoffman state that atom transfers via a unimolecular process are allowed when m = 4q + 2, where m is the number of π electrons and q is an integer (Scheme 2.13, A). Several reactions demonstrating this concerted intramolecular elimination have been reported that have established a similar mechanism to what we suggest for the formation of the naphthalene; specifically, each involves the evolution of hydrogen gas to achieve aromatization. One such example was published by Wellington and Walters, where thermal decomposition of 2,5-dihydrofuran showed production of both furan and hydrogen gas in equal amounts as detected by gas chromatography and mass spectrometry (Scheme 2.13, B); the same reaction was conducted with 2,3-dihydrofuran and did not result in the production of furan.[75] Similar reports that were published independently by Ellis and Frey or Benson and Shaw demonstrated a related unimolecular elimination of hydrogen gas for 1,4-cyclohexadiene in the generation of benzene (Scheme 2.13, C).[76] These authors also determined that this elimination was not applicable to the oxidation of 1,3-cyclohexadiene, which was determined to proceed via a radical mechanism.[76a,77]

Matsubara et al. were the first to propose that a similar intermediate to the tetraene **2.28** would undergo reverse hydrogenation of the diene, and they reported brief DFT calculations which supported this claim.[47] Despite the positive results of these initial calculations, Matsubara et al. did not conduct any experiments to show that hydrogen gas was being evolved in the DDDA reaction of styrene-ynes to form naphthalenes.

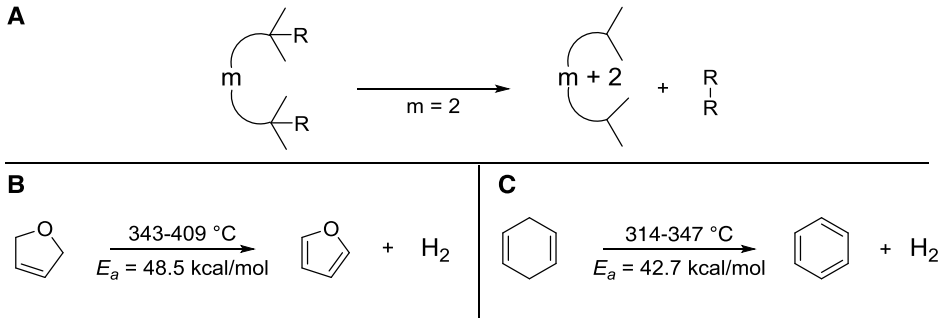

Scheme 2.13. Rules for unimolecular atom transfers and relevant examples.
(A) Woodward-Hoffmann rules of conservation of orbital symmetry for a unimolecular process; (B) thermal decomposition of 2,5-dihydrofuran; (C) thermal decomposition of 1,4-cyclohexadiene

To test the hypothesis that the tetraene intermediate **2.28** would undergo an intramolecular concerted elimination of hydrogen gas to generate naphthalene **1.146**, we performed several DDDA reactions with the goal of detecting hydrogen gas. Our earlier studies established that conventional heating and microwave irradiation provided nearly identical ratios and yields of naphthalene and dihydronaphthalene products in the DDDA reaction of styrene-yne **1.132a** in *o*-DCB-d_4. We envisioned that by conducting the DDDA reaction in a sealed NMR tube via conventional heating, we could potentially observe the production of hydrogen gas by ^{1}H NMR spectroscopy. First, a ^{1}H NMR spectrum was obtained of **1.132a** in *o*-DCB-d_4 in a

sealed NMR tube (Scheme 2.14, A). The solution of **1.132a** was then heated in the NMR tube at 180 °C for 2 min in an oil bath, and a ^{1}H NMR spectrum of the reaction mixture was immediately acquired. The ^{1}H NMR spectrum showed the presence of a new singlet at δ 4.73 that was not attributed to the naphthalene **1.146** or dihydronaphthalene **1.147** products; this resonance was assumed to correspond to hydrogen gas that was formed during the reaction in a 1:11 ratio with **1.146** (Scheme 2.14, B). To confirm that this resonance was hydrogen gas and not an impurity, hydrogen gas was bubbled through the reaction mixture and a new ^{1}H NMR spectrum was obtained which showed an increase in the integration value for the peak designated as hydrogen gas from 0.05 to 0.09; this increase was indicative of a 1:6 ratio of hydrogen gas to naphthalene **1.146** (Scheme 2.14, C). Finally, as an additional measure to ensure that the resonance at δ 4.73 was hydrogen gas, argon was bubbled through the reaction mixture which resulted in the disappearance of this resonance from the ^{1}H NMR spectrum (Scheme 2.14, D). The information obtained from the study of the DDDA reaction by ^{1}H NMR spectroscopy supported our hypothesis that hydrogen gas was being produced during the reaction; however, the quantity of hydrogen gas generated could not be determined using this qualitative approach.

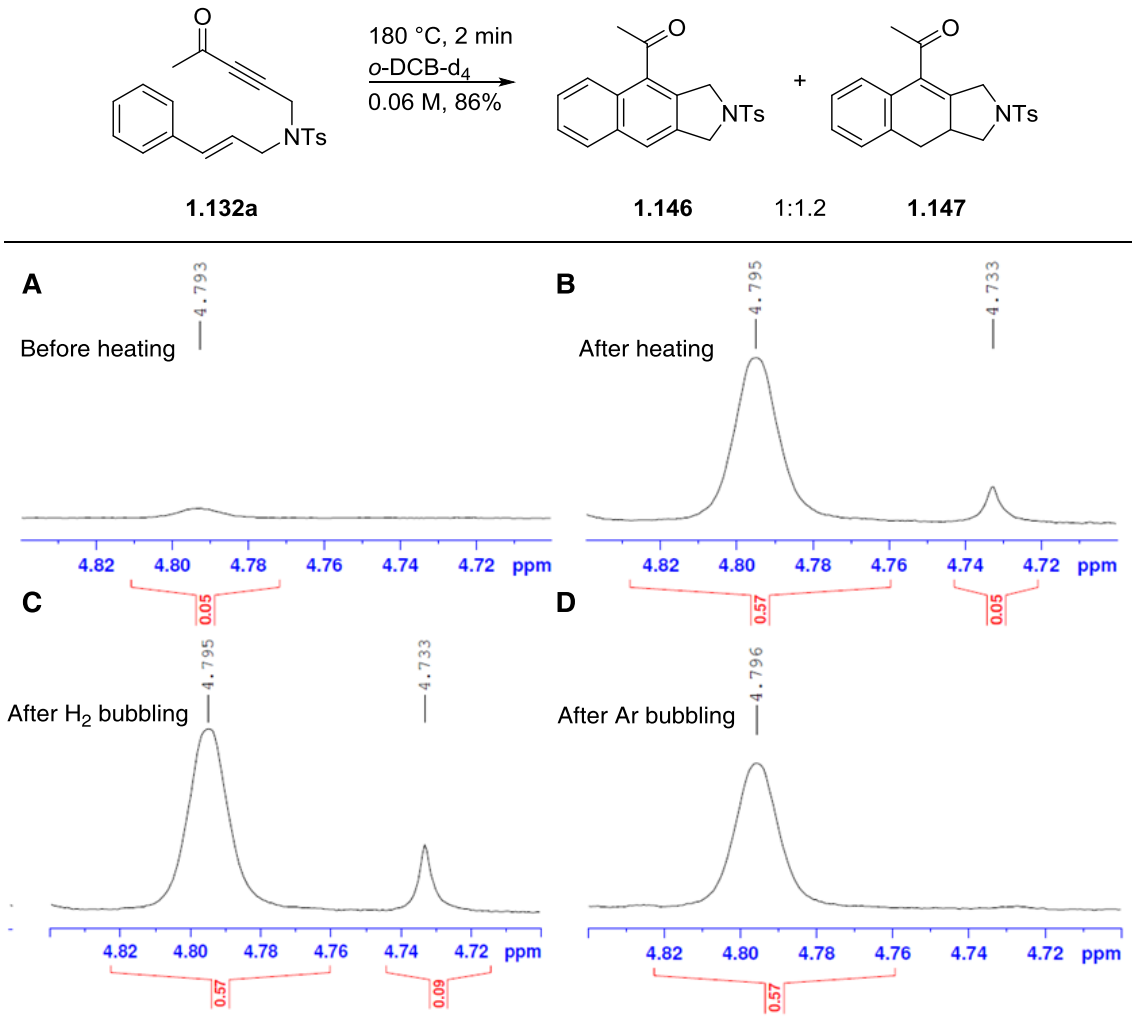

Scheme 2.14. Detection of hydrogen gas by ^{1}H NMR spectroscopy.
^{1}H NMR spectra were taken (A) before heating; (B) after heating; (C) after bubbling with hydrogen gas; (C) after bubbling with argon

In order to quantify the amount of hydrogen gas that was produced during the DDDA reaction, gas chromatography was utilized. For the gas chromatography experiments, styrene-yne **1.132a** was irradiated for 1 min at 180 °C in *o*-DCB (Scheme 2.15, A). An aliquot of the headspace in the reaction vessel was then injected into a gas chromatograph, and the amount of hydrogen gas produced during the DDDA reaction was measured by our collaborators Husain Kagalwala and Professor Stefan Bernhard at Carnegie Mellon University. Based upon the

average 80% combined yield and 1:1.2 ratio of naphthalene **1.146** and dihydronaphthalene **1.147** products typically generated upon irradiation of styrene-yne **1.132a** under these reaction conditions, the theoretical yield of hydrogen gas expected and the percent yield of hydrogen gas detected were calculated. Overall, a 39-48% yield of hydrogen gas was determined by gas chromatography for two experiments (for experiment details and calculations see section 2.4.14). Additionally, the same technique was used in the detection of HD gas for the DDDA reaction of styrene-yne-d_1 **2.14**, and an approximate 32% yield of HD gas was calculated (Scheme 2.15, B). In this case, the detector response for the chromatograph was different due to the heavier mass of HD, so the yield of HD was underestimated and should be more comparable to that obtained for detection of hydrogen gas. Overall, these results indicate that a substantial amount of hydrogen gas is produced during the DDDA reaction, and that our original hypothesis in which the naphthalene product is formed via intramolecular concerted elimination of hydrogen gas from tetraene intermediate **2.28** is supported (Scheme 2.12).

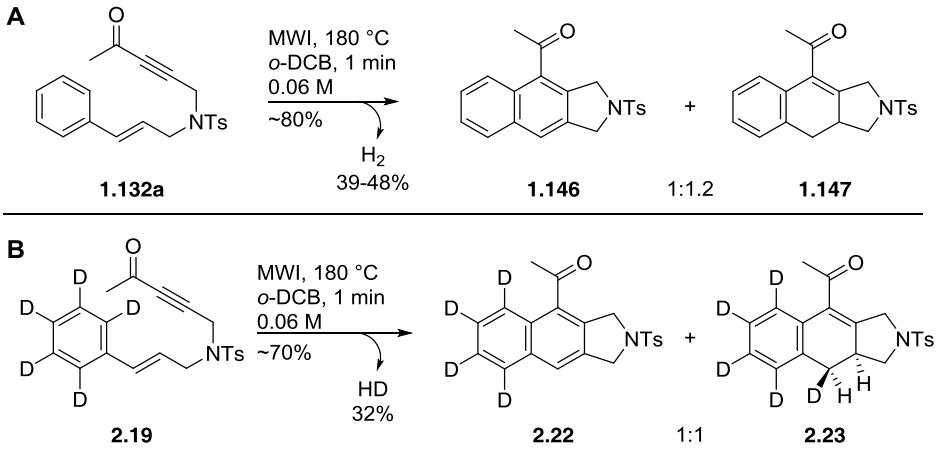

Scheme 2.15. Analysis of DDDA reaction for (A) H_2 and (B) HD gas by GC

2.3 CONCLUSIONS

In conclusion, the mechanism of the DDDA reaction was investigated to gain a better understanding of the product selectivity observed and how to control it. Styrene-ynes that contained a sulfonamide-substituted tether were chosen as the subjects of these mechanistic studies because of their propensity to produce mixtures of naphthalene and dihydronaphthalene products under our original DDDA reaction conditions. Variations to the reaction conditions of the DDDA reaction were explored to aid in the determination of how the naphthalene and dihydronaphthalene products were generated. These studies led to the discovery of reaction conditions that allowed for the selective formation of either the naphthalene or dihydronaphthalene products; changing the reaction solvent from *o*-DCB to $PhNO_2$ produced naphthalene compounds exclusively in the DDDA reaction, while employing DMF as the solvent afforded dihydronaphthalene substrates in greater than 10:1 selectivity. The ability to generate the naphthalene and dihydronaphthalene compounds selectively and in high yields significantly enhances the synthetic utility of the DDDA reaction.

Additionally, isotopic labeling studies were conducted and were found to be instrumental for the determination of the mechanism of dihydronaphthalene formation. Based on a key crossover experiment, we established that dihydronaphthalene substrates were being produced via an intermolecular hydrogen atom transfer process that was initiated by triplet oxygen. Concentration studies provided further support for the radical mechanism proposed. Moreover, we demonstrated that the dihydronaphthalene and naphthalene products were afforded by diverging mechanistic pathways, where the naphthalene was not directly generated from the dihydronaphthalene substrate, but rather provided by concerted intramolecular elimination of hydrogen gas from of a common intermediate. Hydrogen gas detection methods, such as ^{1}H

NMR spectroscopy and gas chromatography were essential in reaching this conclusion, and provided both qualitative and quantitative measures of the amount of hydrogen gas produced during the DDDA reaction.

While we have acquired a substantial amount of experimental evidence supporting our proposed mechanisms for the formation of the naphthalene and dihydronaphthalene compounds, there are still aspects of the DDDA reaction and its product selectivity that we have yet to understand. Currently, our efforts are focused on learning more about the solvent effect observed in the DDDA reaction and its effect on the product selectivity and diastereoselectivity obtained in the formation of the dihydronaphthalene compound. Additionally, we are interested in investigating the difference in product selectivity observed in the DDDA reaction for precursors containing all carbon or heteroatom-substituted styrene-yne tethers. To this end, we have enlisted the assistance of our collaborator Professor Dean Tantillo at UC Davis who is performing DFT calculations to better comprehend the experimental results that we have obtained.

2.4 EXPERIMENTAL

2.4.1 General methods

All commercially available compounds were used as received unless otherwise noted. Dichloromethane (DCM) and tetrahydrofuran (THF) were purified by passing through alumina using the Sol-Tek ST-002 solvent purification system. Triethylamine was freshly distilled from CaH_2 prior to use. Deuterated chloroform ($CDCl_3$) was stored over 3 Å molecular sieves. Purification of the compounds by flash column chromatography was performed using silica gel

(40-63 μm particle size, 60 Å pore size) purchased from Sorbent Technologies. TLC analyses were performed on Silicycle SiliaPlate G silica gel glass plates (250 μm thickness). ^{1}H NMR and ^{13}C NMR spectra were recorded on Bruker Avance 300, 400, 500, or 700 MHz spectrometers. Spectra were referenced to residual chloroform (7.26 ppm, ^{1}H, 77.16 ppm, ^{13}C), 1,2-dichlorobenzene (7.14 ppm, 2H), or *N*,*N*-dimethylformamide (8.38 ppm, 1H). Chemical shifts are reported in ppm, multiplicities are indicated by s (singlet), b s (broad singlet), d (doublet), t (triplet), q (quartet), p (pentet), and m (multiplet). Coupling constants, *J*, are reported in hertz (Hz). All NMR spectra were obtained at rt. In experiments where yields were determined by ^{1}H NMR spectroscopy, *p*-dimethoxybenzene was used as an internal standard and its resonance at 6.94 ppm was chosen for integration to a constant value because it showed minimal overlap with products or byproducts of the reaction, unlike the resonance at 3.80 ppm. A standard solution of *p*-dimethoxybenzene (20 mg) in *o*-DCB-d_4 (0.5 mL) was prepared so that mg quantities of *p*-dimethoxybenzene could be accurately measured. Arrows in the ^{1}H NMR spectra indicate product resonances that were chosen for calculation of product ratios and/or yields. ^{1}H and ^{13}C NMR spectra can be found in Appendix B. IR spectra were obtained using a Nicolet Avatar E.S.P. 360 FT-IR. ES mass spectroscopy was performed on a Waters Q-TOF Ultima API, Micromass UK Limited high resolution mass spectrometer. All microwave-mediated reactions were conducted in either a Biotage Initiator Exp microwave synthesizer using 0.5-2 mL conical and 2-5 mL cylindrical microwave irradiation vials, or in an Anton-Paar Monowave 300 microwave synthesizer using G4 and G10 cylindrical microwave irradiation vials. The temperature of reactions in the Monowave 300 was monitored internally by a ruby sensor fiber optic probe, unless otherwise specified. The microwave parameters were set to variable power, constant temperature, stirring on, and a fixed hold time. Separation of naphthalene and

dihydronaphthalene products was performed on a Varian Prostar HPLC chromatograph using a Varian Dynamax Microsorb 100-5 Si column.

2.4.2 Experimental procedures detailed in published papers

Characterization and conditions for the preparation of the following naphthalenes and dihydronaphthalenes, including syntheses and characterization of all precursors and spectral data, were previously published and can be found in the Supporting Information of Kocsis, L. S.; Benedetti, E.; Brummond, K. M. A Thermal Dehydrogenative Diels–Alder Reaction of Styrenes for the Concise Synthesis of Functionalized Naphthalenes. *Org. Lett.* **2012**, *14*, 4430-4433 (Figure 2.5). The characterization data of **1.146** and **1.147**, along with their ^{1}H and ^{13}C NMR spectra, are provided herein for ease of comparison with other experimental results.

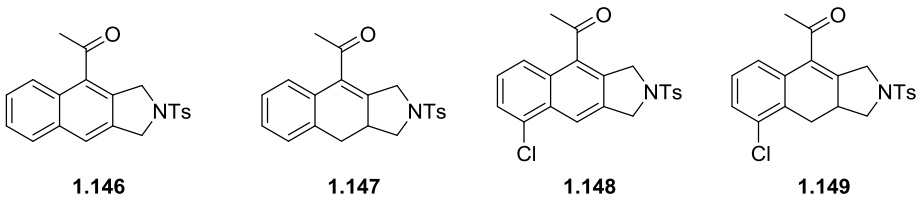

1.146 **1.147** **1.148** **1.149**

Figure 2.5. Previously published naphthalenes and dihydronaphthalenes. Syntheses and characterization can be found in *Org. Lett.* **2012**, *14*, 4430-4433.

2.4.3 Synthesis of styrene-ynes

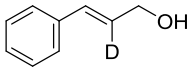

2.10

(*E*)-3-Phenylprop-2-en-2-*d*-1-ol (2.10). To a flame-dried two-neck 100 mL round-bottomed flask equipped with a condenser and a septum under an atmosphere of argon was added lithium aluminum deuteride (0.877 g, 20.9 mmol). The round-bottomed flask was evacuated and refilled with argon (3x), and THF (35 mL) was added via syringe with stirring. 3-Phenyl-2-propyn-1-ol **2.9** (2.0 mL, 16 mmol) in THF (5 mL) was then added slowly dropwise via syringe, and bubbling occurred along with a color change from dark to light grey. The reaction mixture was heated to reflux in an oil bath for 5 h, turning the reaction mixture brown, followed by cooling to rt then 0 °C in an ice bath. To quench the reaction, water was added *slowly* dropwise and vigorous bubbling occurred. Once bubbling had ceased and the reaction mixture had become white in color, diethyl ether was added and the aqueous layer was separated. The aqueous layer was then extracted with diethyl ether (2x), and the combined organic layers were washed with brine, dried over magnesium sulfate, gravity filtered, and concentrated under reduced pressure to yield the title compound as a clear oil (2.23 g, quant). The crude material was carried on without purification.

Data **2.10**

^{1}H NMR (500 MHz, $CDCl_3$)

7.39 (d, *J* = 7.5 Hz, 2H), 7.32 (t, *J* = 7.5 Hz, 2H), 7.26 (t, *J* = 7.5 Hz, 1H), 6.61 (s, 1H), 4.32 (s, 2H) ppm

^{13}C NMR (100 MHz, $CDCl_3$)

136.8, 131.2, 128.7 (2C), 128.3 (t, *J* = 24.0 Hz, 1C), 127.8 (2C), 126.6, 63.8 ppm

IR (thin film)

3338, 3080, 3059, 2919, 2863, 1600, 1493, 1449 cm^{-1}

HRMS (ESI)

$[M-H]^+$ calcd for C_9H_8DO: 134.0722, found 134.0711

TLC R_f = 0.4 (40% ethyl acetate/hexanes) [silica gel, UV]

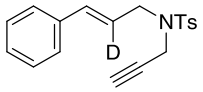

2.12

(*E*)-4-Methyl-*N*-(3-phenylallyl-2-*d*)-*N*-(prop-2-yn-1-yl)benzenesulfonamide (2.12). To a flame-dried two-neck 100 mL round-bottomed flask equipped with an argon inlet adapter and a septum was added (*E*)-3-phenylprop-2-en-2-*d*-1-ol (**2.10**) (1.00 g, 7.40 mmol), 4-methyl-*N*-(prop-2-yn-1-yl)benzenesulfonamide (**2.11**) (1.55 g, 7.40 mmol), and triphenylphosphine (1.94 g, 7.40 mmol). The round-bottomed flask was evacuated and refilled with argon (3x), and THF (69 mL) was added via syringe with stirring. Diisopropyl azodicarboxylate (1.46 mL, 7.40 mmol) was added dropwise via syringe, and the reaction mixture turned bright yellow in color. The reaction mixture was stirred at rt for 20 h, and was then concentrated under reduced pressure. The crude material was purified by silica gel flash column chromatography (5 cm column, 5-15% ethyl acetate/hexanes) to yield the title compound as a white solid (2.04 g, 85%). The preparation of 4-methyl-*N*-(prop-2-yn-1-yl)benzenesulfonamide (**2.11**) followed the procedure reported by Gilbertson.[78]

Data **2.12**

MP 74-75 °C

^{1}H NMR (300 MHz, $CDCl_3$)

7.77 (d, J = 8.1 Hz, 2H), 7.35-7.26 (m, 7H), 6.56 (s, 1H), 4.13 (d, J = 2.4 Hz, 2H), 3.99 (s, 2H), 2.44 (s, 3H), 2.04 (t, J = 2.4 Hz, 1H) ppm

^{13}C NMR (100 MHz, $CDCl_3$)

143.7, 136.2 (2C), 134.9, 129.6 (2C), 128.7 (2C), 128.2, 127.9 (2C), 126.7 (2C), 122.7 (t, J = 24.0 Hz, 1C), 76.8, 74.0, 48.6, 36.0, 21.7 ppm

IR (thin film)

3026, 2921, 2119, 1598, 1495, 1348, 1162 cm^{-1}

HRMS (ESI)

$[M + H]^+$ calcd for $C_{19}H_{19}DO_2NS$: 327.1278, found 327.1269

TLC R_f = 0.5 (25% ethyl acetate/hexanes) [silica gel, UV]

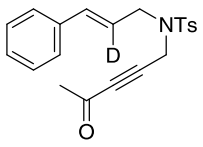

2.14

(*E*)-4-Methyl-*N*-(4-oxopent-2-yn-1-yl)-*N*-(3-phenylallyl-2-*d*)benzenesulfonamide (2.14). To a flame-dried two-neck 15 mL round-bottomed flask equipped with an argon inlet adapter and a septum was added enyne **2.12** (0.112 g, 0.34 mmol) in THF (7.8 mL). The solution was cooled to -78 °C in a dry ice-acetone bath, and then lithium diisopropylamide (0.17 mL of a 2.0 M solution in THF/heptanes/ethylbenzene, 0.34 mmol) was added slowly dropwise via syringe, turning the reaction mixture dark purple. The reaction mixture was stirred at -78 °C for 1 h and became green in color. *N*-Methoxy-*N*-methylacetamide (**2.13**) (33 μL, 0.31 mmol) was subsequently added via syringe and the reaction mixture turned light purple. The reaction mixture was stirred at -78 °C for 15 min and at rt for 1.5 h, and overtime the color became a dark brown. The reaction mixture was poured into brine, and sat'd aq ammonium chloride was added. The

aqueous layer was separated and extracted with ethyl acetate (2x), and the combined organic layers were washed with brine, dried over magnesium sulfate, gravity filtered, and concentrated under reduced pressure. The crude material was purified by silica gel flash column chromatography (2.5 cm column, 15% ethyl acetate/hexanes) to yield the title compound as a light yellow solid (0.052 g, 46%).

Data **2.14**

MP 93-94 °C

^{1}H NMR (400 MHz, $CDCl_3$)

7.76 (d, *J* = 8.0 Hz, 2H), 7.35-7.24 (m, 7H), 6.55 (s, 1H), 4.27 (s, 2H), 3.99 (s, 2H), 2.43 (s, 3H), 2.10 (s, 3H) ppm

^{13}C NMR (100 MHz, $CDCl_3$)

183.3, 144.2, 135.9, 135.7, 135.4, 129.9 (2C), 128.8 (2C), 128.4, 127.9 (2C), 126.7 (2C), 122.2 (t, *J* = 24.0 Hz, 1C), 84.9, 84.4, 49.3, 36.2, 32.4, 21.6 ppm

IR (thin film)

3026, 2921, 2210, 1679, 1597, 1495, 1350, 1163 cm^{-1}

HRMS (ESI)

$[M + H]^+$ calcd for $C_{21}H_{21}DO_3NS$: 369.1374, found 369.1383

TLC R_f = 0.3 (25% ethyl acetate/hexanes) [silica gel, UV]

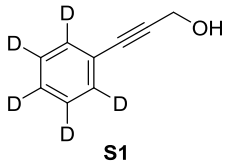

S1

3-(Phenyl-*d*5)prop-2-yn-1-ol (S1). To a flame-dried two-neck 50 mL round-bottomed flask equipped with an argon inlet adapter and a septum was added bromobenzene-d_5 (**2.15**) (1.30 mL,

12.3 mmol) and water (62 mL). Propargyl alcohol (**2.16)** (1.1 mL, 19 mmol), pyrrolidine (1.52 mL, 18.5 mmol), tetrakis(triphenylphosphine)palladium(0) (0.071 g, 0.062 mmol), and copper(I) iodide (0.023 g, 0.12 mmol) were added sequentially. The reaction mixture was stirred at 70 °C for 1 h, turning the reaction mixture from yellow to light green. The reaction mixture was then cooled to rt and diethyl ether was added. The aqueous layer was separated and extracted with diethyl ether (2x), and the combined organic layers were washed with water and brine, dried over magnesium sulfate, gravity filtered, and concentrated under reduced pressure. The crude material was filtered through a pad of silica gel with diethyl ether washings, and then was placed under high vacuum to yield the title compound as a yellow oil (0.844 g, 50%.). Characterization data is consistent with previously reported literature data.[79]

Data **S1**

^{1}H NMR (300 MHz, $CDCl_3$)

4.51 (s, 2H), 1.64 (bs, 1H) ppm

TLC R_f = 0.3 (20% ethyl acetate/hexanes) [silica gel, UV]

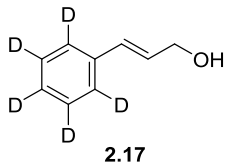

2.17

(*E*)-3-(Phenyl-*d*5)prop-2-en-1-ol (2.17). To a flame-dried two-neck 15 mL round-bottomed flask equipped with a condenser and a septum under an atmosphere of argon was added lithium aluminum hydride (0.164 g, 4.33 mmol). The round-bottomed flask was evacuated and refilled with argon (3x), and THF (7.2 mL) was added via syringe with stirring. 3-(Phenyl-*d*5)prop-2-yn-1-ol (**S1**) (0.457 g, 3.33 mmol) in THF (1.1 mL) was then added slowly dropwise via syringe, and bubbling occurred. The reaction mixture was heated to reflux in an oil bath for 1 h, turning

the reaction mixture from light grey to light brown, followed by cooling to rt then 0 °C in an ice bath. To quench the reaction, water was added *slowly* dropwise and vigorous bubbling occurred. Once bubbling had ceased and the reaction mixture had become white in color, diethyl ether was added and the aqueous layer was separated. The aqueous layer was then extracted with diethyl ether (4x), and the combined organic layers were washed with brine, dried over magnesium sulfate, gravity filtered, and concentrated under reduced pressure to yield the title compound as an amber oil (0.257 g, 56%). The crude material was carried on without purification.

Data **2.17**

^{1}H NMR (300 MHz, $CDCl_3$)

6.63 (d, J = 15.9 Hz, 1H), 6.37 (dt, J = 15.9, 5.4 Hz, 1H), 4.33 (d, J = 5.4 Hz, 2H), 1.55 (bs, 1H) ppm

TLC R_f = 0.2 (20% ethyl acetate/hexanes) [silica gel, UV]

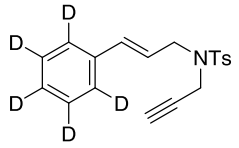

2.18

(*E*)-4-Methyl-*N*-(3-(phenyl-*d*5)allyl)-*N*-(prop-2-yn-1-yl)benzenesulfonamide (2.18). To a flame-dried two-neck 25 mL round-bottomed flask equipped with an argon inlet adapter and a septum was added (*E*)-3-(phenyl-*d*5)prop-2-en-1-ol (**2.17**) (0.253 g, 1.82 mmol), 4-methyl-*N*-(prop-2-yn-1-yl)benzenesulfonamide (**2.11**) (0.381 g, 1.82 mmol), and triphenylphosphine (0.478 g, 1.82 mmol). The round-bottomed flask was evacuated and refilled with argon (3x), and THF (17 mL) was added via syringe with stirring. Diisopropyl azodicarboxylate (0.36 mL, 1.82 mmol) was added dropwise via syringe, and the reaction mixture turned bright yellow in color.

The reaction mixture was stirred at rt for 16 h, and was then concentrated under reduced pressure. The crude material was purified by silica gel flash column chromatography (2.5 cm column, 15% ethyl acetate/hexanes) to yield the title compound as an off-white solid (0.517 g, 86%).

Data **2.18**

MP 69-71 °C

^{1}H NMR (300 MHz, $CDCl_3$)

7.77 (dd, *J* = 8.4, 1.8 Hz, 2H), 7.31 (d, *J* = 8.4 Hz, 2H), 6.58 (td, *J* = 15.9, 1.2 Hz, 1H), 6.08 (dt, *J* = 15.9, 6.9 Hz, 1H), 4.13 (d, *J* = 2.4 Hz, 2H), 3.99 (dd, *J* = 6.9, 1.2 Hz, 2H), 2.44 (s, 3H), 2.04 (t, *J* = 1.2 Hz, 1H) ppm

^{13}C NMR (100 MHz, $CDCl_3$)

143.7, 136.2, 136.1, 135.0, 129.6 (2C), 128.5-127.5 (m, 5C), 126.2 (t, *J* = 24.0 Hz, 2C), 123.0, 76.7, 73.9, 48.7, 36.0, 21.7 ppm

IR (thin film)

3289, 3034, 2923, 2276, 2118, 1598, 1494, 1346, 1161 cm^{-1}

HRMS (ESIMSMS)

$[M + H]^+$ calcd for $C_{19}H_{15}D_5O_2NS$: 331.1518, found 331.1529

TLC R_f = 0.5 (25% ethyl acetate/hexanes) [silica gel, UV]

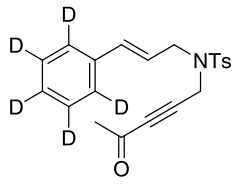

2.19

(*E*)-4-Methyl-*N*-(4-oxopent-2-yn-1-yl)-*N*-(3-(phenyl-*d*5)allyl)benzenesulfonamide (2.19). To a flame-dried two-neck 25 mL round-bottomed flask equipped with an argon inlet adapter and a septum was added enyne **2.18** (0.200 g, 0.61 mmol) in THF (14 mL). The solution was cooled to -78 °C in a dry ice-acetone bath, and then lithium diisopropylamide (0.30 mL of a 2.0 M solution in THF/heptanes/ethylbenzene, 0.61 mmol) was added slowly dropwise via syringe, turning the reaction mixture dark purple. The reaction mixture was stirred at -78 °C for 80 min and became light yellow. *N*-Methoxy-*N*-methylacetamide (**2.13**) (58 μL, 0.55 mmol) was subsequently added dropwise via syringe and the reaction mixture was stirred at -78 °C for 15 min and at rt for 1 h. Over time, the color of the reaction mixture turned reddish in color. The reaction mixture was quenched with sat'd aq ammonium chloride, and the aqueous layer was separated and extracted with ethyl acetate (2x). The combined organic layers were washed with brine, dried over magnesium sulfate, gravity filtered, and concentrated under reduced pressure. The crude material was purified by silica gel flash column chromatography (2.5 cm column, 15% ethyl acetate/hexanes) to yield the title compound as a white solid (0.163 g, 80%).

Data **2.19**

MP 84-86 °C

^{1}H NMR (300 MHz, $CDCl_3$)

7.77 (d, *J* = 8.2 Hz, 2H), 7.34 (d, *J* = 8.2 Hz, 2H), 6.57 (d, *J* = 15.9 Hz, 1H), 6.08 (dt, *J* = 15.9, 6.9 Hz, 1H), 4.27 (s, 2H), 4.00 (dd, *J* = 6.9, 0.9 Hz, 2H), 2.44 (s, 3H), 2.10 (s, 3H) ppm

^{13}C NMR (100 MHz, $CDCl_3$)

183.3, 144.2, 135.8 (2C), 135.4, 129.9 (2C), 128.5-127.6 (m, 5C), 126.3 (t, J = 24.0 Hz, 2C), 122.5, 84.9, 84.4, 49.4, 36.2, 32.4, 21.6 ppm

IR (thin film)

3031, 2922, 2246, 2209, 1670, 1597, 1494, 1349, 1163 cm^{-1}

HRMS (ESIMSMS)

$[M + H]^+$ calcd for $C_{21}H_{17}D_5O_3NS$: 373.1622, found 373.1634

TLC R_f = 0.3 (25% ethyl acetate/hexanes) [silica gel, UV]

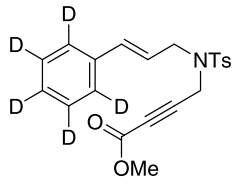

2.20

Methyl (*E*)-4-((4-methyl-*N*-(3-(phenyl-*d*5)allyl)phenyl)sulfonamido)but-2-ynoate (2.20). To a flame-dried two-neck 5 mL round-bottomed flask equipped with an argon inlet adapter and a septum was added enyne **2.18** (0.100 g, 0.30 mmol) in THF (1.5 mL). The solution was cooled to -78 °C in a dry ice-acetone bath, and then *n*-butyllithium (0.21 mL of a 1.6 M solution hexanes, 0.33 mmol) was added slowly dropwise via syringe, turning the reaction mixture dark purple. The reaction mixture was stirred at -78 °C for 45 min and became light brown. Methyl chloroformate (30 μL, 0.39 mmol) was subsequently added dropwise via syringe and the reaction mixture was stirred at -78 °C for 1 h, becoming darker brown over time. The reaction mixture was allowed to warm slowly to -10 °C and sat'd aq ammonium chloride was added. The aqueous layer was separated and extracted with ethyl acetate (2x), and the combined organic layers were washed with brine, dried over magnesium sulfate, gravity filtered, and concentrated under

reduced pressure. The crude material was purified by silica gel flash column chromatography (2.5 cm column, 10% ethyl acetate/hexanes) to yield the title compound as a clear oil (0.065 g, 55%).

Data **2.20**

^{1}H NMR (400 MHz, $CDCl_3$)

7.76 (d, *J* = 8.2 Hz, 2H), 7.33 (d, *J* = 8.2 Hz, 2H), 6.58 (td, *J* = 16.0, 1.2 Hz, 1H), 6.07 (dt, *J* = 16.0, 6.8 Hz, 1H), 4.24 (s, 2H), 3.98 (dd, *J* = 6.8, 0.8 Hz, 2H), 3.71 (s, 3H), 2.44 (s, 3H) ppm

^{13}C NMR (125 MHz, $CDCl_3$)

153.2, 144.2, 135.9, 135.6 (2C), 129.9 (2C), 128.5-127.8 (m, 5C), 126.3 (t, *J* = 24.0 Hz, 2C), 122.6, 80.8 (2C), 52.9, 49.4, 36.1, 21.7 ppm

IR (thin film)

2954, 2240, 1717, 1597, 1435, 1258, 1162 cm^{-1}

HRMS (ESI)

$[M + H]^+$ calcd for $C_{21}H_{17}D_5O_4NS$: 389.1556, found 389.1583

TLC R_f = 0.3 (25% ethyl acetate/hexanes) [silica gel, UV]

2.4.4 General microwave irradiation procedure

To a microwave irradiation vial was added styrene-yne and the reaction solvent. The solution was irradiated at 180 °C for 1 min, followed by concentration of the reaction mixture under high vacuum. The crude material was purified by silica gel column chromatography to yield the naphthalene and/or dihydronaphthalene as a solid. Mixtures of products were separated for characterization by HPLC with a Varian Prostar HPLC chromatograph using 10% ethyl

acetate/hexanes as the eluent and a flow rate of 4 mL/min on a Varian Dynamax Microsorb 100-5 Si column. Experiments conducted under argon involved initial degassing of the starting solution by bubbling with argon through the septum of the microwave irradiation vial for 30 min prior to irradiation.

2.4.5 Conventional heating experiment

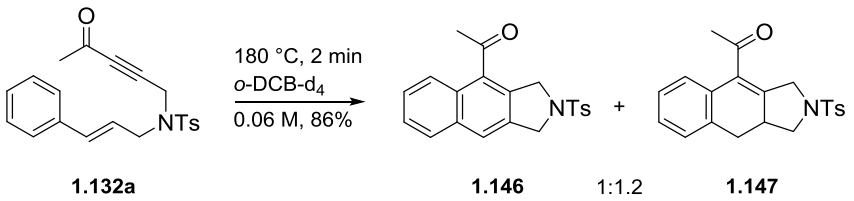

1.132a **1.146** 1:1.2 **1.147**

1-(2-Tosyl-2,3-dihydro-1*H*-benzo[*f*]isoindol-4-yl)ethan-1-one (1.146) and 1-(2-Tosyl-2,3,9,9a-tetrahydro-1*H*-benzo[*f*]isoindol-4-yl)ethan-1-one (**1.147**). To a sealed NMR tube was added styrene-yne **1.132a** (0.013 g, 0.036 mmol), *o*-DCB-d_4 (0.55 mL), and a solution of *p*-dimethoxybenzene in *o*-DCB-d_4 (50 μL, 0.002 g) as an internal standard. A ^{1}H NMR spectrum of the starting solution was obtained. The solution was then heated at 180 °C for 2 min in an oil bath, turning the reaction mixture brown in color. A ^{1}H NMR spectrum of the reaction mixture was obtained showing conversion of the starting material **1.132a** to the products **1.146** and **1.147** as a 1:1.2 mixture in 86% combined yield. Both **1.146** and **1.147** were previously characterized.[64]

The ^{1}H NMR spectrum of the products also showed the presence of H_2 in solution as a singlet integrating for 0.05H at 4.73 ppm, which indicated an 11:1 ratio of **1.146**:H_2. To confirm that this corresponded to H_2, H_2 was bubbled through the reaction mixture and another ^{1}H NMR spectrum was obtained, showing an increase in the integration of the resonance corresponding to

the H_2 to 0.09H, representing a 6:1 ratio of **1.146**:H_2. Argon was then bubbled through the reaction mixture and the resonance corresponding to H_2 disappeared (see Scheme 2.14).

Data **1.146**

^{1}H NMR (400 MHz, $CDCl_3$)

7.85-7.79 (m, 4H), 7.70 (s, 1H), 7.54-7.47 (m, 2H), 7.32 (d, *J* = 8.2 Hz, 2H), 4.73 (s, 2H), 4.70 (s, 2H), 2.66 (s, 3H), 2.39 (s, 3H) ppm

^{13}C NMR (100 MHz, $CDCl_3$)

204.1, 144.1, 134.9, 133.8, 133.6, 133.3, 133.0, 130.1 (2C), 129.1, 128.7, 127.9 (2C), 127.4, 126.6, 124.8, 123.8, 53.0, 52.9, 32.1, 21.7 ppm

Data **1.147**

^{1}H NMR (400 MHz, $CDCl_3$)

7.75 (d, *J* = 8.2 Hz, 2H), 7.34 (d, *J* = 8.2 Hz, 2H), 7.24-7.16 (m, 3H), 7.09 (d, *J* = 6.9 Hz, 1H), 4.53 (dd, *J* = 18.0, 1.6 Hz, 1H), 3.95 (dd, *J* = 9.4, 8.2 Hz, 1H), 3.90 (dd, *J* = 18.0, 2.8 Hz, 1H), 3.02-2.93 (m, 1H), 2.86 (app t, *J* = 9.2 Hz, 1H), 2.82 (dd, *J* = 14.8, 6.4 Hz, 1H), 2.51 (app t, *J* = 14.8 Hz, 1H), 2.44 (s, 3H), 2.34 (s, 3H) ppm

^{13}C NMR (100 MHz, $CDCl_3$)

200.9, 148.1, 144.0, 134.7, 133.1, 132.1 (2C), 130.0 (2C), 128.2, 128.1, 128.0 (2C), 127.3, 125.8, 53.1, 51.8, 40.2, 32.4, 30.2, 21.7 ppm

2.4.6 Irradiation of 1.132a in DMF-d_7

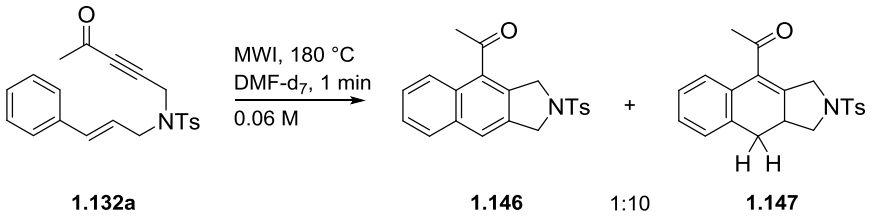

1.132a **1.146** 1:10 **1.147**

1-(2-Tosyl-2,3-dihydro-1*H*-benzo[*f*]isoindol-4-yl)ethan-1-one (1.146) and 1-(2-Tosyl-2,3,9,9a-tetrahydro-1*H*-benzo[*f*]isoindol-4-yl)ethan-1-one (**1.147**). To a G4 Anton-Paar microwave irradiation vial was added styrene-yne **1.132a** (0.020 g, 0.054 mmol) and DMF-d_7 (0.91 mL). The solution was irradiated at 180 °C for 1 min, turning the reaction mixture orange in color. The reaction mixture was then concentrated under high vacuum and the crude material purified by silica gel flash column chromatography (1.5 cm, 20% ethyl acetate/hexanes) to yield the title compounds as a white solid and as a 1:10 mixture of **1.146**:**1.147** (0.015 g, 75%). These products were separated for characterization by HPLC, utilizing 10% ethyl acetate/hexanes as the eluent and a flow rate of 4 mL/min. The HPLC retention time of naphthalene **1.146** was 34.2 min and the retention time of dihydronaphthalene **1.147** was 38.2 min. A ^{1}H NMR spectrum of the dihydronaphthalene product **1.147** showed no deuterium incorporation. Both **1.146** and **1.147** were previously characterized.[64]

2.4.7 Irradiation of 1.132a in presence of 1,4-cyclohexadiene

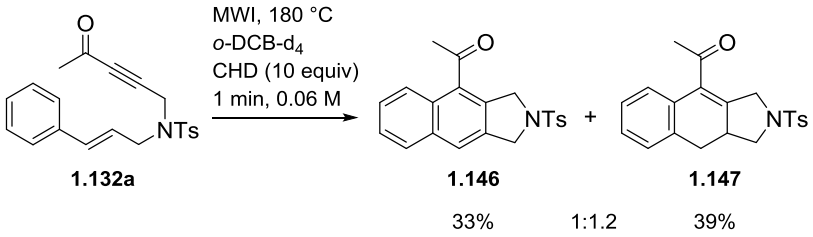

1-(2-Tosyl-2,3-dihydro-1*H*-benzo[*f*]isoindol-4-yl)ethan-1-one (1.146) and 1-(2-Tosyl-2,3,9,9a-tetrahydro-1*H*-benzo[*f*]isoindol-4-yl)ethan-1-one (**1.147**). To a NMR tube was added styrene-yne **1.132a** (0.013 g, 0.036 mmol), *o*-DCB-d_4 (0.55 mL), and a solution of *p*-dimethoxybenzene in *o*-DCB-d_4 (50 μL, 0.002 g) as an internal standard. A ^{1}H NMR spectrum of the solution was obtained, followed by transfer of the solution to a G4 Anton-Paar microwave irradiation vial and addition of 1,4-cyclohexadiene (34 μL, 0.36 mmol). The solution was then irradiated at 180 °C for 1 min, turning the reaction mixture light brown in color. The reaction mixture was then transferred to an NMR tube, and a ^{1}H NMR spectrum was obtained showing conversion of the starting material **1.132a** to the title compounds **1.146** and **1.147** as a 1:1.2 mixture in 72% combined yield as determined by ^{1}H NMR spectroscopy. Naphthalene **1.146** and dihydronaphthalene **1.147** were previously characterized.[64]

2.4.8 Irradiation of 1.132a in the presence of TEMPO

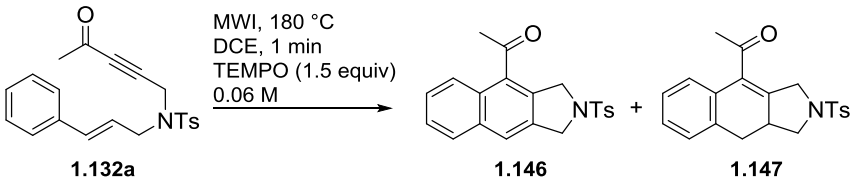

1.132a **1.146** **1.147**

52% 0%

1-(2-Tosyl-2,3-dihydro-1*H*-benzo[*f*]isoindol-4-yl)ethan-1-one (1.146). To a 0.5-2 mL Biotage microwave irradiation vial was added styrene-yne **1.132a** (0.022 g, 0.060 mmol), DCE (1.0 mL), and (2,2,6,6-tetramethylpiperidin-1-yl)oxy (0.014 g, 0.090 mmol). The solution was then irradiated at 180 °C for 1 min, turning the reaction mixture dark brown in color. The reaction mixture was concentrated under reduced pressure and the crude material purified by silica gel flash column chromatography (10% ethyl acetate hexanes) to yield the title compound as a light yellow solid (0.011 g, 52%). Naphthalene **1.146** was previously characterized.[64]

2.4.9 Irradiation of 2.14 in *o*-DCB-d_4

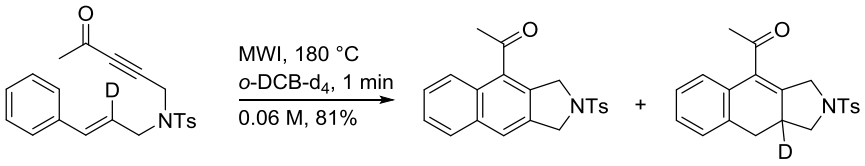

2.14 **1.146** 1:5.2 **2.21**

1-(2-Tosyl-2,3-dihydro-1*H*-benzo[*f*]isoindol-4-yl)ethan-1-one (1.146) and 1-(2-tosyl-2,3,9,9a-tetrahydro-1*H*-benzo[*f*]isoindol-4-yl-9a-*d*)ethan-1-one (2.21). To a NMR tube was added the styrene-yne **2.14** (0.013 g, 0.036 mmol), *o*-DCB-d_4 (0.60 mL), and a solution of *p*-dimethoxybenzene in *o*-DCB-d_4 (50 μL, 0.002 g) as an internal standard. A ^{1}H NMR spectrum of the solution was obtained, followed by transfer of the solution to a G4 Anton-Paar microwave

irradiation vial which was irradiated at 180 °C for 1 min, turning the reaction mixture brown in color. The reaction mixture was then transferred to an NMR tube, and a ^{1}H NMR spectrum was obtained showing conversion of the starting material **2.14** to the products **1.146** and **2.21** as a 1:5.2 mixture in 81% combined yield as determined by ^{1}H NMR spectroscopy. The reaction mixture was then concentrated under high vacuum and a portion of the mixture was separated by HPLC for characterization, utilizing 10% ethyl acetate/hexanes as the eluent and a flow rate of 4 mL/min. Naphthalene **1.146** was previously characterized and its HPLC retention time was 33.9 min.[64]

Data **2.21**

HPLC 38.2 min retention time

MP 154-156 °C

^{1}H NMR (400 MHz, $CDCl_3$)

7.75 (d, *J* = 8.0 Hz, 2H), 7.34 (d, *J* = 8.0 Hz, 2H), 7.26-7.18 (m, 3H), 7.09 (dd, *J* = 6.8, 2.0 Hz, 1H), 4.52 (d, *J* = 18.0 Hz, 1H), 3.94 (d, *J* = 9.6 Hz, 1H), 3.90 (d, *J* = 18.0 Hz, 1H), 2.86 (d, *J* = 9.6 Hz, 1H), 2.81 (d, *J* = 14.6 Hz, 1H), 2.51 (d, *J* = 14.6 Hz, 1H), 2.43 (s, 3H), 2.34 (s, 3H) ppm

^{13}C NMR (125 MHz, $CDCl_3$)

200.9, 147.9, 144.0, 134.7, 133.2 (2C), 132.2, 130.0 (2C), 128.3, 128.1, 128.0 (2C), 127.3, 125.8, 53.0, 51.8, 39.8 (t, *J* = 20 Hz, 1C), 32.4, 30.2, 21.7 ppm

IR (thin film)

3059, 2925, 2255, 1682, 1622, 1598, 1347, 1163 cm^{-1}

HRMS (ESI)

$[M + H]^+$ calcd for $C_{21}H_{21}DO_3NS$: 369.1383, found 369.1370

TLC R_f = 0.5 (35% ethyl acetate/hexanes) [silica gel, UV]

2.4.10 Irradiation of 2.19 in *o*-DCB-d_4

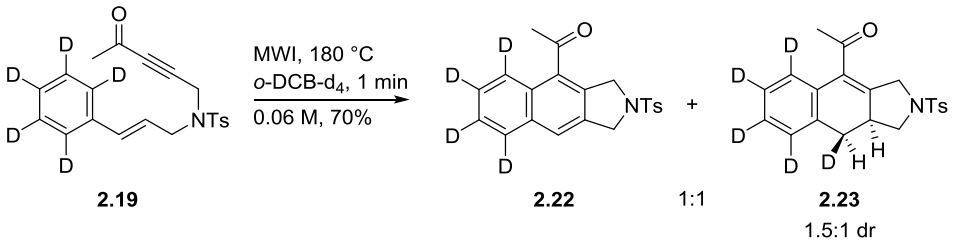

1-(2-Tosyl-2,3-dihydro-1*H*-benzo[*f*]isoindol-4-yl-5,6,7,8-*d*4)ethan-1-one (2.22) and 1-(2-tosyl-2,3,9,9a-tetrahydro-1*H*-benzo[*f*]isoindol-4-yl-5,6,7,8,9-*d*5)ethan-1-one (2.23). To a NMR tube was added the styrene-yne **2.19** (0.013 g, 0.036 mmol), *o*-DCB-d_4 (0.60 mL), and a solution of *p*-dimethoxybenzene in *o*-DCB-d_4 (50 μL, 0.002 g) as an internal standard. A ^{1}H NMR spectrum of the solution was obtained, followed by transfer of the solution to a G4 Anton-Paar microwave irradiation vial which was irradiated at 180 °C for 1 min. The reaction mixture was then transferred to an NMR tube, and a ^{1}H NMR spectrum was obtained showing conversion of the starting material **2.19** to the products **2.22** and **2.23** as a 1:1 mixture in 70% combined yield as determined by ^{1}H NMR spectroscopy. The reaction mixture was then concentrated under high vacuum and a portion of the mixture was separated by HPLC for characterization, utilizing 10% ethyl acetate/hexanes as the eluent and a flow rate of 4 mL/min. Dihydronaphthalene **2.23** was formed as a 1.5:1 ratio of diastereomers, as evidenced by ^{1}H NMR spectroscopy after chromatography (major diastereomer shown). The diastereomers were not separable by HPLC.

Data **2.22**

HPLC 35.0 min retention time

MP 134-136 °C

^{1}H NMR (300 MHz, $CDCl_3$)

7.81 (d, *J* = 8.1 Hz, 2H), 7.72 (s, 1H), 7.33 (d, *J* = 8.1 Hz, 2H), 4.74 (s, 2H), 4.72 (s, 2H), 2.67 (s, 3H), 2.40 (s, 3H) ppm

^{13}C NMR (125 MHz, $CDCl_3$)

204.0, 144.1, 134.9, 133.7, 133.5, 133.3, 133.0, 130.1, 129.0 (2C), 128.3 (t, *J* = 24.3 Hz, 1C), 127.9 (2C), 126.9 (t, *J* = 24.3 Hz, 1C), 126.1 (t, *J* = 24.3 Hz, 1C), 124.3 (t, *J* = 24.3 Hz, 1C), 123.8, 53.0, 52.9, 32.1, 21.7 ppm

IR (thin film)

2926, 2258, 1685, 1597, 1461, 1346, 1163 cm^{-1}

HRMS (ESI)

$[M + H]^+$ calcd for $C_{21}H_{16}D_4O_3NS$: 370.1415, found 370.1404

TLC R_f = 0.5 (35% ethyl acetate/hexanes) [silica gel, UV]

Data **2.23**

HPLC 38.8 min retention time

MP 159-160 °C

^{1}H NMR (400 MHz, $CDCl_3$)

7.75 (d, *J* = 8.0 Hz, 2H), 7.34 (d, *J* = 8.0 Hz, 2H), 4.53 (dd, *J* = 18.0, 1.6 Hz, 1H), 3.95 (dd, *J* = 9.6, 8.4 Hz, 1H), 3.90 (dd, *J* = 18.0, 2.8 Hz, 1H), 3.01-2.93 (m, 1H), 2.85 (app t, *J* = 9.6 Hz, 1H), 2.80 (d, *J* = 6.4, 0.69H), 2.49 (d, *J* = 14.8 Hz, 0.47H), 2.43 (s, 3H), 2.34 (s, 3H) ppm

^{13}C NMR (175 MHz, $CDCl_3$)

200.9, 148.1, 144.0, 134.5, 133.1 (2C), 132.0, 130.0 (2C), 128.0 (2C), 127.8-127.4 (m, 2C), 126.7 (t, J = 24.0 Hz, 1C), 125.4 (t, J = 24.0 Hz, 1C), 53.1, 51.8, 40.2, 32.0 (t, J = 19.3 Hz, 1C), 30.2, 21.7 ppm

IR (thin film)

2925, 2255, 1682, 1598, 1494, 1346, 1162 cm^{-1}

HRMS (ESI)

$[M + H]^+$ calcd for $C_{21}H_{17}D_5O_3NS$: 373.1634, found 373.1621

TLC R_f = 0.5 (35% ethyl acetate/hexanes) [silica gel, UV]

2.4.11 Irradiation of 2.19 in DMF

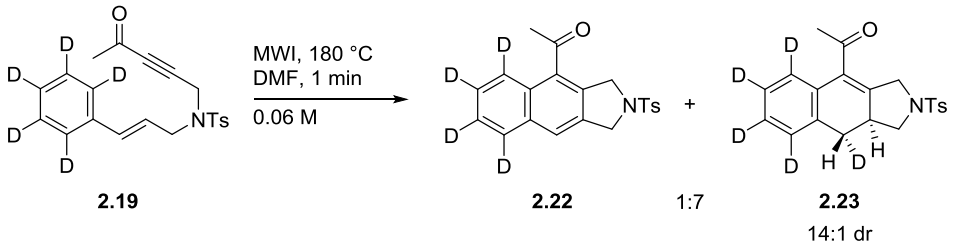

1-(2-Tosyl-2,3-dihydro-1*H*-benzo[*f*]isoindol-4-yl-5,6,7,8-*d*4)ethan-1-one (2.22) and 1-(2-tosyl-2,3,9,9a-tetrahydro-1*H*-benzo[*f*]isoindol-4-yl-5,6,7,8,9-*d*5)ethan-1-one (2.23). To a G4 Anton-Paar microwave irradiation vial was added styrene-yne **2.19** (0.015 g, 0.040 mmol) and DMF (0.67 mL). The solution was irradiated at 180 °C for 1 min and became orange in color. The temperature of the reaction was monitored by IR sensor (no ruby sensor probe). The reaction mixture was then concentrated under high vacuum, and a ^{1}H NMR spectrum of the crude material was obtained which showed a 1:7 mixture of **2.22** and **2.23**. Purification by silica gel flash column chromatography (10% ethyl acetate/hexanes) yielded the mixture as a white solid (0.013 g). The mixture was then separated by HPLC for characterization, utilizing 10% ethyl

acetate/hexanes as the eluent and a flow rate of 4 mL/min. Dihydronaphthalene **2.23** was formed as a 14:1 ratio of diastereomers (major diastereomer shown), as evidenced by ^{1}H NMR spectroscopy after chromatography. The diastereomers were not separable by HPLC.

Data **2.23**

^{1}H NMR (400 MHz, $CDCl_3$)

7.75 (d, *J* = 8.2 Hz, 2H), 7.34 (d, *J* = 8.2 Hz, 2H), 4.53 (dd, *J* = 18.0, 1.6 Hz, 1H), 3.95 (dd, *J* = 9.6, 8.8 Hz, 1H), 3.90 (dd, *J* = 18.0, 2.8 Hz, 1H), 3.00-2.90 (m, 1H), 2.85 (app t, *J* = 9.6 Hz, 1H), 2.80 (d, *J* = 6.4 Hz, 0.07H), 2.49 (d, *J* = 15.2 Hz, 0.95H), 2.43 (s, 3H), 2.34 (s, 3H) ppm

2.4.12 Irradiation of 2.20 in o-DCB-d_4

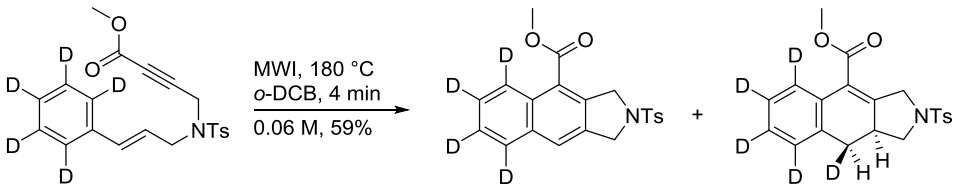

Methyl 2-tosyl-2,3-dihydro-1*H*-benzo[*f*]isoindole-4-carboxylate-5,6,7,8-*d*4 (2.25) and methyl 2-tosyl-2,3,9,9a-tetrahydro-1*H*-benzo[*f*]isoindole-4-carboxylate-5,6,7,8,9-*d*5 (2.26). To a G4 Anton-Paar microwave irradiation vial was added styrene-yne **2.20** (0.022 g, 0.057 mmol) and *o*-DCB (0.95 mL). The solution was irradiated at 180 °C for 4 min and became orange/brown in color. The temperature in this experiment was monitored by IR sensor (no ruby sensor probe). The reaction mixture was then concentrated under high vacuum, and a ^{1}H NMR of the crude material was obtained which showed a 1:1.1 mixture of **2.25** of **2.26**. Purification by silica gel flash column chromatography (1.5 cm column, 10-15% ethyl acetate/hexanes) yielded the

mixture as a white solid (0.013 g, 59%). The mixture was then separated by HPLC for characterization, utilizing 10% ethyl acetate/hexanes as the eluent and a flow rate of 4 mL/min. Dihydronaphthalene **2.26** was formed as a 2.6:1 ratio of diastereomers, as evidenced by ^{1}H and ^{2}H NMR spectroscopy after chromatography (major diastereomer shown). The diastereomers were not separable by HPLC.

Data **2.25**

HPLC 27.3 min retention time

MP 193-195 °C

^{1}H NMR (300 MHz, $CDCl_3$)

7.80 (d, J = 8.1 Hz, 2H), 7.76 (s, 1H), 7.32 (d, J = 8.1 Hz, 2H), 4.92 (s, 2H), 4.74 (d, J = 0.9 Hz, 2H), 4.03 (s, 3H), 2.39 (s, 3H) ppm

^{13}C NMR (175 MHz, $CDCl_3$)

167.4, 144.0, 138.3, 134.6, 133.6, 133.4, 130.1, 128.1-127.8 (m, 3C), 127.3 (t, J = 22.2 Hz, 1C), 126.1 (t, J = 22.2 Hz, 1C), 125.7 (2C), 125.4 (t, J = 22.2 Hz, 1C), 54.8, 52.9, 52.5, 21.7 ppm

HRMS (ESI)

$[M + H]^+$ calcd for $C_{21}H_{16}D_4O_4NS$: 386.13586, found 386.13791

TLC R_f = 0.2 (15% ethyl acetate/hexanes) [silica gel, UV]

Data **2.26**

HPLC 28.7 min retention time

MP 148-150 °C

^{1}H NMR (300 MHz, $CDCl_3$)

7.76 (d, *J* = 8.1 Hz, 2H), 7.35 (d, *J* = 8.1 Hz, 2H), 4.68 (dd, *J* = 18.6, 1.5 Hz, 1H), 4.07 (dd, *J* = 18.6, 3.0 Hz, 1H), 3.99 (dd, *J* = 9.3, 9.3 Hz, 1H), 3.86 (s, 3H), 3.07-2.94 (m, 1H), 2.83-2.75 (m, 1.9H), 2.52-2.42 (m, 3.4H) ppm

^{2}H NMR (300 MHz, $CHCl_3$)

7.22-6.82 (m, 4H), 2.41 (s, 0.17 H), 2.08 (s, 0.44 H)

^{13}C NMR (175 MHz, $CDCl_3$)

166.2, 152.8, 144.1, 134.1, 132.8, 130.0 (2C), 128.0 (2C), 127.5-127.2 (m, 2C), 126.8-126.2 (m, 2C), 123.4, 53.4, 52.8, 52.0, 40.7, 31.6 (t, *J* = 19.0 Hz, 1C), 29.8 (grease), 22.8 (hexanes), 21.7, 14.3 (hexanes) ppm

HRMS (ESI)

$[M + H]^+$ calcd for $C_{21}H_{17}D_5O_4NS$: 389.15779, found 389.15740

TLC R_f = 0.2 (15% ethyl acetate/hexanes) [silica gel, UV]

2.4.13 Crossover experiment

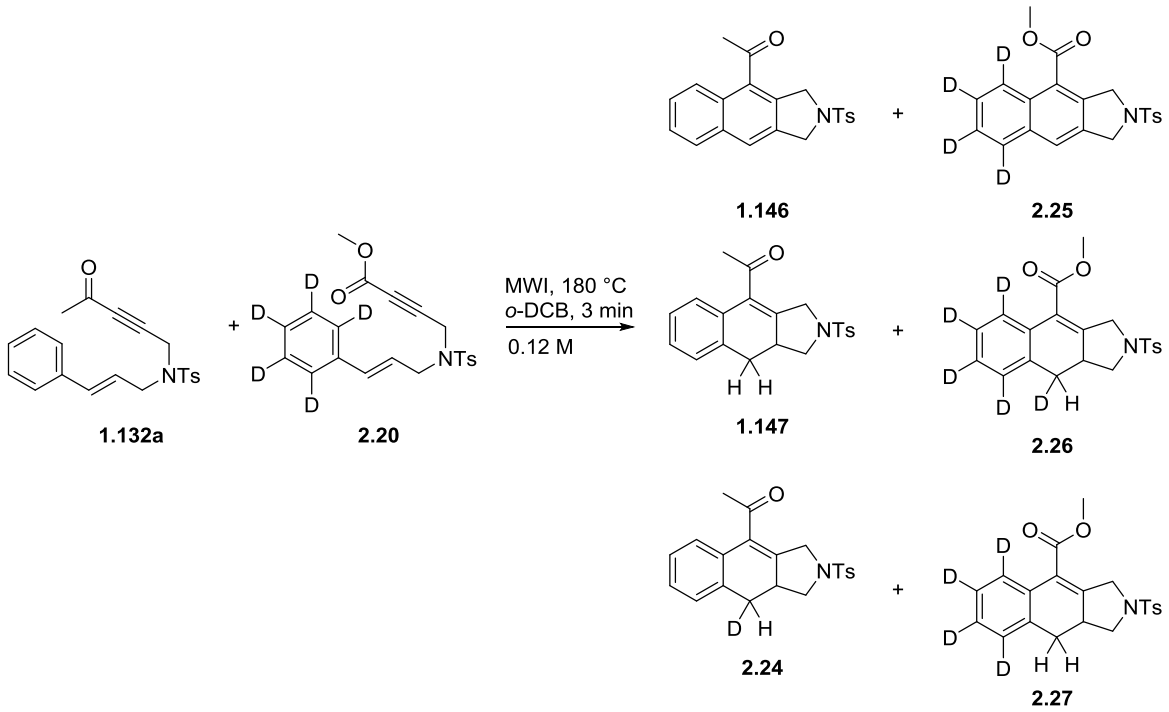

To a G4 Anton-Parr microwave irradiation vial was added styrene-ynes **1.132a** (6.6 mg, 0.018 mmol) and **2.20** (7.0 mg, 0.018 mmol) in *o*-DCB (0.3 mL). The solution was irradiated at 180 °C. After 1 min, the reaction of **1.132a** was complete by TLC, but a significant amount of **2.20** remained. The reaction was irradiated for an additional 2 min until complete by TLC. After irradiation, the reaction mixture was orange/brown in color. The reaction mixture was then concentrated under high vacuum, and the crude oil was subjected to HPLC, utilizing 10% ethyl acetate/hexanes as the eluent and a flow rate of 4 mL/min. The HPLC chromatogram showed four major peaks with retention times of 27.284, 28.707, 34.210, and 38.200 min, which were collected and characterized by ESI MS (see Figure 2.3). Characterization showed that all six potential compounds of the crossover experiment were present within the four HPLC peaks

isolated. The data pertaining to which HPLC peaks contained which products, as well as comparison of found masses to calculated masses, are listed in Table 2.4.

2.4.14 Hydrogen gas detection by gas chromatography

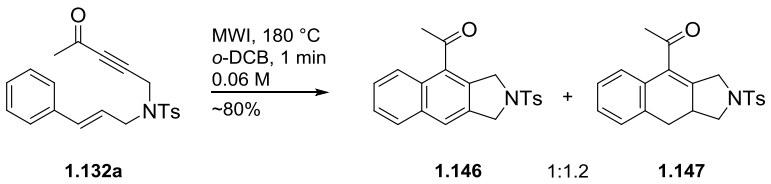

1.132a **1.146** 1:1.2 **1.147**

1-(2-Tosyl-2,3-dihydro-1*H*-benzo[*f*]isoindol-4-yl)ethan-1-one (1.146) and 1-(2-Tosyl-2,3,9,9a-tetrahydro-1*H*-benzo[*f*]isoindol-4-yl)ethan-1-one (**1.147**). To a 0.5-2 mL Biotage microwave irradiation vial was added styrene-yne **1.132a** and *o*-DCB (0.06 M). The solution was irradiated at 180 °C for 1 min, turning the reaction mixture brown. A 0.51 mL aliquot of the headspace of the reaction vessel was extracted via a gas tight syringe through the septum of the microwave vial and injected into a gas chromatograph that was calibrated for hydrogen gas detection. The quantity of hydrogen gas detected for each experiment is displayed in Table 2.5. Based upon the average 80% yield and 1:1.2 ratio of naphthalene **1.146** to dihydronaphthalene **1.147** products typically observed upon irradiation of styrene-yne **1.132a** under these reaction conditions, the theoretical yield of hydrogen gas expected and percent yield of hydrogen gas detected were calculated (Table 2.5). A percent yield of hydrogen gas ranging from approximately 39-48% was determined for the two experiments performed.

Table 2.5. Quantification of hydrogen gas released in the DDDA reaction of **1.132a** by GC

entry	mmol **1.132a**	theoretical yield (mmol) **1.146**/H_2	mL (mmol) H_2 detected	% yield H_2 for 100% reaction yield	% yield H_2 for 80% reaction yield
1	0.125	0.055-0.057	0.51 (0.021)	37-38%	47-48%
2	0.090	0.040-0.041	0.32 (0.013)	32-33%	39-41%

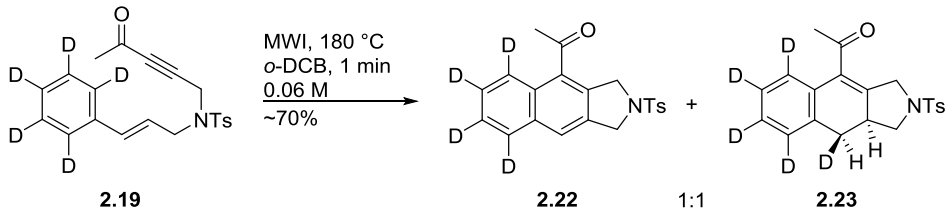

1-(2-Tosyl-2,3-dihydro-1*H*-benzo[*f*]isoindol-4-yl-5,6,7,8-*d*4)ethan-1-one (2.22) and 1-(2-tosyl-2,3,9,9a-tetrahydro-1*H*-benzo[*f*]isoindol-4-yl-5,6,7,8,9-*d*5)ethan-1-one (2.23). To 0.5-2 mL Biotage microwave irradiation vial was added styrene-yne **2.19** (0.034 g, 0.090 mmol) and *o*-DCB (1.5 mL). The solution was irradiated at 180 °C for 1 min, turning the reaction mixture brown. A 1.0 mL aliquot of the headspace of the reaction vessel was extracted via a gas tight syringe through the septum of the microwave vial and injected into a gas chromatograph that was calibrated for hydrogen gas detection. The quantity of HD gas detected for the experiment was 0.24 mL (0.010 mmol). Based upon the average 70% yield and 1:1 ratio of naphthalene **2.22** to dihydronaphthalene **2.23** products typically observed upon irradiation of styrene-yne **2.19** under these reaction conditions, the theoretical yield of HD gas expected and percent yield of HD gas detected were calculated (Table 2.6). A percent yield of HD gas of approximately 32% was determined.

Table 2.6. Quantification of HD gas released in the DDDA reaction of **2.19** by GC

mmol **2.19**	theoretical yield (mmol) **2.22**/HD	mL (mmol) HD detected	% yield HD for 100% reaction yield	% yield HD for 70% reaction yield
0.090	0.045	0.24 (0.010)	22%	32%

3.0 INTRAMOLECULAR DEHYDRO-DIELS-ALDER REACTIONS FOR THE SELECTIVE SYNTHESIS OF ARYLNAPHTHALENE OR ARYLDIHYDRONAPHTHALENE LIGNAN NATURAL PRODUCTS

This chapter is based on the results presented in:

Kocsis, L. S.; Brummond, K. M. Intramolecular Dehydro-Diels-Alder Reaction Affords Selective Entry to Arylnaphthalene or Aryldihydronaphthalene Lignans. *Org. Lett.* **2014**, *16*, 4158-4161.

3.1 INTRODUCTION

3.1.1 Biological Significance of Lignans

Arylnaphthalene lignans and their dihydro- and tetrahydronaphthalene derivatives are medicinally relevant compounds with a wide range of pharmacalogical activity. Diphyllin and justicidin B are both cytotoxic compounds and demonstrate anticancer,[80] antiparasitic,[81] antiviral,[82] and antirheumatic activities (Figure 3.1).[83] β-Apopicropodophyllin displays pronounced activity against the fifth-instar larvae of *Brontispa longissima*,[84] revealing the potential of podophyllotoxins as insecticides, in addition to their possible application as immunosuppressive agents.[85] The most studied compound of this class is etoposide, an approved

anticancer drug for breast cancer, testicular cancer, small cell lung cancer, lymphoma, Kaposi's sarcoma, and childhood leukemia that functions as a topoisomerase inhibitor.[86] While etoposide and derivatives thereof are used extensively in the clinic, several toxic side-effects such as bone-marrow depression, increased risk of secondary acute myelogenous leukemia, and acquired drug resistance have resulted in a continued search for a better drug.[87] Diphyllin D11, a glycosylated derivative of diphyllin, has recently been shown to selectively inhibit topoisomerase IIα[88] despite its structural simplicity compared to etoposide, highlighting the need for diphyllin analogs.

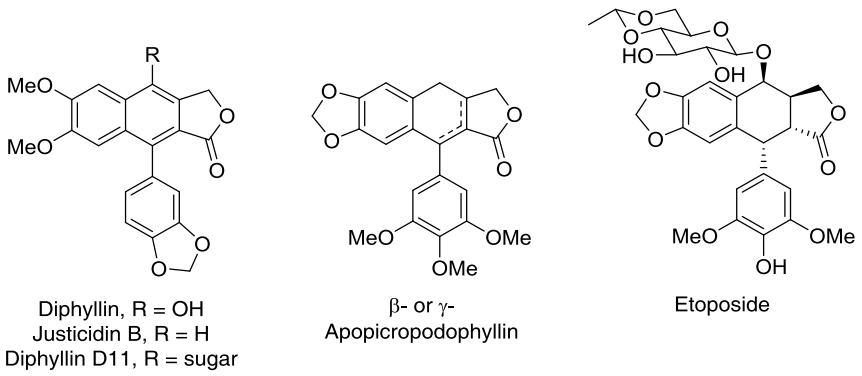

Figure 3.1. Representative structures of arylnaphthalene lignans and their derivatives

3.1.2 Previous syntheses of arylnaphthalene lignans

Synthetic strategies used to prepare arylnaphthalene lignans can be broadly categorized into three different classes of reactions, the first of which involves intermolecular DA reactions of isobenzofurans **3.1** with dialkylacetylene dicarboxylates to generate naphthyl diesters **3.2** (Scheme 3.1).[89] Selective hydrolysis of the C-3 ester of **3.2**, followed by reduction of the

resulting carboxylic acid and subsequent acid-assisted lactonization yields the lignan derivatives **3.3**.[89a,17] To initially access the isobenzofuran **3.1**, additional synthetic steps are required, such as a condensation reaction of hydroxyaldehyde **3.4**[89b] or a Pummerer reaction of sulfoxide **3.5**.[89a] The former route offers entry into analogs of diphyllin upon DA reaction, while the latter case results in an aryl sulfide that can be desulfurized with Raney nickel.[89a] The desirability of naphthyl diesters **3.2** as intermediates to lignan products inspired additional routes to their synthesis, in addition to intermolecular DA reactions. These include acid-catalyzed cyclization/oxidation reactions of alcohol **3.6**,[90] as well as a tandem Horner-Emmons-Claisen condensation reaction sequence of ketoaldehyde **3.7**.[17]

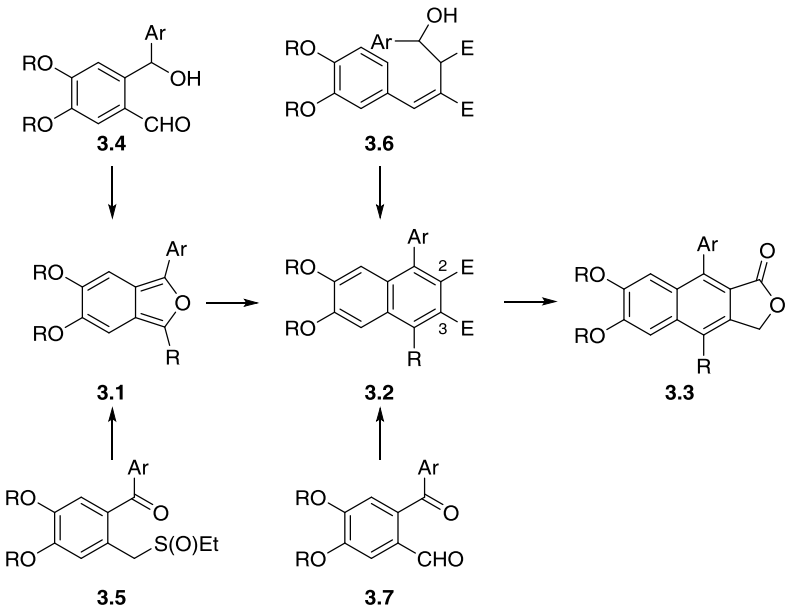

Scheme 3.1. Synthesis of arylnaphthalene lignans via benzannulation strategies

A second common strategy for arylnaphthalene lignan synthesis is by transition metal-catalyzed multicomponent cycloaddition reactions (Scheme 3.2). Reaction of diene **3.8** with $Pd_2(dba)_3$ and benzyne intermediate **3.9**, generated *in situ* from an aryl silyl triflate, produces naphthalene **3.2** after air oxidation.[91] Conversion of the diester of **3.2** to lactone **3.3** was accomplished in a manner analogous to that described previously (Scheme 3.1). Reaction of diyne **3.10** with benzyne **3.9** and the same palladium catalyst yields arylnaphthalene lactone **3.3** directly.[16]

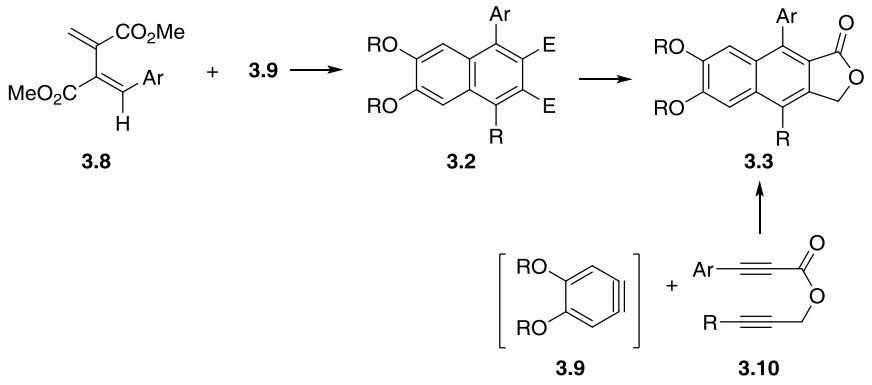

Scheme 3.2. Synthesis of arylnaphthalene lignans via cycloaddition reactions

The third class of reactions that are frequently utilized in the formation of lignan products are intramolecular dehydro-Diels-Alder (DDA) reactions. While there have been many recent developments in syntheses of arylnaphthalene lignans, early examples showed that intramolecular DDA reactions of styrene-yne **3.11** could be performed to provide dihydronaphthalene products **3.12** (Scheme 3.3). These cycloadducts were then either oxidized in a second step to produce arylnaphthalene lignans **3.13**, or reduced to generate

tetrahydronaphthalene structures belonging to the podophyllotoxin class of natural products. Klemm was the first to recognize the potential of this strategy by refluxing **3.11** in acetic anhydride to provide multiple dihydronaphthalene products that were then oxidized with DDQ to arylnaphthalene lignans.[40-41,42,92] Others have since validated this approach,[41b,63,93] but low yields, mixtures of naphthalene and dihydronaphthalene products, and mixtures of regioisomers are commonly obtained from the DDA reaction.[94] To alleviate the need for an additional oxidation step, DDA reactions of diynes have been implemented to access arylnaphthalene lignans **3.13** directly, but this also leads to regio- and retroisomeric mixtures of products. For example, refluxing **3.14** in xylenes affords the DDA product **3.13** and its regio- and retroisomers.[20]

In addition to thermal DDA reactions, base-assisted methods for conversion of styrene-ynes and diynes to aryldihydronaphthalenes and arylnaphthalenes, respectively, have also been developed. One example is a base-catalyzed cyclization employing a catalytic quantity of an organic phosphazene superbase (P_4-*t*-Bu) to effect the conversion of styrene-yne **3.11** to **3.12** (Scheme 3.3).[95] Additionally, a Garratt-Braverman reaction using potassium *tert*-butoxide converts diyne **3.15** to dihydronaphthofuran **3.16**, which is then oxidized to arylnaphthalene lignan **3.13** in varying yields.[96] Despite the many synthetic strategies outlined, there remains no single-step protocol to access arylnaphthalene lignans selectively from a styrenyl precursor; either a second oxidation step is needed, or a diyne precursor must be utilized in place of styrene-yne.

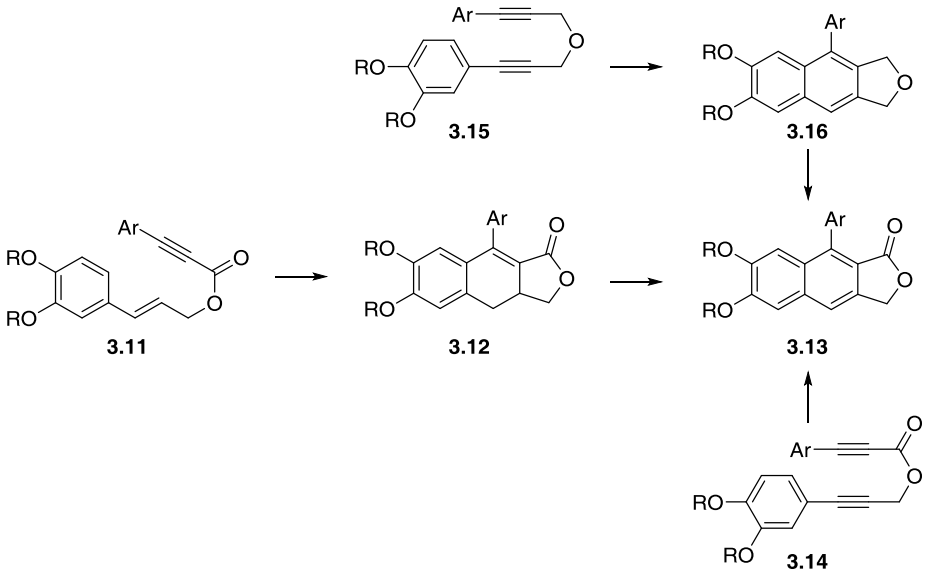

Scheme 3.3. Synthesis of arylnaphthalene lignans via intramolecular Diels-Alder reactions

3.2 RESULTS AND DISCUSSION

3.2.1 Controlling product selectivity of the DDA reaction

Based on previously reported results from our laboratory, we envisioned that a DDA reaction could be utilized to obtain both arylnaphthalene and aryldihydronaphthalene lactones selectively from a single precursor in only one synthetic step.[64] This methodology could then be applied to the synthesis of diphyllin D11 analogs, such as the eight arylnaphthalene and aryldihydronaphthalene lignan natural products **3.17**-**3.24** depicted in Figure 3.2. To test the feasibility of this strategy, styrene-yne **3.27** was prepared in 86% yield from commercially available cinnamyl alcohol (**3.25**) and phenylpropiolic acid (**3.26**) via a DCC coupling reaction (Scheme 3.4). Employing our standard reaction conditions, the styrene-yne **3.27** was subjected to MWI at 180 °C for 20 min in *o*-DCB-d_4 to afford arylnaphthalene lactone **3.28** and

aryldihydronaphthalene lactone **3.29** in a combined 75% yield and a 2:1 ratio, respectively, as determined by ^{1}H NMR spectroscopy. While the reaction showed little product selectivity, these results are consistent with previous reports where precursors containing heteroatoms, esters, or amides in the styrenyl tether led to mixtures of naphthalene and dihydronaphthalene products upon heating.[40-41,42,92,44-45,97]

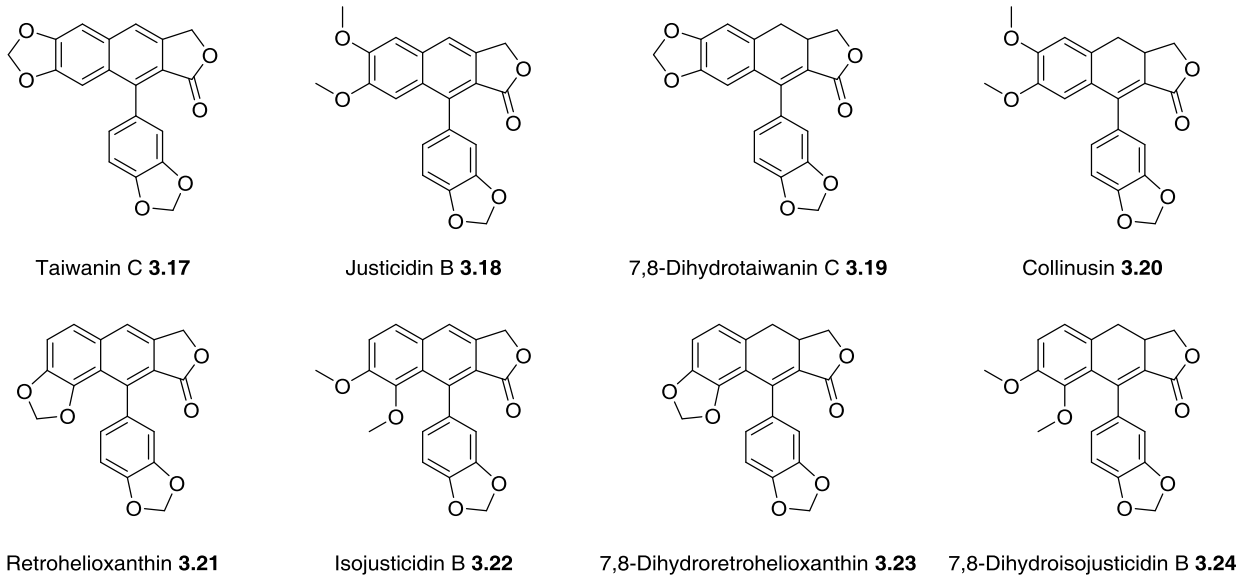

Figure 3.2. Arylnaphthalene and aryldihydronaphthalene lignan products targeted for synthesis by utilizing a DDA reaction of styrene-ynes

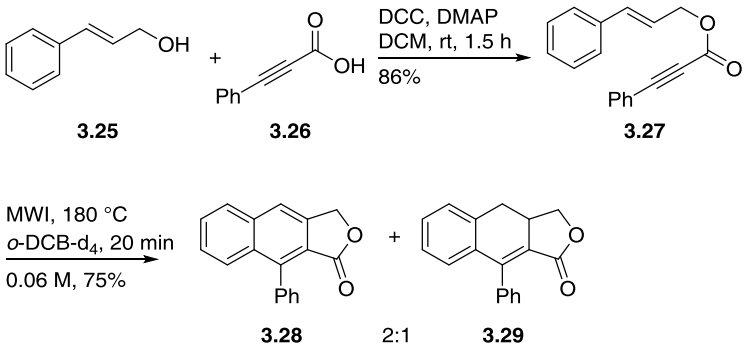

Scheme 3.4. Initial DDA reaction for lactone formation

Next, variations to the reaction conditions were made in an attempt to provide either naphthalene **3.28** or dihydronaphthalene **3.29** selectively. Increasing the concentration of the reaction mixture resulted in an increase in ratio of dihydronaphthalene **3.29** to naphthalene **3.28**. For example, dilute reaction conditions of 0.06 M in *o*-DCB-d_4 produced a 2:1 ratio of **3.28**:**3.29**, while more concentrated conditions of 0.12 or 0.45 M yielded a 1:1 ratio of **3.28**:**3.29** (entries 1-3, Table 3.1). Altering the reaction temperature also had an effect on product selectivity. Decreasing the reaction temperature to 150 °C resulted in a 1:1 mixture of **3.28**:**3.29**, but gave a 41% yield of unreacted starting material as determined by ^{1}H NMR spectroscopy (entry 1 versus 4). Irradiating this same sample for an additional 35 min (70 min total) resulted in a decrease in the amount of starting material and an increase in naphthalene **3.28**; however, the quantity of dihydronaphthalene **3.29** remained constant. The lower overall yield for this reaction indicated that dihydronaphthalene **3.29** was decomposing with longer reaction times (entry 5). When the reaction was performed at 225 °C or 245 °C for 0.5-1 min, naphthalene **3.28** was observed as the major product in a 7:1 ratio of **3.28**:**3.29** (entries 6-7).

Table 3.1. Controlling selectivity of the DDA reaction by varying the reaction conditions

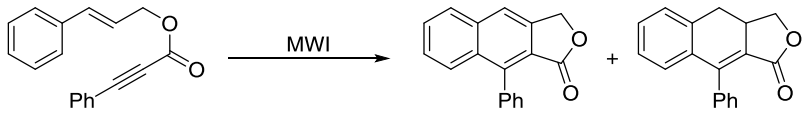

3.27 **3.28** **3.29**

entry	solvent	T (°C)	time (min)	[M]	yield **3.27**	yield **3.28**	yield **3.29**	total yield	**3.28**:**3.29**[c]
1[a]	*o*-DCB-d_4	180	20	0.06	7%	44%	24%	75%	2:1
2[a]	*o*-DCB-d_4	180	20	0.12	0%	35%	36%	71%	1:1
3[a]	*o*-DCB-d_4	180	20	0.45	0%	37%	29%	66%	1:1
4[a]	*o*-DCB-d_4	150	35	0.06	41%	21%	20%	82%	1:1
5[a]	*o*-DCB-d_4	150	70	0.06	18%	31%	20%	69%	1.5:1
6[a]	*o*-DCB-d_4	225	1	0.06	0%	72%	11%	83%	7:1
7[a]	*o*-DCB-d_4	245	0.5	0.06	0%	73%	10%	83%	7:1
8[b]	DMF	180	15	0.06	0%	0%	90%	90%	0:1
9[a]	DMF	135	150	0.06	10%	-	-	-	0:1
10	DMF	225	1	0.06	-	-	-	-	0:1
11[b]	DMF	180	15	0.12	0%	0%	91%	91%	0:1
12[b]	DMF	180	15	0.50	6%	0%	87%	93%	0:1
13[b]	$PhNO_2$	180	15	0.06	-	93%	-	93%	1:0
14[b]	$PhNO_2$	300	1	0.06	-	87%	-	87%	1:0
15	$PhNO_2$	180	15	0.24	-	-	-	-	2.5:1
16	NMP	180	10	0.06	-	-	-	-	1:12

[a]Percent yield determined by ^{1}H NMR spectroscopy using *p*-dimethoxybenzene as an internal standard; [b]isolated yield; [c]ratios of **3.28**:**3.29** determined by ^{1}H NMR spectroscopy.

Modifying the solvent from *o*-DCB (ε = 9.93) to the more polar DMF (ε = 36.7) resulted in exclusive formation of dihydronaphthalene **3.29** in 90% isolated yield after irradiation for 15 min at 180 °C (entry 8, Table 3.1). Decreasing or increasing the reaction temperature to 135 or 225 °C, respectively, did not affect the product selectivity; only dihydronaphthalene **3.29** was obtained (entries 9 and 10). Likewise, increasing the reaction concentration from 0.06 to 0.50 M in DMF generated **3.29** in approximately 90% yield; no naphthalene **3.28** was observed (entries 8, 11, 12). $PhNO_2$ (ε = 34.8) was also tested as a reaction solvent because of its similar dielectric constant to DMF. Irradiation of styrene-yne **3.27** for 15 min at 180 °C in $PhNO_2$ produced

naphthalene **3.28** exclusively in 93% yield (entry 13). While increasing the temperature of the reaction to 300 °C did not affect the selectivity or yield of the reaction in $PhNO_2$ (entry 14), increasing the reaction concentration to 0.24 M did result in decreased selectivity for the naphthalene product, producing a 2.5:1 mixture of **3.28**:**3.29** (entry 15). Despite the observed selectivity for **3.28** and **3.29** in $PhNO_2$ and DMF, respectively, conducting the reaction in NMP ($\varepsilon = 32.2$) resulted in a 1:12 mixture of **3.28**:**3.29**, indicating that DMF and $PhNO_2$ are necessary for exclusive formation of each product (entry 16).

The complete selectivity for arylnaphthalene products in the presence of $PhNO_2$ as the reaction solvent can be explained by the oxidative ability of $PhNO_2$. It has previously been shown that $PhNO_2$ can act as an oxidant to form heteroaromatic systems, such as benzothiazoles[66b] and benzimidazoles,[66a] when utilized as the reaction solvent. Since $PhNO_2$ is acting as an oxidant, we envisioned that it need not be the primary solvent, and that the quantity present in the reaction mixture could be lessened. To test this hypothesis, incremental reductions were made to the amount of $PhNO_2$ added to a reaction mixture of **3.27** in *o*-DCB, and the effect on the product selectivity of the DDDA reaction was observed. Reducing the amount of $PhNO_2$ to 5% (v/v %) in *o*-DCB still favored selectivity for the arylnaphthalene lactone **3.28** over the dihydronaphthalene lactone **3.29** product by 7:1 (entry 1, Table 3.2), while doubling the concentration of $PhNO_2$ in the reaction mixture resulted in an almost proportional increase in the ratio of **3.28**:**3.29** to 13:1 (entry 2). Increasing the concentration of $PhNO_2$ further to 20% produced only the oxidized product **3.28**, indicating that a 1:5 ratio of $PhNO_2$ to *o*-DCB is the minimal amount of $PhNO_2$ required to achieve complete selectivity for the arylnaphthalene lactone (entry 3). Although $PhNO_2$ is vital as an oxidant to achieve exclusive formation of the

naphthalene product in the DDDA reaction, it can be utilized in smaller quantities as an additive to the reaction, rather than as the sole reaction solvent, as demonstrated by the above results.

Table 3.2. Minimal amount of $PhNO_2$ required for exclusive naphthalene formation

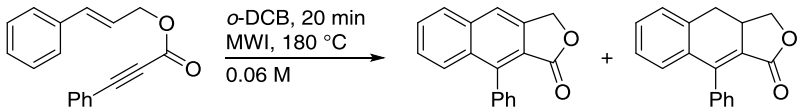

3.27 **3.28** **3.29**

entry	$PhNO_2$	yield	**3.28**:**3.29**
1	5% (8 equiv)	75%	7:1
2	10% (16 equiv)	75%	13:1
3	20% (32 equiv)	70%	1:0

3.2.2 Application of the DDA reaction to the synthesis of lignan natural products

With conditions in hand to prepare either the naphthalene or dihydronaphthalene lactone products selectively from a common precursor, we set out to explore this reaction in the synthesis of more functionalized substrates. The highly oxygenated structures of many arylnaphthalene lignans and their derivatives inspired us to prepare styrene-ynes **3.33a-c** containing 3,4-methylenedioxy and 3,4-dimethoxy functionalities (Scheme 3.5). Esterification of commercially available 3,4-(methylenedioxy)cinnamic (**3.30a**) and 3,4-dimethoxycinnamic acid (**3.30b**) using sulfuric acid and methanol, followed by reduction with DIBAL-H generated cinnamyl alcohols **3.31a** and **3.31b** in 76% and quantitative yields, respectively, over 2 steps. The cinammyl alcohols were then coupled with either phenylpropiolic acid (**3.26**) or arylpropiolic acid **3.32** via reaction with DCC to produce styrene-ynes **3.33a-c** in 66-85% yield.

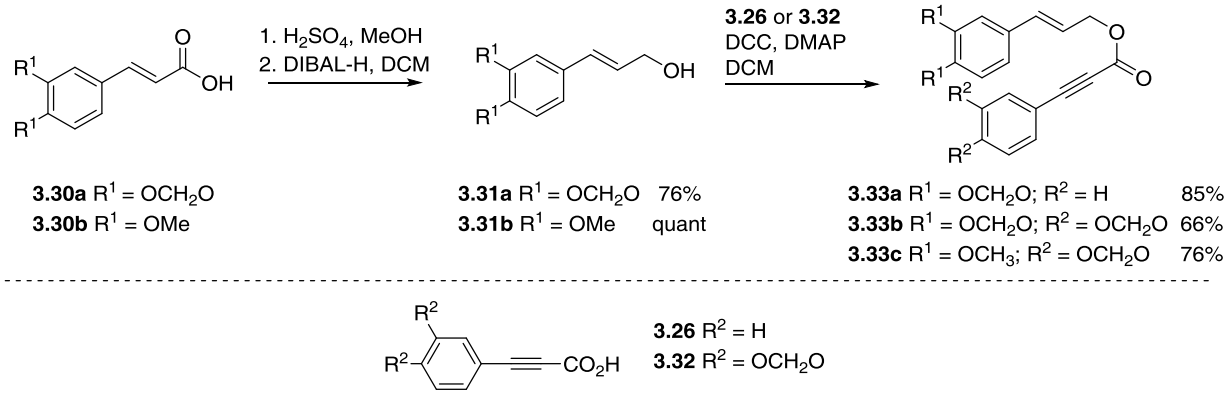

Scheme 3.5. Synthesis of styrene-ynes **3.33a-c**

Arylpropiolic acid **3.32** was prepared by first subjecting 1-iodo-3,4-methylenedioxybenzene (**3.34**) to Sonogashira coupling with trimethylsilylacetylene to generate **3.35** in 96% yield (Scheme 3.6). Removal of the trimethylsilyl group in the presence of 10% sodium hydroxide, followed by treatment of the lithium acetylide of **3.36** with solid carbon dioxide produced **3.32** in 82% yield over 2 steps. Alternatively, **3.32** can be synthesized in one step via a Sonogashira coupling of **3.34** with propiolic acid; however, the yield of this reaction (20-73%), as well as the quality of the product obtained, was not reproducible. Additionally, EDCI•HCl and BOP-Cl were employed as alternate coupling reagents to DCC to circumvent problems associated with separation of styrene-yne **3.33c** from *N*,*N*'-dicyclohexylurea byproduct. Both EDCI•HCl and BOP-Cl produced **3.33c** in equivalent, if not higher yields compared to coupling with DCC (70-86%), as well as in higher purity.

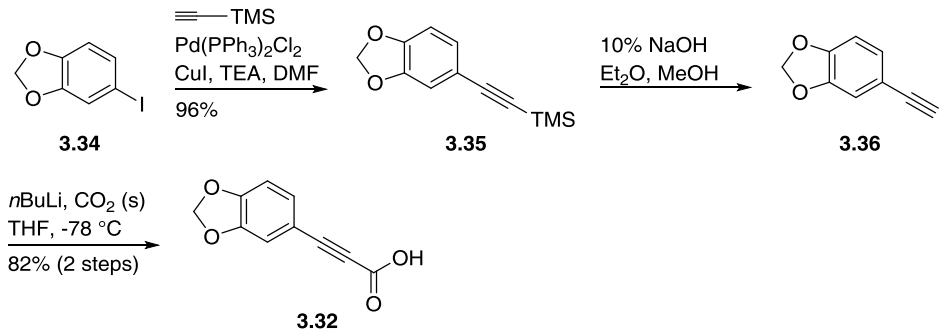

Scheme 3.6. Synthesis of arylpropiolic acid **3.32**

Styrene-yne **3.33a** was subjected first to the optimized DDA reaction conditions. Irradiation of **3.33a** in $PhNO_2$ for 5 min at 180 °C resulted in quantitative formation of the naphthalene product **3.37** as a 2:1 mixture with its regioisomer **3.38** (Scheme 3.7). Alternatively, irradiation of **3.33a** in DMF at 180 °C for 5 min afforded dihydronaphthalene **3.39** in 90% yield as a 2:1 mixture with **3.40**.

Synthesis of arylnaphthalene and aryldihydronaphthalene lignan natural products was achieved by irradiation of **3.33b** and **3.33c** under similar reaction conditions. Irradiation of **3.33b** in $PhNO_2$ for 5 min at 180 °C afforded an 83% yield of the arylnaphthalene lignan taiwanin C (**3.17**) as a 2:1 mixture with retrohelioxanthin (**3.21**), which was then separated by HPLC for characterization (Scheme 3.7). Likewise, irradiation of **3.33c** under the same reaction conditions resulted in a similar 2.3:1 ratio of arylnaphthalene lignans justicidin B (**3.18**) and isojusticidin B (**3.22**) in 83% yield, which were readily separable by column chromatography. Thus, four arylnaphthalene lignan natural products were formed in short reaction time and in high combined yields. Attempts to increase the regioselectivity of the DDA reaction by adding bulkier functionality to the arylpropiolate, such as a 3,4-dimethoxy moiety, were not successful.

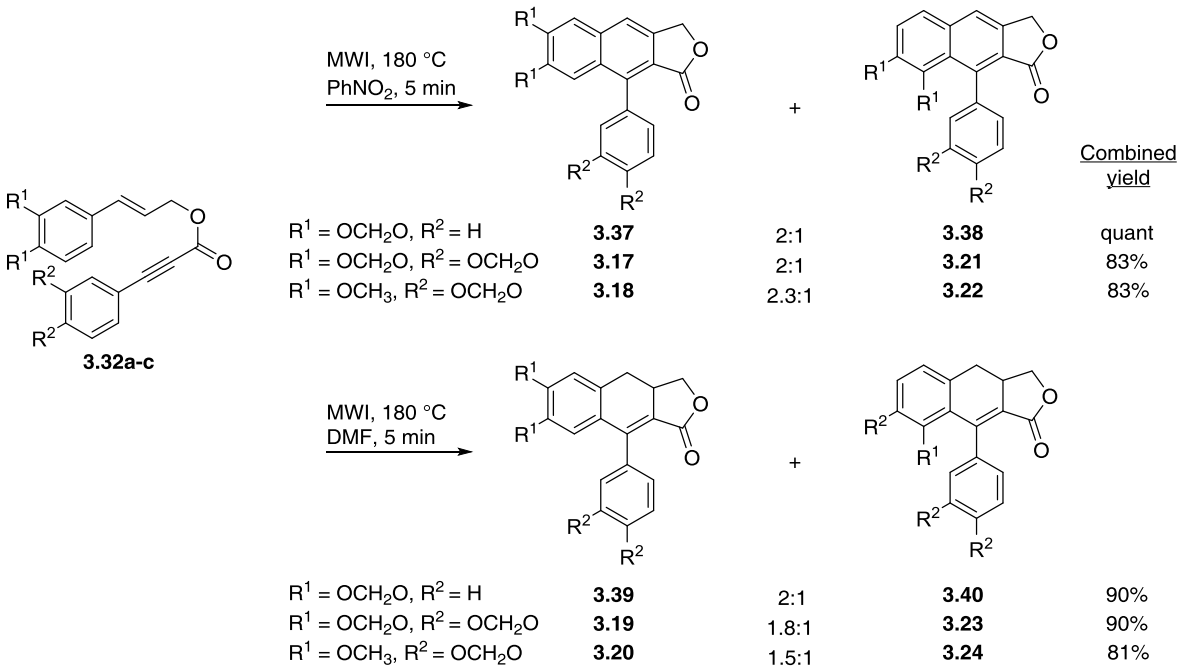

Scheme 3.7. DDA reactions to produce taiwanin C, justicidin B, and their derivatives

Similarly, irradiation of **3.33b** for 5 min at 180 °C in DMF led to formation of 7,8-dihydrotaiwanin C (**3.19**) in 90% yield as a 1.8:1 mixture with 7,8-dihydroretrohelioxanthin (**3.23**) (Scheme 3.7). Irradiation of **3.33c** gave collinusin (**3.20**) and 7,8-dihydroisojusticidin B (**3.24**) in 81% yield as a 1.5:1 ratio. A recent report by Seo and Shin demonstrated that microwave irradiation of **3.33b** in Ac_2O at 140 °C led to the regioselective production of dihydronaphthalene **3.19**, which was then oxidized with DDQ to taiwanin C (**3.17**) in 85% yield over 2 steps.[41b] Under the reaction conditions reported herein, mixtures of regioisomers were always observed when employing DMF or $PhNO_2$ as solvents. In our hands, irradiation of **3.33b** utilizing the same conditions reported by Seo and Shin resulted in a 1.6:1 mixture of **3.19**:**3.23**, a similar ratio to what was obtained by irradiation in DMF.

3.2.3 Discrimination of lignan regioisomers by computational methods

Confirming the identity of lignan regioisomers based on their NMR spectra was sometimes challenging, as these spectra were closely related due to the similarity of the lignan structures and because the majority of ^{13}C NMR resonances fell within 120-150 ppm, a small range of the available spectrum. Similar structural assignment challenges for natural and synthetic products have been addressed by utilizing modern computational methods.[98] In this manner, predicted NMR spectra are compared with experiment to ascertain whether experimental results match a proposed structure. In light of these studies, predictions of NMR spectra were conducted using Spartan 10 software for the eight lignans synthesized via the DDA reaction to confirm the identity of each regioisomer (Figure 3.2).

Lowest energy conformers were first determined by executing molecular mechanics (MMFF) calculations. ^{1}H and ^{13}C NMR spectra were predicted with either EDF2/6-31G* and/or B3LYP/6-31G* methods. 2D NMR spectra of the synthesized lignans were not obtained, thus structural assignments of resonances to all carbon or hydrogen atoms could not be accurately drawn. As a result, experimental and calculated ^{13}C NMR spectra were matched directly by descending order of chemical shift, similar to the protocol employed by Goodman for when structural assignments are lacking.[98d] Calculated chemical shifts were then scaled, and an average chemical shift deviation ($\Delta\delta$) was found between the predicted and experimental values. The average $\Delta\delta$, maximum $\Delta\delta$, and coefficient of determination (R^2) determined from linear correlation plots of experimental versus calculated data were used as measures of how accurately the predicted spectra matched experimental results.

Comparison of the EDF2 and B3LYP functionals for taiwanin C derivatives showed that the EDF2 functional had an average $\Delta\delta$ 2-6 times lower than the B3LYP functional for ^{13}C NMR

data, indicating that a more accurate prediction was obtained using the EDF2 method (entries 1-14, Table 3.3). As a graphical representation of the disparity between the EDF2 and B3LYP methods, Figure 3.3 depicts the error associated for each carbon in taiwanin C (**3.17**), where carbon 1 denotes the most downfield resonance. Considerably higher deviations were observed for the B3LYP than the EDF2 functional for most carbons. Also, maximum Δδ of calculated and experimental values were significantly lower and R^2 values higher for the EDF2 functional. Reports by Bifulco[99] and Rychnovsky[98b] indicated that R^2 values greater than 0.995 and an average Δδ of less than 2 ppm, respectively, represent a good match between predicted and experimental spectra, which is consistent with the EDF2 results. In examples where multiple conformers exist, as for the justicidin B analogs, a ^{13}C NMR spectrum was also predicted for a Boltzmann distribution of the conformers. In most cases, the lowest energy conformers had an average Δδ of less than 2 ppm and high R^2 values of greater than 0.995, fitting the above criteria; however, Boltzmann distribution predicted spectra typically showed lower average Δδ and greater R^2 values indicative of a better match with experimental spectra (entries 15-25). Computational predictions of ^{1}H NMR spectra were also conducted for taiwanin C derivatives, and the average Δδ were similar for both the EDF2 and B3LYP functionals, with B3LYP being slightly favored (Table 3.4). For both functionals, R^2 values were less than 0.99, which indicates that these computational methods for prediction of ^{1}H NMR spectra are less accurate than for prediction of ^{13}C NMR chemical shifts.

Table 3.3. Calculated ^{13}C NMR spectroscopic data for lignan natural products

entry	lignan	conformer[a]	functional	average Δδ	max Δδ	R^2
	taiwanin C Derivatives					
1	taiwanin C (**3.17**)	1	EDF2	1.03	2.95	0.9968
2		1	B3LYP	2.56	5.59	0.9834
3	7,8-dihydrotaiwanin C (**3.19**)	1	EDF2	0.74	2.28	0.9993
4		1	B3LYP	2.28	6.81	0.9937
5		2	EDF2	1.34	5.31	0.9972
6		2	B3LYP	2.34	4.26	0.9941
7		BD	EDF2	1.0	2.7	0.9987
8	retrohelioxanthin (**3.21**)	1	EDF2	1.10	2.88	0.9961
9		1	B3LYP	2.20	6.27	0.9845
10	7,8-dihydroretrohelioxanthin (**3.23**)	1	EDF2	0.96	3.73	0.9987
11		1	B3LYP	2.33	4.77	0.9939
12		2	EDF2	0.91	3.61	0.9988
13		2	B3LYP	2.27	4.79	0.9944
14		BD	EDF2	0.9	2.0	0.9992
	justicidin B Derivatives					
15	justicidin B (**3.18**)	1	EDF2	1.55	7.01	0.9941
16		2	EDF2	1.53	6.94	0.9942
17		BD	EDF2	1.0	3.2	0.9984
18	collinusin (**3.20**)	1	EDF2	1.38	5.00	0.9979
19		BD	EDF2	1.7	7.7	0.9958
20	isojusticidin B (**3.22**)	1	EDF2	1.37	4.05	0.9963
21		2	EDF2	1.27	3.88	0.9967
22		BD	EDF2	0.9	2.8	0.9982
23	7,8-dihydroisojusticidin B (**3.24**)	1	EDF2	1.85	7.88	0.9958
24		2	EDF2	1.76	8.31	0.9956
25		BD	EDF2	1.1	3.3	0.9988

[a]Conformer 1 indicates lowest energy conformer and conformer 2 indicates second lowest energy conformer. BD indicates a Boltzmann distribution.

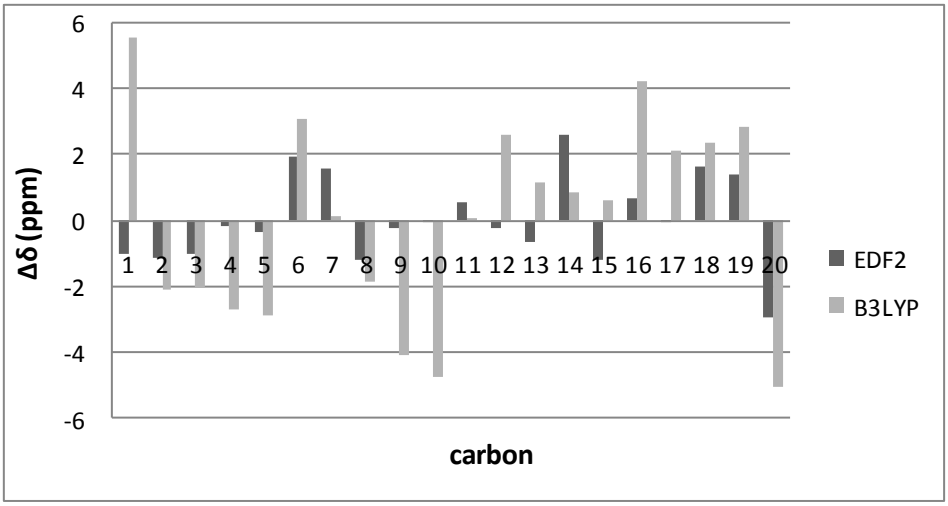

Figure 3.3. Average chemical shift deviation per carbon in taiwanin C (**3.17**) for EDF2 and B3LYP functionals

Table 3.4. Calculated ^{1}H NMR spectroscopic data for lignan natural products

entry	lignan	conformer[a]	method	average Δδ	max Δδ	R^2
1	taiwanin C (**3.17**)	1	EDF2	0.21	0.35	0.9047
2		1	B3LYP	0.15	0.24	0.9456
3	7,8-dihydrotaiwanin C (**3.19**)	1	EDF2	0.19	0.40	0.9762
4		1	B3LYP	0.16	0.40	0.9842
5		2	EDF2	0.20	0.37	0.9767
6		2	B3LYP	0.15	0.29	0.9864
7	retrohelioxanthin (**3.21**)	1	EDF2	0.19	0.37	0.9228
8		1	B3LYP	0.14	0.23	0.9588
9	7,8-dihydroretrohelioxanthin (**3.23**)	1	EDF2	0.19	0.54	0.9750
10		1	B3LYP	0.16	0.37	0.9846
11		2	EDF2	0.19	0.38	0.9776
12		2	B3LYP	0.16	0.29	0.9854

[a]Conformer 1 indicates lowest energy conformer and conformer 2 indicates second lowest energy conformer.

To verify that each EDF2 predicted spectra was representative of the desired lignan and could not also provide a match to its regioisomer, experimental ^{13}C NMR spectral data of the taiwanin C derivatives were compared to predicted spectra of their regioisomers. The average $\Delta\delta$ and R^2 values for the matched and mismatched data were then evaluated. For each example, the experimental and predicted spectra matching the lignan in question had lower average $\Delta\delta$ by a factor of 2 and higher R^2 values than for the mismatched regioisomer (Table 3.5). Also, the experimental spectrum of each lignan was compared with its predicted data and that predicted for its regioisomer using the Goodman D4 applet,[98d] and a 100% probability was determined for the experimental spectra of each lignan matching that of the expected structure, rather than that of the regioisomer. Overall, these results indicate that the EDF2 functional can be used to distinguish between regioisomeric lignans based on their ^{13}C NMR spectra.

Table 3.5. Matched and mismatched ^{13}C NMR spectroscopic data for taiwanin C derivatives

entry	experimental data	predicted data	average Δδ	max Δδ	R^2
1	taiwanin C (**3.17**)	taiwanin C (**3.17**)	1.03	2.95	0.9968
2		retrohelioxanthin (**3.21**)	2.55	7.95	0.9783
3	retrohelioxanthin (**3.21**)	retrohelioxanthin (**3.21**)	1.10	2.88	0.9961
4		taiwanin C (**3.17**)	2.54	6.19	0.9801
5	dihydrotaiwanin C (**3.19**)	dihydrotaiwanin C (**3.19**)	0.74	2.28	0.9993
6		dihydroretrohelioxanthin (**3.23**)	1.55	10.74	0.9935
7	dihydroretrohelioxanthin (**3.23**)	dihydroretrohelioxanthin (**3.23**)	0.96	3.73	0.9987
8		dihydrotaiwanin C (**3.19**)	1.91	9.33	0.9934

One final measure to determine the accuracy of the EDF2 method for discriminating between lignan regioisomers was by comparing structurally assigned experimental spectral data

of lignans with the predicted results. Since no 2D NMR structural analyses were performed in our studies, we did not obtain structural assignments, and the experimental and predicted resonances were matched by descending order of chemical shift for calculations of average Δδ. This method of comparing spectral data could possibly lead to overestimation or underestimation of the match between experimental and calculated results.[98d] However, a previous study by da Silva et al. did confirm the structural assignment of each carbon in taiwanin C (**3.17**) and justicidin B (**3.18**) using 2D NMR analyses.[100] Comparing these literature structural assignments with our predicted ^{13}C NMR data revealed no significant change in average Δδ or R^2 values for taiwanin C (**3.17**) (entries 1 and 2, Table 3.6). The results for comparison with the lowest energy conformer of justicidin B (**3.18**) showed one outlying value that perturbed the R^2 and the max Δδ values (entries 3 and 4). A more accurate correlation of the structurally assigned literature data with our predicted chemical shifts for justicidin B (**3.18**) may be achieved by comparison with the EDF2 predicted Boltzmann distribution ^{13}C NMR spectra; however, Spartan does not allow for structural assignments in Boltzmann distribution calculations, so a comparison could not be made. These results signify that our computational methods are valid for accurate prediction of lignan ^{13}C NMR spectra that can aid in structural determination without the need for additional 2D NMR studies. This computational protocol can be applied to distinguish regioisomers of new lignan analogs that are difficult to discriminate by experimental NMR techniques alone.

Table 3.6. Structurally assigned ^{13}C NMR experimental spectral data versus predicted results

entry	lignan	experimental data	average[a] Δδ	max Δδ	R^2
1	taiwanin C (**3.17**)	structural assignments	1.0	3.0	0.997
2		no structural assignments	1.1	3.2	0.996
3	justicidin B (**3.18**)	structural assignments	1.6	7.0	0.994
4		no structural assignments	1.8	13.3	0.988

[a]Determined from comparison of experimental data with the lowest energy conformer of predicted data.

3.3 CONCLUSION

In conclusion, solvent was shown to have a determinate effect on product selectivity in the microwave-assisted intramolecular DDA reaction of styrene-ynes. Employing DMF as the reaction solvent allowed for exclusive formation of aryldihydronaphthalene lactones, while $PhNO_2$ afforded arylnaphthalene lactones selectively. This constitutes the first report of an entirely selective formation of arylnaphthalene lactones utilizing a DDA reaction of styrene-ynes. The synthetic potential of these selective DDA reactions was realized by the preparation of eight natural products from two precursors, including taiwanin C (**3.17**) and justicidin B (**3.18**), which have previously demonstrated desirable biological activity. The DDA approach to arylnaphthalene and aryldihydronaphthalene lignans is currently being investigated for the preparation of novel topoisomerase inhibitors. Computational EDF2 methods were also developed for prediction of lignan ^{13}C NMR spectra and demonstrated good correlation with experimental spectra, often showing a less than 1 ppm deviation. This computational protocol can be applied in future synthetic studies to aid in the identification of new lignan analogs that have similar and difficult to differentiate structures.

3.4 EXPERIMENTAL

3.4.1 General Synthetic Methods

All commercially available compounds were used as received unless otherwise noted. DCM and THF were purified by passing through alumina using the Sol-Tek ST-002 solvent purification system. Triethylamine was freshly distilled from CaH_2 prior to use. $CDCl_3$ was stored over 3 Å molecular sieves. Purification of the compounds by flash column chromatography was performed using silica gel (40-63 μm particle size, 60 Å pore size) purchased from Sorbent Technologies. TLC analyses were performed on Silicycle SiliaPlate G silica gel glass plates (250 μm thickness). ^{1}H NMR and ^{13}C NMR spectra were recorded on Bruker Avance 300 MHz, 400 MHz, 500 MHz, or 700 MHz spectrometers. Spectra were referenced to residual chloroform (7.26 ppm, ^{1}H, 77.16 ppm, ^{13}C). Chemical shifts are reported in ppm, multiplicities are indicated by s (singlet), b s (broad singlet), d (doublet), t (triplet), q (quartet), p (pentet), and m (multiplet). Coupling constants, *J*, are reported in hertz (Hz). All NMR spectra were obtained at rt. ^{1}H and ^{13}C NMR spectra can be found in Appendix B. IR spectra were obtained using a Nicolet Avatar E.S.P. 360 FT-IR. ES mass spectroscopy was performed on a Waters Q-TOF Ultima API, Micromass UK Limited high resolution mass spectrometer. All microwave-mediated reactions were conducted in either a Biotage Initiator Exp microwave synthesizer using 0.5-2 mL conical and 2-5 mL cylindrical microwave irradiation vials, or in an Anton-Paar Monowave 300 microwave synthesizer using G4 and G10 cylindrical microwave irradiation vials. The temperature of reactions in the Monowave 300 was monitored internally by a ruby sensor fiber optic probe, unless otherwise specified. The microwave parameters were set to variable power, constant temperature, stirring on, and a fixed hold time. Separation of naphthalene and

dihydronaphthalene products was performed on a Varian Prostar HPLC chromatograph using a Varian Dynamax Microsorb 100-5 Si column.

3.4.2 General Computational Methods

All calculations were performed using Wavefunction Spartan 10 software for Windows. Lowest energy conformers were first determined by executing conformer distribution calculations using molecular mechanics and MMFF. With all conformers in hand, global calculations for prediction of ^{1}H and ^{13}C NMR spectra were performed using either EDF2/6-31G* (subset of equilibrium geometry and density functional theory) or B3LYP/6-31G* (subset of energy and density functional theory) functionals under vacuum. Each EDF2/6-31G* calculation required approximately 2.5 h per conformer, while B3LYP/6-31G* calculations required approximately 0.5 h per conformer. Uncorrected chemical shifts were available via the output file, but corrected chemical shifts,[101] which were used for subsequent calculations, could be found as atom labels on the drawn structure (these labels are shown by clicking Model > Configure > Chem Shift). 2D NMR spectra of the lignans were not obtained, thus structural assignments of resonances to all carbon or hydrogen atoms could not be accurately drawn. As a result, experimental and calculated ^{13}C NMR spectra were matched directly by descending order of chemical shift, similar to the protocol employed by the DP4 applet created by Goodman for when structural assignments are lacking.[98d] In some cases, resonances for ^{1}H NMR data could be assigned, and the remaining unassigned resonances were matched by decreasing order of chemical shift as was done for the ^{13}C NMR data. Experimental results were then plotted against predicted results (δ_{calc}) using Excel and fitted with a linear least squares regression. Scaled chemical shifts were determined for each hydrogen or carbon by the equation $\delta_{scaled} = (\delta_{calculated}\text{-intercept})/\text{slope}$,

following the procedure of Goodman.[98d,99] Intercept and slope were determined from linear least-squares regression analysis. Next, the difference ($\Delta\delta_{scaled}$) was calculated between each predicted (δ_{scaled}) and experimental resonance (δ_{exp}). Absolute values of these differences (|$\Delta\delta_{scaled}$ erew (| then averaged to represent a general deviation of the predicted spectra from the experimental spectra. The EDF2/6-31G* model is designed to provide corrected ^{13}C NMR shifts within error of approximately 1.7 ppm for Spartan 10 software, while the B3LYP/6-31G* model has an accuracy within 2.5 ppm (this latter model was originally optimized for Spartan 08).[101] Our predicted results fall within these levels of error. The chemical shifts reported for ^{1}H NMR spectra in Spartan 10 do not undergo a correction, and typically show a larger degree of deviation from experimental results than the ^{13}C NMR predicted chemical shifts. For all calculations, only errors associated with the lowest energy conformers of each substrate are reported. In cases where there are multiple conformers, such as for the justicidin B derivatives, the spectra predicted for a Boltzmann distribution of the conformers was also studied and compared with experimental results. The values of chemical shift reported for the Boltzmann distribution were obtained directly from the predicted spectra, not from atom labels as was done for lowest energy conformers.

3.4.3 Experimental procedures detailed in published papers

Characterization and conditions for the preparation of the following arylnaphthalene and aryldihydronaphthalene lactones and lignans, including syntheses and characterization of all precursors and spectral data, were recently published and can be found in the Supporting Information of Kocsis, L. S.; Brummond, K. M. Intramolecular Dehydro-Diels-Alder Reaction Affords Selective Entry to Arylnaphthalene or Aryldihydronaphthalene Lignans. *Org. Lett.* **2014**,

16, 4158-4161 (Figure 3.4). Additionally, data and calculations pertaining to the computational aspect of this chapter are also detailed in the Supporting Information of the aforementioned publication.

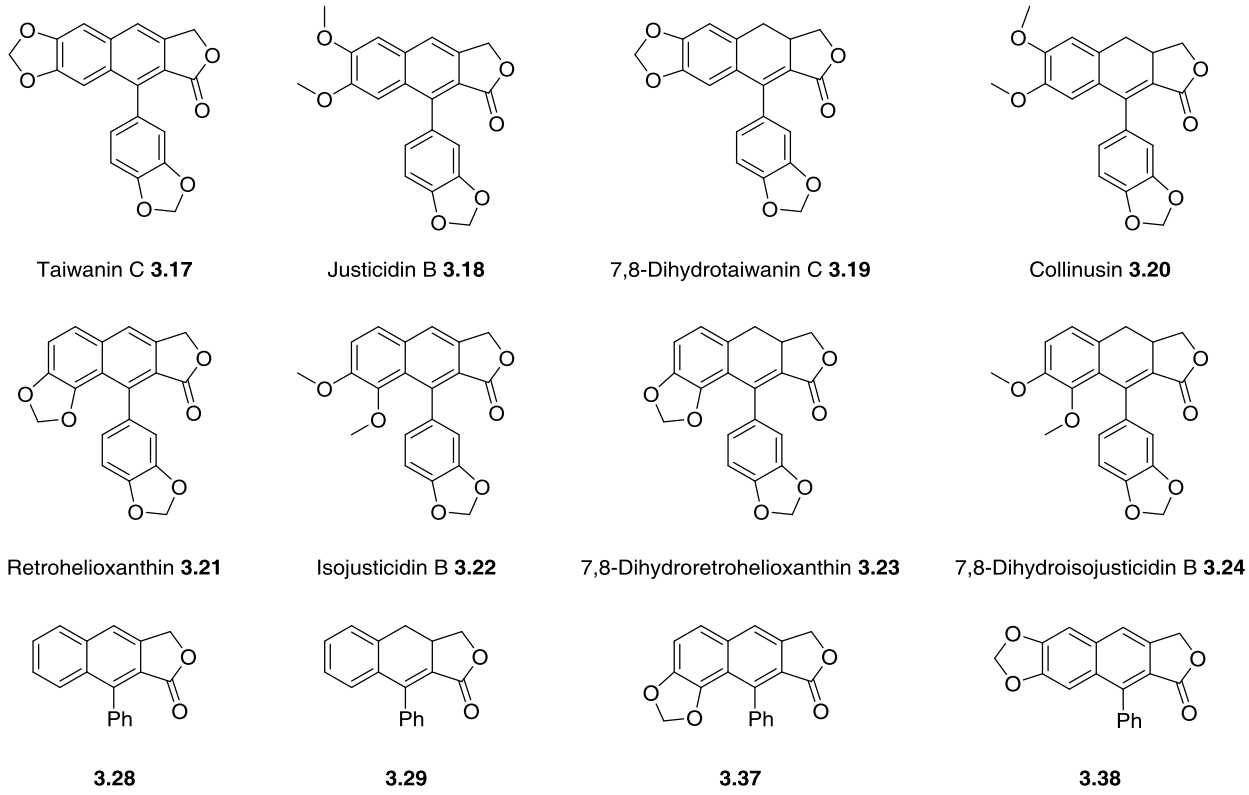

Figure 3.4. Previously published **a**rylnaphthalene and aryldihydronaphthalene lactones. Syntheses and characterization can be found in *Org. Lett*. **2014**, *16*, 4158-4161.

4.0 APPLICATION OF THE DDDA REACTION TO THE SYNTHESIS OF SOLVATOCHROMIC FLUOROPHORES AND THE STUDY OF STRUCTURE-PHOTOPHYSICAL PROPERTY RELATIONSHIPS IN FLUORESCENT DYES

This chapter is partially based on the results presented in:

Benedetti, E.; Kocsis, L. S.; Brummond, K. M. Synthesis and Photophysical Properties of a Series of Cyclopenta[*b*]naphthalene Solvatochromic Fluorophores. *J. Am. Chem. Soc.* **2012**, *134*, 12418-12421.

4.1 INTRODUCTION

Fluorescent compounds are valuable tools for elucidating and understanding biological systems, and they are widely used to monitor environments of biological events.[102] Fluorescence is utilized for a variety of reasons because of the nondestructive nature of these measurements. Of the fluorescent probes available, small organic fluorophores are gaining popularity due to their ease of handling and rapid response times for monitoring real-time events, such as protein trafficking, small molecule signaling, organelle distribution, and cell viability, with excellent spatial and temporal resolution.[103] In addition, their relatively small size minimizes disruption of the environment being studied. The widespread use of these probes is enabled by the commercial availability of hundreds of fluorescent dyes at low costs, as well as advancements in

instrumentation, such as confocal microscopy, single molecule microscopy, and expression microarrays.[9] However, there are many elements to consider when choosing the optimal fluorescent tool, including quantum yield, extinction coefficient, absorption and emission wavelengths, photo- and chemical stability, and Stokes shift, to name a few. Each of the commercially available dyes comes with a list of advantages and compromises that must be weighed for any application. Thus, new small molecule-based fluorescent probes are continually being developed to encompass all the desired elements while minimizing compromises.[104]

A common structural feature of many fluorophores is a conjugated π-system functionalized with both an electron-donating and an electron-withdrawing group, known collectively as donor-π-acceptor dyes. For many of these fluorescent compounds, the π-system is a naphthalene moiety (Figure 1.3). The synthesis of these fluorescent chromophores usually begins by making variations to commercially available naphthalene derivatives; alternatively, new naphthalene-based dyes are developed by a reverse-engineering approach, whereby modifications are made to an existing fluorophore. An excellent example of these protocols involves the synthesis of the solvatochromic fluorophore PRODAN (**1.8**)[7a] and its derivatives, such as the lipophilic LAURDAN (**4.1**),[7b] the thiol-reactive Acrylodan (**4.2**)[105] and Badan (**4.3**),[106] the amino acid-containing Aladan (**4.4**),[107] and the anthracene-based Anthradan (**4.5**) (Figure 4.1).[108] For example, PRODAN (**1.8**) was originally synthesized by Weber et al. by Friedel-Crafts acylation of 2-methoxynaphthalene (**4.6**) with propionyl chloride to provide **4.7**, followed by aromatic substitution with lithium dimethylamide (Scheme 4.1, A).[7a] A more recent approach begins by a Bucherer reaction of 6-bromo-2-naphthol (**4.8**) using sodium metabisulfite and methylamine hydrochloride to yield 6-bromo-*N*-methylnaphthalen-2-amine (**4.9**).[109] Both acylation/reduction[109] and alkylation/dealkylation[110] protocols have been employed to afford the

dimethylaminonaphthalene **4.10**, which can then be acylated by conversion of **4.10** to an aryllithium, followed by addition of *N*-propionylpyrrole to produce PRODAN (**1.8**) (Scheme 4.1, B).[110] In addition to modifying commercially available naphthalene substrates to generate PRODAN (**1.8**), subsequent transformations may be applied directly to PRODAN to create dye derivatives, one example being Acrylodan (**4.2**). Subjecting the lithium enolate of **1.8** to selenation conditions with phenylselenyl bromide, followed by oxidation with sodium periodate and *syn* elimination produces Acrylodan (**4.2**) in a high yield of 89% (Scheme 4.1, C).[105]

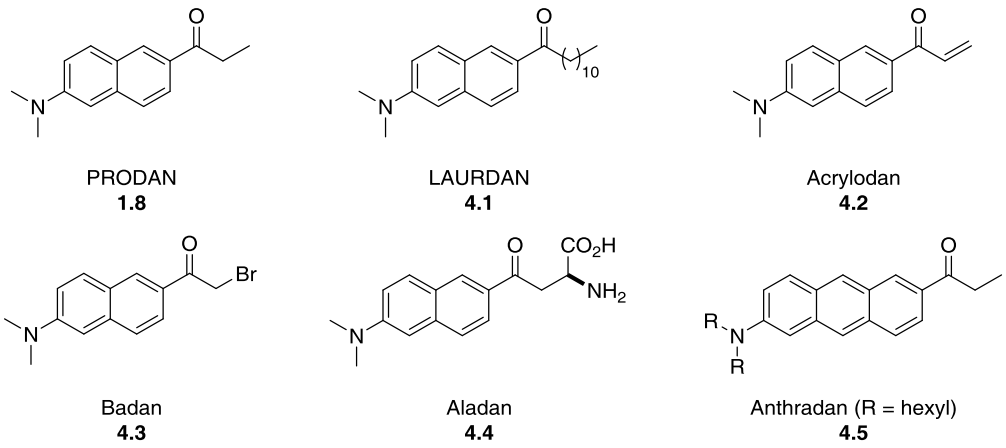

Figure 4.1. PRODAN and its derivatives

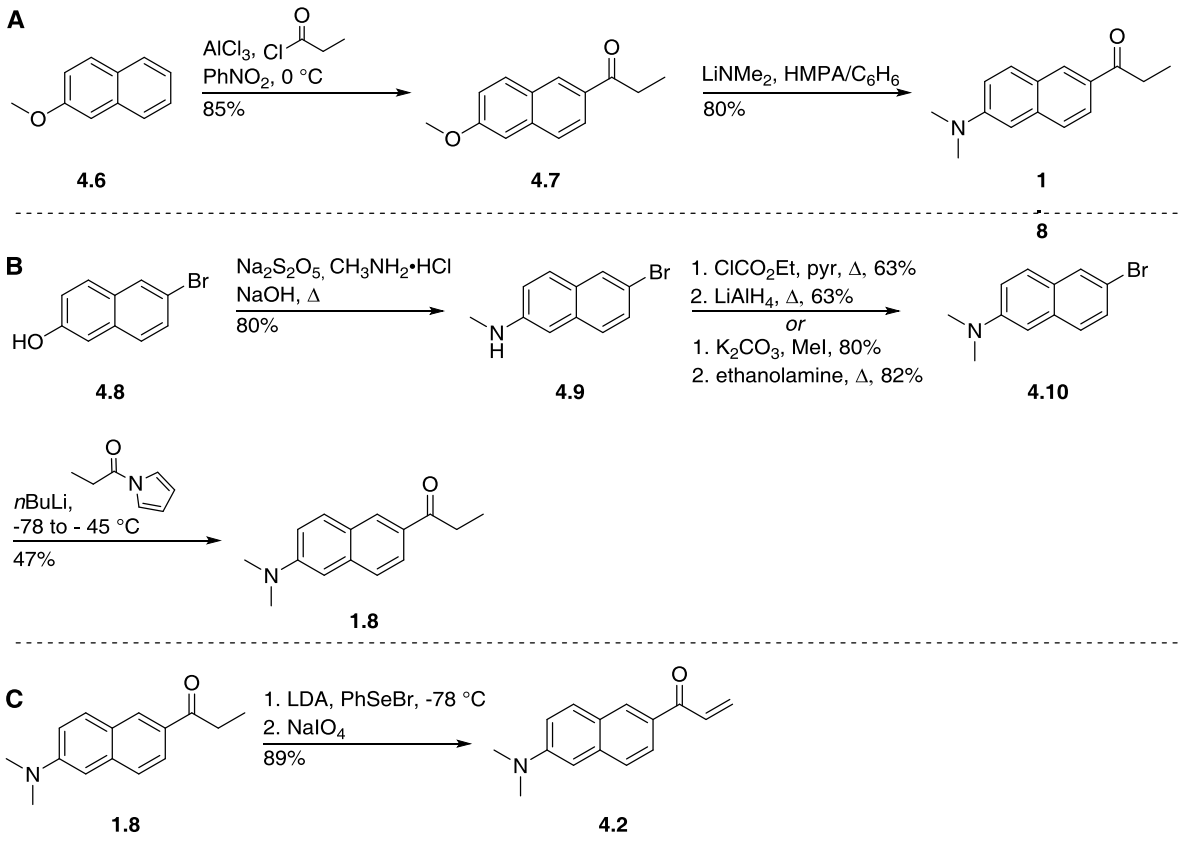

Scheme 4.1 Synthesis of PRODAN and Acrylodan from preexisting naphthalene frameworks

Although the strategies detailed for the synthesis of PRODAN (**1.8**) and Acrylodan (**4.2**) are representative examples of how many fluorescent dyes are assembled, and only require 2-4 synthetic steps to prepare from commercially available materials, the diversity that can be incorporated into the dye scaffold is very limited. A *de novo* synthesis of these naphthalene-based fluorophores would allow for more functional group variation in terms of identity of the functionality and its location within the dye. More importantly, a *de novo* synthetic strategy would not only afford more diversely functionalized scaffolds, but also potentially permit systematic variations to the dye's structure allowing for correlation of structure with photophysical properties. An understanding of structure-photophysical property relationships

(SPPR) is important because it can provide a general set of rules that can then be utilized to tune the chemical and photophysical properties of fluorescent dyes for specific applications. This allows for maximization of the benefits associated with fluorescent dyes while minimizing the compromises that usually accompany selecting a dye that is commercially available.

Despite the advantages associated with determining SPPR of fluorescent dyes, especially by employing *de novo* synthetic strategies, this concept remains relatively unexplored, which can be partially attributed to the convenience of commercially available dyes. However, SPPR studies of fluorescent dyes with an emphasis on using calculations to predict or explain the absorption and/or emission wavelengths have been reported more recently. One example was demonstrated by Baudequin et al. using push-triazole-pull (PTP) chromophores **4.11** that were synthesized via a Cu(I)-mediated Huisgen 1,3-dipolar cycloaddition; this approach allowed for variations in the donor, linker, and acceptor units of the fluorophore (Figure 4.2).[111] Baudequin et al. found that increasing the strength of the donor resulted in red-shifted absorption and emission and increased quantum yield, while changing the linker from a triazole to acetylene, as in **4.12**, significantly decreased quantum yield and Stokes shift, increased molar absorptivity, and red-shifted the absorption maximum. Changes in absorption maxima with variations in structure were explained by TD-DFT/B3LYP calculations of HOMO-LUMO energy gaps for each fluorophore.

A more comprehensive study was conducted by Park et al. on 9-aryl-1,2-dihydropyrrolo[3,4-b]indolizin-3-one derivatives **4.13**, collectively named Seoul-Fluor dyes, that were prepared via a *de novo* synthetic strategy beginning from varyingly substituted amines and cinnamaldehydes.[112] Park et al. prepared 68 Seoul-Fluor analogs in which a correlation was found between the dye's photophysical properties and the electronic nature of the substituents, as

well as their location on the chromophore (Figure 4.2). In these studies, DFT calculations were used to determine which atoms of the dye had the largest HOMO and LUMO coefficients, while the Hammett-constant was employed as a guide to systematically vary electron densities at these positions. Specifically, incorporating more electron-rich or electron-deficient substituents on carbons containing a large HOMO or LUMO coefficient, respectively, resulted in bathochromic shifts in emission maxima by decreasing the HOMO-LUMO energy gap. One particularly important aspect of this work was the ability to predict and tune emission wavelengths of the Seoul-Fluor dyes based on the electronic nature of their substituents by correlating emission wavelengths for the dye library with each dye's respective HOMO-LUMO energy gap. This is the first example of prediction of emission by utilizing computational methods.

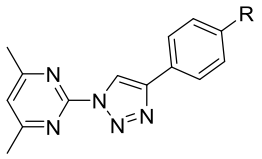

4.11

R	λ_{abs} (nm)	λ_{em} (nm)	Φ_F	ε (M^{-1} cm^{-1})
NMe_2	289	486	0.47	24386
OMe	254	389	0.01	46211
Me	250	364	<0.01	18943

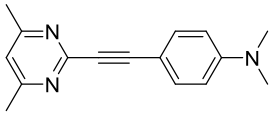

4.12

λ_{abs} (nm)	λ_{em} (nm)	Φ_F	ε (M^{-1} cm^{-1})
357	447	0.04	42161

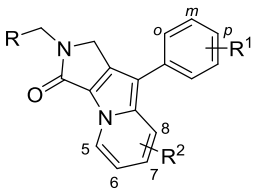

4.13

p-R^1	7-R^2	λ_{abs} (nm)	λ_{em} (nm)	Δ (eV)
CN	COMe	407	494	2.96
Me	COMe	408	509	2.93
Me	OMe	337	485	3.25
NPh_2	COMe	428	579	2.49

Figure 4.2. Previous examples of SPPR studies

While the above examples are directed toward very specific and lesser known dye frameworks, more extensive SPPR studies have been conducted on the popular and commonly

used BODIPY and cyanine fluorescent dyes. For the BODIPY dyes, numerous variations have been made at all positions of the dye scaffold, which have allowed for changes in the electronic nature and number of the subsitutents, conjugation length, and applications of these fluorophores.[113] By appropriately modifying the substituents on the BODIPY substrates, a wide range of absorption and emission properties can be accessed, with the emission red-shifting toward the near-IR. Similar systematic modifications have been incorporated into the cyanine[114] and merocyanine dyes,[115] with an additional emphasis on exploring the effect of charged versus neutral dye frameworks on photophysical properties, as well as the results of increasing or decreasing the length of the polymethine chain. Computational studies have also been utilized for the cyanine dyes to predict and to understand the SPPRs as a means of increasing their utility toward optical[116] or biological sensing applications.[117]

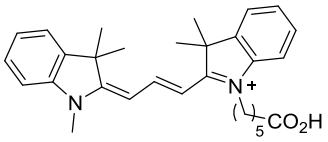

Cyanine Dye
Cy3

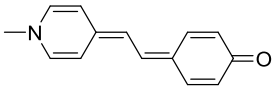

Merocyanine Dye
Brooker's merocyanine

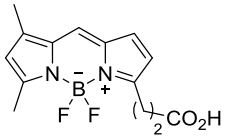

BODIPY
BODIPY R6G

We envisioned that our *de novo* synthesis of naphthalenes via the DDDA reaction could be utilized to generate a new framework of cyclopenta[*b*]naphthalene-based fluorescent dyes that could be readily diversified, and the substituents systematically varied, in order to study SPPR in a similar manner to the reports described above. The synthetic versatility of the DDDA reaction allows for incorporation of a variety of functional groups onto a naphthalene core that could act

as donors and acceptors to create donor-π-acceptor dyes, as well as for the addition of further subsitutents that could be used to tune the properties of the fluorophore. Moreover, donors and acceptors could readily be placed at different positions along the naphthalene ring using the DDDA reaction, increasing the value of this methodology for the study of SPPR. By comparing the frameworks of cyclopenta[*b*]naphthalene compounds **1.94d** and **1.144** that we have already accessed via the DDDA reaction to the commercially available and commonly used dye PRODAN (**1.8**), similarities between the structures become apparent, especially if the halogens are converted to a dimethylamine donor (Scheme 4.2).

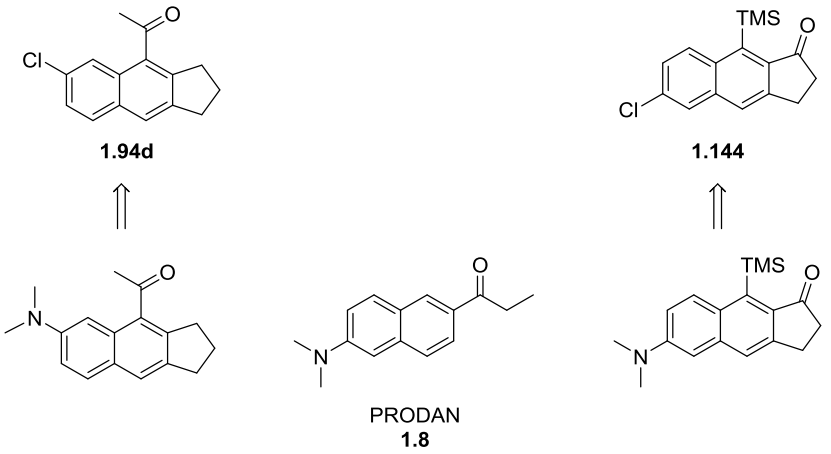

Scheme 4.2. Structural similarity of naphthalenes **1.94d** and **1.144** to PRODAN

We were especially interested in the application of the DDDA reaction to the synthesis and study of PRODAN derivatives, as these dyes are widely used in biological systems, especially for the study of the local environment of proteins,[118] DNA,[119] and lipid membranes.[7b,120] Upon absorption of a photon by PRODAN, an intramolecular charge transfer occurs that results in a charge-separated excited state of the dye with an increased dipole moment

compared to the ground state. The solvent molecules can then reorient dipoles around the fluorophore, resulting in a more ordered arrangement that stabilizes the excited state while destabilizing the ground state (Figure 4.3). The decreased energetic gap leads to a red-shifted emission, the degree of which depends on the polarity of the solvent, with more polar solvents producing larger bathochromic shifts. Applying these solvatochromic dyes to biological systems allows for hydrophobic and hydrophilic environments to be distinguished based on changes in the fluorophore's emission wavelength or intensity as local or conformational changes occur. Specifically, hypsochromic shifts in emission occur when the dye is in a hydrophobic environment, such as hydrophobic pocket of a protein, while bathochromic shifts are observed with incorporation of the dye into hydrophilic environments, such as in a disordered lipid phase. We postulated that appropriately functionalized cyclopenta[*b*]naphthalene substrates generated via the DDDA reaction would emit via a similar intramolecular charge transfer mechanism as PRODAN (**1.8**); therefore, they may have photophysical properties similar to PRODAN and its derivatives, which would allow for their use in related biological applications. Additionally, the synthetic versatility of the DDDA reaction allows for modifications to be made to the cyclopenta[*b*]naphthalene dye scaffold, which could lead to derivatives with even more desirable photophysical properties compared to PRODAN (**1.8**) that could be tuned for specific biological applications.

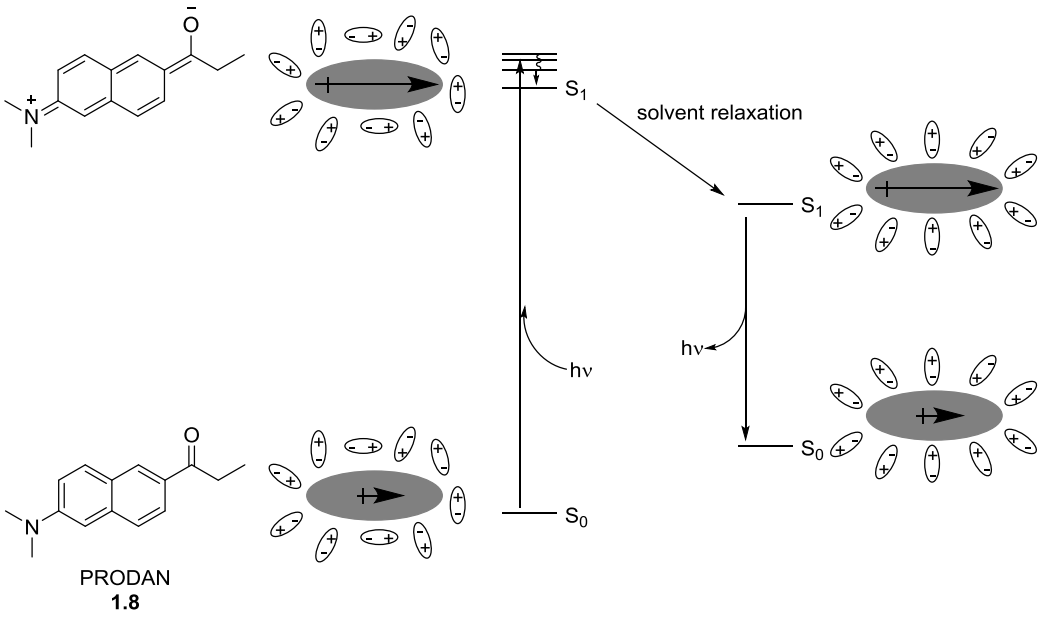

Figure 4.3. Mechanism of solvent relaxation leading to solvatochromism in PRODAN (**1.8**)

4.2 SYNTHESIS OF A CYCLOPENTA[*B*]NAPHTHALENE DYE

To test the feasibility of utilizing cyclopenta[*b*]naphthalene substrates generated via the DDDA reaction as solvatochromic fluorescent dyes, halogenated naphthalenes needed to first be converted to naphthalenes bearing an electron-donating moiety, such as an amine. A Buchwald-Hartwig palladium-catalyzed cross-coupling reaction was selected for this purpose because of the success that was previously demonstrated by Buchwald et al. for its application to an array of chloro-substituted benzene compounds using a variety of amines as coupling partners.[121] As an initial study, Dr. Erica Benedetti, a postdoctoral fellow in our laboratory, subjected chloronaphthalene **1.94d** to Buchwald-Hartwig reaction conditions of RuPhos palladacycle (**4.14**), lithium hexamethyldisilylazide (LHMDS), and dimethylamine to afford cyclopenta[*b*]naphthalene **4.15** in 70% yield (Scheme 4.3). We were pleased by the success of

this initial reaction because cross-coupling reactions of chloronaphthalenes with aliphatic amines have scarcely been reported,[122] and also because this allowed us to continue using chloro- rather than bromonaphthalenes. Bromonaphthalenes are advantageous in cross-coupling reactions due to their increased reactivity, but for the same reason the bromo substituent also becomes a liability during earlier stages of the naphthalene synthesis, especially when metal-halogen exchange can occur.

With our donor-π-acceptor substrate in hand, we measured the absorption and fluorescence spectra of cyclopenta[*b*]naphthalene **4.15** in dichloromethane and determined that the compound had an absorption maximum at 377 nm and an emission maximum at 510 nm (Scheme 4.3). These results demonstrated that not only was the dimethylamine-substituted cyclopenta[*b*]naphthalene compound fluorescent, but it displayed a bathochromic shift in photophysical properties compared to PRODAN (**1.8**) whose absorption and emission maxima in dichloromethane occur at 355 and 440 nm, respectively.[7a] A much larger Stokes shift of 6917 cm^{-1} was also determined for **4.15**, whereas the Stokes shift of PRODAN (**1.8**) was 5442 cm^{-1}. Such large shifts in emission maxima for PRODAN derivatives were only previously found by inserting an additional aromatic ring between the donor and acceptor moieties, as in Anthradan (**4.5**, λ_{em} = 536 nm).[108] However, unlike Anthradan (**4.5**), **4.15** is relatively small, thereby lessening potential disruption to biological systems being studied with this dye. Furthermore, the bathochromic shift of absorption of **4.15** (22 nm) into the visible region allows for excitation with visible light, whereas PRODAN (**1.8**) absorbs light in the UV range, which limits the uses of PRODAN in biological systems.

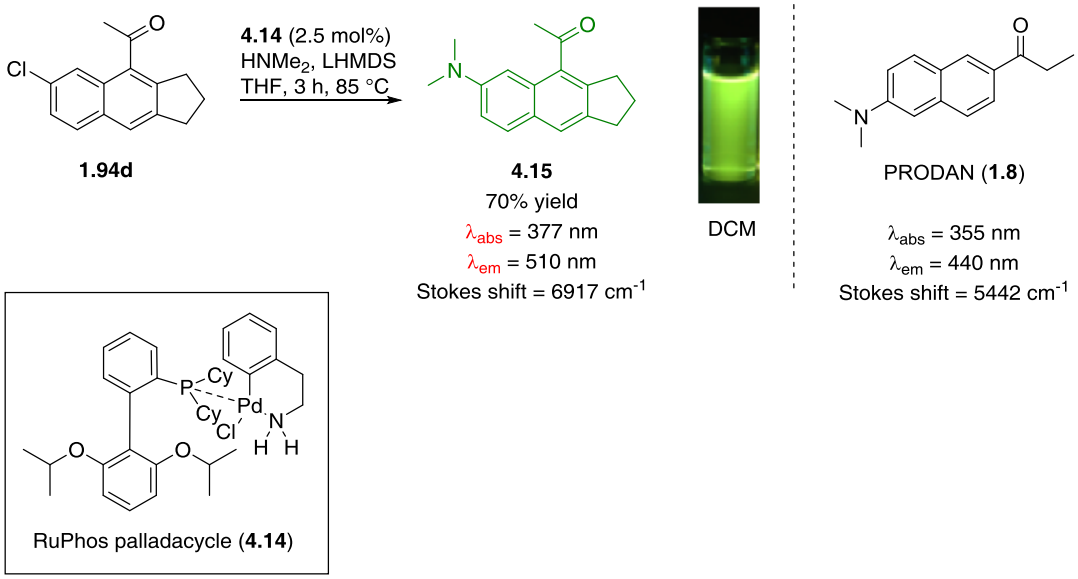

Scheme 4.3. Buchwald-Hartwig reaction to produce a cyclopenta[*b*]naphthalene dye

Next, the solvatochromism of **4.15** was measured so that a comparison could once again be made to PRODAN (**1.8**). PRODAN is commonly utilized in studies of local biological environments because of its sensitivity to polarity, and if we were to apply our dyes to related systems, they would need to display a similar solvatochromic behavior. The maximum emission wavelength of **4.15** was evaluated in 9 solvents ranging in polarity from the non-polar cyclohexane to the polar protic ethanol. A large bathochromic shift of emission of 88 nm was observed when the fluorescence of **4.15** was measured in toluene (λ_{em} = 490 nm) and ethanol (λ_{em} = 578 nm); the emission spectra of PRODAN (**1.8**) only displayed a 69 nm red-shift when studied using the same solvent systems (Figure 4.4).[7a] PRODAN (**1.8**) was insoluble in cyclohexane, so a direct comparison to **4.15** (λ_{em} = 466 nm in cyclohexane) was not made for this solvent. Unlike PRODAN (**1.8**), which displayed a 22 nm red-shift in absorption maxima from toluene to ethanol, the absorption spectra of **4.15** did not change when solvent polarity was

increased. The larger solvatochromic shift in emission observed for **4.15** compared to PRODAN (**1.8**) indicates that **4.15** can detect changes in polarity in a similar manner as PRODAN, and that cyclopenta[*b*]naphthalene dyes may potentially be valuable as biological polarity sensors.

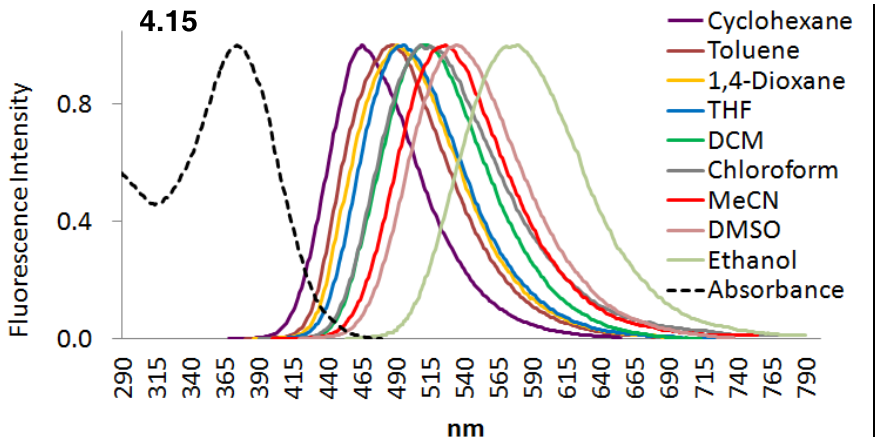

solvent	λ_{em} (nm) **4.15**	λ_{em} (nm) **1.8**
cyclohexane	466	-
toluene	490	416
1,4-dioxane	495	422
THF	497	430
DCM	510	440
chloroform	516	-
MeCN	529	455
DMSO	536	462
Ethanol	578	485

Figure 4.4. Solvatochromic shift in emission wavelength of **4.15**

4.3 SYNTHESIS AND PHOTOPHYSICAL INVESTIGATION OF CYCLOPENTA[*B*]NAPHTHALENE DYE DERIVATIVES

The interesting photophysical properties of cyclopenta[*b*]naphthalene dye **4.15** identified during our initial studies prompted us to prepare a number of structurally related compounds in a search for fluorescent dyes with superior photophysical properties. The first modifications that we were interested in making to the cyclopenta[*b*]naphthalene scaffold were changes to the donor and acceptor of the fluorophore. We envisioned that the substituents of the amine donor could be readily varied by utilizing different primary and secondary amines as coupling partners in the

Buchwald-Hartwig cross-coupling reaction,[121] along with the reaction conditions that were previously established in the conversion of 7-chloronaphthalene **1.94d** to dye **4.15** (Scheme 4.3). While the Buchwald-Hartwig cross-coupling reaction could be employed for changes in the donor, the synthetic versatility of the DDDA reaction enabled changes in the dye's acceptor moiety. Earlier studies of the DDDA reaction of styrene-ynes led to the successful formation of a number of cyclopenta[*b*]naphthalenes in high yields and short microwave irradiation times which contained varied electron-withdrawing functionality, including an aldehyde **1.106**, ester **1.107**, sulfone **1.109**, and phosphonate **1.111** (Scheme 1.25). Additionally, cyclopenta[*b*]naphthalenone **1.139** containing the acceptor at a different position of the naphthalene was also previously synthesized via the DDDA reaction, and could potentially be converted to a fluorescent dye by a Buchwald-Hartwig cross-coupling reaction (Scheme 1.31).

4.3.1 Synthesis of cyclopenta[*b*]naphthalenes with varied donor and acceptor moieties

Cyclopenta[*b*]naphthalene fluorescent dyes in which the substituents of the amine donors were varied were synthesized by Buchwald-Hartwig cross-coupling reactions of 7-chloronaphthalene **1.94d** with several primary and secondary amines. Each reaction was performed using the same conditions of RuPhos palladacycle (2.5 mol%) and LHMDS that previously resulted in a 70% yield of the dimethylamine-substituted dye **4.15** (Scheme 4.3). The secondary amines employed as cross-coupling partners in the Buchwald-Hartwig cross-coupling reaction of **1.94d** were pyrrolidine, piperidine, and morpholine, while the primary amines chosen were benzylamine, aniline, and *para*-methoxyaniline. The secondary amines were successfully coupled to **1.94d** to produce the 7-aminonaphthalene dyes **4.16**-**4.18** in moderate yields of 45-59% (Scheme 4.4). Primary amines appeared to undergo the Buchwald-Hartwig cross-coupling reaction more

efficiently, as the yield of these three reactions to produce **4.19**-**4.21** were higher yielding (71-89%).

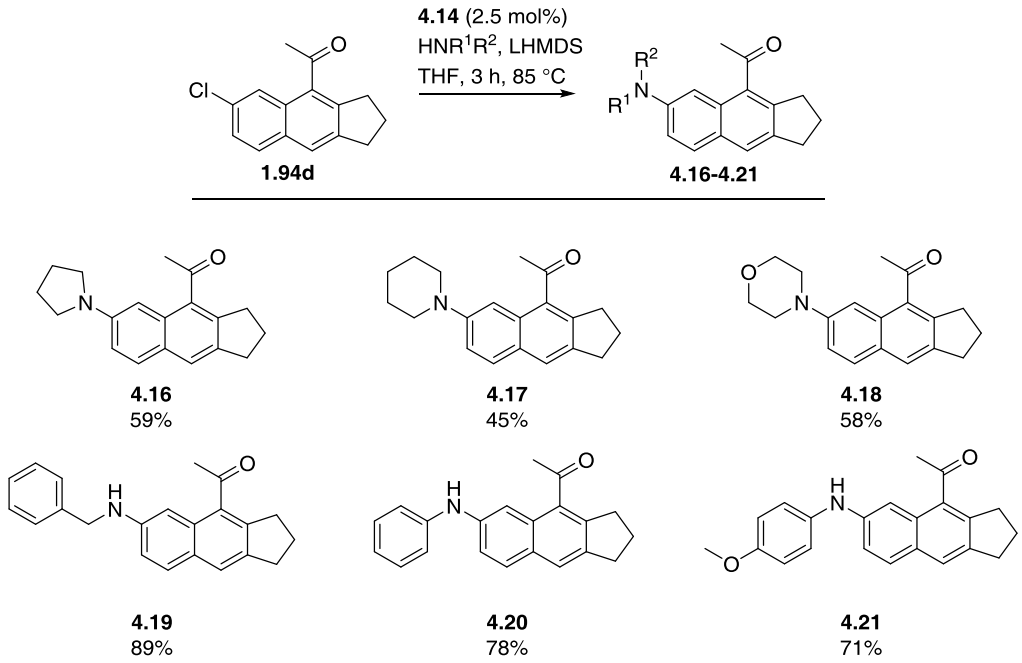

Scheme 4.4. Buchwald-Hartwig reaction of **1.94d** with varied primary and secondary amines

Variations were also made to the acceptor functionality of the dye by performing Buchwald-Hartwig cross-coupling reactions of dimethylamine or pyrrolidine with the 7-chlorocyclopenta[*b*]naphthalenes **1.106**, **1.107**, **1.109**, **1.111**, **1.139**, and **1.143** previously generated via the DDDA reaction. While Buchwald-Hartwig cross-coupling reactions employing LHMDS as base were successful for dyes bearing a methyl ketone, these conditions were not suitable to afford dyes containing different electron-withdrawing functionality as the acceptor, such as aldehydes, esters, sulfones, and phosphonates; each of these reactions resulted in less

than 20% yield of the desired products **4.22-4.26** (Scheme 4.5). However, the 7-chlorocyclopenta[*b*]naphthalenone **1.139** did undergo the Buchwald-Hartwig cross-coupling reaction using LHMDS as base to produce dimethylamine-substituted naphthalene **4.27** in 63% yield. To improve the yield of the Buchwald-Hartwig reaction toward the generation of fluorescent dyes incorporating acceptors other than ketones, cesium carbonate was tested as the base because of its previous success when used in Buchwald-Hartwig reactions of aryl groups substituted with electron-deficient functionality.[121] For cyclopenta[*b*]naphthalenes containing aldehydes **4.22**, sulfones **4.25**, and phosphonates **4.26** as the acceptor moiety, yields were approximately 2-4 times greater when cesium carbonate was employed as a base in the cross-coupling reaction (44-74% yield). Cesium carbonate was not tested in the Buchwald-Hartwig cross-coupling reaction of the ester-substituted 7-chlorocyclopenta[*b*]naphthalene to form **4.24**, or for the generation of 7-dimethylaminocyclopenta[*b*]naphthalenone **4.27**, which was already produced in decent yield by using LHMDS.

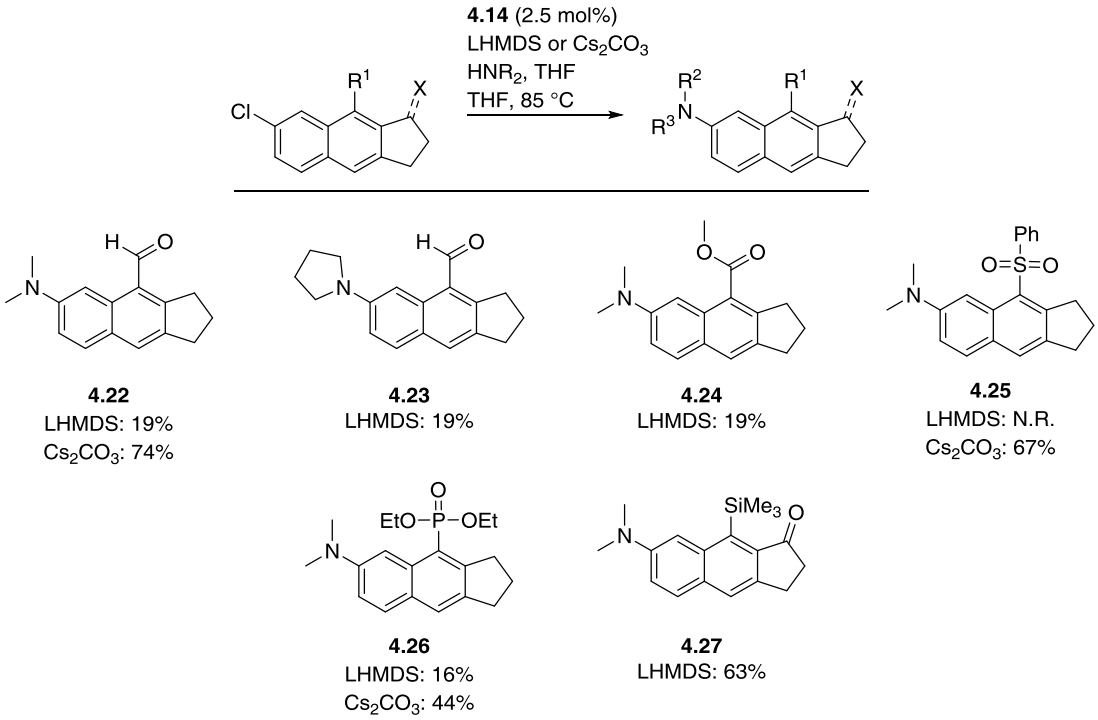

Scheme 4.5. Buchwald-Hartwig reaction of naphthalenes containing different EWGs

4.3.2 Photophysical properties of cyclopenta[*b*]naphthalene fluorescent dyes with varied donor and acceptor moieties

With the cyclopenta[*b*]naphthalene fluorescent dye derivatives in hand, the photophysical properties of each dye were measured in dichloromethane and comparisons were made between changes in structure and the resulting photophysical properties. Changing the number or type of substituents on the amine donor, as in **4.16**-**4.21**, had little overall effect on the photophysical properties of the cyclopenta[*b*]naphthalene dyes (Figure 4.5). The incorporation of pyrrolidine, piperidine, and morpholine as donors, rather than dimethylamine, produced dyes with very similar emission to that of **4.15** (λ_{em} = 508-515 nm). Absorption did vary to a degree for each of these dyes, with the pyrrolidine-substituted derivative **4.16** showing the most red-shifted

absorption maxima at 390 nm, while piperidine- and morpholine-substituted dyes **4.17** and **4.18** displayed more blue-shifted absorption maxima of 362 and 355 nm, respectively, than either **4.15** or **4.16**. The hypsochromic shift in absorption maxima observed for **4.17** and **4.18** also led to each of these dyes having a large Stokes shift of 8207 and 8484 cm^{-1}, respectively; this was a 1289-1567 cm^{-1} increase in Stokes shift compared to dimethylamine-substituted dye **4.15**. Dyes containing secondary amines as donors, such as those substituted with benzylamine **4.19**, aniline **4.20**, and *para*-methoxyaniline **4.21**, did not show substantial deviation in absorption maxima when compared to each other or to **4.15** (λ_{abs} = 367-372 nm); however, the emission was significantly blue-shifted when compared to the dyes incorporating tertiary amine donors. Each dye containing a secondary amine donor was characterized by emission maxima in the range of 482-495 nm, which is a 13-33 nm difference in emission compared to the tertiary amine derivatives. The blue-shift in emission observed for **4.19**-**4.21** can be explained by the absence of two electron-releasing substituents on the amine, which lessens the donating ability of the amine into the conjugated system. Donors that are more electron-releasing typically result in more red-shifted emission spectra.[111]

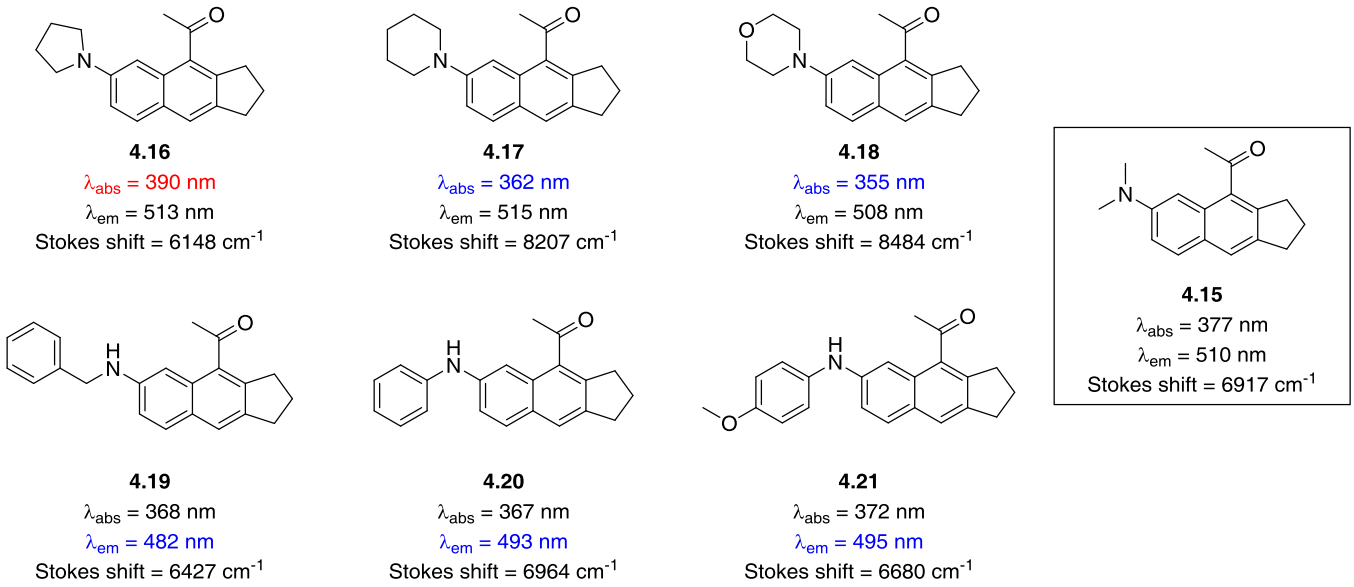

Figure 4.5. Effect of donor substituents on photophysical properties of naphthalene dyes

The photophysical properties of dyes incorporating various EWGs as acceptors were also examined. In these examples, more variation in absorption and emission maxima was noted by changing the identity or location of the acceptor moiety than was observed by changing the substituents of the amine donor. Exchanging the methyl ketone of **4.15** for an aldehyde as the acceptor in **4.22** resulted in a bathochromic shift in both the absorption and emission maxima of 60 and 30 nm, respectively (Figure 4.6). This large shift in absorption maxima now placed the absorption spectrum of **4.22** in the visible region, rather than the UV, highlighting this particular dye as more amenable for application in biological systems. Despite the red-shift of 13 nm observed when dimethylamine was varied to pyrrolidine in systems containing a methyl ketone as the acceptor (**4.15** versus **4.16**), this same trend was not recognized for dyes in which an aldehyde was the acceptor, as **4.23** displayed almost the same photophysical properties as **4.22**. Incorporating an ester, as in **4.24**, which would be a weaker electron acceptor than both the

aldehyde **4.22** and the methyl ketone **4.15**, showed a similar absorption maximum to **4.15**, but an emission maximum that was blue-shifted by 22 nm (λ_{em} = 488 nm). The photophysical properties when a sulfone **4.25** and a phosphonate **4.26** were utilized as acceptors on the cyclopenta[*b*]naphthalene dyes were also investigated, and a hypsochromic shift in emission maxima of 24 and 50 nm, respectively, was noted compared to **4.15**. While the phosphonate-substituted dye **4.26** maintained a similar absorption maximum to **4.15** (λ_{abs} = 384 nm), the absorption maximum of sulfone-substituted **4.25** was red-shifted by 29 nm (λ_{abs} = 406 nm). One final dye that was examined and showed optimal photophysical properties that were nearly identical to that of the aldehyde-bearing cyclopenta[*b*]naphthalene **4.22** was cyclopenta[*b*]naphthalenone **4.27**, which not only contained the acceptor at a different position on the naphthalene, but also incorporated additional functionality in the form of a TMS group on the naphthalene ring.

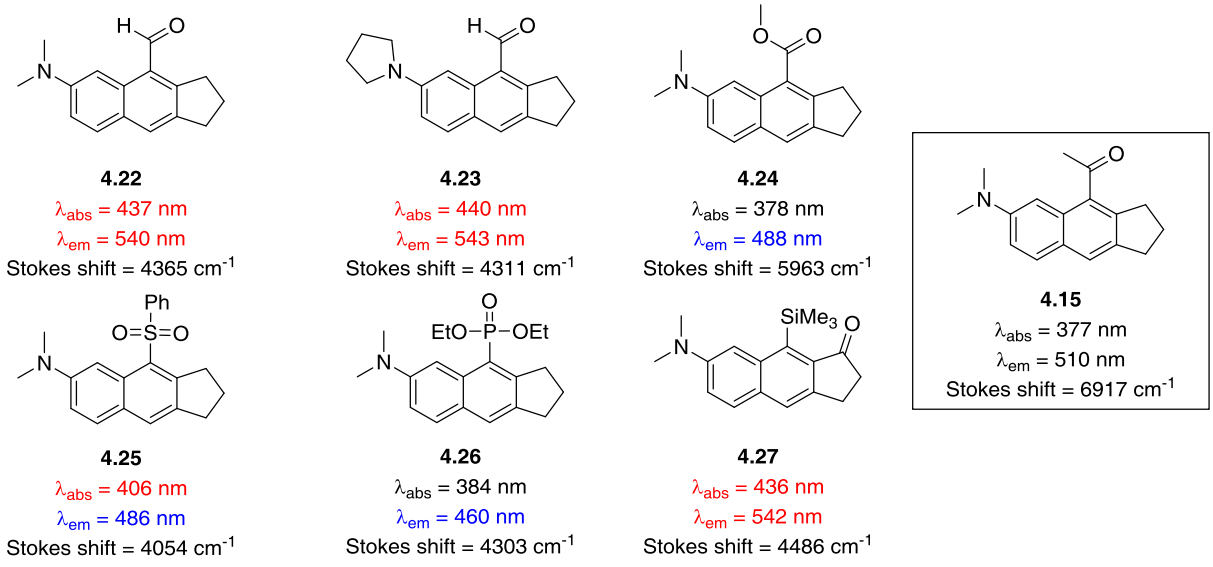

Figure 4.6. Effect of different acceptors on photophysical properties of naphthalene dyes

Of all the dyes for which the donor and acceptors were varied and the photophysical properties investigated, aldehyde-substituted cyclopenta[*b*]naphthalene **4.22** and cyclopenta[*b*]naphthalenone **4.27** displayed the most desirable absorption and emission maxima that were equivalent to one another, but red-shifted considerably from the other dyes in the series. Red-shifted absorbance and emission maxima are desirable when using dyes to study biological systems because less damage is caused to the cellular environment by excitation of the dye with lower energy visible light, rather than UV light, and also there is less signal overlap from autofluorescence when the emission spectrum occurs at lower energies. Based upon these results and our desire to perform more in-depth SPPR studies on these cyclopenta[*b*]naphthalene dyes in order to rationally design and tune the properties of future analogs, the cyclopenta[*b*]naphthalenone scaffold was chosen for further investigation. The cyclopenta[*b*]naphthalenone dyes have structures that are the most similar to PRODAN (**1.8**), and would allow for a direct comparison of the properties of our dyes to those of PRODAN.

4.4 SPPR STUDIES OF CYCLOPENTA[*B*]NAPHTHALENONE DYES

The photophysical properties of PRODAN (**1.8**) have been well documented over the past several decades. Of special interest has been the solvatochromic behavior of PRODAN (**1.8**) and its application to biological systems, as previously discussed, as well as the nature of PRODAN's excited states. There has been much debate whether PRODAN emits from a planar intramolecular charge transfer state (PICT) where the amine is planar with the naphthalene ring, or from a twisted intramolecular charge transfer (TICT) state where the amine is at a 90° angle. In the case of the latter, nearly full charge transfer is proposed to occur from the amine donor to

the carbonyl acceptor in a similar mechanism to that accepted for dimethylaminobenzonitrile (DMABN).[123] Previous theoretical investigations of PRODAN (**1.8**) support the formation of a TICT state;[124] however, experimental evidence, such as solvatochromic studies[125] or dielectric loss measurements,[126] indicates a PICT geometry of the excited state. Through SPPR studies where PRODAN derivatives were synthesized in which the amine donor and carbonyl acceptor were either forced into planar or twisted conformations, Abelt et al. provided evidence for emission of PRODAN (**1.8**) from a PICT excited state. In examples where the amine was constrained to coplanarity with the aromatic system, such as **4.28**, the photophysical and solvatochromic properties observed were similar to those of PRODAN (**1.8**);[127] however, amines forced into twisted conformations (**4.30**) exhibited very different spectral properties (Figure 4.7).[128] Placing the carbonyl acceptor in a planar or twisted position relative to the naphthalene, as in **4.29** and **4.31**, respectively, also showed that the properties of **4.29** more closely matched those of PRODAN (**1.8**).[129] In addition to studying conformations of the donor and acceptor to determine the geometry of the excited state, Abelt et al. also altered the location of the acceptor by placing it in a *peri*-position on the naphthalene **4.32**; this change in position of the acceptor had a large effect on the absorption and emission maxima by red-shifting both values significantly.[130] Despite these few examples of SPPR studies conducted for PRODAN derivatives, other systematic variations to the PRODAN framework have not been investigated. Notably, no research has been performed to explore the effect of donor position on the emissive properties of PRODAN (**1.8**), or the effect of additional substituents on the naphthalene ring. We envisioned that by once again utilizing the synthetic versatility of the DDDA reaction coupled with the Buchwald-Hartwig cross-coupling reaction, we could study these effects on a PRODAN derivative by systematically varying the cyclopenta[*b*]naphthalenone dye scaffold. In this

manner, SPPR could be concluded, allowing for the future rational design of fluorescent dyes for specific applications.

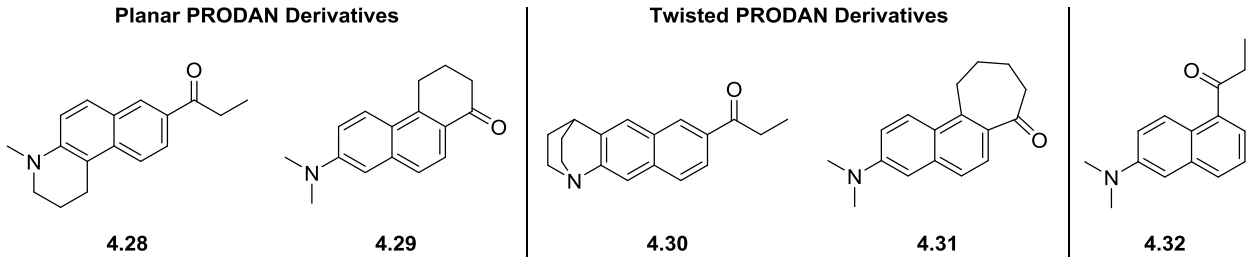

Figure 4.7. Previous SPPR studies of PRODAN derivatives

4.4.1 Synthesis of cyclopenta[*b*]naphthalenone fluorophores

The preparation of a series of cyclopenta[*b*]naphthalenone-based fluorophores that are systematically varied in structure and functionality was performed by a microwave-assisted DDDA reaction of styrene-ynes **1.123a-c** and **1.124a-c** to yield the phenyl- and TMS-substituted cyclopenta[*b*]naphthalenones **1.138-1.145**, as previously described (Scheme 1.31). Desilylation of the TMS-substituted cyclopenta[*b*]naphthalenones **1.142-1.145** was then achieved with tetra-*n*-butylammonium fluoride (TBAF) to generate **4.33-4.35** in 51-65% yield (Scheme 4.6). A subsequent Buchwald-Hartwig cross-coupling reaction of the chloro-substituted cyclopenta[*b*]naphthalenones **1.138-1.145** and **4.33-4.35** with dimethylamine using RuPhos palladacycle (**4.14**) as the catalyst and either LHMDS or cesium carbonate as the base resulted in the formation of the cyclopenta[*b*]naphthalenone fluorescent dyes **4.36**, **4.37**, and **4.39-4.46** (Scheme 4.7). Dye **4.38** was afforded by desilylation of the TMS-substituted

cyclopenta[*b*]naphthalenone dye **4.27** with TBAF in 60% yield (not shown). All fluorescent dyes were synthesized in 48-85% yield, except for phenyl-substituted substrate **4.41**, which was isolated in 20% yield. The low yield observed for the Buchwald-Hartwig cross-coupling reaction to generate **4.41** was likely the result of the poor solubility of its precursor **1.140** in THF. The 8-chlorocyclopenta[*b*]naphthalenone compounds **1.141** and **1.145** failed to undergo the amine cross-coupling reaction to afford **4.47** and **4.48**, which was attributed to the steric hindrance imposed by the TMS and phenyl substituents *peri* to the chloro group on the naphthalene ring. Further attempts to obtain **4.47** and **4.48** by utilizing the less sterically hindered SPhos palladacycle catalyst (**4.49**) in the Buchwald-Hartwig cross-coupling reaction, which has been previously shown to work better than RuPhos palladacycle (**4.14**) for coupling of amines with *ortho*-chloro-substituted aryl systems, also failed.[121b]

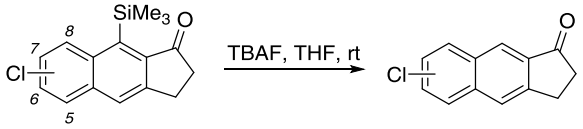

5-Cl **1.142**
6-Cl **1.144**
8-Cl **1.145**

5-Cl **4.33** 51%
6-Cl **4.34** 51%
8-Cl **4.35** 65%

Scheme 4.6. Desilylation of TMS-substituted cyclopenta[*b*]naphthalenone substrates

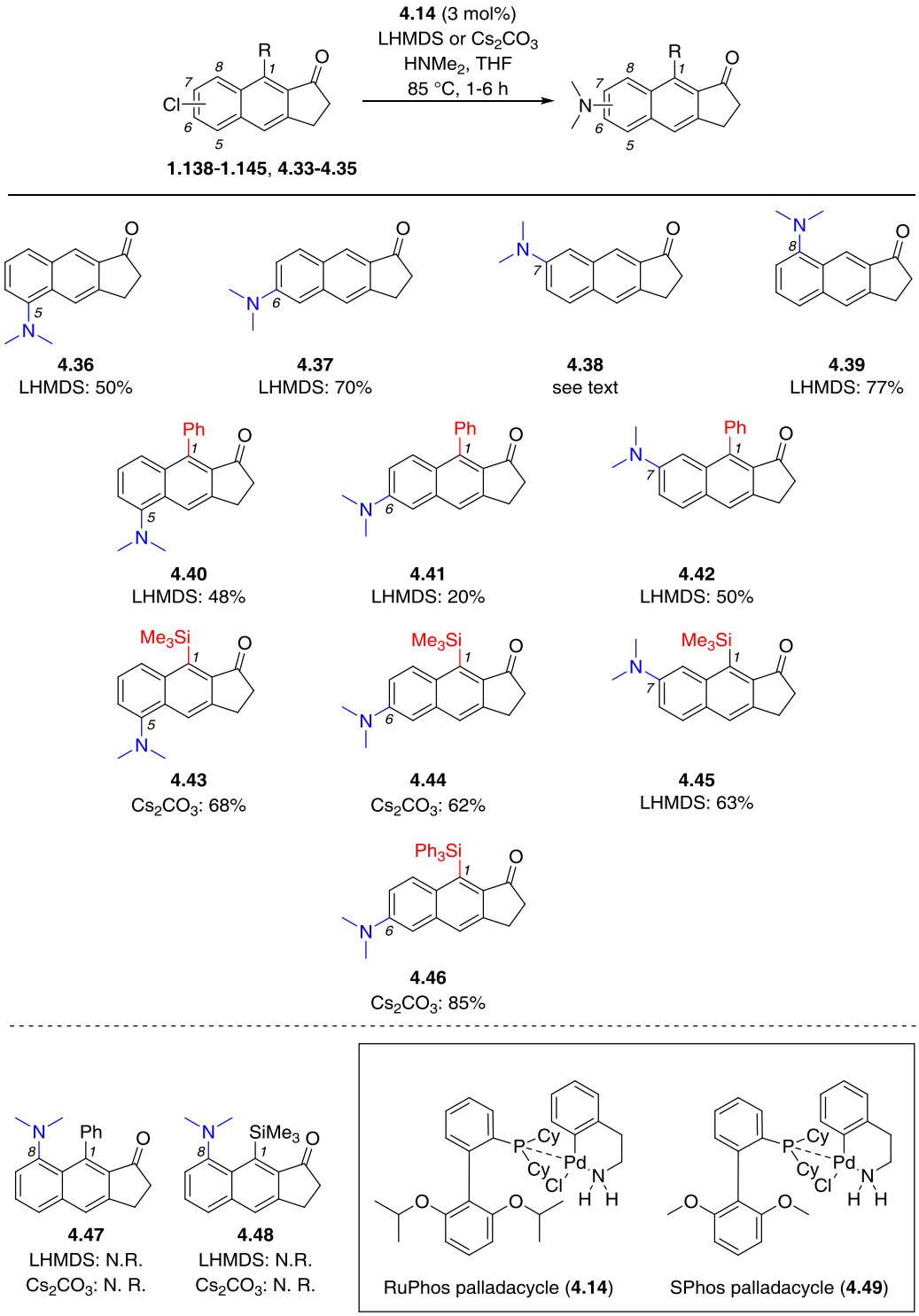

Scheme 4.7. Buchwald-Hartwig reaction to yield cyclopenta[*b*]naphthalenone dyes

4.4.2 Effect of donor position on photophysical properties of cyclopenta[*b*]naphthalenone dyes

Absorption, emission, Stokes shift and spectral width. Determining SPPR for the cyclopenta[*b*]naphthalenone dyes began by examining the effect of donor position on photophysical properties. To this end, the photophysical properties of **4.36**-**4.39**, which only contained a dimethylamine donor on the cyclopenta[*b*]naphthalenone framework, were studied in dichloromethane. It was discovered that modifying the position of the dimethylamine donor on the cyclopenta[*b*]naphthalenone ring resulted in substantial changes to the spectral characteristics of the fluorescent dyes, including absorption and emission wavelength, Stokes shift, and emission spectral width (defined as the full-width-at-half-maximum, FWHM). For example, a dramatic bathochromic shift in the absorption maxima from 374 to 423 nm was observed when the amine donor was moved from the 5- to the 7-position of the naphthalene ring in **4.36** and **4.38**, respectively (entry 1, Table 4.1). The 6- and 8-substituted cyclopenta[*b*]naphthalenone dyes **4.37** and **4.38** exhibited intermediate properties by comparison. While the absorption maximum was the most blue-shifted for **4.36** (λ_{abs} = 374 nm), the emission maximum of 547 nm was among the most red-shifted for the series (entry 2). This large red-shift in emission led to **4.36** also having the largest Stokes shift of 8456 cm^{-1} (entry 3). A similarly red-shifted emission wavelength (λ_{em} = 548 nm) and large Stokes shift (7794 cm^{-1}) were observed for **4.39** (entries 2 and 3). Substitution of the amine at the 6-position, as in **4.37**, produced the most blue-shifted emission maximum for the cyclopenta[*b*]naphthalenone dyes (λ_{em} = 461 nm); consequently, **4.37** had the smallest Stokes shift of 3753 cm^{-1}, significantly smaller than that of **4.36** and **4.39**. Once again, **4.38** displayed intermediate emission (λ_{em} = 522 nm) and Stokes shift values (4484 cm^{-1}) compared to the other dye derivatives. The emission spectral width followed a similar trend to

that found for the emission maxima and Stokes shift; namely, **4.36** and **4.39** displayed the broadest emission spectra, **4.37** the narrowest emission spectra, and **4.38** showed a median value comparatively (entry 4). Normalized absorption and emission spectra for **4.36**-**4.39** in dichloromethane are depicted in Figure 4.8, providing a visual representation of how the donor position on the naphthalene ring shifts both the absorption and emission maxima. These results demonstrate that by altering the position of the donor on the fluorophore, different photophysical properties can be realized, thus allowing for a range of absorption and emission maxima spanning 49 and 87 nm, respectively.

Table 4.1. Photophysical properties for naphthalene dyes with varied donor positions

		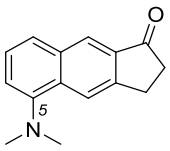	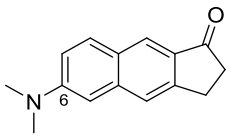	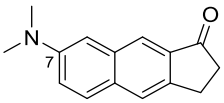	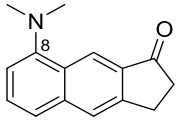
entry	property[a]	**4.36**	**4.37**	**4.38**	**4.39**
1	λ_{abs} (nm)	374	393	423	384
2	λ_{em} (nm)	547	461	522	548
3	Stokes shift (cm^{-1})	8456	3753	4484	7794
4	FWHM (nm)	111	61	86	103
5	Φ_F	0.33	0.64	0.53	0.53

[a]Photophysical properties were measured for samples in DCM; the excitation wavelength was chosen as the maximum absorption wavelength.

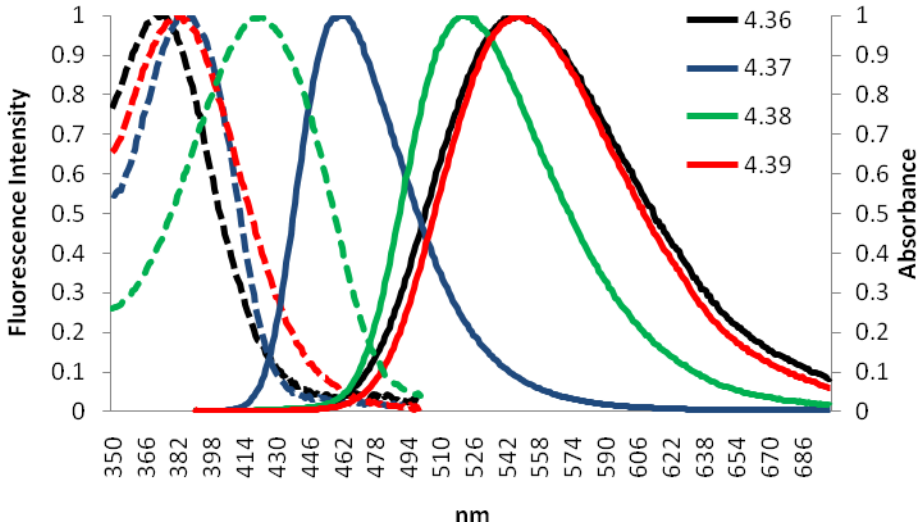

Figure 4.8. Absorption and emission spectra for dyes **4.36**-**4.39** containing donors at varying positions of the naphthalene. Spectra were obtained for samples in DCM. Dashed and solid lines indicate absorption and emission spectra, respectively. Emission spectra were obtained by exciting at the absorption maxima.

Quantum yield. The fluorescence quantum yields (Φ_F) of cyclopenta[*b*]naphthalenone dyes **4.36**-**4.39** were also found to vary with the position of the amine donor. The highest quantum yield was observed for **4.37** containing a 6-substituted amine donor, while substitution of the amine at the 5-position (**4.36**) resulted in a reduced quantum yield of 0.33 (entry 5, Table 4.1). For example, the quantum yield of **4.37** was determined to be 0.64, nearly double that of **4.36**. Intermediate quantum yield values relative to **4.36** and **4.37** were found for substitution of the amine at the 7- or 8-position of the naphthalene, as in **4.38** and **4.39**.

Fluorescence lifetimes and molecular brightness. Additional experiments to measure fluorescence lifetimes (τ) and molar absorptivity (ε), as well as to calculate molecular brightness (*B*), were also conducted for cyclopenta[*b*]naphthalenone dyes bearing the amine donor at different positions of the naphthalene ring. However, rather than using derivatives **4.36**-**4.39**, TMS-substituted cyclopenta[*b*]naphthalenone dyes **4.43**-**4.45** were utilized in these

measurements because of their red-shifted absorption and emission properties (detailed in section 4.4.3) and the larger amount of material that we had available. Fluorescence lifetimes were measured by Xing Yin and Dr. David Waldeck (University of Pittsburgh), and were found to depend strongly on the position of the amine donor. While the emission lifetimes were very similar for **4.43** and **4.44** (~42 ns), the emission lifetime of **4.44** was five times shorter (~8 ns) (Table 4.2). Considering the quantum yields determined for dyes **4.43**-**4.45**, also reported in Table 4.2, these lifetime differences imply a radiative rate that is 4-5 times higher for **4.44** than for **4.43** and **4.45**. The emission lifetime of PRODAN (**1.8**) is measured to be 3.3 ns,[7a] which is more comparable to **4.44** than **4.43** and **4.45**.

The molar absorptivities determined for 5- and 7-substituted cyclopenta[*b*]naphthalenone dyes **4.43** and **4.45** were found to be comparable at 2,500-2,700 M^{-1} cm^{-1}, leading to similar molecular brightness values of 1,100 and 1,600 M^{-1} cm^{-1}, respectively (Table 4.2). Molecular brightness (*B*) is a product of molar absorptivity (ε) and quantum yield (Φ_F), so if one of these individual values increases, so does the overall brightness of the molecule ($B = \Phi_F \cdot \varepsilon$). Substitution of the amine at the 6-position of the naphthalene ring, as in **4.44**, produced not only the most fluorescent dye in the TMS series ($\Phi_F = 0.66$), but also the dye with the highest molar absorptivity of 14,000 M^{-1} cm^{-1} and molecular brightness of 9,200 M^{-1} cm^{-1}. In comparison, **4.44** was almost one order of magnitude brighter than **4.43** and **4.45**, once again demonstrating the substantial effect of donor position on photophysical properties. These observations are consistent with the higher radiative rate found for **4.44**. Unfortunately, 8-TMS-substituted cyclopenta[*b*]naphthalenone dye **4.48** was not available to be measured for fluorescence lifetime or molecular brightness due to the unsuccessful Buchwald-Hartwig cross-coupling reaction of **1.145** (Scheme 4.7).

Table 4.2. Fluorescence lifetimes and brightness of TMS-substituted naphthalenone dyes

dye[a]		τ (ns)	Φ_F	ε (M^{-1} cm^{-1})	*B* (10^2 M^{-1} cm^{-1})[b]
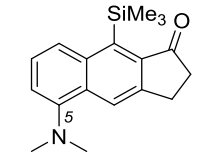	**4.43**	42.0	0.41	2,700	11
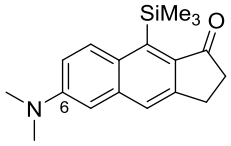	**4.44**	8.0	0.66	14,000	92
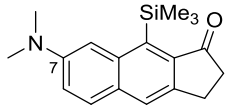	**4.45**	42.2	0.65	2,500	16

[a]Photophysical properties were measured for samples in DCM; the excitation wavelength was chosen as the maximum absorption wavelength; [b]$B = \Phi_F \cdot \varepsilon$.

Solvatochromism. In addition to the effect that changing the position of the amine donor had on the photophysical properties of cyclopenta[*b*]naphthalenone fluorescent dyes, these subtle changes in structure also significantly affected the solvatochromism of this class of dyes. To study the effect of donor position on solvatochromism, the absorption and fluorescence maxima of **4.43**, **4.44**, and **4.45** were investigated in 5 solvents of increasing polarity: cyclohexane (Cy), toluene (PhMe), dichloromethane (DCM), dimethylsulfoxide (DMSO), and ethanol (EtOH) (Table 4.3). The dye **4.43**, which contained an amine located at the 5-position of the naphthalene, showed the largest solvatochromic shift in emission of 147 nm from cyclohexane (λ_{em} = 480 nm) to ethanol (λ_{em} = 627 nm). Dye **4.45**, incorporating a 7-substituted amine donor, displayed a slightly smaller solvatochromic shift in emission of 130 nm from cyclohexane (λ_{em} = 474 nm) to ethanol (λ_{em} = 604 nm). Unlike **4.43**, a small red-shifted shoulder was observed in the emission spectra of **4.45** in cyclohexane. Both **4.43** and **4.45** showed similar solvatochromic shifts in absorption of 11 and 12 nm, respectively. Slight blue-shifts in the absorption maxima were noted

when changing the solvent from dimethylsulfoxide to ethanol for each of these substrates, which may be attributed to the hydrogen bonding ability of ethanol, and a solute-solvent interaction of the dye.[127,129,131] The smallest solvatochromic shift belonged to 6-substituted amine derivative **4.44**, in which the emission was only red-shifted by 91 nm from cyclohexane (λ_{em} = 436 nm) to ethanol (λ_{em} = 527 nm). However, a more substantial bathochromic shift in absorption of 22 nm was noted. The solvatochromic trends in absorption and emission determined for **4.44** were strikingly similar to those of PRODAN (**1.8**) (Table 4.3). Spectra displaying the solvatochromic shifts in absorption and emission maxima for **4.43**-**4.45** are shown in Figure 4.9.

Table 4.3. Photophysical properties for naphthalenone dyes in solvents of increasing polarity

	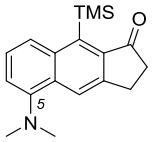			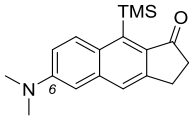			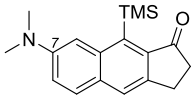			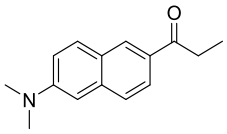		
	4.43			**4.44**			**4.45**			**PRODAN (1.8)**		
solvent[a,b]	λ_{abs} (nm)	λ_{em} (nm)	I/I_{max}	λ_{abs} (nm)	λ_{em} (nm)	I/I_{max}	λ_{abs} (nm)	λ_{em} (nm)	I/I_{max}	λ_{abs} (nm)	λ_{em} (nm)	I/I_{max}[c]
Cy	378	480	1.00	388	436	0.69	427	474	0.86	342[d]	401[d]	0.01
PhMe	381	522	0.83	398	467	0.96	432	508	1.00	346	416	0.32
DCM	386	572	0.60	405	489	1.00	436	542	0.98	355	440	0.75
DMSO	389	616	0.17	410	524	0.94	439	583	0.87	357	462	0.87
EtOH	382	627	0.02	408	527	0.94	435	604	0.20	362	496[d]	1.00
Δ[e]	11	147	-	22	91	-	12	130	-	20	95	-

[a]Solvatochromic studies were conducted in cyclohexane (Cy), toluene (PhMe), dichloromethane (DCM), dimethylsulfoxide (DMSO), and ethanol (EtOH); [b]Sample concentrations were $3.5x10^{-5}$ M for **4.43** and **4.45** and $5.0x10^{-6}$ M for **4.44**; [c]I/I_{max} values for PRODAN (**1.8**) were reported by Abelt et al.;[129] [d]values as reported by Weber et al.;[7a] [e]Δ represents largest overall shift from Cy to EtOH.

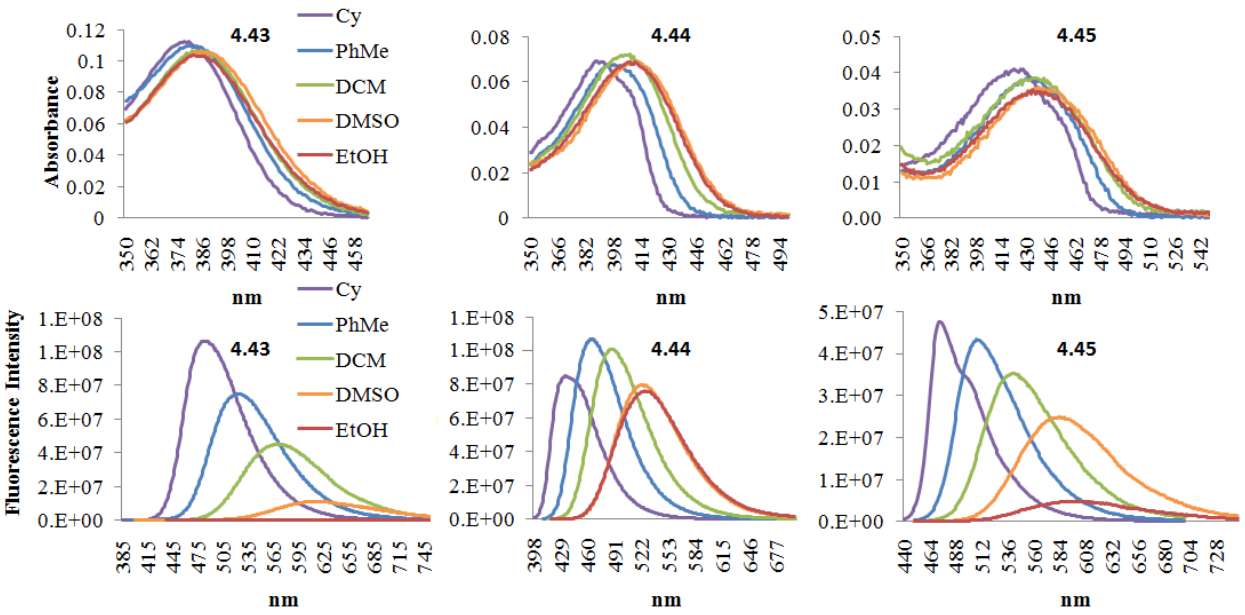

Figure 4.9. Absorption and emission spectra of **4.43**-**4.45** in solvents of increasing polarity. Absorption spectra (top) and emission spectra (bottom). Cyclohexane (Cy), toluene (PhMe), dichloromethane (DCM), dimethylsulfoxide (DMSO), and ethanol (EtOH).

The emission intensity of the cyclopenta[*b*]naphthalenone fluorophores in increasingly polar solvents was also dependent upon the position of the donor (Table 4.3). Both **4.43** and **4.45** were strongly emissive in non-polar solvents; **4.43** displayed the highest emission in cyclohexane, while **4.45** was most fluorescent in toluene (I/I_{max} = 1.00). However, as the solvent polarity increased, the emission intensity of these two dyes decreased. While **4.43** showed a dramatic decrease in emission intensity as solvent polarity increased and near complete fluorescence quenching in ethanol (I/I_{max} = 0.02), the fluorescence intensity of **4.45** decreased more gradually, and was still substantially fluorescent in ethanol (I/I_{max} = 0.20). Unlike **4.43** and **4.45**, **4.44** was strongly fluorescent in polar solvents, similar to the solvatochromic behavior of PRODAN (**1.8**), which has similar donor (amine) and acceptor (carbonyl) placement on the naphthalene ring. Whereas the emission of PRODAN (**1.8**) was considerably weaker in non-

polar solvents (see Table 4.3), **4.44** showed a much higher fluorescence intensity; emission in cyclohexane is the weakest at I/I_{max} = 0.69. Dye **4.45** was comparable to **4.44** in that its emission intensity in cyclohexane was lessened compared to that in toluene and dichloromethane. A visualization of the change in emission intensity by increasing solvent polarity is provided in Figure 4.9.

Difference between ground and excited state dipole moments. With solvatochromic data in hand, differences between ground and excited state dipole moments ($\mu^* - \mu$) for the TMS-substituted cyclopenta[*b*]naphthalenones **4.43**-**4.45** could be calculated using the Lippert-Mataga equation[132] depicted in equation 1, A; $\mu^* - \mu$ can be solved for by rearrangement of the variables in this equation, as shown in equation 1, B. The first step in the Lippert-Mataga calculations was generating a Lippert-Mataga plot, where Stokes shifts in wavenumbers ($\Delta\tilde{\nu}$) were plotted versus the orientation polarizability factor (Δf) of each solvent in which the dye's photophysical properties were measured. Orientation polarizability of a solvent can be determined using equation 1, C, where ε and n denote the dielectric constant and refractive index of the solvent, respectively. The orientation polarizability factors of cyclohexane, toluene, dichloromethane, and dimethylsulfoxide were found to be -0.001, 0.013, 0.219, and 0.265, respectively. Results in ethanol were not incorporated into the Lippert-Mataga plots because of the possible solvent-solute interactions that may occur due to the hydrogen-bonding ability of ethanol.[131,133] The results of the Lippert-Mataga plots of cyclopenta[*b*]naphthalenones **4.43**-**4.45** are displayed in Figure 4.10. Using linear regression, slopes for the best fit lines of the Lippert-Mataga plots were determined, which could then be substituted as the variable $(\Delta\tilde{\nu}$ - const.$)/\Delta f$ in equation 1, B. A larger number of data points, corresponding to the study of the photophysical properties of each dye in a greater number of solvents, would most likely assist in obtaining a better correlation for

the linear regression; however, the scatter associated with these results is also observed in the Lippert-Mataga plots of PRODAN derivatives performed by Abelt et al.[127,129] Based on these results, slopes of 11,400, 6,800, and 9,600 cm^{-1} were found for dyes **4.43**, **4.44**, and **4.45**, respectively.

With the slopes obtained from linear regression analysis of the Lippert-Mataga plots in hand, the Lippert-Mataga equation could almost be solved for μ* - μ; however, one last variable, the Onsager radius (*a*), needed to be calculated. The Onsager radii of **4.43**-**4.45** were determined to be 4.99 Å using the mass-density formula shown in equation 1, D, where M_M is the molecular mass of the dye, *N* is Avogadro's number, and ρ_M is the molecular density, which was assumed as 0.95 g mL^{-1}.[130,134] Finally, the difference in ground and excited state dipole moments (μ* - μ) for **4.43**-**4.45** was determined by utilizing both the calculated slope and the Onsager radius values in the Lippert-Mataga formula (equation 1, B). Differences between the dipole moments of the ground and excited states were found to be 11.8, 9.1, and 10.9 D for cyclopenta[*b*]naphthalenones **4.43**, **4.44**, and **4.45**, respectively. These values were slightly larger, yet comparable, to those reported by Abelt et al. for similar PRODAN derivatives (Figure 4.7).[127,130] In addition to having a substantial effect on almost all photophysical properties of the cyclopenta[*b*]naphthalenone dyes, these results demonstrate that altering the position of the amine donor on the naphthalene ring also changes the difference between ground and excited state dipole moments, which affects the solvatochromic behavior for each dye derivative.

$$\Delta\tilde{\nu} = \frac{2}{4\pi\varepsilon_0 hca^3}(\mu^* - \mu)^2\Delta f + \text{const.} \qquad \text{(A)}$$

ε_0 = vacuum permittivity constant
= 8.854 x 10^{-12} $C^2 \cdot J^{-1}$ m^{-1}
h = Planck's constant
= 6.626 x 10^{-34} J·s
c = velocity of light
= 2.99 x 10^8 m·s^{-1}
$4\pi\varepsilon_0 hc$ = 2.204 x 10^{-35} C^2
N = Avogadro's constant
= 6.022 x 10^{23} mol^{-1}
1 D = 3.3356 x 10^{-28} C·cm

$$\mu^* - \mu = \left(\frac{(\Delta\tilde{\nu} - \text{const.})}{\Delta f} \cdot \frac{4\pi\varepsilon_0 hca^3}{2}\right)^{1/2} \qquad \text{(B)}$$

$$\Delta f = \frac{\varepsilon - 1}{2\varepsilon + 1} - \frac{n^2 - 1}{2n^2 + 1} \qquad \text{(C)}$$

$$a^3 = \frac{3M_M}{4\pi N\rho_M} \qquad \text{(D)}$$

Equation 4.1. Lippert-Mataga and related equations
(A and B) Lippert-Mataga calculations; (C) orientation polarizability calculation; (D) mass-density calculation

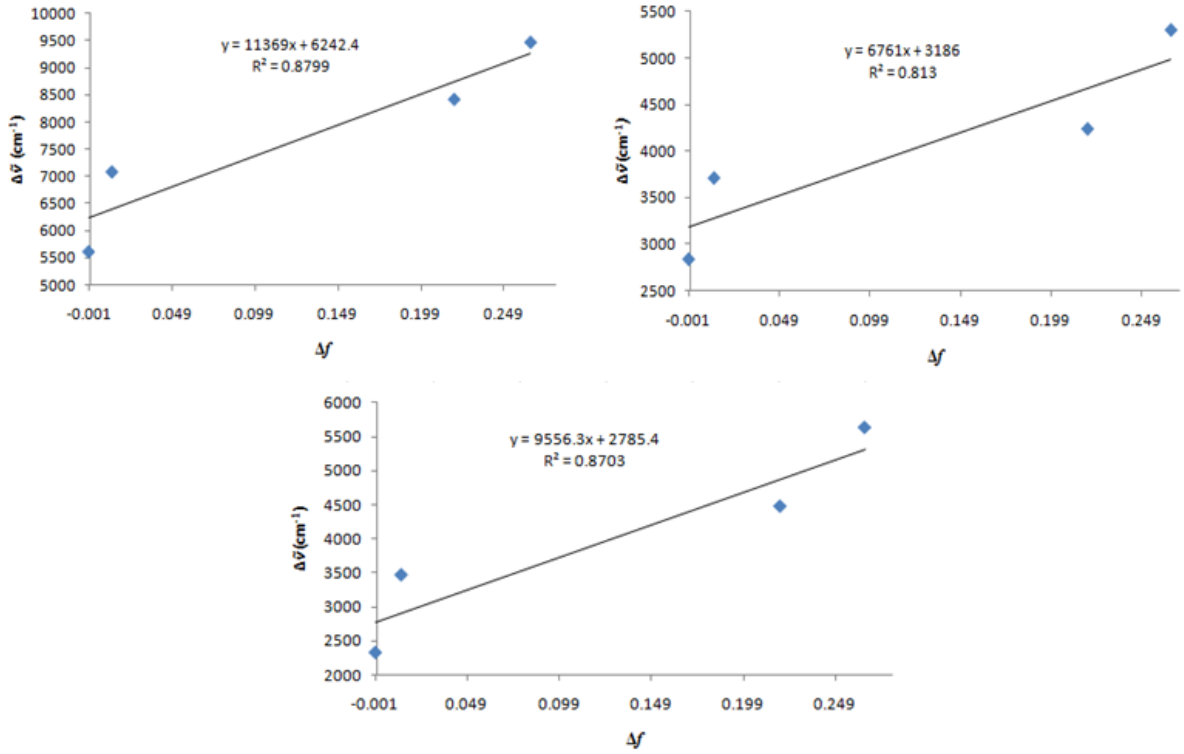

Figure 4.10. Lippert-Mataga plots of **4.43** (top, left), **4.44** (top, right), and **4.45** (bottom)

Discussion. It is clear from the above photophysical studies that the position of the amine donor on the naphthalene ring of the cyclopenta[*b*]naphthalenone dyes has a dramatic impact on the dyes' photophysical properties. By making subtle alterations to the fluorophore framework, large changes in absorption and emission maxima occur. For example, changing the amine from the 6- to the 5- position on the naphthalene ring results in a blue-shift of the absorption maximum by 19 nm and a red-shift of the emission maximum by 86 nm (Table 4.1); however, why varying the amine position has such a substantial effect on the dye's photophysical properties is still unknown. We hypothesize that the amine donor has different planar and non-planar ground state conformations depending upon the positioning of the amine on the naphthalene ring, which possibly accounts for the variation in photophysical properties observed.

By comparing the structures of the 5-, 6-, 7-, and 8-substituted amine derivatives, some similarities and differences become apparent. First, the ground state conformation of dyes in which the amine is located at the 5- or 8-position on the naphthalene ring will be influenced by *peri* interactions of these amines with the proton at the 4-position of the naphthalene.[135] This steric interaction will result in the amine adopting a non-planar, or twisted, conformation in the ground state. Both the 5- and 8-substituted dyes **4.36** and **4.39** exhibit very similar photophysical properties, characterized by blue-shifted absorption and red-shifted emission values compared to other dyes in the series, which may be a result of the twisting of the dimethylamine donor in the ground state.

On the other hand, we believe the ground state conformations of the amine donors in both the 6- and 7-substituted cyclopenta[*b*]naphthalenone derivatives **4.37** and **4.38** to be more planar because they lack the steric influence of a *peri*-interaction. Abelt et al. have reported several experimental studies which support that the amine donor in PRODAN (**1.8**) maintains a planar

conformation in both the ground and excited states.[127-128] The structure of the 6-substituted dye **4.37** is very similar to that of PRODAN (**1.8**), and only differs by the substitution of the carbonyl acceptor, which has been shown to have little effect on the photophysical properties of PRODAN derivatives.[129] Based on the results of Abelt, and the similarity of certain photophysical properties of **4.37** to PRODAN (**1.8**), such as solvatochromic behavior (Table 4.3), we believe that **4.37** also exists in a planar ground state, and most likely a planar excited state conformation.

A contributing factor to the planarity of **4.37**, not found in the other dyes of the series, is the delocalization of charge that occurs between the donor and the acceptor in the ground state, resulting in an additional resonance structure. This additional resonance form shows a partial sp^2 hybridization of the amine of **4.37**, which supports the planarity of this structure in the ground state. The delocalization of charge in **4.37** accounts for the decreased fluorescence lifetime and increased extinction coefficient, quantum yield, and molecular brightness of 6-substitued cyclopenta[*b*]naphthalenone dyes compared to those substituted with donors at the 5- or 7-positions which cannot donate charge directly from the amine to the carbonyl (Table 4.2). The 8-substituted dye **4.39** also has the amine positioned on the naphthalene ring so that delocalization of charge from the donor to the acceptor is possible; however, the steric influence of the *peri* hydrogen results in a larger degree of twisting for the 8-substituted amine donor than that predicted for the 6-substituted derivative. This deviation from planarity has an effect on the dye's photophysical properties, which is represented by a decreased quantum yield for **4.39** compared to **4.37** (Table 4.1). Extinction coefficient and molecular brightness were not determined for the 8-substituted amine donors, so comparisons could not be made.

Previously reported computational studies have shown that dyes with twisted ground state conformations become more planar in the excited state.[124] Based on these results, we may

expect a larger conformational change from the ground to the excited states when the amine donor is in the 5-position, as in **4.36** and **4.43**, since this dye has a twisted conformation in the ground state that can become more planar when excited. However, if the 6-substituted amine donor derivatives **4.37** and **4.44** are already very planar in the ground state due to the absence of a *peri* interaction, as well as the effect of delocalization of charge between the donor and the acceptor moieties, a smaller conformational change would be expected to occur upon excitation. The large conformational change from ground to excited state for dyes in which the amine is located at the 5-position of the naphthalene could account for the dramatic changes in emission maxima, Stokes shift, and solvatochromism associated with these dyes compared to the photophysical properties observed for **4.37**, **4.44**, and PRODAN (**1.8**). Investigations are currently underway to better understand the relationship between donor position and the photophysical properties observed for this series of dyes. Our collaborators Xing Yin and Professor David Waldeck (University of Pittsburgh) are exploring these results using computational methods, and preliminary calculations support the hypothesis that different ground and excited state conformations of the amines are contributing factors to the varied photophysical properties determined for these dyes.

4.4.3 Effect of phenyl and silyl substituents on photophysical properties of cyclopenta[*b*]naphthalenone dyes

Absorption, emission, and Stokes shift. In addition to altering the location of the amine donor, functionalization of the naphthalene moiety of the cyclopenta[*b*]naphthalenone dyes could be used to manipulate the dye's spectral properties. Incorporation of either a phenyl or a silyl substituent at the 1-position of the naphthalene ring caused changes in both the maximum

absorption and emission wavelengths (Scheme 4.7). While incorporation of a phenyl moiety onto the naphthalene ring (**4.40**-**4.42**) had little effect on the absorption maxima, the presence of a TMS group (**4.43**-**4.45**) produced a 12-13 nm bathochromic shift in absorption that was independent of amine position (entries 1-3, Table 4.4). Introduction of a triphenylsilyl group, as in **4.46**, served to further red-shift the absorption by 8 nm from that of **4.44** (λ_{abs} = 413 nm), making it the dye with the most red-shifted absorption in the series (entry 4). Similarly, the addition of silyl substituents to the cyclopenta[*b*]naphthalenone fluorophore resulted in red-shifted emission by 20-33 nm (entries 7 and 8). Once again, the triphenylsilyl-substituted dye **4.46** displayed the most red-shifted properties, with the emission maximum at 494 nm (entry 8); the TMS-substituted dye **4.44** was closely related with a maximum emission wavelength at 489 nm (entry 7). Although phenyl substitution of the naphthalene ring did not have an effect on the absorption maxima, it did induce an 11-15 nm red-shift in the emission maxima, which was a smaller red-shift than when the naphthalene was substituted with a TMS moiety (entry 6). As representative examples that depict the bathochromic shift that occurs in the maximum absorption and emission wavelength with functionalization by phenyl and TMS, the absorption and emission spectra of **4.37**, **4.41**, and **4.44** in dichloromethane are displayed in Figure 4.11.

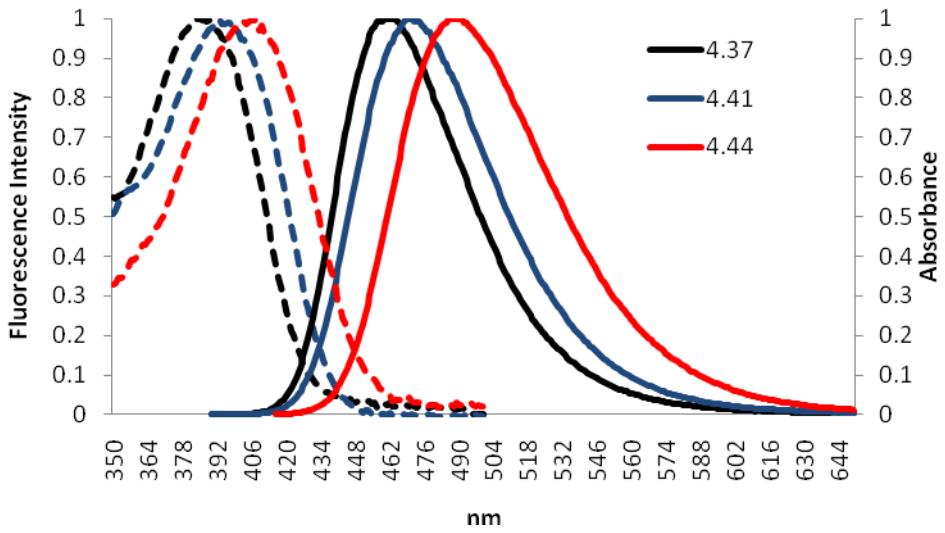

Figure 4.11. Absorption and emission spectra of **4.37**, **4.41**, and **4.44**.
Spectra of naphthalenes functionalized at the 1-position with phenyl or TMS groups were obtained in DCM. Dashed and solid lines represent absorption and emission spectra, respectively. Emission spectra were obtained by exciting at the absorption maxima.

Table 4.4. Spectral properties of naphthalenone dyes containing phenyl or TMS substituents

		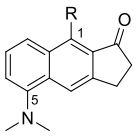		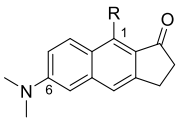		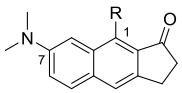	
entry[a]	R	dye	λ_{abs} (nm)	dye	λ_{abs} (nm)	dye	λ_{abs} (nm)
1	H	**4.36**	374	**4.37**	393	**4.38**	423
2	Ph	**4.40**	377	**4.41**	395	**4.42**	427
3	$SiMe_3$	**4.43**	386	**4.44**	405	**4.45**	436
4	$SiPh_3$	-	-	**4.46**	413	-	-
			λ_{em} (nm)		λ_{em} (nm)		λ_{em} (nm)
5	H	**4.36**	547	**4.37**	461	**4.38**	522
6	Ph	**4.40**	562	**4.41**	472	**4.42**	535
7	$SiMe_3$	**4.43**	572	**4.44**	489	**4.45**	542
8	$SiPh_3$	-	-	**4.46**	494	-	-
			Stokes shift (cm^{-1})		Stokes shift (cm^{-1})		Stokes shift (cm^{-1})
9	H	**4.36**	8456	**4.37**	3753	**4.38**	4484
10	Ph	**4.40**	8732	**4.41**	4130	**4.42**	4728
11	$SiMe_3$	**4.43**	8424	**4.44**	4242	**4.45**	4486
12	$SiPh_3$	-	-	**4.46**	3970	-	-
			FWHM[b] (nm)		FWHM (nm)		FWHM (nm)
13	H	**4.36**	111	**4.37**	61	**4.38**	86
14	Ph	**4.40**	114	**4.41**	66	**4.42**	83
15	$SiMe_3$	**4.43**	115	**4.44**	79	**4.45**	86
16	$SiPh_3$	-	-	**4.46**	75	-	-
			Φ_F		Φ_F		Φ_F
17	H	**4.36**	0.33	**4.37**	0.64	**4.38**	0.53
18	Ph	**4.40**	0.44	**4.41**	0.65	**4.42**	0.50[c]
19	$SiMe_3$	**4.43**	0.41	**4.44**	0.66	**4.45**	0.65
20	$SiPh_3$	-	-	**4.46**	0.70	-	-

[a]Photophysical studies were conducted in DCM; [b]full-width-at-half-maximum; [c]value is representative of a structurally similarly fluorophore (R = $HOCH_2C_6H_4$) for which Φ_F was previously reported;[59g] Φ_F is not expected to vary significantly with this slight structural change.

Discussion. The bathochromic shifts in absorption and emission observed when the cyclopenta[*b*]naphthalenone dyes were substituted with phenyl or TMS moieties have also been witnessed for other classes of fluorophores. For example, anthracene **4.47** that is disubstituted in the 9- and 10-positions with TMS groups showed a 28 nm red-shift in the absorption maximum and also a 39 nm red-shift in emission when compared with dyes that were not TMS-substituted (Figure 4.12).[136] This amounts to a red-shift of approximately 14 and 20 nm for the absorption and emission maxima, respectively, per silyl group, which correlates well with the changes that were observed for incorporation of a TMS moiety on our naphthalene substrates. Moreover, in the same example, disubstitution of the anthracene with triphenylsilyl rather than TMS groups resulted in even more red-shifted absorption and emission maxima by 39 and 64 nm, respectively (approximately 20 and 32 nm per silyl group). This once again matches very closely with our photophysical data. Similar reports also exist for TMS-substituted naphthalenes,[137] pyrenes,[138] α,ω-dinaphthylorganosilanes,[139] and thiophenes,[140] although the effect on the maximum emission wavelength is less dramatic. One example of silyl-substituted cyclopentadithiophenes demonstrated that exchanging a TMS for a triphenylsilyl group dramatically increased the quantum yield of the dye.[141] Unfortunately, we did not observe such a trend from **4.44** to **4.46**, possibly because of our already high quantum yield values (Table 4.4). The reasoning behind the bathochromic shifts associated with incorporation of silyl substituents has also been investigated and is commonly believed to occur by the silyl group acting as an extension of the conjugated system through σ*-π* conjugation. This interaction of the π* orbitals of the aromatic ring with the σ* orbitals of the Si-C(methyl) bonds serves to stabilize the LUMO,[138,140,142] while σ-π conjugation by the same groups destabilizes the HOMO,[140,143] all of which results in a smaller HOMO-LUMO gap and red-shifted spectral properties.

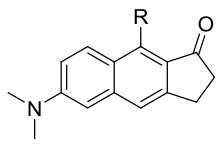

4.44

R	λ_{abs} (nm)	λ_{em} (nm)
H	393	461
$SiMe_3$	405	489
$SiPh_3$	413	494

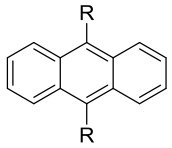

4.47

R	λ_{abs} (nm)	λ_{em} (nm)
H	375	379
$SiMe_3$	403	418
$SiPh_3$	414	443

Figure 4.12. Effect of silyl substitution on photophysical properties of aromatic compounds

The effects of phenyl groups as subsitutents on aromatic dyes have also been studied previously, and it has been found that if the phenyl substituent is not planar with the chromophore, meaning that the angle between the chromophore and phenyl is approximately 60° or greater, then the phenyl ring is not part of the conjugated system and only small shifts in spectra up to 10 nm occur.[144] This data also correlates well with our results where the phenyl moiety has very little effect on the photophysical properties of the cyclopenta[*b*]naphthalenone dyes. The positioning of the phenyl at the 1-position of the cyclopenta[*b*]naphthalenone places it *peri* to not only a hydrogen atom of the naphthalene, but also to the carbonyl of the cyclopentenone ring. Based on the steric hindrance surrounding the phenyl substituent, it would not be expected to be planar with the aromatic system and exhibit large red-shifts in absorption or emission.

4.5 CONCLUSIONS

In conclusion, the synthetic utility of the DDDA reaction was realized by its application to the synthesis of solvatochromic fluorescent dyes. The chloro-substituted cyclopenta[*b*]naphthalene products generated from the DDDA reaction were subjected to a Buchwald-Hartwig cross-coupling reaction to install an amine donor onto the cyclopenta[*b*]naphthalene framework. This synthetic transformation allowed for the creation of a library of donor-π-acceptor fluorophores with more desirable photophysical properties compared to the structurally similar fluorescent probe PRODAN (**1.8**), which is commercially available and commonly used for the study of biological environments. The structural diversity that can be incorporated by this *de novo* synthesis of fluorescent dyes is not attainable employing traditional strategies for dye modification, which usually involve altering a preexisting dye scaffold.

By combination of the DDDA reaction with the Buchwald-Hartwig cross-coupling reaction, initial variations were made to the substituents of the amine donor, as well as to the type of electron acceptor and its placement on the naphthalene ring. From these studies, it was determined that tertiary amines were ideal donors, as secondary amines blue-shifted the maximum emission wavelengths significantly. Substituting the cyclopenta[*b*]naphthalene with an aldehyde acceptor, or changing the position of the acceptor, as in cyclopenta[*b*]naphthalenones, proved to red-shift the absorption and emission properties of the dye considerably, placing the absorption maxima of these dyes well into the visible region. Based on these results and the closer structural resemblance of the cyclopenta[*b*]naphthalenone fluorophores to PRODAN (**1.8**), these dyes were chosen for more intensive SPPR studies, which included systematic variation of the amine donor on the naphthalene ring. The position of the donor was found to have a substantial effect on all photophysical properties of the dye, with the most notable effects being

on the absorption and emission maxima. By subtly changing the amine position, absorption and emission maxima spanning 49 and 87 nm were obtained. These results were especially valuable considering that the effect of donor position on photophysical properties has rarely been investigated, yet it was shown by our studies to have a significant impact. We also investigated the incorporation of additional functionality, such as phenyl and TMS groups, onto the cyclopenta[*b*]naphthalenone framework, which served to further red-shift the absorption and emission properties of these dyes.

Current studies are focused on understanding why donor position has such a dramatic effect on the photophysical properties of the cyclopenta[*b*]naphthalenone dyes. We believe that the twisted or planar conformation of the amine donors in the ground state could be the primary cause for the observed changes in photophysical properties, and we are now investigating these effects computationally with the aid of Xing Yin and Professor David Waldeck at the University of Pittsburgh. Future aims of this research include applying the cyclopenta[*b*]naphthalenone dyes to biological systems to determine their value as biological probes compared to PRODAN (**1.8**).

This research on expanding the scope of the DDDA reaction was not performed alone, and Dr. Erica Benedetti contributed significantly to this work by synthesizing and studying our first fluorescent dye **4.15**, as well as synthesizing and characterizing the cyclopenta[*b*]naphthalene fluorescent dyes **4.16-4.21**.

4.6 EXPERIMENTAL

4.6.1 General Methods

All commercially available compounds were purchased and used as received unless otherwise specified. THF, Et_2O, and DCM were purified by passing through alumina using a Sol-Tek ST-002 solvent purification system. Triethylamine (Et_3N) and acetonitrile (MeCN) were distilled over calcium hydride and deuterated chloroform ($CDCl_3$) was dried over 3 Å molecular sieves. Purification of the compounds by flash column chromatography was performed using silica gel (40-63 μm particle size, 60 Å pore size), or by using a Biotage Horizon flash purification system with either Biotage SNAP KP-SIL or Silicycle SiliaSep silica flash cartridges. TLC analyses were performed on silica gel F_{254} glass plates (250 μm thickness). ^{1}H NMR and ^{13}C NMR spectra were recorded on Bruker Avance 300, 400, 500, 600, or 700 MHz spectrometers. Spectra were referenced to residual chloroform (7.26 ppm, ^{1}H; 77.16 ppm, ^{13}C) or benzene (7.16 ppm, ^{1}H; 128.0 ppm, ^{13}C). Chemical shifts are reported in ppm, multiplicities are indicated by s (singlet), d (doublet), t (triplet), q (quartet), p (pentet), and m (multiplet). Coupling constants, *J*, are reported in hertz (Hz). All NMR spectra were obtained at room temperature unless otherwise specified. ^{1}H and ^{13}C NMR spectra can be found in Appendix B. IR spectra were obtained using a Nicolet Avatar E.S.P. 360 FT-IR. EI mass spectroscopy was performed on a Waters Micromass GCT high resolution mass spectrometer, while ES mass spectroscopy was performed on a Waters Q-TOF Ultima API, Micromass UK Limited high resolution mass spectrometer. All microwave-mediated reactions were conducted in either a Biotage Initiator Exp microwave synthesizer using 0.5-2 mL conical and 2-5 mL cylindrical microwave irradiation vials, or in an Anton-Paar Monowave 300 microwave synthesizer using G4 and G10 cylindrical microwave

irradiation vials. The temperature of reactions in the Monowave 300 was monitored internally by a ruby sensor fiber optic probe, unless otherwise specified. The microwave parameters were set to variable power, constant temperature, stirring on, and a fixed hold time. Absorption and fluorescence spectra were recorded on a Lambda 9 spectrophotometer (Perkin Elmer) and FluoroMax-3 spectrofluorometer (Jobin Yvon Horiba), respectively. Only spectral grade solvents were employed. For spectroscopic measurements, 10 mm quartz-cuvettes were used and all samples were degassed by bubbling with argon prior to study for a minimum of 20 min. Fluorescence measurements were conducted with slit widths open to 2 nm, scanning increments of 1 nm, and the excitation wavelength set as the absorption maximum for each dye. Solvatochromic studies were conducted using spectral grade cyclohexane (Cy), toluene (PhMe), dichloromethane (DCM), dimethyl sulfoxide (DMSO), and ethanol (EtOH). Fluorescence measurements were obtained by exciting at the absorption maximum found for the dyes in each solvent. Individual spectra were overlaid, but not normalized as to show accurate emission intensities. Fluorescence lifetimes were calculated by degassing solutions of **4.43** (3.0×10^{-5} M solution; λ_{ex} = 378 nm), **4.44** (7.0×10^{-6} M solution; λ_{ex} = 378 nm), and **4.45** (3.0×10^{-5} M solution; λ_{ex} = 440 nm) in DCM by freeze-pump-thaw.

4.6.2 Experimental procedures detailed in published papers

Characterization and conditions for the preparation of the following cyclopenta[*b*]naphthalene dyes, including syntheses and characterization of all precursors and spectral data, were recently published and can be found in the Supporting Information of Benedetti, E.; Kocsis, L. S.; Brummond, K. M. Synthesis and Photophysical Properties of a Series of

Cyclopenta[*b*]naphthalene Solvatochromic Fluorophores. *J. Am. Chem. Soc.* **2012**, *134*, 12418-12421 (Figure 4.13).

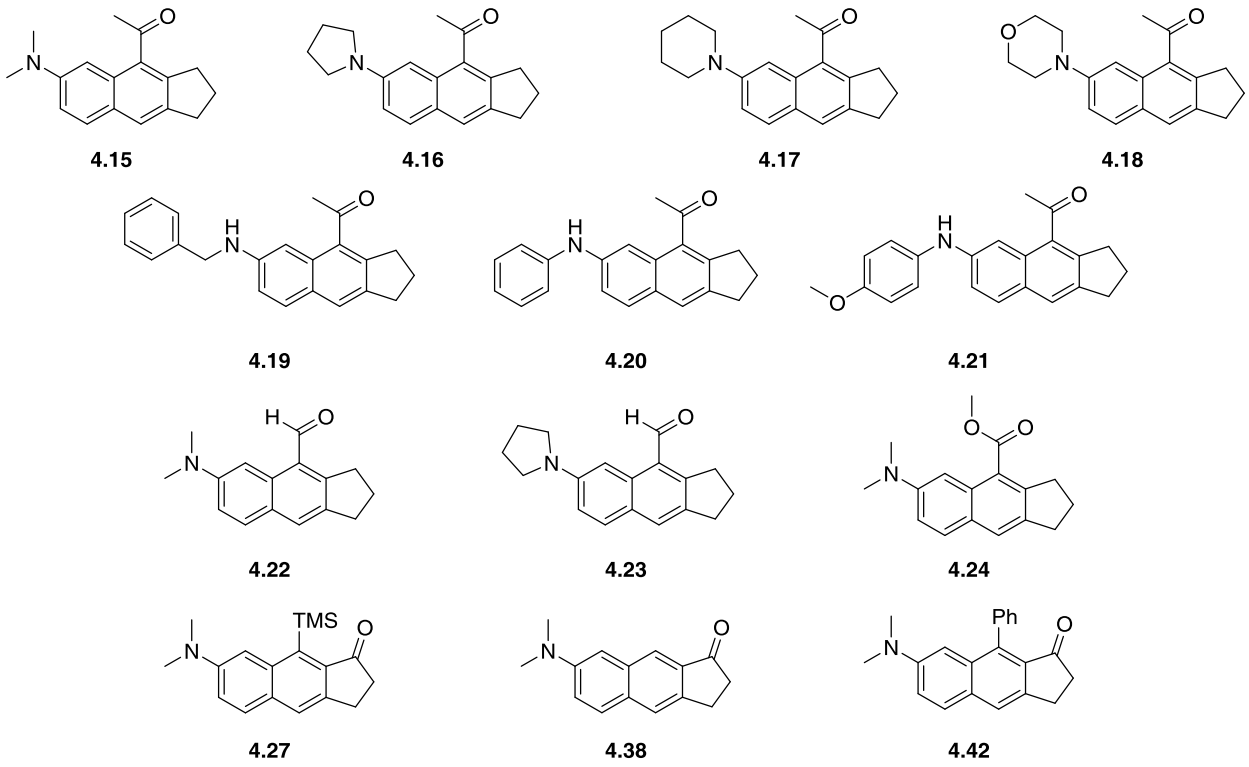

Figure 4.13. Previously published cyclopenta[*b*]naphthalene dyes. Syntheses and characterization can be found in Benedetti, E.; Kocsis, L. S.; Brummond, K. M. Synthesis and Photophysical Properties of a Series of Cyclopenta[*b*]naphthalene Solvatochromic Fluorophores. *J. Am. Chem. Soc.* **2012**, *134*, 12418-12421.

4.6.3 General procedures

General Procedure A: Desilylation of cyclopenta[*b*]naphthalenones. To a two-neck round-bottomed flask equipped with an argon inlet adapter, a septum, and a stir bar was added cyclopenta[*b*]naphthalenone (1.0 equiv) in THF (0.06-0.08 M). TBAF (2.0-3.0 equiv of a 1.0 M

solution in THF) was added dropwise with stirring, turning the reaction mixture purple then brown in color. The reaction mixture was stirred at rt for 30 min and was quenched with sat'd aq ammonium chloride. The aqueous layer was separated and extracted with ethyl acetate (3x). The combined organic layers were washed with brine, dried over magnesium sulfate, gravity filtered, and concentrated under reduced pressure. The crude product was purified by silica gel flash column chromatography to yield the title compound.

General procedure B: Buchwald-Hartwig cross-coupling reactions employing lithium bis(trimethylsilyl)amide

To an oven-dried 0.5-2 mL microwave irradiation vial equipped with a stir bar was added RuPhos palladacycle (0.025-0.060 equiv). The microwave irradiation vial was capped and then evacuated and refilled with argon or nitrogen (3x) through a small gauge needle piercing the vial cap. Lithium bis(trimethylsilyl)amide (2.0 equiv of a 1.0 M solution in THF) was added all at once with stirring, turning the reaction mixture red. Cyclopenta[*b*]naphthalenone (1.0 equiv) in THF (0.14-0.36 M) was added all at once via syringe turning the reaction mixture red-brown in color. Finally, dimethylamine (1.5-4.4 equiv of a 2.0 M solution in THF) was added via syringe. Once all reagents were added, the needle serving as an argon inlet was removed and the reaction mixture was lowered into a preheated 85 °C oil bath and heated until complete by TLC. The reaction mixture was then cooled to rt, diluted with sat'd aq ammonium chloride solution, and extracted with ethyl acetate (3x). The combined organic layers were washed with brine, dried over $MgSO_4$, gravity filtered, and concentrated under reduced pressure. The crude product was purified by silica gel flash column chromatography to yield the title compound.

General procedure C: Buchwald-Hartwig cross-coupling reactions employing cesium carbonate

To an oven-dried 0.5-2 mL microwave irradiation vial equipped with a stir bar was added RuPhos palladacycle (0.025-0.030 equiv), cesium carbonate (2.0 equiv), and cyclopenta[*b*]naphthalenone (1.0 equiv). The microwave irradiation vial was capped and then evacuated and refilled with argon (3x) through a small gauge needle piercing the vial cap. THF (0.25-0.50 M) was added all at once via syringe, followed by dimethylamine (1.5-5.0 equiv of a 2.0 M solution in THF). Once all reagents were added, the needle serving as an argon inlet was removed and the reaction mixture was lowered into a preheated 85 °C oil bath and heated until complete by TLC. The reaction mixture was then cooled to rt, diluted with sat'd aq ammonium chloride solution, and extracted with ethyl acetate (3x). The combined organic layers were washed with brine, dried over $MgSO_4$, gravity filtered, and concentrated under reduced pressure. The crude product was purified by silica gel flash column chromatography to yield the title compound.

4.6.4 Desilylation of TMS-substituted cyclopenta[*b*]naphthalenones

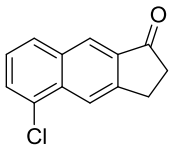

4.33

5-Chloro-2,3-dihydro-1*H*-cyclopenta[*b*]naphthalen-1-one (4.33). Follows general procedure A: naphthalene **1.142** (0.046 g, 0.16 mmol), THF (2.0 mL), and TBAF (0.35 mL, 0.35 mmol, 2.2 equiv). The crude product was purified by silica gel flash column chromatography (4 g silica

cartridge, 0-10% ethyl acetate/hexanes) to yield the title compound as a light yellow solid (18 mg, 51%).

Data **4.33**

MP 154-155 °C

^{1}H NMR (400 MHz, $CDCl_3$)

8.31 (s, 1H), 8.28 (s, 1H), 7.88 (d, *J* = 8.4 Hz, 1H), 7.66 (d, *J* = 7.5 Hz, 1H), 7.39 (t, *J* = 7.5 Hz, 1H), 3.37-3.34 (m, 2H), 2.83-2.80 (m, 2H) ppm

^{13}C NMR (100 MHz, $CDCl_3$)

206.9, 149.1, 135.3, 134.3, 133.5, 131.7, 129.6, 128.7, 125.9, 124.6, 121.8, 36.9, 25.6 ppm

IR (thin film)

3056, 2958, 2921, 2839, 1710, 1625, 1593, 1497, 1159 cm^{-1}

LRMS (TOF MSMS ES+ ASAP)

m/z (%): 216 (100), 188 (3), 181 (2)

HRMS (TOF MS ES+ ASAP)

[M] calcd for $C_{13}H_9OCl$: 216.0342; found, 216.0340

TLC R_f = 0.4 (10% ethyl acetate/hexanes) [silica gel, UV, $KMnO_4$ stain]

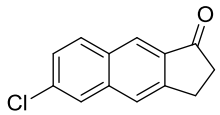

4.34

6-Chloro-2,3-dihydro-1*H*-cyclopenta[*b*]naphthalen-1-one (4.34). Follows general procedure A: naphthalene **1.144** (0.058 g, 0.20 mmol), THF (3.3 mL), and TBAF (0.60 mL, 0.60 mmol, 3.0 equiv). The crude product was purified by silica gel flash column chromatography (2.5 cm

column, 5-10% ethyl acetate/hexanes) to yield the title compound as a light brown solid (22 mg, 51%).

Data **4.34**

MP 172-175 °C

^{1}H NMR (300 MHz, $CDCl_3$)

8.29 (s, 1H), 7.92 (d, *J* = 8.8 Hz, 1H), 7.85 (s, 1H), 7.81 (s, 1H), 7.44 (dd, *J* = 8.8, 2.0 Hz, 1H), 3.35-3.31 (m, 2H), 2.83-2.79 (m, 2H) ppm

^{13}C NMR (100 MHz, $CDCl_3$)

206.8, 149.1, 137.6, 135.0, 134.5, 131.8, 130.5, 127.2, 126.4, 124.3, 124.0, 36.9, 25.4 ppm

IR (thin film)

3068, 3019, 2953, 2922, 2847, 1710, 1628, 1492 cm^{-1}

LRMS (TOF MSMS ES+ ASAP)

m/z (%): 217 (100), 199 (7), 188 (8), 175 (15)

HRMS (TOF MS ES+ ASAP)

$[M+H]^+$ calcd for $C_{13}H_{10}OCl$: 217.0420; found, 217.0404

TLC R_f = 0.1 (10% ethyl acetate/hexanes) [silica gel, UV, $KMnO_4$ stain]

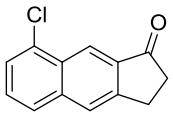

4.35

8-Chloro-2,3-dihydro-1*H*-cyclopenta[*b*]naphthalen-1-one (4.35). Follows general procedure A: naphthalene **1.145** (0.035 g, 0.12 mmol), THF (2.0 mL), and TBAF (0.24 mL, 0.24 mmol, 2.0 equiv). The crude product was purified by silica gel flash column chromatography (1.5 cm

column, 10% ethyl acetate/hexanes) to yield the title compound as a light brown solid (17 mg, 65%).

Data **4.35**

MP 118-122 °C

^{1}H NMR (300 MHz, $CDCl_3$)

8.78 (s, 1H), 7.93 (s, 1H), 7.79 (dd, *J* = 8.1 Hz, 1H), 7.59 (d, *J* = 6.9 Hz, 1H), 7.49 (t, *J* = 8.1 Hz, 1H), 3.37-3.33 (m, 2H), 2.86-2.82 (m, 2H) ppm

^{13}C NMR (100 MHz, $CDCl_3$)

206.9, 148.7, 138.1, 135.5, 134.4, 130.0, 128.3, 126.9, 126.3, 125.3, 121.2, 36.9, 25.2 ppm

IR (thin film)

2956, 2925, 2851, 1709, 1626, 1596, 1496 cm^{-1}

LRMS (TOF MSMS ES+ ASAP)

m/z (%): 217 (100), 216 (12), 199 (5), 188 (30), 175 (13)

HRMS (TOF MS ES+ ASAP)

$[M+H]^+$ calcd for $C_{13}H_{10}OCl$: 217.0420; found, 217.0412

TLC R_f = 0.1 (10% ethyl acetate/hexanes) [silica gel, UV, $KMnO_4$ stain]

4.6.5 Synthesis of cyclopenta[*b*]naphthalene dyes via Buchwald-Hartwig reactions

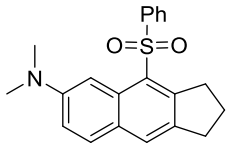

4.25

***N*,*N*-Dimethyl-4-(phenylsulfonyl)-2,3-dihydro-1*H*-cyclopenta[*b*]naphthalen-6-amine (4.25)**. Follows general procedure C: RuPhos palladacycle (0.003 g, 0.004 mmol), cesium carbonate (0.085 g, 0.26 mmol), cyclopenta[*b*]naphthalene **1.109** (0.044 g, 0.13 mmol), THF (0.26 mL), and dimethylamine (95 μL, 0.19 mmol). The reaction mixture was heated at 85 °C for 2 h, turning the reaction mixture from grey to yellow. The crude material was purified by silica gel flash column chromatography (1.5 cm column, 20-30% Et_2O/pentane) to yield the title compound as a yellow solid (30 mg, 67%).

Data **4.25**

MP 206-208 °C

^{1}H NMR (300 MHz, $CDCl_3$)

7.91 (d, *J* = 6.9 Hz, 2H), 7.71 (s, 2H), 7.59 (d, *J* = 9.1 Hz, 1H), 7.49-7.40 (m, 3H), 7.04 (dd, *J* = 9.1, 2.4 Hz, 1H), 3.69 (t, *J* = 7.5 Hz, 2H), 3.04-3.00 (m, 7H), 2.14 (p, *J* = 7.5 Hz, 2H) ppm

^{13}C NMR (100 MHz, $CDCl_3$)

149.1, 148.8, 143.7, 139.4, 132.6, 130.7, 129.3, 129.2, 129.0 (2C), 127.2, 127.0, 126.5 (2C), 115.5, 103.8, 40.7 (2C), 35.3, 32.1, 25.8 ppm

IR (thin film)

2922, 1616, 1516, 1144 cm^{-1}

HRMS (TOF MS ES+)

[M] calcd for $C_{21}H_{21}NO_2S$: 351.1293; found, 351.1324

TLC R_f = 0.3 (20% ethyl acetate/hexanes) [silica gel, UV, $KMnO_4$ stain]

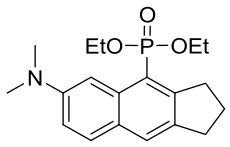

4.26

Diethyl (6-(dimethylamino)-2,3-dihydro-1*H*-cyclopenta[*b*]naphthalen-4-yl)phosphonate (4.26). Follows general procedure C: RuPhos palladacycle (0.002 g, 0.003 mmol), cesium carbonate (0.063 g, 0.19 mmol), cyclopenta[*b*]naphthalene **1.111** (0.033 g, 0.097 mmol), THF (0.20 mL), and dimethylamine (75 μL, 0.15 mmol). The reaction mixture was heated at 85 °C for 3 h, turning the reaction mixture from grey to dark yellow. The crude material was purified by silica gel flash column chromatography (4 g silica cartridge, 0-60% ethyl acetate/hexanes) to yield the title compound as a yellow solid (15 mg, 44%).

Data **4.26**

^{1}H NMR (300 MHz, $CDCl_3$)

7.97 (s, 1H), 7.67 (s, 1H), 7.61 (dd, *J* = 9.0, 2.4 Hz, 1H), 7.11 (dd, *J* = 9.0, 2.4 Hz, 1H), 4.25-3.95 (m, 4H), 3.43 (dt, *J* = 7.5, 2.4 Hz, 2H), 3.07 (s, 6H), 2.97 (t, *J* = 7.5 Hz, 2H), 2.07 (p, *J* = 7.5 Hz, 2H), 1.30 (t, *J* = 7.2 Hz, 6H) ppm

^{13}C NMR (100 MHz, $CDCl_3$)

153.1 (d, *J* = 11.0 Hz), 148.9, 139.1 (d, *J* = 15.0 Hz), 134.9 (d, *J* = 13.0 Hz), 129.0, 127.7 (d, *J* = 3.0 Hz), 126.3 (d, *J* = 12.0 Hz), 116.7, 115.4, 114.9, 106.5,

61.4 (d, J = 5.0 Hz), 41.0 (2C), 35.4 (d, J = 2.0 Hz), 32.2, 25.8, 16.6 (d, J = 7.0 Hz) ppm

IR (thin film)

2979, 1622, 1514, 1022 cm^{-1}

HRMS (TOF MS ES+)

[M] calcd for $C_{19}H_{26}NO_3P$: 347.1650; found, 347.1674

TLC R_f = 0.3 (50% ethyl acetate/hexanes) [silica gel, UV, $KMnO_4$ stain]

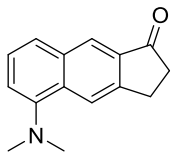

4.36

5-(Dimethylamino)-2,3-dihydro-1*H*-cyclopenta[*b*]naphthalen-1-one (4.36). Follows general procedure B: Ruphos palladacycle (0.0015 g, 0.0020 mmol, 0.028 equiv), lithium bis(trimethylsilyl)amide (0.14 mL, 0.14 mmol), cyclopenta[*b*]naphthalenone **4.33** (0.016 g, 0.072 mmol), THF (0.20 mL, 0.36 M), and dimethylamine (54 μL, 0.11 mmol, 1.5 equiv). The reaction mixture was heated at 85 °C for 1.5 h, turning the reaction mixture dark brown over time. The crude product was purified by silica gel flash column chromatography (1.5 cm, 5% ethyl acetate/hexanes) to yield the title compound as a yellow solid (8 mg, 50%).

Data **4.36**

MP 95-98 °C

^{1}H NMR (300 MHz, $CDCl_3$)

8.32-8.29 (m, 2H), 7.66 (d, J = 7.8 Hz, 1H), 7.41 (t, J = 7.8 Hz, 1H), 7.19 (d, J = 7.8 Hz, 1H), 3.37-3.33 (m, 2H), 2.91 (s, 6H), 2.83-2.78 (m, 2H) ppm

^{13}C NMR (100 MHz, $CDCl_3$)

207.6, 150.7, 147.6, 134.5, 133.7, 133.0, 126.0, 125.3, 124.7, 121.3, 116.8, 45.2 (2C), 37.1, 25.7 ppm

IR (thin film)

3056, 2925, 2852, 2823, 2786, 1712, 1626, 1601, 1503 cm^{-1}

LRMS (TOF MSMS ES+ ASAP)

m/z (%): 225 (100), 224 (35), 196 (3), 182 (10)

HRMS (TOF MS ES+ ASAP)

[M] calcd for $C_{15}H_{15}NO$: 225.1154; found, 225.1147

TLC R_f = 0.1 (10% ethyl acetate/hexanes) [silica gel, UV, $KMnO_4$ stain]

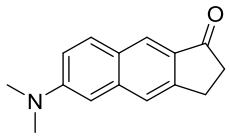

4.37

6-(Dimethylamino)-2,3-dihydro-1*H*-cyclopenta[*b*]naphthalen-1-one (4.37). Follows general procedure B: RuPhos palladacycle (0.0020 g, 0.0027 mmol, 0.059 equiv), lithium bis(trimethylsilyl)amide (92 μL, 0.092 mmol), cyclopenta[*b*]naphthalenone **4.34** (0.010 g, 0.046 mmol), THF (0.30 mL, 0.15 M), and dimethylamine (0.10 mL, 0.20 mmol, 4.4 equiv). The reaction mixture was heated at 85 °C for 1 h, turning the reaction mixture amber over time. The crude product was purified by silica gel flash column chromatography (1.5 cm, 10-15% ethyl acetate/hexanes) to yield the title compound as a yellow solid (7 mg, 70%).

Data **4.37**

MP 188-190 °C

^{1}H NMR (300 MHz, $CDCl_3$)

8.16 (s, 1H), 7.81 (d, *J* = 9.1 Hz, 1H), 7.60 (s, 1H), 7.14 (dd, *J* = 9.1, 2.3 Hz, 1H), 6.82 (d, *J* = 2.3 Hz, 1H), 3.26-3.21 (m, 2H), 3.12 (s, 6H), 2.77-2.72 (m, 2H) ppm

^{13}C NMR (100 MHz, $CDCl_3$)

207.0, 150.2, 149.0, 139.5, 131.5, 131.2, 125.4, 124.4, 121.8, 116.3, 104.6, 40.4 (2C), 36.9, 25.3 ppm

IR (thin film)

2959, 2918, 2851, 1693, 1614, 1512 cm^{-1}

LRMS (TOF MSMS ES+ ASAP)

m/z (%): 225 (31), 224 (100), 209 (32), 196 (5), 184 (17)

HRMS (TOF MS ES+ ASAP)

$[M+H]^+$ calcd for $C_{15}H_{16}NO$: 226.1232; found, 226.1189

TLC R_f = 0.1 (15% ethyl acetate/hexanes) [silica gel, UV, $KMnO_4$ stain]

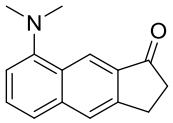

4.39

8-(Dimethylamino)-2,3-dihydro-1*H*-cyclopenta[*b*]naphthalen-1-one (4.39). Follows general procedure B: RuPhos palladacycle (0.0015 g, 0.0020 mmol, 0.027 equiv), lithium bis(trimethylsilyl)amide (0.15 mL, 0.15 mmol), cyclopenta[*b*]naphthalenone **4.35** (0.016 g, 0.074 mmol), THF (0.30 mL, 0.25 M), and dimethylamine (0.11 mL, 0.22 mmol, 3.0 equiv). The reaction mixture was heated at 85 °C for 2.5 h, turning the reaction mixture dark brown over time. The crude product was purified by silica gel flash column chromatography (1.5 cm, 5% ethyl acetate/hexanes) to yield the title compound as a yellow solid (13 mg, 77%).

Data **4.39**

MP 97-100 °C

^{1}H NMR (300 MHz, $CDCl_3$)

8.74 (s, 1H), 7.85 (s, 1H), 7.49-7.47 (m, 2H), 7.03 (dd, *J* = 5.8, 2.6 Hz, 1H), 3.32-3.29 (m, 2H), 2.91 (s, 6H), 2.82-2.79 (m, 2H) ppm

^{13}C NMR (100 MHz, $CDCl_3$)

207.5, 153.4, 147.9, 138.8, 133.9, 128.7, 128.1, 125.1, 122.2, 121.4, 113.9, 45.3 (2C), 37.0, 25.2 ppm

IR (thin film)

3053, 2936, 2867, 2837, 1710, 1623, 1595, 1575, 1501 cm^{-1}

LRMS (TOF MSMS ES+ ASAP)

m/z (%): 226 (16), 225 (67), 211 (100)

HRMS (TOF MS ES+ ASAP)

$[M+H]^+$ calcd for $C_{15}H_{16}NO$: 226.1232; found, 226.1193

TLC R_f = 0.1 (10% ethyl acetate/hexanes) [silica gel, UV, $KMnO_4$ stain]

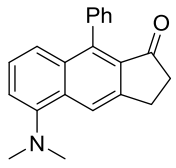

4.40

5-(Dimethylamino)-9-phenyl-2,3-dihydro-1*H*-cyclopenta[*b*]naphthalen-1-one (4.40).

Follows general procedure B: RuPhos palladacycle (0.0040 g, 0.0053 mmol, 0.025 equiv), lithium bis(trimethylsilyl)amide (0.42 mL, 0.42 mmol), cyclopenta[*b*]naphthalenone **1.138** (0.060 g, 0.21 mmol), THF (0.8 mL, 0.26 M), and dimethylamine (0.16 mL, 0.32 mmol, 1.5 equiv). The reaction mixture was heated at 85 °C for 1 h, turning the reaction mixture black. The

crude product was purified by silica gel flash column chromatography (12 g silica cartridge, 0-15% ethyl acetate/hexanes) to yield the title compound as a dark yellow solid (0.030 g, 48%).

Data **4.40**

MP 152-155 °C

^{1}H NMR (300 MHz, $CDCl_3$)

8.37 (s, 1H), 7.51-7.46 (m, 3H), 7.35 (d, *J* = 8.4 Hz, 1H), 7.31-7.27 (m, 3H), 7.18 (dd, *J* = 7.2, 1.2 Hz, 1H), 3.36-3.32 (m, 2H), 2.93 (s, 6H), 2.75-2.71 (m, 2H) ppm

^{13}C NMR (100 MHz, $CDCl_3$)

206.2, 150.6, 147.6, 140.1, 136.8, 133.4, 132.7, 130.8, 129.8 (2C), 127.9 (2C), 127.6, 125.7, 123.3, 120.8, 116.5, 45.4 (2C), 37.6, 25.1 ppm

IR (thin film)

3062, 2991, 2955, 2829, 2786, 1717, 1609, 1591, 1489 cm^{-1}

LRMS (TOF MSMS ES+ ESI)

m/z (%): 302 (30), 287 (100)

HRMS (TOF MS ES+ ESI)

$[M+H]^+$ calcd for $C_{21}H_{20}NO$: 302.1545; found, 302.1559

TLC R_f = 0.1 (10% ethyl acetate/hexanes) [silica gel, UV, $KMnO_4$ stain]

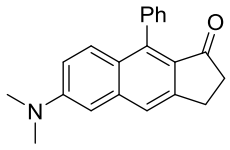

4.41

6-(Dimethylamino)-9-phenyl-2,3-dihydro-1*H*-cyclopenta[*b*]naphthalen-1-one (4.41).

Follows general procedure B: RuPhos palladacycle (0.0015 g, 0.0020 mmol, 0.029 equiv),

lithium bis(trimethylsilyl)amide (0.14 mL, 0.14 mmol), cyclopenta[*b*]naphthalenone **1.140** (0.020 g, 0.068 mmol), THF (0.50 mL, 0.14 M), and dimethylamine (0.10 mL, 0.20 mmol, 3.0 equiv). Naphthalene **1.140** was not very soluble in THF, so a larger quantity of THF was used than in the general procedure. The reaction mixture was heated at 85 °C for 2 h, turning the reaction mixture black. The crude product was purified by silica gel flash column chromatography (1.5 cm column, 10-20% ethyl acetate/hexanes) to yield the title compound as a yellow solid (4 mg, 20%). The lower yield of this reaction was attributed to the poor solubility of naphthalene **1.140** in THF.

Data **4.41**

MP 172-174 °C

^{1}H NMR (300 MHz, $CDCl_3$)

7.65 (s, 1H), 7.54 (d, *J* = 9.6 Hz, 1H), 7.51-7.47 (m, 3H), 7.31-7.26 (m, 2H), 7.03 (dd, *J* = 9.6, 2.4 Hz, 1H), 6.91 (s, 1H), 3.23 (t, *J* = 6.9 Hz, 2H), 3.10 (s, 6H), 2.68 (t, *J* = 6.9 Hz, 2H) ppm

^{13}C NMR (175 MHz, $CDCl_3$)

205.5, 149.8, 149.1 140.0, 139.1, 136.7, 129.7 (2C), 129.5, 127.7 (2C), 127.4 (2C), 124.8, 121.6, 115.9, 104.5, 40.3 (2C), 37.4, 24.7 ppm

LRMS (TOF MSMS ES+ ASAP)

m/z (%): 301 (100), 300 (28)

HRMS (TOF MS ES+ ASAP)

[M] calcd for $C_{21}H_{19}NO$: 301.1467; found, 301.1469

TLC R_f = 0.2 (15% ethyl acetate/hexanes) [silica gel, UV, $KMnO_4$ stain]

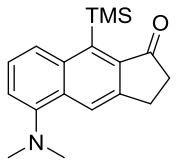

4.43

5-(Dimethylamino)-9-(trimethylsilyl)-2,3-dihydro-1*H*-cyclopenta[*b*]naphthalen-1-one (4.43). Follows general procedure C: RuPhos palladacycle (0.0015 g, 0.0020 mmol, 0.029 equiv), cesium carbonate (0.045 g, 0.14 mmol), cyclopenta[*b*]naphthalenone **1.142** (0.020 g, 0.069 mmol), THF (0.25 mL, 0.25 M), and dimethylamine (0.11 mL, 0.21 mmol, 3.0 equiv). The reaction mixture was heated at 85 °C for 3.5 h, turning the reaction mixture from cloudy orange to dark brown. The crude product was purified by silica gel flash column chromatography (1.25 cm, 3% ethyl acetate/hexanes) to yield the title compound as a yellow solid (14 mg, 68%).

Data **4.43**

MP 95-97 °C

^{1}H NMR (700 MHz, $CDCl_3$)

8.37 (s, 1H), 8.11 (d, *J* = 8.4 Hz, 1H), 7.36 (t, *J* = 7.7 Hz, 1H), 7.15 (d, *J* = 7.7 Hz, 1H), 3.32-3.30 (m, 2H), 2.89 (s, 6H), 2.77-2.75 (m, 2H), 0.53 (s, 9H) ppm

^{13}C NMR (175 MHz, $CDCl_3$)

208.2, 150.8, 147.2, 142.7, 141.4, 138.7, 131.9, 125.9, 124.7, 122.7, 115.8, 45.4 (2C), 37.1, 29.7 (grease), 25.6, 3.03 (3C) ppm

IR (thin film)

2940, 2792, 1715, 1592, 1490, 1454 cm^{-1}

LRMS (TOF MSMS ES+ ESI)

m/z (%): 298 (20), 283 (11), 268 (100), 209 (7)

HRMS (TOF MS ES+ ESI)

$[M+H]^+$ calcd for $C_{18}H_{24}NOSi$: 298.1627; found, 298.1616

TLC R_f = 0.3 (10% ethyl acetate/hexanes) [silica gel, UV, $KMnO_4$ stain]

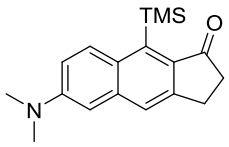

4.44

6-(Dimethylamino)-9-(trimethylsilyl)-2,3-dihydro-1*H*-cyclopenta[*b*]naphthalen-1-one (4.44). Follows general procedure C: RuPhos palladacycle (0.010 g, 0.013 mmol, 0.030 equiv), cesium carbonate (0.280 g, 0.86 mmol), cyclopenta[*b*]naphthalenone **1.144** (0.125 g, 0.43 mmol), THF (0.86 mL, 0.50 M), and dimethylamine (0.65 mL, 1.29 mmol, 3.0 equiv). The reaction mixture was heated at 85 °C for 6 h, turning the reaction mixture from red to dark brown over time. The crude product was purified by silica gel flash column chromatography (2.0 cm, 4% ethyl acetate/hexanes) to yield the title compound as a yellow solid (80 mg, 62%).

Data **4.44**

MP 168-171 °C

^{1}H NMR (300 MHz, $CDCl_3$)

8.32 (d, *J* = 9.3 Hz, 1H), 7.61 (bs, 1H), 7.11 (dd, *J* = 9.3, 2.8 Hz, 1H), 6.80 (d, *J* = 2.8 Hz, 1H), 3.23-3.21 (m, 2H), 3.10 (s, 6H), 2.72-2.68 (m, 2H), 0.52 (s, 9H) ppm

^{13}C NMR (100 MHz, $CDCl_3$)

207.4, 149.1, 148.8, 142.2, 138.5, 137.9, 131.8, 130.6, 123.8, 115.3, 105.2, 40.3 (2C), 36.8, 25.2, 3.1 (3C) ppm

IR (thin film)

2956, 2923, 2887, 2851, 1696, 1616, 1507 cm^{-1}

LRMS (TOF MSMS ES+ ESI)

m/z (%): 297 (100), 281 (5)

HRMS (TOF MS ES+ ESI)

$[M+H]^+$ calcd for $C_{18}H_{24}NOSi$: 298.1627; found, 298.1630

TLC R_f = 0.2 (10% ethyl acetate/hexanes) [silica gel, UV, $KMnO_4$ stain]

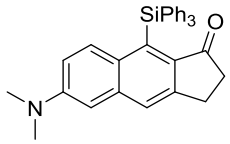

4.46

6-(Dimethylamino)-9-(triphenylsilyl)-2,3-dihydro-1*H*-cyclopenta[*b*]naphthalen-1-one (4.46). Follows general procedure C: RuPhos palladacycle (0.001 g, 0.0013 mmol, 0.030 equiv), cesium carbonate (0.027 g, 0.084 mmol), cyclopenta[*b*]naphthalenone **1.144** (0.020 g, 0.042 mmol), THF (0.10 mL, 0.42 M), and dimethylamine (0.11 mL, 0.21 mmol, 5.0 equiv). The reaction mixture was heated at 85 °C for 2.5 h, turning the reaction mixture red, and then at 95 °C for 1 h, turning the reaction mixture to brown. The crude product was purified by silica gel flash column chromatography (1.5 cm, 5-10% ethyl acetate/hexanes) to yield the title compound as a yellow solid (17 mg, 85%). The product was further purified by HPLC for characterization (5% ethyl acetate/hexanes for 10 min, 5-10% ethyl acetate/hexanes over 30 min, flow rate of 4 mL/min, elution at 32.2 min).

Data **4.46**

MP >260 °C

^{1}H NMR (300 MHz, $CDCl_3$)

7.76 (s, 1H), 7.72 (d, J = 9.6 Hz, 1H), 7.60 (dd, J = 7.5, 1.8 Hz, 6H), 7.35-7.26 (m, 9H), 6.83 (d, J = 3.0 Hz, 1H), 6.63 (d, J = 9.6, 3.0 Hz, 1H), 3.23-3.19 (m, 2H), 3.02 (s, 6H), 2.46-2.41 (m, 2H) ppm

^{13}C NMR (150 MHz, $CDCl_3$)

205.2, 149.1, 148.1, 139.6, 138.9, 137.8 (3C), 135.5 (6C), 134.4, 132.6, 131.6, 128.6 (3C), 127.5 (6C), 125.2, 115.2, 105.1, 40.2 (2C), 36.3, 25.4 ppm

IR (thin film)

3058, 2989, 2922, 2845, 1698, 1615, 1509, 699 cm^{-1}

HRMS (TOF MS ES+ ASAP)

[M] calcd for $C_{33}H_{29}NOSi$: 483.2018; found, 483.2030

TLC R_f = 0.1 (10% ethyl acetate/hexanes) [silica gel, UV, $KMnO_4$ stain]

4.6.6 Normalized absorption and emission spectra

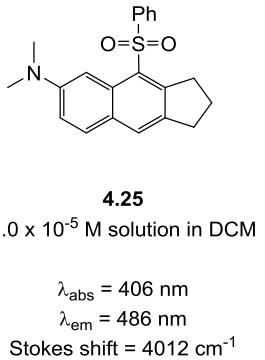

4.25
1.0 x 10^{-5} M solution in DCM

λ_{abs} = 406 nm
λ_{em} = 486 nm
Stokes shift = 4012 cm^{-1}

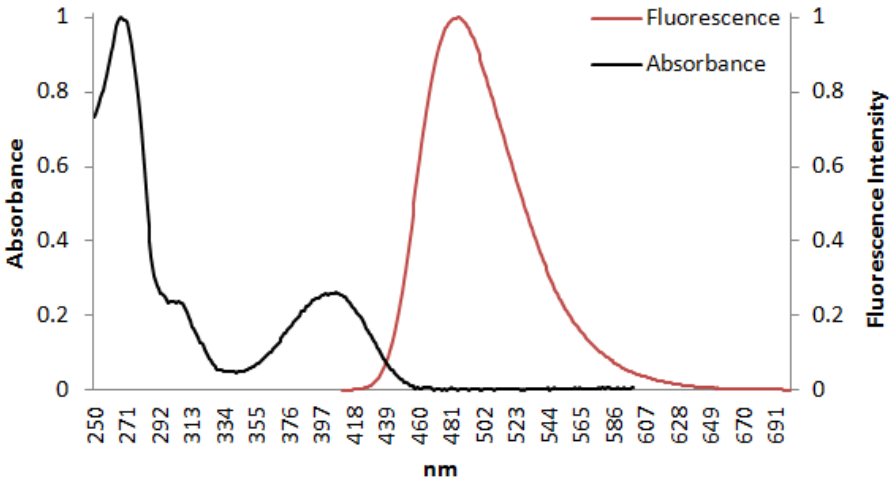

Figure 4.14. Normalized absorbance and fluorescence spectra of **4.25** in DCM

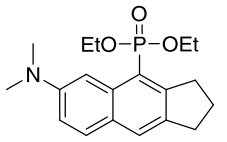

4.26

λ_{abs} = 384 nm

λ_{em} = 460 nm

Stokes shift = 4303 cm^{-1}

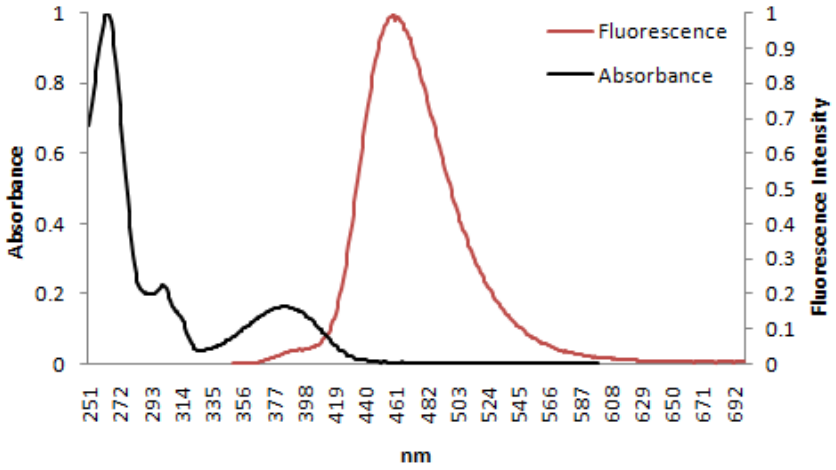

Figure 4.15. Normalized absorbance and fluorescence spectra of **4.26** in DCM

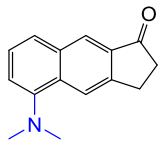

4.36

3.0 x 10^{-5} M solution in DCM

λ_{abs} = 374 nm

λ_{em} = 547 nm

Stokes shift = 8456 cm^{-1}

Spectral width (FWHM) = 111 nm

Φ_F = 0.33

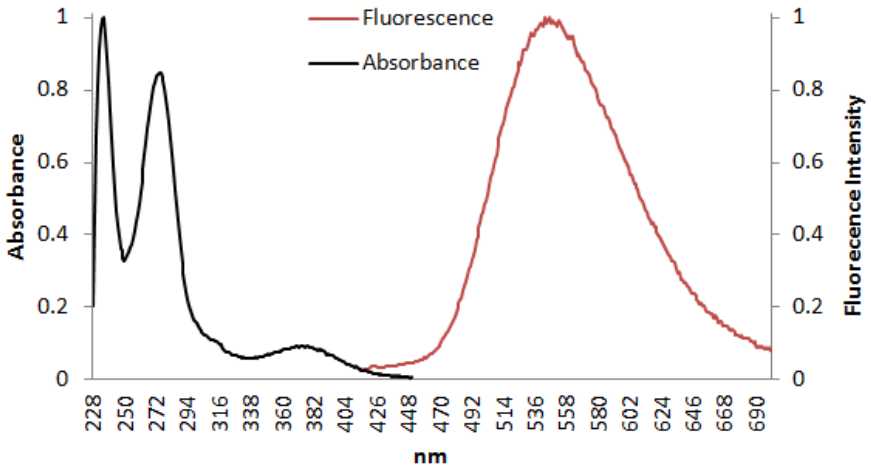

Figure 4.16. Normalized absorbance and fluorescence spectra of **4.36** in DCM

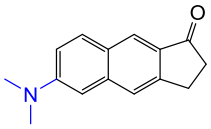

4.37

3.5 x 10^{-6} M solution in DCM

λ_{abs} = 393 nm

λ_{em} = 461 nm

Stokes shift = 3753 cm^{-1}

Spectral width (FWHM) = 61 nm

Φ_F = 0.64

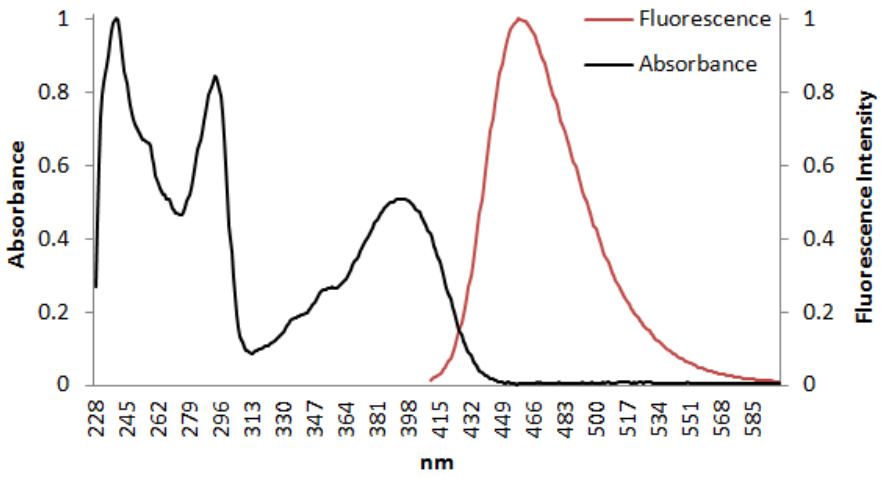

Figure 4.17. Normalized absorbance and fluorescence spectra of **4.37** in DCM

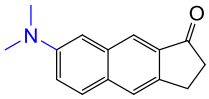

4.38

5.0 x 10^{-5} M solution in DCM

λ_{abs} = 423 nm

λ_{em} = 522 nm

Stokes shift = 4484 cm^{-1}

Spectral width (FWHM) = 86 nm

Φ_F = 0.53

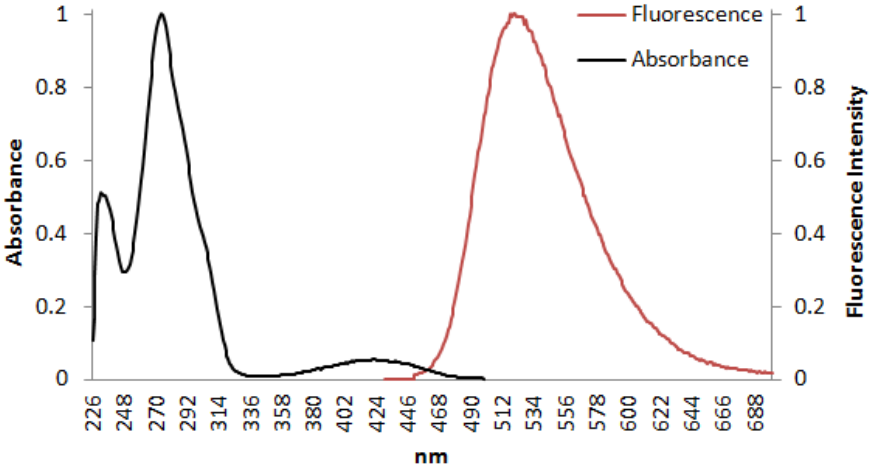

Figure 4.18. Normalized absorbance and fluorescence spectra of **4.38** in DCM

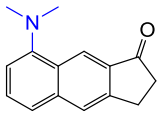

4.39
3.0 x 10^{-5} M solution in DCM

λ_{abs} = 384 nm
λ_{em} = 548 nm
Stokes shift = 7793 cm^{-1}
Spectral width (FWHM) = 103 nm
Φ_F = 0.53

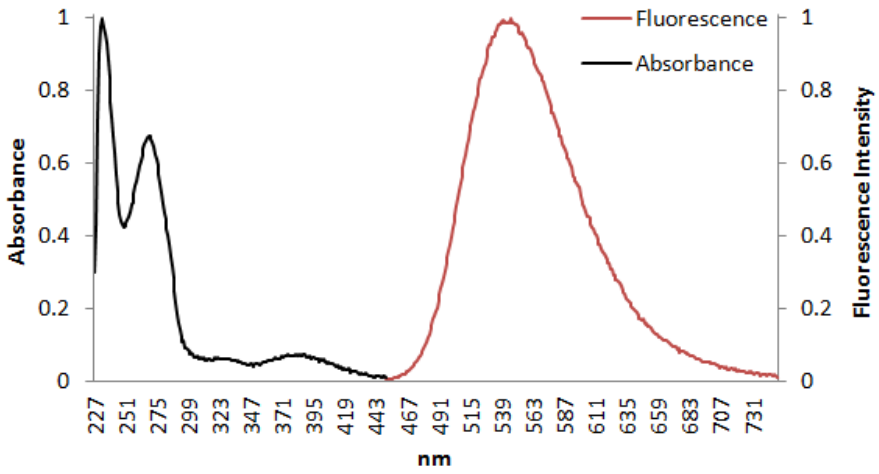

Figure 4.19. Normalized absorbance and fluorescence spectra of **4.39** in DCM

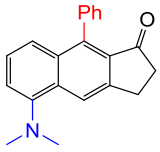

4.40
3.0 x 10^{-5} M solution in DCM

λ_{abs} = 377 nm
λ_{em} = 562 nm
Stokes shift = 8732 cm^{-1}
Spectral width (FWHM) = 114 nm
Φ_F = 0.44

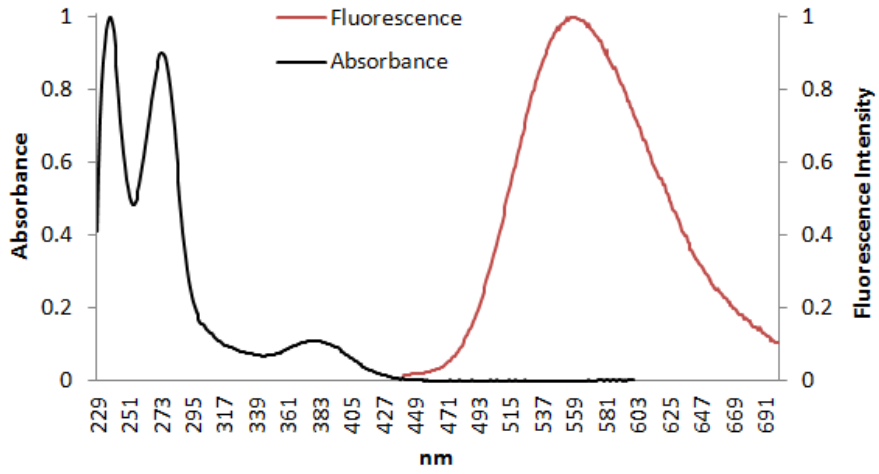

Figure 4.20. Normalized absorbance and fluorescence spectra of **4.40** in DCM

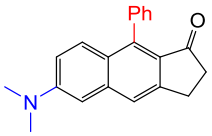

4.41
1.0 x 10^{-5} M solution in DCM

λ_{abs} = 395 nm
λ_{em} = 472 nm
Stokes shift = 4130 cm^{-1}
Spectral width (FWHM) = 66 nm
Φ_F = 0.65

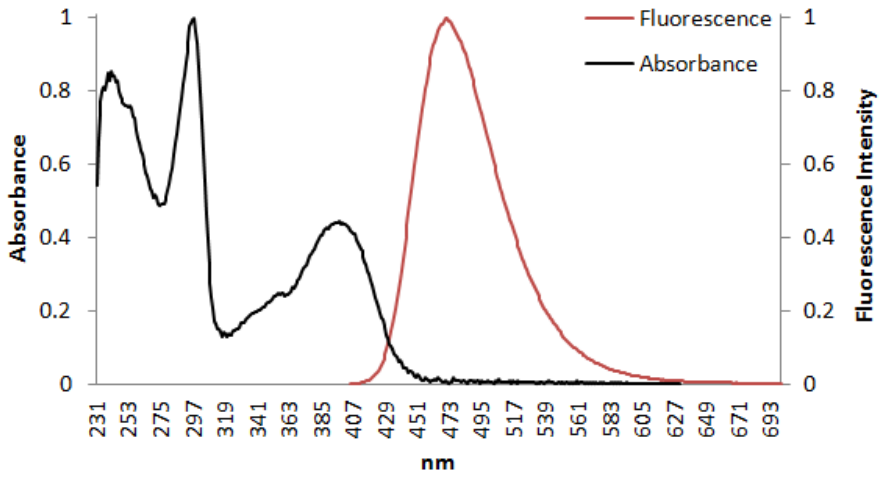

Figure 4.21. Normalized absorbance and fluorescence spectra of **4.41** in DCM

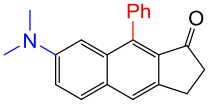

4.42
1.0 x 10^{-5} M solution in DCM

λ_{abs} = 427 nm
λ_{em} = 535 nm
Stokes shift = 4728 cm^{-1}
Spectral width (FWHM) = 83 nm

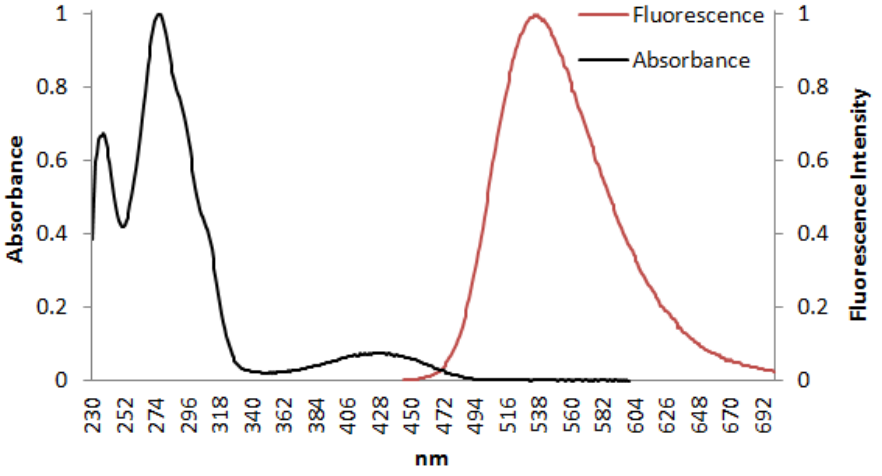

Figure 4.22. Normalized absorbance and fluorescence spectra of **4.42** in DCM

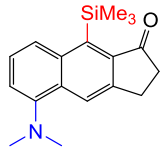

4.43

3.0 x 10^{-5} M solution in DCM

λ_{abs} = 386 nm
λ_{em} = 572 nm
Stokes shift = 8424 cm^{-1}
Spectral width (FWHM) = 115 nm
Φ_F = 0.41

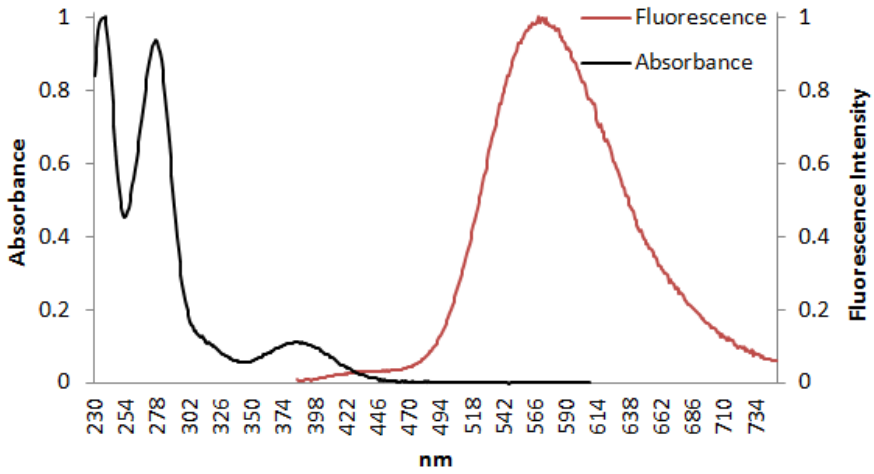

Figure 4.23. Normalized absorbance and fluorescence spectra of **4.43** in DCM

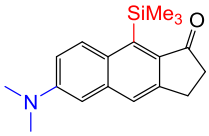

4.44

7.0 x 10^{-6} M solution in DCM

λ_{abs} = 405 nm
λ_{em} = 489 nm
Stokes shift = 4242 cm^{-1}
Spectral width (FWHM) = 79 nm
Φ_F = 0.66

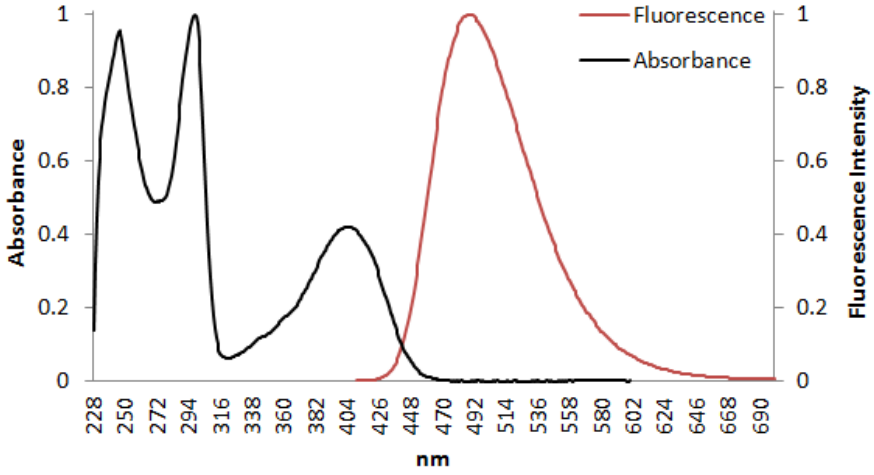

Figure 4.24. Normalized absorbance and fluorescence spectra of **4.44** in DCM

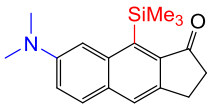

4.45
3.0 x 10^{-5} M solution in DCM

λ_{abs} = 436 nm
λ_{em} = 542 nm
Stokes shift = 4486 cm^{-1}
Spectral width (FWHM) = 86 nm
Φ_F = 0.65

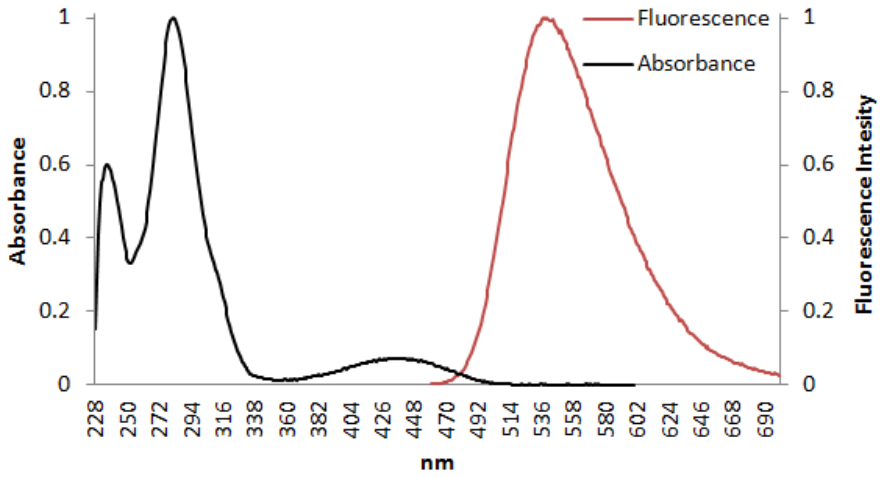

Figure 4.25. Normalized absorbance and fluorescence spectra of **4.45** in DCM

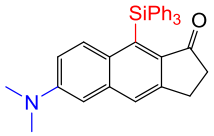

4.46
1.5 x 10^{-5} M solution in DCM

λ_{abs} = 413 nm
λ_{em} = 494 nm
Stokes shift = 3970 cm^{-1}
Spectral width (FWHM) = 75 nm
Φ_F = 0.70

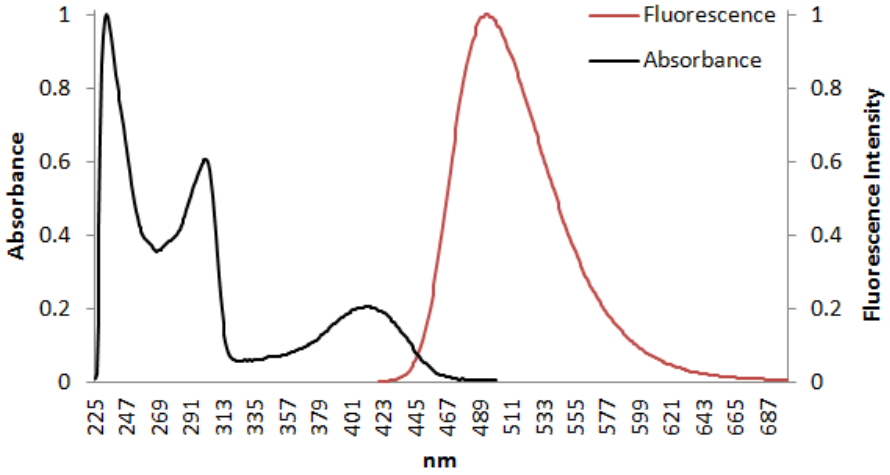

Figure 4.26. Normalized absorbance and fluorescence spectra of **4.46** in DCM

4.6.7 Calculation of quantum yield

The relative quantum yields of the cyclopenta[*b*]naphthalenone dyes were calculated by comparing their fluorescence emission against two standards, either coumarin 6 (Φ_F = 0.78 in ethanol), coumarin 314 (Φ_F = 0.68 in ethanol), or coumarin 153 (Φ_F = 0.53 in ethanol).[145] The reported quantum yield for each cyclopenta[*b*]naphthalenone dye is an average of these two quantum yield values. The standards were chosen based on their similar absorption and emission wavelengths to the reported fluorescent dyes (coumarin 6: λ_{abs} = 458 nm, λ_{em} = 505 nm; coumarin 314: λ_{abs} = 436 nm, λ_{em} = 480 nm; coumarin 153: λ_{abs} = 422 nm, λ_{em} = 532 nm). All samples were first degassed by bubbling with argon, followed by dilution to volume with additional degassed solvent and storage under an atmosphere of argon until all data had been collected. Quantum yields were calculated according to the following equation:

$$\mathbf{\Phi_x = \Phi_{st} \bullet (I_x/I_{st}) \bullet (A_{st}/A_x) \bullet (\eta^2_x/\eta^2_{st})}$$

where Φ is the quantum yield, I is the integrated fluorescent intensity (area under the emission curve), A is the optical density (absorption) at the excitation wavelength, and η is the refractive index of the solvent employed to dissolve the sample. The subscript x denotes values for the fluorescent dye being analyzed, and the subscript st indicates values for the standard sample.

The excitation wavelength was chosen by overlaying the absorption spectra of the most red-shifted absorption band of the fluorescent dye with the absorption spectra of each standard and locating the wavelength at which they intersect. Intersection points to determine excitation

wavelength were chosen near the blue region of the absorption band when possible to ensure that a full emission curve was collected. The concentrations of the standard and fluorescent dye samples were chosen as to maintain an absorbance maximum intensity for the most red-shifted absorption band of less than 0.1 to avoid reabsorption effects.[145b] Standard deviations are shown for samples for which quantum yield calculations were performed on multiple samples.

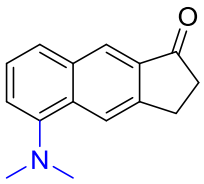

4.36

3.0×10^{-5} M solution in DCM

Φ_x vs. coumarin 6 in ethanol = 0.34 (λ_{ex} = 396 nm)

Φ_x vs. coumarin 314 in ethanol = 0.31 (λ_{ex} = 384 nm)

Figure 4.27. Calculated quantum yield values of **4.36** in DCM

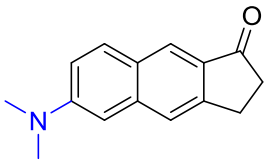

4.37

3.5×10^{-6} M solution in DCM

Φ_x vs. coumarin 6 in ethanol = 0.61 (λ_{ex} = 420 nm)

Φ_x vs. coumarin 153 in ethanol = 0.66 (λ_{ex} = 396 nm)

Figure 4.28. Calculated quantum yield values of **4.37** in DCM

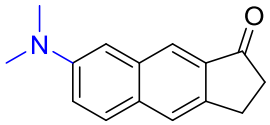

4.38

5.0 x 10^{-5} M solution in DCM

Φ_x vs. coumarin 6 in ethanol = 0.55 (λ_{ex} = 408 nm)

Φ_x vs. coumarin 314 in ethanol = 0.51 (λ_{ex} = 376 nm)

Figure 4.29. Calculated quantum yield values of **4.38** in DCM

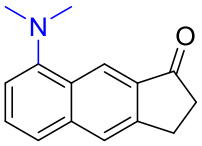

4.39

3.0 x 10^{-5} M solution in DCM

Φ_x vs. coumarin 6 in ethanol = 0.54 (λ_{ex} = 402 nm)

Φ_x vs. coumarin 314 in ethanol = 0.51 (λ_{ex} = 386 nm)

Figure 4.30. Calculated quantum yield values of **4.39** in DCM

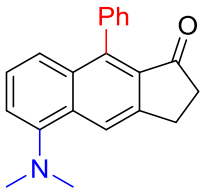

4.40

3.0 x 10^{-5} M solution in DCM

Φ_x vs. coumarin 6 in ethanol = 0.46 (λ_{ex} = 403 nm)

Φ_x vs. coumarin 314 in ethanol = 0.43 (λ_{ex} = 388 nm)

Figure 4.31. Calculated quantum yield values of **4.40** in DCM

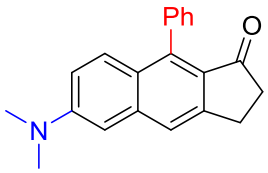

4.41

1.0 x 10^{-5} M solution in DCM

Φ_x vs. coumarin 6 in ethanol = 0.65 (λ_{ex} = 408 nm)

Φ_x vs. coumarin 314 in ethanol = 0.64 (λ_{ex} = 384 nm)

Figure 4.32. Calculated quantum yield values of **4.41** in DCM

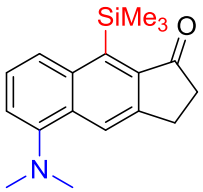

4.43

3.0 x 10^{-5} M solution in DCM

Φ_x vs. coumarin 6 in ethanol = 0.43 (λ_{ex} = 404 nm)

Φ_x vs. coumarin 314 in ethanol = 0.39 (λ_{ex} = 387 nm)

Figure 4.33. Calculated quantum yield values of **4.43** in DCM

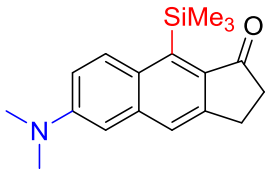

4.44

7.0 x 10^{-6} M solution in DCM

Φ_x vs. coumarin 6 in ethanol = 0.61 ± 0.029 (λ_{ex} = 432 nm)

Φ_x vs. coumarin 153 in ethanol = 0.71 ± 0.006 (λ_{ex} = 410 nm)

Figure 4.34. Calculated quantum yield values of **4.44** in DCM

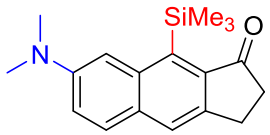

4.45

3.0 x 10^{-5} M solution in DCM

Φ_x vs. coumarin 6 in ethanol = 0.61 ± 0.063 (λ_{ex} = 451 nm)

Φ_x vs. coumarin 153 in ethanol = 0.69 ± 0.036 (λ_{ex} = 447 nm)

Figure 4.35. Calculated quantum yield values of **4.45** in DCM

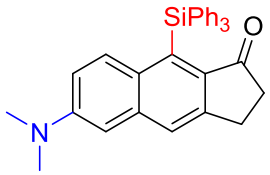

4.46

1.5 x 10^{-5} M solution in DCM

Φ_x vs. coumarin 6 in ethanol = 0.67 ± 0.04 (λ_{ex} = 435 nm)

Φ_x vs. coumarin 153 in ethanol = 0.73 ± 0.04 (λ_{ex} = 414 nm)

Figure 4.36. Calculated quantum yield values of **4.46** in DCM

4.6.8 Calculation of molar absorptivity

Extinction coefficients were determined by preparing 9-12 solutions of increasing concentration for cyclopenta[*b*]naphthalenone dyes in DCM and measuring their individual absorbance spectra. Concentrations were chosen as not to exceed an absorbance maximum of 1.0. Each solution was prepared individually from dilution of an aliquot of a stock solution. Concentration of the

samples (x-axis) was plotted against the corresponding absorbance intensity at the absorbance maximum (y-axis) as an Excel scatter plot. The resulting plot was fitted with using linear regression analysis, the slope of which represented the molar absorptivity of the fluorescent dye according to Beer's Law.

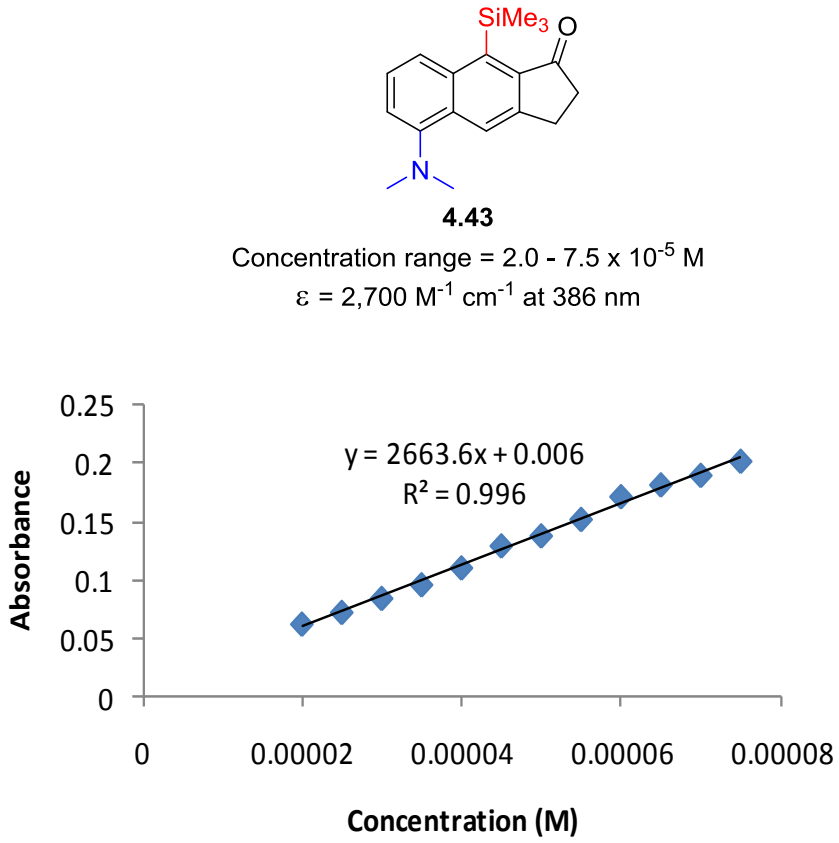

Figure 4.37. Calculation of molar absorptivity for **4.43** in DCM

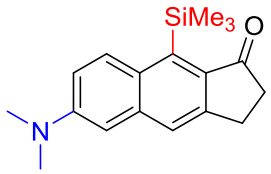

4.44

Concentration range = 0.25 - 5.0 x 10^{-5} M

ε = 14,000 M^{-1} cm^{-1} at 403 nm

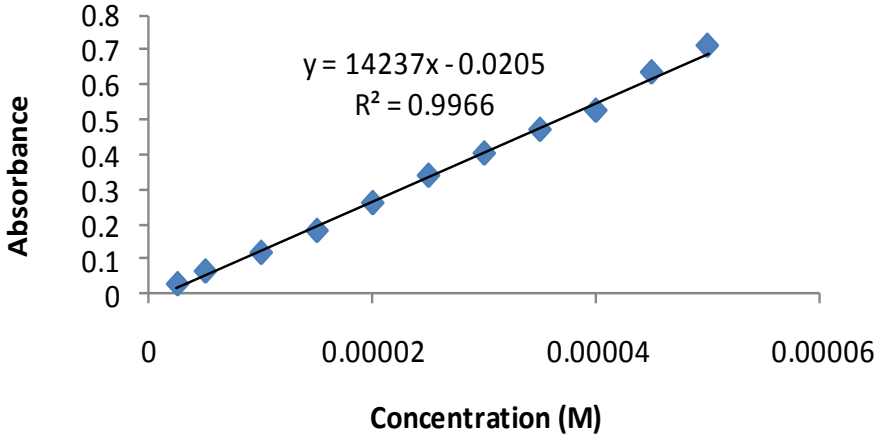

Figure 4.38. Calculation of molar absorptivity for **4.44** in DCM

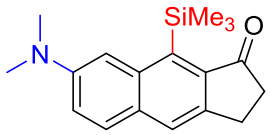

4.45

Concentration range = 0.50 - 5.0 x 10^{-5} M

ε = 2,500 M^{-1} cm^{-1} at 436 nm

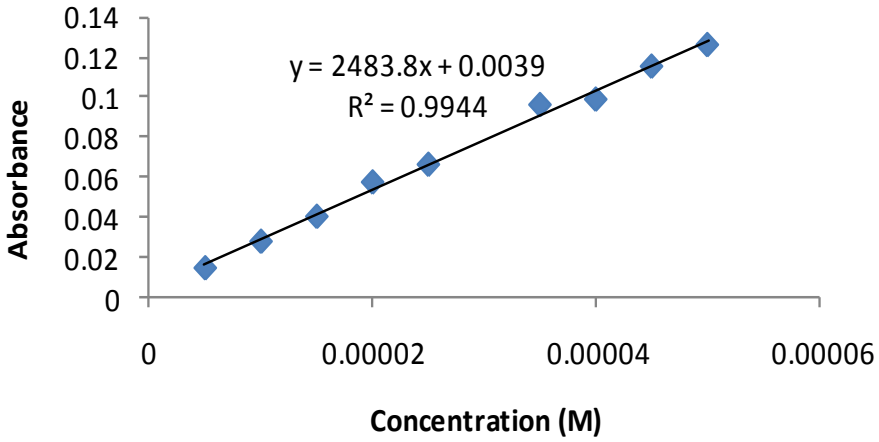

Figure 4.39. Calculation of molar absorptivity for **4.45** in DCM

5.0 SUBMISSION OF SUBSTRATES TO THE NIH MLSMR

Several substrates were submitted to the National Institute of Health's Molecular Libraries Small Molecule Repository (MLSMR) on October 17, 2013. The notebook page or compound number, structure, and MLSMR identifiers for each compound submitted are displayed in Table 5.1. On August 25, 2014 the Pubchem database was checked to determine if these substrates had been distributed or tested; however, as of this date, no biological testing had been logged for these compounds. To check for updates on these compounds, perform a substance search in Pubchem on either the SMRID or MLSID identifiers.

Table 5.1. Compounds submitted to the NIH MLSMR

Notebook Page or Compound Number	Structure	SMRID	MLSID
LSK-3-057	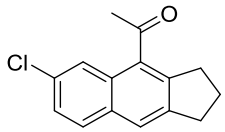	SMR003642950	MLS004883395
LSK-3-204	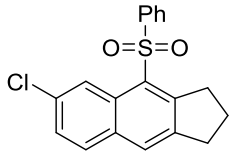	SMR003642944	MLS004883389
LSK-4-010	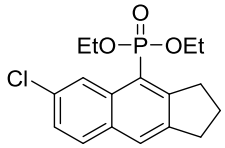	SMR003642946	MLS004883391
LSK-4-015	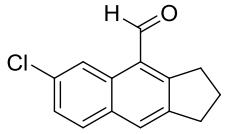	SMR003642945	MLS004883390
LSK-4-073	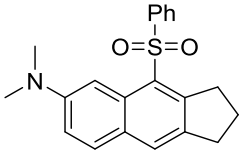	SMR003642947	MLS004883392
EB-010	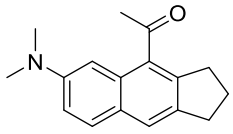	SMR003642951	MLS004883396
EB-242	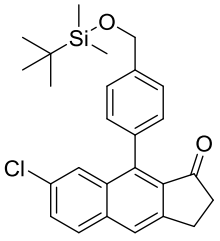	SMR003642953	MLS004883398
AV-036	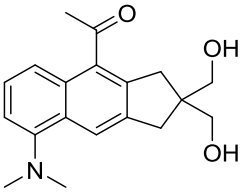	SMR003642949	MLS004883394

APPENDIX A

^{1}H AND ^{13}C NMR SPECTRA OF SYNTHETICALLY PREPARED MOLECULES

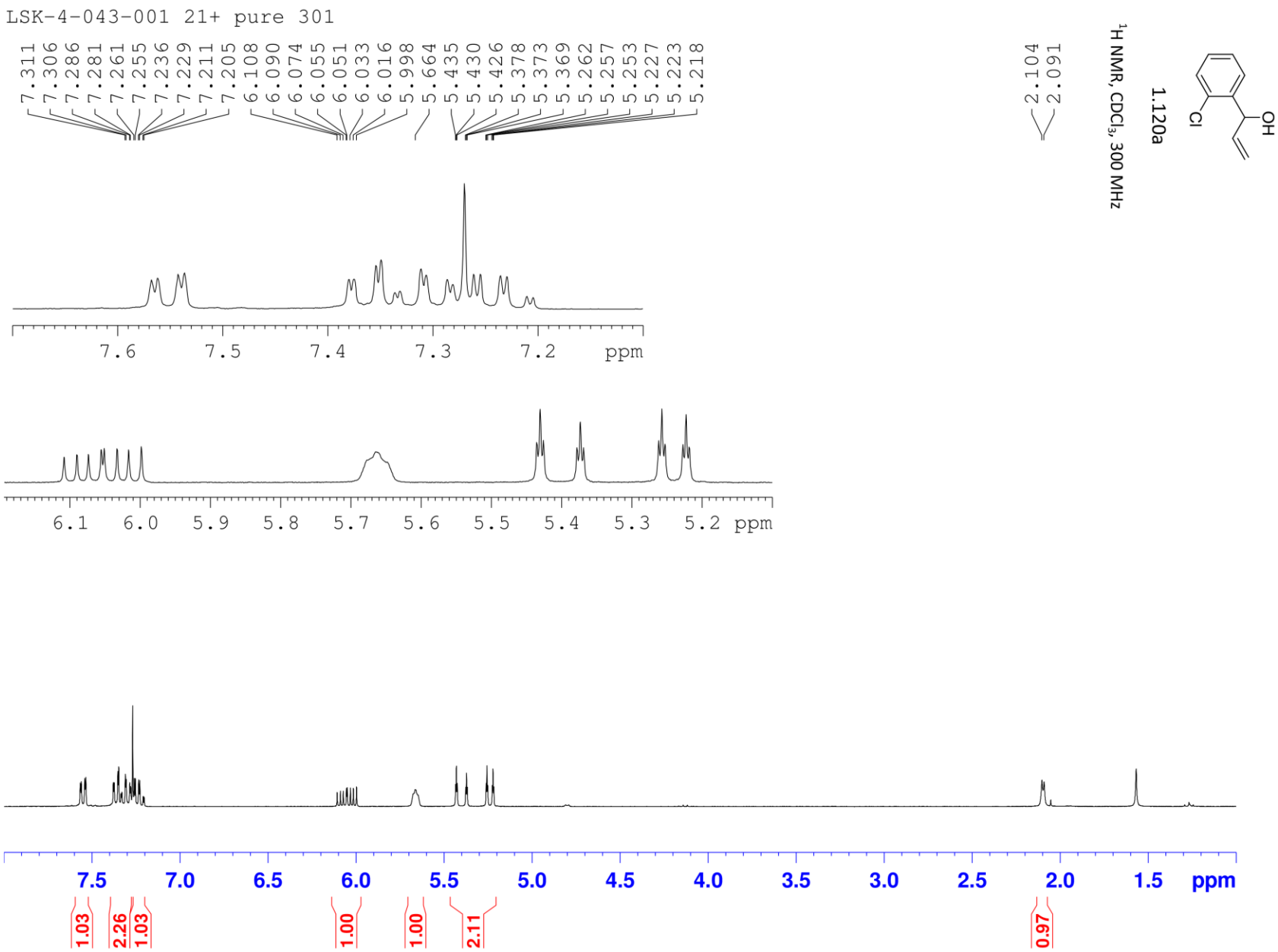
LSK-4-043-001 21+ pure 301
7.311
7.306
7.286
7.281
7.261
7.255
7.236
7.229
7.211
7.205
6.108
6.090
6.074
6.055
6.051
6.033
6.016
5.998
5.664
5.435
5.430
5.426
5.378
5.373
5.369
5.262
5.257
5.253
5.227
5.223
5.218
2.104
2.091
1H NMR, CDCl3, 300 MHz
1.120a
Cl
OH
7.6
7.5
7.4
7.3
7.2
ppm
6.1
6.0
5.9
5.8
5.7
5.6
5.5
5.4
5.3
5.2
ppm
7.5
7.0
6.5
6.0
5.5
5.0
4.5
4.0
3.5
3.0
2.5
2.0
1.5
ppm
1.03
2.26
1.03
1.00
1.00
2.11
0.97

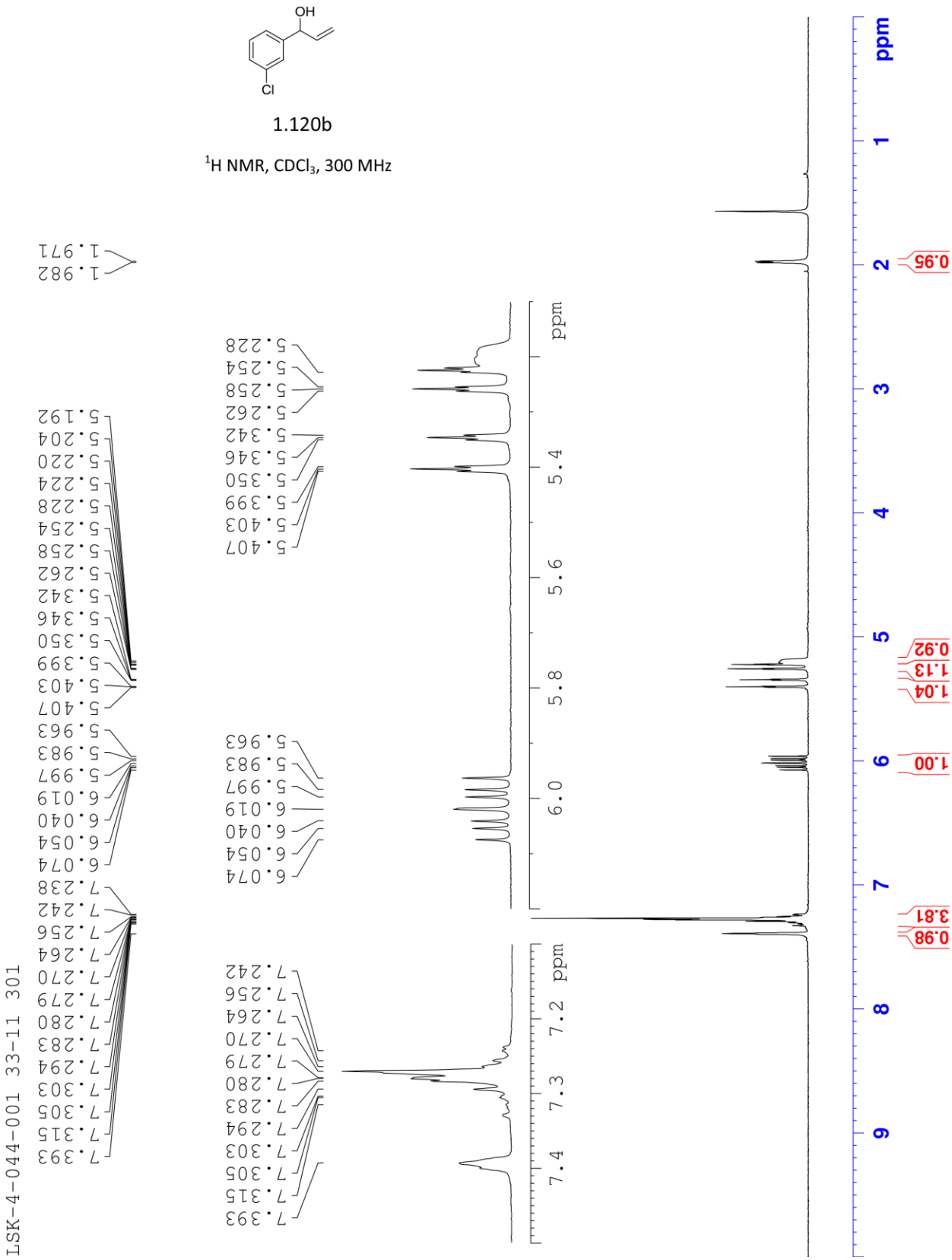
OH
Cl
1.120b
^{1}H NMR, CDCl$_3$, 300 MHz
LSK-4-044-001 33-11 301
ppm
0.95
1.04
1.13
0.92
1.00
0.98
3.81

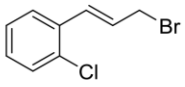

1.121a

^{1}H NMR, $CDCl_3$, 400 MHz

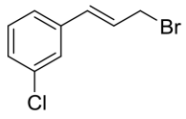

1.121b

^{1}H NMR, $CDCl_3$, 300 MHz

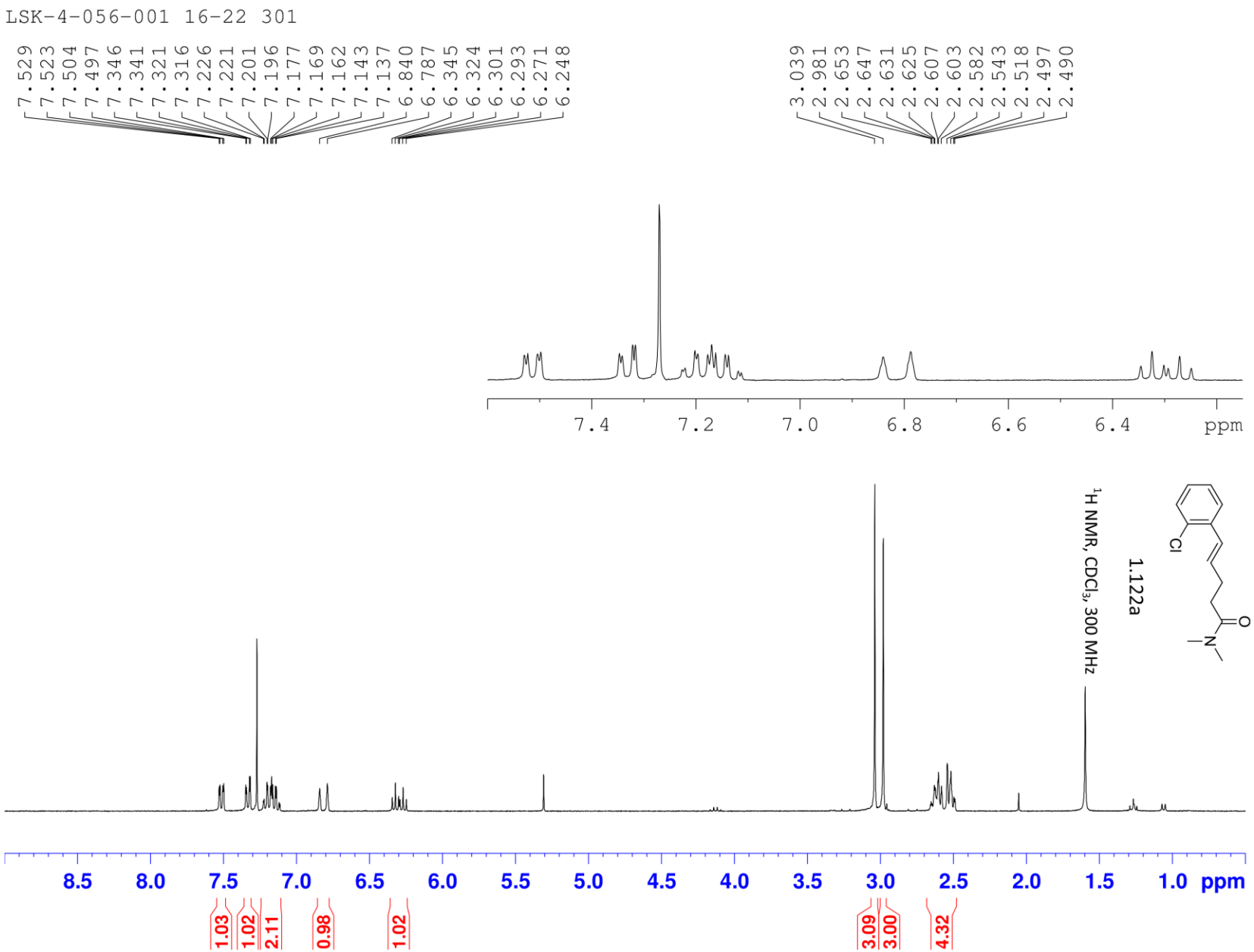
LSK-4-056-001 16-22 301
7.529
7.523
7.504
7.497
7.346
7.341
7.321
7.316
7.226
7.221
7.201
7.196
7.177
7.169
7.162
7.143
7.137
6.840
6.787
6.345
6.324
6.301
6.293
6.271
6.248
3.039
2.981
2.653
2.647
2.631
2.625
2.607
2.603
2.582
2.543
2.518
2.497
2.490
7.4
7.2
7.0
6.8
6.6
6.4
ppm
1H NMR, CDCl3, 300 MHz
1.122a
Cl
O
N
8.5
8.0
7.5
7.0
6.5
6.0
5.5
5.0
4.5
4.0
3.5
3.0
2.5
2.0
1.5
1.0
ppm
1.03
1.02
2.11
0.98
1.02
3.09
3.00
4.32

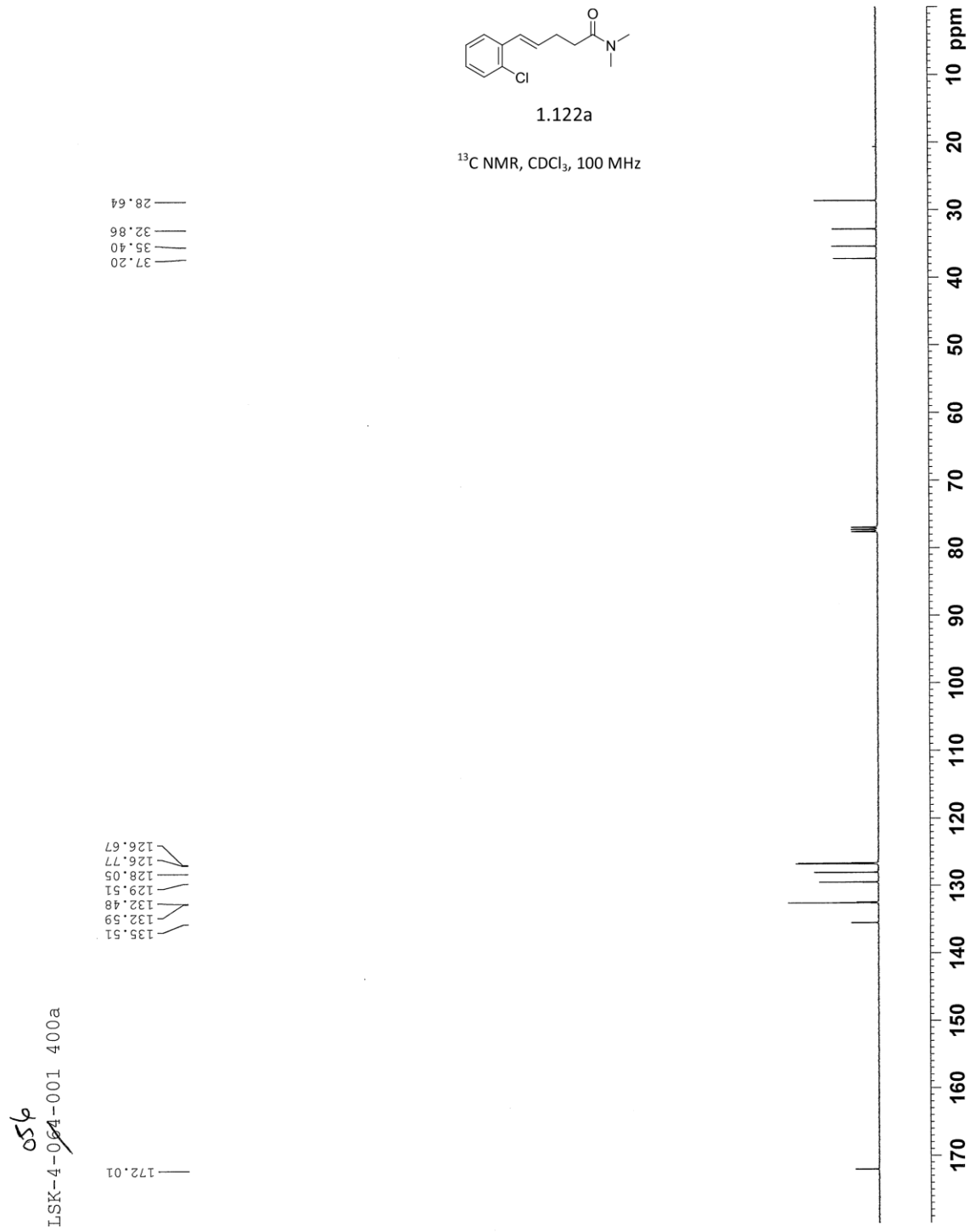
O
N
Cl
1.122a
^{13}C NMR, $CDCl_3$, 100 MHz
28.64
32.86
35.40
37.20
126.67
126.77
128.05
129.51
132.48
132.59
135.51
172.01
LSK-4-064-001 400a
056
10 ppm
20
30
40
50
60
70
80
90
100
110
120
130
140
150
160
170

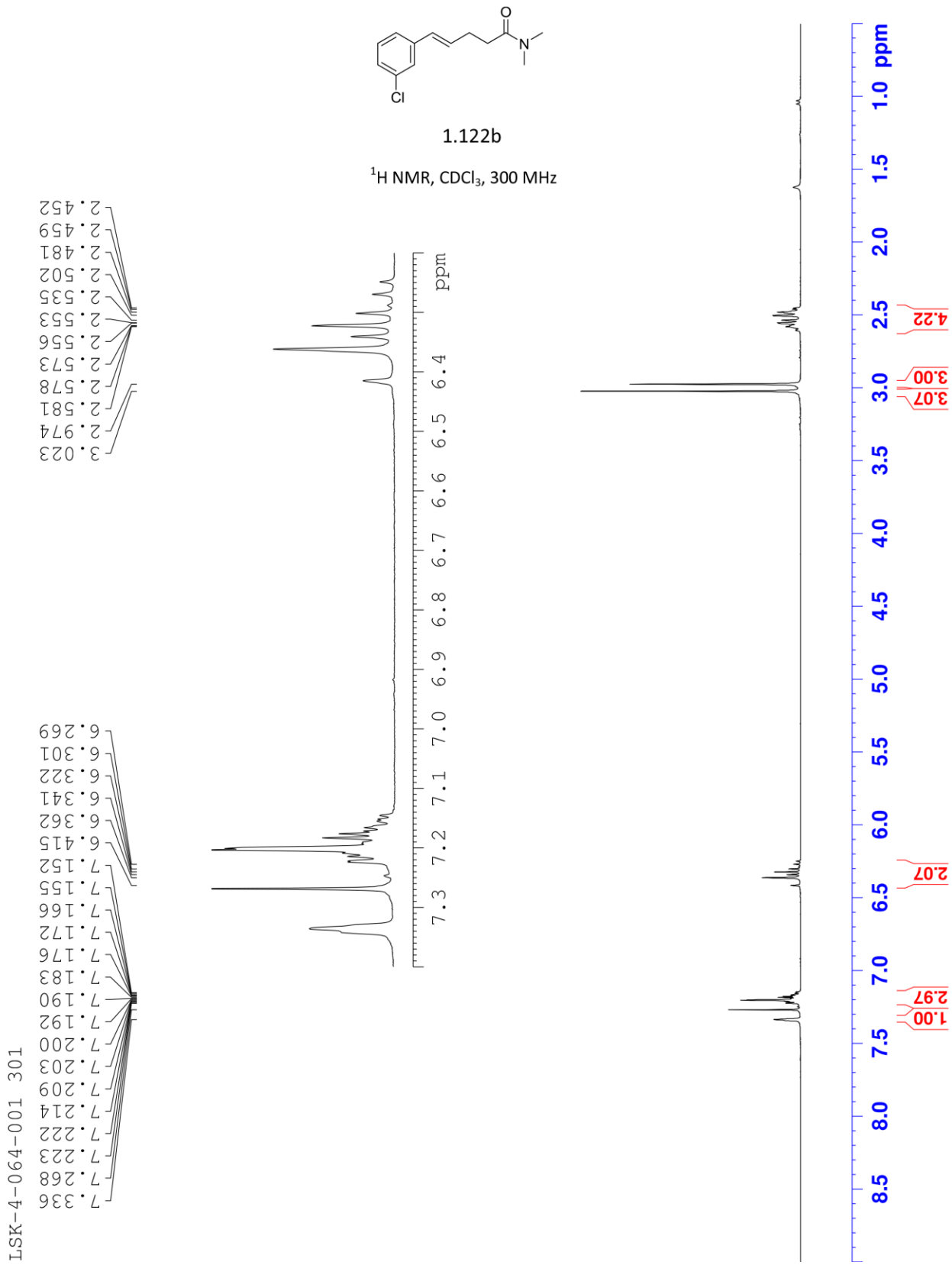
O
N
Cl
1.122b
^{1}H NMR, $CDCl_3$, 300 MHz
LSK-4-064-001 301
7.336
7.268
7.223
7.222
7.214
7.209
7.203
7.200
7.192
7.190
7.183
7.176
7.172
7.166
7.155
7.152
6.415
6.362
6.341
6.322
6.301
6.269
3.023
2.974
2.581
2.578
2.573
2.556
2.553
2.535
2.502
2.481
2.459
2.452
ppm
7.3
7.2
7.1
7.0
6.9
6.8
6.7
6.6
6.5
6.4
ppm
8.5
8.0
7.5
7.0
6.5
6.0
5.5
5.0
4.5
4.0
3.5
3.0
2.5
2.0
1.5
1.0
4.22
3.00
3.07
2.07
1.00
2.97

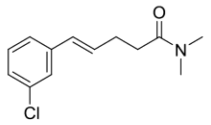

1.122b

^{13}C NMR, $CDCl_3$, 100 MHz

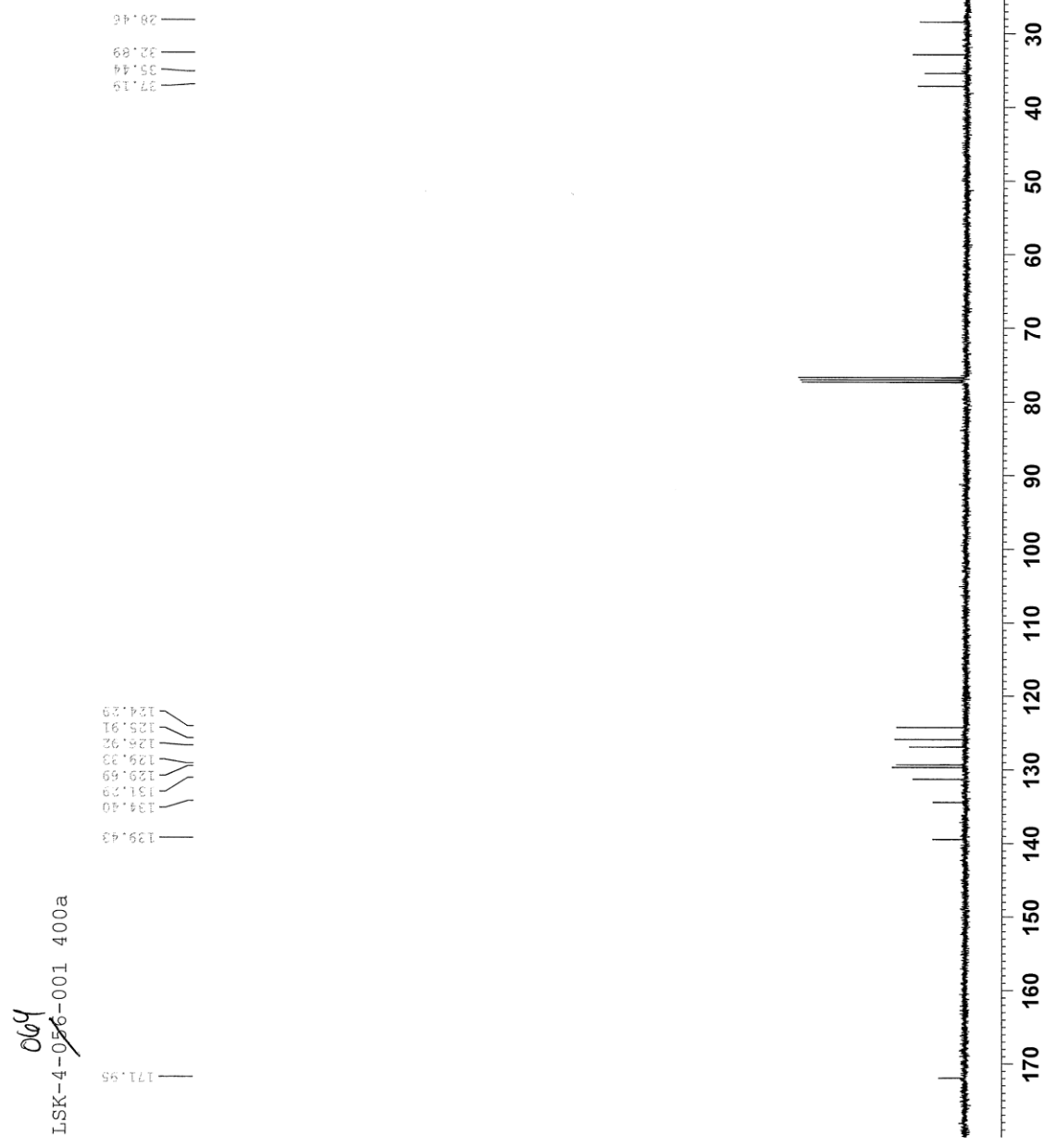

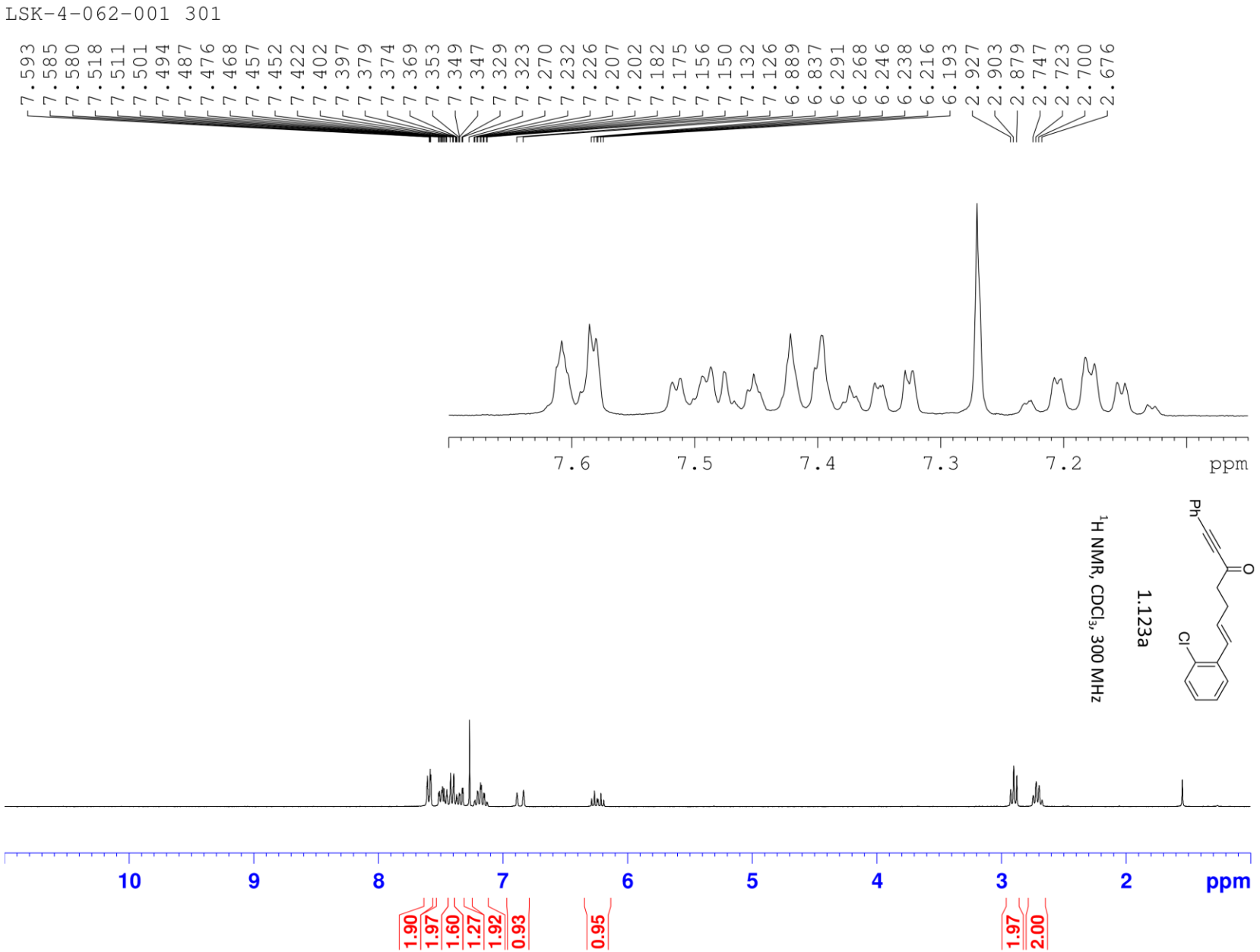
LSK-4-062-001 301
7.593
7.585
7.580
7.518
7.511
7.501
7.494
7.487
7.476
7.468
7.457
7.452
7.422
7.402
7.397
7.379
7.374
7.369
7.353
7.349
7.347
7.329
7.323
7.270
7.232
7.226
7.207
7.202
7.182
7.175
7.156
7.150
7.132
7.126
6.889
6.837
6.291
6.268
6.246
6.238
6.216
6.193
2.927
2.903
2.879
2.747
2.723
2.700
2.676
7.6
7.5
7.4
7.3
7.2
ppm
Ph
O
Cl
1.123a
^{1}H NMR, $CDCl_3$, 300 MHz
10
9
8
7
6
5
4
3
2
ppm
1.90
1.97
1.60
1.27
1.92
0.93
0.95
1.97
2.00

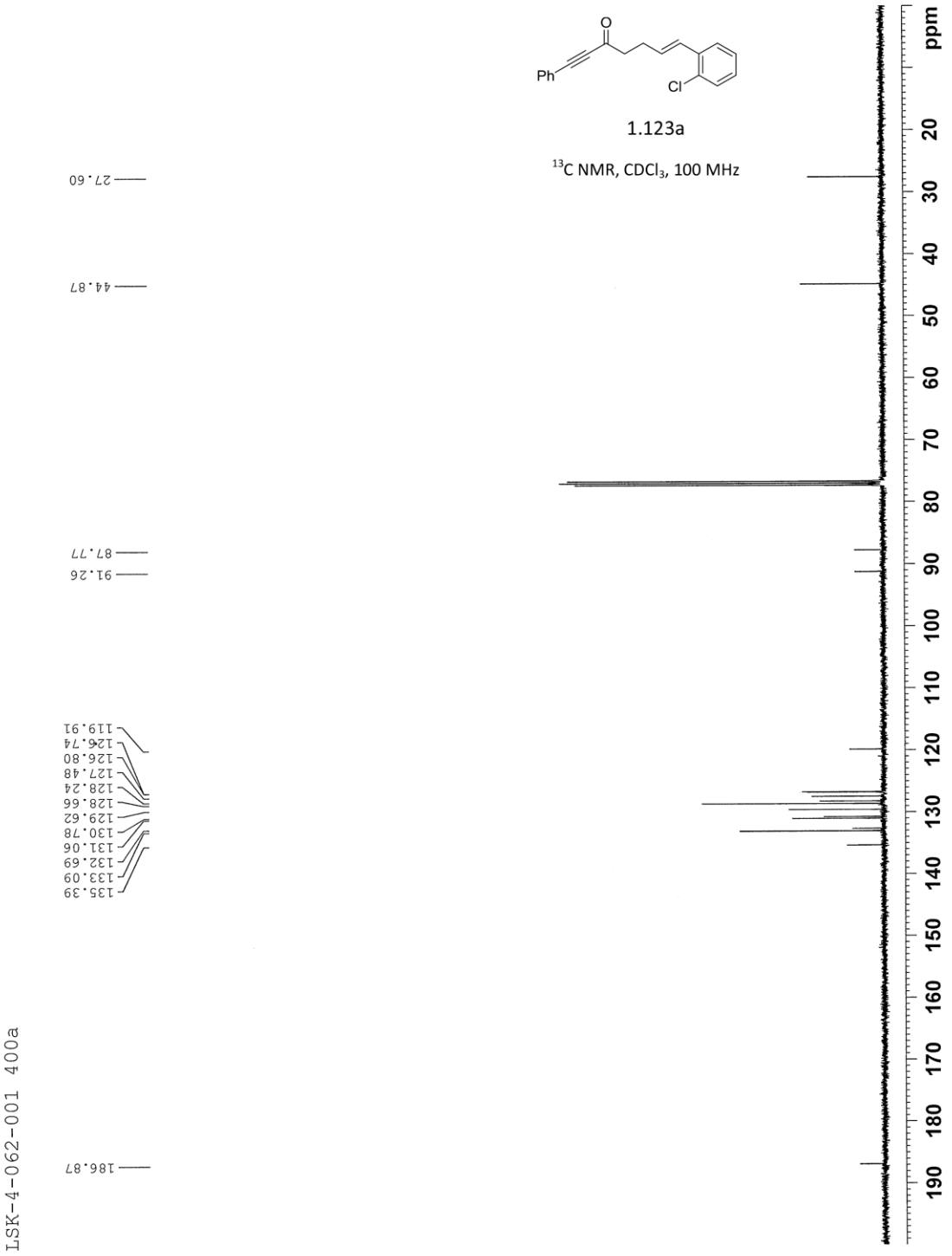
O
Ph
Cl
1.123a
^{13}C NMR, CDCl$_3$, 100 MHz
27.60
44.87
87.77
91.26
119.91
126.74
126.80
127.48
128.24
128.66
129.62
130.78
131.06
132.69
133.09
135.39
186.87
LSK-4-062-001 400a
ppm
20
30
40
50
60
70
80
90
100
110
120
130
140
150
160
170
180
190

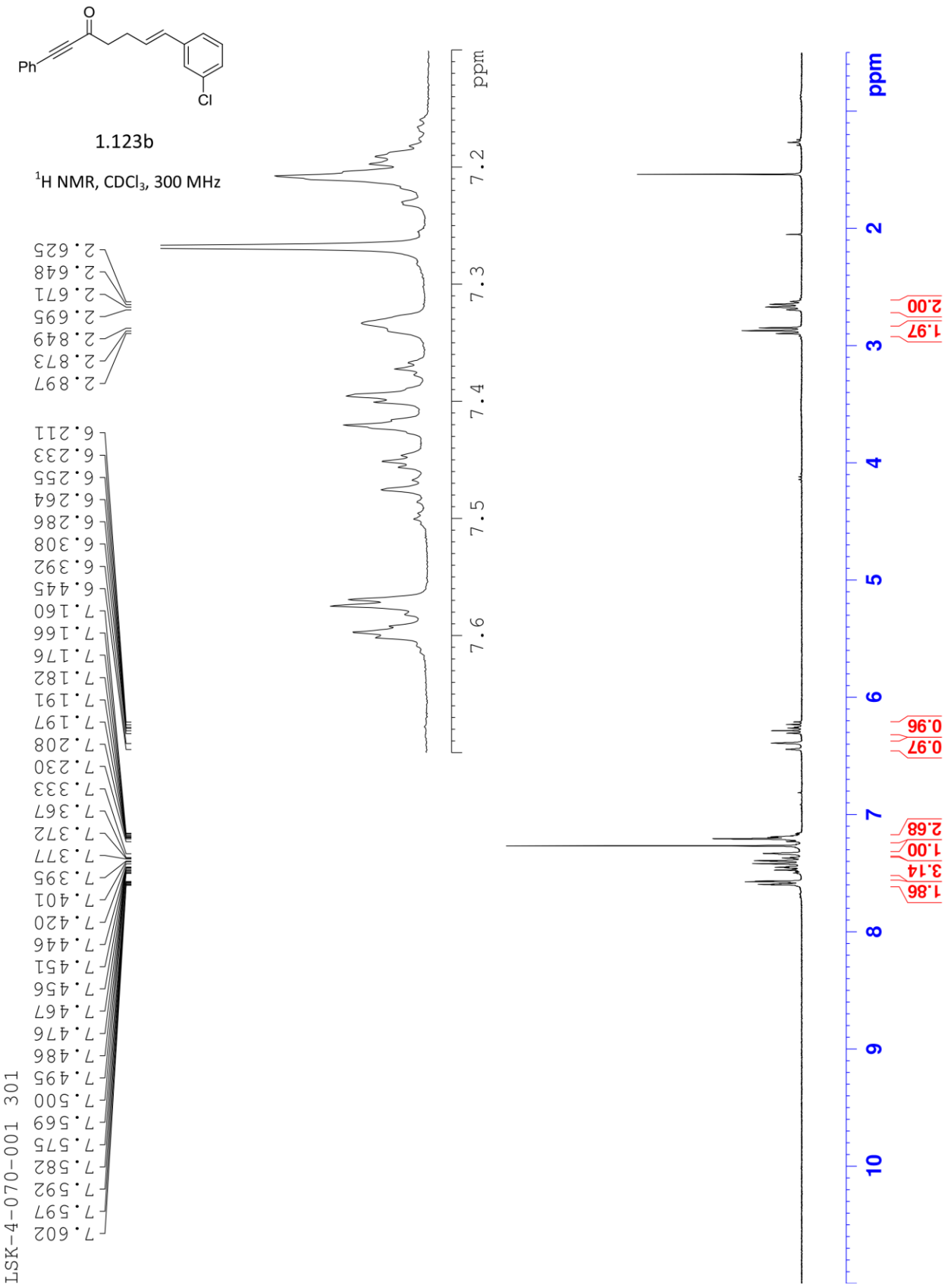
O
Ph
Cl
1.123b
^{1}H NMR, $CDCl_3$, 300 MHz
LSK-4-070-001 301
7.602
7.597
7.592
7.582
7.575
7.569
7.500
7.495
7.486
7.476
7.467
7.456
7.451
7.446
7.420
7.401
7.395
7.377
7.372
7.367
7.333
7.230
7.208
7.197
7.191
7.182
7.176
7.166
7.160
6.445
6.392
6.308
6.286
6.264
6.255
6.233
6.211
2.897
2.873
2.849
2.695
2.671
2.648
2.625
ppm
7.6
7.5
7.4
7.3
7.2
ppm
10
9
8
7
6
5
4
3
2
1.86
3.14
1.00
2.68
0.97
0.96
1.97
2.00

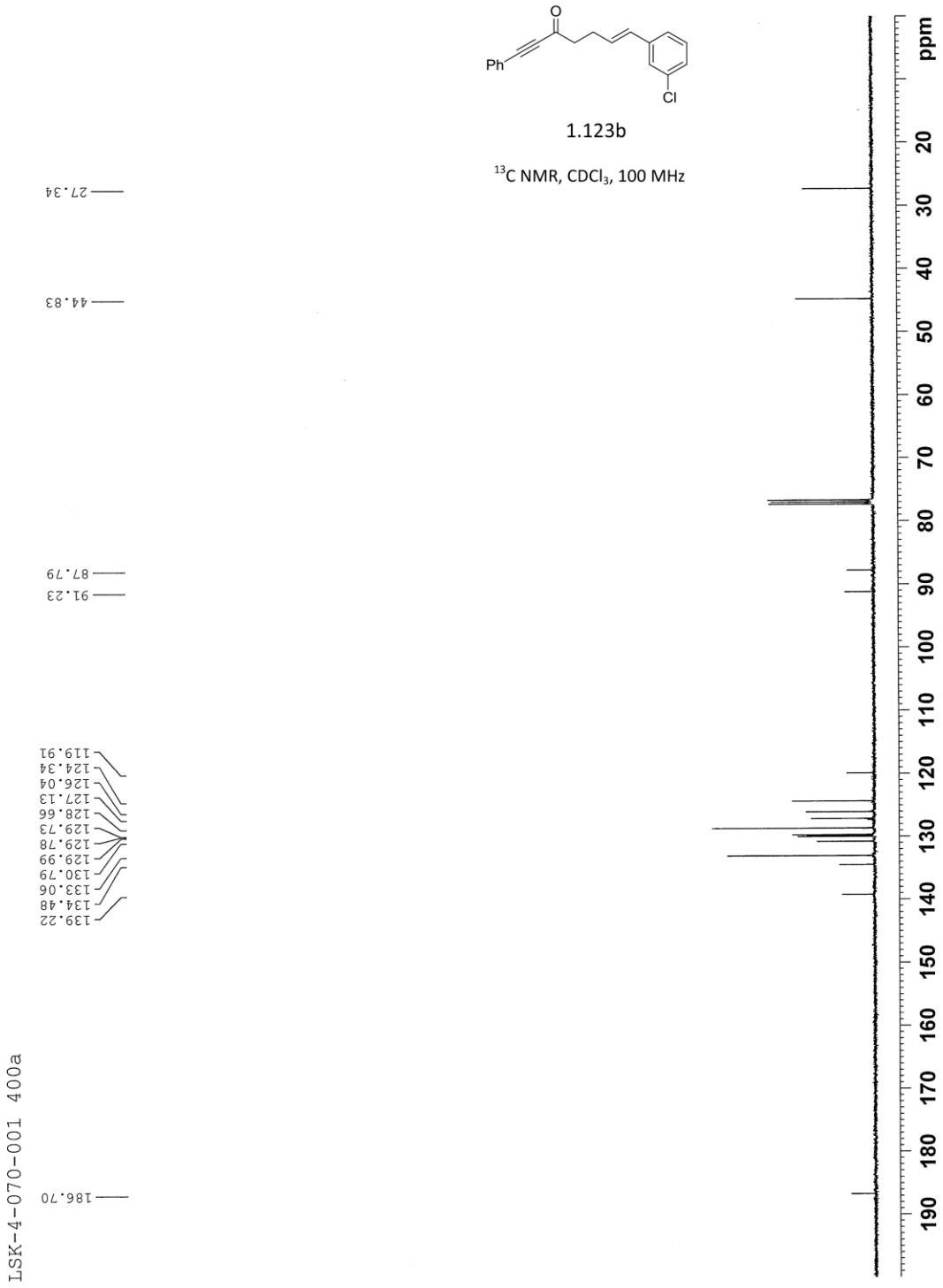
O
Ph
Cl
1.123b
^{13}C NMR, $CDCl_3$, 100 MHz
LSK-4-070-001 400a
27.34
44.83
87.79
91.23
119.91
124.34
126.04
127.13
128.66
129.73
129.78
129.99
130.79
133.06
134.48
139.22
186.70
ppm
20
30
40
50
60
70
80
90
100
110
120
130
140
150
160
170
180
190

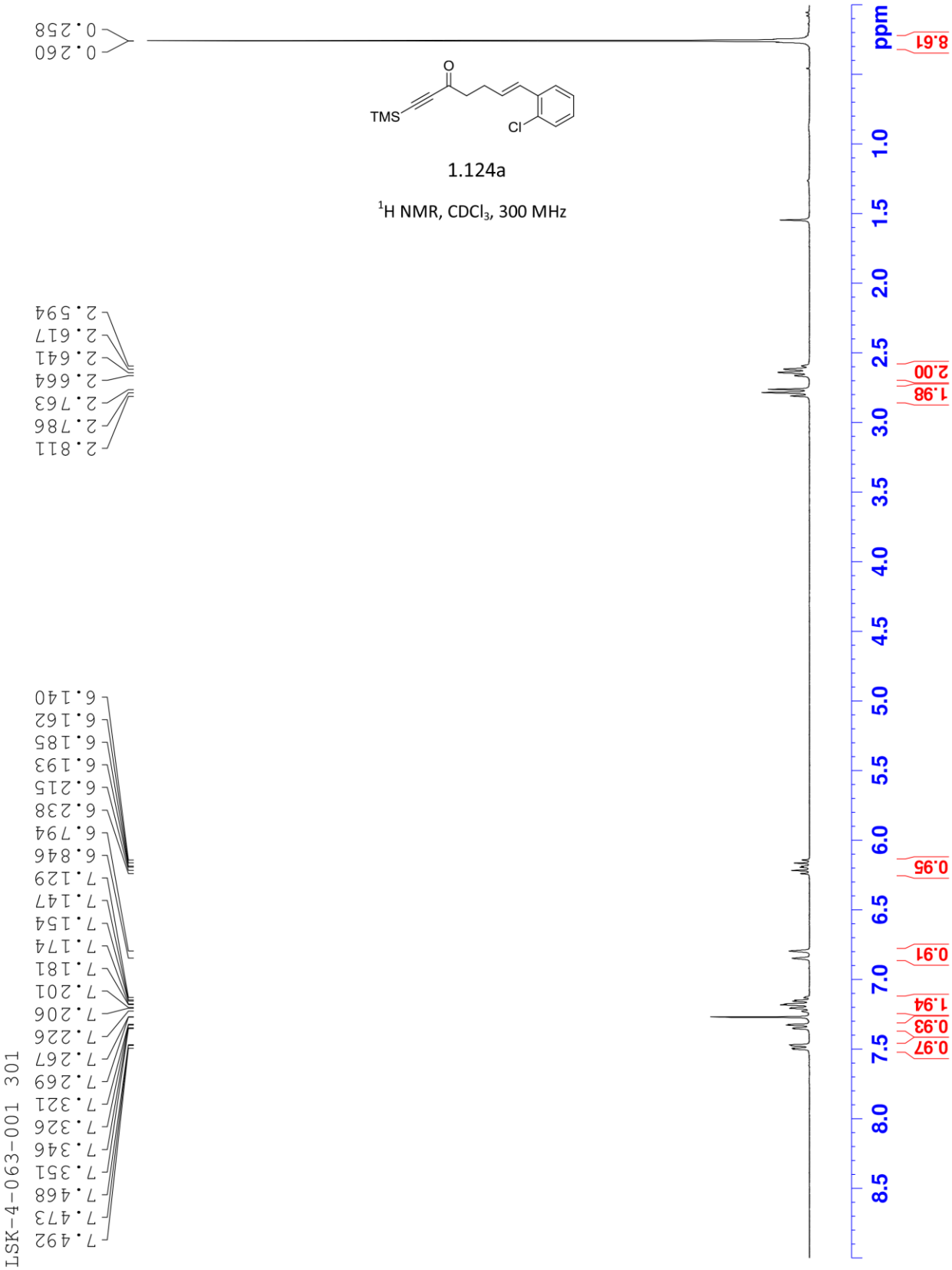
TMS
Cl
1.124a
^{1}H NMR, $CDCl_3$, 300 MHz
LSK-4-063-001 301
ppm

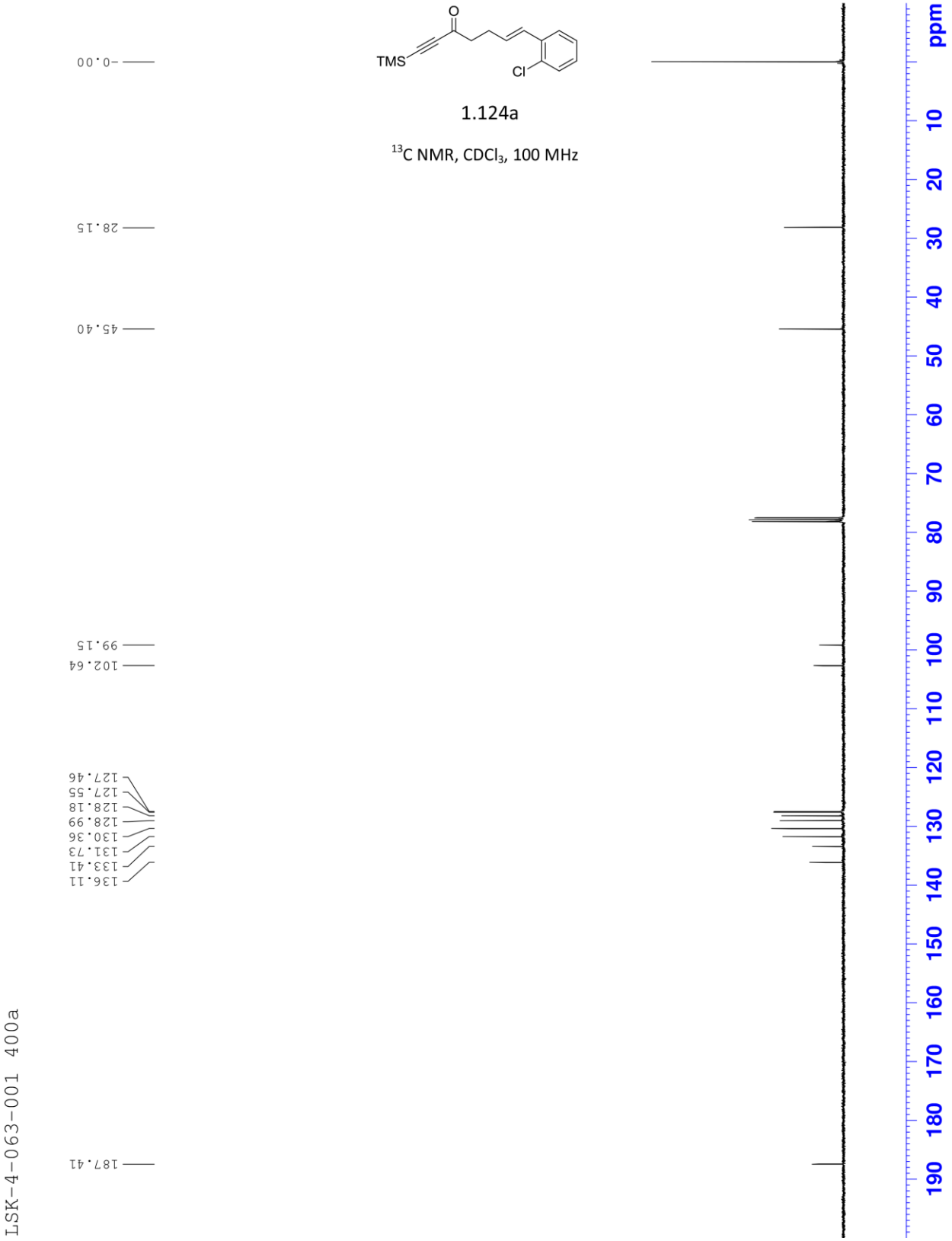
TMS
O
Cl
1.124a
^{13}C NMR, $CDCl_3$, 100 MHz
0.00
28.15
45.40
99.15
102.64
127.46
127.55
128.18
128.99
130.36
131.73
133.41
136.11
187.41
ppm
10
20
30
40
50
60
70
80
90
100
110
120
130
140
150
160
170
180
190
LSK-4-063-001 400a

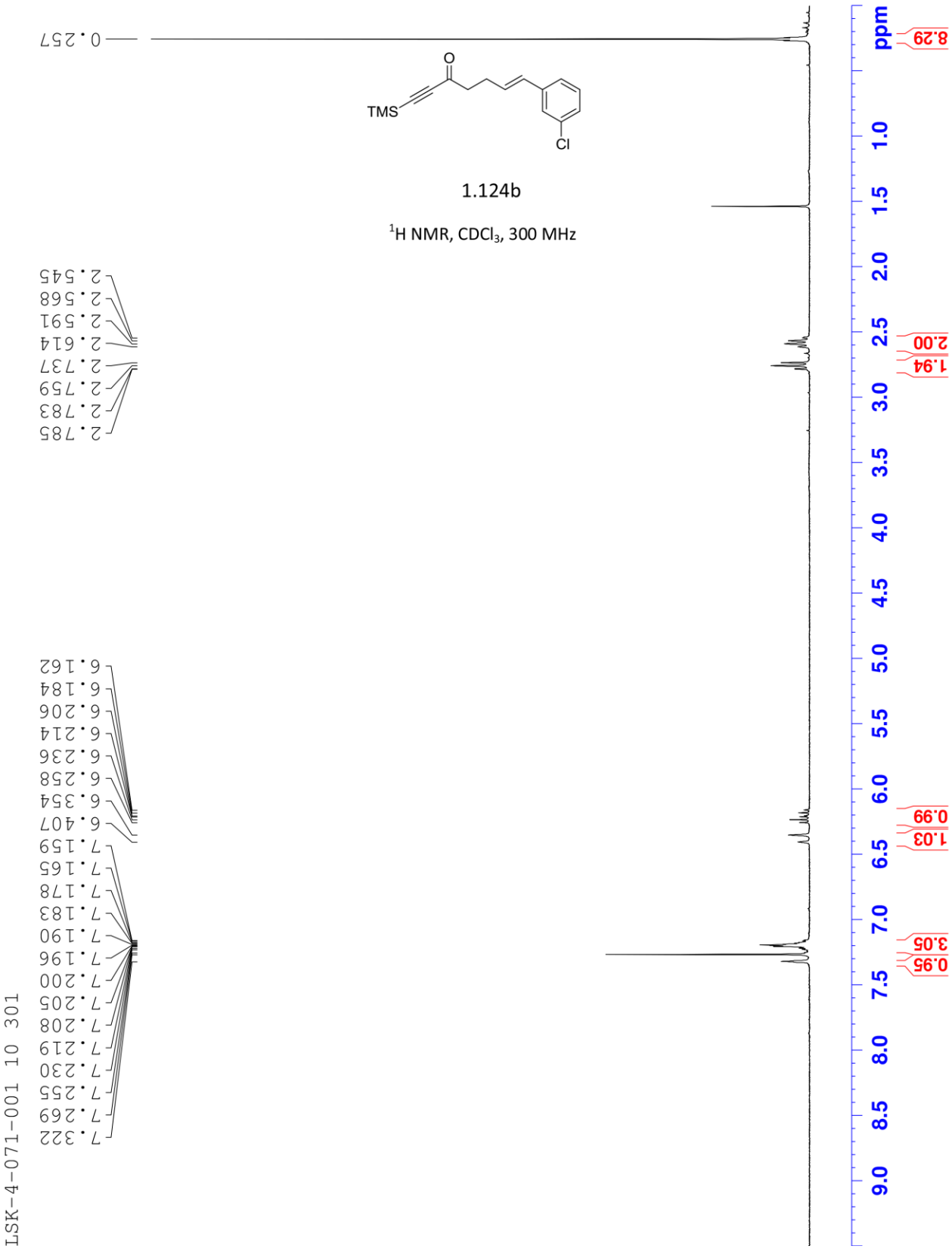
0.257
TMS
O
Cl
1.124b
^{1}H NMR, CDCl$_3$, 300 MHz
2.545
2.568
2.591
2.614
2.737
2.759
2.783
2.785
6.162
6.184
6.206
6.214
6.236
6.258
6.354
6.407
7.159
7.165
7.178
7.183
7.190
7.196
7.200
7.205
7.208
7.219
7.230
7.255
7.269
7.322
LSK-4-071-001 10 301
ppm
8.29
2.00
1.94
1.03
0.99
3.05
0.95

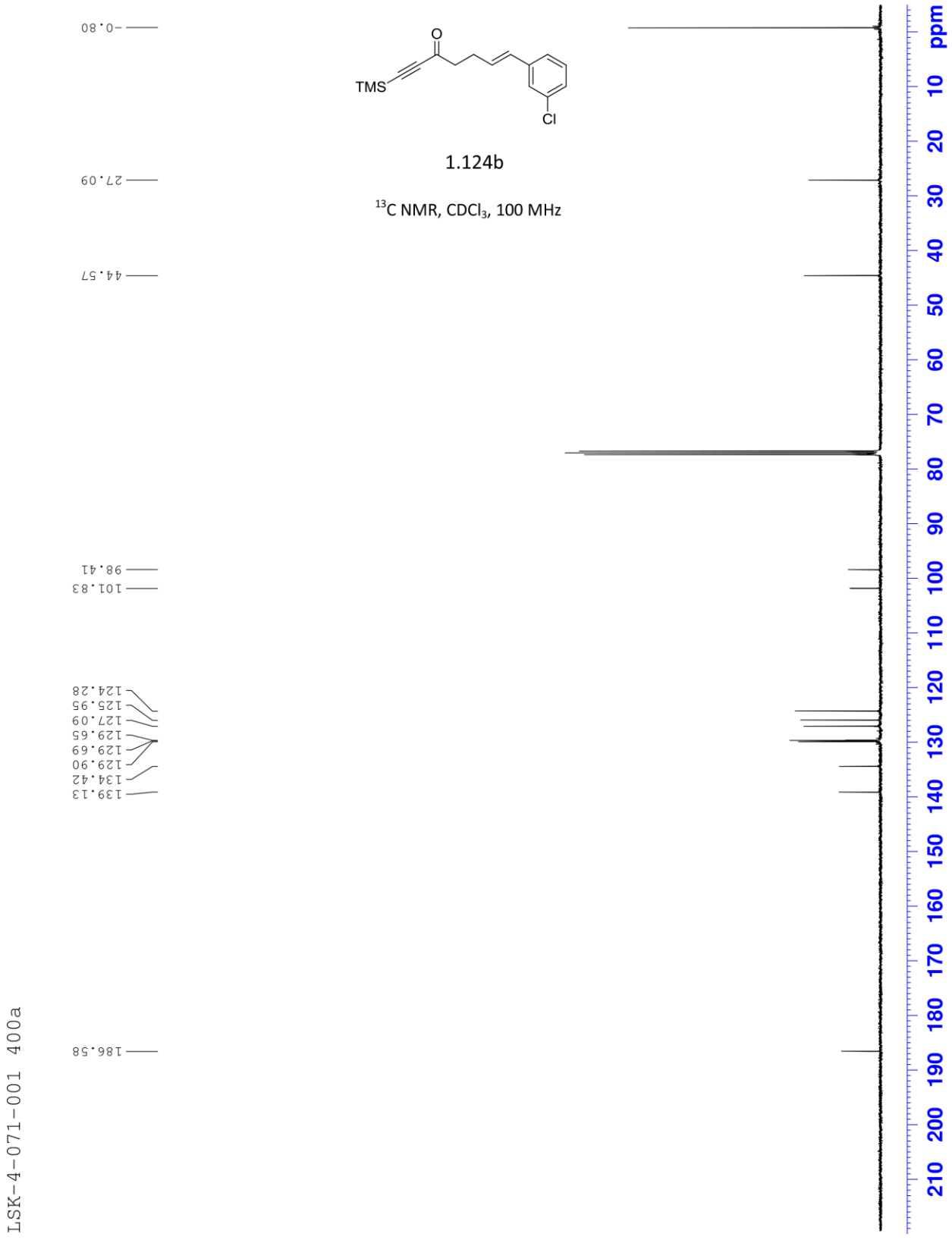
TMS
Cl
O
1.124b
^{13}C NMR, $CDCl_3$, 100 MHz
LSK-4-071-001 400a
-0.80
27.09
44.57
98.41
101.83
124.28
125.95
127.09
129.65
129.69
129.90
134.42
139.13
186.58
ppm

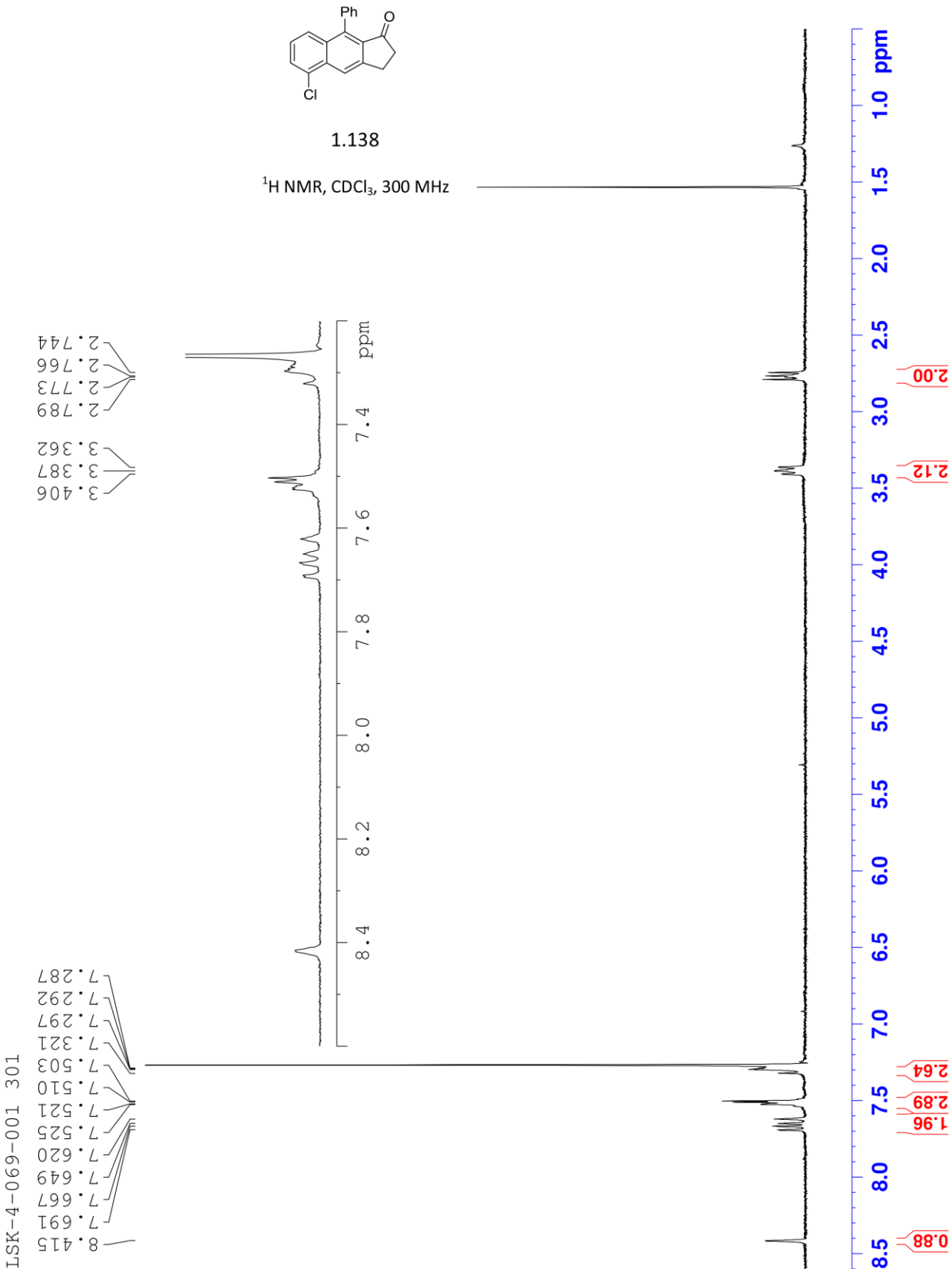
Ph
O
Cl
1.138
^{1}H NMR, $CDCl_3$, 300 MHz
LSK-4-069-001 301
8.415
7.691
7.667
7.649
7.620
7.525
7.521
7.510
7.503
7.321
7.297
7.292
7.287
3.406
3.387
3.362
2.789
2.773
2.766
2.744
ppm
8.4
8.2
8.0
7.8
7.6
7.4
ppm
8.5
8.0
7.5
7.0
6.5
6.0
5.5
5.0
4.5
4.0
3.5
3.0
2.5
2.0
1.5
1.0
0.88
1.96
2.89
2.64
2.12
2.00

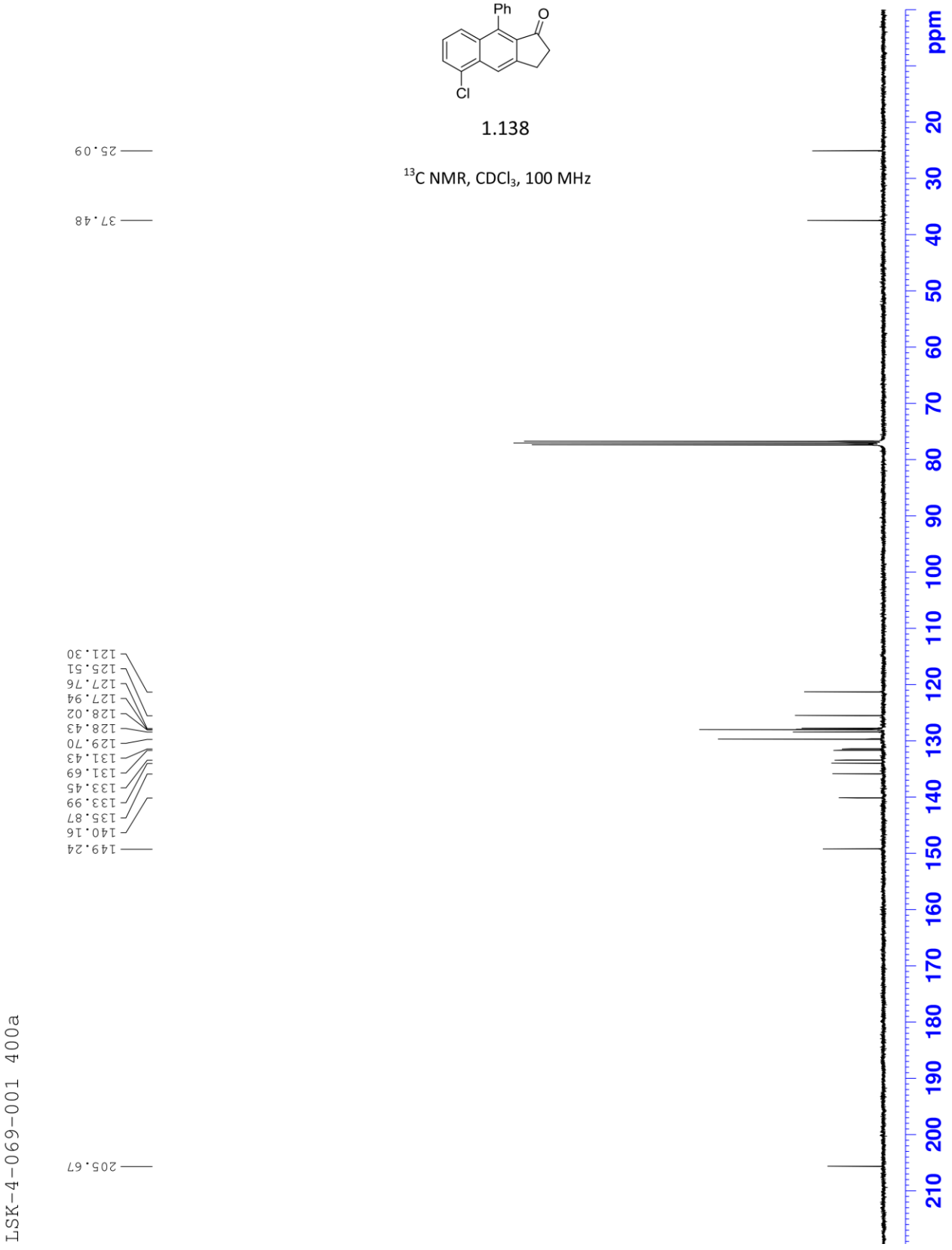
Ph
O
Cl
1.138
^{13}C NMR, $CDCl_3$, 100 MHz
25.09
37.48
121.30
125.51
127.76
127.94
128.02
128.43
129.70
131.43
131.69
133.45
133.99
135.87
140.16
149.24
205.67
LSK-4-069-001 400a
ppm
20
30
40
50
60
70
80
90
100
110
120
130
140
150
160
170
180
190
200
210

1.140

^{1}H NMR, C_6D_6, 400 MHz

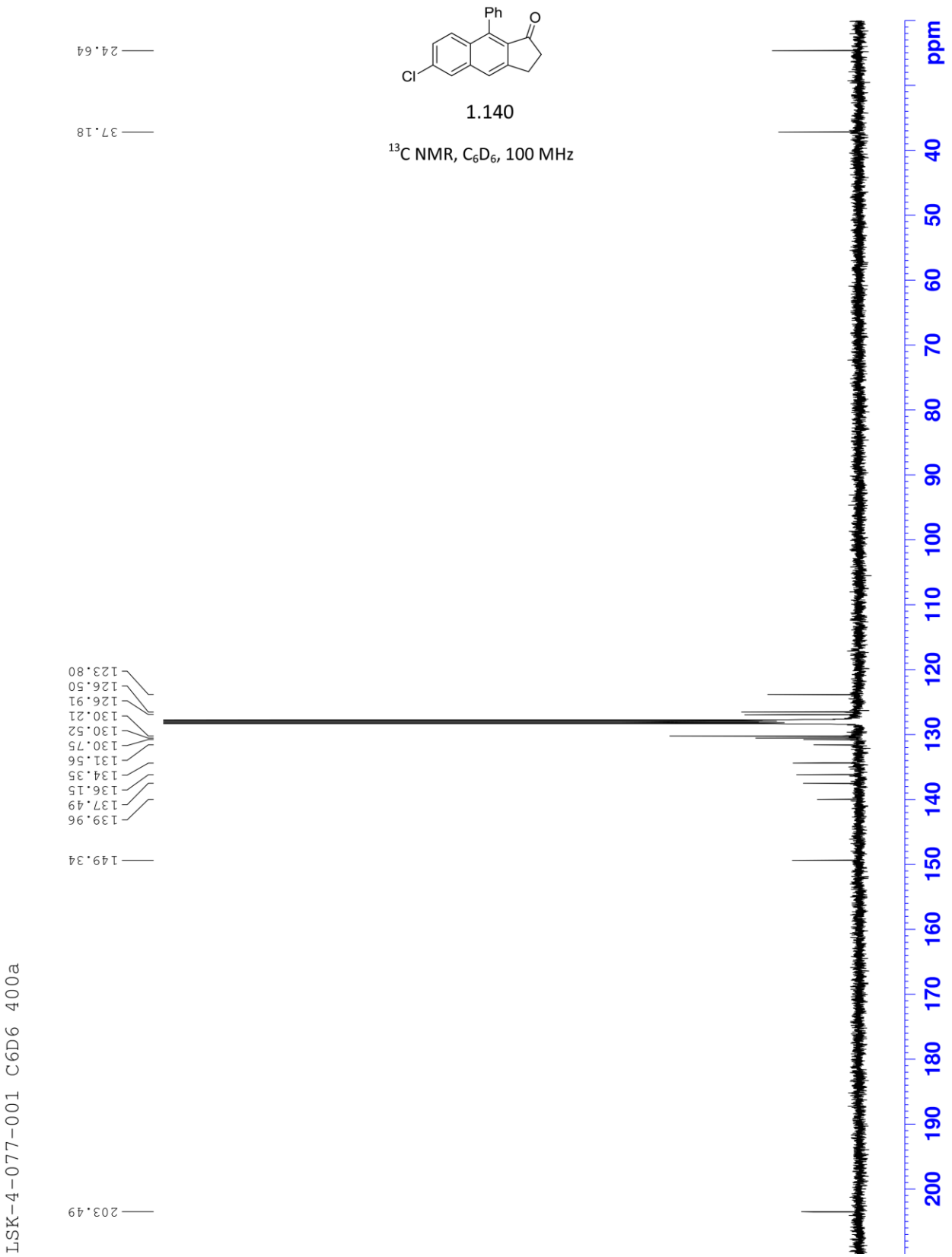
Ph
O
Cl
1.140
^{13}C NMR, C_6D_6, 100 MHz
24.64
37.18
123.80
126.50
126.91
130.21
130.52
130.75
131.56
134.35
136.15
137.49
139.96
149.34
203.49
ppm
40
50
60
70
80
90
100
110
120
130
140
150
160
170
180
190
200
LSK-4-077-001 C6D6 400a

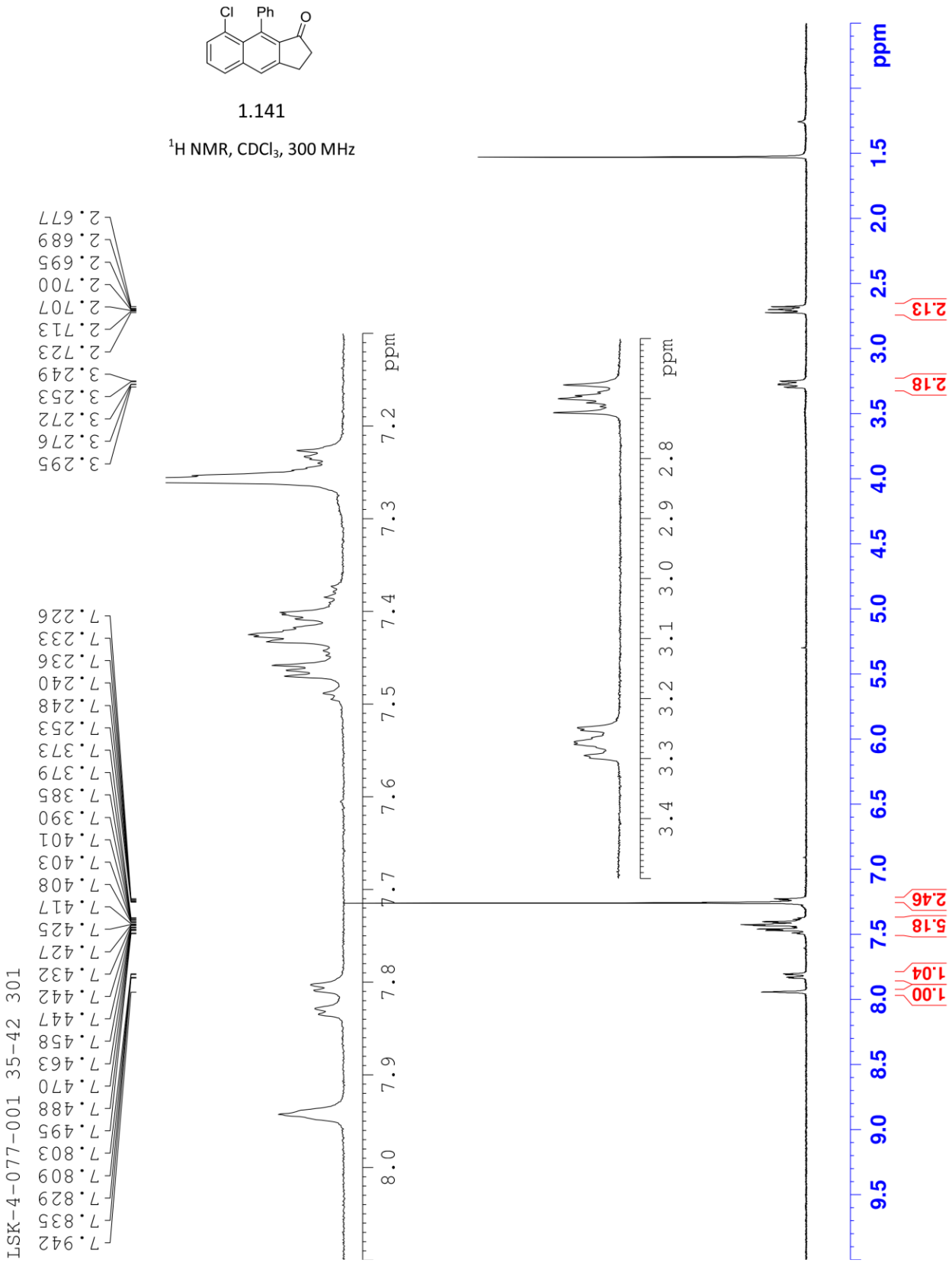
Cl
Ph
O
1.141
^{1}H NMR, CDCl$_3$, 300 MHz
LSK-4-077-001 35-42 301
ppm
2.13
2.18
2.46
5.18
1.00
1.04

1.141

^{13}C NMR, $CDCl_3$, 100 MHz

LSK-4-077-001 34-42 400a

1.142

^{1}H NMR, $CDCl_3$, 300 MHz

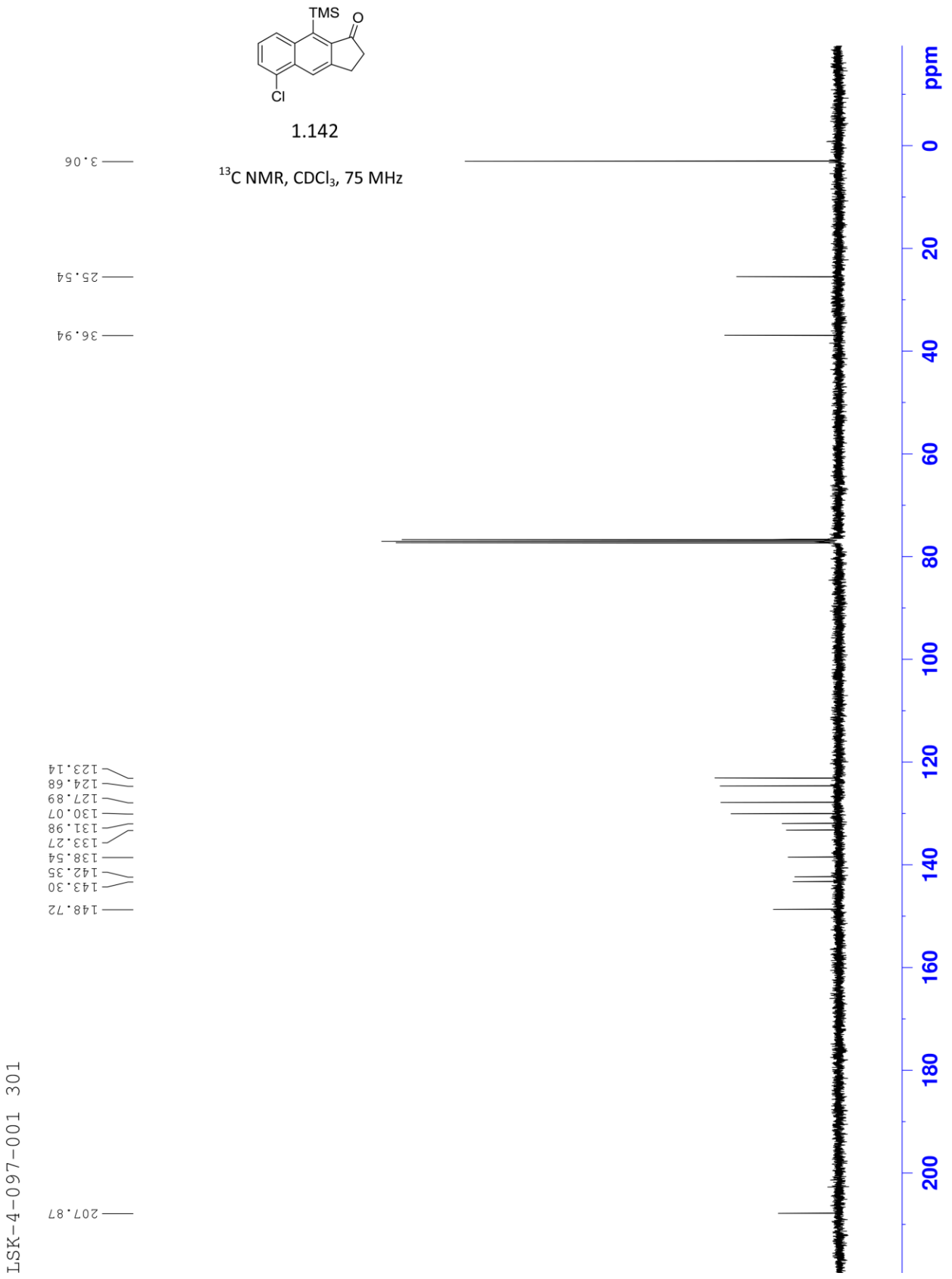
TMS
O
Cl
1.142
^{13}C NMR, $CDCl_3$, 75 MHz
3.06
25.54
36.94
123.14
124.68
127.89
130.07
131.98
133.27
138.54
142.35
143.30
148.72
207.87
LSK-4-097-001 301
ppm
0
20
40
60
80
100
120
140
160
180
200

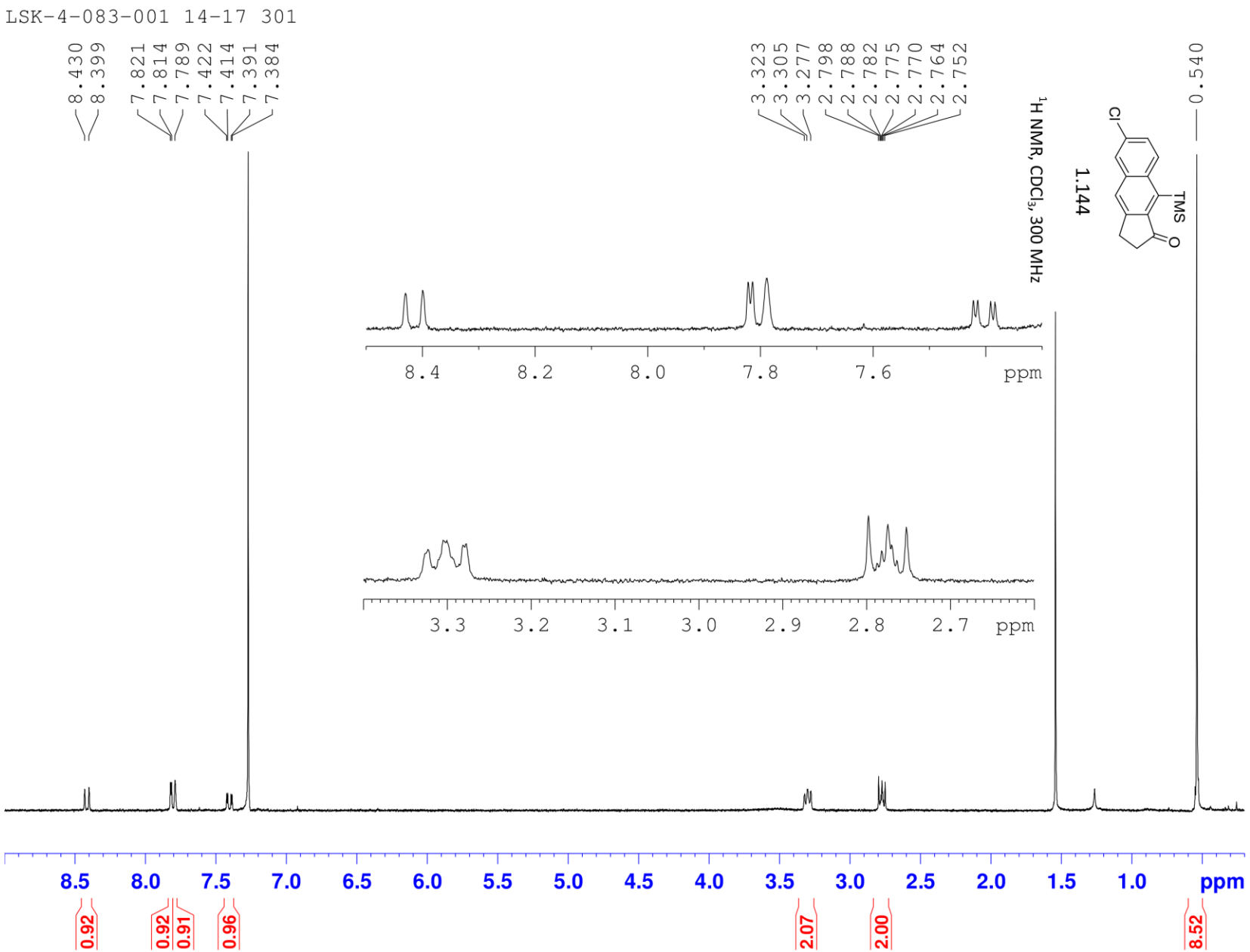
LSK-4-083-001 14-17 301
8.430
8.399
7.821
7.814
7.789
7.422
7.414
7.391
7.384
3.323
3.305
3.277
2.798
2.788
2.782
2.775
2.770
2.764
2.752
0.540
^{1}H NMR, CDCl$_3$, 300 MHz
1.144
Cl
TMS
O
8.4
8.2
8.0
7.8
7.6
ppm
3.3
3.2
3.1
3.0
2.9
2.8
2.7
ppm
8.5
8.0
7.5
7.0
6.5
6.0
5.5
5.0
4.5
4.0
3.5
3.0
2.5
2.0
1.5
1.0
ppm
0.92
0.92
0.91
0.96
2.07
2.00
8.52

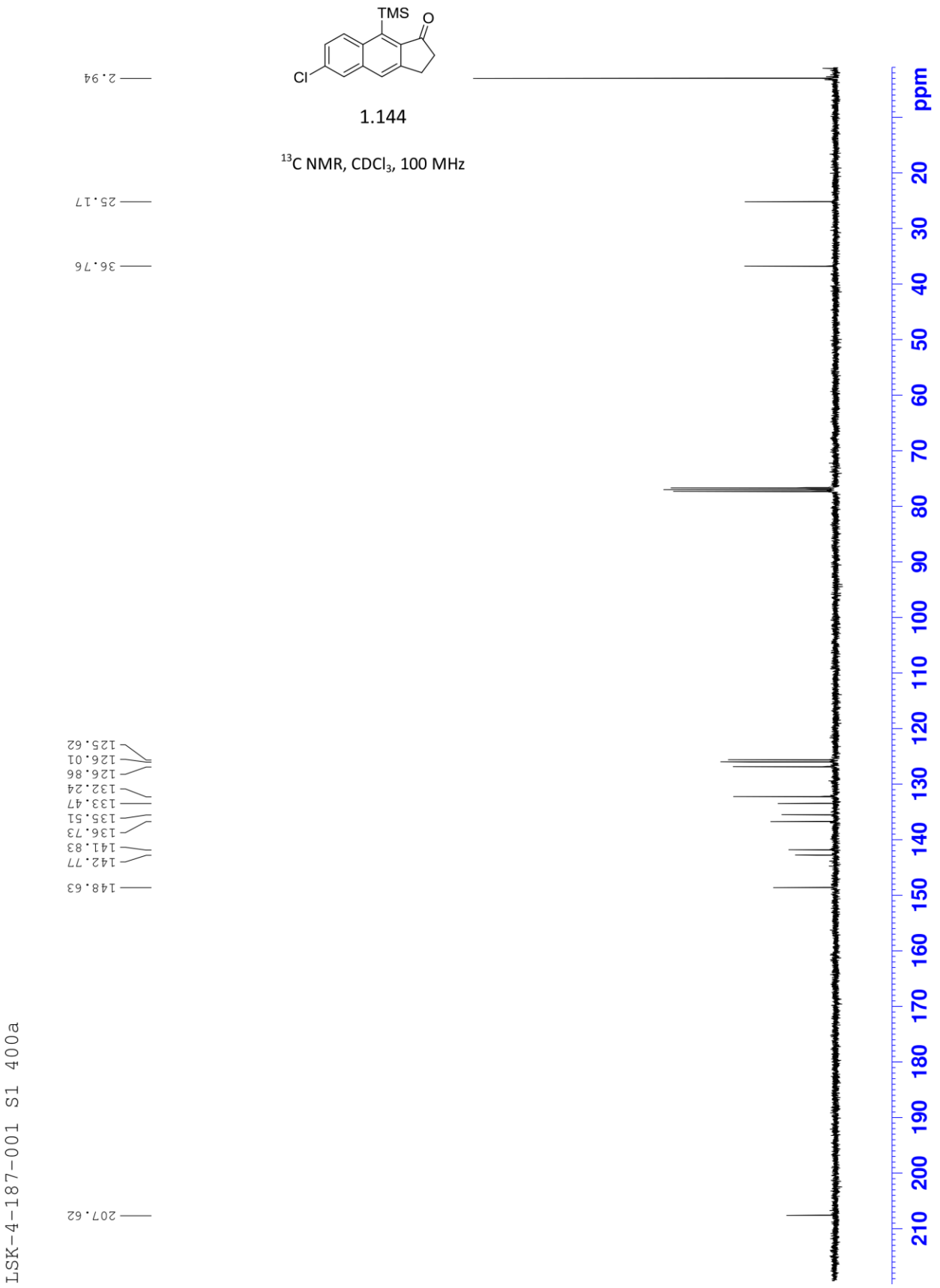
TMS
O
Cl
1.144
^{13}C NMR, $CDCl_3$, 100 MHz
2.94
25.17
36.76
125.62
126.01
126.86
132.24
133.47
135.51
136.73
141.83
142.77
148.63
207.62
ppm
LSK-4-187-001 S1 400a

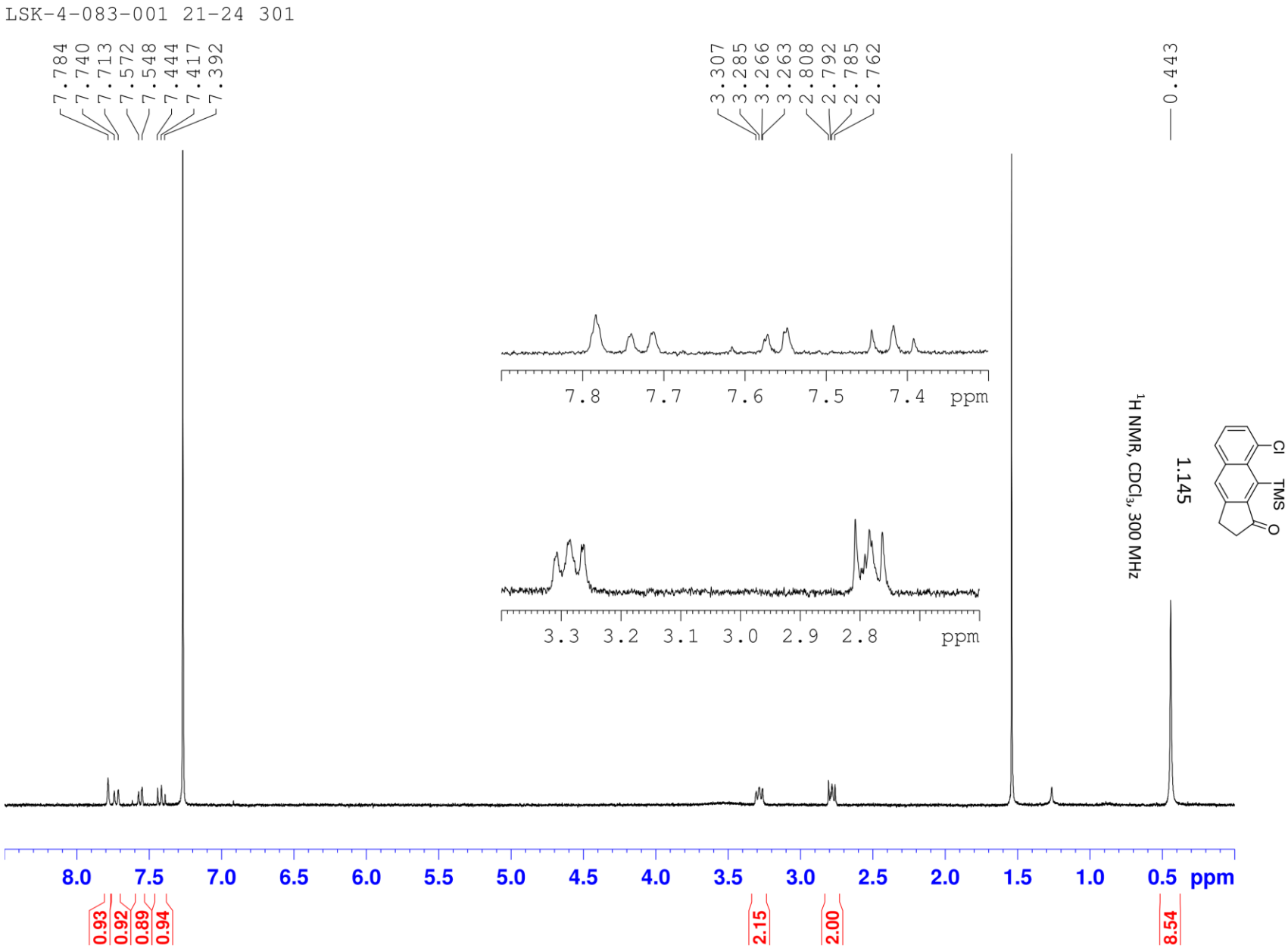
LSK-4-083-001 21-24 301
7.784
7.740
7.713
7.572
7.548
7.444
7.417
7.392
3.307
3.285
3.266
3.263
2.808
2.792
2.785
2.762
0.443
7.8 7.7 7.6 7.5 7.4 ppm
3.3 3.2 3.1 3.0 2.9 2.8 ppm
^{1}H NMR, $CDCl_3$, 300 MHz
1.145
Cl
TMS
O
8.0 7.5 7.0 6.5 6.0 5.5 5.0 4.5 4.0 3.5 3.0 2.5 2.0 1.5 1.0 0.5 ppm
0.93
0.92
0.89
0.94
2.15
2.00
8.54

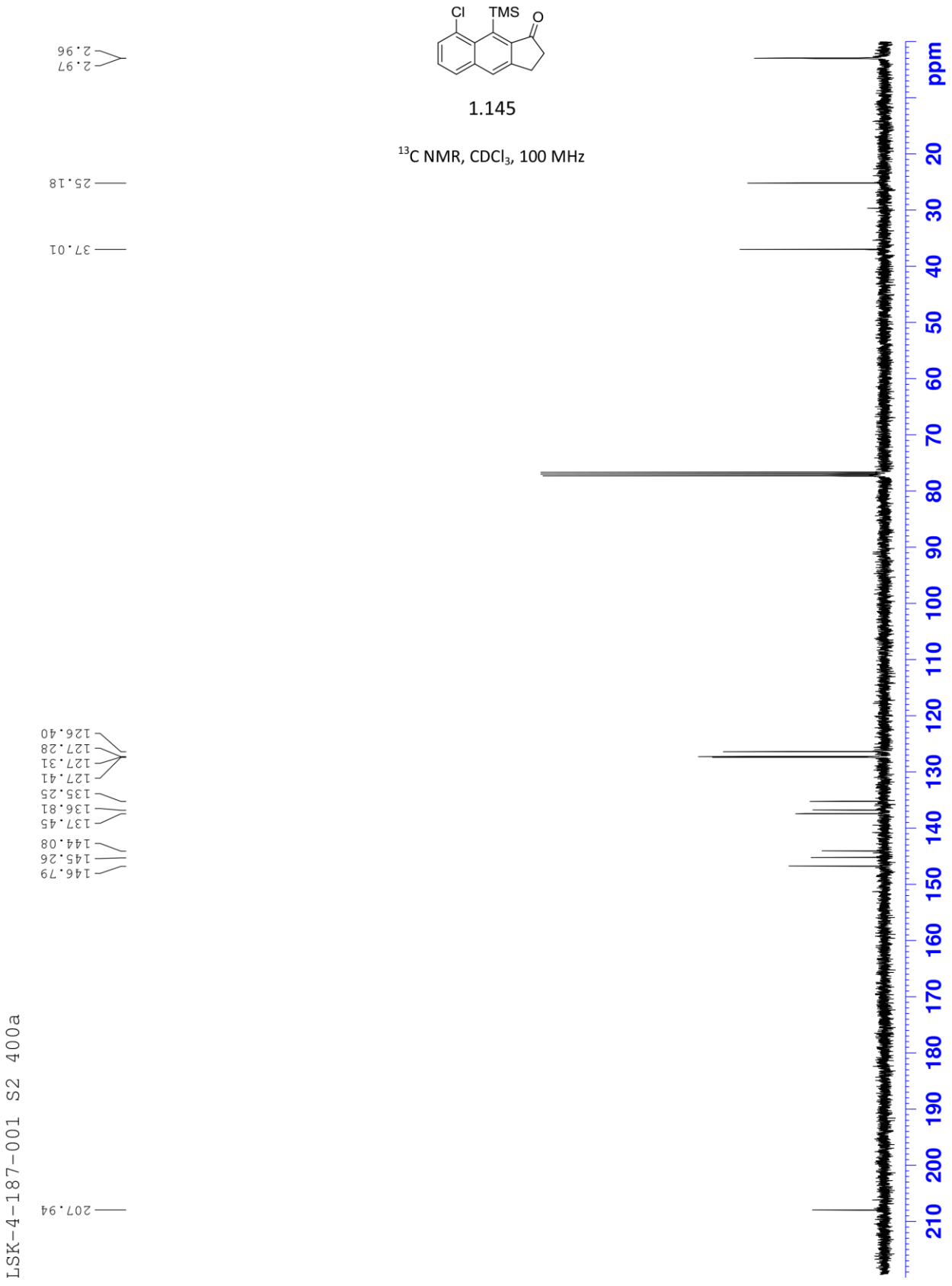
Cl
TMS
O
1.145
^{13}C NMR, $CDCl_3$, 100 MHz
2.96
2.97
25.18
37.01
126.40
127.28
127.31
127.41
135.25
136.81
137.45
144.08
145.26
146.79
207.94
LSK-4-187-001 S2 400a
ppm
20
30
40
50
60
70
80
90
100
110
120
130
140
150
160
170
180
190
200
210

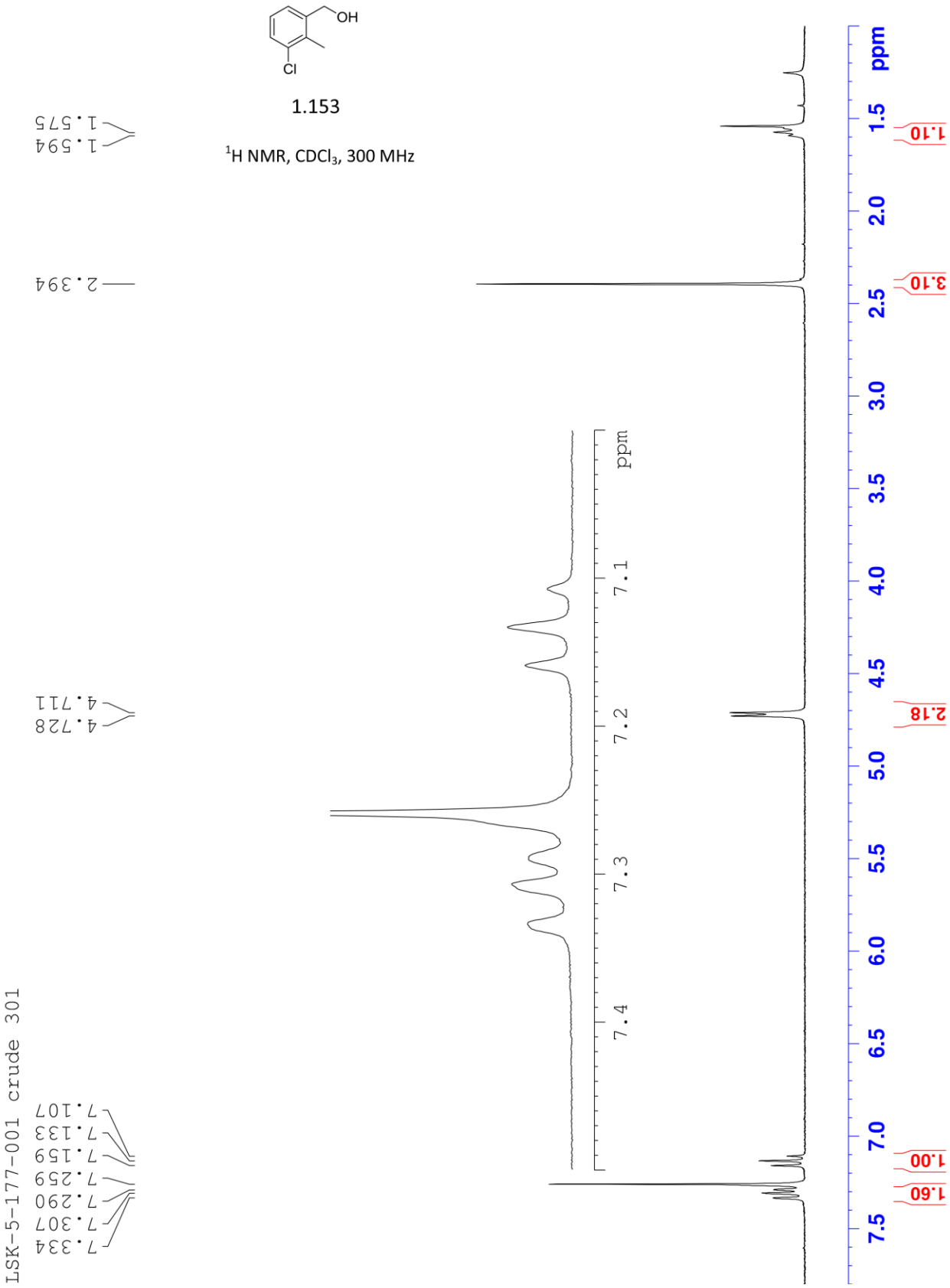
OH
Cl
1.153
^{1}H NMR, CDCl$_3$, 300 MHz
LSK-5-177-001 crude 301
7.334
7.307
7.290
7.259
7.159
7.133
7.107
4.728
4.711
2.394
1.594
1.575
ppm
7.4
7.3
7.2
7.1
ppm
7.5
7.0
6.5
6.0
5.5
5.0
4.5
4.0
3.5
3.0
2.5
2.0
1.5
1.60
1.00
2.18
3.10
1.10

1.154

^{1}H NMR, $CDCl_3$, 300 MHz

LSK-5-189-001 crude 301

10.279
2.718
7.736
7.732
7.710
7.707
7.611
7.608
7.585
7.581
7.334
7.308
7.260
7.736
7.732
7.710
7.707
7.611
7.608
7.585
7.581
7.334
7.308
7.260
7.9 7.8 7.7 7.6 7.5 7.4 7.3 7.2 ppm
ppm
1 2 3 4 5 6 7 8 9 10
1.00
2.91
0.96
0.96
1.00

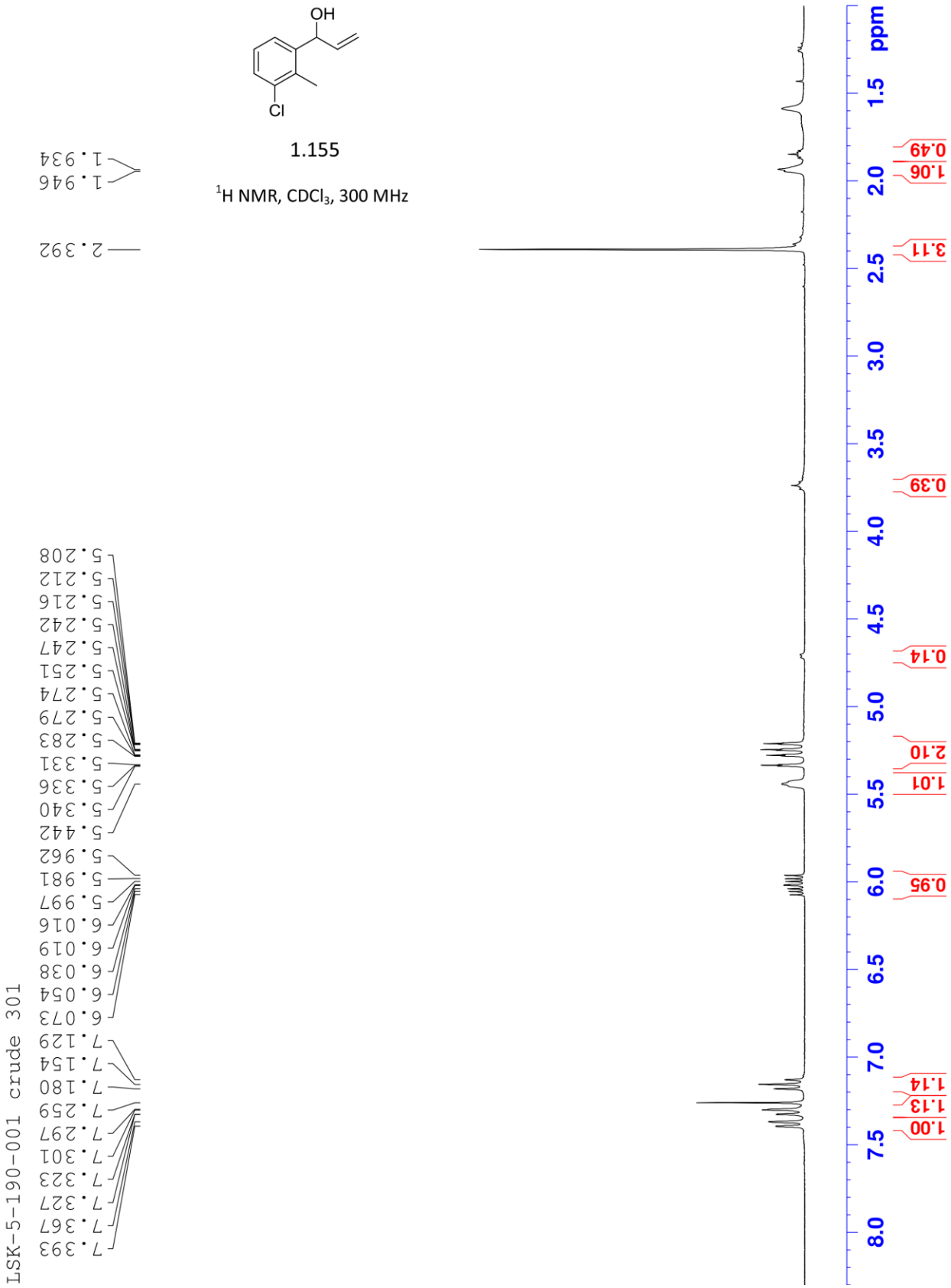
OH
Cl
1.155
^{1}H NMR, CDCl$_3$, 300 MHz
LSK-5-190-001 crude 301
7.393
7.367
7.327
7.323
7.301
7.297
7.259
7.180
7.154
7.129
6.073
6.054
6.038
6.019
6.016
5.997
5.981
5.962
5.442
5.340
5.336
5.331
5.283
5.279
5.274
5.251
5.247
5.242
5.216
5.212
5.208
2.392
1.946
1.934
ppm
0.49
1.06
3.11
0.39
0.14
2.10
1.01
0.95
1.14
1.13
1.00

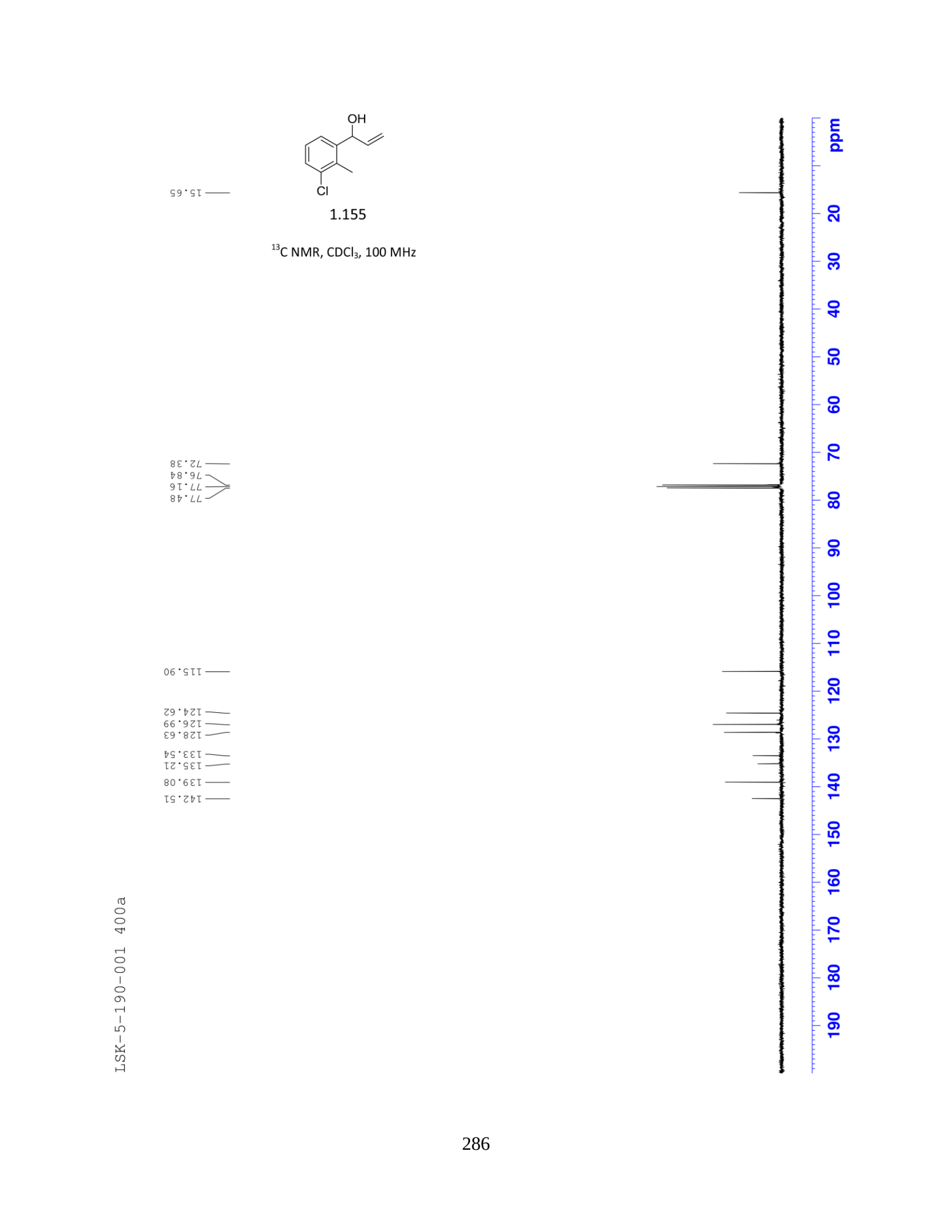
OH
Cl
1.155
^{13}C NMR, $CDCl_3$, 100 MHz
15.65
72.38
76.84
77.16
77.48
115.90
124.62
126.99
128.63
133.54
135.21
139.08
142.51
ppm
LSK-5-190-001 400a

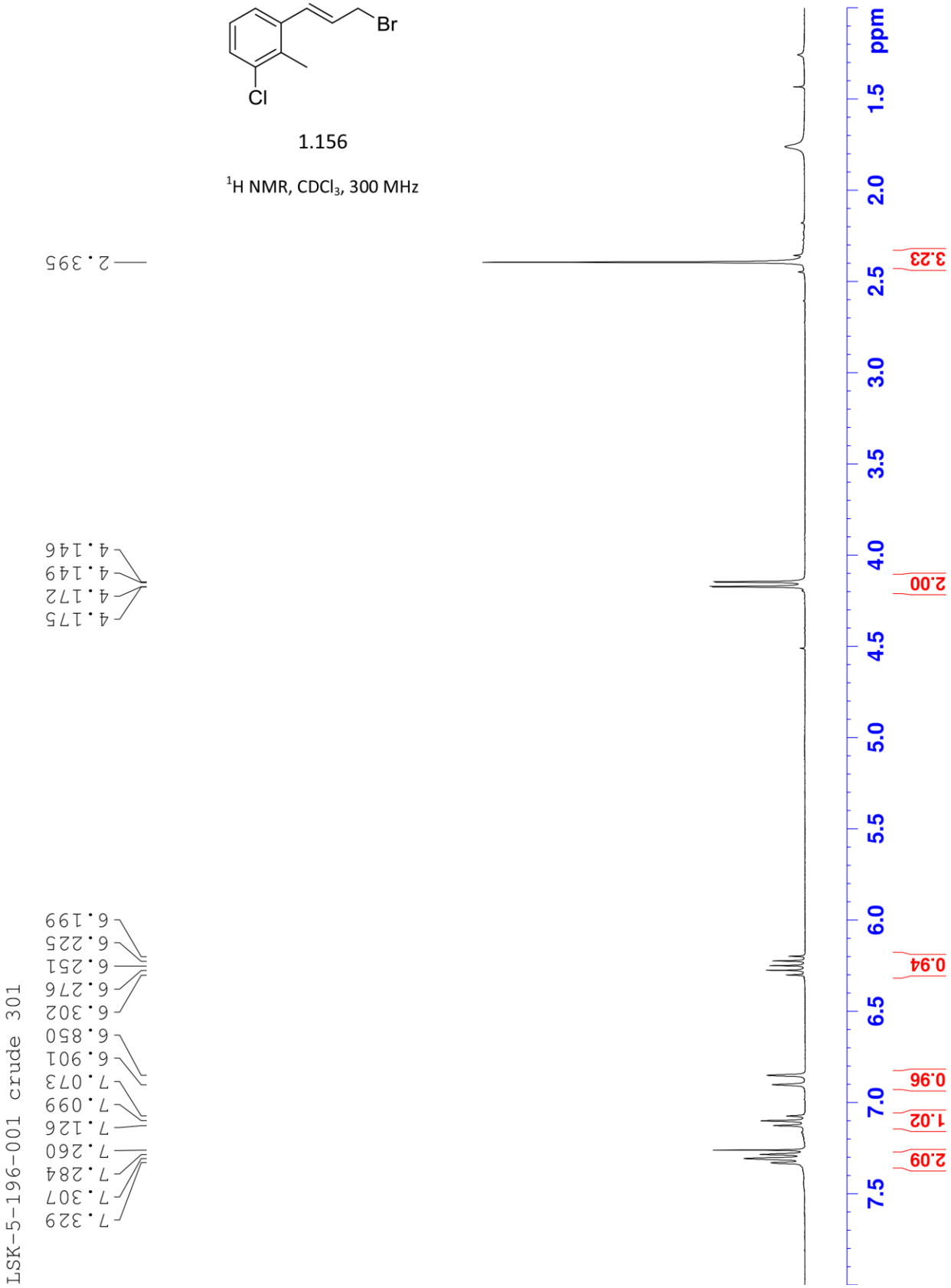
Br
Cl
1.156
^{1}H NMR, $CDCl_3$, 300 MHz
LSK-5-196-001 crude 301
7.329
7.307
7.284
7.260
7.126
7.099
7.073
6.901
6.850
6.302
6.276
6.251
6.225
6.199
4.175
4.172
4.149
4.146
2.395
ppm
7.5
7.0
6.5
6.0
5.5
5.0
4.5
4.0
3.5
3.0
2.5
2.0
1.5
2.09
1.02
0.96
0.94
2.00
3.23

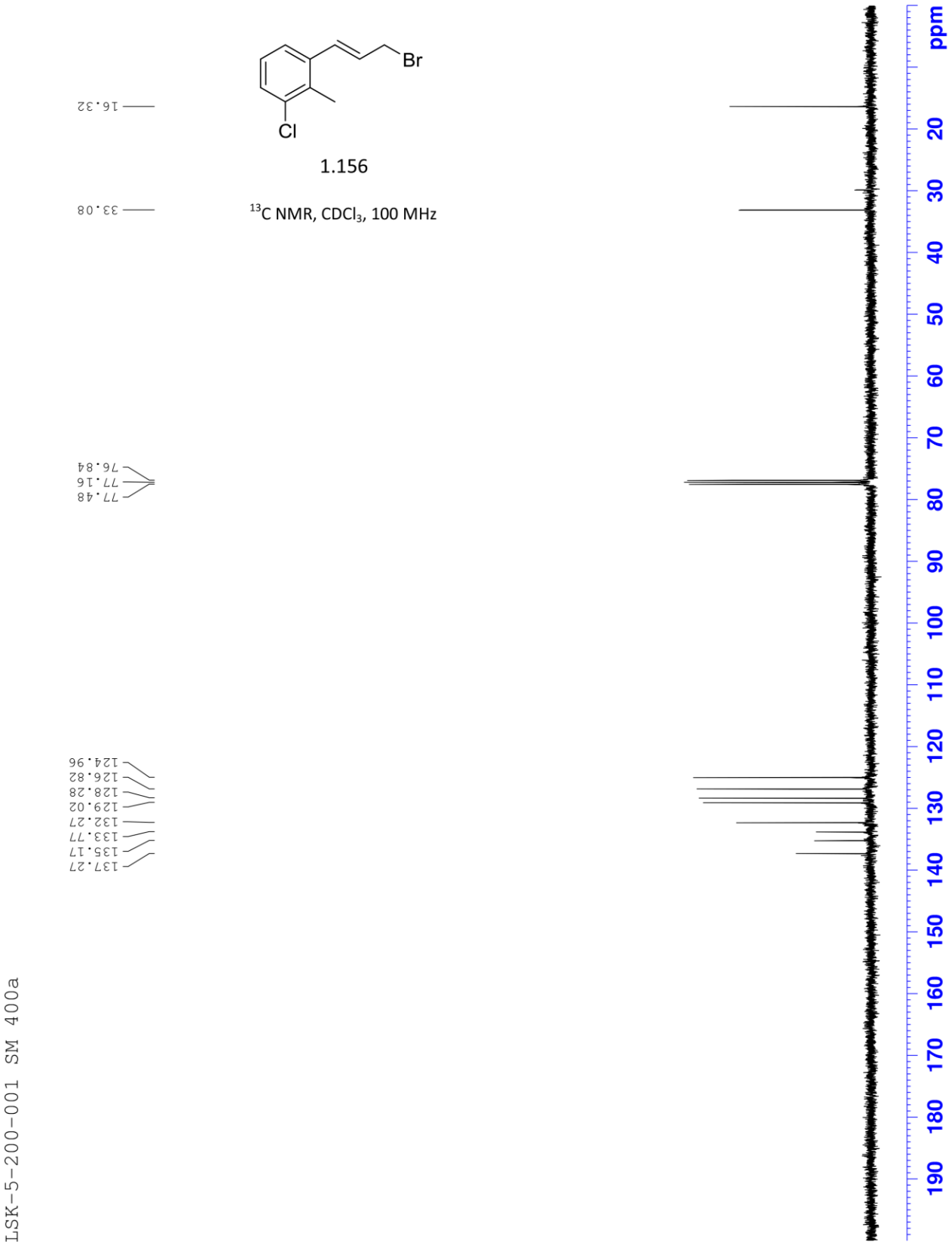
Br
Cl
1.156
^{13}C NMR, $CDCl_3$, 100 MHz
16.32
33.08
76.84
77.16
77.48
124.96
126.82
128.28
129.02
132.27
133.77
135.17
137.27
ppm
20
30
40
50
60
70
80
90
100
110
120
130
140
150
160
170
180
190
LSK-5-200-001 SM 400a

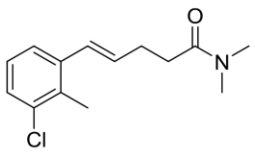

1.157

^{1}H NMR, $CDCl_3$, 300 MHz

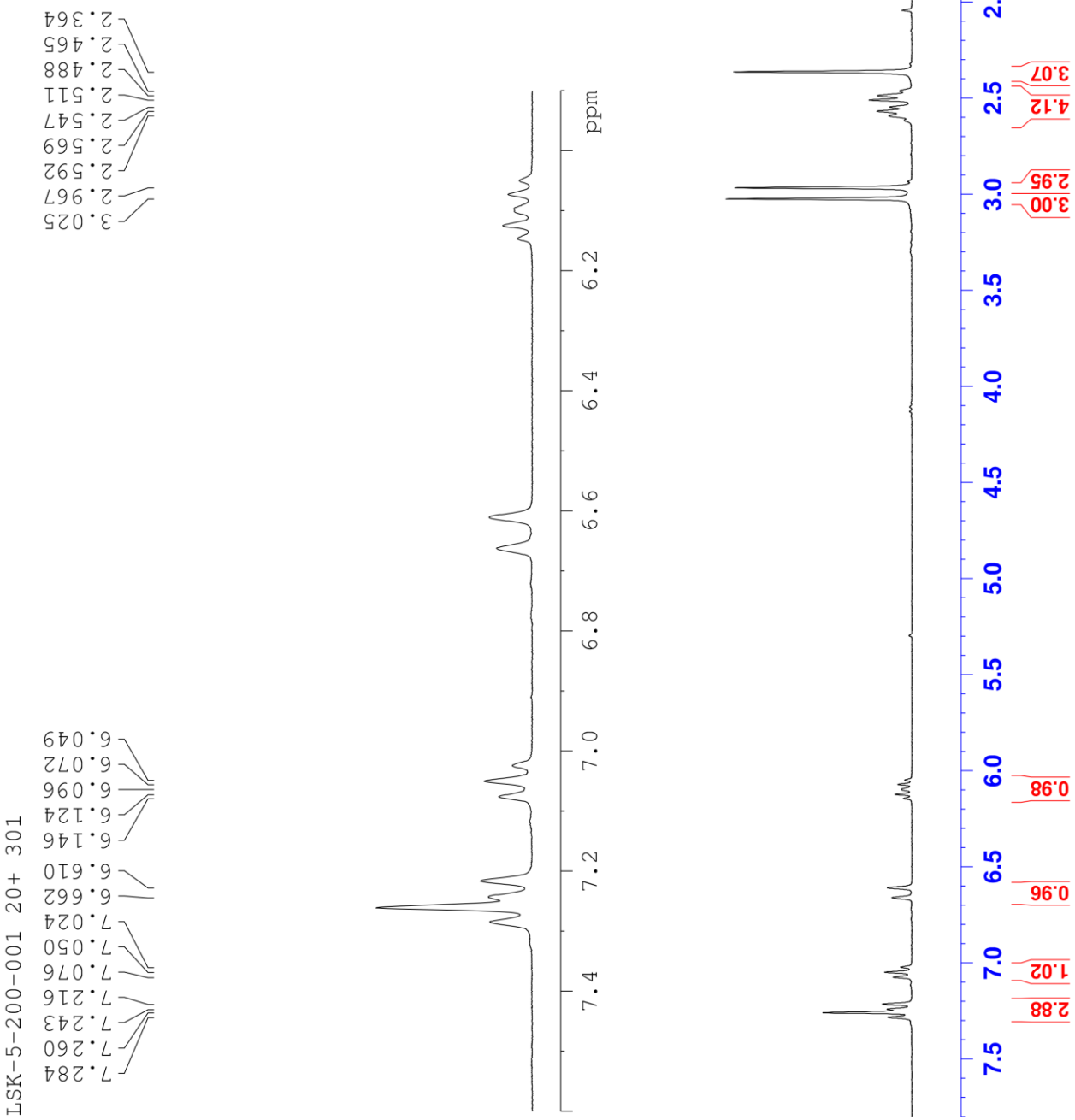

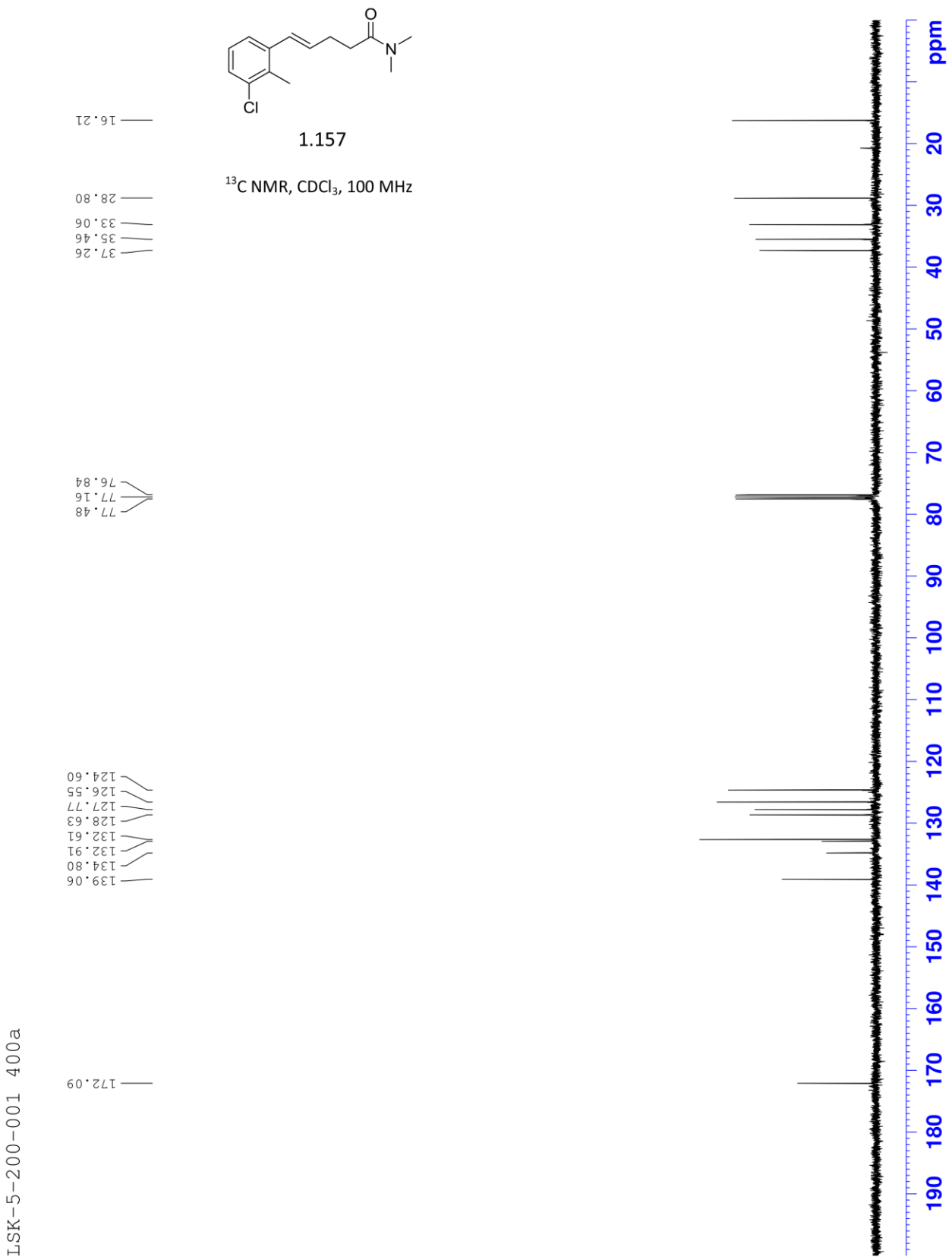
O
N
Cl
1.157
^{13}C NMR, $CDCl_3$, 100 MHz
16.21
28.80
33.06
35.46
37.26
76.84
77.16
77.48
124.60
126.55
127.77
128.63
132.61
132.91
134.80
139.06
172.09
LSK-5-200-001 400a
ppm

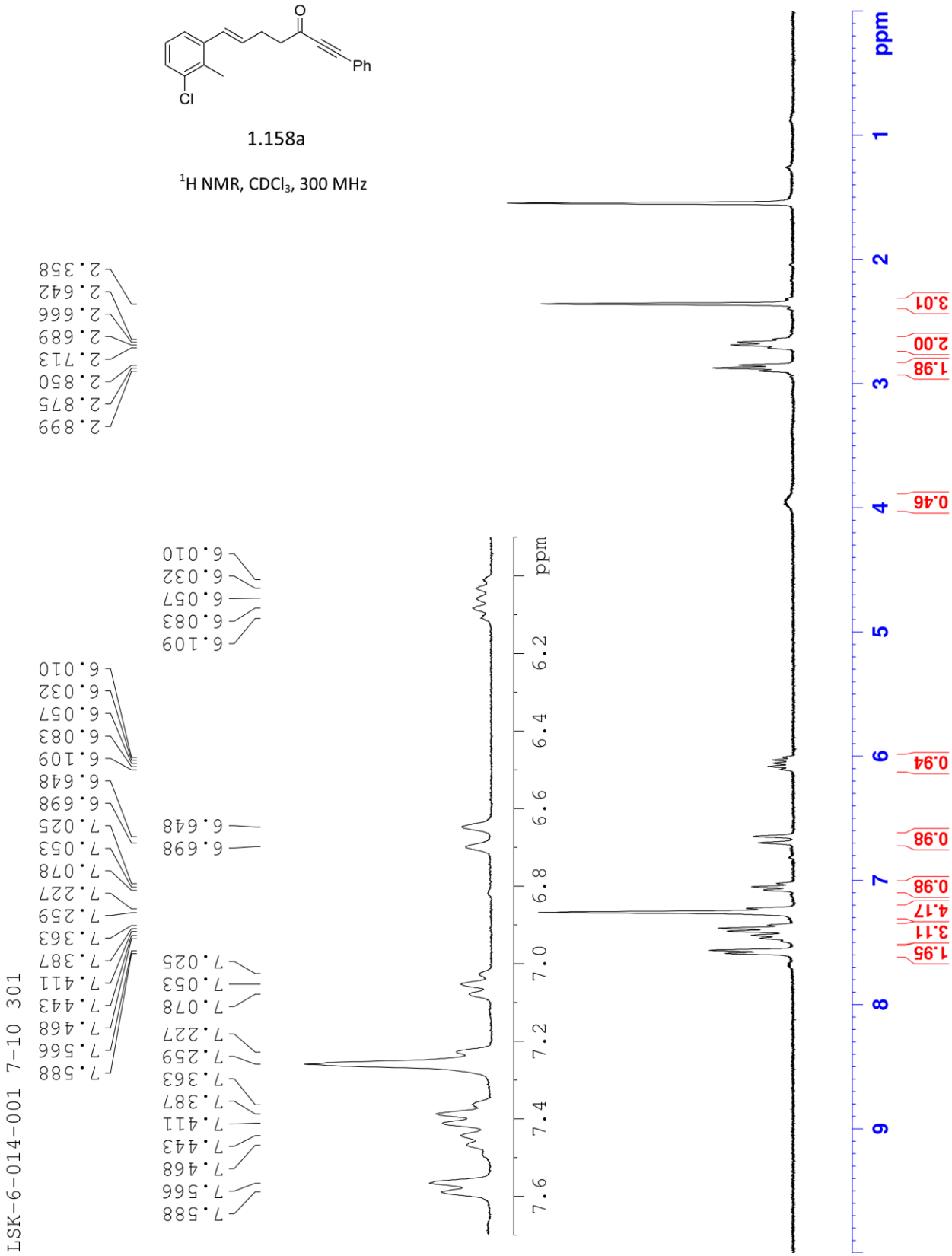
O
Ph
Cl
1.158a
^{1}H NMR, CDCl$_3$, 300 MHz
LSK-6-014-001 7-10 301
ppm
3.01
2.00
1.98
0.46
0.94
0.98
0.98
4.17
3.11
1.95

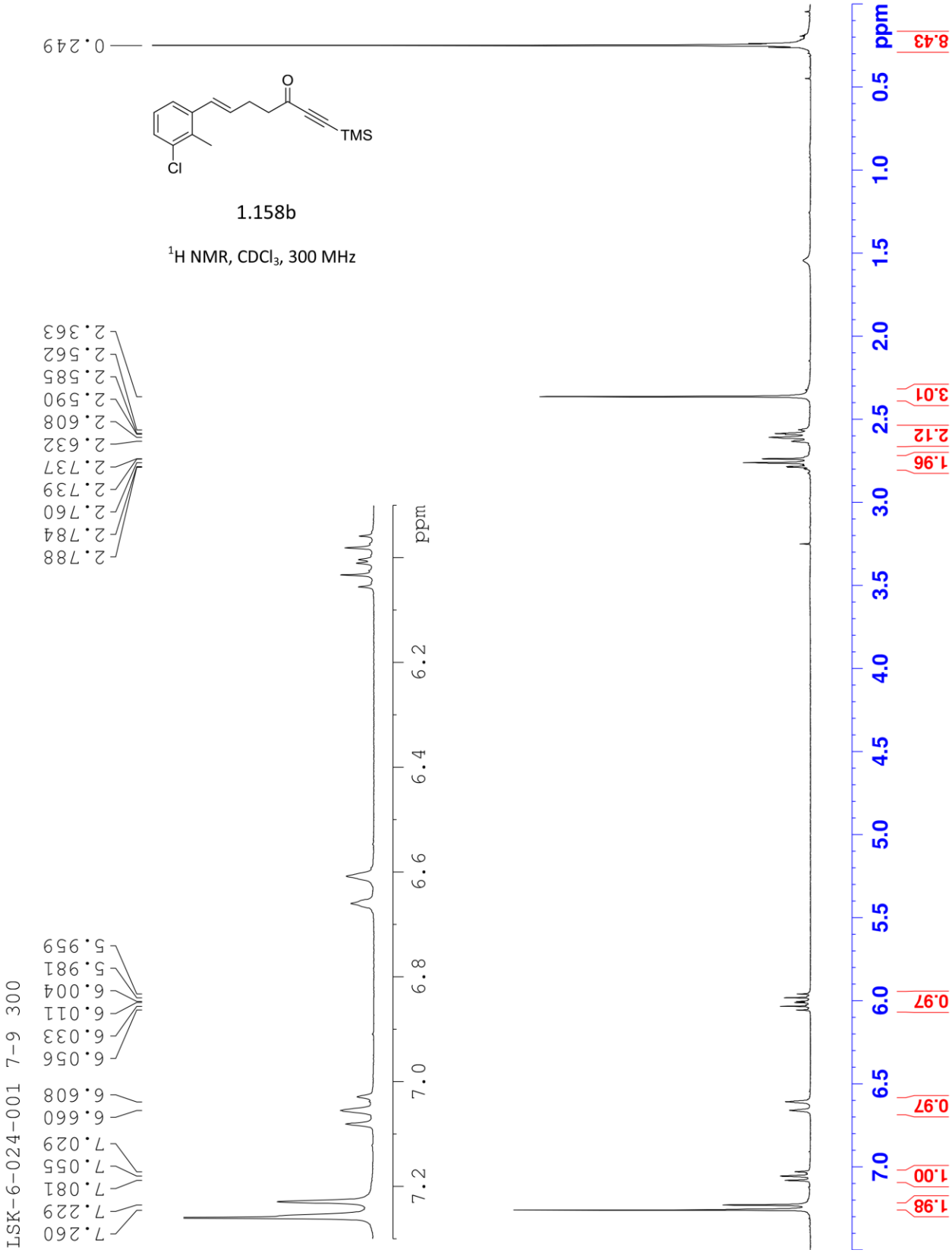
0.249
O
TMS
Cl
1.158b
^{1}H NMR, $CDCl_3$, 300 MHz
2.363
2.562
2.585
2.590
2.609
2.632
2.737
2.739
2.760
2.784
2.788
6.056
6.033
6.011
6.004
5.981
5.959
7.260
7.229
7.081
7.055
7.029
6.660
6.608
LSK-6-024-001 7-9 300
ppm
7.2
7.0
6.8
6.6
6.4
6.2
ppm
8.43
3.01
2.12
1.96
0.97
0.97
1.00
1.98

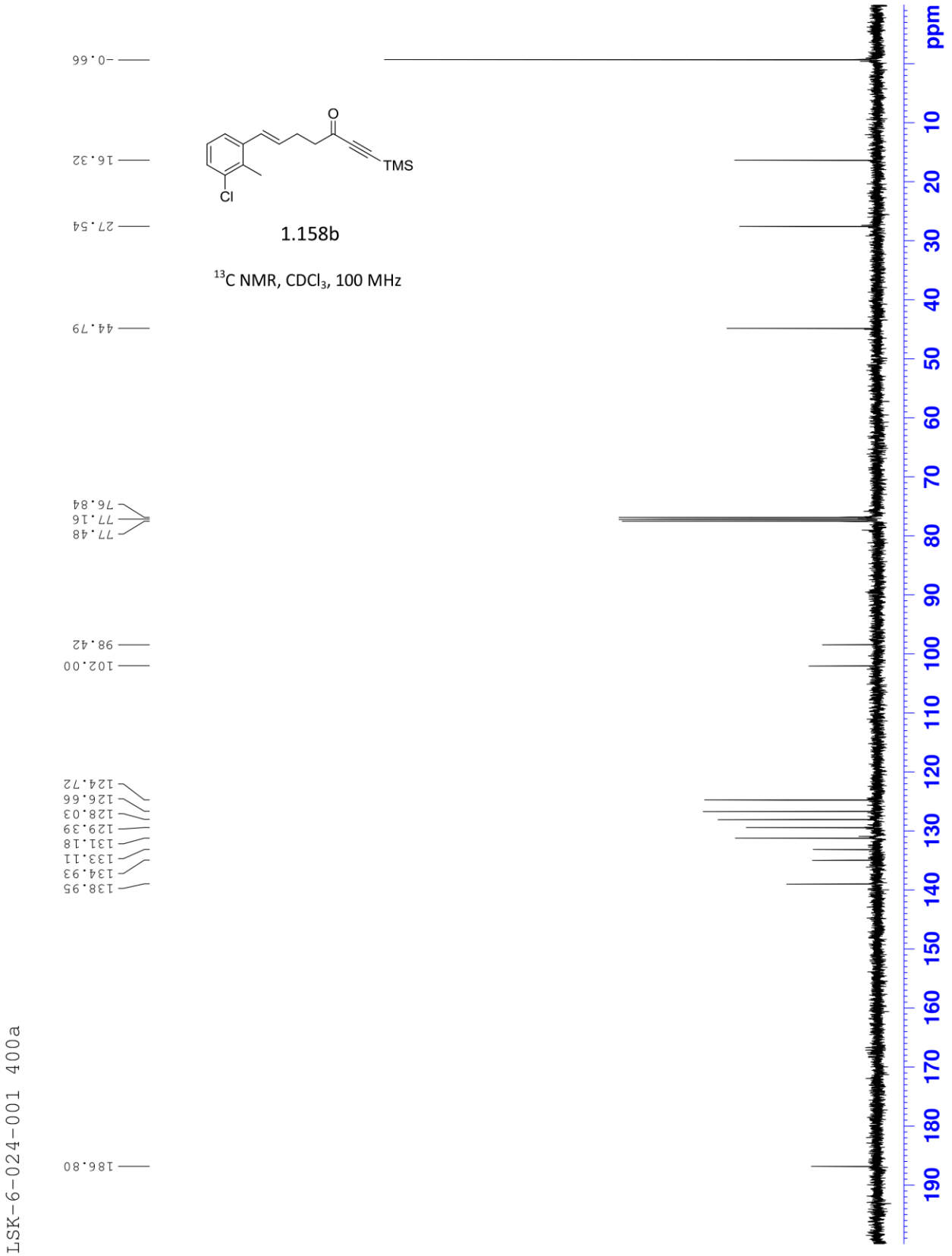
O
TMS
Cl
1.158b
^{13}C NMR, $CDCl_3$, 100 MHz
LSK-6-024-001 400a
ppm

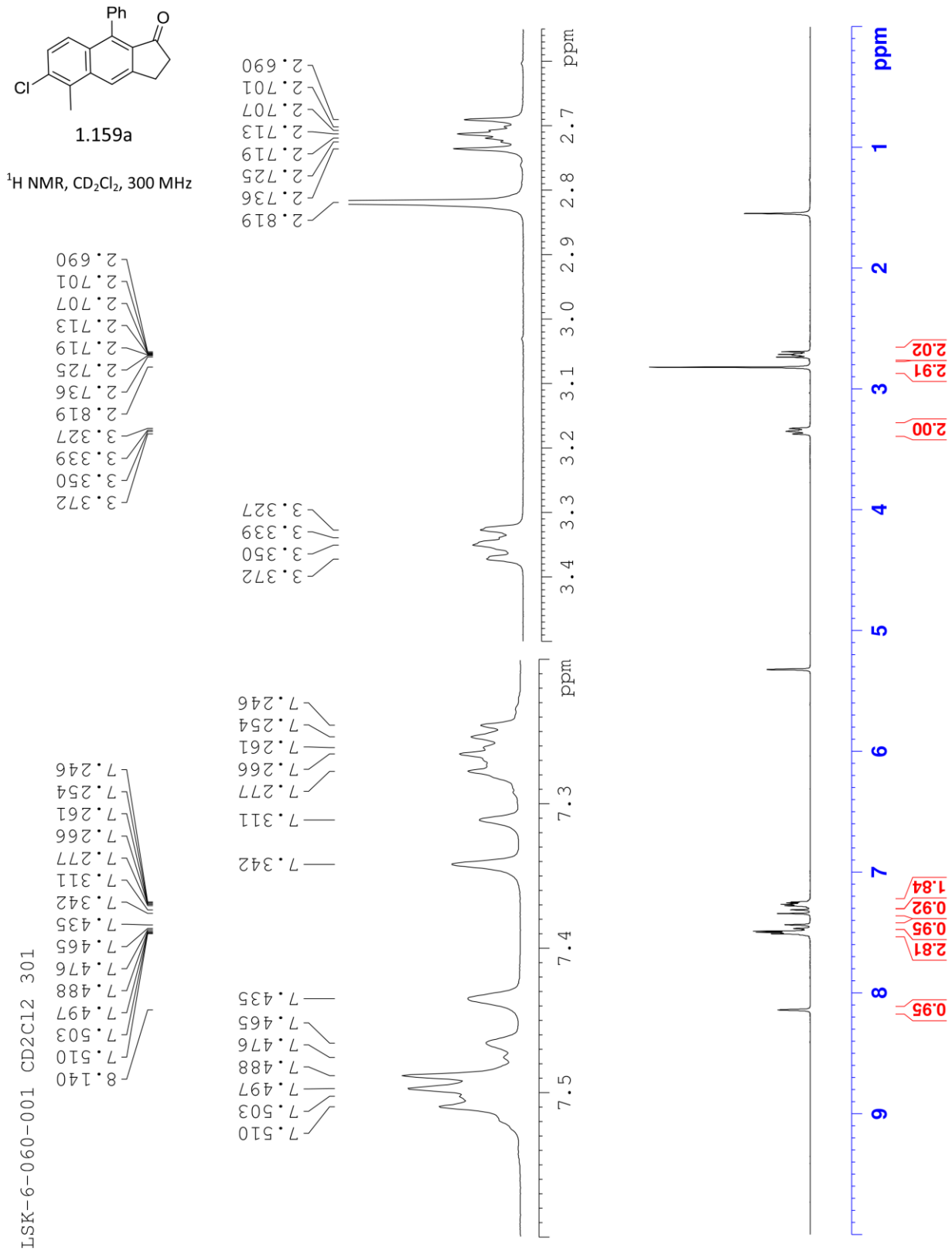
Ph
O
Cl
1.159a
^{1}H NMR, CD_2Cl_2, 300 MHz
LSK-6-060-001 CD2C12 301
ppm
2.81
0.95
0.92
0.95
1.84
2.00
2.91
2.02

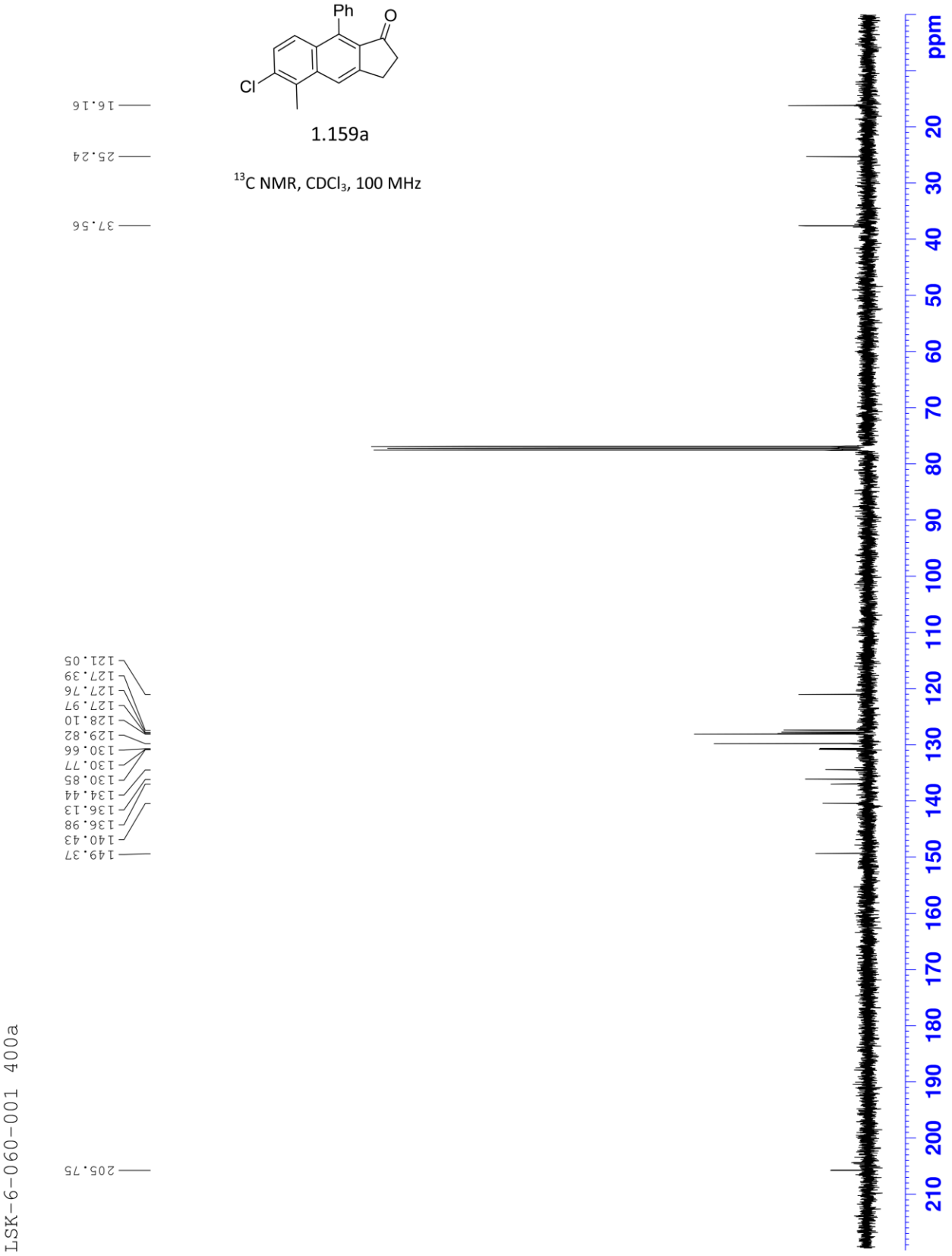
Ph
O
Cl
1.159a
^{13}C NMR, $CDCl_3$, 100 MHz
16.16
25.24
37.56
121.05
127.39
127.76
127.97
128.10
129.82
130.66
130.77
130.85
134.44
136.13
136.98
140.43
149.37
205.75
LSK-6-060-001 400a
ppm

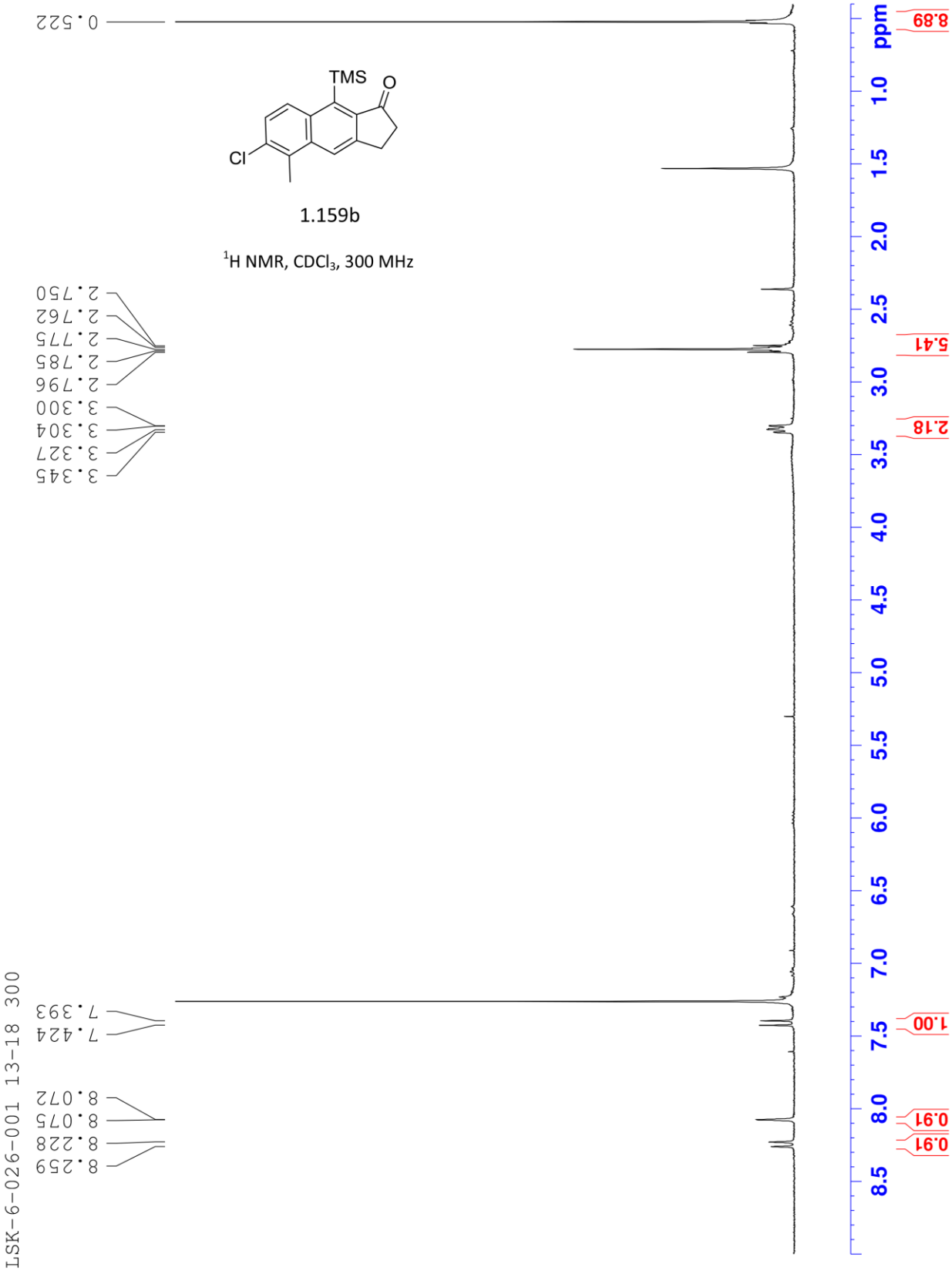
TMS
O
Cl
1.159b
^{1}H NMR, $CDCl_3$, 300 MHz
LSK-6-026-001 13-18 300
0.522
2.750
2.762
2.775
2.785
2.796
3.300
3.304
3.327
3.345
7.393
7.424
8.072
8.075
8.228
8.259
ppm
8.89
5.41
2.18
1.00
0.91
0.91

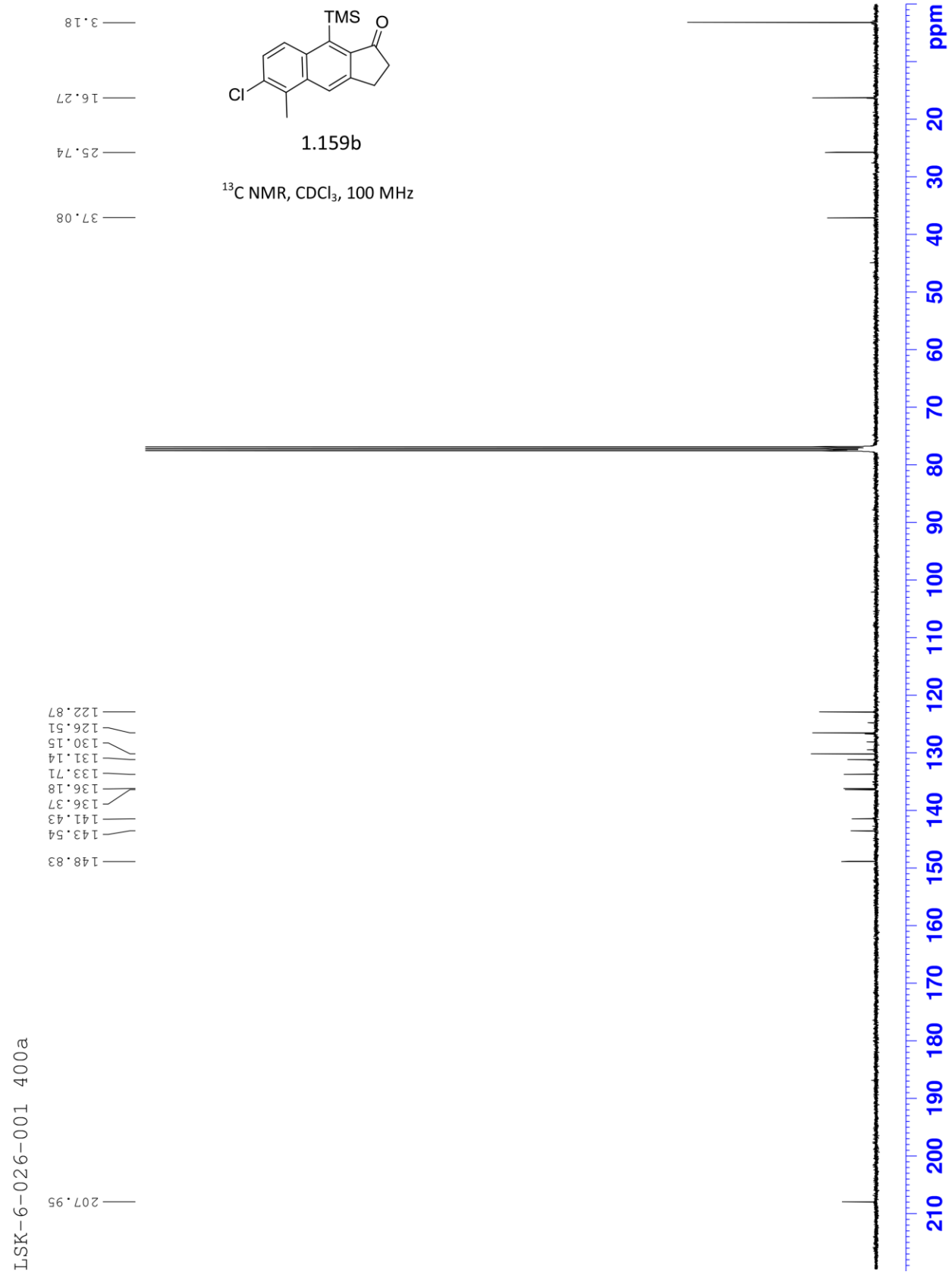
TMS
O
Cl
1.159b
^{13}C NMR, $CDCl_3$, 100 MHz
3.18
16.27
25.74
37.08
122.87
126.51
130.15
131.14
133.71
136.18
136.37
141.43
143.54
148.83
207.95
LSK-6-026-001 400a
ppm

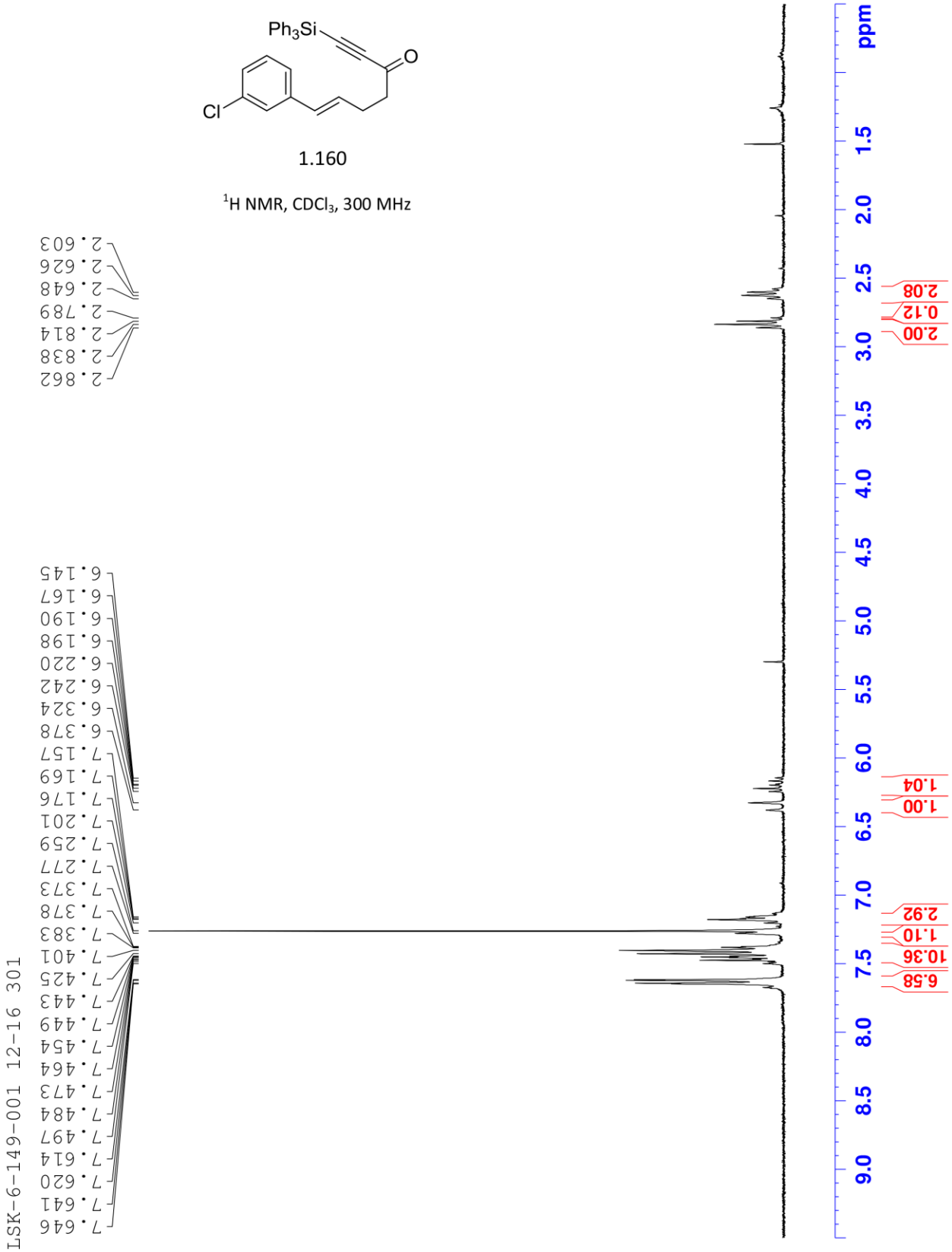
Ph3Si
O
Cl
1.160
1H NMR, CDCl3, 300 MHz
LSK-6-149-001 12-16 301
ppm
2.08
0.12
2.00
1.04
1.00
2.92
1.10
10.36
6.58

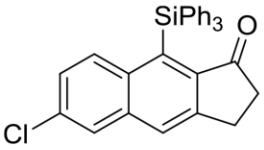

1.161

^{1}H NMR, $CDCl_3$, 600 MHz

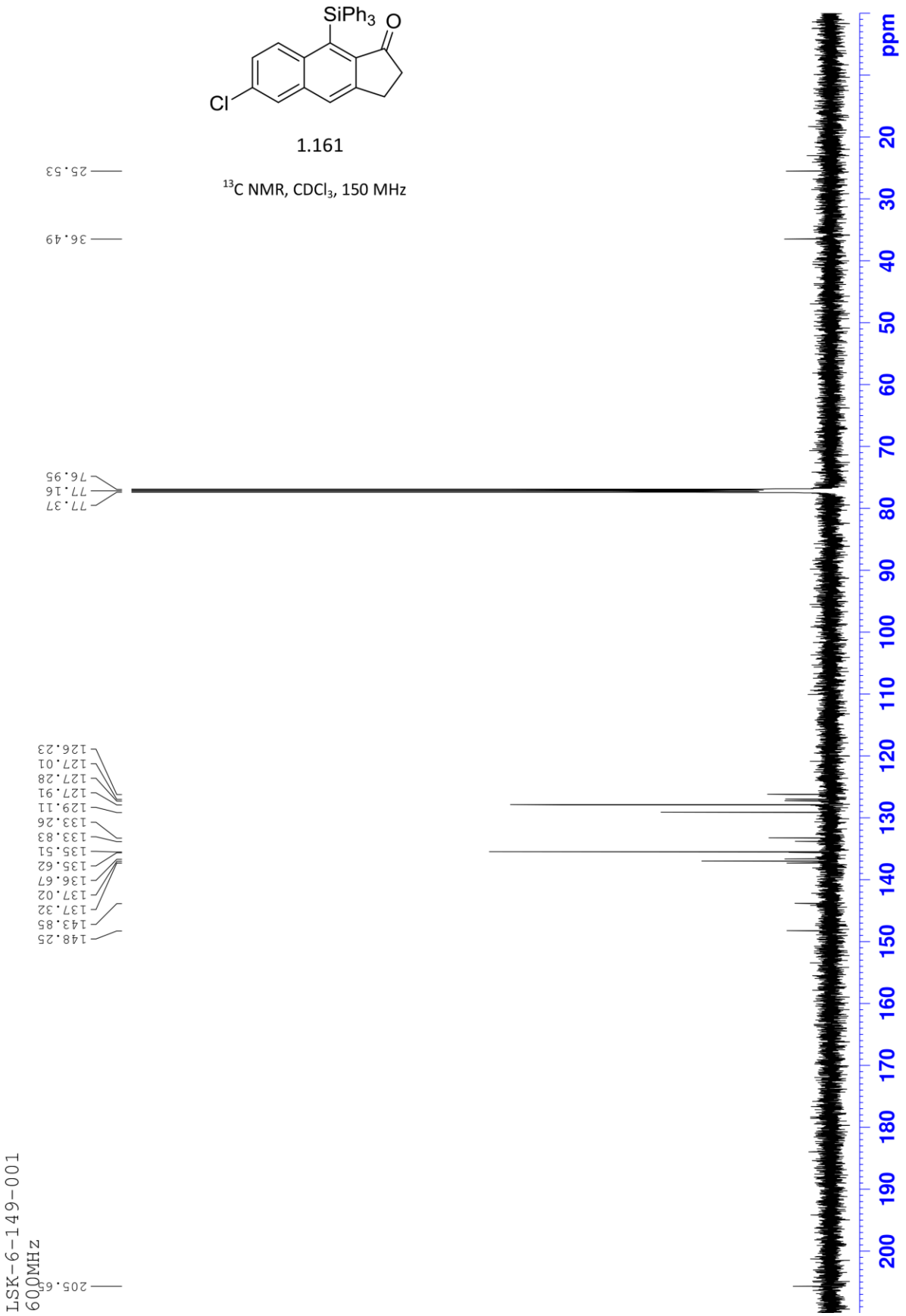
SiPh3
O
Cl
1.161
13C NMR, CDCl3, 150 MHz
25.53
36.49
76.95
77.16
77.37
126.23
127.01
127.28
127.91
129.11
133.26
133.83
135.51
135.62
136.67
137.02
137.32
143.85
148.25
205.67
LSK-6-149-001
60.0MHz
ppm
20
30
40
50
60
70
80
90
100
110
120
130
140
150
160
170
180
190
200

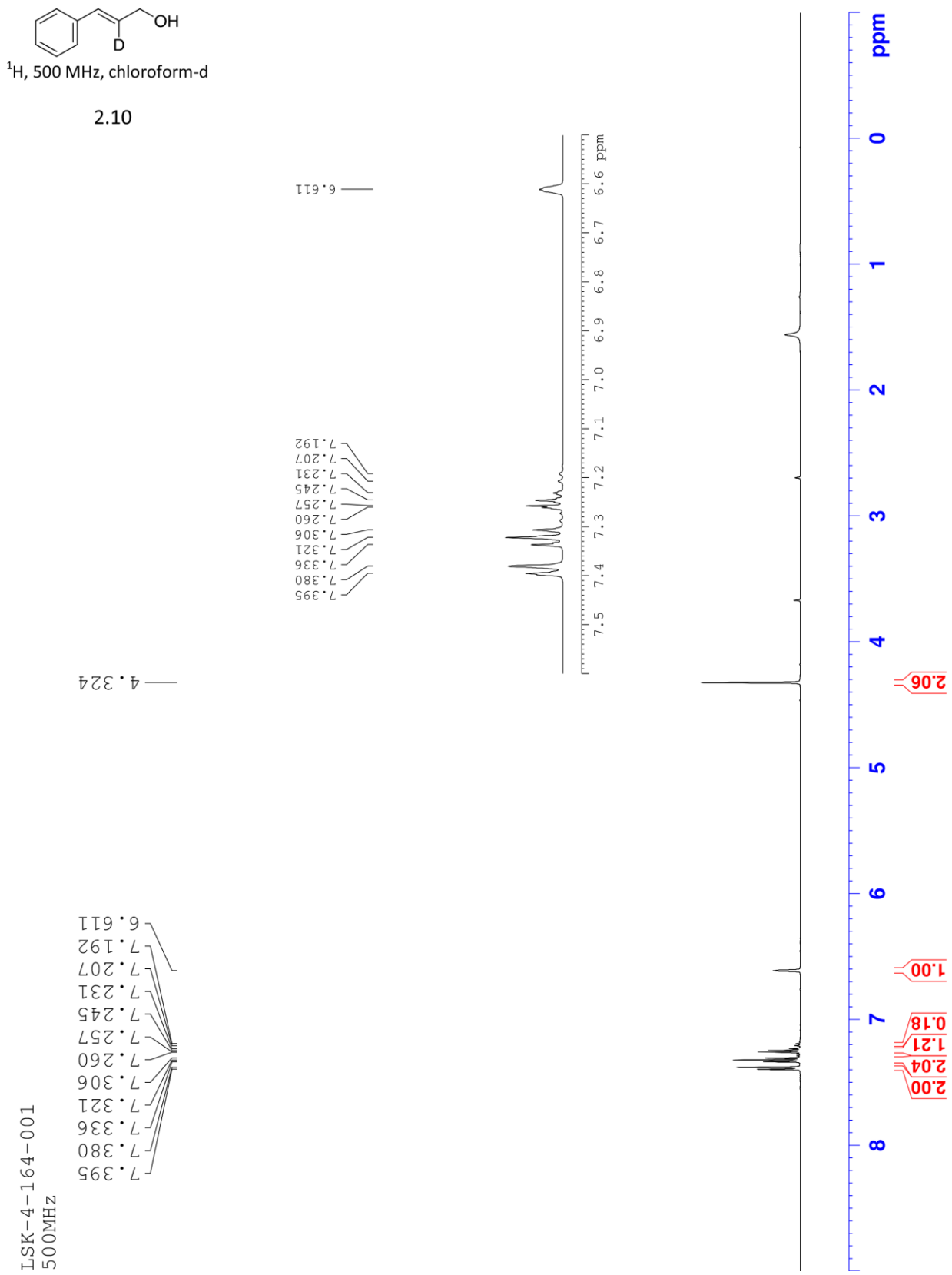
OH
D
1H, 500 MHz, chloroform-d
2.10
LSK-4-164-001
500MHz
7.395
7.380
7.336
7.321
7.306
7.260
7.257
7.245
7.231
7.207
7.192
6.611
4.324
ppm
2.00
2.04
1.21
0.18
1.00
2.06

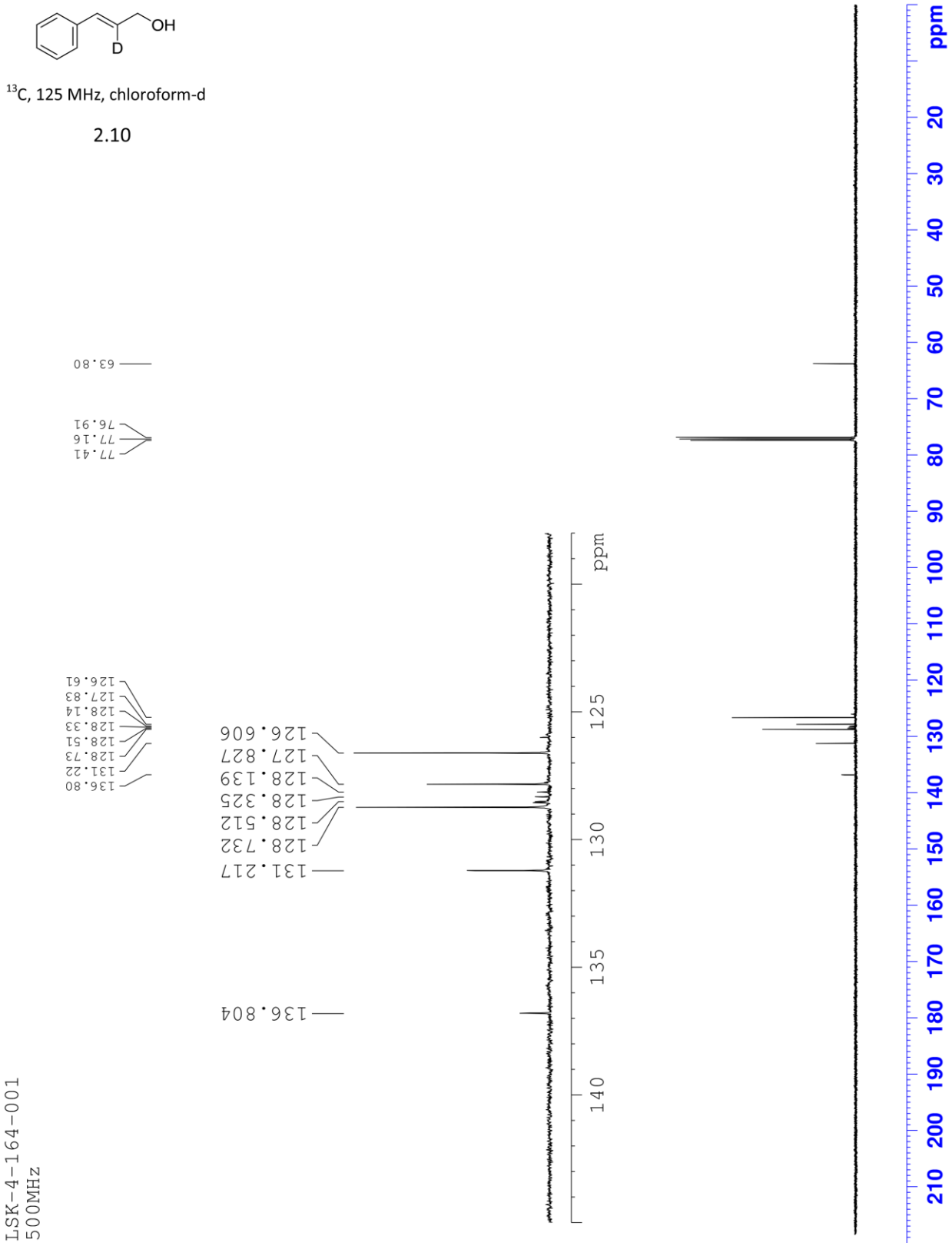
OH
D
^{13}C, 125 MHz, chloroform-d
2.10
LSK-4-164-001
500MHz
63.80
77.41
77.16
76.91
136.80
131.22
128.73
128.51
128.33
128.14
127.83
126.61
136.804
131.217
128.732
128.512
128.325
128.139
127.827
126.606
ppm
125
130
135
140
ppm
20
30
40
50
60
70
80
90
100
110
120
130
140
150
160
170
180
190
200
210

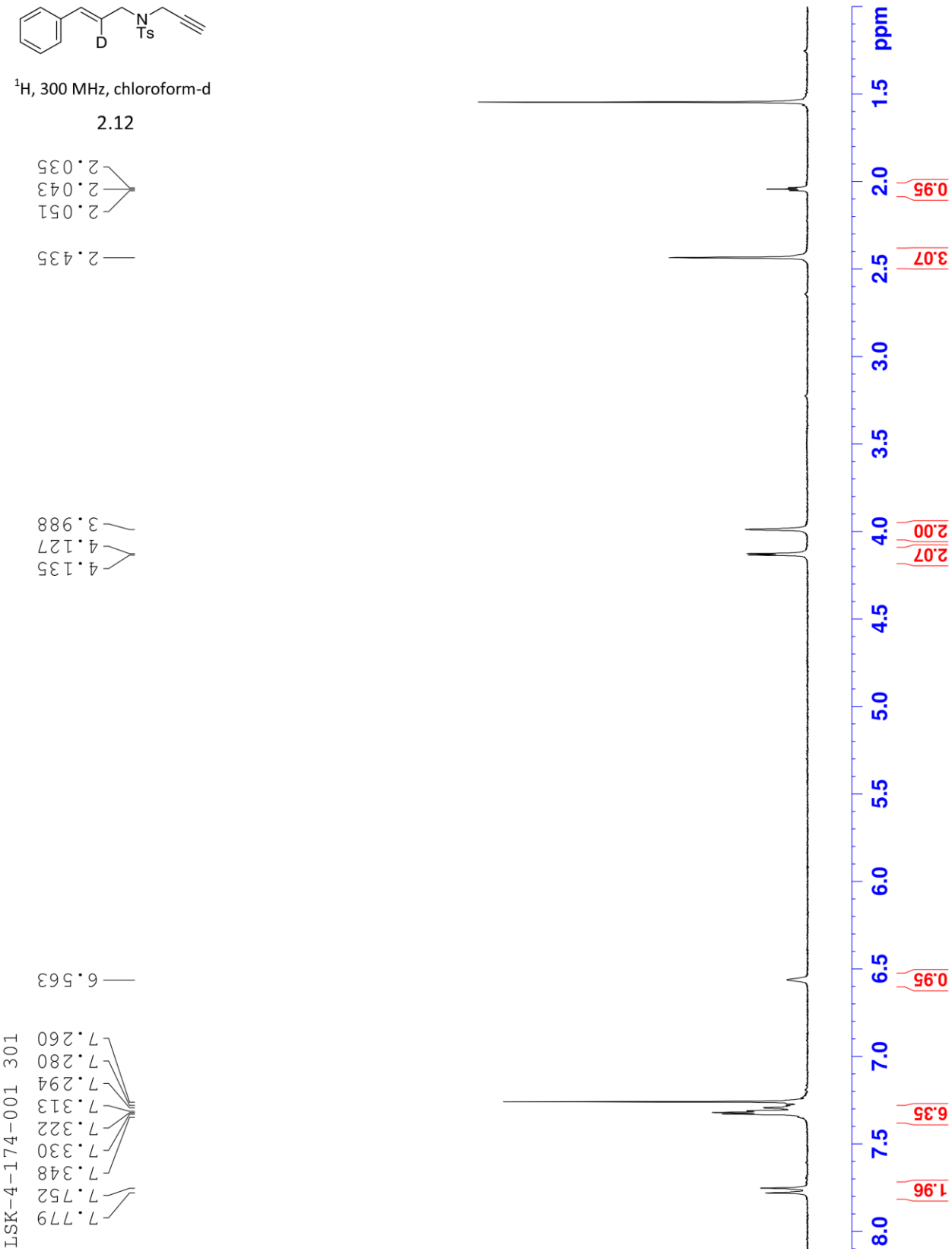
N
Ts
D
1H, 300 MHz, chloroform-d
2.12
LSK-4-174-001 301
7.779
7.752
7.348
7.330
7.322
7.313
7.294
7.280
7.260
6.563
4.135
4.127
3.988
2.435
2.051
2.043
2.035
ppm
1.5
2.0
2.5
3.0
3.5
4.0
4.5
5.0
5.5
6.0
6.5
7.0
7.5
8.0
0.95
3.07
2.00
2.07
0.95
6.35
1.96

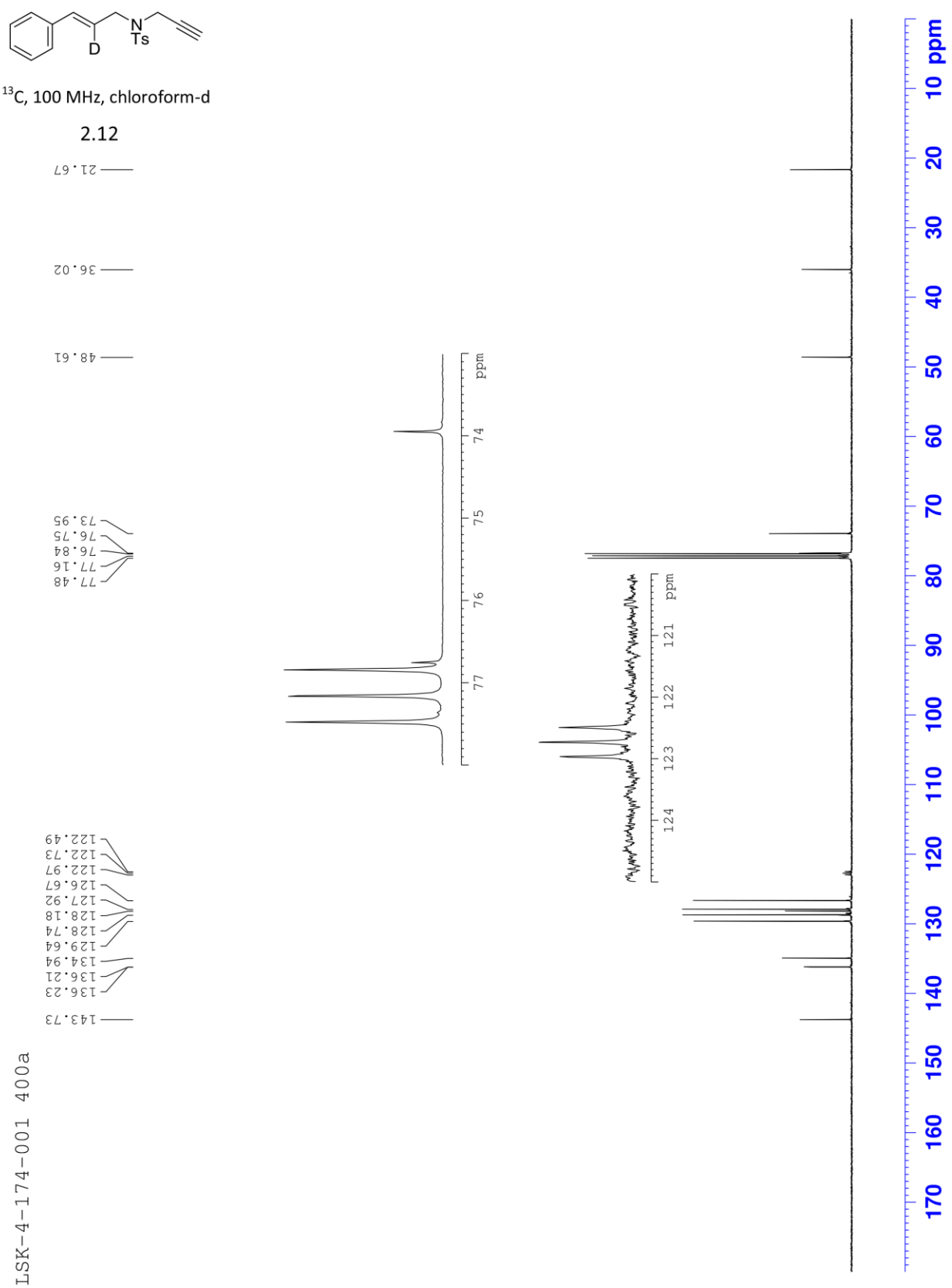
D
N
Ts
13C, 100 MHz, chloroform-d
2.12
LSK-4-174-001 400a
21.67
36.02
48.61
73.95
76.75
76.84
77.16
77.48
122.49
122.73
122.97
126.67
127.92
128.18
128.74
129.64
134.94
136.21
136.23
143.73
ppm
ppm

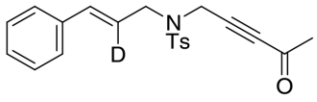

^{1}H, 400 MHz, chloroform-d

2.14

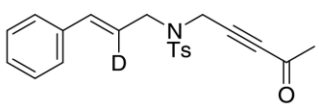

^{13}C, 100 MHz, chloroform-d

2.14

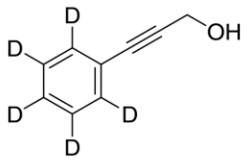

^{1}H, 300 MHz, chloroform-d

S1

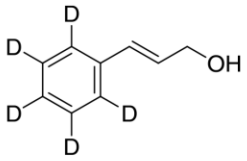

^{1}H, 300 MHz, chloroform-d

2.17

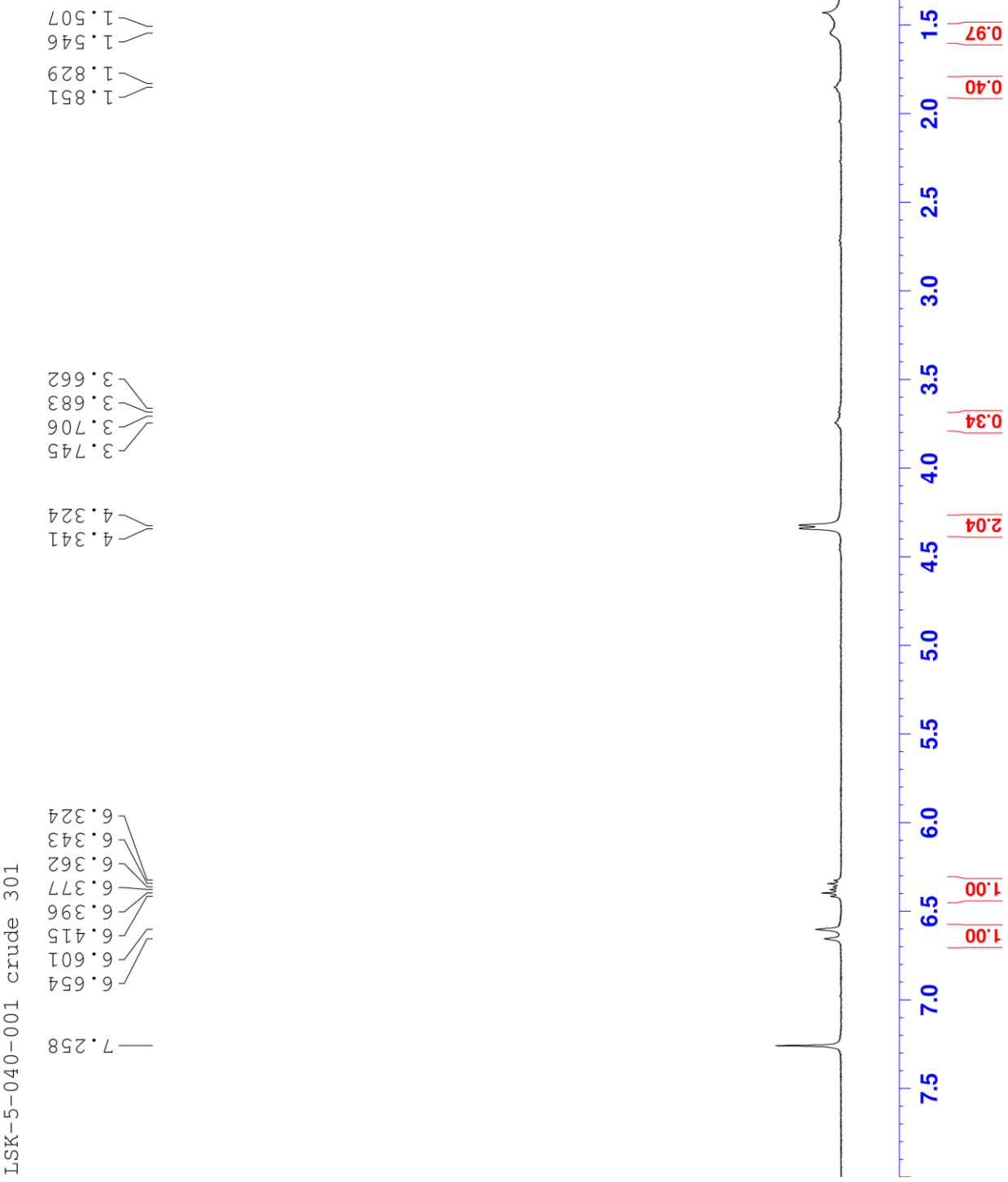

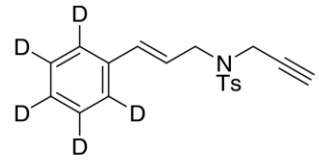

^{1}H, 300 MHz, chloroform-d

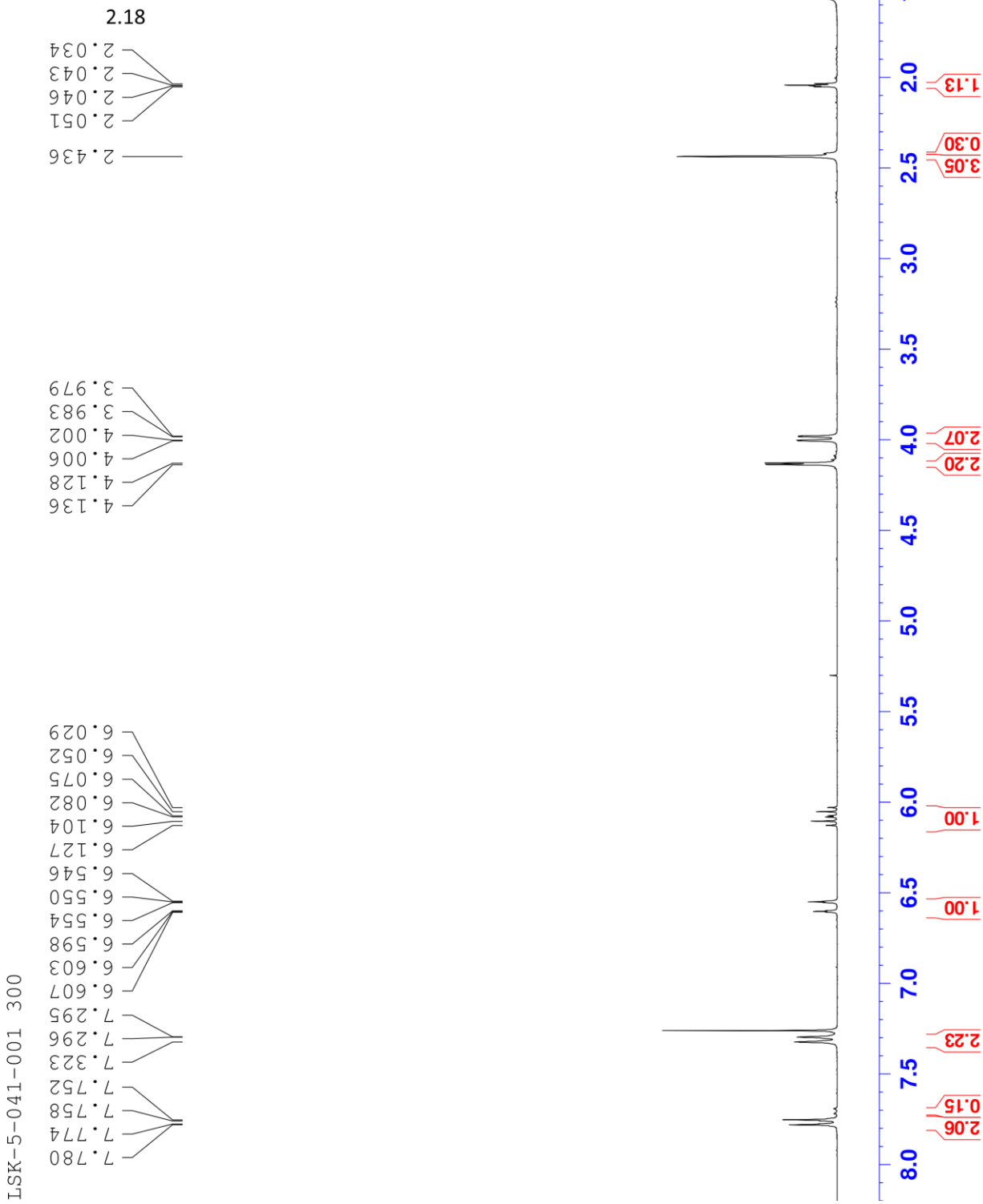

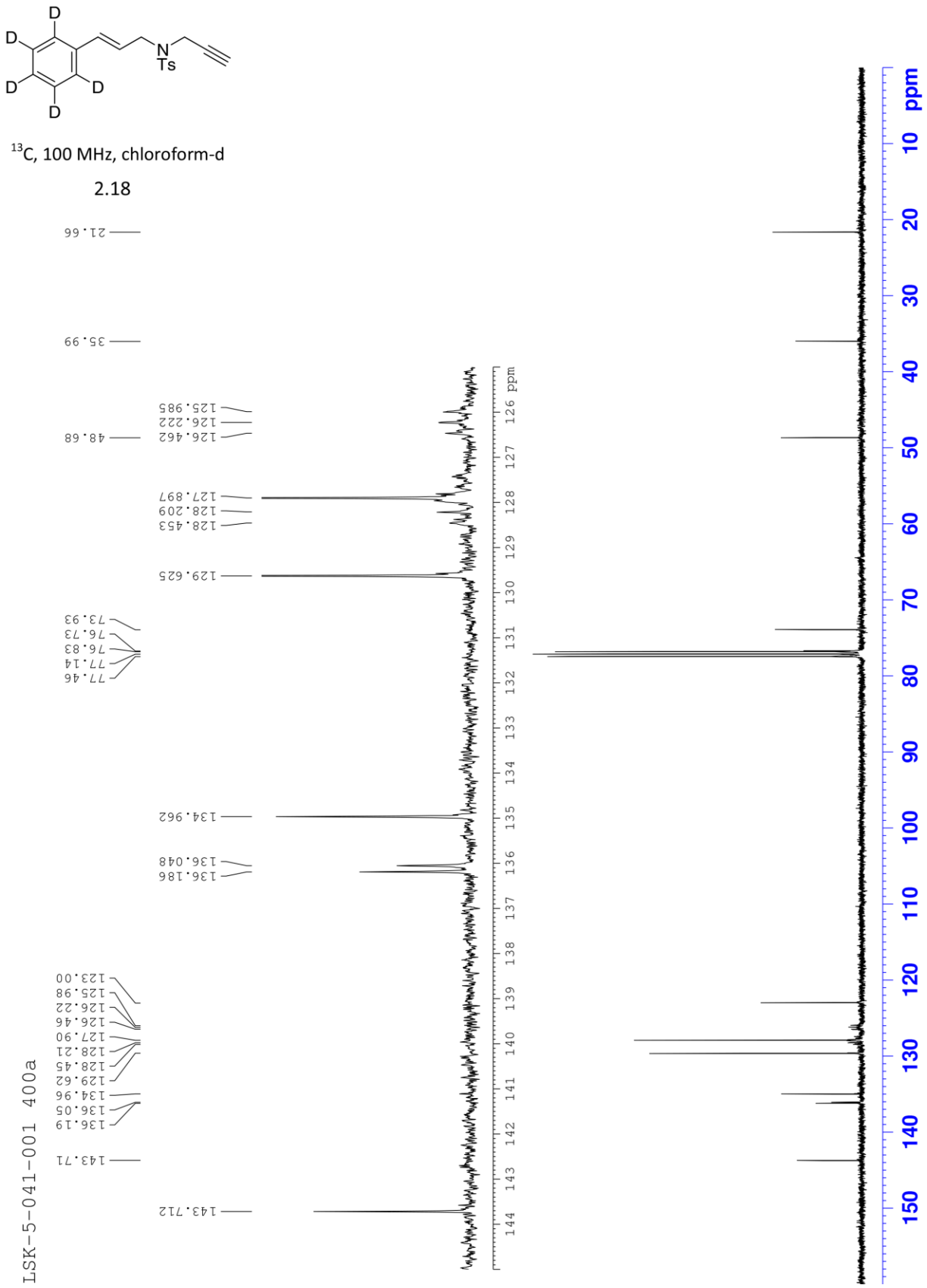
D
D
D
D
D
N
Ts
^{13}C, 100 MHz, chloroform-d
2.18
LSK-5-041-001 400a
21.66
35.99
48.68
73.93
76.73
76.83
77.14
77.46
123.00
125.98
126.22
126.46
127.90
128.21
128.45
129.62
134.96
136.05
136.19
143.71
125.985
126.222
126.462
127.897
128.209
128.453
129.625
134.962
136.048
136.186
143.712
ppm

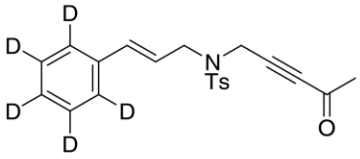

^{1}H, 300 MHz, chloroform-d

2.19

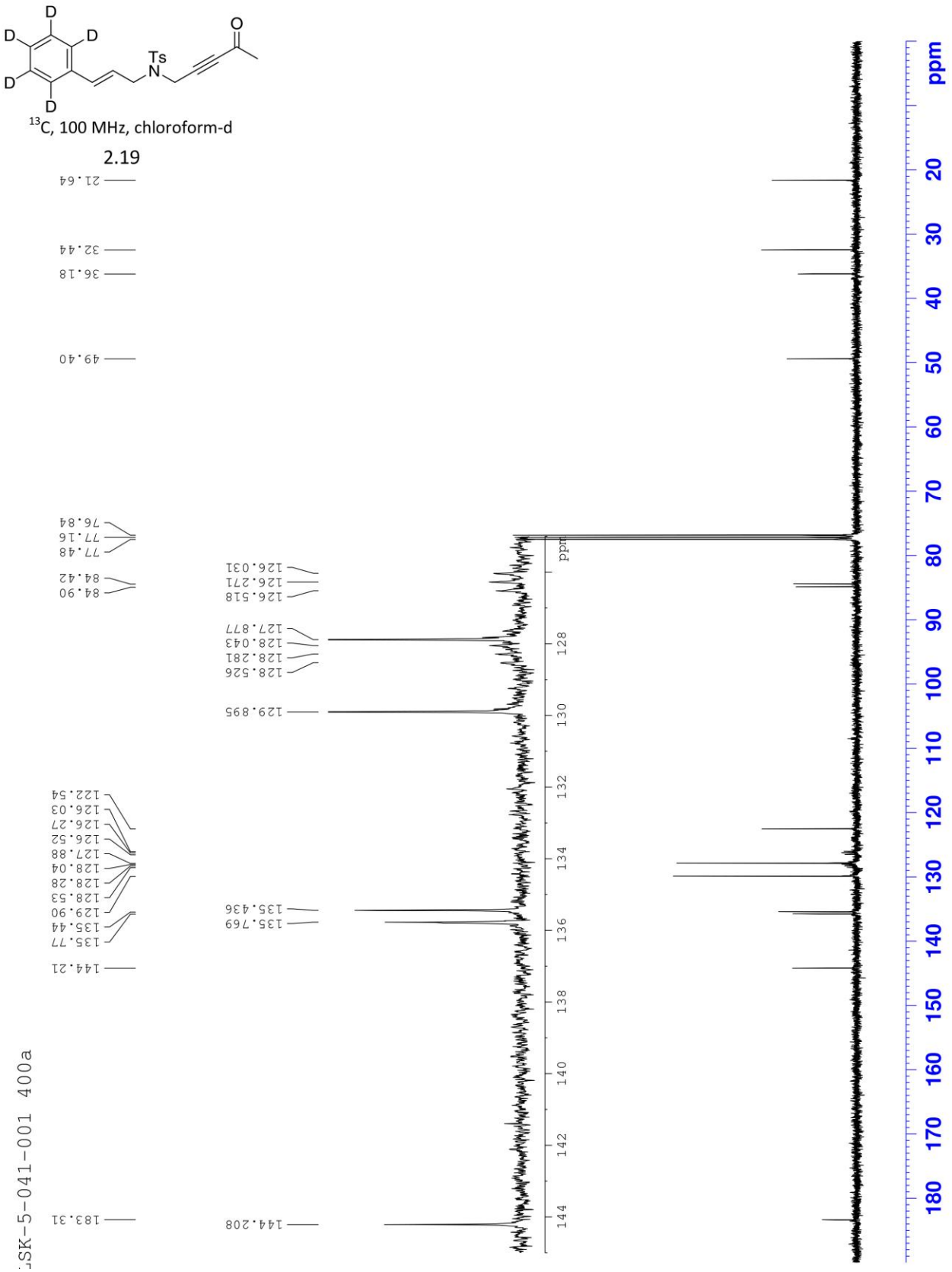
D
D
D
D
D
Ts
N
O
13C, 100 MHz, chloroform-d
2.19
21.64
32.44
36.18
49.40
76.84
77.16
77.48
84.42
84.90
122.54
126.03
126.27
126.52
127.88
128.04
128.28
128.53
129.90
135.44
135.77
144.21
183.31
126.031
126.271
126.518
127.877
128.043
128.281
128.526
129.895
135.436
135.769
144.208
ppm
ppm
SK-5-041-001 400a

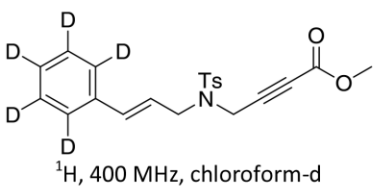

^{1}H, 400 MHz, chloroform-d

2.20

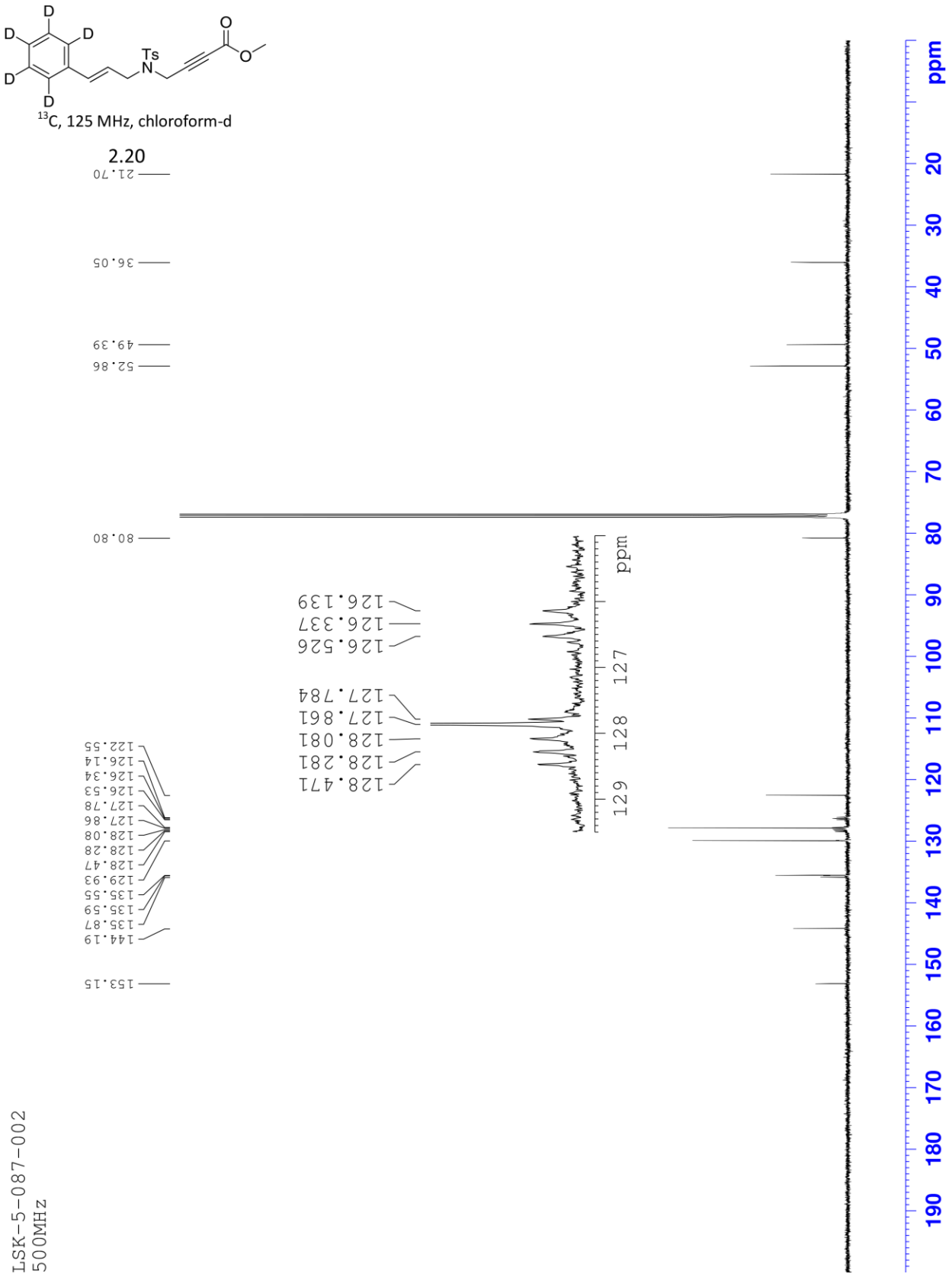
D
D
D
D
D
Ts
N
O
O
13C, 125 MHz, chloroform-d
2.20
21.70
36.05
49.39
52.86
80.80
122.55
126.14
126.34
126.53
127.78
127.86
128.08
128.28
128.47
129.93
135.55
135.59
135.87
144.19
153.15
126.139
126.337
126.526
127.784
127.861
128.081
128.281
128.471
129 128 127 ppm
ppm
LSK-5-087-002
500MHz

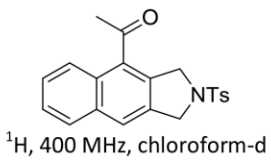

^{1}H, 400 MHz, chloroform-d

1.146

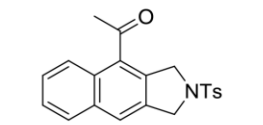

^{13}C, 100 MHz, chloroform-d

1.146

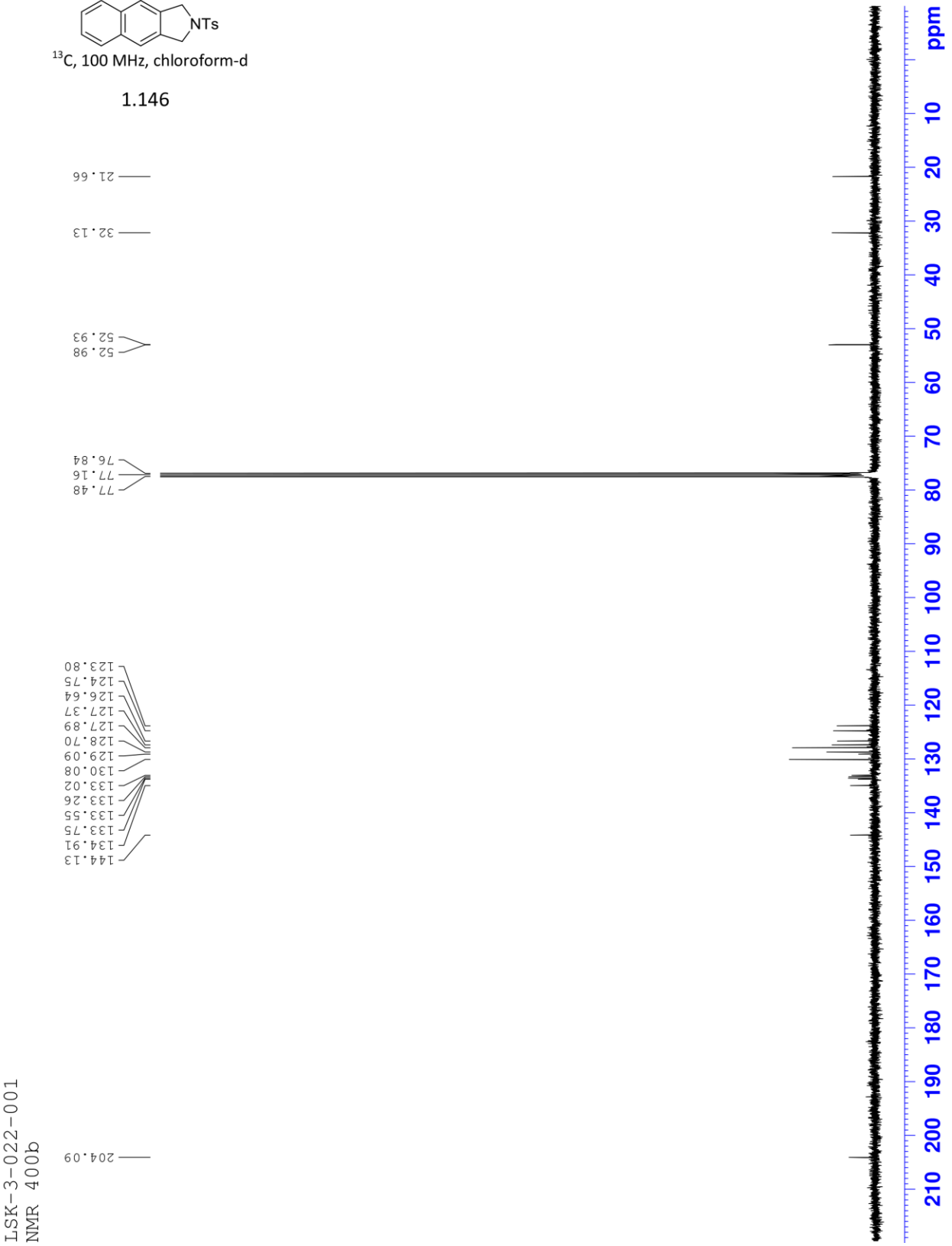

LSK-3-022-001
NMR 400b

O
NTs
1H, 400 MHz, chloroform-d
1.147
ppm

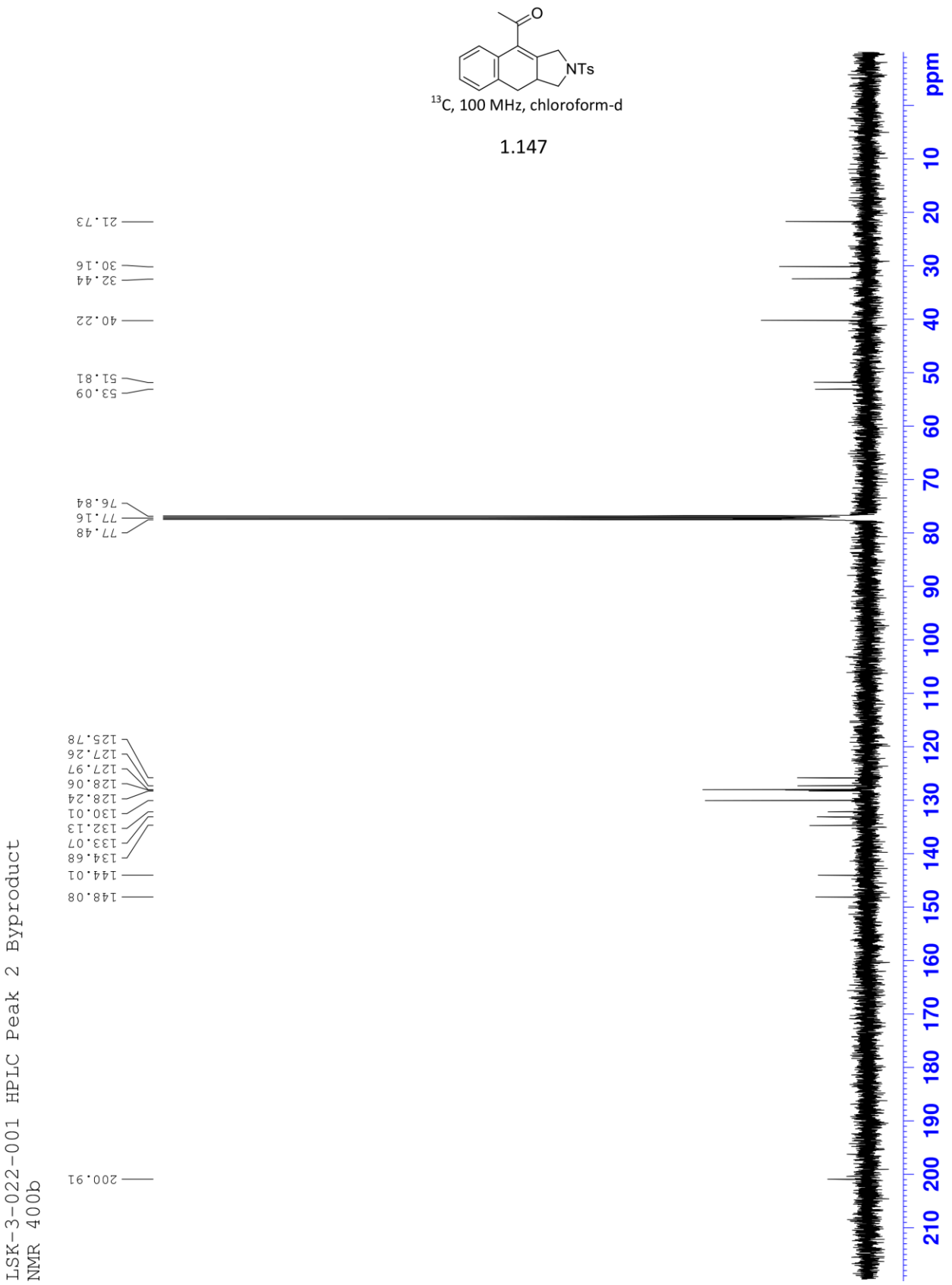
O
NTs
13C, 100 MHz, chloroform-d
1.147
LSK-3-022-001 HPLC Peak 2 Byproduct
NMR 400b
21.73
30.16
32.44
40.22
51.81
53.09
76.84
77.16
77.48
125.78
127.26
127.97
128.06
128.24
130.01
132.13
133.07
134.68
144.01
148.08
200.91
ppm
10
20
30
40
50
60
70
80
90
100
110
120
130
140
150
160
170
180
190
200
210

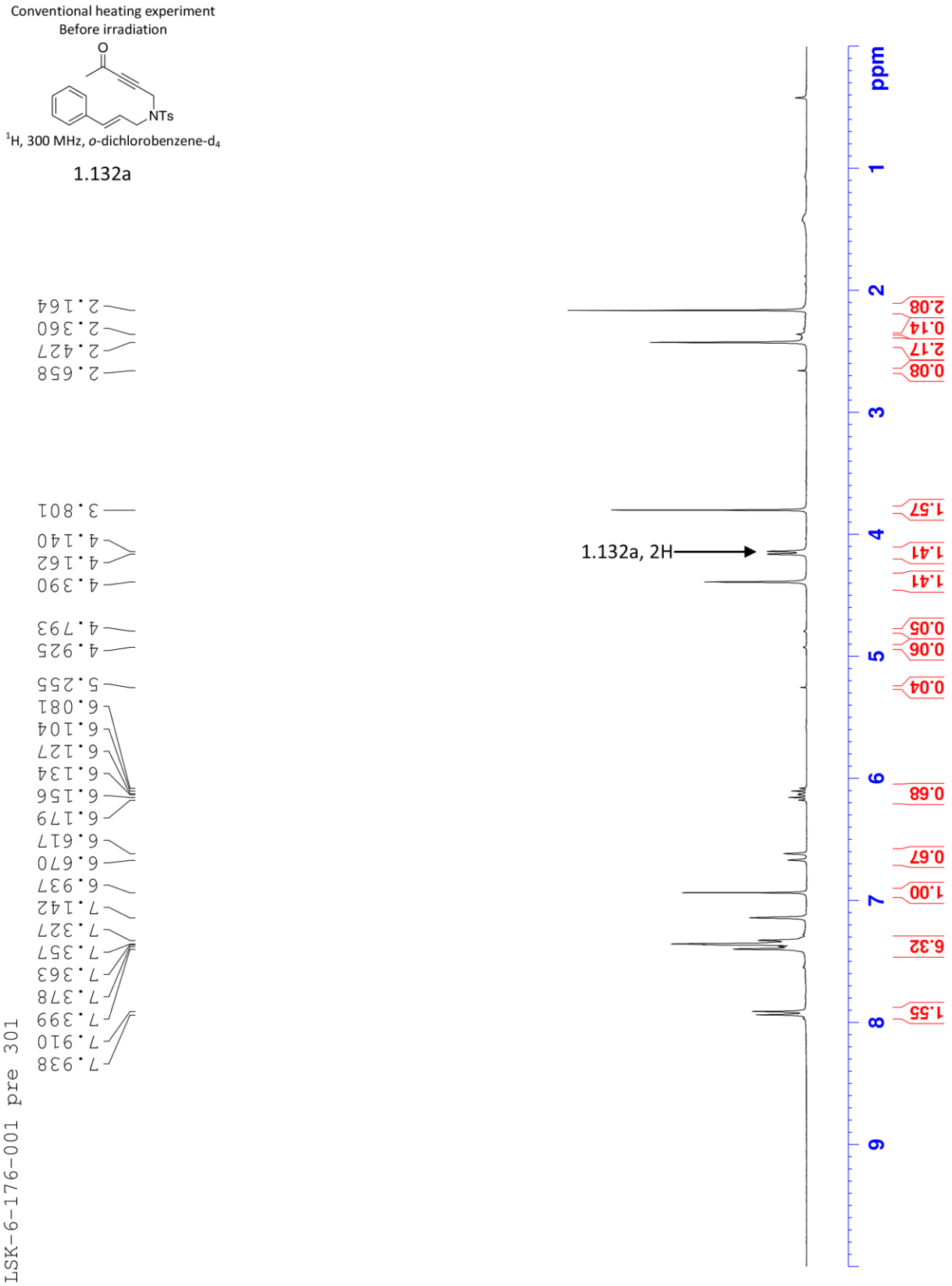
Conventional heating experiment
Before irradiation
O
NTs
^{1}H, 300 MHz, *o*-dichlorobenzene-d$_4$
1.132a
LSK-6-176-001 pre 301
2.164
2.360
2.427
2.658
3.801
4.140
4.162
4.390
4.793
4.925
5.255
6.081
6.104
6.127
6.134
6.156
6.179
6.617
6.670
6.937
7.142
7.327
7.357
7.363
7.378
7.399
7.910
7.938
1.132a, 2H
ppm
1
2
3
4
5
6
7
8
9
2.08
0.14
2.17
0.08
1.57
1.41
1.41
0.05
0.06
0.04
0.68
0.67
1.00
6.32
1.55

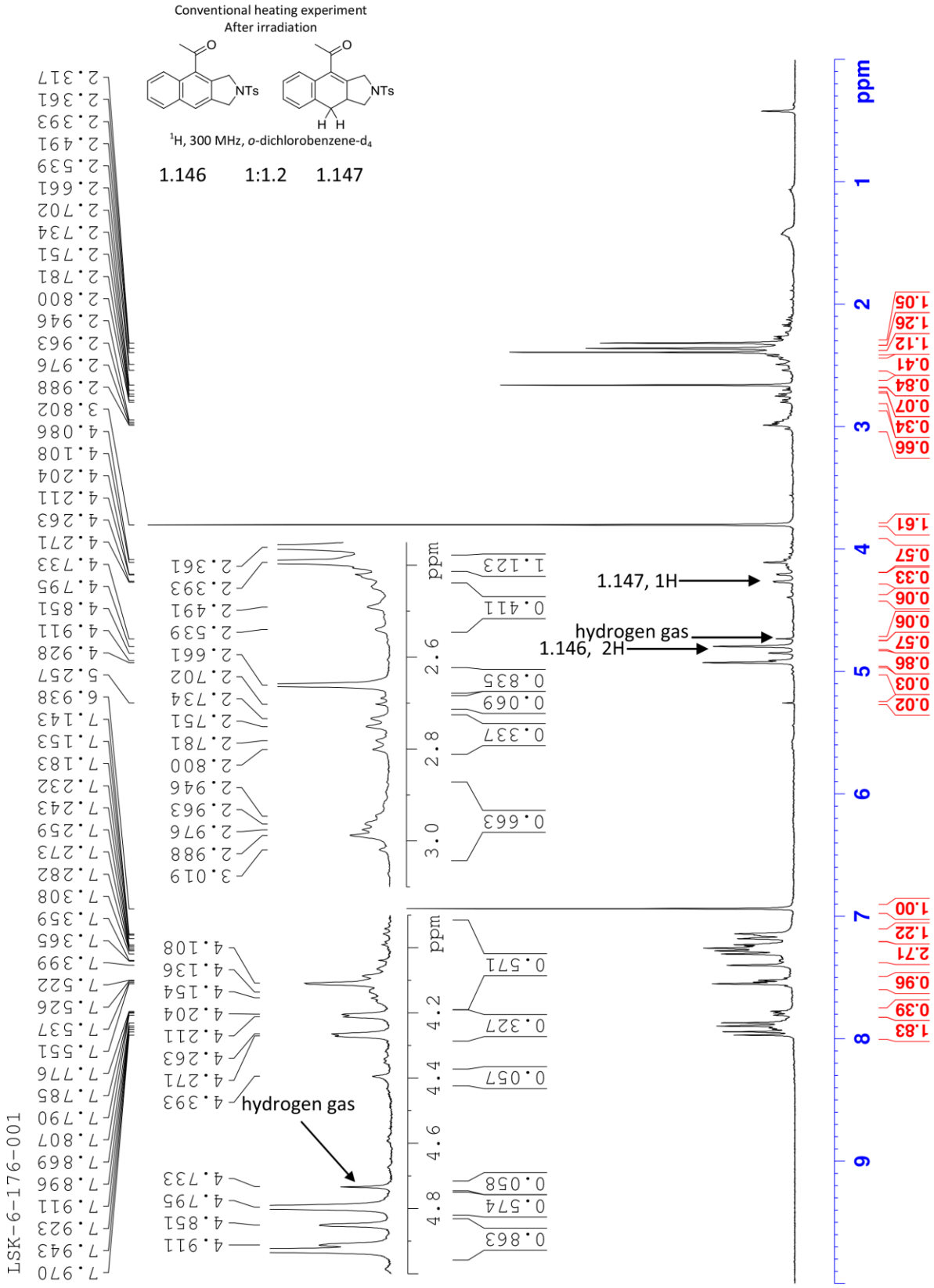
Conventional heating experiment
After irradiation
NTs
NTs
H H
^{1}H, 300 MHz, *o*-dichlorobenzene-d$_4$
1.146 1:1.2 1.147
1.147, 1H
hydrogen gas
1.146, 2H
hydrogen gas
LSK-6-176-001
ppm

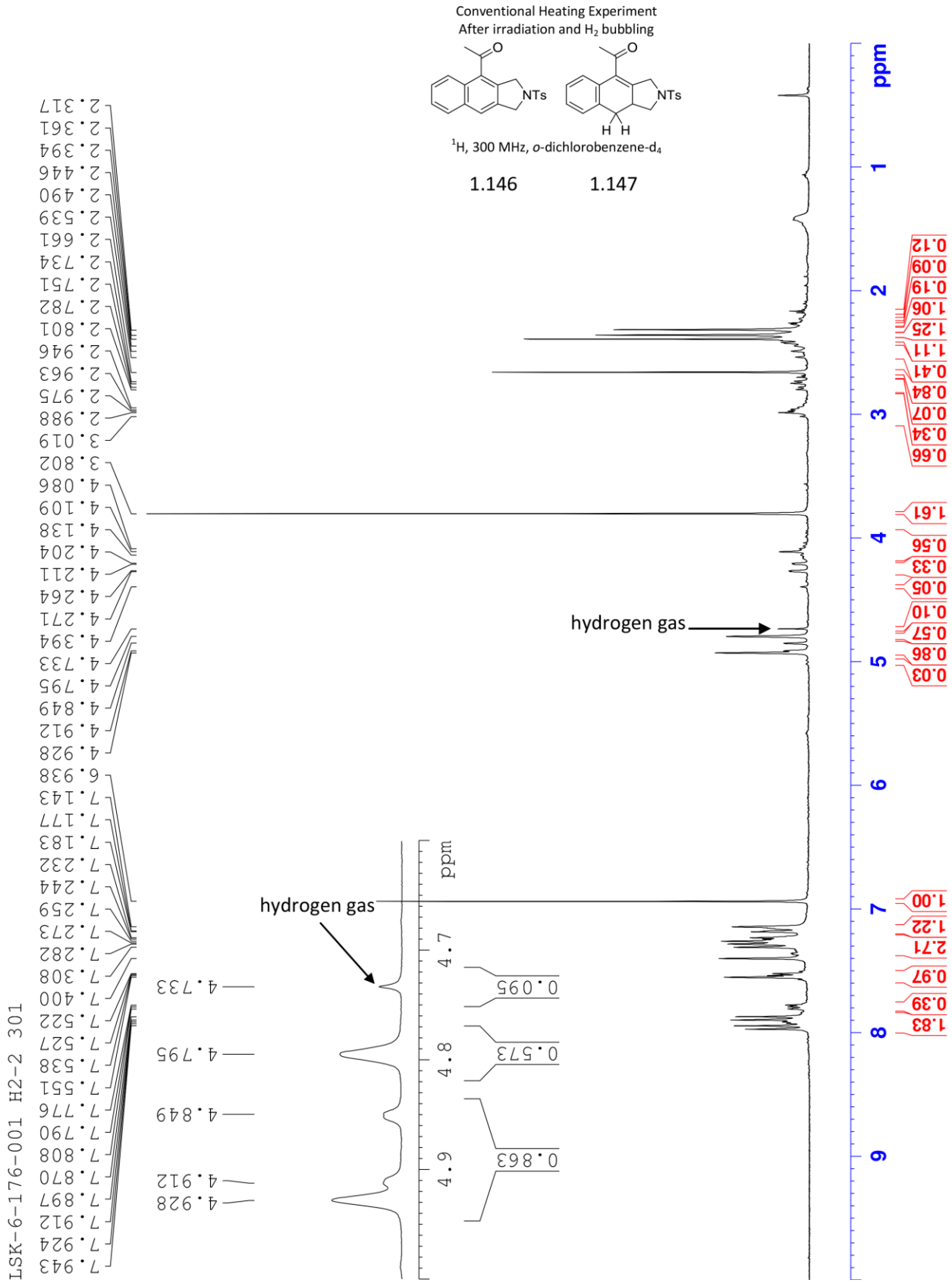
Conventional Heating Experiment
After irradiation and H_2 bubbling
NTs
NTs
H H
^{1}H, 300 MHz, *o*-dichlorobenzene-d_4
1.146
1.147
hydrogen gas
hydrogen gas
ppm
LSK-6-176-001 H2-2 301

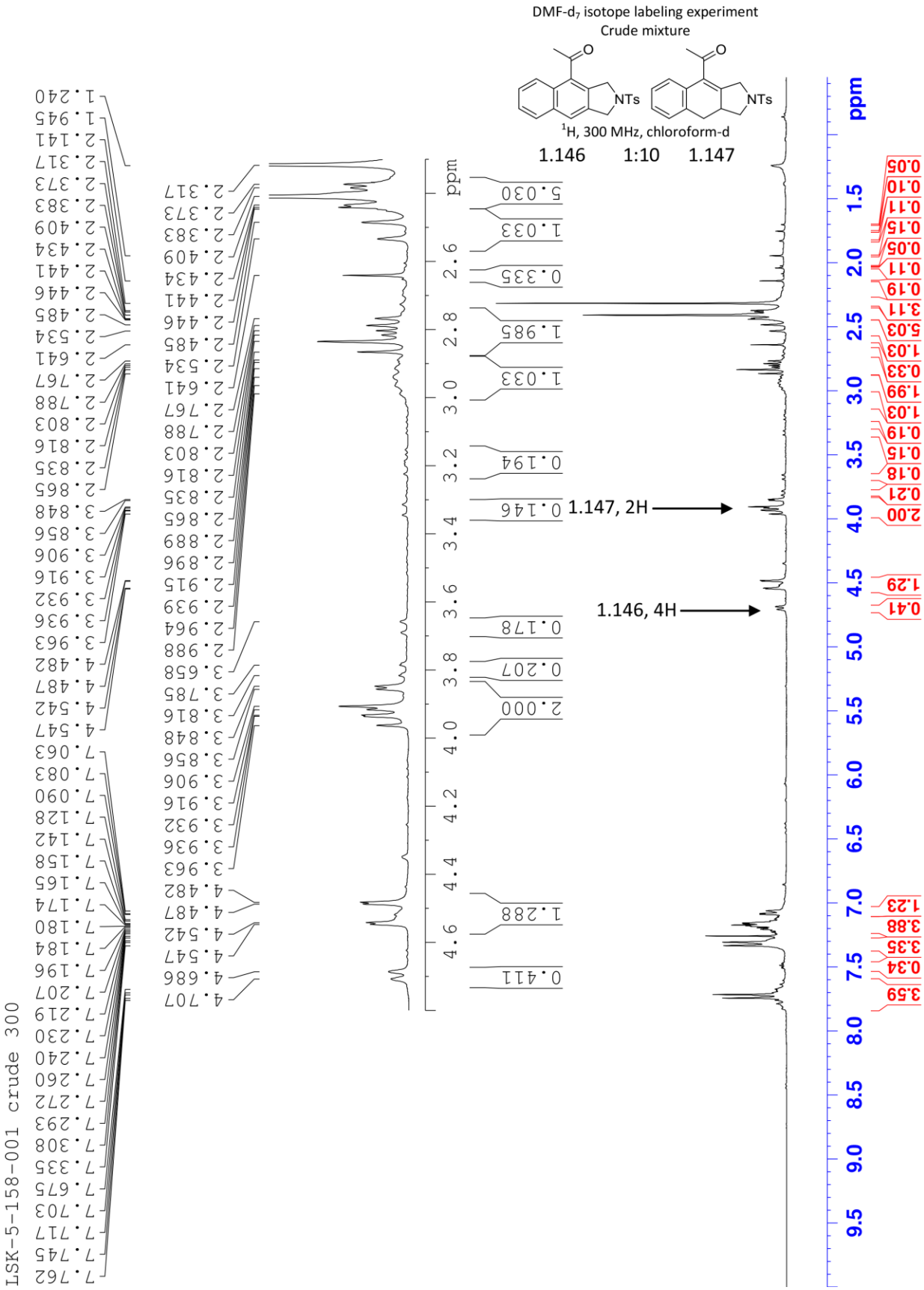
DMF-d7 isotope labeling experiment
Crude mixture
NTs
NTs
1H, 300 MHz, chloroform-d
1.146 1:10 1.147
1.147, 2H
1.146, 4H
LSK-5-158-001 crude 300
ppm

LSK-5-158-001 HPLC 400a
DMF-d7 isotope labeling experiment
Purification by HPLC
1H, 400 MHz, chloroform-d
1.147
NTs
O
H H
ppm

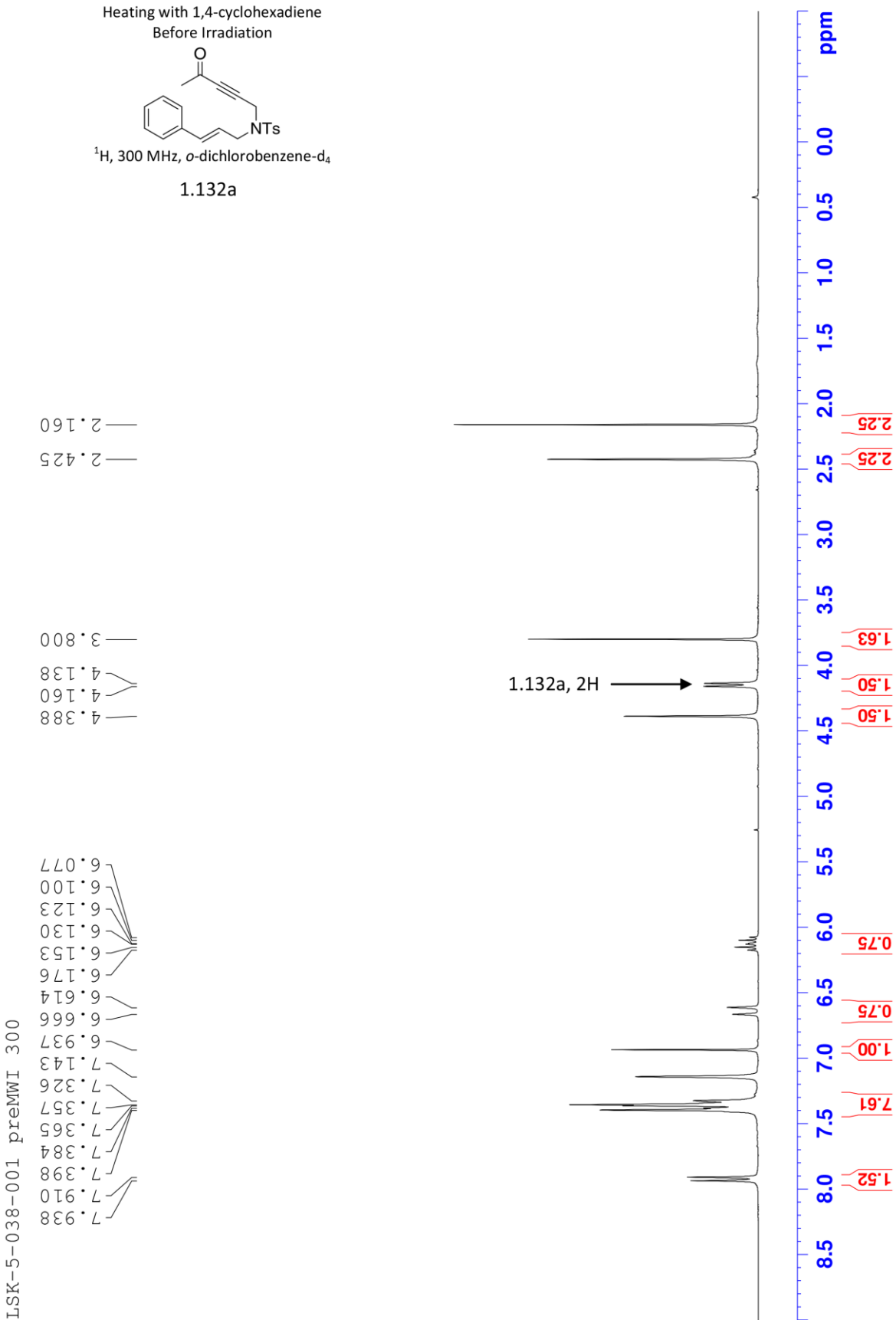
Heating with 1,4-cyclohexadiene
Before Irradiation
O
NTs
^{1}H, 300 MHz, *o*-dichlorobenzene-d$_4$
1.132a
1.132a, 2H
LSK-5-038-001 preMWI 300
2.160
2.425
3.800
4.138
4.160
4.388
6.077
6.100
6.123
6.130
6.153
6.176
6.614
6.666
6.937
7.143
7.326
7.357
7.365
7.384
7.398
7.910
7.938
ppm
0.0
0.5
1.0
1.5
2.0
2.5
3.0
3.5
4.0
4.5
5.0
5.5
6.0
6.5
7.0
7.5
8.0
8.5
2.25
2.25
1.63
1.50
1.50
0.75
0.75
1.00
7.61
1.52

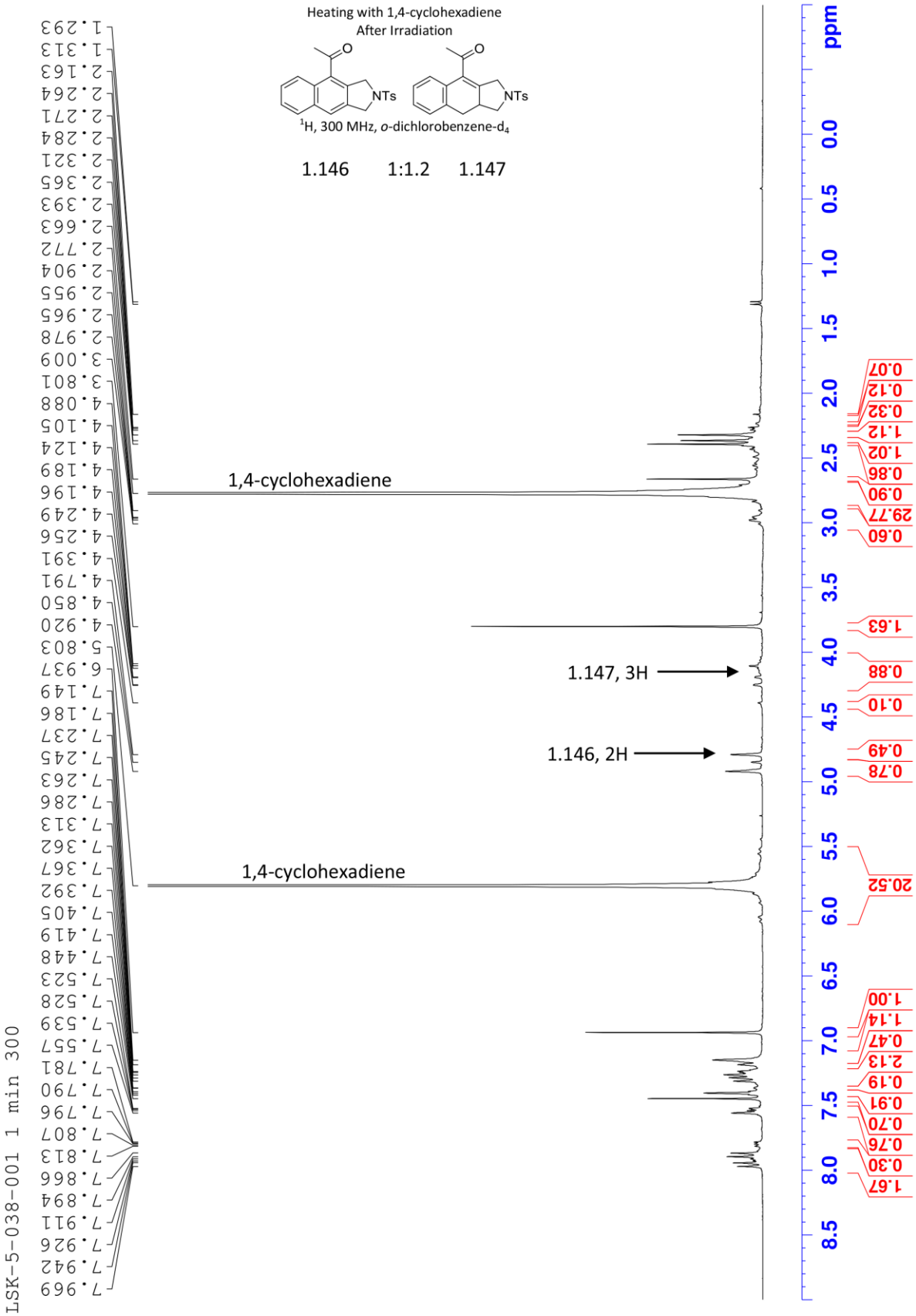
Heating with 1,4-cyclohexadiene
After Irradiation
NTs
NTs
^{1}H, 300 MHz, *o*-dichlorobenzene-d$_4$
1.146 1:1.2 1.147
1,4-cyclohexadiene
1.147, 3H
1.146, 2H
1,4-cyclohexadiene
LSK-5-038-001 1 min 300
ppm

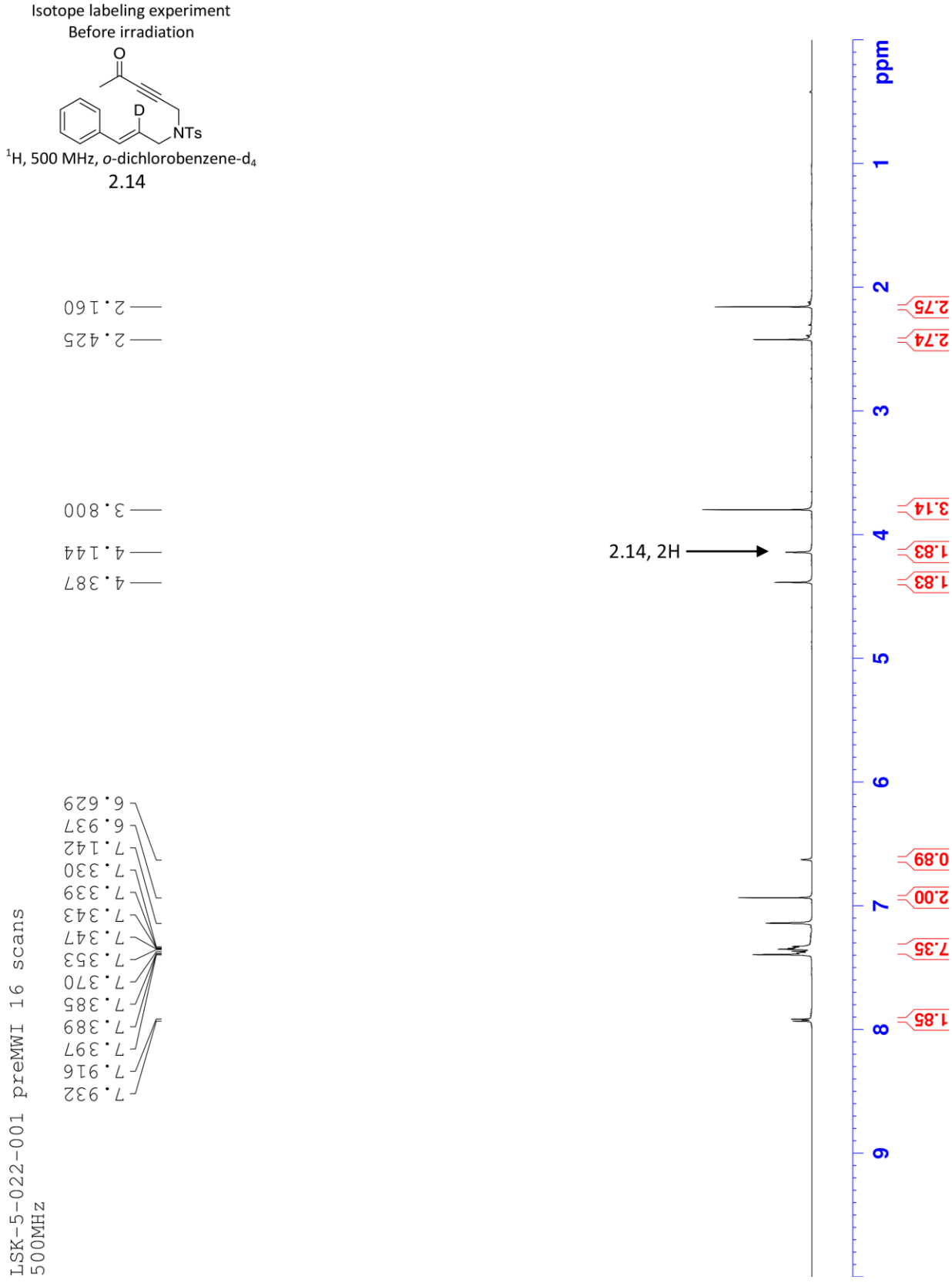
Isotope labeling experiment
Before irradiation
O
D
NTs
1H, 500 MHz, o-dichlorobenzene-d4
2.14
2.160
2.425
3.800
4.144
4.387
6.629
6.937
7.142
7.330
7.339
7.343
7.347
7.353
7.370
7.385
7.389
7.397
7.916
7.932
LSK-5-022-001 preMWI 16 scans
500MHz
2.14, 2H
ppm
1
2
3
4
5
6
7
8
9
2.75
2.74
3.14
1.83
1.83
0.89
2.00
7.35
1.85

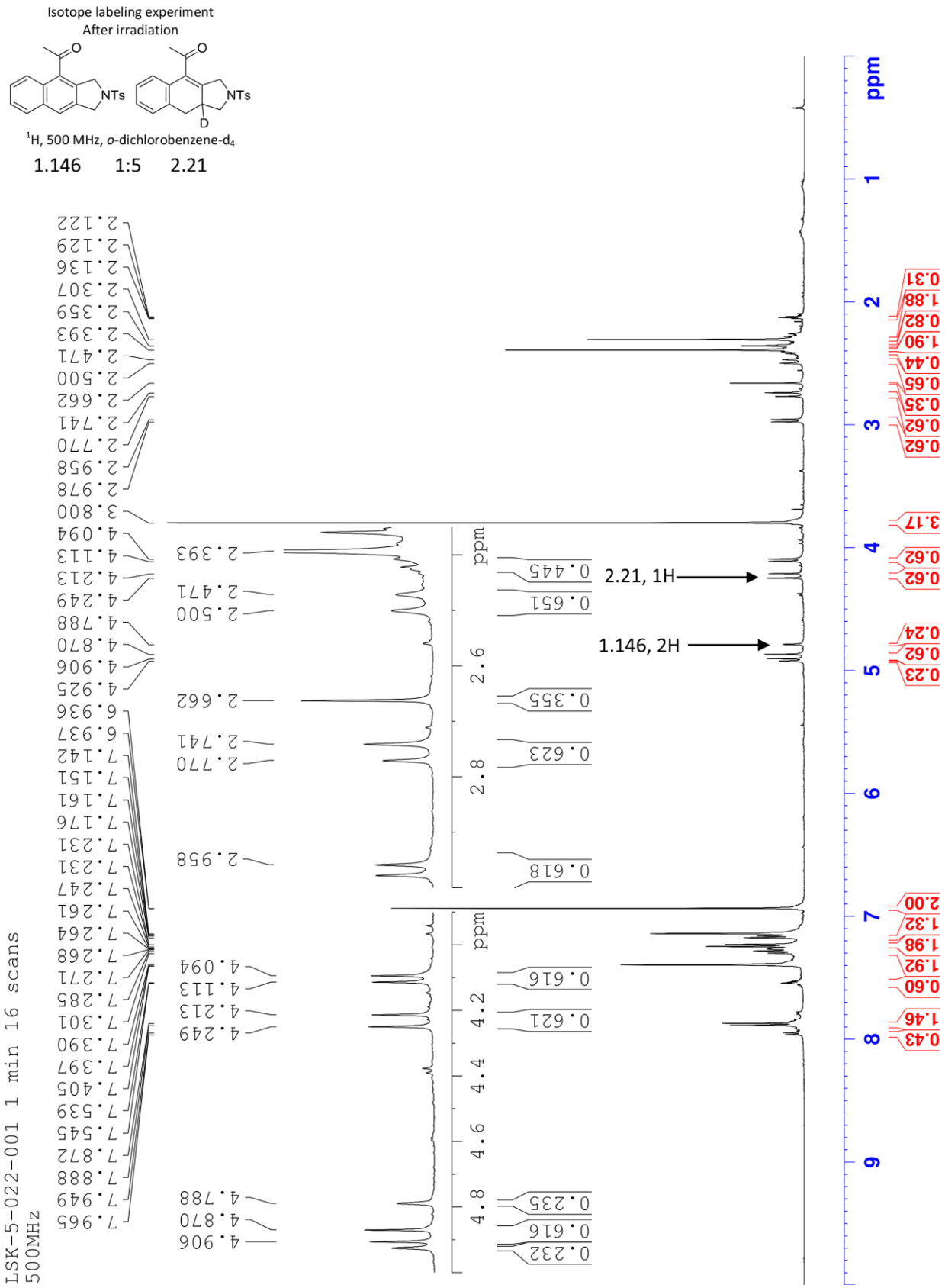
Isotope labeling experiment
After irradiation
NTs
NTs
D
^{1}H, 500 MHz, *o*-dichlorobenzene-d$_4$
1.146 1:5 2.21
LSK-5-022-001 1 min 16 scans
500MHz
2.21, 1H
1.146, 2H
ppm

Isotope labeling experiment
After HPLC

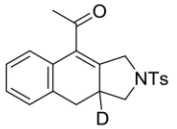

^{1}H, 400 MHz, chloroform-d

2.21

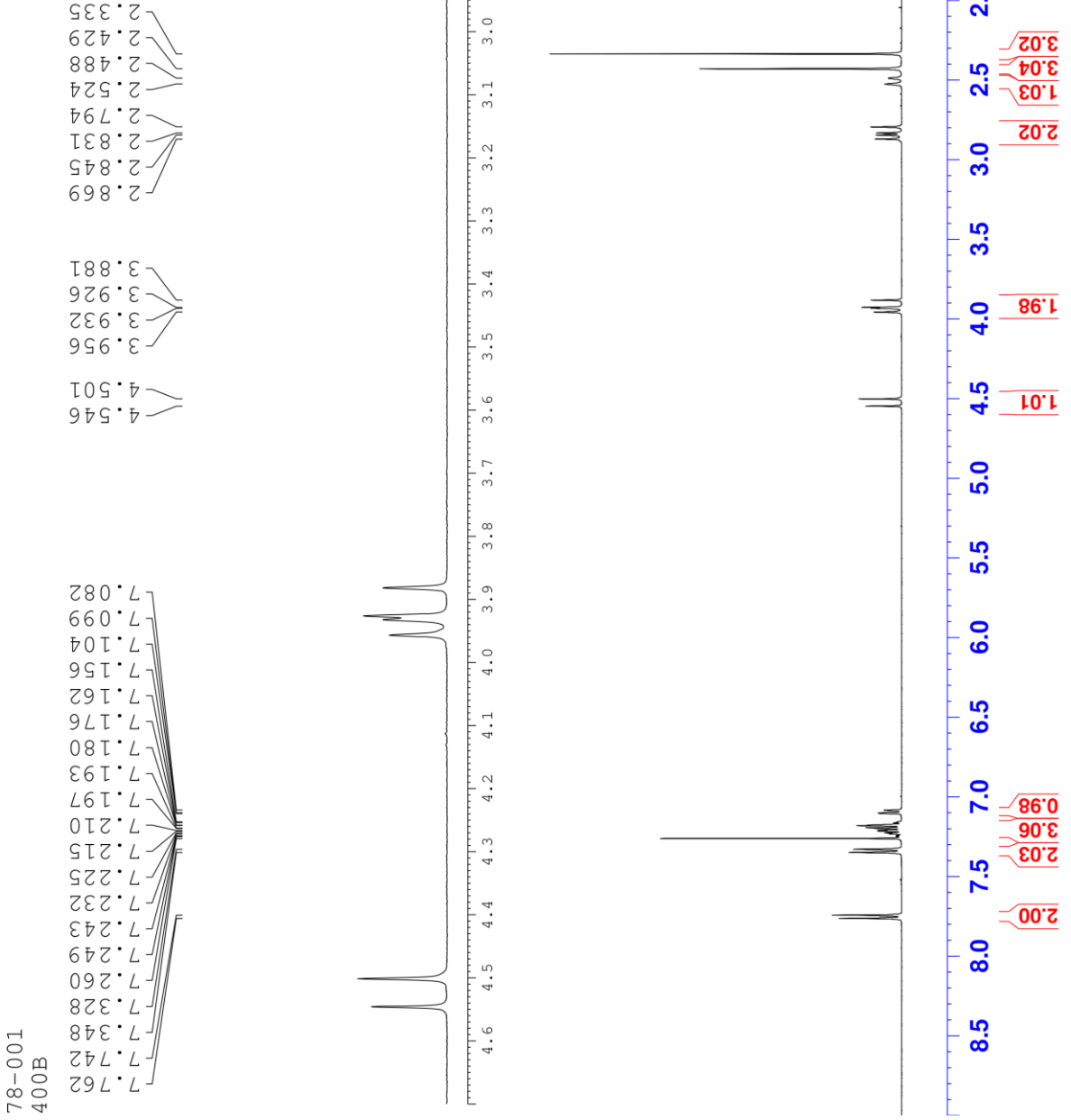

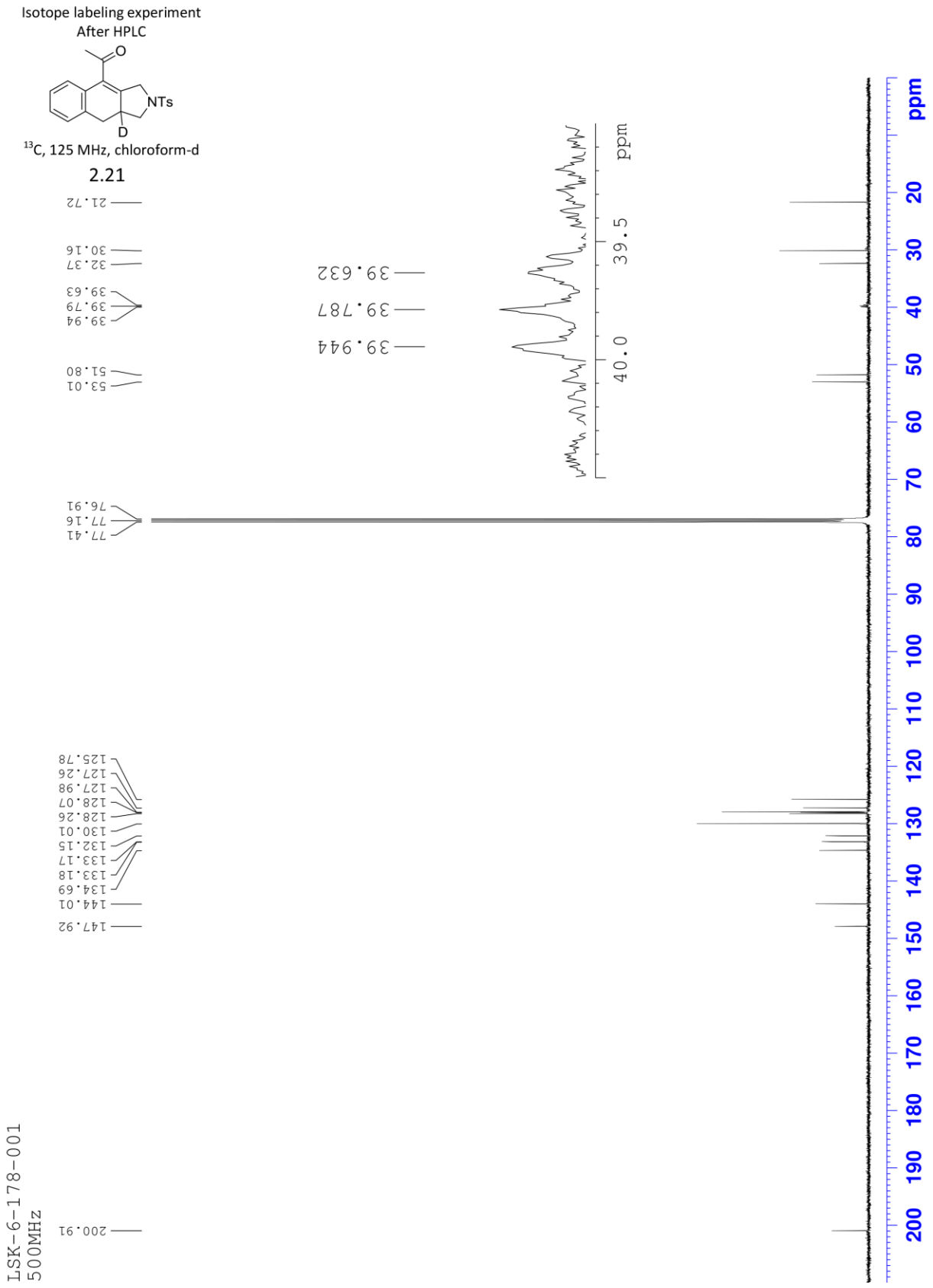
Isotope labeling experiment
After HPLC
O
NTs
D
^{13}C, 125 MHz, chloroform-d
2.21
21.72
30.16
32.37
39.63
39.79
39.94
51.80
53.01
76.91
77.16
77.41
125.78
127.26
127.98
128.07
128.26
130.01
132.15
133.17
133.18
134.69
144.01
147.92
200.91
39.632
39.787
39.944
40.0
39.5
ppm
LSK-6-178-001
500MHz
ppm

Isotope labeling experiment
Before irradiation

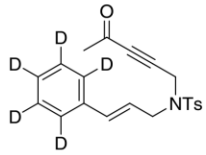

^{1}H, 300 MHz, *o*-dichlorobenzene-d$_4$

2.19

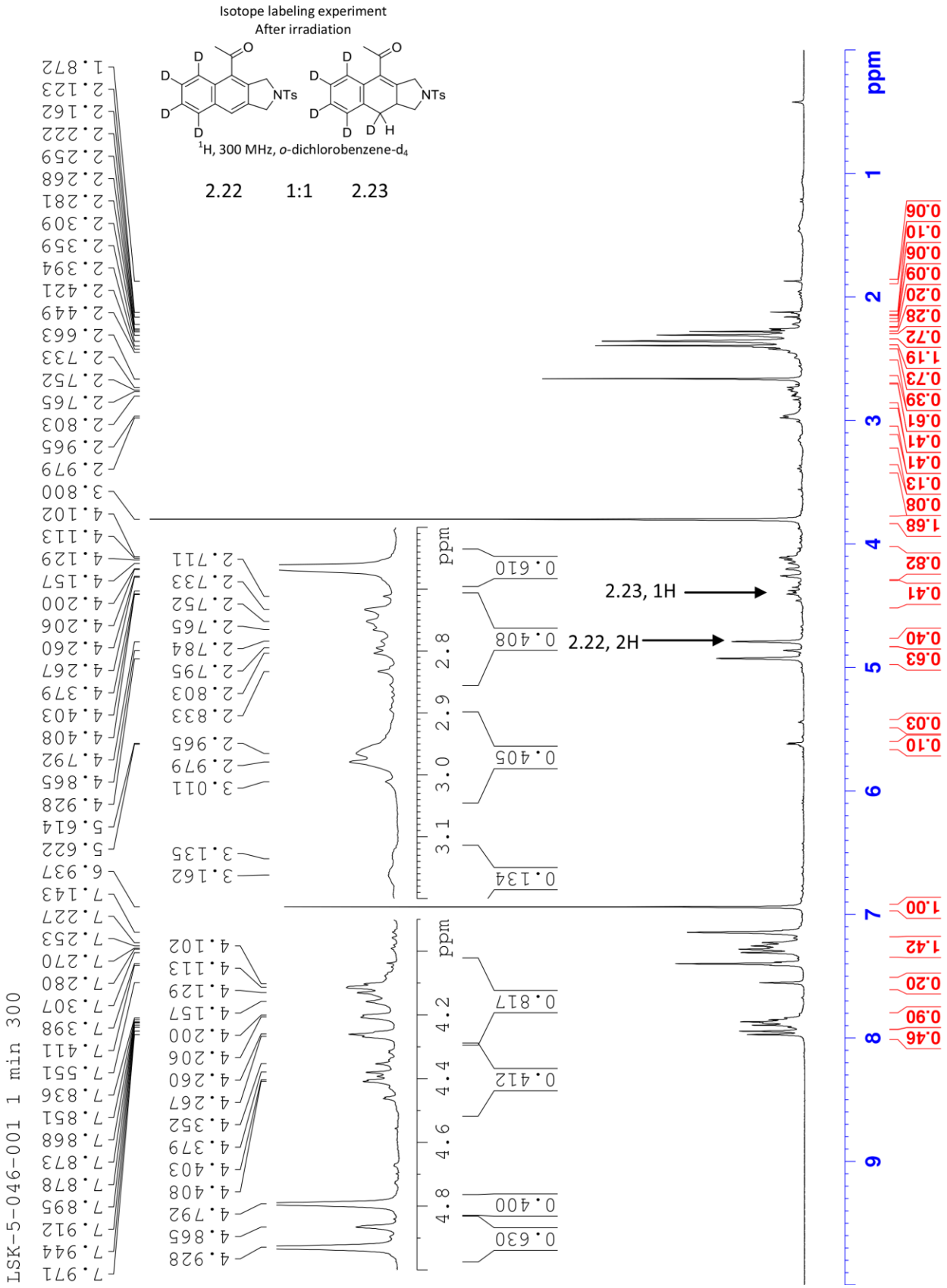
Isotope labeling experiment
After irradiation
NTs
NTs
^{1}H, 300 MHz, *o*-dichlorobenzene-d$_4$
2.22 1:1 2.23
2.23, 1H
2.22, 2H
LSK-5-046-001 1 min 300
ppm

Isotope labeling experiment
After HPLC

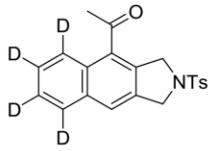

^{1}H, 300 MHz, chloroform-d

2.22

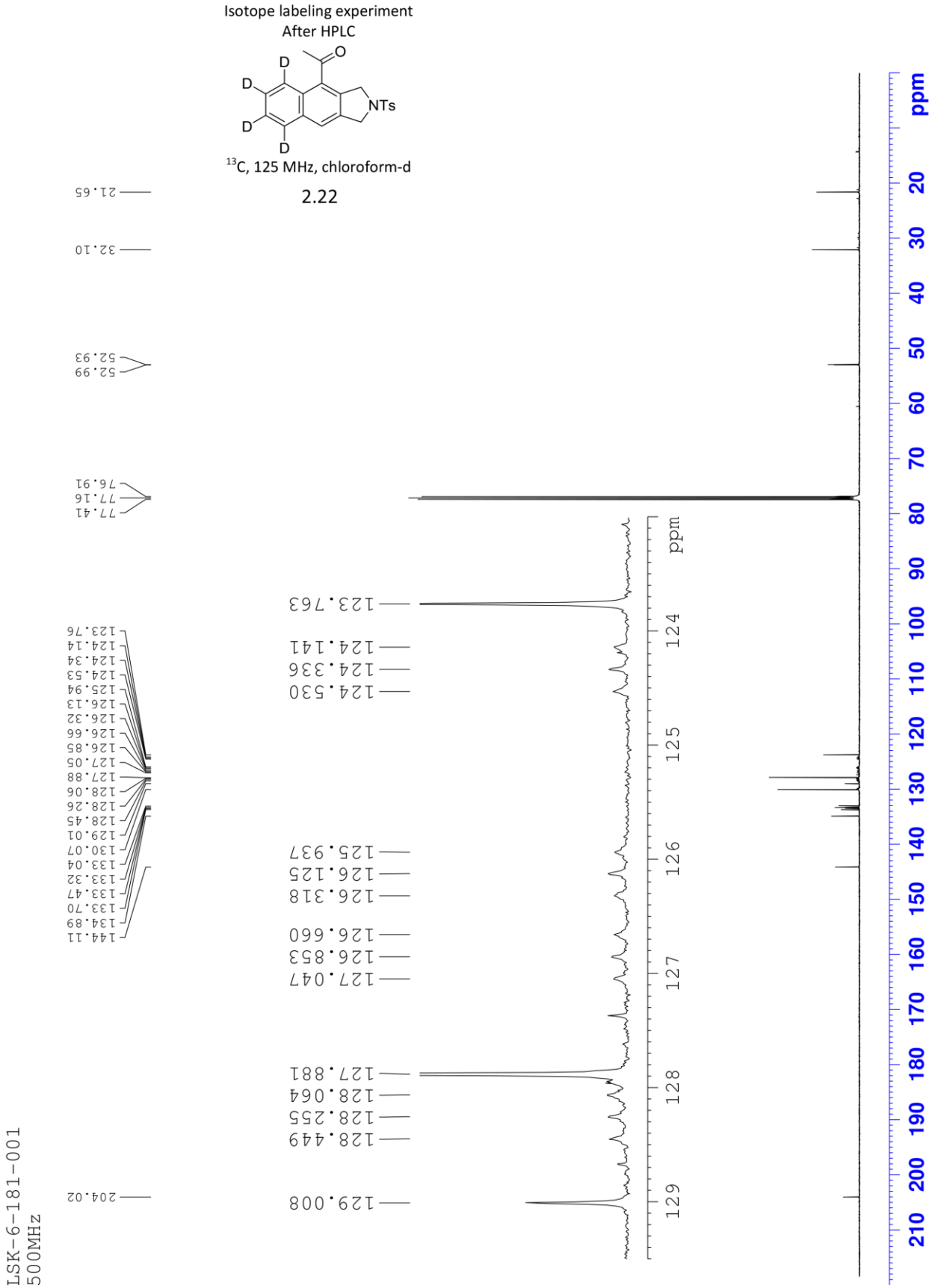
Isotope labeling experiment
After HPLC
D
D
D
D
O
NTs
^{13}C, 125 MHz, chloroform-d
2.22
LSK-6-181-001
500MHz
ppm

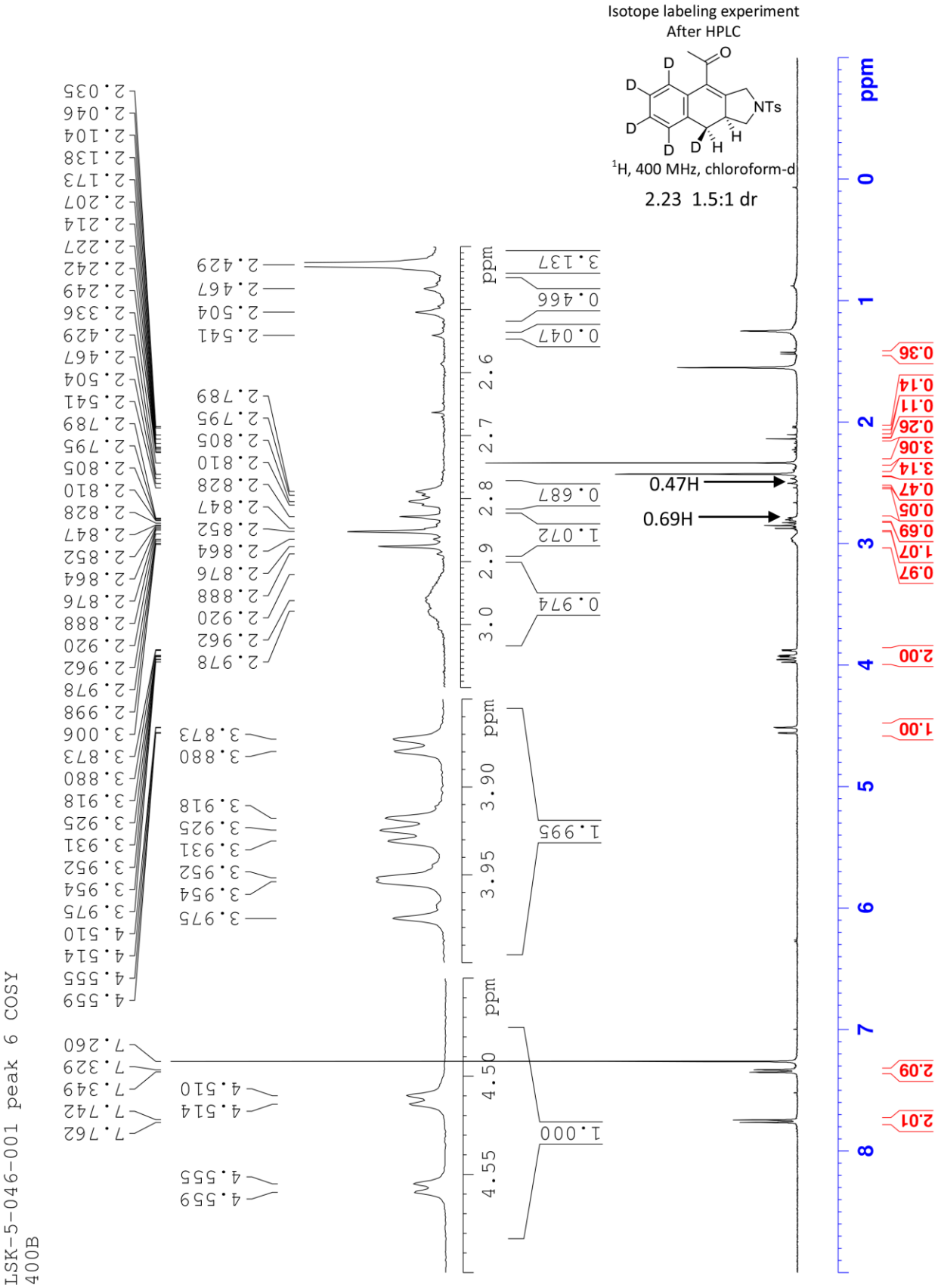
Isotope labeling experiment
After HPLC
D
D
D
D
O
NTs
D
D
H
H
1H, 400 MHz, chloroform-d
2.23 1.5:1 dr
0.47H
0.69H
ppm
LSK-5-046-001 peak 6 COSY
400B

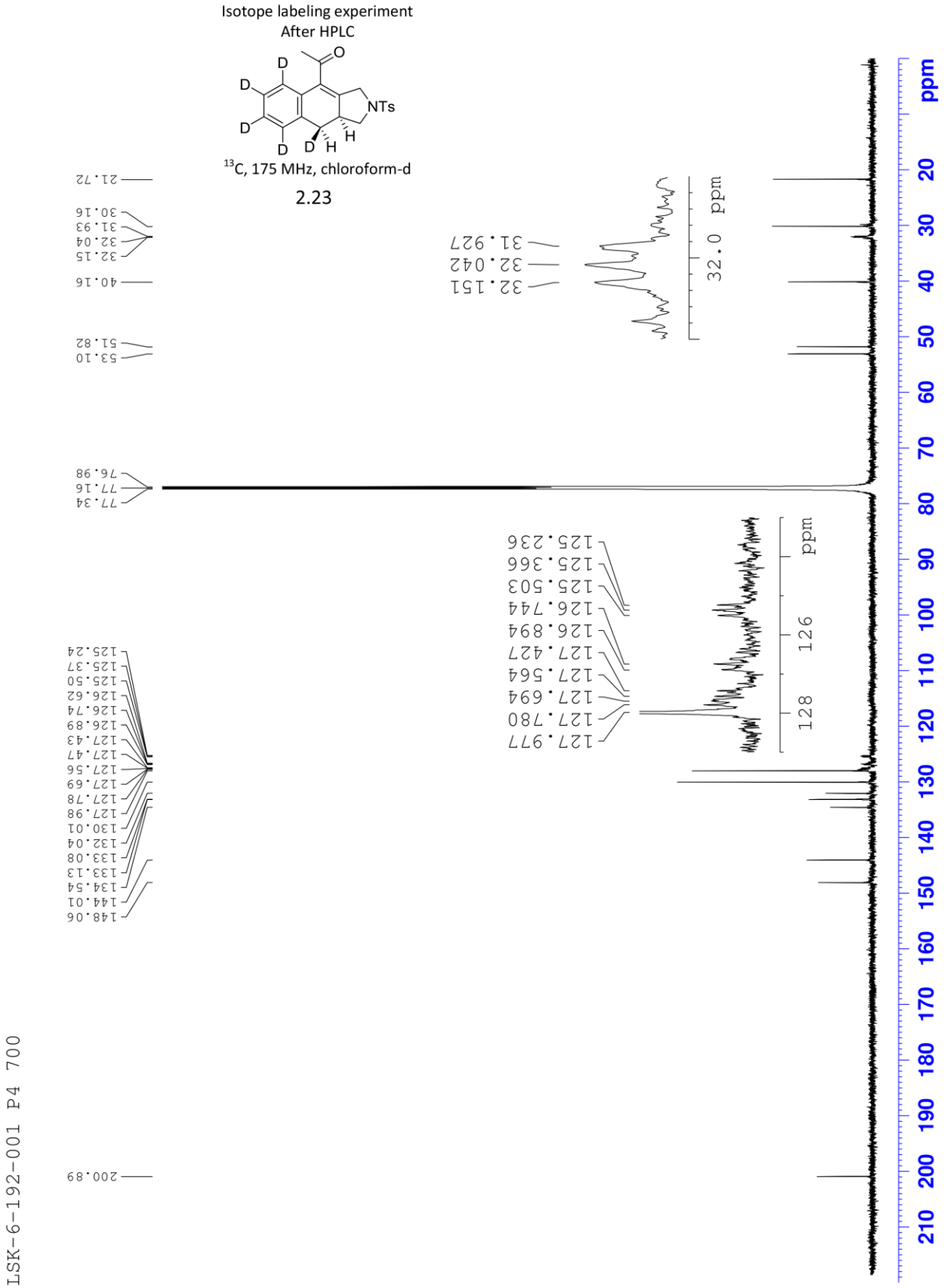
Isotope labeling experiment
After HPLC
^{13}C, 175 MHz, chloroform-d
2.23
LSK-6-192-001 P4 700
ppm

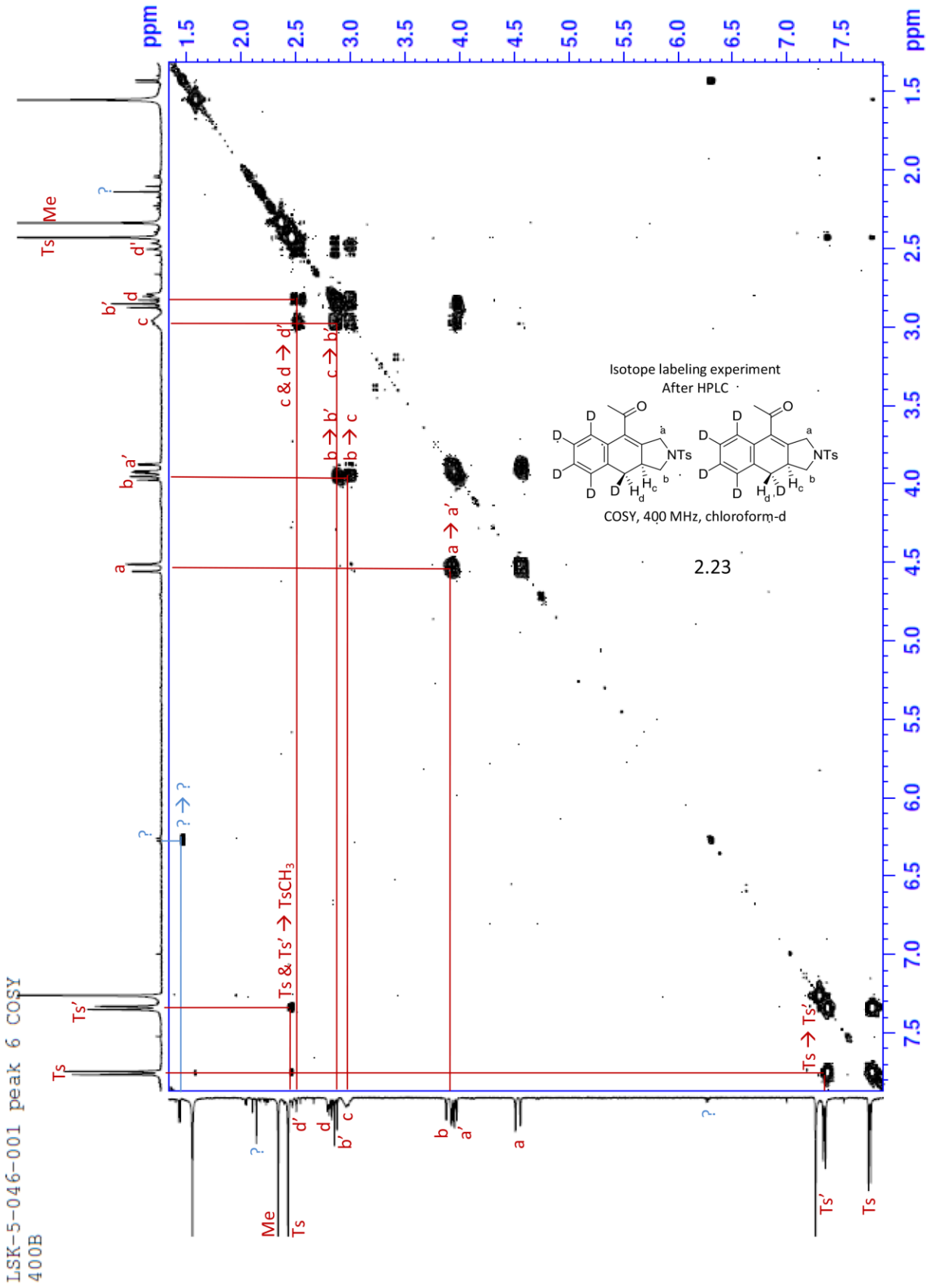
LSK-5-046-001 peak 6 COSY
400B
Isotope labeling experiment
After HPLC
COSY, 400 MHz, chloroform-d
2.23
Ts
Me
Ts'
a
a'
b
b'
c
d
d'
?
? → ?
Ts & Ts' → TsCH3
c & d → d'
c → b'
b → b'
b → c
a → a'
Ts → Ts'
NTs
D
O
ppm

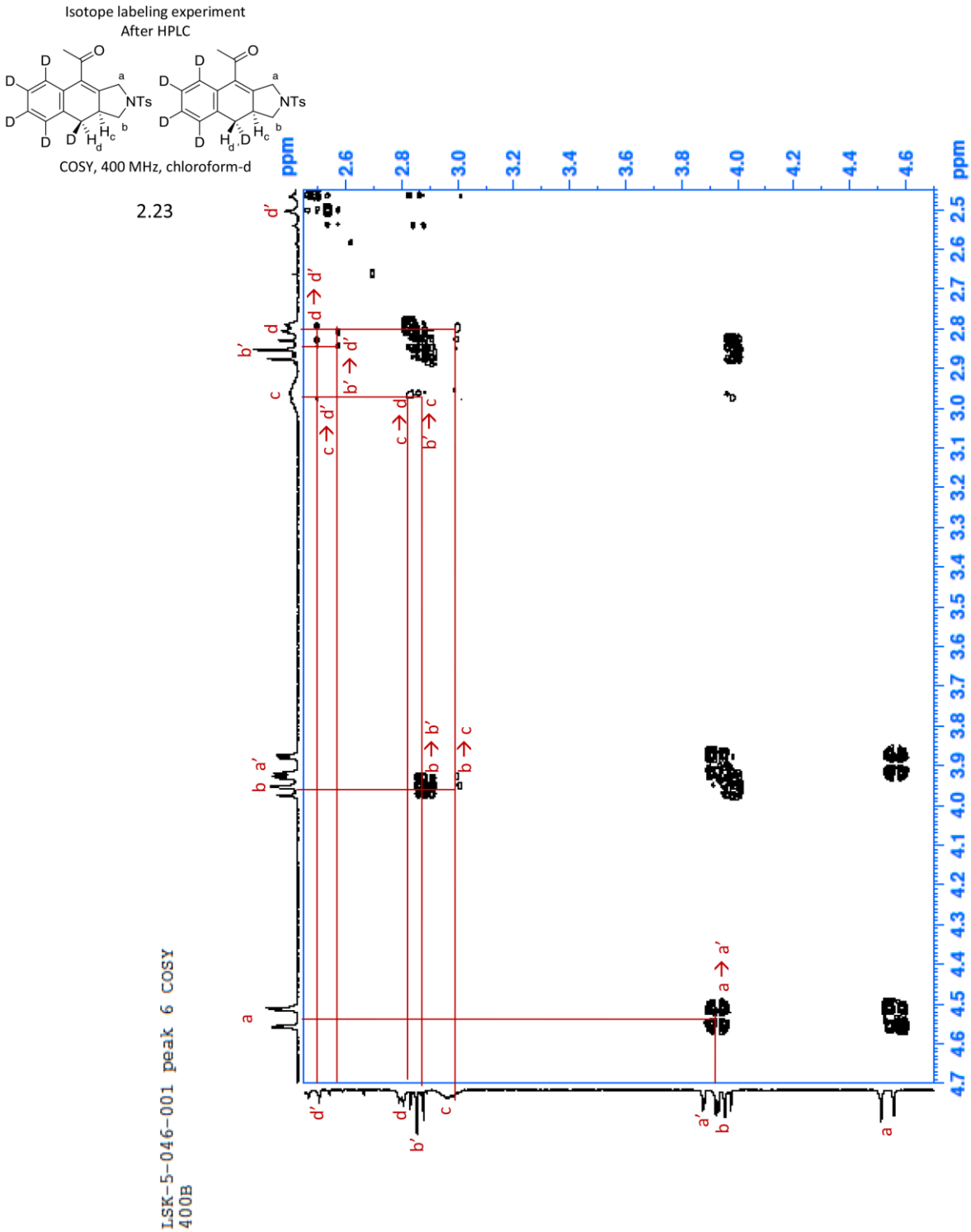
Isotope labeling experiment
After HPLC
COSY, 400 MHz, chloroform-d
2.23
ppm
LSK-5-046-001 peak 6 COSY
400B

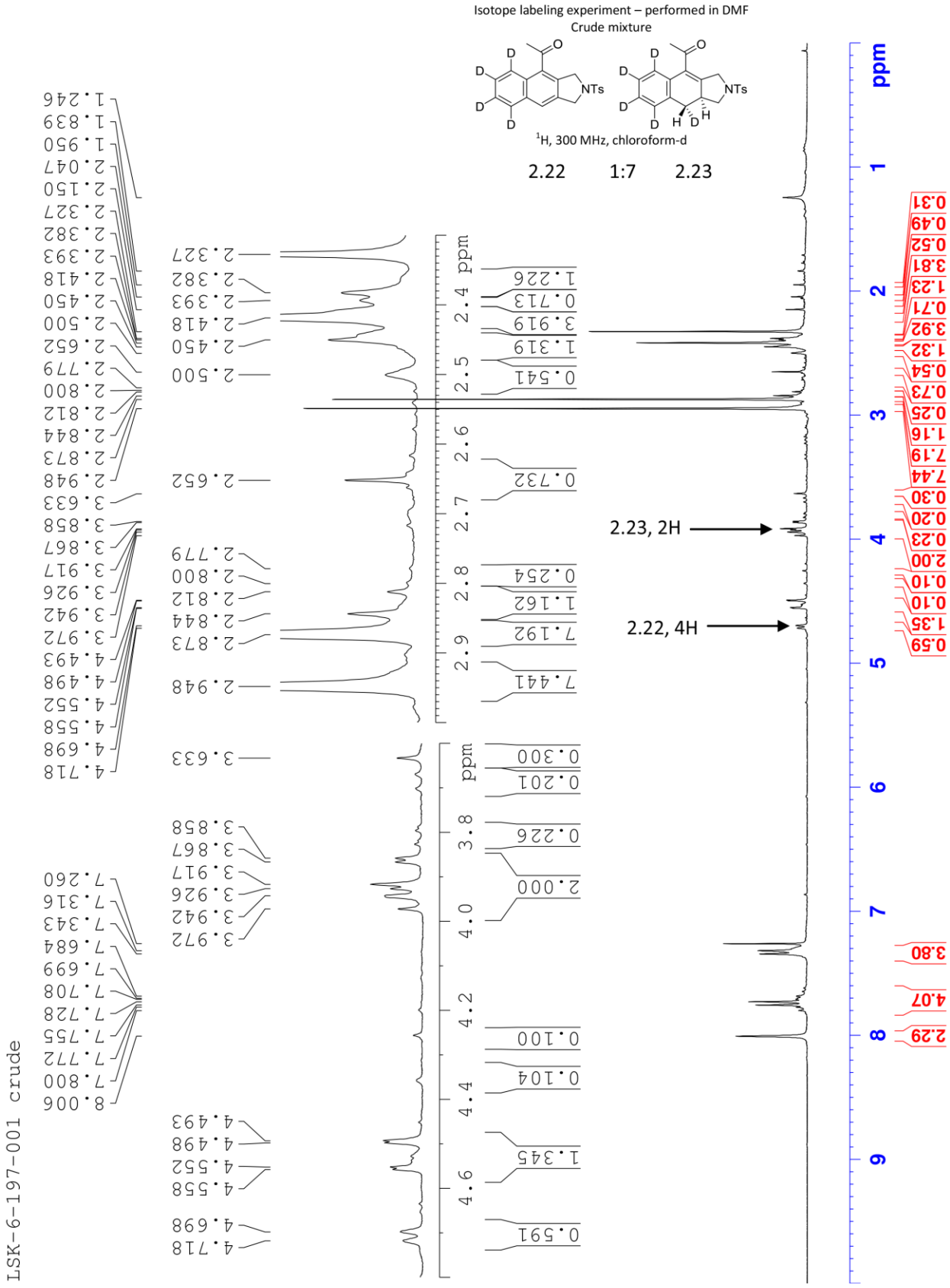
Isotope labeling experiment – performed in DMF
Crude mixture
NTs
NTs
^{1}H, 300 MHz, chloroform-d
2.22
1:7
2.23
2.23, 2H
2.22, 4H
LSK-6-197-001 crude
ppm

Isotope labeling experiment – performed in DMF
After HPLC
^{1}H, 400 MHz, chloroform-d
2.23 14:1 dr
0.95H
0.07H
LSK-6-192-001 HPLC 4 400a

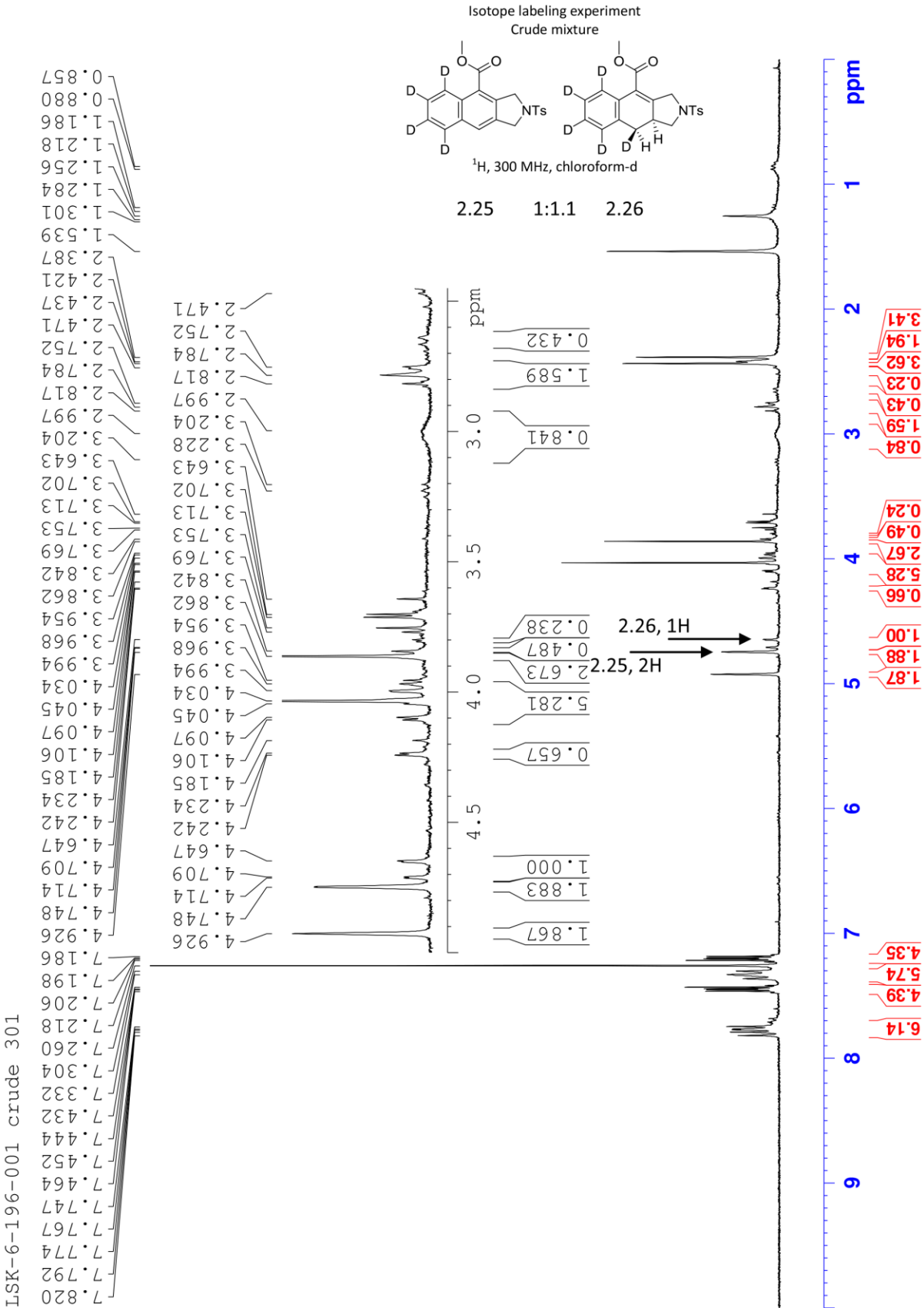
Isotope labeling experiment
Crude mixture
NTs
NTs
^{1}H, 300 MHz, chloroform-d
2.25 1:1.1 2.26
2.26, 1H
2.25, 2H
LSK-6-196-001 crude 301
ppm

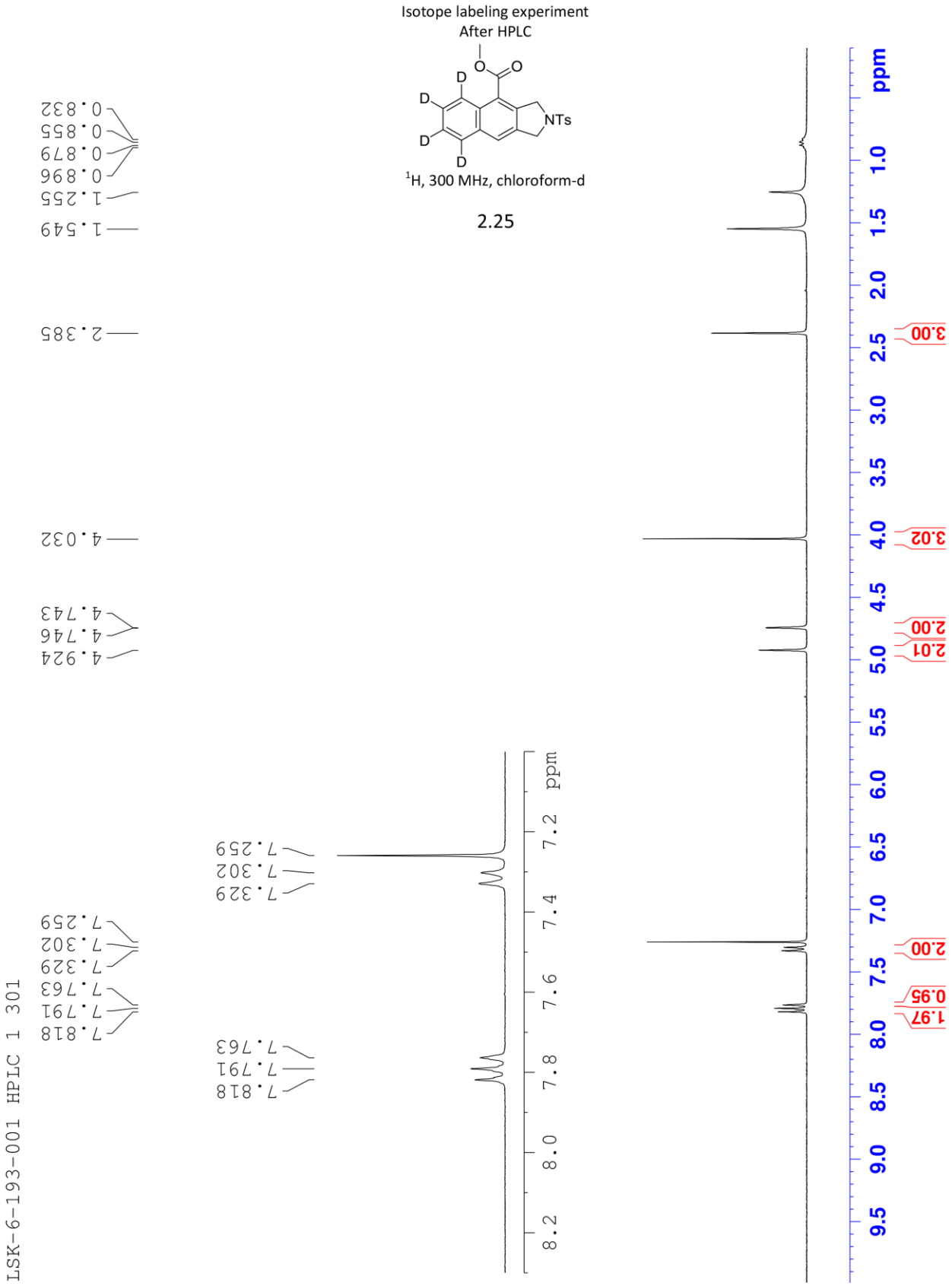
Isotope labeling experiment
After HPLC
D
D
D
D
O
O
NTs
1H, 300 MHz, chloroform-d
2.25
LSK-6-193-001 HPLC 1 301
7.818
7.791
7.763
7.329
7.302
7.259
4.924
4.746
4.743
4.032
2.385
1.549
1.255
0.896
0.879
0.855
0.832
ppm
3.00
3.02
2.00
2.01
2.00
0.95
1.97

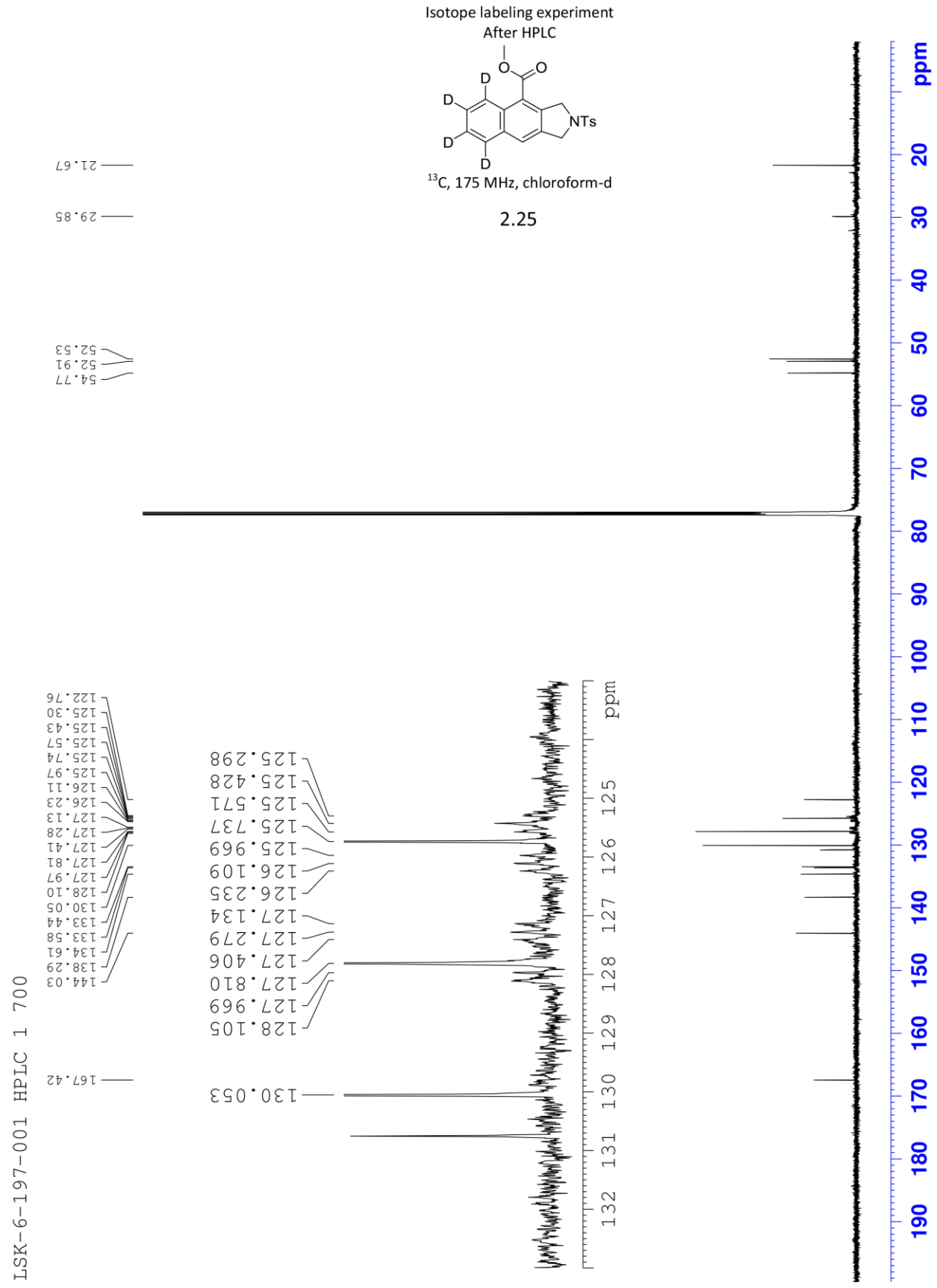
Isotope labeling experiment
After HPLC
^{13}C, 175 MHz, chloroform-d
2.25
LSK-6-197-001 HPLC 1 700
ppm

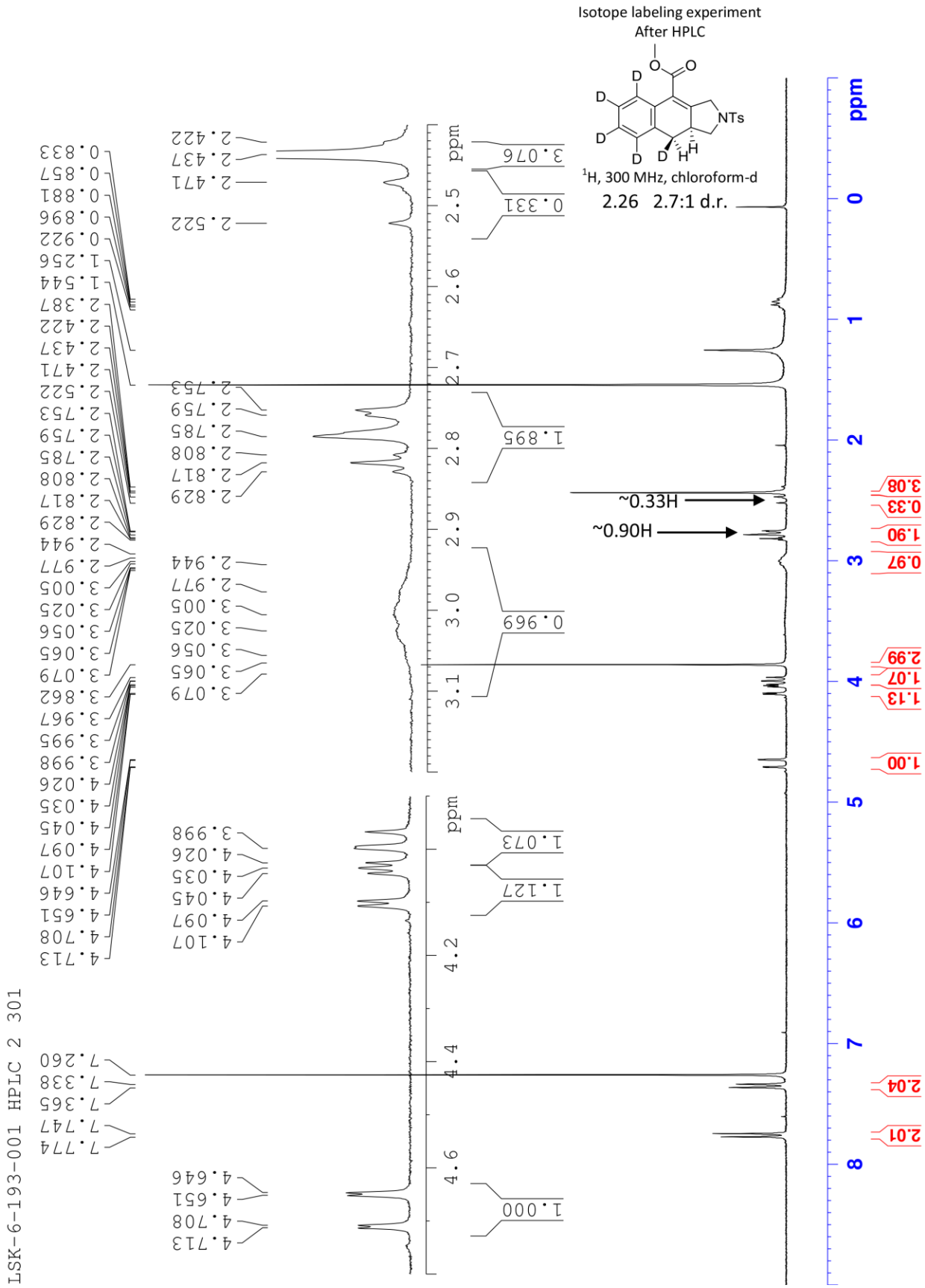
Isotope labeling experiment
After HPLC
NTs
D
H
^{1}H, 300 MHz, chloroform-d
2.26 2.7:1 d.r.
~0.33H
~0.90H
LSK-6-193-001 HPLC 2 301
ppm

Isotope labeling experiment
After HPLC

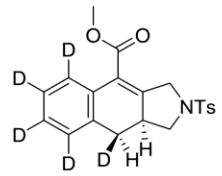

^{2}H, 700 MHz, chloroform-d

2.26 2.6:1 dr

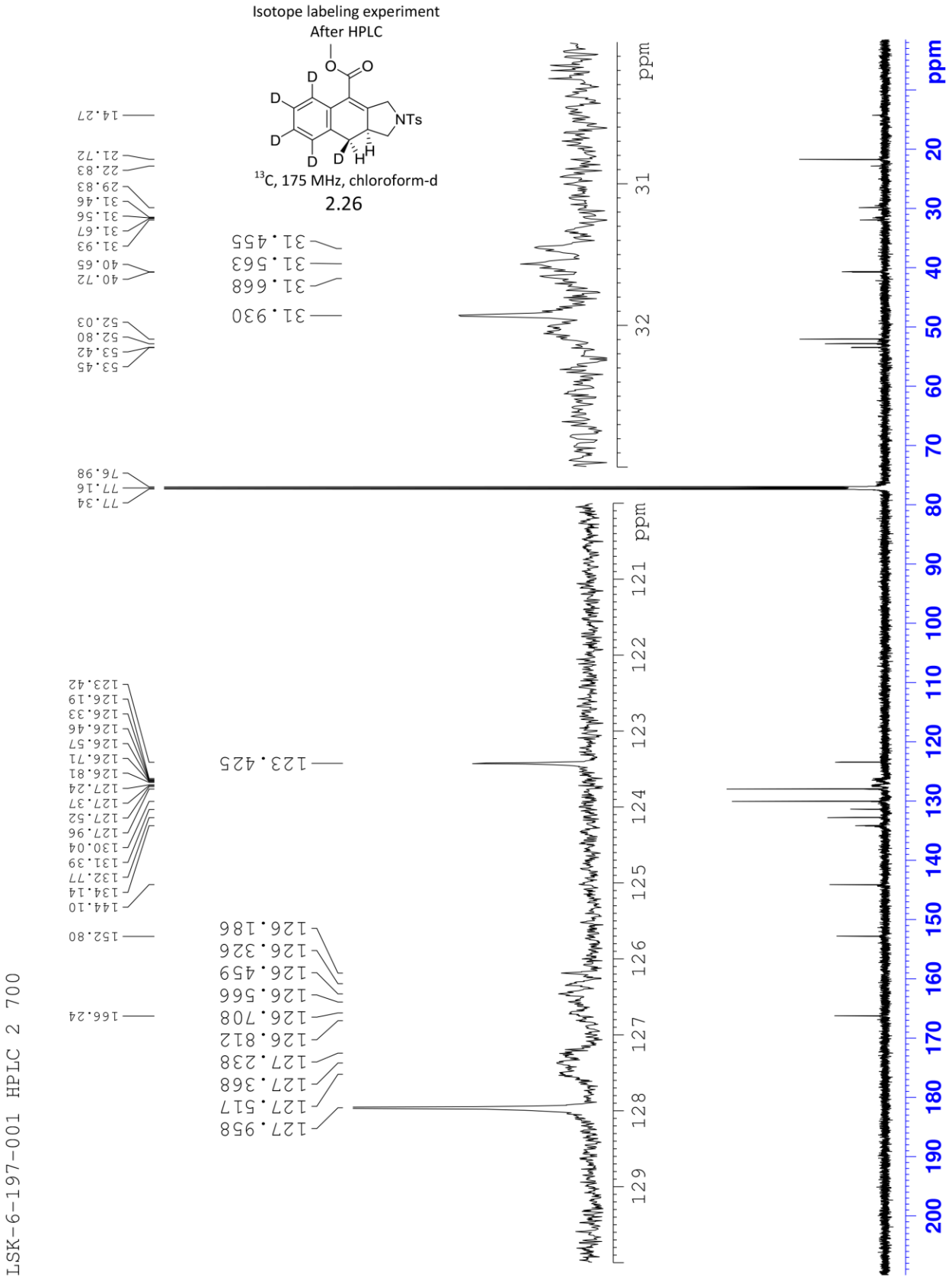
LSK-6-197-001 HPLC 2 700
Isotope labeling experiment
After HPLC
^{13}C, 175 MHz, chloroform-d
2.26
ppm

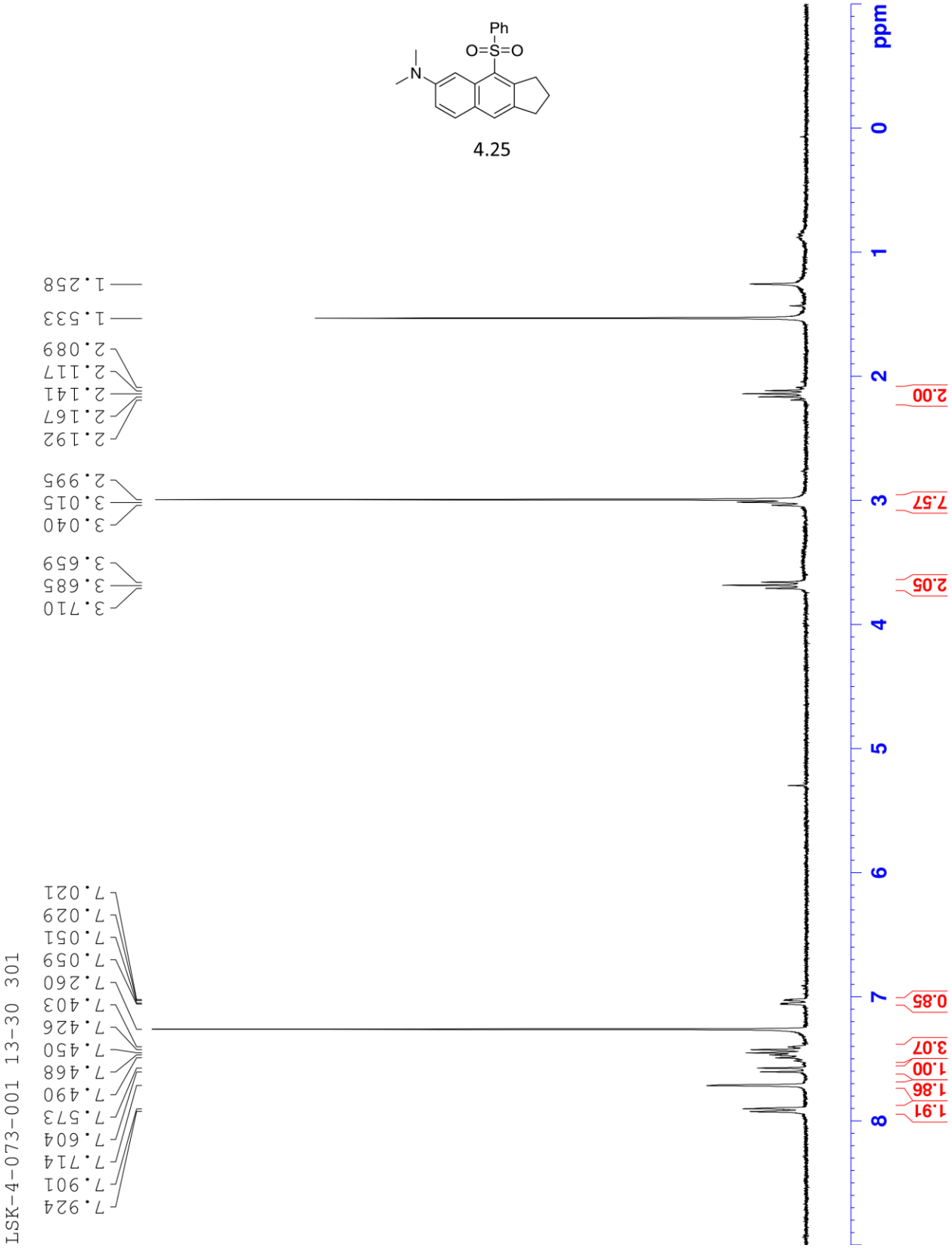
Ph
O=S=O
N
4.25
LSK-4-073-001 13-30 301
7.924
7.901
7.714
7.604
7.573
7.490
7.468
7.450
7.426
7.403
7.260
7.059
7.051
7.029
7.021
3.710
3.685
3.659
3.040
3.015
2.995
2.192
2.167
2.141
2.117
2.089
1.533
1.258
ppm
0
1
2
3
4
5
6
7
8
2.00
7.57
2.05
0.85
3.07
1.00
1.86
1.91

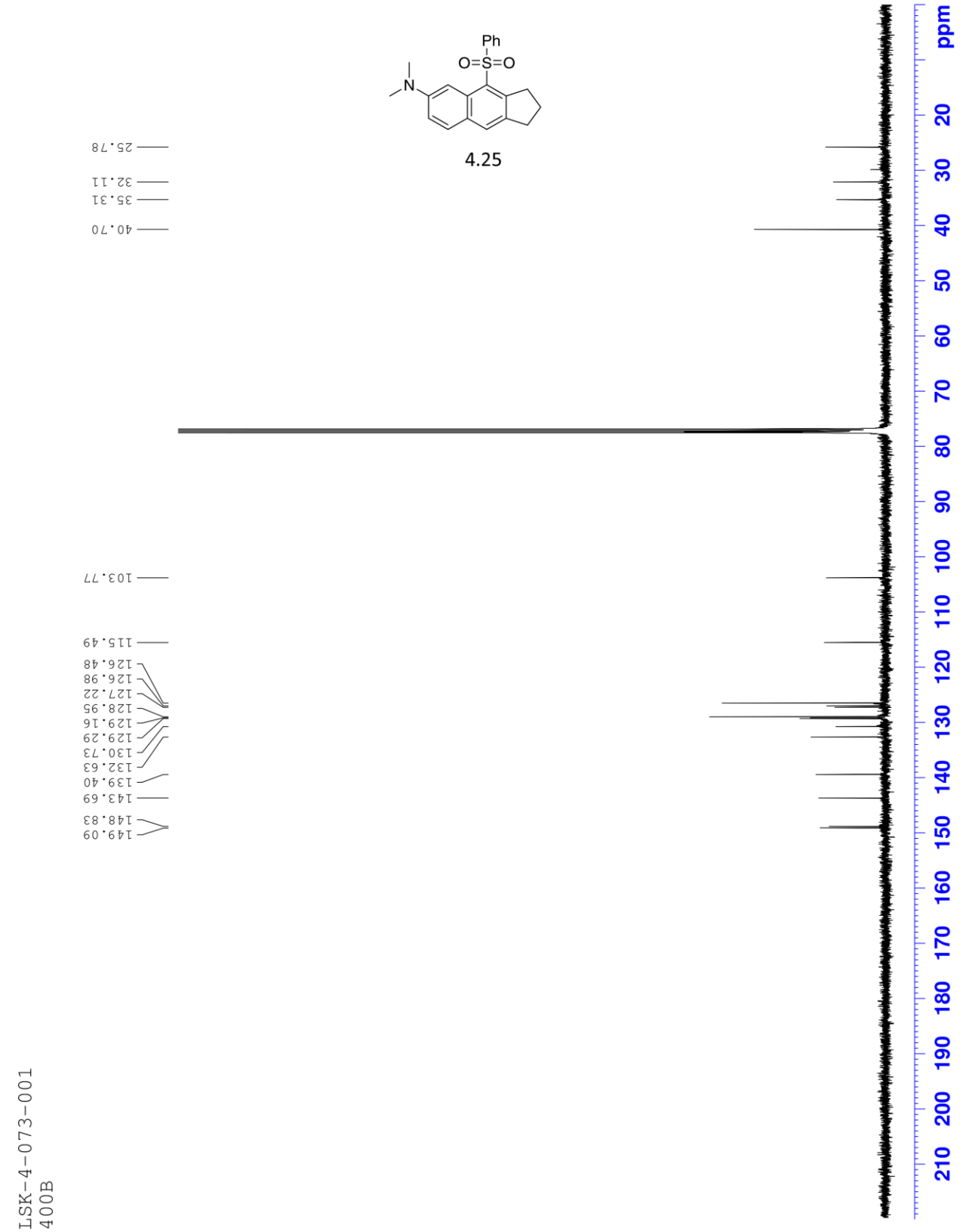
Ph
O=S=O
N
4.25
25.78
32.11
35.31
40.70
103.77
115.49
126.48
126.98
127.22
128.95
129.16
129.29
130.73
132.63
139.40
143.69
148.83
149.09
ppm
20
30
40
50
60
70
80
90
100
110
120
130
140
150
160
170
180
190
200
210
LSK-4-073-001
400B

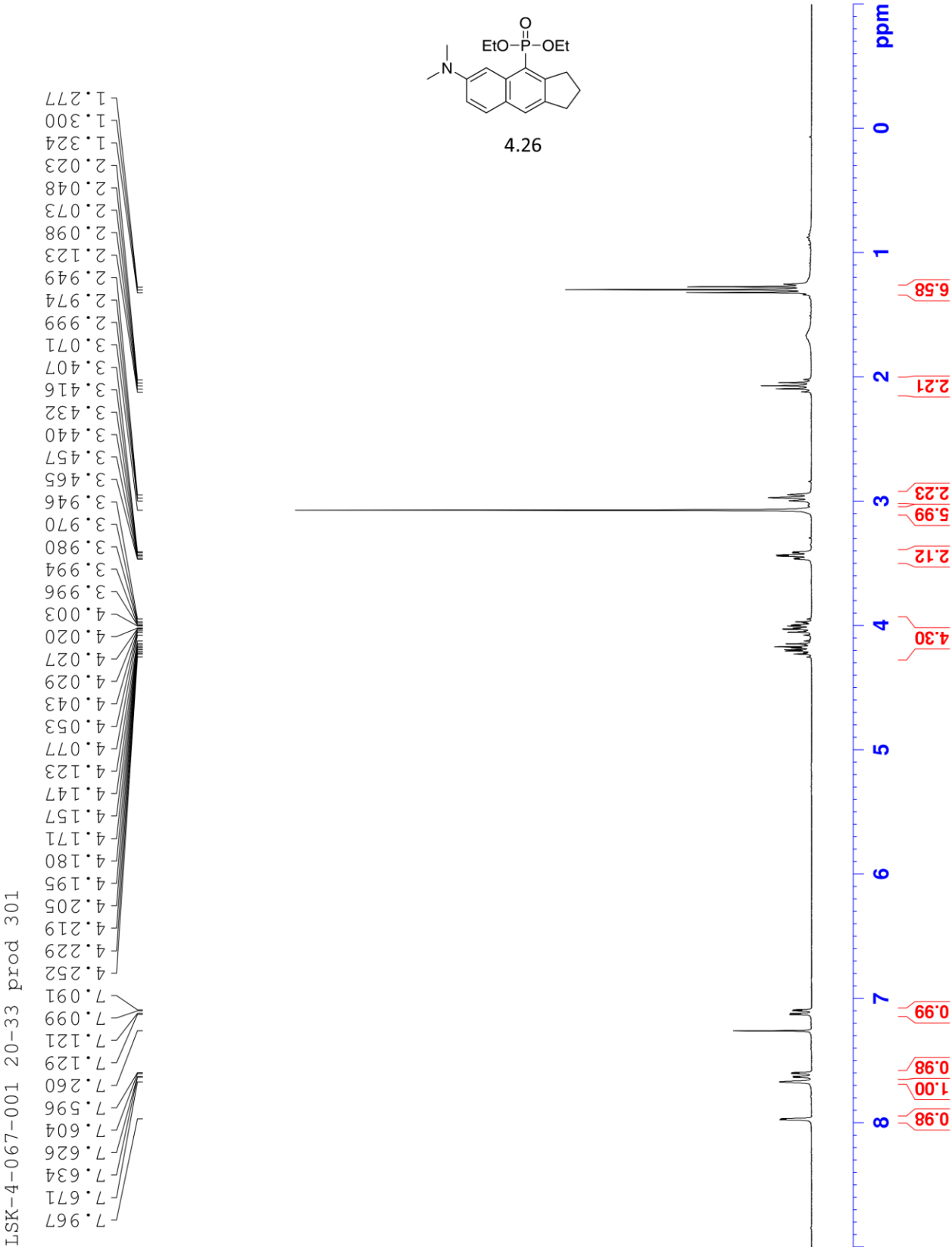
LSK-4-067-001 20-33 prod 301
1.277
1.300
1.324
2.023
2.048
2.073
2.098
2.123
2.949
2.974
2.999
3.071
3.407
3.416
3.432
3.440
3.457
3.465
3.946
3.970
3.980
3.994
3.996
4.003
4.020
4.027
4.029
4.043
4.053
4.077
4.123
4.147
4.157
4.171
4.180
4.195
4.205
4.219
4.229
4.252
7.091
7.099
7.121
7.129
7.260
7.596
7.604
7.626
7.634
7.671
7.967
EtO–P–OEt
O
N
4.26
ppm
0
1
2
3
4
5
6
7
8
6.58
2.21
2.23
5.99
2.12
4.30
0.99
0.98
1.00
0.98

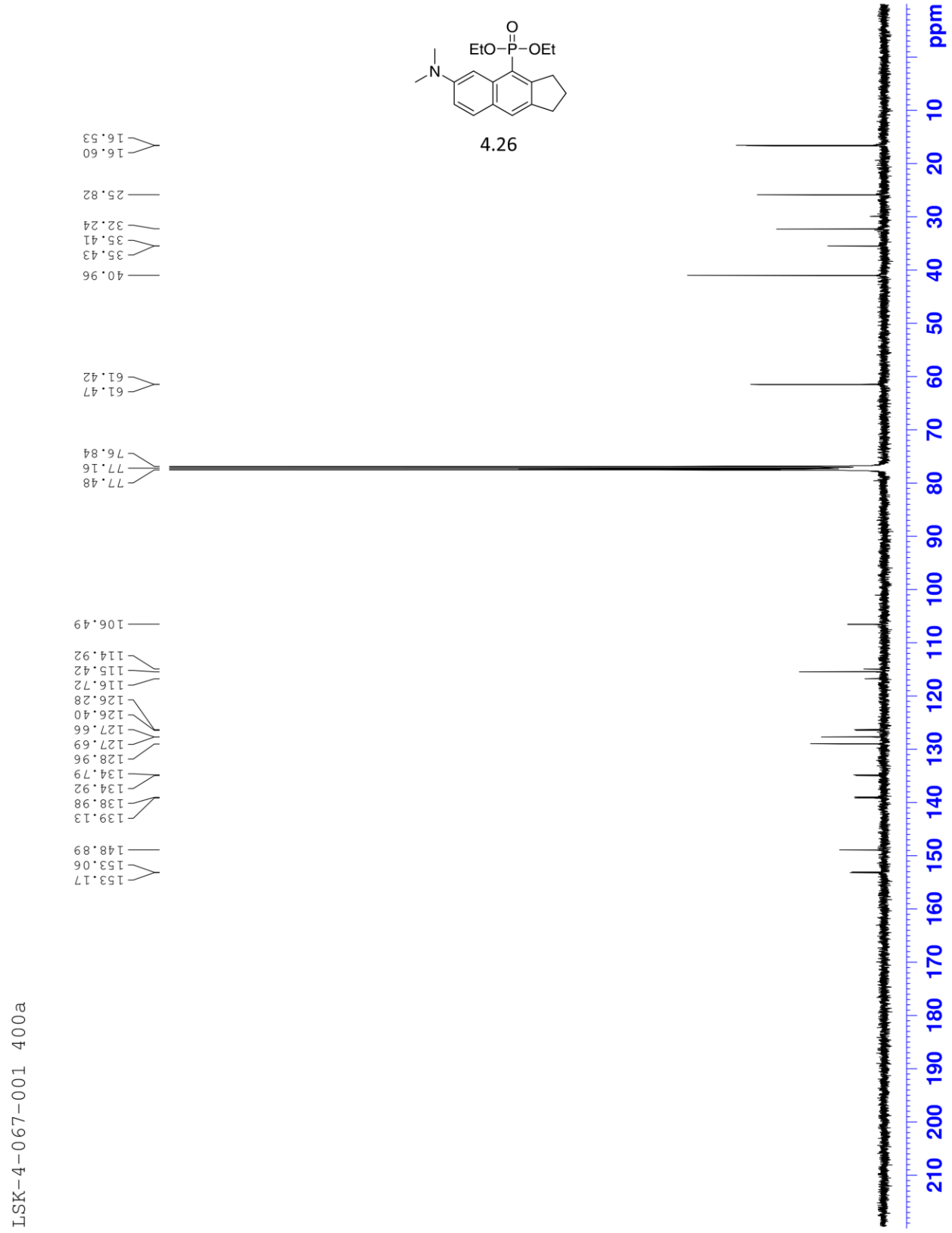
LSK-4-067-001 400a
4.26
EtO–P–OEt
O
N
16.53
16.60
25.82
32.24
35.41
35.43
40.96
61.42
61.47
76.84
77.16
77.48
106.49
114.92
115.42
116.72
126.28
126.40
127.66
127.69
128.96
134.79
134.92
138.98
139.13
148.89
153.06
153.17
ppm
10
20
30
40
50
60
70
80
90
100
110
120
130
140
150
160
170
180
190
200
210

LSK-4-099-001 400a

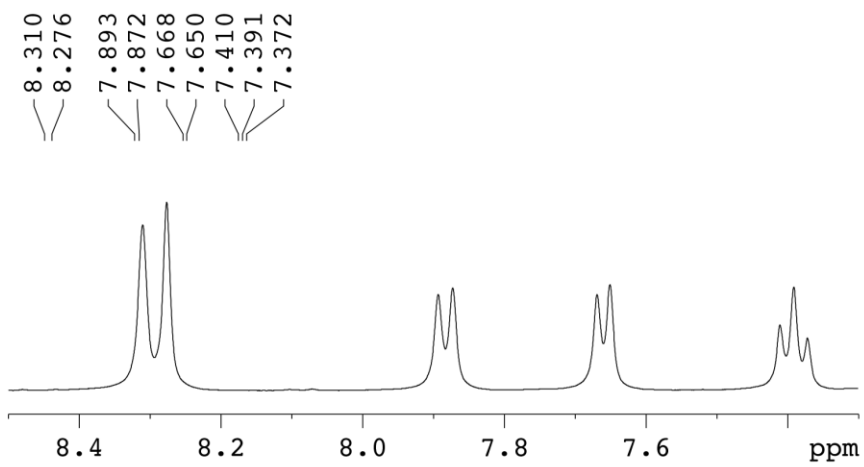

4.33

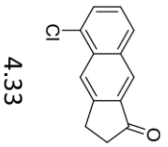

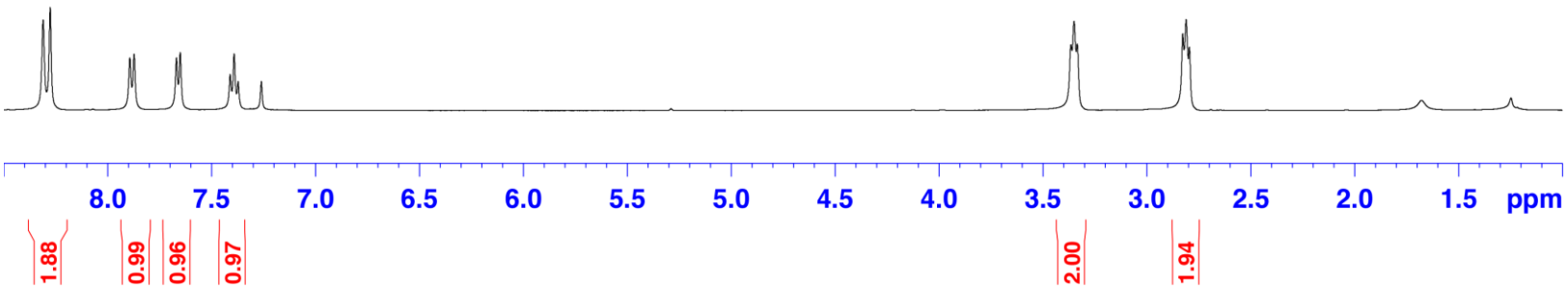

LSK-4-099-001 400a

149.13
135.31
134.30
133.48
131.73
129.60
128.70
125.89
124.58
121.78
36.93
25.63

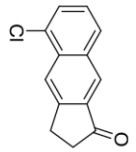

4.33

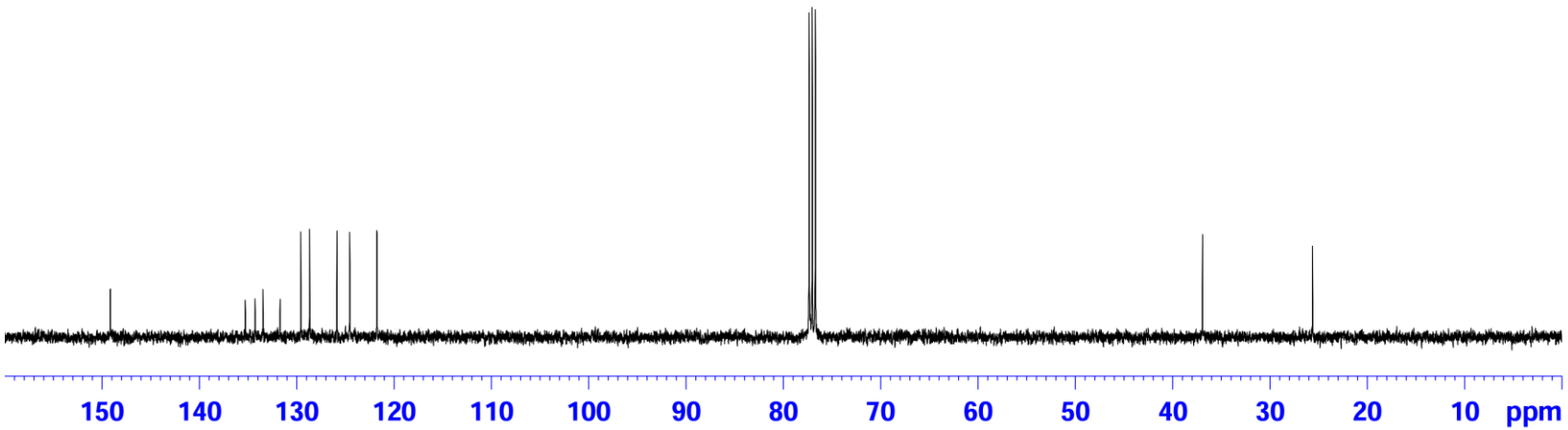

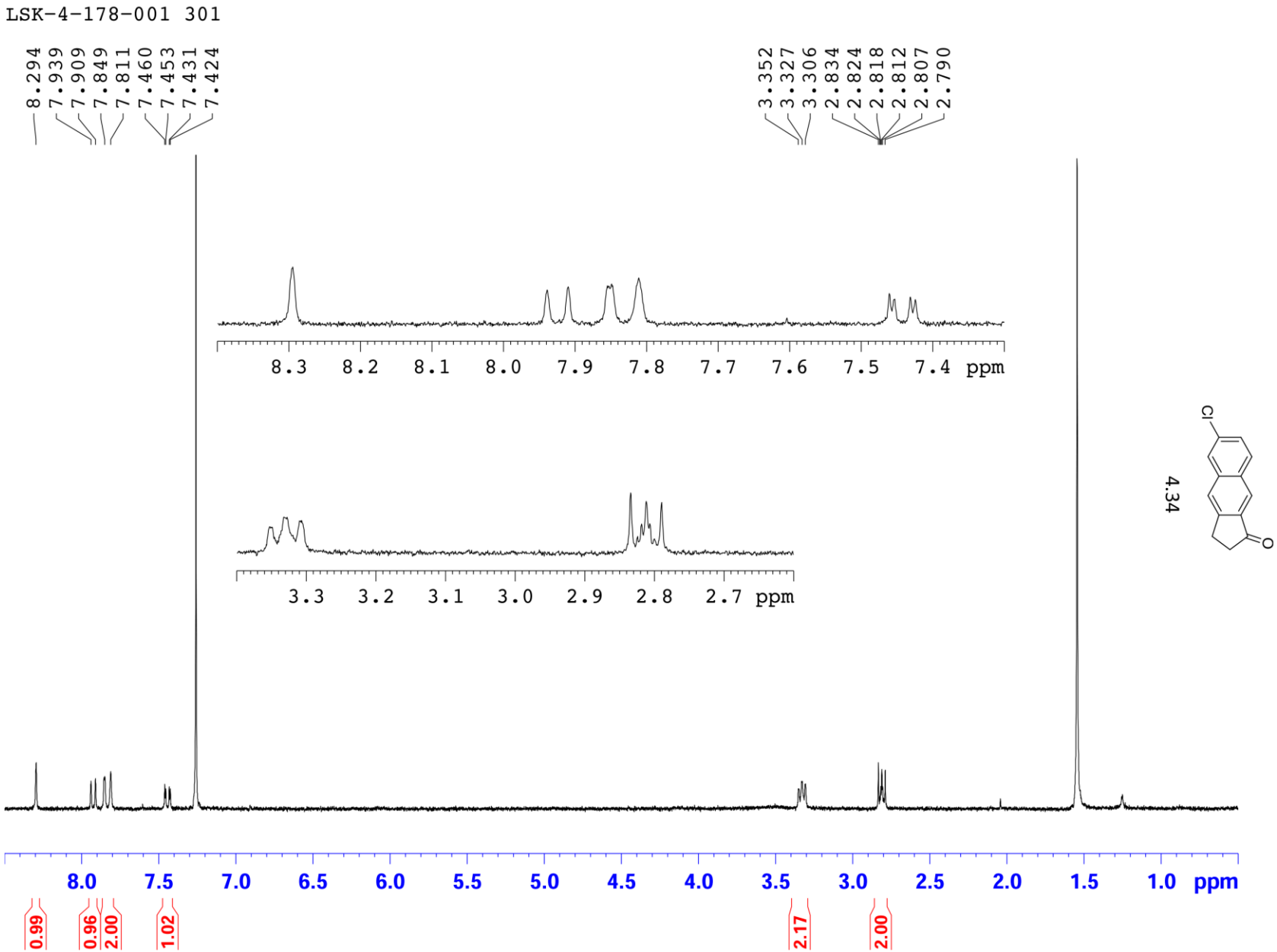
LSK-4-178-001 301
8.294
7.939
7.909
7.849
7.811
7.460
7.453
7.431
7.424
3.352
3.327
3.306
2.834
2.824
2.818
2.812
2.807
2.790
8.3 8.2 8.1 8.0 7.9 7.8 7.7 7.6 7.5 7.4 ppm
3.3 3.2 3.1 3.0 2.9 2.8 2.7 ppm
Cl
O
4.34
8.0 7.5 7.0 6.5 6.0 5.5 5.0 4.5 4.0 3.5 3.0 2.5 2.0 1.5 1.0 ppm
0.99
0.96
2.00
1.02
2.17
2.00

LSK-4-178-001
400B

206.79
149.05
137.58
135.00
134.54
131.78
130.52
127.18
126.43
124.25
124.00
36.85
25.35

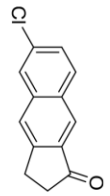

4.34

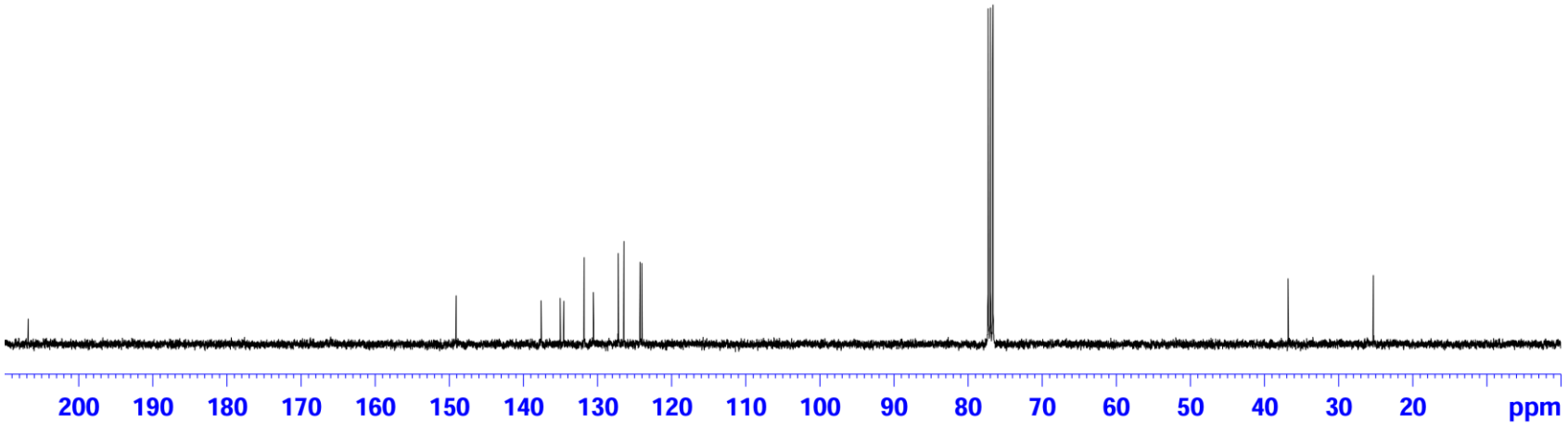

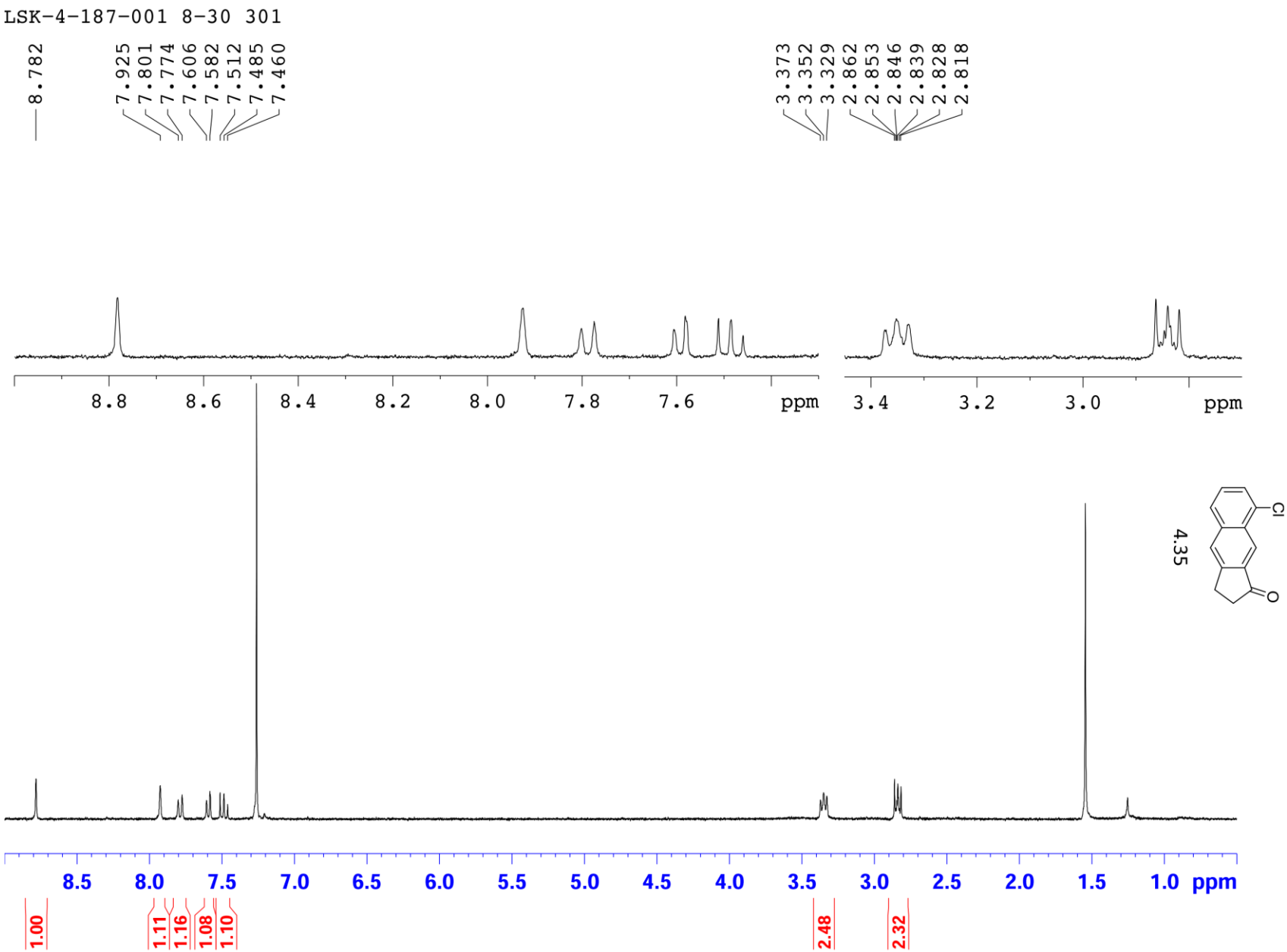
LSK-4-187-001 8-30 301
8.782
7.925
7.801
7.774
7.606
7.582
7.512
7.485
7.460
3.373
3.352
3.329
2.862
2.853
2.846
2.839
2.828
2.818
8.8
8.6
8.4
8.2
8.0
7.8
7.6
ppm
3.4
3.2
3.0
ppm
4.35
Cl
O
8.5
8.0
7.5
7.0
6.5
6.0
5.5
5.0
4.5
4.0
3.5
3.0
2.5
2.0
1.5
1.0
ppm
1.00
1.11
1.16
1.08
1.10
2.48
2.32

LSK-4-187-001 8′-30′ 400a

214.20
206.94
148.70
138.12
135.48
134.41
129.98
128.25
126.94
126.31
125.34
121.24
36.88
25.23

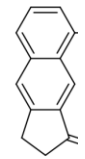

4.35

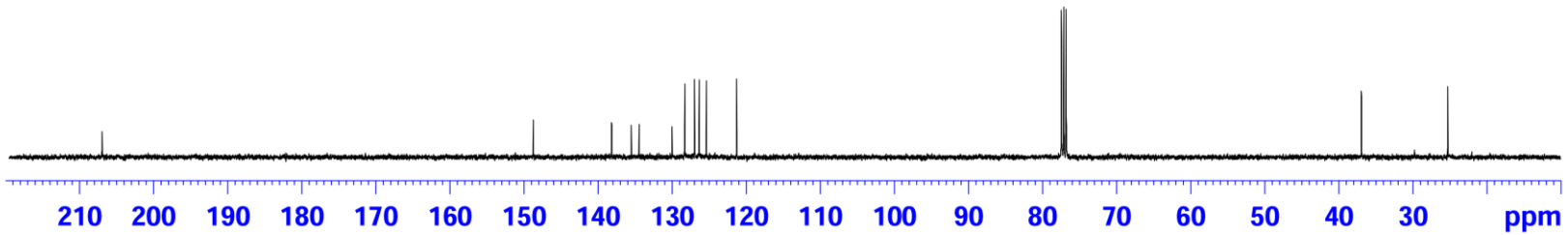

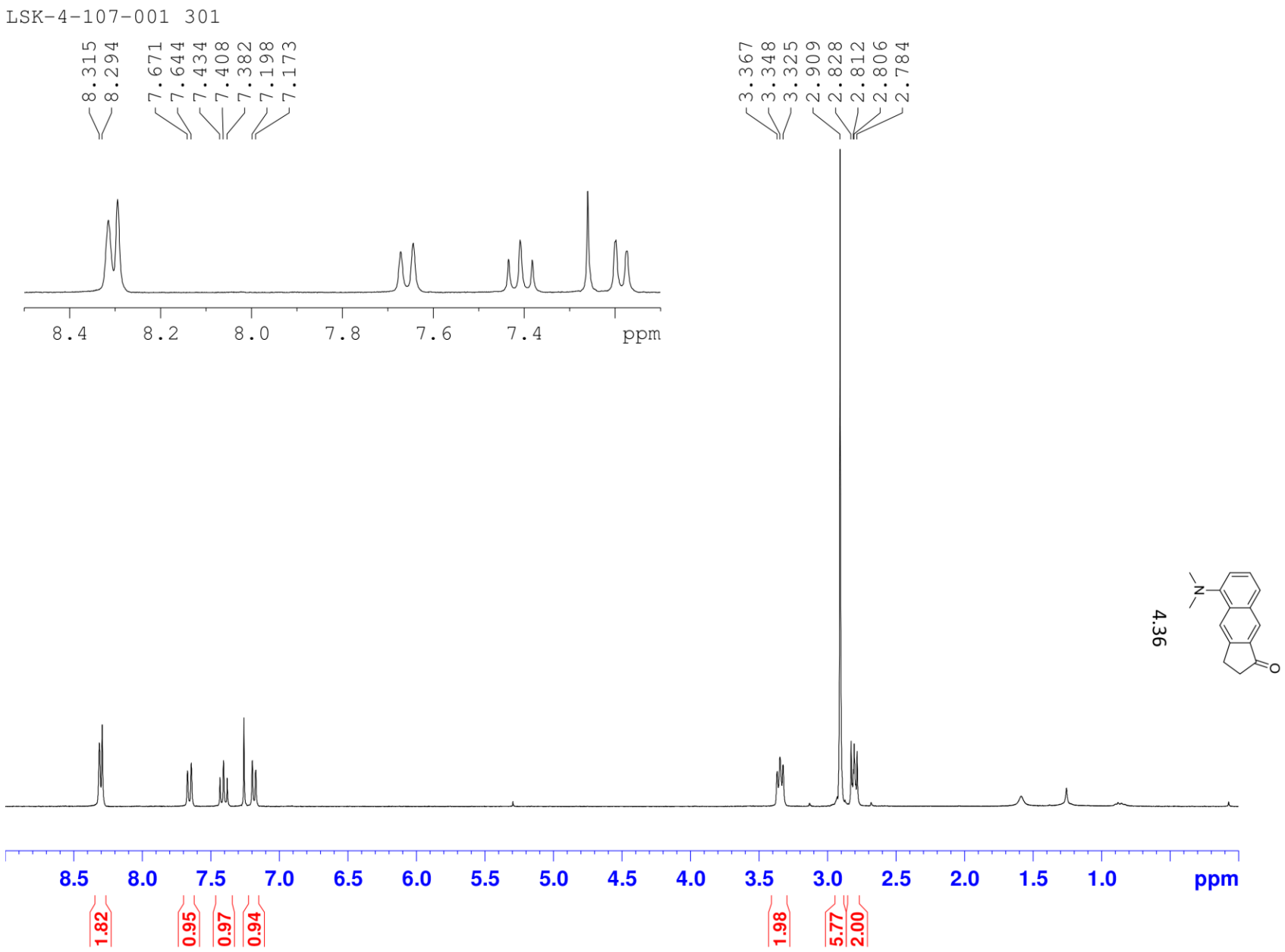
LSK-4-107-001 301
8.315
8.294
7.671
7.644
7.434
7.408
7.382
7.198
7.173
3.367
3.348
3.325
2.909
2.828
2.812
2.806
2.784
8.4
8.2
8.0
7.8
7.6
7.4
ppm
4.36
8.5
8.0
7.5
7.0
6.5
6.0
5.5
5.0
4.5
4.0
3.5
3.0
2.5
2.0
1.5
1.0
ppm
1.82
0.95
0.97
0.94
1.98
5.77
2.00

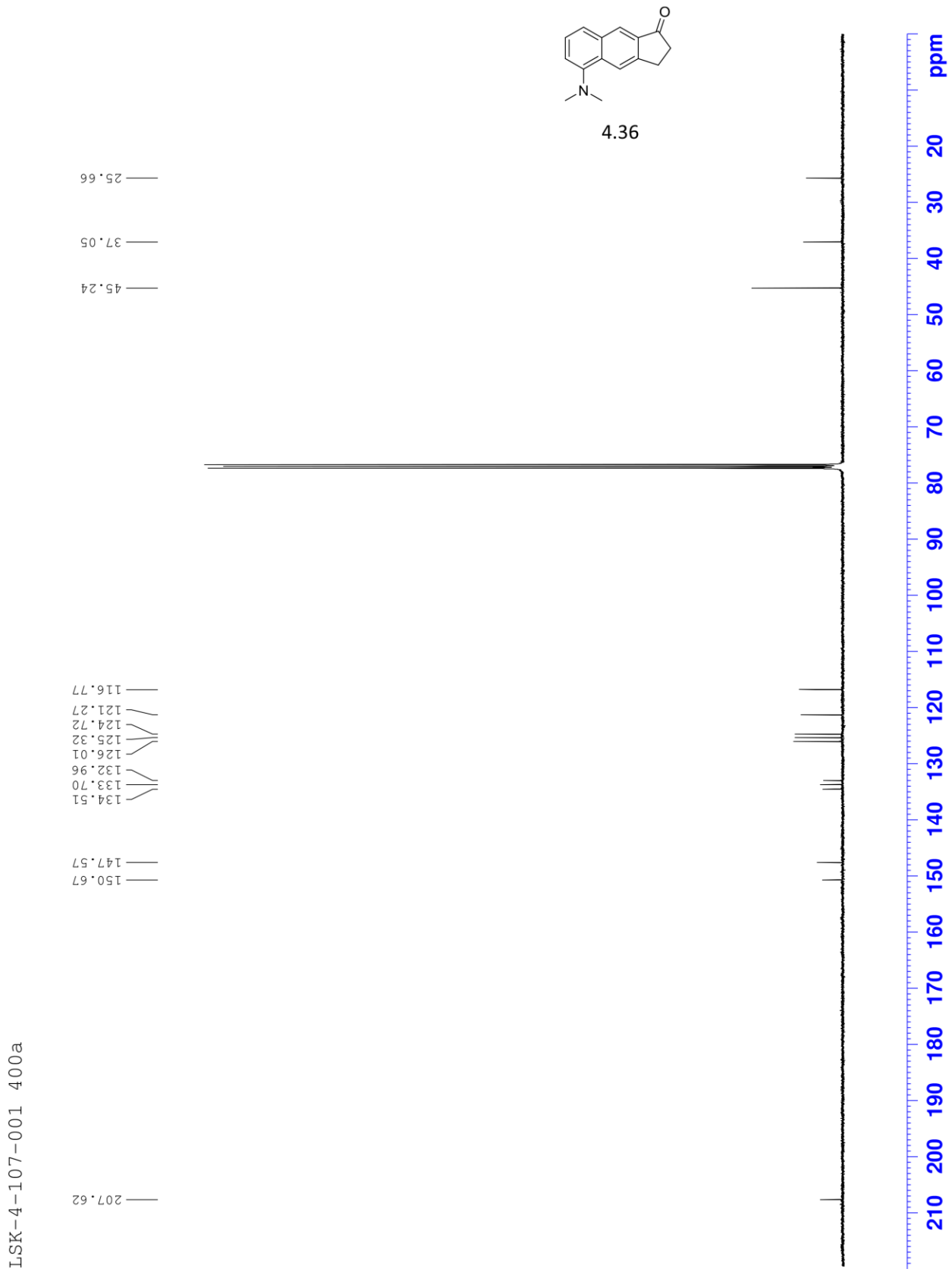
LSK-4-107-001 400a
207.62
150.67
147.57
134.51
133.70
132.96
126.01
125.32
124.72
121.27
116.77
45.24
37.05
25.66
4.36
ppm

LSK-4-184-001 301

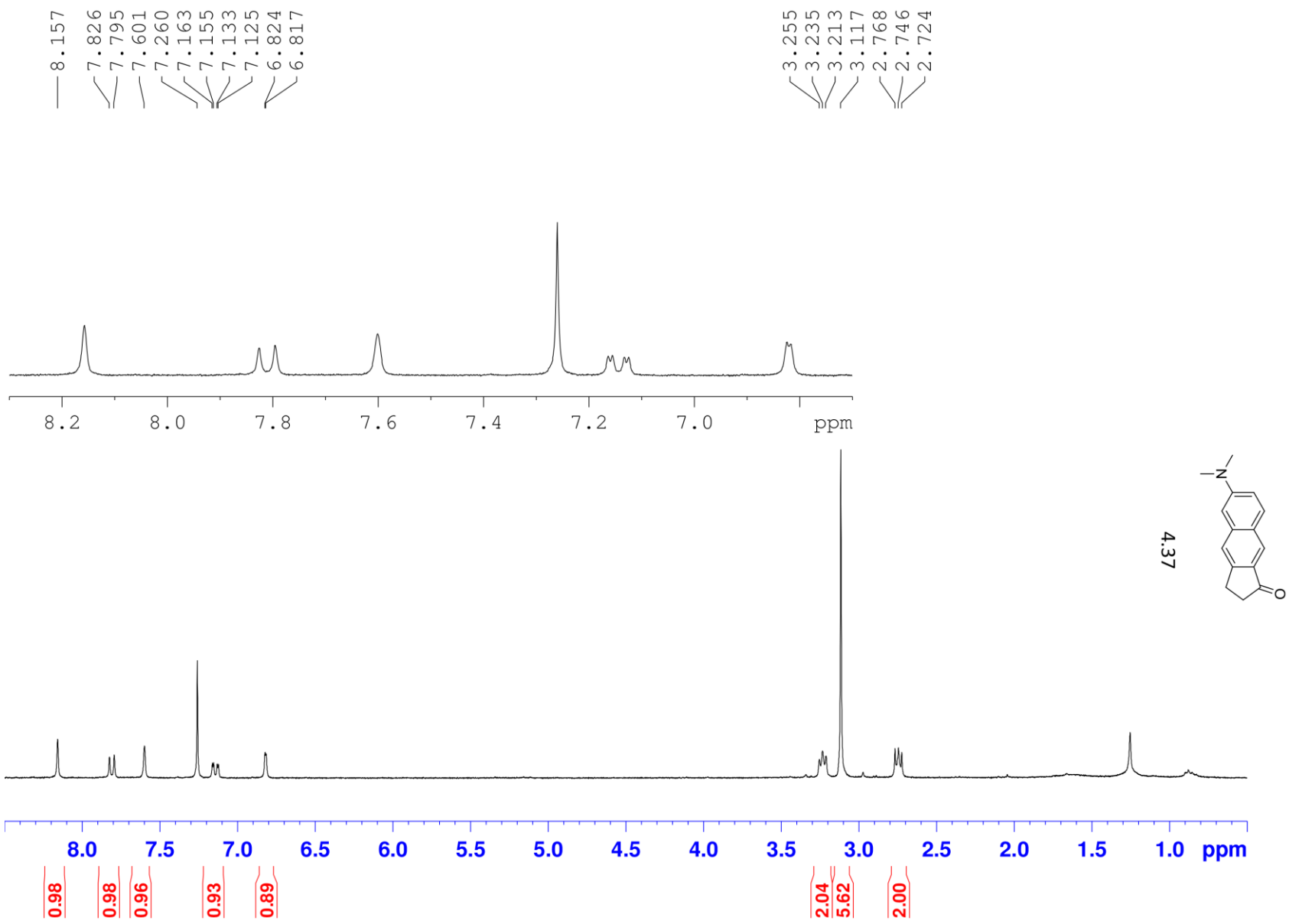

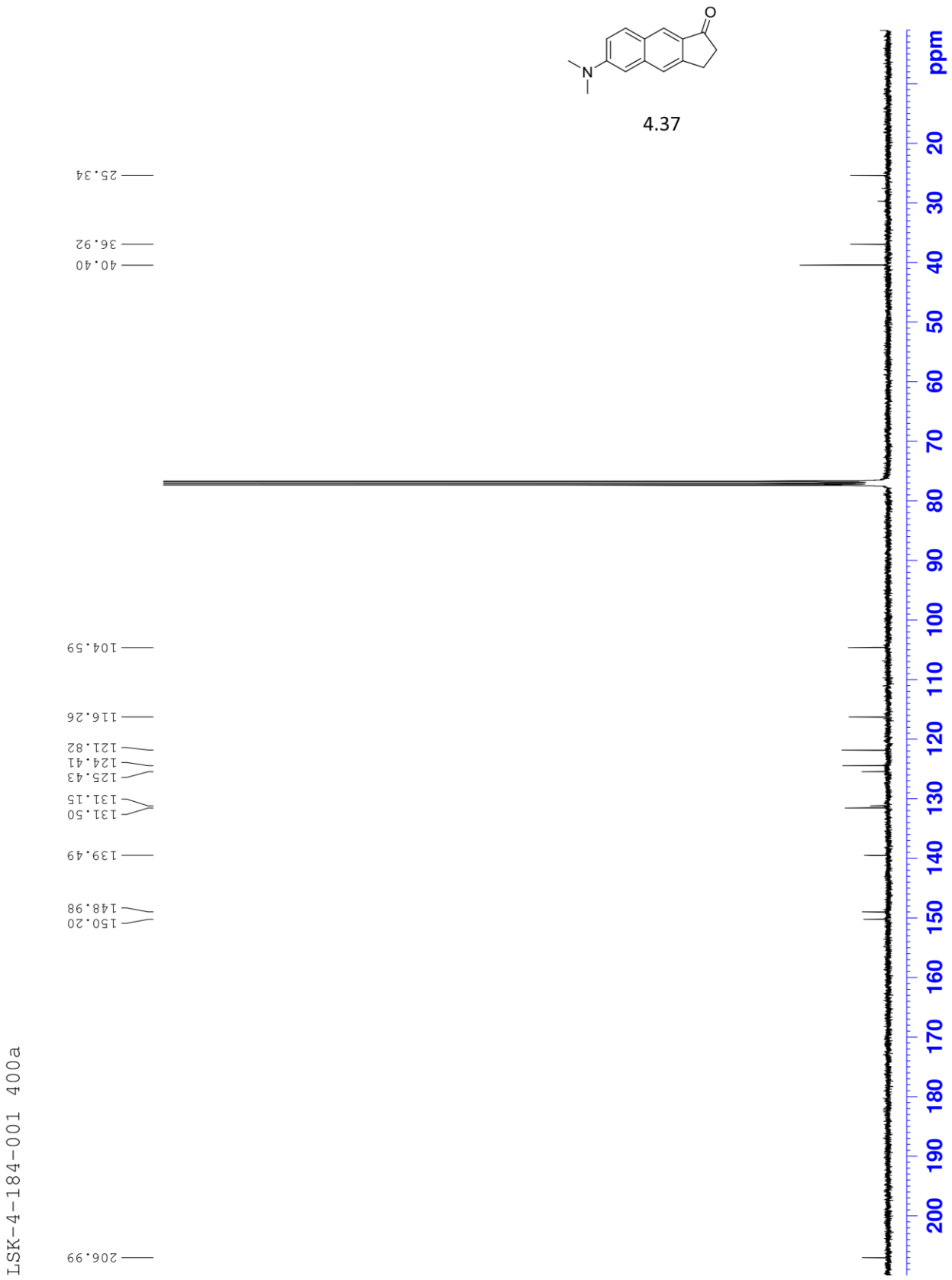
LSK-4-184-001 400a
206.99
150.20
148.98
139.49
131.50
131.15
125.43
124.41
121.82
116.26
104.59
40.40
36.92
25.34
4.37
ppm

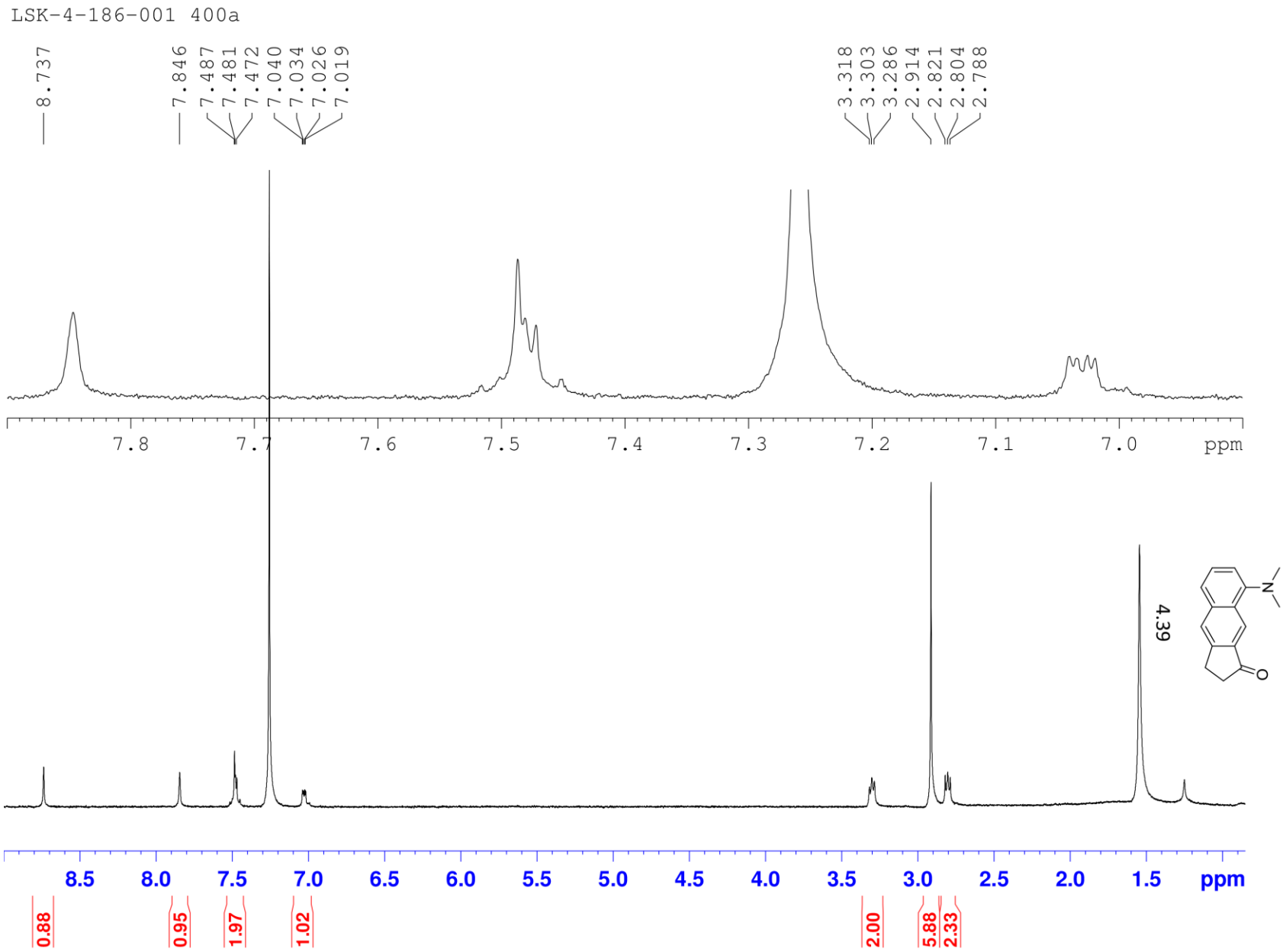
LSK-4-186-001 400a
8.737
7.846
7.487
7.481
7.472
7.040
7.034
7.026
7.019
3.318
3.303
3.286
2.914
2.821
2.804
2.788
7.8
7.7
7.6
7.5
7.4
7.3
7.2
7.1
7.0
ppm
4.39
N
O
8.5
8.0
7.5
7.0
6.5
6.0
5.5
5.0
4.5
4.0
3.5
3.0
2.5
2.0
1.5
ppm
0.88
0.95
1.97
1.02
2.00
5.88
2.33

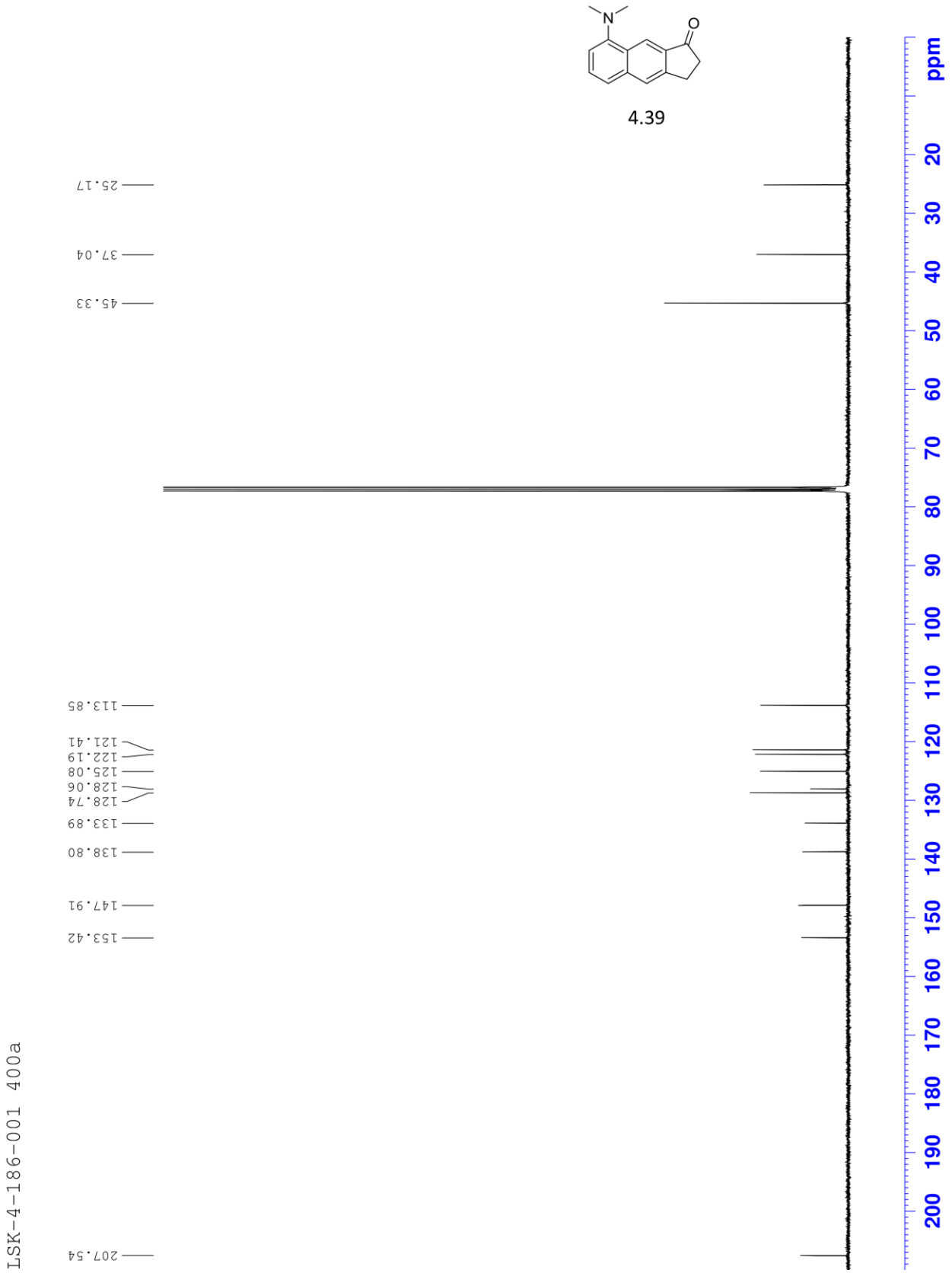
LSK-4-186-001 400a
207.54
153.42
147.91
138.80
133.89
128.74
128.06
125.08
122.19
121.41
113.85
45.33
37.04
25.17
4.39
ppm

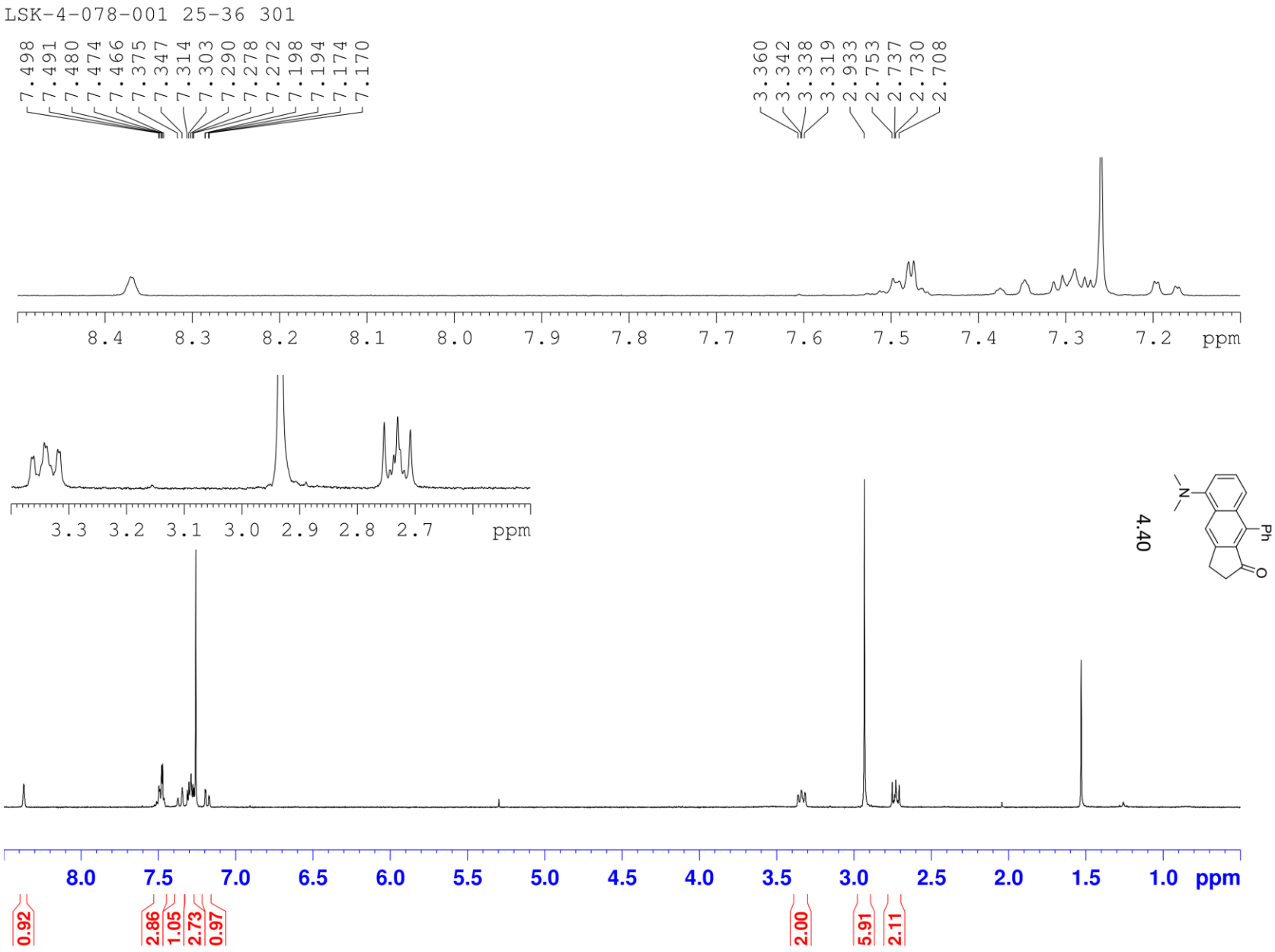
LSK-4-078-001 25-36 301
7.498
7.491
7.480
7.474
7.466
7.375
7.347
7.314
7.303
7.290
7.278
7.272
7.198
7.194
7.174
7.170
3.360
3.342
3.338
3.319
2.933
2.753
2.737
2.730
2.708
8.4 8.3 8.2 8.1 8.0 7.9 7.8 7.7 7.6 7.5 7.4 7.3 7.2 ppm
3.3 3.2 3.1 3.0 2.9 2.8 2.7 ppm
4.40
Ph
O
8.0 7.5 7.0 6.5 6.0 5.5 5.0 4.5 4.0 3.5 3.0 2.5 2.0 1.5 1.0 ppm
0.92
2.86
1.05
2.73
0.97
2.00
5.91
2.11

LSK-4-078-001 400a

206.16

150.56
147.62
140.08
136.78
133.41
132.67
130.75
129.77
127.87
127.58
125.68
123.34
120.82
116.52

45.41
37.58
25.12

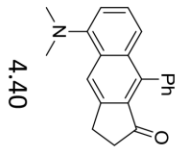

4.40

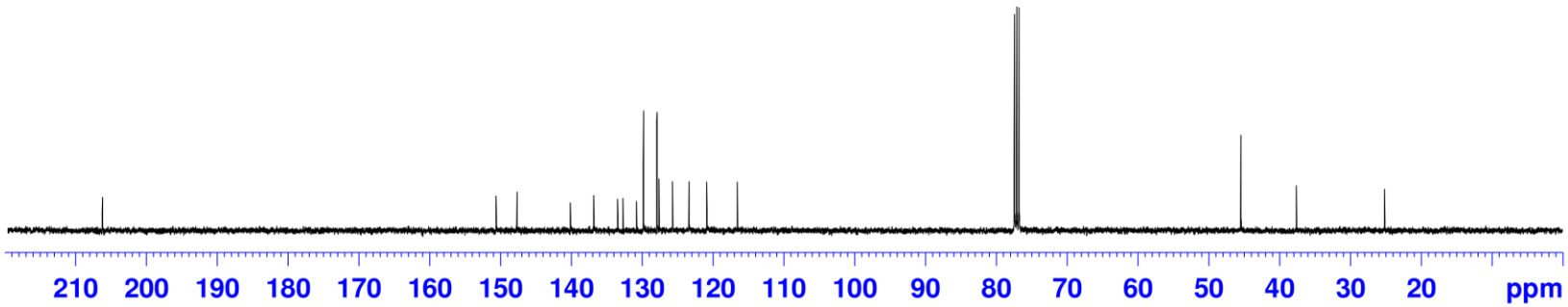

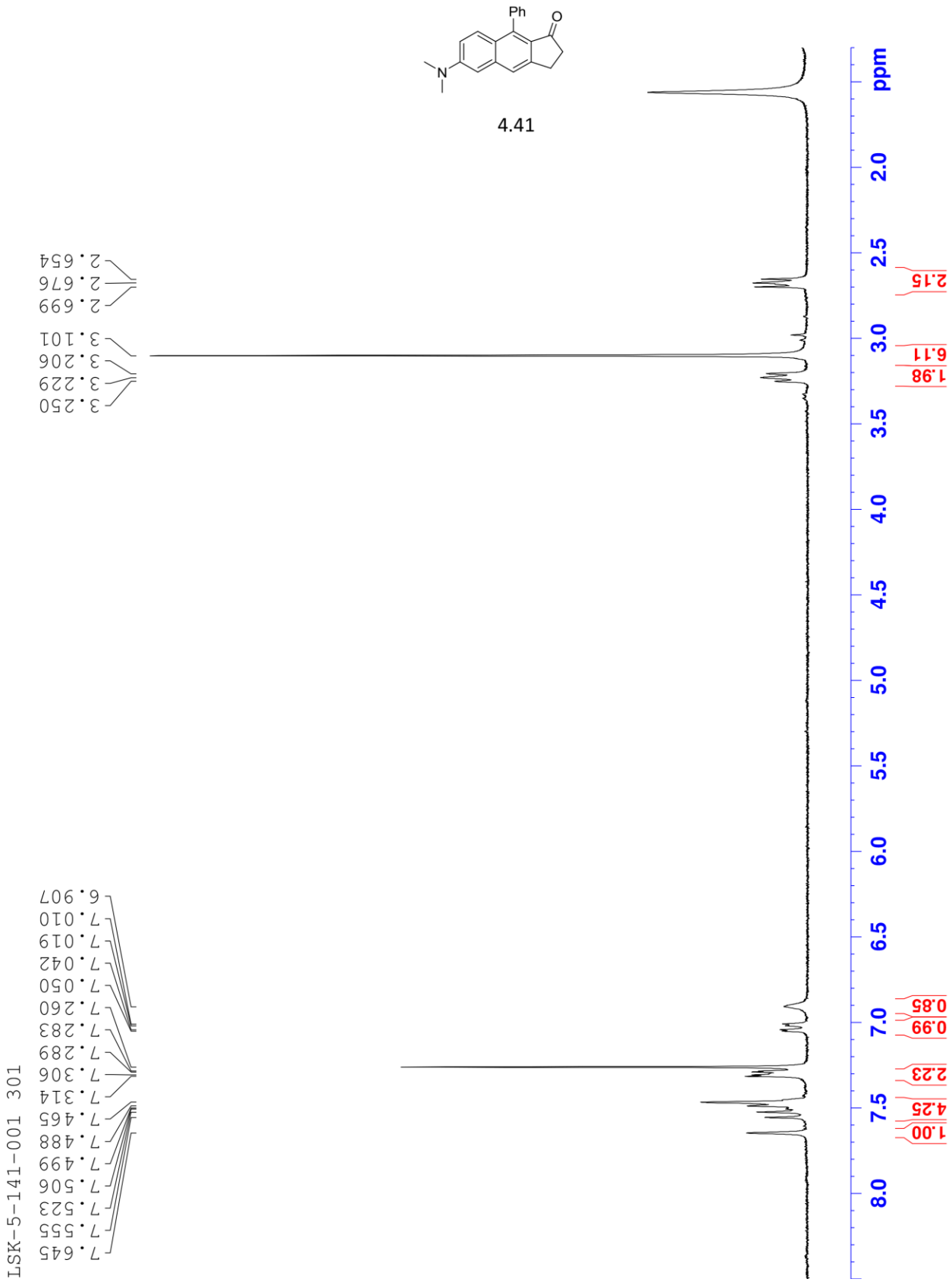
Ph
O
N
4.41
LSK-5-141-001 301
7.645
7.555
7.523
7.506
7.499
7.488
7.465
7.314
7.306
7.289
7.283
7.260
7.050
7.042
7.019
7.010
6.907
3.250
3.229
3.206
3.101
2.699
2.676
2.654
ppm
8.0
7.5
7.0
6.5
6.0
5.5
5.0
4.5
4.0
3.5
3.0
2.5
2.0
1.00
4.25
2.23
0.99
0.85
1.98
6.11
2.15

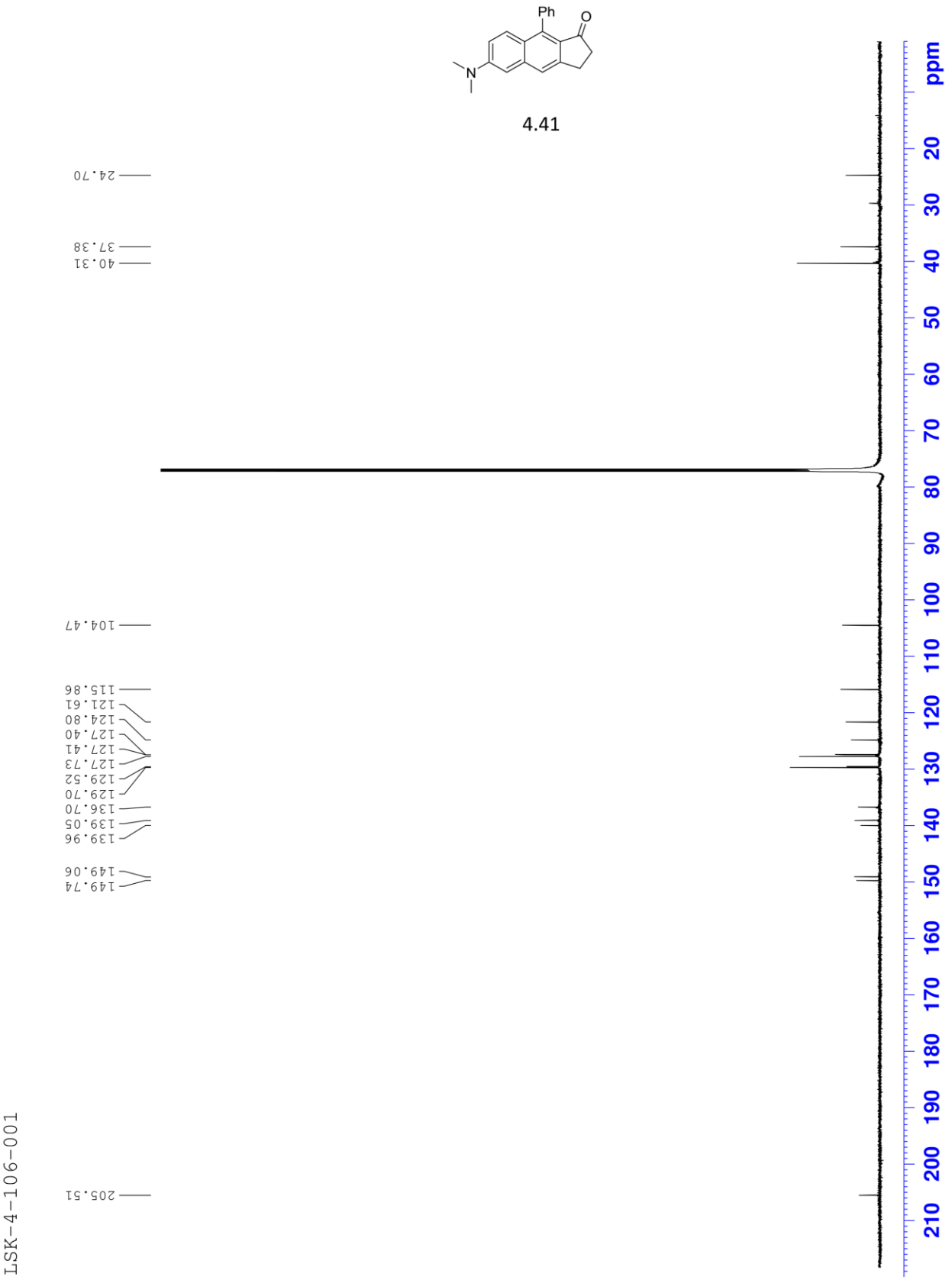
Ph
O
N
4.41
24.70
37.38
40.31
104.47
115.86
121.61
124.80
127.40
127.41
127.73
129.52
129.70
136.70
139.05
139.96
149.06
149.74
205.51
ppm
20
30
40
50
60
70
80
90
100
110
120
130
140
150
160
170
180
190
200
210
LSK-4-106-001

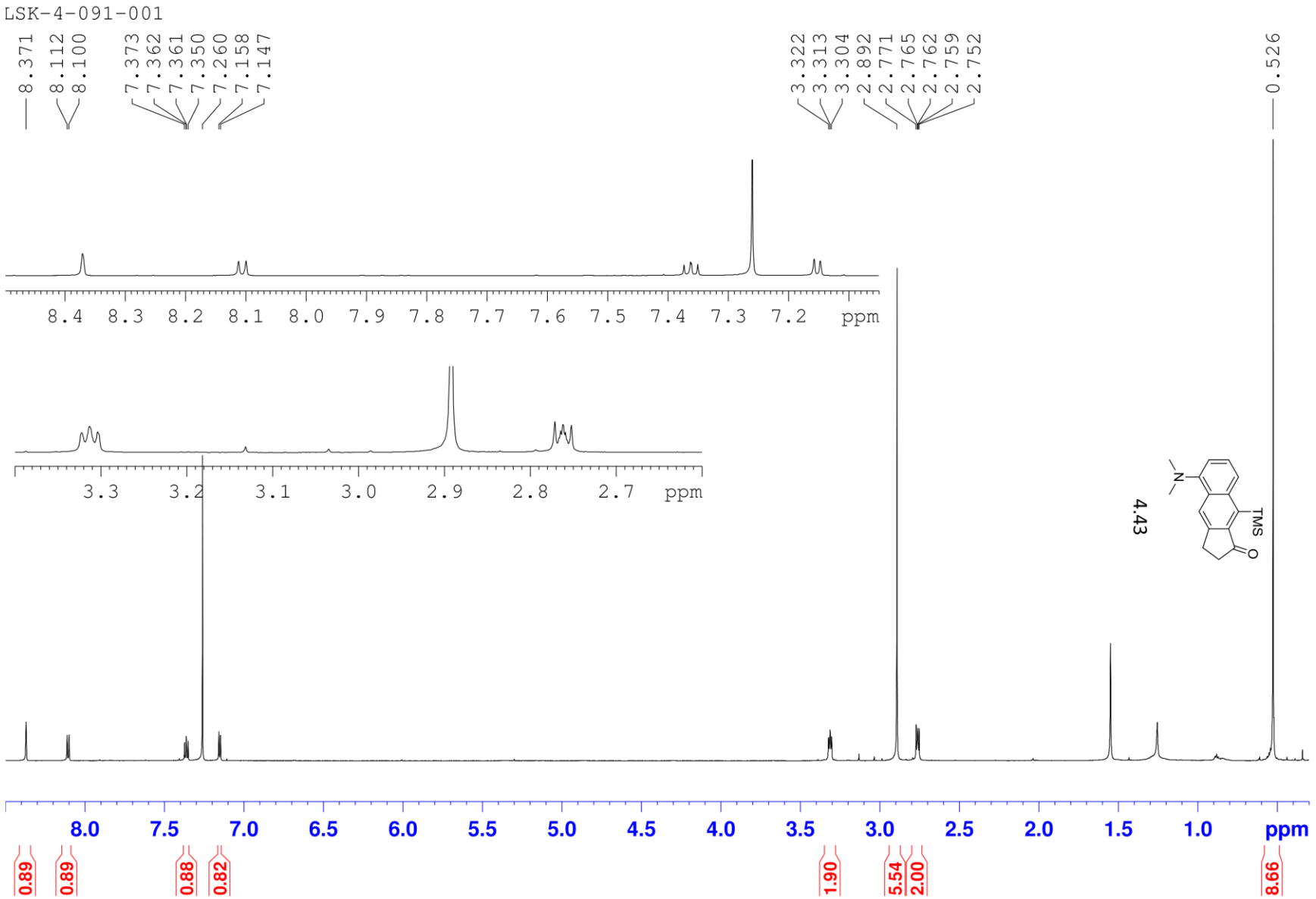
LSK-4-091-001
8.371
8.112
8.100
7.373
7.362
7.361
7.350
7.260
7.158
7.147
3.322
3.313
3.304
2.892
2.771
2.765
2.762
2.759
2.752
0.526
8.4 8.3 8.2 8.1 8.0 7.9 7.8 7.7 7.6 7.5 7.4 7.3 7.2 ppm
3.3 3.2 3.1 3.0 2.9 2.8 2.7 ppm
4.43
TMS
O
8.0 7.5 7.0 6.5 6.0 5.5 5.0 4.5 4.0 3.5 3.0 2.5 2.0 1.5 1.0 ppm
0.89
0.89
0.88
0.82
1.90
5.54
2.00
8.66

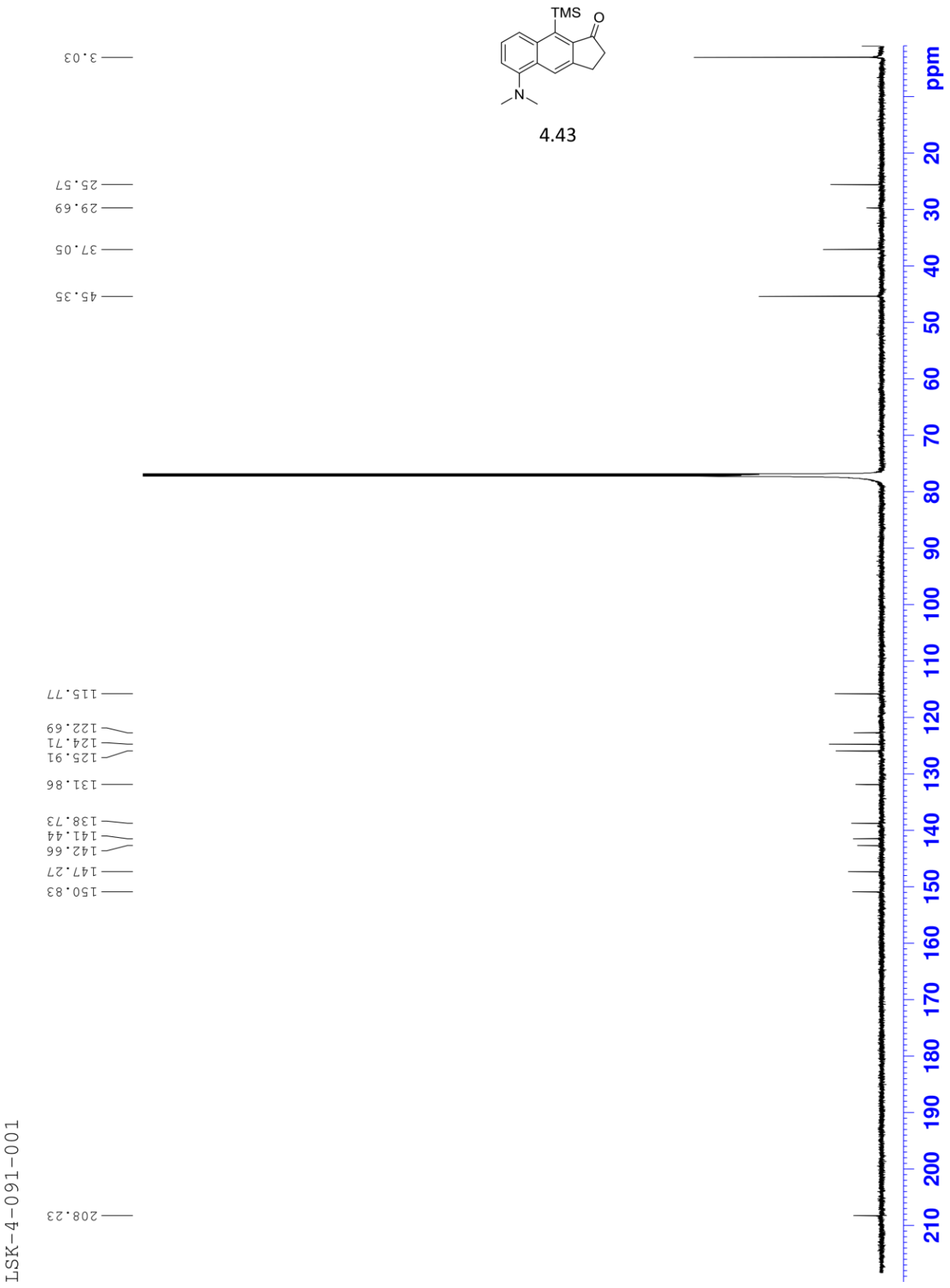
TMS
O
N
4.43
LSK-4-091-001
3.03
25.57
29.69
37.05
45.35
115.77
122.69
124.71
125.91
131.86
138.73
141.44
142.66
147.27
150.83
208.23
ppm

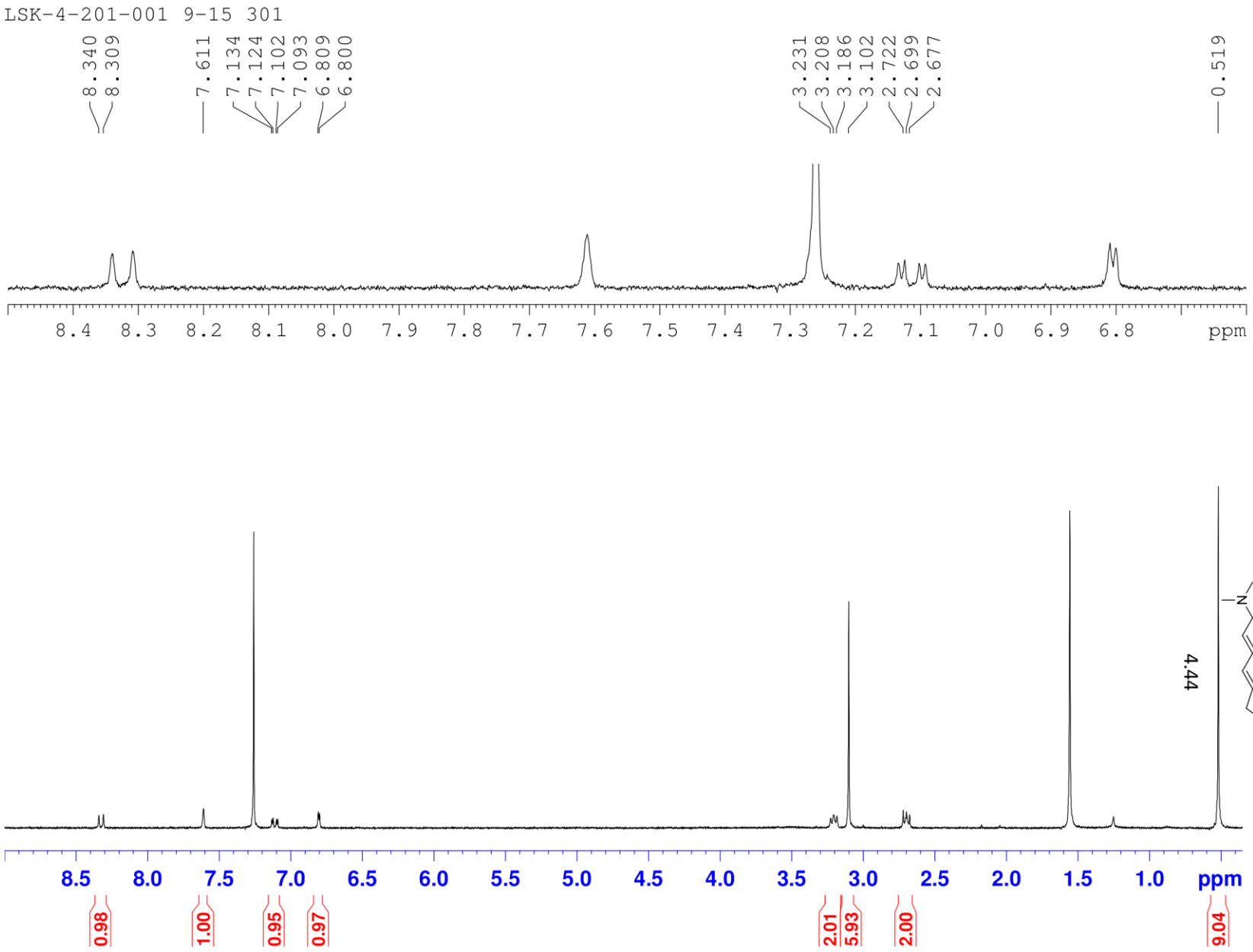
LSK-4-201-001 9-15 301
8.340
8.309
7.611
7.134
7.124
7.102
7.093
6.809
6.800
3.231
3.208
3.186
3.102
2.722
2.699
2.677
0.519
8.4 8.3 8.2 8.1 8.0 7.9 7.8 7.7 7.6 7.5 7.4 7.3 7.2 7.1 7.0 6.9 6.8 ppm
4.44
TMS
O
8.5 8.0 7.5 7.0 6.5 6.0 5.5 5.0 4.5 4.0 3.5 3.0 2.5 2.0 1.5 1.0 ppm
0.98
1.00
0.95
0.97
2.01
5.93
2.00
9.04

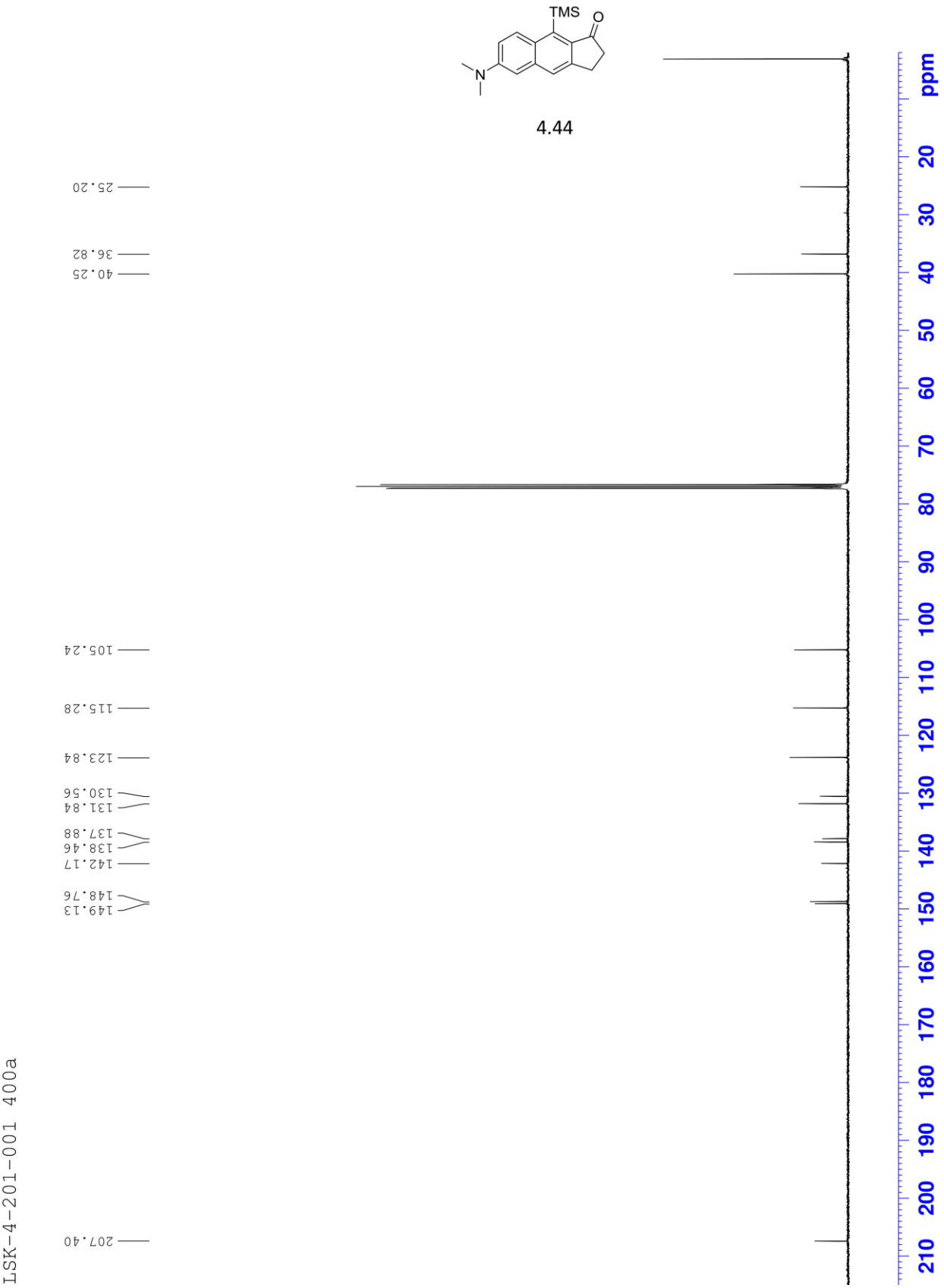
TMS
O
N
4.44
LSK-4-201-001 400a
207.40
149.13
148.76
142.17
138.46
137.88
131.84
130.56
123.84
115.28
105.24
40.25
36.82
25.20
ppm
210
200
190
180
170
160
150
140
130
120
110
100
90
80
70
60
50
40
30
20

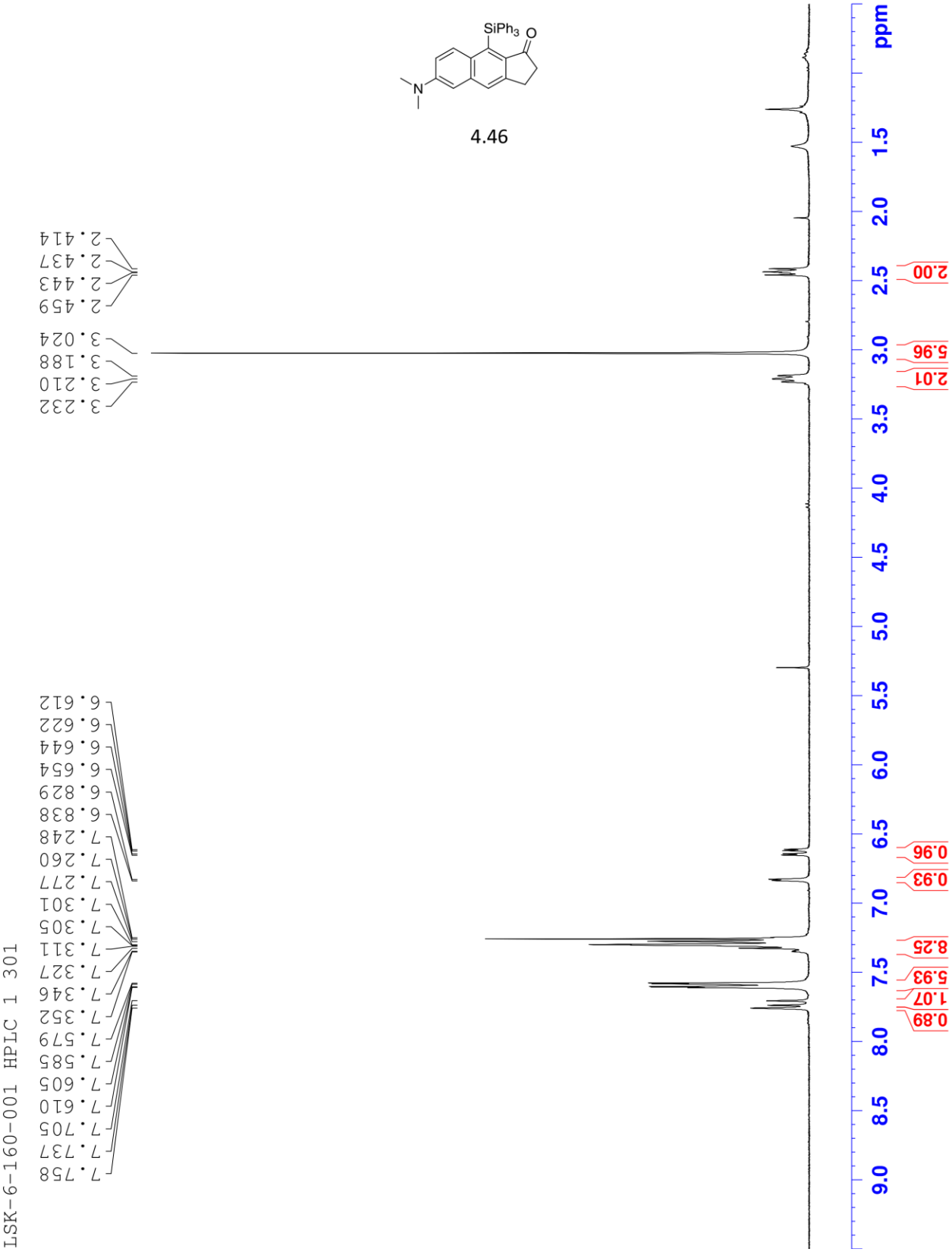
SiPh3
O
N
4.46
LSK-6-160-001 HPLC 1 301
7.758
7.737
7.705
7.610
7.605
7.585
7.579
7.352
7.346
7.327
7.311
7.305
7.301
7.277
7.260
7.248
6.838
6.829
6.654
6.644
6.622
6.612
3.232
3.210
3.188
3.024
2.459
2.443
2.437
2.414
ppm
9.0
8.5
8.0
7.5
7.0
6.5
6.0
5.5
5.0
4.5
4.0
3.5
3.0
2.5
2.0
1.5
2.00
5.96
2.01
0.96
0.93
8.25
5.93
1.07
0.89

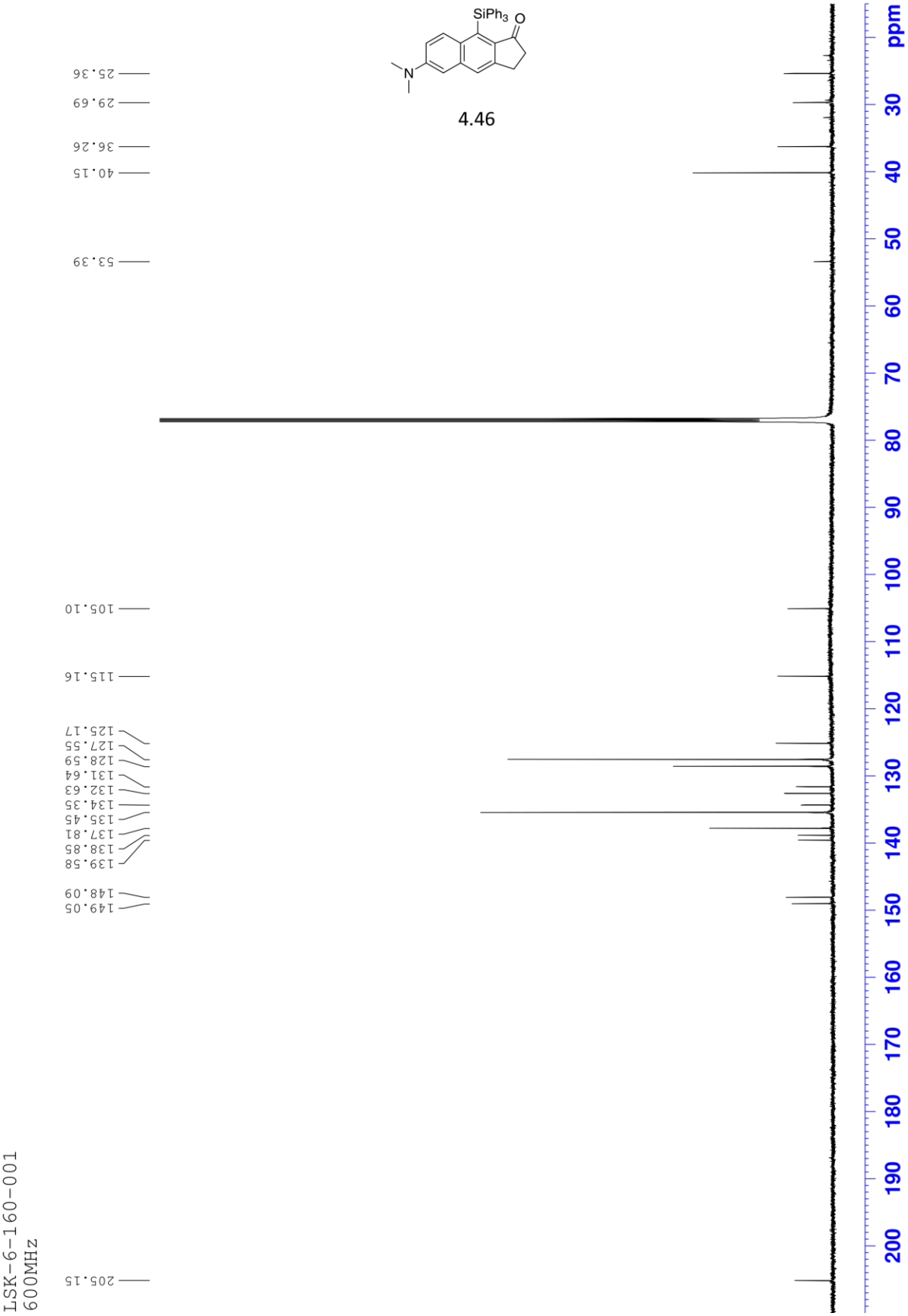
SiPh3
O
N
4.46
25.36
29.69
36.26
40.15
53.39
105.10
115.16
125.17
127.55
128.59
131.64
132.63
134.35
135.45
137.81
138.85
139.58
148.09
149.05
205.15
ppm
LSK-6-160-001
600MHz

BIBLIOGRAPHY

1. (a) Lester, W. Rifampin: A Semisynthetic Derivative of Rifamycin-A Prototype for the Future. *Annu. Rev. Microbiol.* **1972**, *26*, 85-102; (b) Boyd, M. R.; Hallock, Y. F.; Cardellina, J. H.; Manfredi, K. P.; Blunt, J. W.; McMahon, J. B.; Buckheit, R. W.; Bringmann, G.; Schaeffer, M. Anti-HIV Michellamines from Ancistrocladus korupensis. *J. Med. Chem.* **1994**, *37*, 1740-1745.

2. (a) Joseph, A. E.; Matlin, S. A.; Knox, P. Cytotoxicity of enantiomers of gossypol. *Br. J. Cancer* **1986**, *54*, 511-513; (b) Lin, T. S.; Schinazi, R.; Griffith, B. P.; August, E. M.; Eriksson, B. F.; Zheng, D. K.; Huang, L. A.; Prusoff, W. H. Selective inhibition of human immunodeficiency virus type 1 replication by the (-) but not the (+) enantiomer of gossypol. *Antimicrob. Agents Chemother.* **1989**, *33*, 2149-2151.

3. (a) Dorsett, P. H.; Kerstine, E. E.; Powers, L. J. Antiviral activity of gossypol and apogossypol. *J. Pharm. Sci.* **1975**, *64*, 1073-1075; (b) Radloff, R. J.; Deck, L. M.; Royer, R. E.; Vander Jagt, D. L. Antiviral activities of gossypol and its derivatives against herpes simplex virus type II. *Pharmacol. Res. Commun.* **1986**, *18*, 1063-1073.

4. (a) Petranyi, G.; Ryder, N.; Stutz, A. Allylamine derivatives: new class of synthetic antifungal agents inhibiting fungal squalene epoxidase. *Science* **1984**, *224*, 1239-1241; (b) Ryder, N. S.; Frank, I.; Dupont, M. C. Ergosterol biosynthesis inhibition by the thiocarbamate antifungal agents tolnaftate and tolciclate. *Antimicrob. Agents Chemother.* **1986**, *29*, 858-860.

5. Duggan, K. C.; Walters, M. J.; Musee, J.; Harp, J. M.; Kiefer, J. R.; Oates, J. A.; Marnett, L. J. Molecular Basis for Cyclooxygenase Inhibition by the Non-steroidal Anti-inflammatory Drug Naproxen. *J. Biol. Chem.* **2010**, *285*, 34950-34959.

6. Tan, A. K.; Fink, A. L. Identification of the site of covalent attachment of nafcillin, a reversible suicide inhibitor of beta-lactamase. *Biochem. J.* **1992**, *281*, 191-196.

7. (a) Weber, G.; Farris, F. J. Synthesis and spectral properties of a hydrophobic fluorescent probe: 6-propionyl-2-(dimethylamino)naphthalene. *Biochemistry* **1979**, *18*, 3075-3078; (b) Parasassi, T.; Krasnowska, E.; Bagatolli, L.; Gratton, E. Laurdan and Prodan as Polarity-Sensitive Fluorescent Membrane Probes. *J. Fluoresc.* **1998**, *8*, 365-373.

8. Hsieh, W. T.; Matthews, K. S. Lactose repressor protein modified with dansyl chloride: activity effects and fluorescence properties. *Biochemistry* **1985**, *24*, 3043-3049.

9. *The Molecular Probes Handbook, A Guide to Fluorescent Probes and Labeling Technologies*. 11 ed.; Life Technologies Corporation: Grand Island, NY, 2010;

10. de Koning, C. B.; Rousseau, A. L.; van Otterlo, W. A. L. Modern methods for the synthesis of substituted naphthalenes. *Tetrahedron* **2003**, *59*, 7-36.

11. G. Ramesh, N.; Iio, K.; Okajima, A.; Akai, S.; Kita, Y. A strong-base induced [4+2] cycloaddition of homophthalic anhydrides with enolizable enones: a direct and efficient synthesis of peri-hydroxy aromatic compounds. *Chem. Commun.* **1998**, 2741-2742.

12. Kita, Y.; Higuchi, K.; Yoshida, Y.; Iio, K.; Kitagaki, S.; Ueda, K.; Akai, S.; Fujioka, H. Enantioselective Total Synthesis of a Potent Antitumor Antibiotic, Fredericamycin A. *J. Am. Chem. Soc.* **2001**, *123*, 3214-3222.

13. Meyers, A. I.; Willemsen, J. J. The synthesis of (*S*)-(+)-gossypol via an asymmetric Ullmann coupling. *Chem. Commun.* **1997**, 1573-1574.

14. Jo Chang, D.; Ser Park, B. Highly efficient photoinduced rearrangement of benzobicyclo[3.1.0]hexenones to 1-naphthols. *Tetrahedron Lett.* **2001**, *42*, 711-713.

15. Peña, D.; Pérez, D.; Guitián, E.; Castedo, L. Selective Palladium-Catalyzed Cocyclotrimerization of Arynes with Dimethyl Acetylenedicarboxylate: A Versatile Method for the Synthesis of Polycyclic Aromatic Hydrocarbons. *J. Org. Chem.* **2000**, *65*, 6944-6950.

16. Sato, Y.; Tamura, T.; Mori, M. Arylnaphthalene Lignans through Pd-Catalyzed [2+2+2] Cocyclization of Arynes and Diynes: Total Synthesis of Taiwanins C and E. *Angew. Chem. Int. Ed.* **2004**, *43*, 2436-2440.

17. Flanagan, S. R.; Harrowven, D. C.; Bradley, M. A new benzannulation reaction and its application in the multiple parallel synthesis of arylnaphthalene lignans. *Tetrahedron* **2002**, *58*, 5989-6001.

18. Ukita, T.; Nakamura, Y.; Kubo, A.; Yamamoto, Y.; Takahashi, M.; Kotera, J.; Ikeo, T. 1-Arylnaphthalene Lignan: A Novel Scaffold for Type 5 Phosphodiesterase Inhibitor. *J. Med. Chem.* **1999**, *42*, 1293-1305.

19. Wessig, P.; Müller, G. The Dehydro-Diels−Alder Reaction. *Chem. Rev.* **2008**, *108*, 2051-2063.

20. Stevenson, R.; Weber, J. V. Improved Methods of Synthesis of Lignan Arylnaphthalene Lactones via Arylpropargyl Arylpropiolate Esters. *J. Nat. Prod.* **1989**, *52*, 367-375.

21. Eckert, T.; Ipaktschi, J. Synthesis of polycyclic aromatic heterocyclic compounds via thermal isomerizations of 1,8-diarylethynylnaphthalenes. *Monatsh. Chem.* **1998**, *129*, 1035-1048.

22. Wessig, P.; Müller, G.; Pick, C.; Matthes, A. The Photo-Dehydro-Diels-Alder (PDDA) Reaction - A Powerful Method for the Preparation of Biaryls. *Synthesis* **2007**, *2007*, 464-477.

23. (a) Kimura, M.; Horino, Y.; Wakamiya, Y.; Okajima, T.; Tamaru, Y. Pronounced Chemo-, Regio-, and Stereoselective [2 + 2] Cycloaddition Reaction of Allenes toward Alkenes and Alkynes. *J. Am. Chem. Soc.* **1997**, *119*, 10869-10870; (b) Ikemoto, C.; Kawano, T.; Ueda, I. Thermal radical cyclization of non-conjugated aromatic enyne-allenes: Synthesis of a Cyclobuta[α]naphthalene skeleton. *Tetrahedron Lett.* **1998**, *39*, 5053-5056; (c) Shen, Q.; Hammond, G. B. Regiospecific Synthesis of Bicyclo- and Heterobicyclo-gem-difluorocyclobutenes Using Functionalized Fluoroallenes and a Novel Mo-Catalyzed Intramolecular [2 + 2] Cycloaddition Reaction. *J. Am. Chem. Soc.* **2002**, *124*, 6534-6535; (d) Cao, H.; Van Ornum, S. G.; Deschamps, J.; Flippen-Anderson, J.; Laib, F.; Cook, J. M. Synthesis of Dicyclopenta[*a*,*e*]pentalenes via a Molybdenum Carbonyl Mediated Tandem Allenic Pauson−Khand Reaction and the X-ray Crystal Structure of a Planar Dicyclopenta[*a*,*e*]pentalene. *J. Am. Chem. Soc.* **2004**, *127*, 933-943.

24. Brummond, K. M.; Chen, D. Microwave-Assisted Intramolecular [2 + 2] Allenic Cycloaddition Reaction for the Rapid Assembly of Bicyclo[4.2.0]octa-1,6-dienes and Bicyclo[5.2.0]nona-1,7-dienes. *Org. Lett.* **2005**, *7*, 3473-3475.

25. Oh, C. H.; Gupta, A. K.; Park, D. I.; Kim, N. Highly efficient [2 + 2] intramolecular cyclizations of allenynes under microwave irradiation: construction of fused bicyclic compounds. *Chem. Commun.* **2005**, 5670-5672.

26. Ohno, H.; Mizutani, T.; Kadoh, Y.; Miyamura, K.; Tanaka, T. Thermal Intramolecular [2+2] Cycloaddition of Allenenes and Allenynes: Diastereoselective Access to Bicyclic Nitrogen Heterocycles. *Angew. Chem. Int. Ed.* **2005**, *44*, 5113-5115.

27. Ovaska, T. V.; Kyne, R. E. Intramolecular thermal allenyne [2+2] cycloadditions: facile construction of the 5–6–4 ring core of sterpurene. *Tetrahedron Lett.* **2008**, *49*, 376-378.

28. Jiang, X.; Ma, S. Intramolecular [2+2]-cycloaddition of propargylic 2,3-allenoates for the efficient synthesis of 3-oxabicyclo[4.2.0]octa-1(8),5-dien-4-ones: a dramatic substituent effect. *Tetrahedron* **2007**, *63*, 7589-7595.

29. Mukai, C.; Hara, Y.; Miyashita, Y.; Inagaki, F. Thermal [2+2] Cycloaddition of Allenynes: Easy Construction of Bicyclo[6.2.0]deca-1,8-dienes, Bicyclo[5.2.0]nona-1,7-dienes, and Bicyclo[4.2.0]octa-1,6-dienes. *J. Org. Chem.* **2007**, *72*, 4454-4461.

30. Buisine, O.; Gandon, V.; Fensterbank, L.; Aubert, C.; Malacria, M. Thermal Intramolecular Alder-Ene Cycloisomerization of 1,6-Allenynes. *Synlett* **2008**, *2008*, 751-754.

31. (a) Baran, P. S.; Richter, J. M. Enantioselective Total Syntheses of Welwitindolinone A and Fischerindoles I and G. *J. Am. Chem. Soc.* **2005**, *127*, 15394-15396; (b) Reisman, S. E.; Ready, J. M.; Hasuoka, A.; Smith, C. J.; Wood, J. L. Total Synthesis of (±)-Welwitindolinone A Isonitrile. *J. Am. Chem. Soc.* **2006**, *128*, 1448-1449.

32. Smith, C. D.; Zilfou, J. T.; Stratmann, K.; Patterson, G. M.; Moore, R. E. Welwitindolinone analogues that reverse P-glycoprotein-mediated multiple drug resistance. *Mol. Pharmacol.* **1995**, *47*, 241-247.

33. Bergman, R. G. Reactive 1,4-dehydroaromatics. *Acc. Chem. Res.* **1973**, *6*, 25-31.

34. (a) Myers, A. G.; Kuo, E. Y.; Finney, N. S. Thermal generation of α–3-dehydrotoluene from (Z)-1,2,4-heptatrien-6-yne. *J. Am. Chem. Soc.* **1989**, *111*, 8057-8059; (b) Nagata, R.; Yamanaka, H.; Okazaki, E.; Saito, I. Biradical formation from acyclic conjugated eneyne-allene system related to neocarzinostatin and esperamicin-calichemicin. *Tetrahedron Lett.* **1989**, *30*, 4995-4998.

35. Schmittel, M.; Strittmatter, M.; Kiau, S. Switching from the Myers reaction to a new thermal cyclization mode in enyne-allenes. *Tetrahedron Lett.* **1995**, *36*, 4975-4978.

36. Siebert, M. R.; Osbourn, J. M.; Brummond, K. M.; Tantillo, D. J. Differentiating Mechanistic Possibilities for the Thermal, Intramolecular [2 + 2] Cycloaddition of Allene−Ynes. *J. Am. Chem. Soc.* **2010**, *132*, 11952-11966.

37. Stille, J. K.; Chung, D. C. Reaction of Vinylidene Cyanide with Styrene. Structure of the Cycloadduct and Copolymer. *Macromolecules* **1975**, *8*, 83-85.

38. (a) Williams, J. K.; Wiley, D. W.; McKusick, B. C. Cyanocarbon Chemistry. XIX. Tetracyanocyclobutanes from Tetracyanoethylene and Electron-rich Alkenes. *J. Am. Chem. Soc.* **1962**, *84*, 2210-2215; (b) Ohno, H.; Mizutani, T.; Kadoh, Y.; Aso, A.; Miyamura, K.; Fujii, N.; Tanaka, T. A Highly Regio- and Stereoselective Formation of Bicyclo[4.2.0]oct-5-ene Derivatives through Thermal Intramolecular [2 + 2] Cycloaddition of Allenes. *J. Org. Chem.* **2007**, *72*, 4378-4389.

39. Bergmann, F.; Pfleiderer, W. Nucleotides. Part XLI. The 2-dansylethoxycarbonyl (2-{[5-(dimethylamino)naphthalen-1-yl]sulfonyl}ethoxycarbonyl; dnseoc) group for protection of the 5′-hydroxy function in oligodeoxyribonucleotide synthesis. *Helv. Chim. Acta* **1994**, *77*, 203-215.

40. (a) Klemm, L. H.; Gopinath, K. W. An intramolecular Diels-Alder reaction. A simple synthesis of γ-apopicropodophyllin. *Tetrahedron Lett.* **1963**, *4*, 1243-1245; (b) Klemm, L. H.; Gopinath, K. W.; Lee, D. H.; Kelly, F. W.; Trod, E.; McGuire, T. M. The intramolecular diels-alder reaction as a route to synthetic lignan lactones. *Tetrahedron* **1966**, *22*, 1797-1808.

41. (a) Klemm, L. H.; Lee, D. H.; Gopinath, K. W.; Klopfenstein, C. E. Intramolecular Diels—Alder Reactions. III. Cyclizations of trans-Cinnamyl and Phenylpropargyl Phenylpropiolates. *J. Org. Chem.* **1966**, *31*, 2376-2380; (b) Park, J.-E.; Lee, J.; Seo, S.-Y.; Shin, D. Regioselective route for arylnaphthalene lactones: convenient synthesis of taiwanin C, justicidin E, and daurinol. *Tetrahedron Lett.* **2014**, *55*, 818-820.

42. Klemm, L. H.; Klemm, R. A.; Santhanam, P. S.; White, D. V. Intramolecular Diels-Alder reactions. VI. Synthesis of 3-hydroxymethyl-2-naphthoic acid lactones. *J. Org. Chem.* **1971**, *36*, 2169-2172.

43. Klemm, L. H.; McGuire, T. M.; Gopinath, K. W. Intramolecular Diels-Alder reactions. 10. Synthesis and cyclizations of some N-(cinnamyl and phenylpropargyl)cinnamamides and phenylpropiolamides. *J. Org. Chem.* **1976**, *41*, 2571-2579.

44. Chackalamannil, S.; Doller, D.; Clasby, M.; Xia, Y.; Eagen, K.; Lin, Y.; Tsai, H.-A.; McPhail, A. T. A facile Diels–Alder route to dihydronaphthofuranones. *Tetrahedron Lett.* **2000**, *41*, 4043-4047.

45. Ruijter, E.; Garcia-Hartjes, J.; Hoffmann, F.; van Wandelen, L. T. M.; de Kanter, F. J. J.; Janssen, E.; Orru, R. V. A. Synthesis of Polycyclic Alkaloid-Type Compounds by an N-Acyliminium Pictet-Spengler/Diels-Alder Sequence. *Synlett* **2010**, *2010*, 2485-2489.

46. Toyota, M.; Terashima, S. A novel synthesis of the basic carbon framework of fredericamycin A. Promising routes for the spiro chiral center construction of the CD-ring system. *Tetrahedron Lett.* **1989**, *30*, 829-832.

47. Ozawa, T.; Kurahashi, T.; Matsubara, S. Dehydrogenative Diels–Alder Reaction. *Org. Lett.* **2011**, *13*, 5390-5393.

48. (a) Cone, M. C.; Melville, C. R.; Gore, M. P.; Gould, S. J. Kinafluorenone, a benzo[b]fluorenone isolated from the kinamycin producer Streptomyces murayamaensis. *J. Org. Chem.* **1993**, *58*, 1058-1061; (b) Ernst-Russell, M. A.; Chai, C. L. L.; Wardlaw, J. H.; Elix, J. A. Euplectin and Coneuplectin, New Naphthopyrones from the Lichen Flavoparmelia euplecta. *J. Nat. Prod.* **2000**, *63*, 129-131.

49. (a) Kappe, C. O. Controlled Microwave Heating in Modern Organic Synthesis. *Angew. Chem. Int. Ed.* **2004**, *43*, 6250-6284; (b) Herrero, M. A.; Kremsner, J. M.; Kappe, C. O. Nonthermal Microwave Effects Revisited: On the Importance of Internal Temperature Monitoring and Agitation in Microwave Chemistry. *J. Org. Chem.* **2007**, *73*, 36-47.

50. Lidström, P.; Tierney, J.; Wathey, B.; Westman, J. Microwave assisted organic synthesis—a review. *Tetrahedron* **2001**, *57*, 9225-9283.

51. (a) Chen, P.-K.; Rosana, M. R.; Dudley, G. B.; Stiegman, A. E. Parameters Affecting the Microwave-Specific Acceleration of a Chemical Reaction. *J. Org. Chem.* **2014**, *79*, 7425-7436; (b) Rosana, M. R.; Hunt, J.; Ferrari, A.; Southworth, T. A.; Tao, Y.; Stiegman, A.

E.; Dudley, G. B. Microwave-Specific Acceleration of a Friedel–Crafts Reaction: Evidence for Selective Heating in Homogeneous Solution. *J. Org. Chem.* **2014**, *79*, 7437-7450.

52. Obermayer, D.; Gutmann, B.; Kappe, C. O. Microwave Chemistry in Silicon Carbide Reaction Vials: Separating Thermal from Nonthermal Effects. *Angew. Chem. Int. Ed.* **2009**, *48*, 8321-8324.

53. van Zijl, A. W.; Arnold, L. A.; Minnaard, A. J.; Feringa, B. L. Highly Enantioselective Copper-Catalyzed Allylic Alkylation with Phosphoramidite Ligands. *Adv. Synth. Catal.* **2004**, *346*, 413-420.

54. Mąkosza, M.; Urbańska, N.; Chesnokov, A. A. Reactions of the carbanion of chloromethyl methyl sulfone with aldehydes and ketones. *Tetrahedron Lett.* **2003**, *44*, 1473-1475.

55. Maytum, H. C.; Francos, J.; Whatrup, D. J.; Williams, J. M. J. 1,4-Butanediol as a Reducing Agent in Transfer Hydrogenation Reactions. *Chem. Asian J.* **2010**, *5*, 538-542.

56. Wiedemann, S. H.; Ellman, J. A.; Bergman, R. G. Rhodium-Catalyzed Direct C−H Addition of 3,4-Dihydroquinazolines to Alkenes and Their Use in the Total Synthesis of Vasicoline. *J. Org. Chem.* **2006**, *71*, 1969-1976.

57. Mitchell, R. H.; Lai, Y. H. Syntheses and reactions of the first dithia[3.1.3.1]metacyclophanes, [2.1.2.1]metacyclophanes, and [2.1.2.1]metacyclophanedienes. *J. Org. Chem.* **1984**, *49*, 2534-2540.

58. (a) Pearson, D. E.; Buehler, C. A. Friedel-Crafts Acylations with Little or No Catalyst. *Synthesis* **1972**, *1972*, 533-542; (b) Taylor, R. *Electrophilic Aromatic Substitution*. John Wiley & Sons: New York, 1990; ; (c) Katritzky, A. R.; Li, J.; Xie, L. [3+3] Benzannulations of benzenoid- and heteroaromatic-ring systems. *Tetrahedron* **1999**, *55*, 8263-8293.

59. (a) Stará, I. G.; Starý, I.; Kollárovič, A.; Teplý, F.; Šaman, D.; Fiedler, P. Coupling reactions of *ortho*-substituted aryl halides with alkynes. The synthesis of functionalized 1-naphthyl-, 1-(1-naphthyl)-2-phenyl-, and 1,2-bis(1-naphthyl)acetylenes. *Tetrahedron* **1998**, *54*, 11209-11234; (b) Suzuki, A. Recent advances in the cross-coupling reactions of organoboron derivatives with organic electrophiles, 1995–1998. *J. Organomet. Chem.* **1999**, *576*, 147-168; (c) Jeffery, T.; Ferber, B. t. One-pot palladium-catalyzed highly chemo-, regio-, and stereoselective synthesis of trans-stilbene derivatives. A concise and convenient synthesis of resveratrol. *Tetrahedron Lett.* **2003**, *44*, 193-197; (d) Ohta, K.; Goto, T.; Endo, Y. 1,2-Dicarba-closo-dodecaboran-1-yl Naphthalene Derivatives. *Inorg. Chem.* **2005**, *44*, 8569-8573; (e) Mei, X.; Liu, S.; Wolf, C. Template-Controlled Face-to-Face Stacking of Olefinic and Aromatic Carboxylic Acids in the Solid State. *Org. Lett.* **2007**, *9*, 2729-2732; (f) Bhosale, S. V.; Kalyankar, M. B.; Bhosale, S. V.; Langford, S. J.; Reid, E. F.; Hogan, C. F. The synthesis of novel core-substituted naphthalene diimides via Suzuki cross-coupling and their properties. *New J. Chem.* **2009**, *33*, 2409-2413; (g)

Benedetti, E.; Kocsis, L. S.; Brummond, K. M. Synthesis and Photophysical Properties of a Series of Cyclopenta[*b*]naphthalene Solvatochromic Fluorophores. *J. Am. Chem. Soc.* **2012**, *134*, 12418-12421.

60. Liljenberg, M.; Brinck, T.; Herschend, B.; Rein, T.; Rockwell, G.; Svensson, M. Validation of a Computational Model for Predicting the Site for Electrophilic Substitution in Aromatic Systems. *J. Org. Chem.* **2010**, *75*, 4696-4705.

61. (a) Asao, N.; Nogami, T.; Lee, S.; Yamamoto, Y. Lewis Acid-Catalyzed Benzannulation via Unprecedented [4+2] Cycloaddition of o-Alkynyl(oxo)benzenes and Enynals with Alkynes. *J. Am. Chem. Soc.* **2003**, *125*, 10921-10925; (b) Dudnik, A. S.; Schwier, T.; Gevorgyan, V. Gold-Catalyzed Double Migration-Benzannulation Cascade toward Naphthalenes. *Org. Lett.* **2008**, *10*, 1465-1468; (c) Hayes, M. E.; Shinokubo, H.; Danheiser, R. L. Intramolecular [4 + 2] Cycloadditions of Benzynes with Conjugated Enynes, Arenynes, and Dienes. *Org. Lett.* **2005**, *7*, 3917-3920; (d) Kang, D.; Kim, J.; Oh, S.; Lee, P. H. Synthesis of Naphthalenes via Platinum-Catalyzed Hydroarylation of Aryl Enynes. *Org. Lett.* **2012**, *14*, 5636-5639.

62. (a) Klemm, L. H.; Gopinath, K. W. Intramolecular Diels-Alder cyclization into the thiophene ring. *J. Heterocycl. Chem.* **1965**, *2*, 225-227; (b) Stevenson, R.; Weber, J. V. Synthesis of Lignan Aryldihydronaphthalene Lactones by Cyclization of Cinnamyl Arylpropiolate Esters: Revised Structure of β-Apopolygamatin. *J. Nat. Prod.* **1991**, *54*, 310-314.

63. Hajbi, Y.; Neagoie, C.; Biannic, B.; Chilloux, A.; Vedrenne, E.; Baldeyrou, B.; Bailly, C.; Mérour, J.-Y.; Rosca, S.; Routier, S.; Lansiaux, A. Synthesis and biological activities of new furo[3,4-b]carbazoles: Potential topoisomerase II inhibitors. *Eur. J. Med. Chem.* **2010**, *45*, 5428-5437.

64. Kocsis, L. S.; Benedetti, E.; Brummond, K. M. A Thermal Dehydrogenative Diels–Alder Reaction of Styrenes for the Concise Synthesis of Functionalized Naphthalenes. *Org. Lett.* **2012**, *14*, 4430-4433.

65. Klemm, L. H.; Olson, D. R.; White, D. V. Intramolecular Diels-Alder reactions. VII. Electroreduction of α,β-Unsaturated Esters. I. A Simple Synthesis of *rac*-deoxypicropodophyllin by Intramolecular Diels-Alder Reaction Plus Trans Addition of Hydrogen. *J. Org. Chem.* **1971**, *36*, 3740-3743.

66. (a) Yadagiri, B.; Lown, J. W. Convenient Routes to Substituted Benzimidazoles and Imidazolo[4,5-b]pyridines Using Nitrobenzene as Oxidant. *Synth. Commun.* **1990**, *20*, 955-963; (b) Charris, J.; Camacho, J.; Ferrer, R.; Lobo, G.; Barazarte, A.; Gamboa, N.; Rodrigues, J.; López, S. A convenient route to 2-substituted benzothiazole-6-carboxylic acids using nitrobenzene as oxidant. *J. Chem. Res.* **2006**, *2006*, 769-770; (c) Sanap, K. K.; Samant, S. D. Synthesis of fluorescent dibenzopyranones by the Diels-Alder reaction of 4-styrylcoumarins and *N*-phenylmaleimide and in situ aromatization using DDQ. *ARKIVOC* **2013**, *iii*, 109-118.

67. (a) Coellen, M.; Rüchardt, C. Transfer Hydrogenation of Nitro-, Nitroso- and Azoarenes by Homolytic Retrodisproportionation. *Chem. Eur. J.* **1995**, *1*, 564-567; (b) Rüchardt, C.; Gerst, M.; Ebenhoch, J. Uncatalyzed Transfer Hydrogenation and Transfer Hydrogenolysis: Two Novel Types of Hydrogen-Transfer Reactions. *Angew. Chem. Int. Ed. Engl.* **1997**, *36*, 1406-1430; (c) Cristiano, M. L. S.; Gago, D. J. P.; Rocha Gonsalves, A. M.; Johnstone, R. A. W.; McCarron, M.; Varejao, J. M. T. B. Investigations into the mechanism of action of nitrobenzene as a mild dehydrogenating agent under acid-catalysed conditions. *Org. Biomol. Chem.* **2003**, *1*, 565-574.

68. Wassmundt, F. W.; Kiesman, W. F. Efficient Catalysis of Hydrodediazoniations in Dimethylformamide. *J. Org. Chem.* **1995**, *60*, 1713-1719.

69. (a) Lin, X.; Stien, D.; Weinreb, S. M. A New Method for the Generation and Cyclization of Iminyl Radicals via the Hudson Reaction. *Org. Lett.* **1999**, *1*, 637-640; (b) Cadot, C.; Dalko, P. I.; Cossy, J.; Ollivier, C.; Chuard, R.; Renaud, P. Free-Radical Hydroxylation Reactions of Alkylboronates. *J. Org. Chem.* **2002**, *67*, 7193-7202; (c) Wetter, C.; Studer, A. Microwave-assisted free radical chemistry using the persistent radical effect. *Chem. Commun.* **2004**, 174-175; (d) Studer, A. Tin-free radical chemistry using the persistent radical effect: alkoxyamine isomerization, addition reactions and polymerizations. *Chem. Soc. Rev.* **2004**, *033*, 267-273.

70. (a) Souaille, M.; Fischer, H. Living Free Radical Polymerizations Mediated by the Reversible Combination of Transient Propagating and Persistent Nitroxide Radicals. The Role of Hydroxylamine and Alkene Formation. *Macromolecules* **2001**, *34*, 2830-2838; (b) Kaim, A. Deactivation reactions in the modeled 2,2,6,6-tetramethyl-1-piperidinyloxy-mediated free-radical polymerization of styrene: A comparative study with the 2,2,6,6-tetramethyl-1-piperidinyloxy/acrylonitrile system. *J. Polym. Sci., Part A: Polym. Chem.* **2007**, *45*, 232-241.

71. Litwinienko, G.; Beckwith, A. L. J.; Ingold, K. U. The frequently overlooked importance of solvent in free radical syntheses. *Chem. Soc. Rev.* **2011**, *40*, 2157-2163.

72. (a) Alfassi, Z. B.; Benson, S. W.; Golden, D. M. Very low pressure pyrolysis of 1,3-cyclohexadiene. Orbital symmetry nonallowed reaction. *J. Am. Chem. Soc.* **1973**, *95*, 4784-4788; (b) Gao, Y.; DeYonker, N. J.; Garrett, E. C.; Wilson, A. K.; Cundari, T. R.; Marshall, P. Enthalpy of Formation of the Cyclohexadienyl Radical and the C−H Bond Enthalpy of 1,4-Cyclohexadiene: An Experimental and Computational Re-Evaluation. *J. Phys. Chem. A* **2009**, *113*, 6955-6963.

73. Hendry, D. G.; Schuetzle, D. Reactions of hydroperoxy radicals. Liquid-phase oxidation of 1,4-cyclohexadiene. *J. Am. Chem. Soc.* **1975**, *97*, 7123-7127.

74. Woodward, R. B.; Hoffmann, R. The Conservation of Orbital Symmetry. *Angew. Chem. Int. Ed. Engl.* **1969**, *8*, 781-853.

75. Wellington, C. A.; Walters, W. D. The Vapor Phase Decomposition of 2,5-Dihydrofuran. *J. Am. Chem. Soc.* **1961**, *83*, 4888-4891.

76. (a) Ellis, R. J.; Frey, H. M. The thermal unimolecular isomerisation of bicyclo[3,1,0]hex-2-ene and decomposition of cyclohexa-1,4-diene. *J. Chem. Soc. A* **1966**, 553-556; (b) Benson, S. W.; Shaw, R. Kinetics and mechanism of the pyrolysis of 1,4-cyclohexadiene. *Trans. Faraday Soc.* **1967**, *63*, 985-992.

77. Benson, S. W.; Shaw, R. Kinetics and Mechanism of the Pyrolysis of 1,3-Cyclohexadiene. A Thermal Source of Cyclohexadienyl Radicals and Hydrogen Atoms. The Addition of Hydrogen Atoms to Benzene and Toluene. *J. Am. Chem. Soc.* **1967**, *89*, 5351-5354.

78. DeBoef, B.; Counts, W. R.; Gilbertson, S. R. Rhodium-Catalyzed Synthesis of Eight-Membered Rings. *J. Org. Chem.* **2007**, *72*, 799-804.

79. Brooner, R. E. M.; Brown, T. J.; Widenhoefer, R. A. Direct Observation of a Cationic Gold(I)–Bicyclo[3.2.0]hept-1(7)-ene Complex Generated in the Cycloisomerization of a 7-Phenyl-1,6-enyne. *Angew. Chem. Int. Ed.* **2013**, *52*, 6259-6261.

80. (a) Vasilev, N.; Elfahmi; Bos, R.; Kayser, O.; Momekov, G.; Konstantinov, S.; Ionkova, I. Production of Justicidin B, a Cytotoxic Arylnaphthalene Lignan from Genetically Transformed Root Cultures of Linum leonii. *J. Nat. Prod.* **2006**, *69*, 1014-1017; (b) Shen, W.; Zou, X.; Chen, M.; Liu, P.; Shen, Y.; Huang, S.; Guo, H.; Zhang, L. Effects of diphyllin as a novel V-ATPase inhibitor on gastric adenocarcinoma. *Eur. J. Pharmacol.* **2011**, *667*, 330-338.

81. (a) Di Giorgio, C.; Delmas, F.; Akhmedjanova, V.; Ollivier, E.; Bessonova, I.; Riad, E.; Timon-David, P. In Vitro Antileishmanial Activity of Diphyllin Isolated from Haplophyllum bucharicum. *Planta Med.* **2005**, *71*, 366-369; (b) Schmidt, T. J.; Khalid, S. A.; Romanha, A. J.; Alves, T. M. A.; Biavatti, M. W.; Brun, R.; Costa, F. B. D.; Castro, S. L. d.; Ferreira, V. F.; Lacerda, M. V. G. d.; Lago, J. H. G.; Leon, L. L.; Lopes, N. P.; Amorim, R. C. d. N.; Niehues, M.; Ogungbe, I. V.; Pohlit, A. M.; Scotti, M. T.; Setzer, W. N.; Soeiro, M. d. N. C.; Steindel, M.; Tempone, A. G. The Potential of Secondary Metabolites from Plants as Drugs or Leads Against Protozoan Neglected Diseases - Part II. *Curr. Med. Chem.* **2012**, *19*, 2176-2228.

82. Asano, J.; Chiba, K.; Tada, M.; Yoshii, T. Antiviral activity of lignans and their glycosides from Justicia procumbens. *Phytochemistry* **1996**, *42*, 713-717.

83. Baba, A.; Kawamura, N.; Makino, H.; Ohta, Y.; Taketomi, S.; Sohda, T. Studies on Disease-Modifying Antirheumatic Drugs: Synthesis of Novel Quinoline and Quinazoline Derivatives and Their Anti-inflammatory Effect. *J. Med. Chem.* **1996**, *39*, 5176-5182.

84. Zhang, J.; Liu, Y.-Q.; Yang, L.; Feng, G. Podophyllotoxin Derivatives Show Activity Against *Brontispa longissima* Larvae. *Nat. Prod. Commun.* **2010**, *5*, 1247-1250.

85. Gordaliza, M.; Faircloth, G. T.; Castro, M. A.; Miguel del Corral, J. M.; López-Vázquez, M. L.; San Feliciano, A. Immunosuppressive Cyclolignans. *J. Med. Chem.* **1996**, *39*, 2865-2868.

86. (a) Hande, K. R. Etoposide: four decades of development of a topoisomerase II inhibitor. *Eur. J. Cancer* **1998**, *34*, 1514-1521; (b) Robinson, M. J.; Osheroff, N. Effects of antineoplastic drugs on the post-strand-passage DNA cleavage/religation equilibrium of topoisomerase II. *Biochemistry* **1991**, *30*, 1807-1813; (c) Wu, C.-C.; Li, T.-K.; Farh, L.; Lin, L.-Y.; Lin, T.-S.; Yu, Y.-J.; Yen, T.-J.; Chiang, C.-W.; Chan, N.-L. Structural Basis of Type II Topoisomerase Inhibition by the Anticancer Drug Etoposide. *Science* **2011**, *333*, 459-462.

87. (a) You, Y. Podophyllotoxin Derivatives: Current Synthetic Approaches for New Anticancer Agents. *Curr. Pharm. Des.* **2005**, *11*, 1695-1717; (b) Jacob, D. A.; Gibson, E. G.; Mercer, S. L.; Deweese, J. E. Etoposide Catechol Is an Oxidizable Topoisomerase II Poison. *Chem. Res. Toxicol.* **2013**, *26*, 1156-1158.

88. Bailly, C. Contemporary Challenges in the Design of Topoisomerase II Inhibitors for Cancer Chemotherapy. *Chem. Rev.* **2012**, *112*, 3611-3640.

89. (a) Cochran, J. E.; Padwa, A. A New Approach to the 1-Arylnaphthalene Lignans Utilizing a Tandem Pummerer-Diels-Alder Reaction Sequence. *J. Org. Chem.* **1995**, *60*, 3938-3939; (b) Hui, J.; Zhao, Y.; Zhu, L. Synthesis and in vitro anticancer activities of novel aryl-naphthalene lignans. *Med. Chem. Res.* **2012**, *21*, 3994-4001.

90. (a) Morimoto, T.; Chiba, M.; Achiwa, K. Efficient asymmetric syntheses of naturally occurring lignan lactones using catalytic asymmetric hydrogenation as a key reaction. *Tetrahedron* **1993**, *49*, 1793-1806; (b) Cow, C.; Leung, C.; Charlton, J. L. Antiviral activity of arylnaphthalene and aryldihydronaphthalene lignans. *Can. J. Chem.* **2000**, *78*, 553-561.

91. Patel, R. M.; Argade, N. P. Palladium-Promoted [2 + 2 + 2] Cocyclization of Arynes and Unsymmetrical Conjugated Dienes: Synthesis of Justicidin B and Retrojusticidin B. *Org. Lett.* **2012**, *15*, 14-17.

92. (a) Klemm, L. H.; Santhanam, P. Intramolecular Diels-Alder reactions. V. Synthesis of dehydro-β-peltatin methyl ether. *J. Org. Chem.* **1968**, *33*, 1268-1269; (b) Klemm, L. H.; Santhanam, P. S. Intramolecular Diels-Alder reactions. VIII. Syntheses of phenolic cyclolignan lactones. *J. Heterocycl. Chem.* **1972**, *9*, 423-426.

93. (a) Joshi, B. S.; Viswanathan, N.; Balakrishnan, V.; Gawad, D. H.; Ravindranath, K. R. Attenuol—structure, stereochemistry and synthesis. *Tetrahedron* **1979**, *35*, 1665-1671; (b) Revesz, L.; Meigel, H. Design and Synthesis of a Potential Dopamine D-1 Antagonist. *Helv. Chim. Acta* **1988**, *71*, 1697-1703.

94. (a) Stevenson, R.; Block, E. Lignan lactones. Synthesis of (+/-)-collinusin and justicidin B. *J. Org. Chem.* **1971**, *36*, 3453-3455; (b) Tanoguchi, M.; Kashima, T.; Saika, H.; Inoue, T.; Arimoto, M.; Yamaguchi, H. Studies on the Constituents of the Seeds of Hernandia ovigera L. VII. : Syntheses of (+/-)-Hernolactone and (+/-)-Hernandin. *Chem. Pharm. Bull.* **1989**, *37*, 68-72; (c) Kashima, T.; Tanoguchi, M.; Arimoto, M.; Yamaguchi, H. Studies on the Constituents of the Seeds of Hernandia ovigera L. VIII. Syntheses of (+/-)-Desoxypodophyllotoxin and β-Peltatin-A Methyl Ether. *Chem. Pharm. Bull.* **1991**, *39*, 192-194.

95. Tang, J.-S.; Xie, Y.-X.; Wang, Z.-Q.; Deng, C.-L.; Li, J.-H. Phosphazene Base-Catalyzed Intramolecular Cascade Reactions of Aryl-Substituted Enynes. *Synthesis* **2010**, *2010*, 3204-3210.

96. Mondal, S.; Maji, M.; Basak, A. A Garratt–Braverman route to aryl naphthalene lignans. *Tetrahedron Lett.* **2011**, *52*, 1183-1186.

97. Clasby, M. C.; Chackalamannil, S.; Czarniecki, M.; Doller, D.; Eagen, K.; Greenlee, W. J.; Lin, Y.; Tagat, J. R.; Tsai, H.; Xia, Y.; Ahn, H.-S.; Agans-Fantuzzi, J.; Boykow, G.; Chintala, M.; Hsieh, Y.; McPhail, A. T. Himbacine derived thrombin receptor antagonists: Discovery of a new tricyclic core. *Bioorg. Med. Chem. Lett.* **2007**, *17*, 3647-3651.

98. (a) Forsyth, D. A.; Sebag, A. B. Computed ^{13}C NMR Chemical Shifts via Empirically Scaled GIAO Shieldings and Molecular Mechanics Geometries. Conformation and Configuration from ^{13}C Shifts. *J. Am. Chem. Soc.* **1997**, *119*, 9483-9494; (b) Rychnovsky, S. D. Predicting NMR Spectra by Computational Methods: Structure Revision of Hexacyclinol. *Org. Lett.* **2006**, *8*, 2895-2898; (c) Nicolaou, K. C.; Frederick, M. O. On the Structure of Maitotoxin. *Angew. Chem. Int. Ed.* **2007**, *46*, 5278-5282; (d) Smith, S. G.; Goodman, J. M. Assigning Stereochemistry to Single Diastereoisomers by GIAO NMR Calculation: The DP4 Probability. *J. Am. Chem. Soc.* **2010**, *132*, 12946-12959; (e) Willoughby, P. H.; Jansma, M. J.; Hoye, T. R. A guide to small-molecule structure assignment through computation of (^{1}H and ^{13}C) NMR chemical shifts. *Nat. Protocols* **2014**, *9*, 643-660.

99. Barone, G.; Gomez-Paloma, L.; Duca, D.; Silvestri, A.; Riccio, R.; Bifulco, G. Structure Validation of Natural Products by Quantum-Mechanical GIAO Calculations of ^{13}C NMR Chemical Shifts. *Chem. Eur. J.* **2002**, *8*, 3233-3239.

100. da Silva, R.; Ruas, M. M.; Donate, P. M. Complete assignments of ^{1}H and ^{13}C NMR spectral data for arylnaphthalene lignan lactones. *Magn. Reson. Chem.* **2007**, *45*, 902-904.

101. *Spartan '10 for Windows, Macintosh, and Linux*. Wavefunction, Inc.: 2011; 485-487.

102. Joseph, R. L. *Principles of Fluorescence Spectroscopy*. 3rd ed.; Springer Science+Business Media, LLC: New York, 2006;

103. (a) Johnsson, N.; Johnsson, K. Chemical Tools for Biomolecular Imaging. *ACS Chem. Biol.* **2007**, *2*, 31-38; (b) Fernandez-Suarez, M.; Ting, A. Y. Fluorescent probes for super-resolution imaging in living cells. *Nat. Rev. Mol. Cell Biol.* **2008**, *9*, 929-943; (c) Im, C.-N.; Kang, N.-Y.; Ha, H.-H.; Bi, X.; Lee, J. J.; Park, S.-J.; Lee, S. Y.; Vendrell, M.; Kim, Y. K.; Lee, J.-S.; Li, J.; Ahn, Y.-H.; Feng, B.; Ng, H.-H.; Yun, S.-W.; Chang, Y.-T. A Fluorescent Rosamine Compound Selectively Stains Pluripotent Stem Cells. *Angew. Chem. Int. Ed.* **2010**, *49*, 7497-7500.

104. Sinkeldam, R. W.; Greco, N. J.; Tor, Y. Fluorescent Analogs of Biomolecular Building Blocks: Design, Properties, and Applications. *Chem. Rev.* **2010**, *110*, 2579-2619.

105. Prendergast, F. G.; Meyer, M.; Carlson, G. L.; Iida, S.; Potter, J. D. Synthesis, spectral properties, and use of 6-acryloyl-2-dimethylaminonaphthalene (Acrylodan). A thiol-selective, polarity-sensitive fluorescent probe. *J. Biol. Chem.* **1983**, *258*, 7541-7544.

106. Gangopadhyay, J. P.; Grabarek, Z.; Ikemoto, N. Fluorescence probe study of Ca^{2+}-dependent interactions of calmodulin with calmodulin-binding peptides of the ryanodine receptor. *Biochem. Biophys. Res. Commun.* **2004**, *323*, 760-768.

107. Cohen, B. E.; McAnaney, T. B.; Park, E. S.; Jan, Y. N.; Boxer, S. G.; Jan, L. Y. Probing Protein Electrostatics with a Synthetic Fluorescent Amino Acid. *Science* **2002**, *296*, 1700-1703.

108. Lu, Z.; Lord, S. J.; Wang, H.; Moerner, W. E.; Twieg, R. J. Long-Wavelength Analogue of PRODAN: Synthesis and Properties of Anthradan, a Fluorophore with a 2,6-Donor−Acceptor Anthracene Structure. *J. Org. Chem.* **2006**, *71*, 9651-9657.

109. Balo, C.; Fernández, F.; García-Mera, X.; López, C. SYNTHESIS OF FLUORESCENCE PROBES WITH A 2,6-AMINONAPHTHALENE-CARBONYL CHROMOPHORE. *Org. Prep. Proced. Int.* **2000**, *32*, 367-372.

110. Silvonek, S. S.; Giller, C. B.; Abelt, C. J. ALTERNATE SYNTHESES OF PRODAN AND ACRYLODAN. *Org. Prep. Proced. Int.* **2005**, *37*, 589-594.

111. Cornec, A.-S.; Baudequin, C.; Fiol-Petit, C.; Plé, N.; Dupas, G.; Ramondenc, Y. One "Click" to Access Push–Triazole–Pull Fluorophores Incorporating a Pyrimidine Moiety: Structure–Photophysical Properties Relationships. *Eur. J. Org. Chem.* **2013**, *2013*, 1908-1915.

112. Kim, E.; Koh, M.; Lim, B. J.; Park, S. B. Emission Wavelength Prediction of a Full-Color-Tunable Fluorescent Core Skeleton, 9-Aryl-1,2-dihydropyrrolo[3,4-b]indolizin-3-one. *J. Am. Chem. Soc.* **2011**, *133*, 6642-6649.

113. Loudet, A.; Burgess, K. BODIPY Dyes and Their Derivatives: Syntheses and Spectroscopic Properties. *Chem. Rev.* **2007**, *107*, 4891-4932.

114. Mishra, A.; Behera, R. K.; Behera, P. K.; Mishra, B. K.; Behera, G. B. Cyanines during the 1990s: A Review. *Chem. Rev.* **2000**, *100*, 1973-2012.

115. Kunlinich, A. V.; Ischenko, A. A. Merocyanine dyes: synthesis, structure, properties, and applications. *Russ. Chem. Rev.* **2009**, *78*, 141-164.

116. Gieseking, R. L.; Mukhopadhyay, S.; Risko, C.; Marder, S. R.; Brédas, J.-L. 25th Anniversary Article: Design of Polymethine Dyes for All-Optical Switching Applications: Guidance from Theoretical and Computational Studies. *Adv. Mater.* **2014**, *26*, 68-84.

117. (a) Silva, G. L.; Ediz, V.; Yaron, D.; Armitage, B. A. Experimental and Computational Investigation of Unsymmetrical Cyanine Dyes: Understanding Torsionally Responsive Fluorogenic Dyes. *J. Am. Chem. Soc.* **2007**, *129*, 5710-5718; (b) Shank, N. I.; Pham, H. H.; Waggoner, A. S.; Armitage, B. A. Twisted Cyanines: A Non-Planar Fluorogenic Dye with Superior Photostability and its Use in a Protein-Based Fluoromodule. *J. Am. Chem. Soc.* **2012**, *135*, 242-251.

118. (a) Macgregor, R. B.; Weber, G. Estimation of the polarity of the protein interior by optical spectroscopy. *Nature* **1986**, *319*, 70-73; (b) Chakrabarti, A. Fluorescence of Spectrin-Bound Prodan. *Biochem. Biophys. Res. Commun.* **1996**, *226*, 495-497.

119. (a) Kimura, T.; Kawai, K.; Majima, T. Probing the microenvironments in the grooves of Z-DNA using dan-modified oligonucleotides. *Chem. Commun.* **2006**, 1542-1544; (b) Tainaka, K.; Tanaka, K.; Ikeda, S.; Nishiza, K.; Unzai, T.; Fujiwara, Y.; Saito, I.; Okamoto, A. PRODAN-Conjugated DNA: Synthesis and Photochemical Properties. *J. Am. Chem. Soc.* **2007**, *129*, 4776-4784.

120. (a) Massey, J. B.; She, H. S.; Pownall, H. J. Interfacial properties of model membranes and plasma lipoproteins containing ether lipids. *Biochemistry* **1985**, *24*, 6973-6978; (b) Bagatolli, L. A. To see or not to see: Lateral organization of biological membranes and fluorescence microscopy. *Biochimica et Biophysica Acta (BBA) - Biomembranes* **2006**, *1758*, 1541-1556; (c) Kim, H. M.; Choo, H.-J.; Jung, S.-Y.; Ko, Y.-G.; Park, W.-H.; Jeon, S.-J.; Kim, C. H.; Joo, T.; Cho, B. R. A Two-Photon Fluorescent Probe for Lipid Raft Imaging: C-Laurdan. *ChemBioChem* **2007**, *8*, 553-559; (d) Demchenko, A. P.; Mély, Y.; Duportail, G.; Klymchenko, A. S. Monitoring Biophysical Properties of Lipid Membranes by Environment-Sensitive Fluorescent Probes. *Biophys. J.* **2009**, *96*, 3461-3470.

121. (a) Surry, D. S.; Buchwald, S. L. Dialkylbiaryl phosphines in Pd-catalyzed amination: a user's guide. *Chem. Sci.* **2011**, *2*, 27-50; (b) Maiti, D.; Fors, B. P.; Henderson, J. L.; Nakamura, Y.; Buchwald, S. L. Palladium-catalyzed coupling of functionalized primary and secondary amines with aryl and heteroaryl halides: two ligands suffice in most cases. *Chem. Sci.* **2011**, *2*, 57-68.

122. Reddy, N. P.; Tanaka, M. Palladium-catalyzed amination of aryl chlorides. *Tetrahedron Lett.* **1997**, *38*, 4807-4810.

123. (a) Grabowski, Z. R.; Rotkiewicz, K.; Siemiarczuk, A.; Cowley, D. J.; Baumann, W. Twisted Intramolecular Charge Transfer States (TICT). A New Class of Excited States with Full Charge Separation. *Nouv. J. Chim.* **1979**, *3*, 443-454; (b) Rotkiewicz, K.; Rubaszewska, W. Intramolecular charge transfer state and unusual fluorescence from an upper excited singlet of a nonplanar derivative of p-cyano-N, N-dimethylaniline. *J. Lumin.* **1982**, *27*, 221-230; (c) Köhler, G.; Rechthaler, K.; Grabner, G.; Luboradzki, R.; Suwińska, K.; Rotkiewicz, K. Structure of Cage Amines as Models for Twisted Intramolecular Charge-Transfer States. *J. Phys. Chem. A* **1997**, *101*, 8518-8525; (d) Okada, T.; Uesugi, M.; Köhler, G.; Rechthaler, K.; Rotkiewicz, K.; Rettig, W.; Grabner, G. Time-resolved spectroscopy of DMABN and its cage derivatives 6-cyanobenzquinuclidine (CBQ) and benzquinuclidine (BQ). *Chem. Phys.* **1999**, *241*, 327-337; (e) Parusel, A. Semiempirical studies of solvent effects on the intramolecular charge transfer of the fluorescence probe PRODAN. *J. Chem. Soc., Faraday Trans.* **1998**, *94*, 2923-2927.

124. (a) Ilich, P.; Prendergast, F. G. Singlet adiabatic states of solvated PRODAN: a semiempirical molecular orbital study. *J. Phys. Chem.* **1989**, *93*, 4441-4447; (b) Parusel, A. B. J.; Schneider, F. W.; Köhler, G. An ab initio study on excited and ground state properties of the organic fluorescence probe PRODAN. *Journal of Molecular Structure: THEOCHEM* **1997**, *398–399*, 341-346.

125. (a) Balter, A.; Nowak, W.; Pawełkiewicz, W.; Kowalczyk, A. Some remarks on the interpretation of the spectral properties of prodan. *Chem. Phys. Lett.* **1988**, *143*, 565-570; (b) Catalan, J.; Perez, P.; Laynez, J.; Blanco, F. G. Analysis of the solvent effect on the photophysics properties of 6-propionyl-2-(dimethylamino)naphthalene (PRODAN). *J. Fluoresc.* **1991**, *1*, 215-223.

126. Samanta, A.; Fessenden, R. W. Excited State Dipole Moment of PRODAN as Determined from Transient Dielectric Loss Measurements. *J. Phys. Chem. A* **2000**, *104*, 8972-8975.

127. Lobo, B. C.; Abelt, C. J. Does PRODAN Possess a Planar or Twisted Charge-Transfer Excited State? Photophysical Properties of Two PRODAN Derivatives. *J. Phys. Chem. A* **2003**, *107*, 10938-10943.

128. Davis, B. N.; Abelt, C. J. Synthesis and Photophysical Properties of Models for Twisted PRODAN and Dimethylaminonaphthonitrile. *J. Phys. Chem. A* **2005**, *109*, 1295-1298.

129. Everett, R. K.; Nguyen, H. A. A.; Abelt, C. J. Does PRODAN Possess an O-TICT Excited State? Synthesis and Properties of Two Constrained Derivatives. *J. Phys. Chem. A* **2010**, *114*, 4946-4950.

130. Abelt, C. J.; Sun, T.; Everett, R. K. 2,5-PRODAN: synthesis and properties. *Photochem. Photobiol. Sci.* **2011**, *10*, 618-622.

131. Chapman, C. F.; Fee, R. S.; Maroncelli, M. Measurements of the Solute Dependence of Solvation Dynamics in 1-Propanol: The Role of Specific Hydrogen-Bonding Interactions. *J. Phys. Chem.* **1995**, *99*, 4811-4819.

132. Mataga, N.; Kaifu, Y.; Koizumi, M. Solvent Effects upon Fluorescence Spectra and the Dipolemoments of Excited Molecules. *Bull. Chem. Soc. Jpn.* **1956**, *29*, 465-470.

133. Cerezo, F. M.; Rocafort, S. C.; Sierra, P. S.; García-Blanco, F.; Oliva, C. D.; Sierra, J. C. Photophysical Study of the Probes Acrylodan (1-[6-(Dimethylamino)naphthalen-2-yl]prop-2-en-1-one), ANS (8-Anilinonaphthalene-1-sulfonate) and Prodan (1-[6-(Dimethylamino)naphthalen-2-yl]propan-1-one) in Aqueous Mixtures of Various Alcohols. *Helv. Chim. Acta* **2001**, *84*, 3306-3312.

134. Roesch, N.; Zerner, M. C. Calculation of Dispersion Energy Shifts in Molecular Electronic Spectra. *J. Phys. Chem.* **1994**, *98*, 5817-5823.

135. Balasubramaniyan, V. *peri* Interaction in Naphthalene Derivatives. *Chem. Rev.* **1966**, *66*, 567-641.

136. Karatsu, T.; Hazuku, R.; Asuke, M.; Nishigaki, A.; Yagai, S.; Suzuri, Y.; Kita, H.; Kitamura, A. Blue electroluminescence of silyl substituted anthracene derivatives. *Org. Electron.* **2007**, *8*, 357-366.

137. (a) Maeda, H.; Maeda, T.; Mizuno, K. Absorption and Fluorescence Spectroscopic Properties of 1- and 1,4-Silyl-Substituted Naphthalene Derivatives. *Molecules* **2012**, *17*, 5108-5125; (b) Maeda, H.; Ishida, H.; Inoue, Y.; Merpuge, A.; Maeda, T.; Mizuno, K. UV absorption and fluorescence properties of fused aromatic hydrocarbons having trimethylsilyl, trimethylgermyl, and trimethylstannyl groups. *Res. Chem. Intermed.* **2009**, *35*, 939-948.

138. Niko, Y.; Kawauchi, S.; Otsu, S.; Tokumaru, K.; Konishi, G.-i. Fluorescence Enhancement of Pyrene Chromophores Induced by Alkyl Groups through σ–π Conjugation: Systematic Synthesis of Primary, Secondary, and Tertiary Alkylated Pyrenes at the 1, 3, 6, and 8 Positions and Their Photophysical Properties. *J. Org. Chem.* **2013**, *78*, 3196-3207.

139. Karatsu, T.; Shibata, T.; Nishigaki, A.; Fukui, K.; Kitamura, A. π–π and σ–π Interactions in α,ω-Dinaphthyl and -Dianthryl Oligosilanes in Solution. *Chem. Lett.* **2001**, *30*, 994-995.

140. Kyushin, S.; Matsuura, T.; Matsumoto, H. 2,3,4,5-Tetrakis(dimethylsilyl)thiophene: The First 2,3,4,5-Tetrasilylthiophene. *Organometallics* **2006**, *25*, 2761-2765.

141. Hanamura, H.; Haneishi, R.; Nemoto, N. Fluorescent cyclopentadithiophene derivatives having phenyl-substituted silyl moieties. *Tetrahedron Lett.* **2011**, *52*, 4039-4041.

142. (a) Yamaguchi, S.; Tamao, K. Theoretical Study of the Electronic Structure of 2,2'-Bisilole in Comparison with 1,1'-Bi-1,3-cyclopentadiene: σ*–π* Conjugation and a Low-Lying LUMO as the Origin of the Unusual Optical Properties of 3,3',4,4'-Tetraphenyl-2,2'-bisilole. *Bull. Chem. Soc. Jpn.* **1996**, *69*, 2327-2334; (b) Bullpitt, M.; Kitching, W.; Adcock, W.; Doddrell, D. Group IVb metalloidal substituent effects studied by carbon-13 nuclear magnetic resonance spectroscopy. *J. Organomet. Chem.* **1976**, *116*, 161-185.

143. Kyushin, S.; Kitahara, T.; Matsumoto, H. Benzo[1,2:4,5]bis(1,1,2,2-tetraisopropyldisilacyclobutene). *Chem. Lett.* **1998**, *27*, 471-472.

144. Berlman, I. B. Empirical correlation between nuclear conformation and certain fluorescence and absorption characteristics of aromatic compounds. *J. Phys. Chem.* **1970**, *74*, 3085-3093.

145. (a) Reynolds, G. A.; Drexhage, K. H. New coumarin dyes with rigidized structure for flashlamp-pumped dye lasers. *Opt. Commun.* **1975**, *13*, 222-225; (b) Würth, C.; Grabolle, M.; Pauli, J.; Spieles, M.; Resch-Genger, U. Relative and absolute determination of fluorescence quantum yields of transparent samples. *Nat. Protocols* **2013**, *8*, 1535-1550.